U.PORTO

FACULDADE DE FARMÁCIA
UNIVERSIDADE DO PORTO

The *Leishmania TDR1* family-related gene: functional studies and evaluation of TDR1 recombinant protein as a vaccine against leishmaniasis

Ana Marta Franco da Silva

Dissertation thesis for the degree of Doctor of Philosophy in Pharmaceutical Sciences – Biochemistry submitted to the Faculty of Pharmacy, University of Porto

Supervisor: Professora Doutora Anabela Cordeiro da Silva - Faculdade de Farmácia da Universidade do Porto

Co-supervisor: Professor Graham H. Coombs - Strathclyde Institute of Pharmacy and Biomedical Sciences, University of Strathclyde

December 2011

AUTHOR'S DECLARATION

Under the terms of the Decree-Law nº 216/92, of October 13th, is hereby declared that the following original articles were prepared in the scope of this dissertation.

PUBLICATIONS

Articles in international peer-reviewed journals

Silva AM, Tavares J, Silvestre R, Ouaissi A, Coombs GH, Cordeiro-da-Silva A
Immunological role of *Leishmania infantum* Thiol Dependent Reductase. 1
Submitted for publication to Parasite Immunology

Silva AM, Cordeiro-da-Silva A, Coombs GH
Deletion of the *TDR1* gene provides evidence of variable ploidy in *Leishmania infantum.*
Submitted for publication to FEMS Microbiology Letters

Silva AM, Westrop GD, Müller S, Cordeiro-da-Silva A, Coombs GH
Thiol Dependent Reductase 1 of *Leishmania* is implicated in the regulation of central metabolism via deglutathionylation.
Submitted for publication to Free Radical Biology & Medicine

Silva AM, Cordeiro-da-Silva A, Coombs GH
Metabolic variation during development in culture of *Leishmania donovani* promastigotes.
PLoS Negl Trop Dis 2011;5(12):e1451.

Fyfe PK, Westrop GD, **Silva AM**, Coombs GH, Hunter WN
Leishmania donovani TDR1, a unique trimeric glutathione transferase evolved by gene duplication then fusion.
To be submitted for publication

Under the terms of the Decree-Law nº 216/92, of October 13th, the author declares that he afforded a major contribution to the conceptual design and technical execution of the work, interpretation of the results and manuscript preparation of the published articles included in this dissertation.

The candidate performed the experimental work with a doctoral fellowship (FCT/ SFRH/ BD/28316/2006) supported by the “Fundação para a Ciência e a Tecnologia”, which also participate with grants to attend in international meetings and for the graphical execution of this thesis. The Faculty of Pharmacy of the University of Porto (Portugal), the Institute for Molecular and Cell Biology of the University of Porto (Portugal) and the Strathclyde Institute of Pharmacy and Biomedical Sciences, University of Strathclyde (United Kindgom) provided the facilities and logistical supports.

À memória do meu pai,

João Costa Silva Júnior

"Eras um pouco de mim… Ficou o teu sorriso no que não esqueço, ficaste todo em mim. Pai. Nunca esquecerei."

(In morreste-me, José Luis Peixoto)

ACKNOWLEDGMENTS

I would like to thank everyone who has contributed to the realization of this thesis.

First, I would like to thank my supervisor, Prof. Anabela Cordeiro da Silva for the opportunity given to work in her research group, which led a couple of years later to the start of this thesis project. Thanks for all the support, guidance, encouragement and trust throughout all the years.

I would like to extend my gratitude to my co-supervisor Professor Graham Coombs for giving me the opportunity to carry out the research for this thesis in his lab and learn from his vast scientific knowledge. Thanks for all the advice, encouragement and guidance.

To all members of the Parasite Disease Group, thanks for your friendship and motivation, in particular to Joana Tavares, Ricardo Silvestre and Nuno Santarém, for the warm welcome when I arrived to the group and also for your patience to teach me the way in the field of parasitology and immunology. Joana, I have no words to thank all you taught me, for your availability, even when it meant a few more hours in the lab and above all your friendship!

I have spent a good part of this work in Glasgow and I would like to thank all the members of Graham's lab. Gareth for everything you taught me, for the patience to answer all my questions and advice. Roderick for your willingness to share ideas, your own work and your availability to hear about my work, even when was all about problems! A thank you also goes to Julien for the nice conversations not only about science and help with the metabolomics work. Thank you to former members Saskia, Ruben and Lesley.

I would like to thank Chris Carter for all the help with the animals experiments but above all for her enthusiasm about science and for the funny environment created in the BPU.

À minha família e amigos agradeço tudo o que consegui, sem o vosso apoio e carinho incondicional tudo teria sido muito mais difícil. Não posso deixar de mencionar em especial a minha avó, os meus tios que sempre cuidaram de mim com um carinho extraordinário e o meu Carlitos que sem saber é uma força especial! Todas as palavras

são poucas para expressar a minha gratidão. Um especial obrigado à D. Gina e ao Sr. Alvarinho que incondicionalmente me apoiaram e acarinharam desde o primeiro momento. À memória do meu avô João, a tua humildade, sacrifício e generosidade ensinaram-me a ser melhor em todos os momentos.

À minha mãe a tua dedicação, força e coragem acompanharam-me durante todo este percurso. Esta tese só foi possível com o teu amor incondicional, todas as palavras são poucas para expressar o quanto te agradeço.

E finalmente, dedico esta tese a ti, Gil com quem partilhei todos os momentos da sua concretização, as frustrações, as angústias, as pequenas vitórias… O teu apoio incondicional, paciência, compreensão, disponibilidade e força permitiram-me chegar ao fim desta etapa…

"Ontem arriscaste mais
Do que uma simples coisa exigia
Deste-me a chave dos sonhos
O caos e a harmonia"

"The important thing in science is not so much to obtain new facts as to discover new ways of thinking about them" (Sir William Bragg)

ABSTRACT

Leishmaniasis is a vector-borne disease caused by protozoan parasites of the genus *Leishmania* that affects millions of people worldwide. The disease can assume different clinical forms depending on the infectious species and also on the immune status of the host. Visceral leishmaniasis, caused by the members of the *L. donovani* complex, is the most severe form of the disease and is fatal if left untreated. Currently there is no effective vaccine available and the chemotherapeutic treatment that exists is expensive, toxic and lacks efficacy; moreover, drug resistance has emerged as a serious problem. Thus novel therapies are urgently required and this will be aided through characterization of the factors involved in parasite survival and virulence.

Leishmania Thiol dependent reductase 1 (TDR1) is parasite-specific enzyme that presents some similarities with human omega glutathione-S-transferase, as demonstrated previously by its thiol transferase and dehydroascorbate reductase activities. This enzyme also catalyzes *in vitro* the conversion of pentavalent antimonials (Sb^V) into a trivalent form, an ability that could be important in the mechanism of action of this drug against *Leishmania*. Alternatively, it could be involved in drug resistance as reduction of Sb^V and conjugation with thiols is used by the parasite to extrude the drug out of the cell.

TDR1's high similarity with a *T. cruzi* enzyme named Tc52 which had been previously reported as a virulence factor led us to analyze the effect of recombinant TDR1 on the immune response in the context of infection with *L. infantum* promastigotes. Balb/c immunization with recombinant TDR1 led to an increase in the CD8-T cell splenic population and decrease in IL-10 production, although the reduction in parasite burden was not sufficient to consider TDR1 as a good antigen to be used in vaccination approaches. Interesting was the finding of an increase in CD8-T cells induced by immunization with TDR1, since CD8-T cell activation and the formation of memory T cells plays an important role against parasitic diseases. These CD8-T cells presented increase expression of memory surface markers, potentially involved in the partial protection obtained at the chronic phase of infection.

In order to provide insights into the functional role of TDR1, attempts were made to delete the gene by homologous recombination in visceral *Leishmania* species (*L. infantum* and *L. donovani*). Unexpectedly, attempts to obtain the *L. donovani* null mutant after two rounds of gene deletion failed. *Leishmania* have been considered diploid organisms, although exceptions were reported and aneuploidy has arisen during attempts to delete essential

genes or in drug-resistant cell lines. The fact that a null mutant was previously obtained in *L. major* after two rounds of gene knockout suggested that the gene was unlikely to be essential in *L.donovani*. Thus we proceeded to the disruption of a third copy of the gene and a null mutant in *L. donovani* was obtained in this way. *L. infantum TDR1* null mutants were obtained both after 2 and 4 rounds of gene deletion, showing that the gene occurs in variable copy number within the same cloned population. *TDR1* null mutant generation has provided more evidence that the *Leishmania* genome has plasticity in terms of ploidy and recently reported genome sequence data for different *Leishmania* species supports this finding. Deletion of *TDR1* did not affect *L. donovani* and *L. infantum* parasites' virulence to macrophages. Further analysis of *L. donovani* null mutants revealed that the null mutants were not more susceptible to oxidative and nitrosative stress, although an increase in sensitivity to trivalent antimony and trivalent arsenite was observed, which could be related with TDR1 detoxification activities. Also, there were no changes in the susceptibility of intracellular parasites of the *TDR1* null mutant in macrophages to Sb^V when compared with the WT parasites. Thus, the results obtained did not support the role of TDR1 in drug activation or in the involvement in resistance to Sb^V.

Analysis of parasite's metabolome, a new approach to detect differences between *Leishmania* null mutants and the WT parent line, revealed few but striking differences in metabolite levels involved in energy and amino acid metabolism. This was interpreted as a metabolic re-configuration in the absence of TDR1, implying the enzyme in the regulation of metabolism through S-glutathionylation. Metabolic re-configuration has been reported in a wide range of organisms and occurs due to inhibition or activation of enzymes activity. S-glutationylation, which occurs in response to oxidative stress or under physiological conditions as a regulatory mechanism, has not yet been reported in *Leishmania* although the effect of *TDR1* deletion strongly suggests it existence. Furthermore, recombinant TDR1 has deglutathionylation activity towards protein and peptide substrates supporting the hypothesis postulated.

Overall, the results presented here provide information on the potential role of TDR1 *in vivo*, through the regulation of enzymes activities by S-glutathionylation. Moreover, *TDR1* gene clearly shows that *Leishmania* copes well with aneuploidy; the challenge now is to understand how the parasite takes advantage of this genomic feature. Metabolomics analysis has shown to be an excellent tool for dissecting differences between mutant or natural lines of *Leishmania*.

Keywords: *Leishmania*, Thiol dependent reductase 1, CD8-T cells, aneuploidy, deglutathionylation

RESUMO

A leishmaniose é uma doença parasitária causada por protozoários do género da *Leishmania.* Esta patologia afecta milhões de pessoas em todo o mundo, e pode assumir diferentes formas clínicas, dependendo da espécie de *Leishmania* que infecta e do estado imunológico do hospedeiro. A leishmaniose visceral, causada por parasitas do complexo *L. donovani,* representa a forma mais severa da doença, letal se não tratada. Actualmente não existe uma vacina contra a leishmaniose humana e os medicamentos disponíveis são dispendiosos, tóxicos, carecem de eficácia e verifica-se um número crescente de casos de resistência aos mesmos.

A "Thiol dependent reductase 1 (TDR1)" é uma enzima especifica do parasita *Leishmania* que apresenta algumas semelhanças com a proteina humana omega glutationa-S-transferase, tendo como actividades a redução do ácido dehidroascórbico e a transferência de tióis. Esta enzima também catalisa a conversão de compostos antimoniais pentavalentes (Sb^V) na sua forma trivalente, actividade que pode ser importante no mecanismo de acção deste medicamento contra o parasita ou estar envolvida na resistência ao mesmo, uma vez que a redução de Sb^V e posterior conjugação com tióis é usada pelo parasita como mecanismo de desintoxicação.
A homologia observada entre a TDR1 e a enzima de *T. cruzi*, designada Tc52, previamente considerada como um factor de virulência, conduziu à análise do efeito da proteína recombinante TDR1 (rTDR1) na resposta imunológica no contexto da infecção com formas promastigotas da *L. infantum.* A imunização de ratinhos Balb/c com rTDR1 induziu um aumento significativo no número das células T-CD8 do baço e uma diminuição na produção da citoquina IL-10 durante a fase crónica de infecção. No entanto a redução da carga parasitária não foi suficiente para considerar a TDR1 como um antigénio adequado para desenvolver uma vacina. Interessante foi o aumento das células T-CD8, uma vez que a activação destas e a formação de células T de memória desempenha um papel importante no controlo das doenças parasitárias. Verificou-se um aumento nos marcadores de superfície nas células T-CD8 característicos de células T centrais de memória, o que poderá ter contribuído para a protecção parcial obtida na fase crónica de infecção.

Com o objectivo de investigar a função da proteína TDR1 nas espécies de *Leishmania* viscerais (*L. donovani* e *L. infantum*) realizaram-se tentativas para remover os alelos que codificam para esta proteína através de recombinação homóloga. A remoção do gene não foi possível após duas rondas de transfecção. A *Leishmania* tem sido considerada

um organismo diplóide, apesar de terem sido já identificadas excepções e casos de aneuploidia detectados durante tentativas para eliminar genes essenciais ou em parasitas resistentes a medicamentos. O facto de um mutante nulo ter sido produzido anteriormente na *L. major*, sugeriu a possibilidade de o gene não ser essencial na *L. donovani,* dada a sua proximidade filogenética. Assim, procedemos a uma terceira ronda de transfecção na qual foi possível remover o último alelo do gene *TDR1.* No caso da *L. infantum*, os mutantes nulos foram obtidos após 2 e 4 rondas de transfecção, mostrando que o gene apresenta um número de cópias variável dentro da mesma população. Estes resultados fornecem evidências de que o genoma da *Leishmania* tem plasticidade em termos de ploidia, suportado pelos recentes dados obtidos na sequenciação do genoma de diferentes espécies de *Leishmania*. A remoção do gene *TDR1* não afectou a capacidade dos parasitas para infectar macrófagos. Uma análise detalhada dos mutantes nulos na *L. donovani* revelou que a remoção do gene alterou a susceptibilidade a compostos antimoniais trivalentes e arsénicos trivalentes, o que pode estar relacionado com a capacidade de desintoxicação da TDR1. Também não foram detectadas alterações na susceptibilidade ao stress oxidativo/nitrosativo e aos Sb^{V} pela forma intracelular do mutante nulo. Assim, os resultados experimentais não suportam a função da TDR1 na activação dos Sb^{V} ou na resistência a estes compostos.

A análise do metaboloma dos mutantes nulos na *L. donovani* revelou importantes diferenças, nos níveis de metabolitos envolvidos na produção de energia e metabolismo de aminoácidos. Estas alterações foram interpretadas como uma re-configuração metabólica, na ausência da TDR1, implicando a enzima na regulação do metabolismo através da modificação pós-traducional designada de S-glutationação. A S-glutationação pode ocorrer em condições de stress oxidativo mas também em condições fisiológicas como um mecanismo de regulação, através da inibição ou activação de enzimas; esta modificação ainda não foi descrita na *Leishmania*, no entanto as alterações detectadas devido à remoção do gene *TDR1* sugerem a sua existência. Além disso, rTDR1 é capaz de reverter a S-glutationação de diferentes substratos, proteínas e péptidos, suportando a hipótese acima descrita. Em suma, os resultados deste estudo fornecem informações sobre a potencial função da proteína TDR1 *in vivo*, como reguladora da actividade enzimática na célula através de S-glutationação. A análise do metaboloma mostrou ser uma excelente ferramenta para investigar as diferenças tanto entre linhas celulares mutantes como selvagens de *Leishmania*.

Palavras-chave: *Leishmania*, Thiol dependent reductase 1, células T-CD8, aneuploidia, glutationação.

TABLE OF CONTENTS

INDEX OF FIGURES

CHAPTER 1 *LEISHMANIA SPP.* AND LEISHMANIASIS

CHAPTER 2 *LEISHMANIA*: FROM GENOME TO METABOLOME

CHAPTER 3 *LEISHMANIA:* THIOL METABOLISM AND ANTIOXIDANT DEFENSE

INDEX OF TABLES

CHAPTER 2 *LEISHMANIA*: FROM GENOME TO METABOLOME

ABBREVIATIONS LIST

A2	amastigote antigen 2
ACR2	arsenate reductase 2
APx	ascorbate peroxidase
AsIII	arsenite
AsV	arsenate
CDNB	1-chloro-2,4-dinitrobenzene
CL	cutaneous leishmaniasis
CR1 or CR3	complement receptor 1 or 3
DAT	direct agglutination test
DC	dendritic cell
DHA	dehydroascorbate
DHAR	dehydroascorbate reductase
DHFR-TS	dihydrofolate-reductase thymidylate synthase
FML	fucose mannose ligand
GADPH	glyceraldehyde-3-phosphate dehydrogenase
GIPL	glycosylinositolphospholipids
GPI	glycosylphosphatidylinositol
GR	glutathione reductase
Grx	glutaredoxin
GSH	reduced glutathione
GSNO	S-nitrosoglutathione
Gsp	mono-glutathionylspermidine
GSSG	oxidized glutathione
GST	glutathione S-transferase
GSTO	omega glutathione S-transferase
H_2O_2	hydrogen peroxide
H_4F	methyl-tetrahydrobiopterin
HASPB1	hydrophilic acylated surface protein B1
HEDS	2-hydroxyethyldisulphide
HIV	human immunodeficiency virus
HMG-CoA	3-hydroxy-3-methylglutaryl-CoA
IFAT	indirect fluorescent antibody test
IPC	inositolphosphorylceramide

kDNA	kinetoplast
KMP-11	kinetoplastid membrane protein 11
LACK	*Leishmania* homologue of receptor for activated C kinase
LC-MS	liquid chromatography–mass spectrometry
LeIF	*Leishmania* elongation and initiation factor
LmSTI1	*Leishmania major* homologue of the eukaryotic stress-inducible protein
LPG	lipophosphoglycan
ML	mucocutaneous leishmaniasis
MPL-SE	monophosphoryl lipid A - stable emulsion
MVT	multi-vesicular tubule (MVT)
NET	neutrophil extracellular traps
NF-kβ	nuclear factor -kappa
$NO^{\cdot}$	nitric oxid
nsGPx	non-selenium glutathione peroxidase
$O_2^{\cdot -}$	superoxide radical
$OH^{\cdot}$	hydroxyl radical
$ONOO^{-}$	peroxynitrite
OvSH	ovothiol
PAPS	phosphoadenylsulfate reductase
PC	phosphatidylcholine
PE	phosphatidylethanolamine
PEP	phosphoenolpyruvate
PG	phosphatidylglycerol
PI	phosphatidylinositol
PKDL	post-kala-azar dermal leishmaniasis
PL	phospholipid
Plrx	plasmoredoxin
PM	peritrophic matrix
PPP	pentose phosphate pathway
PS	phosphatidylserine
PSA-2	parasite surface antigen 2
PSG	promastigote secretory gel
PTM	post-translational modification
PTR1	pterin reductase 1
PV	parasitophorous vesicle
RNAi	interference RNA
RNS	reactive nitrogen species

ROS	reactive oxygen species
RR	ribonucleotide reductase
SAM	S-adenosyl-methionine
Sb^{III}	trivalent antimonial
Sb^{V}	pentavalent antimonial
SIR2	silent information regulator 2
SL	sphingolipid
SNPs	single nucleotide polymorphisms
SO_2H	sulfinic acid
SO_3H	sulfonic acid
SOH	sulfenic acid
SSG	sodium stibogluconate
$T(SH)_2$	trypanothione
TCA	tricarboxylic acid
TDR1	thiol dependent reductase 1
TGF	transforming growth factor
TNF	tumor necrosis factor
TR	thioredoxin reductase
Trx	thoredoxin
TryR	trypanothione reductase
TryS	trypanothione synthetase
TSA	thiol-specific-antioxidant
TXN	tryparedoxin
TXNPx	tryparedoxin peroxidase
UMSBP	universal minicircle sequence binding protein
UTR	untranslated region
VL	visceral leishmaniasis
WHO	World Health Organization

CHAPTER 1

LEISHMANIA SPP. AND LEISHMANIASIS

1.1 The *Leishmania* parasite

1.1.1 History and taxonomy

Leishmania parasite was first described in 1885 by Cunningham in India from a tissue taken from a sore called the Delhi boil, which at the time was thought to have fungal origin. Later, in 1898, Borovsky reported that the causative agent was a protozoan and described the anatomy of the organism. William Leishman and Charles Donovan were the first to attribute to the parasite the etiology of the disease, after independently discovering the parasite in the spleens of patients with kala azar, nowadays called visceral leishmaniasis[1]. In 1904, the organism responsible for the disease was recognised as being protozoan in nature, named "Leishman-Donovan bodies" and received the taxonomic designation of *Leishmania donovani*. In 1924, John Sinton proposed the theory that the sand fly was the vector of the Kala-azar parasite, *L. donovani* and only later, Robert Knowles and scientists at the Calcutta School of Tropical Medicine gave evidence to support Sinton's theory, by detection of *Leishmania* parasites in sand flies that had been fed on patients. The first experimental evidence of transmission of leishmaniasis by the bite of sand flies was by Shortt et al in 1931, who achieved the transmission of *L. donovani* to hamsters by the bite of *Phlebotomus argentipes*[2]. Since then, *Leishmania* has been found to be a complex grouping of species, more than 20 species transmitted to humans by species of phlebotomine sandflies, which cause several diverse clinical manifestations[3]. Currently there are two groups of *Leishmania* parasites, subgenera Leishmania and Vianna, classified based on which part of the sand fly gut is colonized by the parasite[4]. This separation was also supported by DNA sequence-based phylogenetic analysis[5] (Figure 1.1).

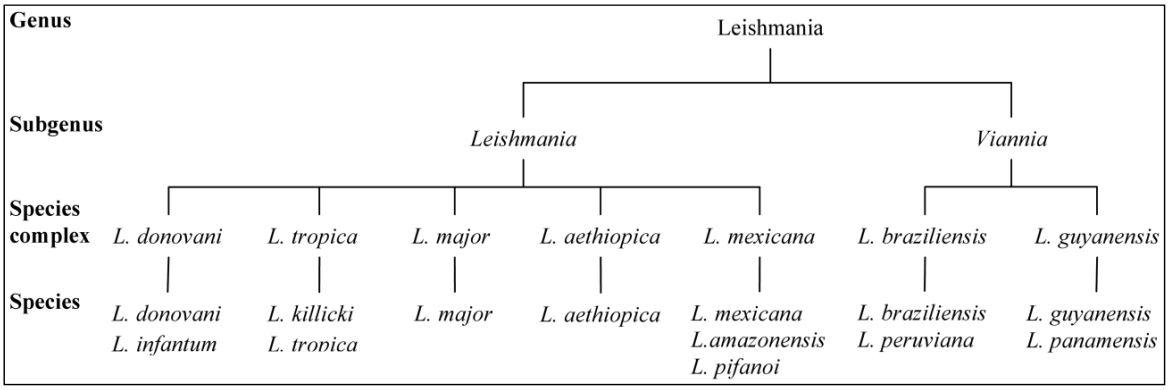

Figure 1.1 The main species of *Leishmania* that affect humans (adapted from WHO[6]).

Members of the subgenus *Leishmania* undergo suprapylarian development taking place exclusively in the midgut and foregut of the vector whereas members of the subgenus Viannia also undergo a period of peripylarian development in the hindgut[5, 7].

1.1.2 Morphology and ultrastructure

Leishmania has a dimorphic life cycle and two main forms can be distinguished: an extracellular promastigote stage that develops within the digestive tract of sand flies and an intracellular amastigotes, which proliferate and multiply within the phagolysosome of mammalian macrophages. The promastigotes have a fusiform shape (5-15μM) while amastigote forms are smaller and present an ovoid shape (3-5μM); both forms possess a specialized invagination of the plasma membrane, named flagellar pocket, at the anterior end of the parasite that encloses the base of the flagellum that in amastigotes is greatly reduced or barely emergent[8], the reason why amastigotes are non-motile forms (Figure 1.2).

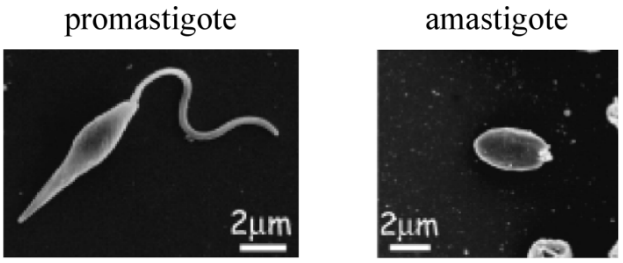

Figure 1.2 Scanning electron microscope images of *Leishmania* main morphological forms: promastigotes and amastigote (adapted from Besteiro *et al.*[9]).

In 1950s, a report by Chang has described the ultrastructure of *L. donovani* as follow: "The structure of the intracellular form of *Leishmania donovani* as seen by the light microscope consists of a nucleus and usually a rod-like kinetoplast within a homogeneous mass of cytoplasm, while the extracellular or culture form has, in addition to these structures, an anterior flagellum" and concluded "intra- and extracellular phases of the parasite possess the same basic structures"[10]. There are considerable variations between different species of kinetoplastids and even between different life cycle stages within a specie; ultrastructure features such as the overall dimension, flagelar morphology and position of kinetoplast (mitochondrial) and flagellar basal body relative position to the nucleus have been used to distinguish the different forms[11]. Nevertheless, research work through the years has shown that the different developmental stages can be distinguished from each other based also on their growth rates, nutritional requirements and the

regulated expression of surface proteins. Moreover, parasite differentiation is often marked by dramatic changes in the morphology and function of organelles in the secretory and endocytic pathways that regulate many of these processes. A schematic representation of the main intracellular organelles from promastigotes and amastigote forms (Figure 1.3) reveals differences between the two forms such as the absence of flagellum in the amastigote form and the presence of multi-vesicular tubule (MVT) lysosome or megasomes in the promastigotes and amastigote form, respectively.

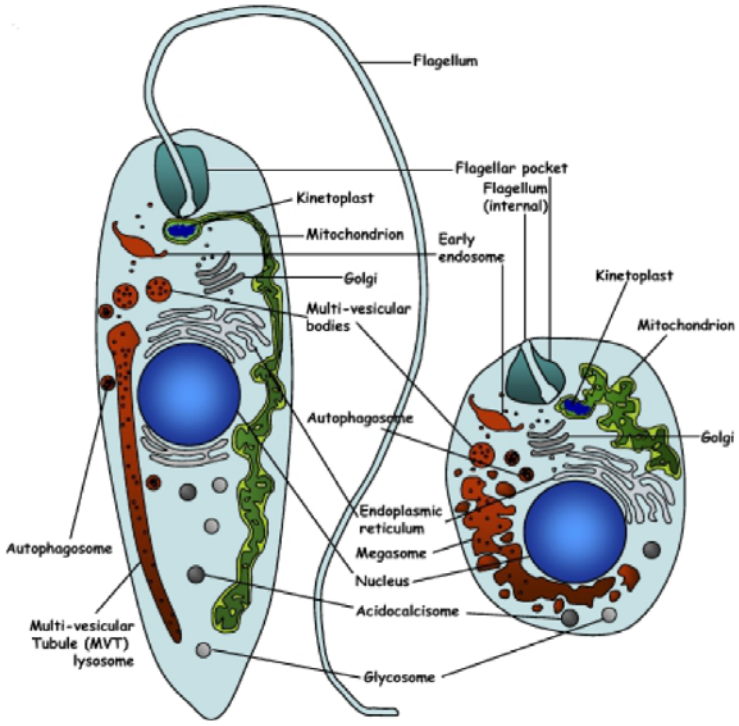

Figure 1.3 Schematic representation of the main intracellular organelles from *Leishmania* promastigote (left) or amastigote (right) forms (adapted from Besteiro *et al.*[9]).

Surface membrane of Kinetoplastids, including *Leishmania*, is divided into 3 morphological distinct subdomains: (i) the flagellum, (ii) the flagellar pocket and (iii) a pellicular plasma membrane[12], which surrounds the body of the cell and is attached to an array of subpeculiar microtubules that underlie the plasma membrane[13]. The flagellum is responsible for parasite motility, but is also involved in the attachment of the parasite to the sand fly[12] and may have a role in environmental sensing, as many nutrients and signaling proteins are targeted to the flagellar membrane[14]. The single flagellum emerges from a deep invagination, named flagellar pocket, which is an important zone of interaction between the parasite and its environment because it is the only site in the cell for endocytosis and exocytosis being responsible for crucial exchanges such as uptake of

nutrients via receptor-mediated endocytosis[15] for secretion of proteins into the extracellular medium, and for integration of membrane proteins into the cell surface[12, 16], which is supported by the fact that the structure is surrounded by several organelles of the secretory and endocytic pathways[13]. Besides the flagellar pocket, *Leishmania* contains other specialized organelles such as the kinetoplast and glycosomes.

The mitochondrial DNA is enclosed in an unusual structure known as the kinetoplast (kDNA), considered one of the unusual characteristic of trypanosomatids. kDNA is a network of thousands of catenated circular DNAs of two types, maxicircles and minicircles. There are several thousand minicircles, which range in size from about 0.5 to 2.5 kb (depending on the species), and a few dozen maxicircles, which usually vary between 20 and 40 kb[17, 18]. The maxicircles are structurally and functionally analogous to the mitochondrial DNA from higher eukaryotes, and they encode rRNAs and subunits of the respiratory complexes. Minicircles encode guide RNAs that modify the maxicircle transcripts by extensive uridylate insertion or deletion in a process known as RNA editing[19].

Another unique feature of trypanosomatids is the compartmentalization of several important metabolic pathways, such as glycolysis, in organelles designated glycosomes[20]. Compartmentation of glycolytic enzymes in *T. brucei* prevents the toxic accumulation of glycolysis metabolism intermediates, as the parasite lacks a feedback regulation of the early steps of glycolysis[21]. The sequestering of pathways of carbohydrate metabolism within the glycosomes may allow a rapid adaptation of parasites to new nutritional conditions during their life cycle[20].

1.1.3 Life cycle

The life cycle of *Leishmania* alternates between a mammalian host and a phlebotomine sand fly (Figure 1.4). Phlebotomies sand flies are the vectors responsible for the transmission to mammalian hosts ranging from desert rats to humans[22], who are often an accidental host. Female sand flies become infected when they feed on an infected host, as free amastigotes or amastigote-infected mononuclear cells are ingested along with the blood meal. Once in the vector, amastigotes will transform into motile and replicative forms called procyclic promastigotes. This development is triggered by a change in environmental conditions such as decrease in temperature and increase in pH[7, 23]. The *Leishmania* procyclic promastigote will differentiate into the infective, non-dividing

metacyclic promastigote, a form characterized by a smaller body and a longer flagellum that undergo significant changes for a successful transmission to the mammalian host.

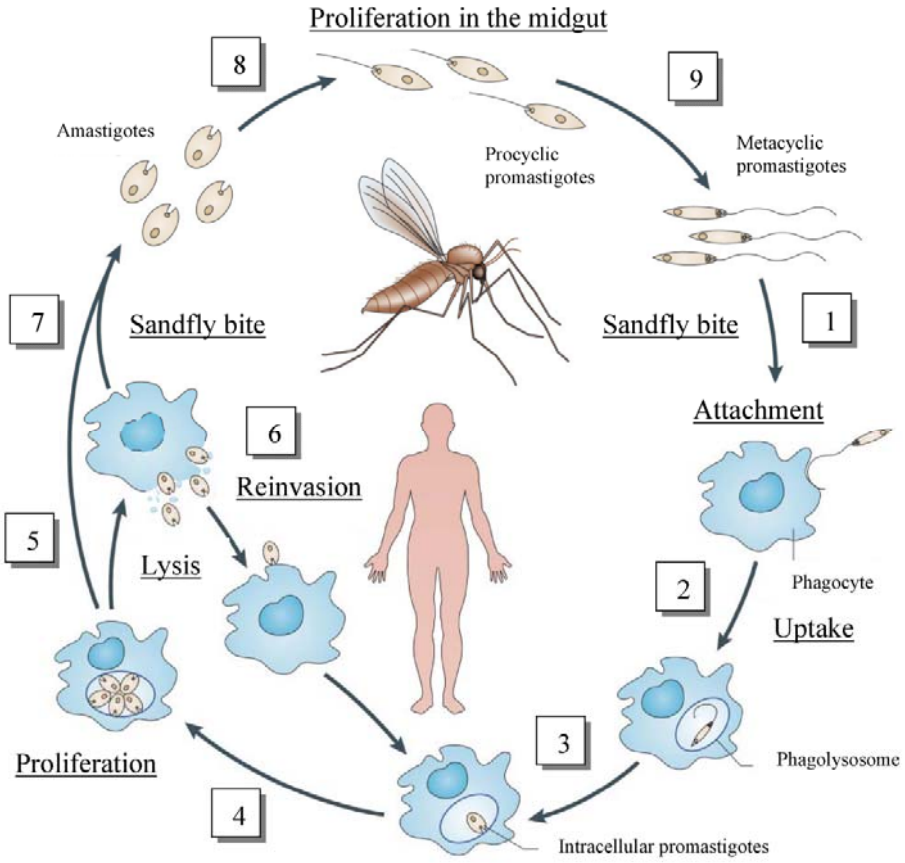

Figure 1.4 The life cycle of *Leishmania* parasites. *Leishmania* metacyclic promastigotes are delivered to the mammalian host through the bite of an infected sandfly (1) followed by the promastigote attachement to the macrophage. Once phagocytised by the macrophage (2), the parasite-containing phagosomes fuse with lysosomes, forming phagolysosomes, where the promastigotes forms differentiate into amastigotes (3), replicate (4), and are released by lysis of the infected macrophages (5), leading to infection of other cells (6). Following ingestion of the parasite by the sandfly during a bloodmeal (7), amastigotes differentiate into procyclic promastigotes (8), which then undergo several changes and develop into the infective metacyclic stage (9) (adapted from Kaye *et al.*[24]).

During another blood feeding, the sandfly regurgitates the metacyclic promastigotes, which are phagocytosed by macrophages or other cell types, such as neutrophils, dendritic cells or fibroblasts found in the local environment. Once inside the macrophage, the promastigotes undergo significant biochemical and metabolic changes, which result in

the intracellular aflagellate amastigote form, which can replicate within the macrophage parasitophorous vacuoles.

1.1.4 *Leishmania*-sand fly interactions

There are approximately 1000 species of sand flies, from which only 70 are proven or probable vectors of *Leishmania*[25]. *Leishmania* vectors are small insects of the order Diptera, subfamily Phlebotominae commonly called phlebotomie sand flies, with a body length of approximately 2−3 mm (Figure 1.5)[26, 27]. There are 3 features that make sand flies easy to recognize as described by Killick-Kendrick *et al* : "when at rest, they characteristically hold their wings at an angle above the abdomen; they are hairy; and, when coming to engorge, they typically hop around on the host before settling down to bite"[26]. The activity of sand flies is crepuscular or nocturnal and diurnal resting places are comparatively cool and humid[26, 28]. Both male and females sand flies feed on natural sugar sources but only females also feed on blood which provides nutrition for the production of eggs[26].

Figure 1.5 A blood-sucking phlebotomine sand fly (adapted from Kato *et al.*[27]).

Many factors can account for the low number of sand fly species that participate in the transmission of leishmaniasis such as a different distribution from that of the reservoir host, inability to support the development of *Leishmania*. To be considered as a *Leishmania* vector, a sand fly must be anthropophilic, bite the reservoir host(s), infected in the nature with the same *Leishmania* as occurs in humans, support the growth of the parasite and be able to transmit the parasite by bitting[26]. Thus *Leishmania* species are restricted to two genera of phlebotomie sand flies: *Phlebotomus*, divided into 12 subgenera, and *Lutzomyia*, divided into 25 subgenera and species groups[26]. The vectors can be further divided into specific or permissive considering the vector competence to

support the growth of only one or more species of *Leishmania.* Some phlebotomine species are considered specific as they can support the growth of only those species of *Leishmania* with which they are infected in nature, such as *Phlebotomus papatasi and Phlebotomus sergenti*; other species such as *Lutzomyia longipalpis* and *Phlebotomus argentipes* are permissive vectors since they are able to develop mature transmissible infections when infected with several *Leishmania* species[29-32]. Vectorial competence is influenced mainly by 3 factors: parasite resistance to the action of digestive enzymes produced in the sand fly midgut, which may inhibit the early growth of parasites in the bloodmeal[33]; the presence on the inner surface of the gut of the vector of the appropriate lipophosphoglycan-binding sites that match the lipophosphoglycan on the surface of the promastigotes, enabling them to attach to the inner surface of the sandfly gut[33, 34] and the complete development of the parasite to produce metacyclic promastigotes, the only form of the parasite that can survive in the vertebrate host[2]. Besides the digestive enzymes, other potential barriers to the complete development of the parasite in the sand fly, such as, the peritrophic membrane (physical barrier to parasite migration out of the abdominal midgut), the excretion of the digested bloodmeal (may result in loss of infection from the gut) and the anatomy and physiology of the anterior gut (may prevent the forward movement of metacyclic promastigotes and their egestion during blood feeding) have likely forced the parasite to express specific molecules in order to survive in the sand fly[2].

In the sand fly, can be distinguished 4 major development forms: procyclic, nectomonad, leptomonad and metacyclic promastigotes. *Leishmania* development in the sand fly is often simplified to two main forms, procyclic and metacyclic, however promastigotes undergo a sequential transformation that is dependent on the nutrient availability and occurs as they migrate from the posterior midgut to the stomodeal valve[5, 7]. These different forms should be taken into account to understand promastigote cell biology and differentiation to the infective stage, metacyclics forms (metacyclogenesis). The time-dependent location of these distinct morphological forms of *Leishmania* promastigotes within the sand fly are shown in Figure 1.6. First, amastigotes differentiate into procyclic promastigotes, the replicative form that multiplies in the bloodmeal and is confined to the peritrophic matrix (PM); PM is produced by epithelial cells and lines the gut lumen of most insects, protecting against rough food particles and pathogens and composed of chitinous microfibrils, proteoglycans and proteins[35]. Procyclic promastigotes will then differentiate into a non-dividing form, nectomonad promastigotes that are responsible for the infection establishment[2] and anterior migration[36] beyond the bloodmeal phase. As soon as nectomonads are released into the midgut lumen they attach between microvilli of epithelial cells to avoid elimination from the midgut during digestion. It was shown for *L.*

major that the abundant surface molecule lipophosphoglycan (LPG) specifically binds to the midgut galectin receptor PpGalec of the sand fly vector *P. papatasi*[37]. Surface molecules such LPG and proteoglycans protect the parasite from the proteolytic activities of the blood-fed midgut besides being responsible for the attachment in order to maintain infection during excretion of the bloodmeal[2].

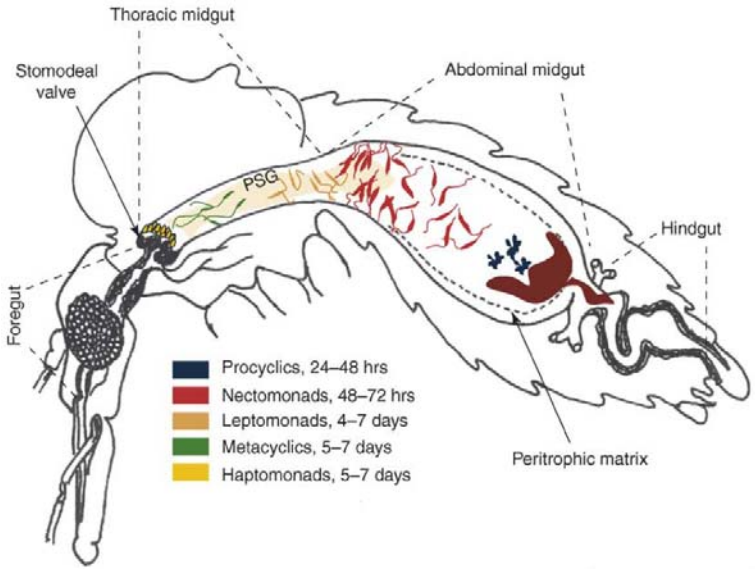

Figure 1.6 Main developmental forms of *Leishmania* promastigotes in the sand fly vector (adapted from Kamhawi *et al.*[7]).

Nectomonads migrate towards the anterior midgut and differentiate into the shorter leptomonads, which go through the second round of multiplication in the insect host called the sugarmeal phase, leading to a massive infection of the anterior midgut. Leptomonads produce the promastigote secretory gel (PSG), a matrix structure composed mainly of filamentous proteophosphoglycan, which is thought to trigger metacyclogenesis and plays an important role in the transmission phase, being responsible for the 'blocked fly' effect[36]. The transformation of leptomonads into non-dividing metacyclics occurs at the stomodeal valve, which separates the midgut from the foregut and the proboscis. Metacyclic forms are highly motile, present a small cell body compared to the elongated flagellum and are resistant to complement-mediated lysis. The other parasite form found at the stomodeal valve, the haptomonad, forms a parasite plug at the stomodeal valve[7].

1.1.5 Reservoirs and transmission modes

According to the source of human infection, leishmaniasis can be an anthroponosis, parasites essentially circulate between humans, or a zoonosis, in which the reservoir

hosts are wild animals and the parasites circulate essentially between those and the sand fly, humans being an accidental host[6]. A reservoir is, from a pratical point of view, a host that fulfills some attributes that favor the maintenance and dissemination of a given disease agent[38]. Many mammals have been described as important reservoirs of *Leishmania* [38-42], including dogs, which are the main reservoir hosts of *L. infantum*, playing an important role in the epidemiology of zoonotic visceral leishmaniasis[38].

1.1.6 Reproduction mode: clonality versus sexuality

In eukaryotes, genetic exchange is crucial for adaptation to new environmental conditions. Since the discovery of *Leishmania* there has been a debate about how these parasites reproduce: clonality versus sexuality[43]. For many years, the "clonal theory" has been accepted as the main mechanism of parasite reproduction[44-47]. The 'clonal theory' of parasitic protozoa which suggests that offsprings are genetically identical to their parents has been based in several criteria (ex. fixed heterozygosity, absence of recombinant genotypes, deviation from Hardy-Weinberg expectations, widespread identical genotypes). The hypothesis of clonality does not rule out the possibility of occasional genetic recombination, but suggests that is not important enough to change the predominant pattern of clonal population structure[47]. However, this theory was challenged over the years by the observation of interspecific, intraspecific hybrids, recombinant genotypes[43, 48-52] and by other studies based on molecular karyotype analysis and multilocus microsatellite typing that argued for a predominance of autogamy (a sexual reproductive mode where zygotes are produced by the fusion of two gametes that were produced by the same parental individual)[53,54, 55] or possible existence of selfing (a sexual reproductive mode where an individual self-fertilizes its own ovules with its own spermatozoids)[53]. The impossibility to obtain clear evidences to support sexuality in *Leishmania*, in part due to technical limitations as the low reliability of the genetic markers used, sampling or data interpretation[53] allowed the clonal theory to persist and be accepted as the main mode of reproduction, with infrequent genetic recombination, until new evidences emerged from experimental data. Using transgenic *Leishmania* strains resistant to different selective drugs, Akopyants *et al* [56] were able to isolate parasites from naturally infected sand fly that result from recombination between the two strains as they contain full genomic complements from both parents, but with kinetoplast DNA maxicircles from only one parent. The generation of a hybrid progeny occurred just in the sand fly vector and the parasites were transmitted to the mammalian host by sand fly bite[56]. This study demonstrated for the first time that genetic exchange occurs during *Leishmania* promastigotes development in the sand fly vector. Although genetic exchange in *T. brucei*

has been demonstrated a long time ago[57], a similar approach was used previously to show that genetic exchange in *T. brucei* takes place in the salivary glands of the tsetse fly vector involving meiosis[58], but the precise mechanism remains unknown. In order to understand the impact of genetic exchange in *Leishmania* epidemiology it is necessary to gain more insights into the process such as when, where (in which part of sand fly gut) and the frequency of hybrids. It may not have much relevance in parasites with exponential growth in an ideal environment, but could become crucial when parasites face changes in the environment[59] as it can potentiate a successful adaptation to new niches, vectors and hosts. A genetic exchange consequence is clearly shown by the fact that *L. infantum*/*L. major* hybrids were transmited by sand fly vector *Phlebotomus papatasi*, which is normally only competent to transmit *L. major*[60].

1.2 Leishmaniasis

1.2.1 Clinical manifestations

Clinical manifestations of *Leishmania* infection range from self-healing cutaneous and mucocutaneous forms to visceral leishmaniasis, which is fatal if left untreated. The clinical outcome is mainly dependent on the infectious species, but other factors such as the host immune status also play a role[3, 61]. Leishmaniasis is classified based on symptomatology in 3 main forms as follows:

- **Visceral leishmaniasis**

Visceral leishmaniasis (VL) is characterized by fever, weight loss, enlargement of the spleen and liver, anemia and this form of the disease is fatal if left untreated[62]. A frequent complication of VL is post-kala-azar dermal leishmaniasis (PKDL) characterized by a macular, maculo-papular or nodular rash, which are highly infectious as the nodular lesions may contain many parasites, being consider as potential reservoirs for anthroponotic VL[62].

- **Cutaneous leishmaniasis**

Cutaneous leishmaniasis (CL) is characterized by the presence of one or several ulcers or nodules in the skin, which heal spontaneously but cause disfiguring scars. Thus CL is not

a life-threatening condition however lesions can lead to significant disfigurement and disability[63, 64].

- **Mucocutaneous leishmaniasis**

Mucocutaneous leishmaniasis (ML) is characterized by destructive ulcerations of the mucosa, which extend from the nose and mouth to the pharynx and larynx. These lesions are not self-healing and are usually caused by inadequate treatment of a primary CL lesion[64, 65].

1.2.2 Disease burden and geographical distribution

Leishmaniasis is still one of the world's most neglected diseases, widely dispersed, with transmission to humans in five continents (endemic in 98 countries or territories), affecting mainly developing countries; 350 million people are considered at risk of contracting the disease, with an estimated incidence of 2 million new cases per year. Leishmaniasis is associated with nearly 2.4 million disability-adjusted life years and 50000 deaths annually, however this numbers may be underestimated mainly due failure to account for secondary effects, such as stigma and the economic effect on households and their treatment, that leads to millions of disable people[6]. Leishmaniasis is also found as an opportunistic disease associated with human immunodeficiency virus (HIV). *Leishmania*–HIV coinfection had been reported in 35 endemic countries, intensifying the burden of leishmaniasis by causing severe forms[6]. Depending on the geographic region the infection is acquired, leishmaniasis have traditionally been classified as *"*Old World*"* forms (Asia, Europe and Africa) and *"*New World*"* forms (Americas)[65].

Visceral leishmaniasis is caused by parasites of the *L. donovani* complex, *L.donovani* and *L. infantum* depending on the geographical area. There are an estimated 0.5 million new cases of VL, over 50,000 deaths each year and more than 90% of the cases are concentrated in Bangladesh, Brazil, Ethiopia, India, Nepal and the Sudan[6] (Figure 1.7).

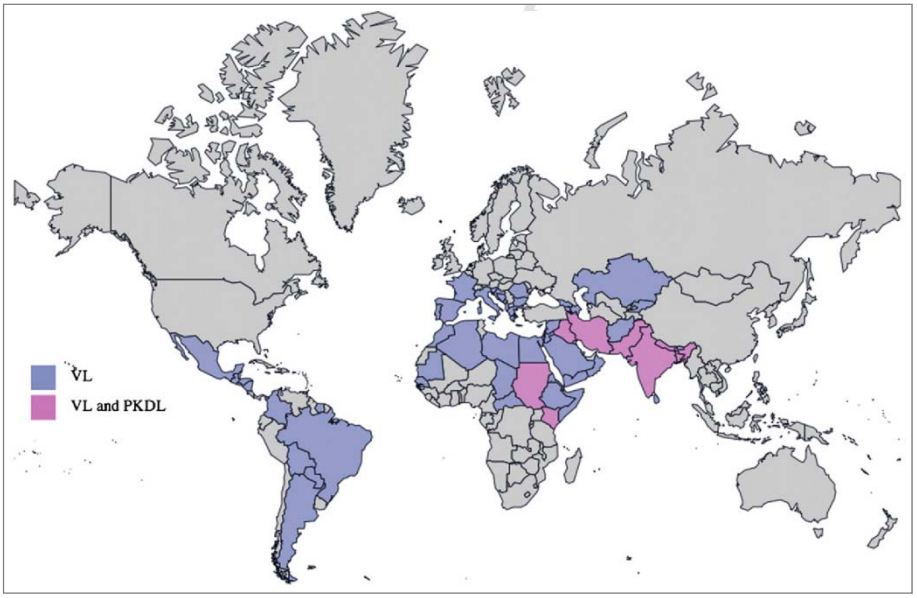

Figure 1.7 Worlwide distribution of visceral (VL) and post kala-azar dermal (PKDL) leishmaniasis (adapted from Duthie *et al.*[66]).

CL is endemic in more than 70 countries worldwide and up to 90% of cases occur in Afghanistan, Algeria, the Islamic Republic of Iran, Saudi Arabia and the Syrian Arab Republic and in Bolivia, Brazil, Colombia, Nicaragua and Peru[6] (Figure 1.8). The distribution of ML is tightly linked to CL. CL is predominantly caused by *L. major* and *L. tropica*, while ML cases are mainly caused by *L. braziliensis* and *L. panamensis.*

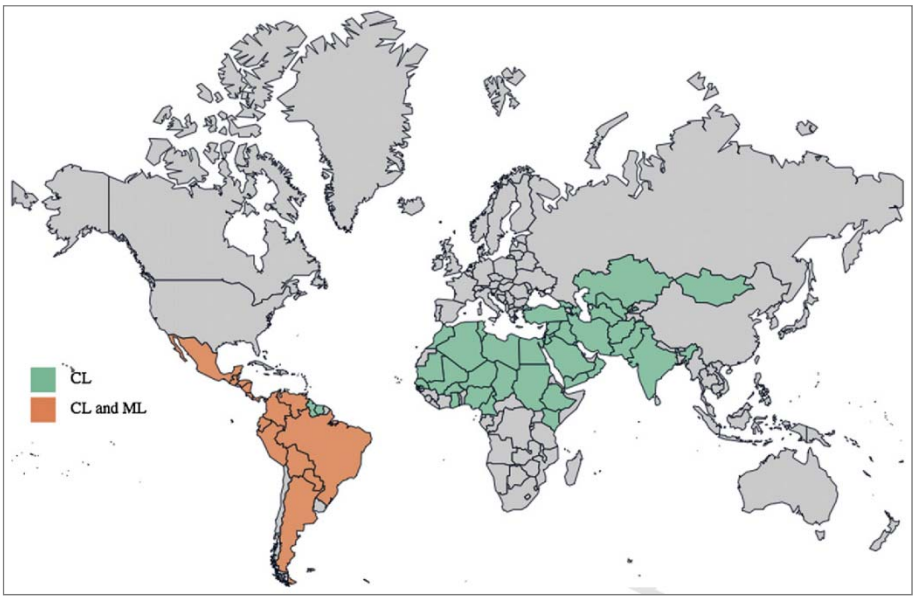

Figure 1.8 Worldwide distribution of cutaneous (CL) and mucocutaneous (ML) leishmaniasis (adapted from Duthie *et al.*[66]).

1.2.3 Diagnosis

The diagnosis of leishmaniasis is considered a complex challenge due to the wide spectrum of clinical manifestations and also the difficulty to distinguish the condition from other diseases as many of the clinical signs is shared with malaria, schistosomiasis, tuberculosis or other systemic infections. Thus, *Leishmania* specific laboratory tests are required for diagnosis confirmation and can be grouped into 3 categories: (i) parasite detection; (ii) antibody-detection tests and (iii) antigen-detection tests[67, 68].

(i) Parasite detection: demonstration of parasite in tissue samples by light microscopic examination, detection of parasite DNA in tissue samples by PCR. The commonly used method for diagnosing VL is the visualization of the amastigote form of the parasite by microscopy examination in tissues aspirates. This method is highly specific; however, sensitivity varies greatly depending on the source[62, 69, 70]. Detection of parasites in blood, serum or organs by PCR[71, 72] offers several advantages over the microcope examination: it is highly specific and sensitive irrespective of species or genus, quick to perform, may allow host tissue quantification of parasites and is able to detect more asymptomatic infections[73].

(ii) Antibody-detection tests: methods based on the presence of specific humoral response[74]. Serological tests based on indirect fluorescent antibody test (IFAT), enzyme linked immunosorbent assay (ELISA) and immunoblotting have shown high accuracy, but are not adapted to field settings. Thus to overcome that problem were specifically developed two tests for field use: direct agglutination test (DAT - based on antigen-antibody reaction) and the rK39 antigen-based immunochromatographic test (a rapid dipstick test based on the recombinant K39 protein)[68, 75, 76]. Although, high sensitivity and specificity were obtained[77], both tests suffer from 2 limitations: specific antibodies remain detectable up to several years after cure so relapse cannot be reliable diagnosed and a significant proportion of healthy people living in endemic areas are positive[76]. Nevertheless, a phase III trial for diagnostics of VL in India have confirmed DAT and rK39 strip tests has an excellent diagnostic tool, with high sensitive and excellent specificity, being rK39 strip test most suitable for the diagnosis of VL in the field conditions as it is easier to perform than DAT[78].

(iii) Antigen-detection tests: detection of parasite antigen in tissue, blood or urine samples, by detection of nonspecific or specific antileishmanial antibodies (immunoglobulin), or by assay for *Leishmania*-specific cell-mediated immunity [67].

1.2.4 Control strategies

The lack of an effective human vaccine or chemotherapy limits the options to prevent leishmaniasis. Thus, control strategies include the elimination of reservoir populations and reduction or interruption of disease transmission through vector control.

Vector control methods available include chemicals, environmental management and personal protection, and although they can have a strong effect when use independently, sand fly control should involve more than one method; vector control "packages" should take into account parameters such as the species involved, habitats, host feeding preferences and resting sites among others[6]. The efficacy of these measure was well demonstrated by almost disappearance of VL in the Indian subcontinent after a large-scale anti-malarial insecticide (dichloro-diphenyl-trichloroethane (DDT)) spraying campaigns implementation in the 1950s and 1960s; the disease quickly re-emerged when the spraying campaigns were discontinued[6, 62]. The main methods for controlling sandflies with insecticides are indoor residual spraying, spraying of resting sites, use of insecticide-impregnated materials such as bednets and curtains, and pyrethroid impregnated dog collars[6, 79]. Vector control through environmental management involves for example the relocation of human settlements away from sandfly habitats and physical modification of the habitats and personal protection measures, such as application of insect repellents on exposed skin and avoiding times of sand fly activity, should be used by people entering or living in highly endemic foci to avoid bites by sandfly vectors of leishmaniasis[6].

In the regions where the dog is the main reservoir, a canine vaccine would be the better solution as it would reduce this reservoir and interrupt transmission of *Leishmania* to humans. Treatment of infected dogs is not effective and canine treatment is performed with the same drugs used in humans increasing the risk of the emergence of drug resistant parasites[80]; the deltamethrin-impregnated collars have been shown to be effective in reducing the risk of infection in dogs[81]. Dog vaccination with Leishmune[82] has shown positives results, with a good correlation in the decrease of both canine and human VL with the increase of the number of vaccinated dogs[83]. Thus it is a promising tool to reduce parasite reservoir and protecting dogs.

1.2.5 Antileishmanial drugs

The lack of vaccines against human leishmaniasis implies that chemotherapy is the only way available to fight the disease. However, the current drugs are far from being

satisfactory with associated high costs and an alarming increase in drug resistance[84-86]. Drug discovery and development has been mainly directed towards treatment of VL since this form of disease is fatal if left untreated. Pentavalent antimonials remain the first-line treatment in most parts of the world despite the requirement for long treatment duration, toxic effects and the development of resistance, particularly in the region of Bihar (India), where 60% of patients do not respond to the treatment[85]. Miltefosine, different formulations of amphotericin B, paromomycin among others are available to use in addition to pentavalent antimonials. Combination therapy for VL is now seen as a way to increase treatment efficacy and tolerance, reduce treatment duration and cost, and reduce the probability of selection for drug resistant parasites. Studies have shown that treatment with oral miltefosine can be shortened when it is combined with single-dose liposomal amphotericin B[87-89].

- **Pentavalent antimonials**

Pentavalent antimonials (Sb^{V}) are available in two formulations: meglumine antimoniate and sodium stibogluconate (SSG). The full mechanism of action of antimonials is not known but the drug inhibits the activity of the glycolytic and fatty acid oxidative pathways in amastigote forms[85]. Antimonials are administered as a produg in pentavalent form, which needs to be reduced to its trivalent form (Sb^{III}) in order to be active against the parasite. Tis reduction can either occur in the macrophage, in the amastigote, or both[85] and it was shown to be catalyzed *in vitro* by parasite-specific enzymes namely thiol dependent reductase 1 (TDR1)[90] and arsenate reductase 2 (ACR2)[91] or non-enzymatically by thiols. In antimonial-sensitive cell lines was observed an accumulation of the trivalent form, which is reduced in resistant cell lines[92]. Resistance to antimonial drugs is thought to be multifactorial but one of the key factors is the concentration of active drug within the parasite, which can be modulated by decreased uptake and increased inactivation of the drug by the parasite. Inactivation can be achieved by the conjugation of Sb^{III} with glutathione or trypanothione, leading to extrusion of the drug out of the cell[93]. Indeed, an increase in total thiols[92] and overexpression of associated enzymes are often observed in metal resistant *Leishmania*[94]. This leads to an imbalance in thiol homeostasis and a consequent accumulation of reactive oxygen species[95, 96]. The mode of action of pentavalent antimonials is also dependent on T-cell subsets and cytokines. SSG was found to inhibit protein tyrosine phosphatases, which leads to an increase in cytokine responses. Also treatment with meglumine antimoniate leads to an increase in the phagocytic capacity of monocytes and neutrophils, suggesting an important role of the host response in the activity of these drugs[97-99].

- **Amphotericin B**

Amphotericin B is available in four different formulations: amphotericin B deoxycholate, liposomal amphotericin, cholesterol dispersion amphotericin and lipid complex amphotericin. The primary target of this drug is membrane ergosterol, which constitute the major surface sterol in *Leishmania* in contrast with cholesterol in human cells[100]. Thus, amphotericin B kills the parasite by destroying the surface membrane, without having to enter it. Given this, resistance to amphotericin B seems unlikely to occur as *Leishmania* parasites would need to generate a new biochemical pathway to replace surface ergosterol[101]. A single-dose of liposomal amphotericin B was considered by the WHO appointed expert committee on control of leishmaniasis the best available therapy for anthroponotic VL in the Indian subcontinent as it is effective and is safer than any other treatment[6].

- **Pentamidine**

Pentamidine is a dicationic drug that interferes with *Leishmania* DNA synthesis, leads to the condensation and disruption of the kinetoplast DNA core and promotes fragmentation of the mithocondrial membrane, killing the parasite[102-104]. Pentamidine has been used with success to treat cutaneous leishmaniasis or ML in some regions of the New World with same efficacy as antimonials[105].

- **Paramomycin**

Paromomycin, is an aminoglycoside that inhibits protein synthesis and modifies membrane fluidity and permeability[106]. Recently was shown that paromomycin drastically alters the accuracy of protein synthesis in *Leishmania*; defective proteins might cause deleterious effects on parasite survival. Paramomycin binds to the parasite ribosomal decoding site, modifying the codon-anticodon recognition process; the effectiveness against leishmaniasis is believed to be due to the ability of paramomycin to discriminate between ribosomes of *Leishmania* and mammalian cells[107]. *L. donovani* promastigotes selected *in vitro* for paramomycin resistance showed reduced accumulation of drug and a significant reduction in the initial binding of drug to the cell surface. Paromomycin resistant cells retained sensitivity to other drugs indicating that if resistance emerge in the field other drugs can be used[108].

- **Miltefosine**

Miltefosine (hexadecylphosphocholine) is an alkyl phospholipid which was first developed as an anticancer agent and the first orally administered drug for VL to be developed. Miltefosine induces an apoptosis-like death in *L. donovani* promastigotes and amastigotes[109, 110]. The mechanism of action involves interaction with lipids and in particular membrane lipids - phospholipids and sterols. Reduction in the membrane sterol content led to a reduction in miltefosine activity of 40%; Leishmania lipid rafts, microdomains enriched in sphingolipids, sterols, LPG and GP63[111], are used as miltefosine reservoirs at the membrane level, contributing for the constant supply of the miltefosine transporter (LdMT), which is responsible for the internalization of the drug within the parasite[112]. *In vitro* resistance to miltefosine was shown to occur through decreased uptake or increased efflux of the drug; experimental mutations at LdMT and its specific beta subunit LdRos3, rendered the parasites less sensitive to miltefosine[113, 114]. Miltefosine resistance induces modifications in C-24 sterol alkylation and fatty acid elongation and saturation. These changes interfere with membrane fluidity and consequently affect drug-membrane interactions[115], essential for an effective action of the drug.

1.2.6 Vaccine development

Studies on antileishmanial vaccine candidates have increased remarkably in the recent years, largely due to a better understanding of the mechanisms necessary to induce immunity and the availability of *Leishmania* genome sequences. Several vaccine formulations provided partial protection, however there is no fully effective vaccine against leishmaniasis. An ideal vaccine should meet several attributes such as safety, low cost, be effective against species causing CL and VL, induce CD8- and CD4-T cell responses and long-term immunological memory[116]. In addition, an effective vaccine should efficiently stimulate dendritic cells as they play a key role in inducing both humoral and cellular responses[117]. In the search for a vaccine against leishmaniasis have been used different strategies, including killed, live attenuated parasites, recombinant proteins or vaccines based on recombinant DNA among others[118].

First generation vaccines

Tthe administration of live virulent parasites, process known as Leishmaniazation constitute the first vaccine against Leishmania. This has been used for over 60 years in several countries, since 1940s but discontinued due to safety issues. In the 1970s and

1980s vaccine trials involving whole and killed parasites were conducted. Recent trials have used inactivated whole parasites, in some cases a mixture of strains, or in the presence of adjuvants but none of those demonstrated protection[119]. However, in Brazil similar vaccines have been used successful for immunotherapy of human CL, leading to the register of a first generation vaccine as an adjunct to antimony therapy[120]. The first generation vaccines also include the use of live attenuated parasites, which are infectious but not pathogenic, an important advantage over the vaccination with live or killed parasites[116]. The ability to manipulate *Leishmania* genome to create genetically modified parasites by introducing or eliminating genes offered a new alternative to develop a vaccine against leishmaniasis. *L. major* parasites lacking dhfr-ts- gene induced substantial protection against a virulent *L. amazonensis* and *L. major* infection in a murine model, although it failed to induce protective immunity in a primate model[121-123]. Immunization with *L. major* parasites lacking the *lpg2*$^{-}$ gene yield different results depending on the susceptibility of the murine model used[124-126]. Deletion of one allele of *SIR2* gene in *L. infantum* affected the development of the intracellular amastigote stage and immunization of Balb/c mice with these mutants induced a high degree of protection against a virulent challenge[127]. Another example involves the disruption of *L. donovani* centrin which also affects the growth of the amastigote stage of the parasite. Mice immunized with centrin null mutant showed early clearance of virulent parasite challenge associated with a significant increase in IFN-γ, IL-2, and TNF production by CD4+T cell population; sustained immunity and cross-protection against infection with *L. braziliensis*, indicates that these live attenuated parasites are effective and a potentially candidate vaccine against VL as well as ML[128]. The use of live parasites is considered important for vaccination as it mimics the natural course of infection, although the possibility that the parasite may revert back to a virulent form or reactivation in immunosupressed individuals is a major concern limiting the use of live attenuated vaccines[129]. Also their large scale distribution represents a major concern.

Second generation vaccines

Second generation vaccines, such as parasite fractions, recombinant proteins or expression in heterologous microbial vector, represent a more feasible option than the first generation vaccines, as they can be produced in a large scale and responses elicited can be potentiated with the use of an adjuvant[130, 131]. Different approaches have been used to identify proteins potentially suitable to be tested as a vaccine candidate[118]; several *Leishmania* proteins were selected including GP63, *Leishmania* homologue of receptor for activated C kinase (LACK), parasite surface antigen 2 (PSA-2), fucose mannose ligand (FML), cysteine proteinase (CP)A and CPB, amastigote antigen 2 (A2), hydrophilic

acylated surface protein B1 (HASPB1), kinetoplastid membrane protein 11 (KMP-11), *L. major* homologue of the eukaryotic thiol-specific-antioxidant (TSA), *L. major* homologue of the eukaryotic stress-inducible protein 1 (LmSTI1) *Leishmania* elongation and initiation factor (LeIF) among others, although only a few formulations have entered clinical or veterinary testing (reviewed by Nagill *et al.*[118], Duthie *et al.*[66], Kaye *et al.*[132], Costa et al.[133]). Analysis of the overall results obtained with these antigens in vaccinations experiments revealed in some cases contradictory results that could be due to different eign-keys><key app="EN" db-id="eevzatx0madrtoeadsections, challenge dose, adjuvants animal model. Also, failure to protect against the different forms of the disease was observed as in the case of LACK immunizations which failed to protect against VL[134]. Another issue with the use of recombinant proteins is that alone they induce weak T cell responses and only the addition of certain adjuvants leads to the generation of effective and durable T cell responses[66].

Currently, there is only one defined vaccine against leishmaniasis entering phase II clinical testing in humans designated LEISH-F1 (also designated as Leish-111f)[135, 136]. LEISH-F1 is a fusion protein of three relatively conserved *Leishmania* proteins (TSA, LmSTI1 and LeIF) formulated with MPL-SE (monophosphoryl lipid A - stable emulsion)[137]. This vaccine candidate protects mice, hamsters, rhesus macaques[137-140]. In mice infected with *L. infantum*, LEISH-F1 + MPL-SE vaccine administration induced a strong humoral and T cell responses; a significant increase in CD4+ T cells producing IFN-γ, IL-2 and TNF was detected, indicative of a Th1-type immune response[137]. Recently was reported that LEISH-F1 + MPL-SE vaccine is safe and immunogenic in human healthy subjects with and without history of previous infection with *L. donovani*[136]. Moreover, the vaccine was considered safe and immunogenic against CL when administered alone[140] or in conjugation with antimonials in human clinical trials[135, 141]. The effect of LEISH-F1 vaccine was also investigated in naturally exposed dogs. As dogs are a very important reservoir, a canine vaccine with the aim to prevent or treat the animals would have beneficial effects through the interruption of the transmission of *Leishmnaia* parasites to humans. However, vaccination with LEISH-F1 did not protected dogs in an extremely high *L. infantum* endemic region[142]. On the other hand, the administration of the fucose mannose ligand (FML)-vaccine induced high levels of protection, since only 8% of the vaccinated dogs showed mild signs of canine leishmaniasis after 2 year, while 33% of the non-vaccinated animals developed clinical or fatal disease associated with *L. donovani* infection[143]. This vaccine is commercially available since 2004 under the name of Leishmune[82] and is considered a transmission blocking vaccine likely due to the fact that vaccinated dogs do not have parasites in their skin even when infected[144] and antibodies raised against

Leishmume are able to block the parasite development in the sand fly rendering the vector non-infectious [145, 146].

Third generation vaccines: DNA vaccines

DNA vaccines are an attractive alternative to conventional methods of vaccination due to several features that include the ability to elicit humoral and cellular immune responses, which can be modulated by the addition of adjuvants such as cytokines or CpG[147, 148]. Prime boosting strategies that involve priming with DNA and boosting with the respective recombinant protein or other antigen delivery systems have also been used[149-152], since heterologous prime-boost leads to a synergistic enhancement of immunity to the target antigen[153]. DNA compared to recombinant protein vaccines present some advantages, largely due to stability and low cost of production. Moreover DNA vaccines may provide better protection as they can induce the expression of *Leishmania* antigens folded in its native conformation and normal posttranslational modifications to occur similar to natural infection and potentially with unaltered antigenecity[147]. Induction of both humoral and cellular immune responses by DNA vaccines is due to the ability of DC to present the encoded antigen in the context of MHC class I and MHC class II (known as cross-priming) as they can be directly transfected with the plasmid or take up soluble proteins and debris from apoptotic transfected cells[117]. Moreover has been suggested that this form of antigen delivery induces longer lasting immune responses[154]. There are many reports involving vaccination with DNA encoding *Leishmania* antigens, some of them tested previously as recombinant proteins, including GP63[155], LACK[156, 157], LmST11 and TSA[158], cysteine proteinases[159], ORFF[160] among others with a wide range of success rate[161, 162].Preclinical experience in other models of leishmaniasis with recombinant adenovirus, vaccinia virus and attenuated Salmonella suggest that these carriers should also be explored against VL[132].

1.3 *Leishmania*-host interactions

Intracellular parasitism poses substantial challenges and to be successful the parasites must be able to enter and/or invade the host cell and escape the mechanisms used by the host to clear the intracellular parasites, such as apoptosis, autophagy, production of oxidative and nitrosative species and recognition by Toll-like receptors[163]. *Leishmania* parasites have adapted to colonize different host cells as a way to invade and evade the host immune response, taking advantage of the interaction between the different cells to establish and promote disease. Moreover, *Leishmania*-host interactions are even more

complex due to the diversity between the parasites themselves and the differences in human versus mouse host cell responses experimentally studied.

Leishmania infection of a mammalian host initiates after a sand fly bite, in which promastigotes are injected into the skin where the parasite uptake by phagocytic cells occurs. The sand fly inoculate has an active role in the modulation of immune response of the host to *Leishmania* and may have a role in the influx of potential host cells. Besides delivering a high number of parasites highly enriched in metacyclic promastigotes, the infective form of the parasite[30, 164], was detected the presence of apoptotic parasites that through the production of TGF-β seems to mediate the silencing of phagocytes and lead to survival of viable parasites[165]. In addition, the infectious inoculum also contains sand fly salivary components and parasite derived molecules such as the filamentous proteophosphoglycan (fPPG), which is a component of the promastigote secretory gel that blocks the anterior midgut of infected *Lutzomyia longipalpis* sand flies[30].

The earliest *Leishmania* interactions with the host take place in the whole blood as the sand fly bite create a hemorrhagic pool in the host skin for feeding. This first contact between *Leishmania* and the mammalian host induces tissue damage, a process that initiates a strong local inflammatory response and the recruitment of neutrophils and monocytes. Parasites react with natural antibodies and are opsonized by complement, binding to erythrocytes through complement receptor 1 (CR1) and after few minutes of infection transferred and internalized by neutrophils and monocytes[166]. Several recent studies have highlighted and reviewed the role of neutrophils in the initial phase of *Leishmania* infection both as a safe target that protects *Leishmania* from the extracellular hostile environment before entering macrophages but also is an important player in the development and modulation of an immune reponse against the parasite[167-175]. The neutrophils classical function is considered to be the capacity to phagocytose and kill microorganisms, contributing to the “first line of defense” against infectious agents[176]. However, the role of neutrophils in *Leishmania* infection goes further as they have been established as early host cells for promastigotes[177] and may also contribute to the development and modulation of immune response against the parasite through the release of chemokines and cytokines[178-183]. *Leishmania* can transiently survive within neutrophils due to the development of protective mechanisms including the prevention of oxidative burst activation, avoiding the generation of toxic ROS[177] and also the ability to be targeted to non-lytic compartment of neutrophils as reported for *L. donovani*[173].

Recruitment of neutrophils to the local of infection occurs as early as 30 min post infection and after 1 day of infection parasites localize mainly inside neutrophils. During the first week, the proportion of infected neutrophils drops and as parasites are released from apoptotic neutrophils they become localized in macrophages. The crucial role of neutrophils after sand fly transmission of *Leishmania* is also shown by reduction of local incidence of infection observed when this cell population was depleted, suggesting that parasite can hide in the neutrophil until the host cell apoptosis forces the parasite to infect a macrophage[171]. On the other hand, passage through neutrophils can render the parasite more infective, as host recognition of phosphatidylserine (PS) on the surface of unicellular parasites is an important feature of the process and progression of infection[184].

The way parasites are transferred from neutrophils to macrophages is not yet clear. A model named “Trojan horse” whereby macrophage can uptake apoptotic neutrophils containing viable *Leishmania* parasites has been shown to occur *in vitro* and considered a mechanism for “silent” entry of parasites into macrophages[175]. However, dynamic intravital microscopy have not shown the phagocytosis of infected neutrophils but that *Leishmania* parasites can escape neutrophils before infecting macrophages[171]. Also arrival of macrophages to the local of infection can induce neutrophils apoptosis. Thus another strategy called “Trojan rabbit” was proposed, in which the parasite hides outside the apoptotic neutrophil to infect the macrophage[169].

Engulfment of apoptotic neutrophils by macrophages can have immunoregulatory or pathogenic roles. BALB/c neutrophils induce a biochemical cascade that deactivates macrophage through the production of TGF-β and increase growth of *L. major* in a manner dependent on PGE2 and TGF-β. In contrast resistant B6 mice interaction of dead neutrophils with macrophage promoted parasite killing[185]. Susceptible Balb/c mice are also less efficient in mediating neutrophil apoptosis as these cells persist much longer in Balb/c than in the resistant B6 mice, suggesting an important role for neutrophil accumulation in the differences observed between the two species[186]. Clearance of neutrophils can have a proinflammatory effect mediated by soluble factors and neutrophil elastase, which activate infected macrophages to eliminate *Leishmania* parasites via TLR4 signaling[187]. Besides the role of neutrophils in the killing of parasites through the activation of macrophages, they have their own microbicidal mechanism such as the release of neutrophil extracellular traps (NETs), which are composed of DNA, histone proteins and antimicrobial peptides[188]. Indeed, *L. amazonensis* induced NET release by human neutrophils in a parasite number- and dose-dependent manner, which in turn led to decrease in parasite viability; the disruption of neutrophil NETs interaction with

Leishmania led to an increase in parasite survival that supports the possible contribution of NETs in the decrease of parasite burden at the site of inoculation[189]. In contrast, another study have shown that *L. donovani* is able to evade the microbicidal effect of NETs, a mechanism dependent on LPG biosynthesis as mutant parasites were highly susceptible to the antimicrobial activity of NETs. As the parasites are only trapped by NETs and not killed, it was proposed that these structures may contribute to the containment of *L. donovani* promastigotes at the site of inoculation, facilitating their uptake by macrophages[190].

Intradermal infection with *L. infantum chagasi*, a visceralizing species, leads to the recruitment of neutrophils to the dermis even later after inoculation and parasites were trafficked through the neutrophils, suggesting that neutrophils may play a role in visceral leishmaniasis[191]. Also, neutrophils seem to have a crucial role during the first weeks of infection with *L. donovani*, as mice in which neutrophils were selectively depleted have shown a significant increase in parasite burden in spleen and bone marrow[172]. Both studies highlight the importance of neutrophils in visceral leishmaniasis and how they may influence the development of a protective response.

Leishmania spp. have also found a way to interfere and/or control neutrophils functions. The infectious inoculum is composed of non-apoptotic and apoptotic cells, the last ones shown to be necessary in the survival of non-apoptotic parasites that were rapidly killed if phagocytosed in the absence of apoptotic promastigotes. This is explained by the induction of higher levels of TGF-β and low levels of TNF-α by apoptotic parasites than non-apoptotic cells, directly related with PS exposure on the parasite surface. The PS recognition is known to suppress phagocytic functions through the release of and down-regulation of TNF-α; TGF-β is likely involved in the silent entry of the parasite and survival in the neutrophils[165]. *Leishmania* is also able to interfere with IFN-γ signaling in neutrophils, working as a potent inhibitor mechanism of the host cell activation[174]. Another strategy of survival used by *Leishmania* is to delay apoptosis of neutrophils, since they are short-lived cells that undergo rapidly spontaneous apoptosis. Infection with *L. major* led to an increase up to 2 days in life span of neutrophils revealing that the parasite can actively modulate the host apoptosis which will probably allow the parasite to adapt and survive before engulfment by macrophages[186]. Infected neutrophils secrete high levels of MIP-1β which attracts macrophages[180], that due to the recognition of PS on the neutrophil surface will proceed to a “silent” clearance of apoptotic neutrophils, since ingestion of apoptotic cells does not result in the activation of antimicrobial effector functions. *Leishmania*-infected neutrophils are able to deactivate the functions of macrophages as the amount of TGF-β secreted by macrophage following the uptake of infected neutrophils was higher

than direct uptake of *L. major* promastigotes, with no significant release of TNF [175]. The ability of the *Leishmania* to survive and maintain infectivity in neutrophils seems to have a crucial role in the establishment of a productive infection in macrophages[174].

Although, in situ imaging has shown that most infected neutrophils release the parasites before being phagocytosed by macrophages and also that parasites numbers in the macrophages of mice did not change after neutrophil depletion[171]. Thus, the contribution of parasites uptake by neutrophils to *Leishmania* infectivity is still controversial and not clear. Indeed reported work suggests that the effects of neutrophil depletion are mouse strain dependent[185].

Another type of cells may be involved in the initiation of a protective immune response directed to *Leishmania*, as infection with *L. major* induced the secretion of immunomodulatory mediators such as IL-12, IL-1 IL-4 and IL-6 by keratinocytes[192]. There still some controversy in the role of DC during early infection, whether these cells are able to uptake the parasite[193-195]. However, recent studies have shown using an intradermal infection model that dermal DCs, a sub-type of dendritic cells found on the dermis, are able to uptake *L. major* parasites shortly after infection[196]. Both infected and non-infected dermal DCs became non-migratory at the inoculation site, suggesting that the inflammatory environment induces the change in dermal DC migratory behavior. However, 20h post-infection the number of parasite-containing dermal DC decreased, suggesting that infected dermal DC leave the dermis in order to migrate to draining lymph nodes[196], supporting previous studies which have shown that DC arrival in draining lymph nodes occurs around 24 hours post-infection[197].

Although *Leishmania* parasites can be found in different types of cells, the macrophage is considered the principal site of parasite proliferation and dissemination. Metacyclic promastigotes can be phagocytised indirectly by macrophages through the uptake of infected neutrophils as detailed above. Macrophages can also be directly phagocytised promastigotes that attach to the host cell via a receptor-mediated mechanism and are taken up via CR3-dependent mechanism, by which *Leishmania* is able to avoid complement mediated lysis. This occurs in part through the activity of *Leishmania* surface protease GP63, which cleaves host complement component C3b into iC3b, preventing complement mediated parasite lysis and, in addition the iC3b deposited on the promastigote surface promotes receptor-mediated uptake through CR1 and CR3[198, 199] . Parasite phagocytosis by macrophage *in vitro* is rapid and can be completed within 10-20 minutes of parasite attachment, occurring similarly when performed by neutrophils or dermal DC[171, 196, 200].

CHAPTER 2

LEISHMANIA: FROM GENOME TO METABOLOME

2.1 *Leishmania* "omics"

Leishmania represents a very diverse group of organisms. In order to characterize *Leishmania* diversity whole-genome sequencing, transcriptomic studies based on whole genome-based DNA arrays and global proteomic studies have already been carried out[201]. Suprisingly, the comparative genomic studies between *L. major*, *L. infantum* and *L. braziliensis* showed a highly conserved gene synteny and a small number of species-specific genes[202], despite an estimated divergence of 46-36 million years[43]. These findings were unexpected as they contrast with the major phenotypic differences caused by each species. Recently, new sequencing technologies allowed a more powerful study of different *Leishmania* species genomes demonstrating that the apparent genetic homogeneity contains features such as aneuploidy, expansion and contraction of genes in tandem arrays and episomes that contributes to genomic diversity and/or plasticity[203, 204]. Transcriptomic studies have been used to determine differences in gene expression between different species and life cycles or associated with drug resistance and clinical polymorphism. Although, due to the fact that regulation in *Leishmania* appears to occur at a post-transcriptional level it was found that the vast majority of the genes are constitutively expressed in all developmental stages and thus transcriptomics alone might not be useful to describe coordinate expression in *Leishmania*. On the other hand, proteomic studies have been useful in the identification of stage specific proteins and have reported a higher percentage of the predicted proteome as stage-specifically regulated at the translational or post-translational level contrary to the data obtained with transcriptomics[201]. Both genomic and proteomic approaches play a role in revealing differences between *Leishmania* species, but are limited in providing contextual and integrative information that is necessary to decipher the mechanisms of cellular function. Metabolites are key in linking together the web of complex interactions, cellular pathways, molecular participants and environmental stimuli. Metabolomics has gained increasing interest in drug discovery, disease diagnostics and treatment, as it allows the measure of metabolites fluctuation that can occur very quickly[205] and is now being applied in parasite research[206-209].

2.2 *Leishmania* genome: gene content and structure

The Leishmania genome is composed of nuclear and kinetoplast DNA, that constitute a unique feature of trypanosomatids. The *L. major* genome was the first to be sequenced[210],

however before the whole-genome sequencing was completed previous studies have already revealed an unusual pattern of gene distribution, in which the genes are aligned in long arrays that appear to be transcribed as a single unit prior to *trans*-splicing and polyadenylation[211]. *L. major* Friendlin genome is 32.8 Mb in size with a karyotype of 36 chromosomes, with 8272 protein encoding genes, of which 36% can be ascribed with a putative function[210]. Comparative genomic analysis of *L. major*, *L. infantum* and *L. braziliensis* showed a high degree of conserved synteny for more than 99% of the genes. Conservation within coding sequences is also high, with an average amino acid identity between *L. major* and *L. infantum* of 92% and between *L. braziliensis and L. infantum* or *L. major of 77%*[202]. Despite a similar DNA content among all *Leishmania* species analyzed, differences were detected in the karyotype, confirming data previously observed by linkage group analysis[212]. *L. infantum* has a haploid content of 36 chromosomes as does *L. major*, while the New World species have 35 or 34 chromosomes, *L. braziliensis* and *L. mexicana* respectively[202]. These differences are due to chromosome fusion events that in *L. braziliensis* involved chromosome 20 with 34 and in *L. mexicana* the chromosome 8 with 29, and 20 with 36[203, 204]. An update on *Leishmania* genomes obtained by recent genome re-sequencing projects, using the Illumina Genome Analyser plataform and the iterative mapping algorithm iCORN[204] is shown in Table 2.1.

Table 2.1 Summary of *Leishmania* genomes

	L. major	***L. infantum***	***L. braziliensis***	***L. mexicana***
Size (Mb)	32.855	32.101	31.997	32.108
Chromosomes	36	36	35	34
GC%	59.7	59.6	57.8	59.7
Predicted protein coding genes	8412	8241	8357	8250
Predicted specific genes	14	19	67	2

(adapted from Rogers *et al.*[204])

This together with new alignments allowed an update in the number of unique genes in each species (Table 2.1) that is even more restricted than the first data provided by the comparative genomic analysis of *L. major*, *L. infantum* and *L. braziliensis*[202] . An interesting finding was that species-specific genes are conserved in isolates from within the same complex (*L. donovani* versus *L. infantum*) and between strains of the same species isolated from different or similar geographical locations[204]. The identification of specie-specific genes is thought to be crucial to determine the possible role of those in the variety of clinical outcomes caused by different *Leishmania* species, particularly the *L.*

donovani genes required for visceral infection. Experimental approaches to identify the role of specie-specific genes have been mainly achieved through the generation of transgenic parasites, such as *L. major* parasites expressing *L. donovani* specific genes[213]. The A2 gene is an example of a *L. donovani* specific gene that encodes an amastigote-specific protein. A2 *L. donovani* deficient amastigotes were severely compromised in their ability to infect mice, indicating the requirement of *A2* for survival in the mammalian host[214, 215]. Introduction of *A2* gene into *L. major* by genetic transfection led to an increase of parasite survival in visceral organs, conferring a change in the virulence phenotype[216]. Furthermore, genome sequencing analysis revealed significant sequence diversity and structural variation at the A2 locus in *L. donovani*[203], in contrast with the conservation observed at the same locus in *L. major*[203], suggesting and re-enforcing the possible role of the gene in infection visceralization. Other examples of potentially interesting specie-specific genes are the cyclopropane fatty acyl phospholipid synthase (*CFAS*) gene present in *L. infantum* and *L. braziliensis* but not in *L. major* and the SEC14-like originally identified in *L. infantum*[202], but which has now been identified also in *L. mexicana*[204]. CFAS orthologue in *Mycobacterium tuberculosis* has been shown to modify cell surface glycolipids and is associated with increased virulence and persistence[203], while Sec14 cytosolic factor has been implicated in the release of secretory vesicles from the transgolgi network[217]. There were no differences in growth and in the ability to infect macrophages between SEC14-like null mutants and the *L. infantum* WT[204]. Other species-specific genes can result from insertions/deletions and sequence rearrangements that contribute to gene degeneration[218] as demonstrated by the identification of *Pfp1* gene, which is expressed in *L. major,* but present in *L. infantum* and *L. braziliensis* as a pseudogene[219]. Unexpected was the fact that genes ubiquitously present in different *Leishmania* species could also have a dramatic effect on parasite tropisms[213]. Zhang and co-workers found that the expression of *L. donovani* Li1040 ortholog gene in *L. major,* which does not belong to the group of specie-specific genes, dramatically increase *L. major* parasite numbers in the liver and spleen[213]. This finding highlight that the factors controlling tropism and virulence are not only related to the species-specific genes, but also to post-transcriptional regulation and gene polymorphisms.

2.3 Genomic features that contribute to *Leishmania* diversity and plasticity

Given the small number of species-specific genes identified, differential gene expression has been investigated as another potential explanation for disease phenotypic differences. DNA microarrays, of varying size and composition, have been used to determine the

global *Leishmania* gene expression, revealing that the vast majority of *Leishmania* genome is constitutively expressed and that only a limited number of genes, ranging from 0.2 to 5.7% depending on the microarray study, showed differential regulation when comparing promastigote and amastigote forms[220-225]. Analysis of *L. major* promastigotes and lesion-derived amastigotes gene expression showed that over 94% of the genes were expressed in both stages, with just 1.5% differential mRNA expression[221]. These results suggest that *Leishmania* is constitutively pre-adapted for survival and replication in different hosts, the constitutive expression of the genome being an advantage of adaptation to the different environments using an appropriate set of genes as necessary[226]. Comparison of *L. donovani* axenic and intracellular amastigotes revealed substantial differences in gene expression regulation, with 40% more genes up-regulated in axenic than in intracellular amastigotes and just 12% of the differential regulated genes were common to both amastigotes preparations[225]. Also for *L. major* the differences obtained when comparing promastigotes to axenic (3.5%) or lesion derived amastigotes (0.2%)[220] point out that the axenic culture conditions may alter the amastigote transcriptomic abundance and that the importance of the host macrophage as a driving force to specific adaptations cannot be disregarded. Indeed, a quantitative proteomic analysis of axenic and splenic *L. donovani* amastigotes revealed important differences, such as in cell volume and nuclear size, A2 protein expression and parasite infectivity, between both amastigote sources[227]. Reduction in A2 expression in the hamster-derived amastigotes suggests that these parasites are adapted to survive under stress conditions, as the A2 protein has been considered a virulence factor required for *L. donovani* intracellular survival and resistance to stress[215]; this is in agreement with the hypothesis suggested by the results obtained when comparing mRNA levels of axenic and intracellular amastigotes, showing that the ones collected from the host are adapted to growth in different environments. This demonstrates that results obtained with axenic amastigotes should be carefully considered as they represent a host free system.

The constitutive expression of the *Leishmania* genome is consistent with the unusual gene organization detected in trypanosomatids. The *Leishmania* genome is organized into large polycistronic gene clusters, comprising of up to hundreds of genes, in the same 5'-3' direction along the chromosome DNA strand[210]. These long arrays are transcribed into polycistronic RNA precursors and further processed into individual mRNAs with a 39-nt 5' capped spliced leader sequence and a 3' poly(A) tail generated from the polycistronic pre-mRNAs via 5' trans-splicing and 3' cleavage polyadenylation reactions[228]. Polycistronic transcription and the lack of RNA polymerase II promotors for protein-coding genes imply that most of the gene regulation occurs post-transcriptionally. Indeed, numerous

sequences located in the 3'UTRs were described as being involved in the control of mRNA stability and translation, even before the *Leishmania* genome sequence was available[229-234]. Advances in the discovery and characterization of these elements occurred due to the complete annotation of *L. major* genome[210]. Stage-specific post-transcriptional regulation is described as being mediated through specific regions (cis-elements) within 3'UTRs of mRNAs[235]. These elements are widely distributed in the 3'UTR and are classified as U-rich instability elements (UREs), short interspersed degenerated retroposons (SIDERs)[236] and individual cis-elements[237]. SIDER elements represent the most abundant transposable elements characterized so far in trypanosomatid genomes; two functional distinct families were described in *Leishmania*: SIDER1, which is implicated in stage-specific translational control and SIDER2 that promotes mRNA destabilization. SIDER2 are cis-acting components of a regulatory pathway that generally down regulates gene expression to ensure rapid turnover of a specific subset of *Leishmania* mRNAs.

Rapid mRNA turnover may be a strategy that allows the parasite to easily adapt its pattern of protein synthesis to the different environments[236]. A well known example of stage-specific regulation in *Leishmania* through conserved elements in the 3′UTR is the amastin gene family, which is expressed preferentially in the mammalian stage[238]. Thus, *Leishmania* genome organization and regulation explains why limited stage-specific differences in mRNA levels are detected. In fact the weak correlation of protein expression with the corresponding mRNA levels, as reported in many other organisms[239-241], confirm the importance of regulation of protein levels in *Leishmania* by mechanisms such as stage-specific translational control or protein stability. A combined proteomic and transcriptomic analysis of *L. infantum* parasites have confirmed the striking lack of correlation in promastigotes between mRNA and protein levels, while for amastigotes it was found to be over 50%[242]. Moreover, a higher number of promastigote- or amastigote-specific protein isoforms were found to be differentially regulated, respectively 6.1% and 12.4%, when comparing with the data obtained from mRNA levels, for which the fold changes observed were more modest than at a protein level. Furthermore, multiple protein spots were found for a single gene and also different isoforms of the same protein are detected as stage-specific, clearly suggesting that protein post-translational modifications occurs playing an essential role on the parasite adaptation to different environments, which might explain the considerable degree of discrepancies between transcriptomics and proteomics as well as the limited number of stage-specific genes. Many other proteomic studies with *L. infantum*, *L. donovani*, *L. mexicana* and *L. panamensis* have also highlighted differences between different life stages: there are subtle differences based on the identification of protein isoforms from the same gene, but

also major differences in protein expression, up- or down regulation of expression, with some being stage-specific[221, 243-248].

Despite considering that different mechanisms of post-transcriptional and post-translational regulation are crucial for species-specific differences, it is still intriguing how an apparent genetic homogeneity between different *Leishmania* species due to the constitutive expression of the genome generates such enormous diversity in disease outcome. The recent re-sequencing genome projects have increased our knowledge about *Leishmania* genome structure and highlighted some features that can contribute for genome diversity and/or plasticity, the most notable being the chromosome copy number variation between *Leishmania* species and strains[203, 204] changing the assumption until now accepted that the *Leishmania* genome was generally diploid[249], since that only two exceptions had been reported in *L. major*, with the detection of triploidy and tetraploidy in chromosome 1[250] and 31[56], respectively. Thus it is clear that the emergence of new and powerful molecular technology will reveal important features of the genome that were likely to be masked by previous approaches, showing that evolutionary changes to reach an adaptive phenotype reflects changes in the karyotype such as gene rearrangement and chromosomal size variation[251]. Several studies, either associated with attempts to knockout essential genes[252-254] or dealing with the mechanisms associated with drug resistance, have highlighted the plasticity of *Leishmania* genome[255, 256]. DNA microarrays have been used to screen for differentially expressed genes in *Leishmania* parasites selected *in vitro* for drug resistance and proven suitable to detect gene amplification events[256-258]. Overexpression of genes such as gamma-glutamylcysteine synthetase (*GSH1*), ABC transporter MRPA (*PGPA*), pterin reductase 1 (*PTR1*) and dihydrofolate-reductase thymidylate synthase (*DHFR-TS)* was found to be due to DNA amplification, a strategy that seems to be used by *Leishmania* parasites to increase expression of certain genes in order to survive under drug pressure[258]. Modulation of gene copy numbers and consequent up or down regulation of gene expression in resistant lines was described as involving gene deletion, extrachromosomal circular or linear amplicons and supernumerary chromosomes[255, 256]. Gene amplification has been described in drug resistant parasites selected *in vitro* for resistance to methotrexate (MTX), in which the target gene *DHFR-TS* or *PTR1* were amplified as part of extrachromosomal circular or linear amplicons[258-260]; also *in vitro* selection of antimony resistance *L. infantum* parasites led to the generation of several supernumerary chromosomes and two haploid chromosomes [255, 256]. Although, a clear pattern of aneuploidy was observed in *L. donovani* clinical lines, isolated from visceral leishmaniasis patients, it was not possible to establish a clear link between supernumerary chromosomes and drug resistance phenotypes[203].

Clearly further work is needed to confirm the generation of aneuploidy with drug resistance emergence in clinical strains, however there are some indications that gene rearrangements and chromosome aneuploidy make part of the mechanisms used in response to drug pressure, demonstrating the plasticity of the *Leishmania* genome and how well these parasites cope with changes that include duplication or deletion of a whole chromosome. Most surprising is the fact that chromosome copy number variation does not occur only under drug pressure. It was revealed by the new sequencing genome projects that included the annotation of *L. mexicana* and *L. donovani* reference genomes for the first time and also the refined versions of *L. major, L. infantum* and *L. braziliensis*, to be a natural genetic feature of *Leishmania* species and apparently the major source of genomic diversity[203, 204]. Variation in chromosome organization and copy number is a common mechanism used by pathogenic fungi to rapidly generate diversity in response to stressful growth conditions [261] This plasticity includes the types of genomic changes frequently observed with cancer cells, including chromosomal rearrangements, aneuploidy, and loss of heterozygosity. Aneuploidy in human cancer cells is very prevalent and increasingly common during the acquisition of drug resistance in cancer cells[262, 263]. Chromosome copy number variation was found in all *Leishmania* species and large differences were detected among the strains and species analyzed, as shown in Table 2.2.

The only supernumerary chromosome found to be common to all species was chromosome 31[204], which has been previously identified as tetraploid in *L. major*[56]. Furthermore, identified in *L. mexicana* and *L. braziliensis* were chromosomes with an intermediate read depth, being neither disomic or trisomic, suggesting a mixture of ploidy in the cloned population as reported for seven chromosomes from individual *L. major* parasites by fluorescent in-situ hybridisation (FISH)[264]. Sterkers and co-workers have, for the first time, shown variable ploidy within the same *L. major* population suggesting that every chromosome was observed in at least two ploidy stages and also that chromosome ploidy distribution was variable among clones and strains[264]. This phenomenon, named chromosomal mosaicism, appeared to be constitutive and potentially responsible for the generation of phenotypic variability from genomic plasticity[264]. Suprisingly, was the observation that *L. braziliensis* strain M2904 is predominantly triploid contrary to what was observed for the other species, containing several tetrasomic chromosomes and six copies of chromosome 31[204].

Table 2.2 Summary of *Leishmania* chromosomes

Species	Strain	No. chrs	Size (mb)[1]	Size (mb)[2]	Intermediate chrs	Trisomic chrs	Tetrasomic chrs or higher
L. major	Friedlin	36	32.8	67.8	-	-	31
L. major	LV39	36	32.8	70.8	-	-	31
L. infantum	JPCM5	36	32.1	72.8	-	6,8,9,17,22,25, 33,35	31
L. donovani	BPK206/0	36	32.1	72.5	1, 5, 6, 9, 11, 35	13,15,20,23, 33	8, 31
L. donovani	LV9	36	32.1	66.5	2, 14	23, 31, 33	-
L. braziliensis	M2904	35	32.0	66.4	5, 14	29	16, 30
L. mexicana	U1103	34	32.1	67.8	2, 4, 6, 7, 8, 12, 14, 15, 17, 26, 27	5, 26	30
L. mexicana	M379	34	32.1	ND	12, 13	16	

All chromosomes disomic unless indicated; Chrs, chromosomes ; [1] sequenced, haploid; [2] adjusted for chromosome number (adapted from Rogers *et al*[204]).

Chromosome ploidy variation was validated for *LinJ*36.0640 and L*inJ*31.3030 genes of *L. infantum* JPCM5 (MCAN/ES/98/LLM-887)[204] by gene deletion, with no differences in growth or infectivity between the null mutants and wild type strains. As shown by the analysis of 17 strains of *L. donovani*, the pattern of aneuploidy is unique for each cell line, impossible to link a given pattern to sodium stibogluconate drug resistance, showing clearly that *Leishmania* genomic plasticity and diversity is a complex phenomenon. It's noteworthy to mention the huge difference in the number of single nucleotide polymorphisms (SNPs) detected in *L. major* (297 SNPs) and *L. infantum* (629 SNPs) compared with *L. mexicana* (12531 SNPs) and *L. braziliensis* (44588 SNPs), revealing a remarkably high level of heterozygosity in *L. braziliensis.* SNPs are the most frequent variation in the human genome, which consist of single base-pair substitutions that occur within and outside genes[265]. As mentioned above, the recent genome sequence revealed that chromosome copy number variation is the major source of genomic diversity in *Leishmania*[203, 204]. Besides chromosome copy number variations, expansion and contraction of genes in tandem arrays also contributes to gene dosage differences[203, 204]. The total number of arrays and the number of gene copies in each array varied among species, with 56 protein-coding genes found to be multicopy in all 4 species studied: *L. major, L. infantum*, *L. donovani* and *L. braziliensis* and *L. mexicana*. Interesting was the fact that multicopy genes were found preferentially on disomic and not in supernumerary chromosomes[204]. The authors of the study suggested that disomic chromosomes containing genes in tandem array are not among those that underwent whole chromosome duplications due to the presence of a higher proportion of dose-sensitive genes[204]. As reported previously drug selection *in vitro* induced the amplification of genes as part of extrachromosomal amplicons[255]. Although the presence of episomal DNA corresponding to the amplification of the MAPK locus in *L. donovani* clinical lines, and the fact that more copies of the MAPK-locus were found in SSG-resistant lines, is evidence for *Leishmania* genomic plasticity and the potentially different mechanisms used to regulate gene dosage. Furthermore, it was shown that the gene dosage in the *L. donovani* reference line strongly correlates with transcription levels and thus the implications of this need to be evaluated at proteome and metabolome levels[203].

2.4 Proteomics meets metabolomics: an integrative approach to understand *Leishmania* metabolism

In *Leishmania,* mRNA levels can be a misleading indication of the protein expression as parasite genome is constitutively expressed and consequently regulation of gene expression in these organisms is post-transcriptional[266]. Thus, mRNA stability, translation rate and post-translation modifications affecting protein function and stability contribute to gene expression modulation. Both changes in transcripts and protein levels are reflected in functionally relevant variation at a metabolite level, making the metabolome the closest "picture" of the phenotype[201]. Metabolic levels are tightly regulated and the unclose of the complex *Leishmania* metabolic network and its associated dynamic will allow the determination of basic biological processes and to be relevant to understand the mechanisms underlying drug resistance, since drugs such as amphotericin B and miltefosine target metabolic processes, ergosterol biosynthesis and phospholipid metabolism, respectively[267, 268]. The annotation of the *Leishmania* genome together with several proteomic and biochemical studies on promastigotes and amastigote forms allowed the prediction of *Leishmania* metabolic potential and also the inference of a wide range of metabolic pathways[269-271].

Proteomics analysis of *Leishmania* spp. have been used to identify stage-specific, immunogenic or secreted/excreted proteins, contributing to an understanding of the changes and/or adaptations underlying, for example, parasite differentiation or drug resistance. Moreover, proteomics has provided crucial data for the prediction of the metabolic pathways present in *Leishmania* spp. Several proteomic studies have been published, reporting the comparison between promastigote and axenic amastigote proteome profile, grown in *in vitro* conditions, which mimic the sand fly and phagolysosome environments, while others have been focused on the analysis of the proteome during differentiation[221, 242-248, 272-279]. All studies revealed differences in protein expression, up-or down- regulation and stage specific expression; however an interesting result was the fact that different protein spots were originated in the same gene, likely due to post-translational modifications (PTM) and consequent detection of different protein isoforms in the different *Leishmania* life stages. PTMs such as phosphorylation, methylation, acetylation and glycosylation are important regulators of protein function, stability and turnover rate[280]. In *Leishmania*, little information is available about PTMs, although recently proteomic approaches have been used to identify sites of PTM in promastigotes and amastigotes, with the aim of determining the changes that occur during

axenic differentiation and also gain insight into the role of these modifications in the regulation of *Leishmania* development[272, 281, 282]. Both phosphorylation and methylation PTMs were more common latter than during the initial differentiation, and in the case of protein methylation, such modification was followed by an increase in protein abundance suggesting a role in protein stability. The notable increase in β-tubulin glycosylation observed 15h post differentiation signals support for the possible role of this modification in parasite cytoskeletal remodeling, since glycosylation of tubulin was reported to inhibit GTP-dependent polymerization[281]. Furthermore, Morales and co-workers have identified phosphoproteins implicated in stress and heat shock response, RNA/protein turnover, metabolism, and signalling. They have reported that in amastigotes relatively more proteins were phosphorylated compared to promastigotes, 4% and 2.6% of total protein content, respectively[272]. Phosphorylation appears to be extremely important in the regulation of *Leishmania* response to stress, as amastigotes phosphoproteins with increasing abundance were almost exclusively protein chaperones such as the HSP90 family member HSP83, various HSP70 family members and the stress induced protein STI1/HOP[282], for which have been shown a largely constitutive expression, not induced by elevated temperatures across promastigotes and amastigotes stages[245]. The importance of chaperone phosphorylation in *L. donovani* viability was shown by mutation of STI1/HOP phosphorylation sites, since a "conditional" *STI1* null mutant required the presence of a functional *STI1/HOP* copy when a mutated copy was added as an episome[282]. Thus, phosphorylation as well as other PTMs constitute an extremely important adaptation of *Leishmania* parasites to constitutive gene expression and absence of transcriptional regulation.

Proteome profiling comparison of promastigote and amastigote forms provide important information, as they represent two different life stages, although the search for differences in protein expression during parasite differentiation and preparation to infect the mammalian host is also of utmost interest. The most comprehensive analysis of protein expression was carried out across seven time points during *in vitro* differentiation of *L. donovani* promastigotes, in order to highlight how promastigotes retool themselves to survive and replicate as an amastigote[245]. This study, used a novel proteomics approach, in which peptides were labeled by the isobaric tags for the relative and absolute quantification (iTRAQ) method, allowing a coverage of 21% of the predicted *Leishmania* proteome, that resulted in the detection of 969 proteins at all time-points, grouped into an amastigote (289 proteins) and promastigote (310 proteins) specific cluster; major changes in protein abundance occurred at 10–15 h post differentiation signals[245]. Many enzymes of the major metabolic pathways were identified and analysis of their pattern provided a

comprehensive view of parasite metabolic and physiological adjustments during differentiation. Parasites down-regulate glycolysis and simultaneously up-regulate gluconeogenesis, in agreement with the scarce availability of glucose in the phagolysosome[283] and the necessary production of sugars from glycerol and amino acids; also notorious is the parasite shift from glucose to fatty acid oxidation as the main source of metabolic energy, by the up-regulation of the majority of the enzymes involved in β-oxidation and down-regulated expression of acetyl-CoA carboxylase, the enzyme that synthesizes a key inhibitor of β-oxidation, 15h after differentiation. Also, enzymes involved in the tricarboxylic acid cycle, mitochondrial respiration and oxidative phosphorylation were up-regulated throughout differentiation, supporting the increase in metabolic energy production, that the authors of the study propose to be necessary to maintain amastigote pH homeostasis[281].

The availability of the *Leishmania* genome sequence and all the information gathered by transcriptomic, proteomic and biochemical studies allowed the construction of a database named LeishCyc, which describes *L. major* genes, gene products, metabolites, their relationships and biochemical organization into metabolic pathways, providing a useful tool for integration of *Leishmania* -omics data (transcriptomics, proteomics, metabolomics) in the context of metabolic pathways[271].

Analysis of the metabolome, the total collection of metabolites in a cell provides a read-out of the metabolite levels in biological samples. Thus, metabolomics gives access to information that both genomics and proteomics do not cover, enabling the analysis of small molecules that reveal new insights into the molecular pathways underlying biological processes. Metabolomics have been applied to the discovery of new biomarkers and also to provide a “fingerprint” that allow the distinction between healthy and unhealthy cells[284], considered as being an excellent tool in the discovery of metabolites and metabolic pathways central to biological regulation, with important applications in the study of disease including the regulation of disease. Metabolomics applied to parasites is now emerging due to availability of new and improved techniques for extraction and identification of metabolites. Some studies have examined the effect of parasite infection *in vivo* by analysis of host biofluids in order to elucidate the metabolic modulation induced by the parasite and identify biomarkers for a variety of diseases caused by *Schistosoma*, *Trichinella* and *Plasmodium*[209, 285, 286]. Other experiments have analyzed the parasite *in vitro*, revealing important aspects of *T. brucei* carbon metabolism[287] or changes in metabolism that may be involved in the generation of *Leishmania* drug resistance[207].

2.5 *Leishmania* metabolome

During its digenetic life cycle, *Leishmania* alternates between the alimentary tract of the sandfly vector and the acidic phagolysosomes of mammalian macrophages. In order to survive in such different environments, *Leishmania* has adapted to exploit multiple carbon sources, possesses a complex transport and salvage pathways to acquire essential nutrients, for which lack the pathways of de novo synthesis, is able to synthesize metabolites involved in cellular oxidative defence, to modulate the host cell metabolic and signalling pathways for their own profit[288, 289]. As a promastigote, *Leishmania* experience nutrient-rich conditions in the digestive tract of the sand-fly either during digestion of the blood meal or sugar meal phase. Although, the parasite has to survive in a nutrient poor environment during the initial phagocytosis by the neutrophils and adapt to the poor content of sugars within the macrophage phagolysosome, where the nutrient composition is heavily dependent on the host immune and activation state of the host cell[283].
The pathways of core metabolism in *Leishmania* occur between two organelles: glycosome and mithocondrion (Figure 2.1). Glycolysis, gluconeogenesis, pentose phosphate and succinate fermentation, that are involved in carbohydrate metabolism take place partially or exclusively in the glycosome while the tricarboxylic acid (TCA) cycle occurs in the mitochondria[269, 290, 291].

Leishmania can use an amylase, many sugar kinases and a sucrose like protein for the digestion of plant starch and disaccharides, likely to be present in the nectar taken by sand flies[269]. Thus, *Leishmania* parasites are well adapted to develop in a glucose rich environment, a fact observed *in vitro* by the preference of glucose and other sugars as carbon sources by both promastigotes and axenic amastigotes[292]. Although, the sugar content in the phagolysosome, in which the amastigote form resides is likely to be scarce and the parasite have adapted to use other sources of carbon such as amino acids and fatty acids, *Leishmania* is still highly dependent on hexoses. Exogenous hexoses may be needed to sustain essential pathways such as the pentose phosphate pathway (PPP), RNA/DNA synthesis, N-glycosylation and myo-inositol synthesis[293, 294]. Hexose transporter-deficient *L. mexicana* mutants could not survive inside macrophages[295]. Also, fructose-1,6-bis-phosphatase (FBP) *L. major* mutants were able to infect but failed to generate normal lesions in mice, revealing the essential role of gluconeogenesis[296]. Indeed, analysis of parasite proteome during *in vitro* differentiation has shown that glycolysis is down-regulated during late differentiation while gluconeogenesis enzymes expression was up-regulated. Co-localization and co-expression of gluconeogenic and glycolytic enzymes may allow the parasites to rapidly adapt to different environments.

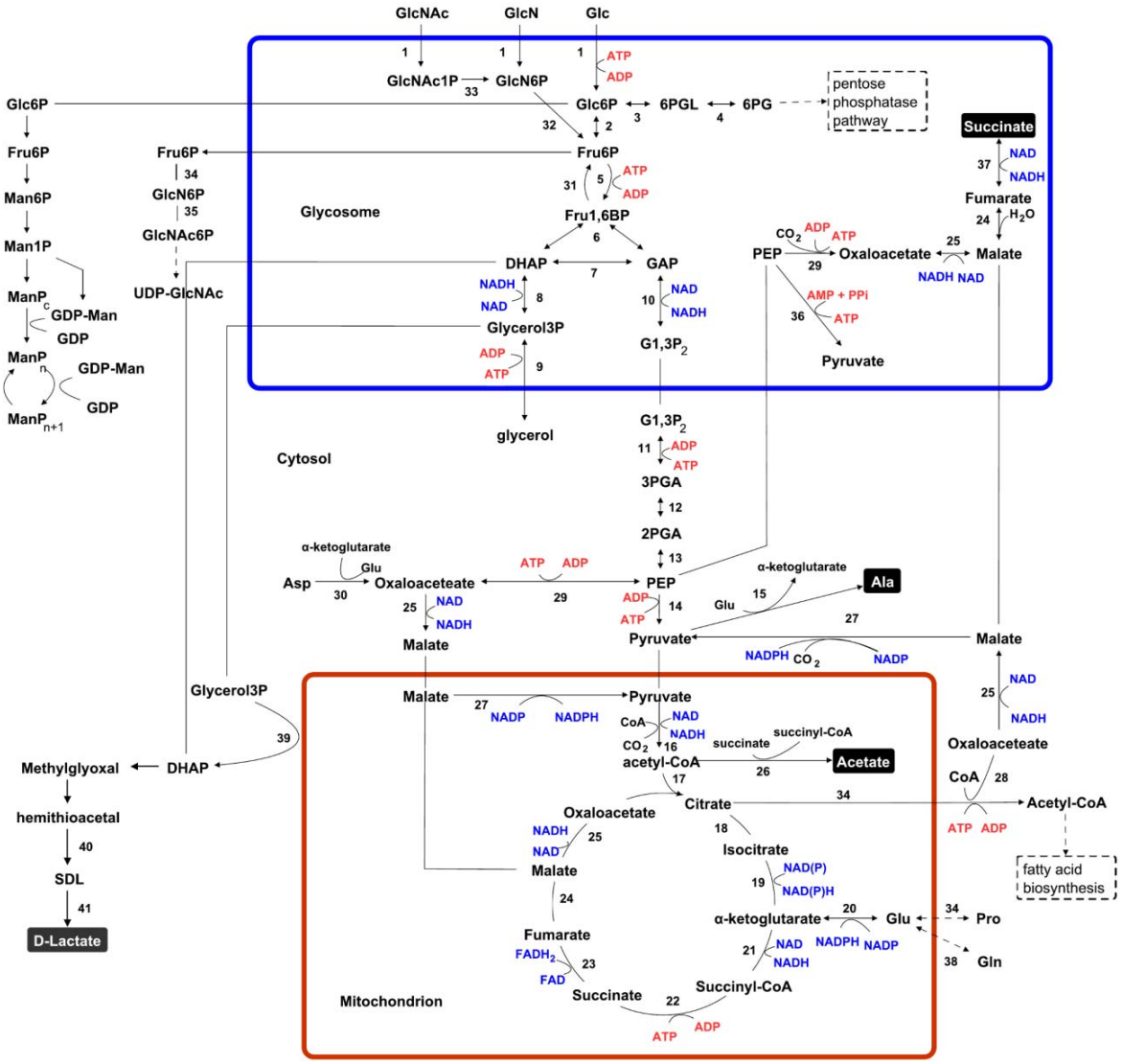

Figure 2.1 Central carbon metabolism in *Leishmania.*

Boxed metabolites are end-products (in black) of metabolism; dotted arrows represent multiple step reactions. Abbreviations: Ala, alanine; Asp, aspartic acid; DHAP, dihydroxyacetone phosphate; Glc, glucose; Fru, fructose; Fru1,6BP, fructose-1,6-bisphosphate; GAP, glyceraldehyde-3-phosphate; G1,3P2, 1,3-biphosphoglycerate; GlcN, glucosamine; GlcNAc, N-acetyl-glucosamine; Glu, glutamic acid; Gln, glutamine; Man6P, mannose-6-phosphate; $ManP_c$, Man1,4-cyclic-phosphate; Man_n, mannogen oligomers $(Man\beta1\text{-}2Man)_n$; PGL, phosphogluconolactone; PG, phosphogluconate; PGA, phosphoglycerate; PEP, phosphoenolpyruvate; Pro, proline; SDL, S-D-lactoyl-conjugate. Enzymes: 1, hexokinase; 2, glucose-6-phosphate dehydrogenase, 3, 6-phosphogluconolactonase; 4, phosphoglucose isomerase; 5, phosphofructokinase; 6, fructose biphosphate aldolase; 7, triosephosphate isomerase; 8, glycerol-3-phosphate dehydrogenase; 9, glycerol kinase; 10, glyceraldehyde-3-phosphate dehydrogenase; 11,

phosphoglycerate kinase; 12, phosphoglycerate mutase; 13, enolase; 14, pyruvate kinase; 15, alanine aminotransferase; 16, pyruvate dehydrogenase; 17, citrate lyase; 18, aconitase; 19, isocitrate dehydrogenase; 20, glutamatedehydrogenase; 21, α-ketoglutarate dehydrogenase; 22, succinyl-CoA ligase; 23, succinate dehydrogenase; 24, fumarate hydratase; 25, malate dehydrogenase; 26, acetate-succinate CoA transferase; 27, malic enzyme; 28, acetyl-CoA synthethase; 29, phosphoenolpyruvate carboxykinase; 30, aspartate aminotransferase; 31, fructose-1,6-bis-phosphatase; 32, glucosamine-6-phosphate deaminase; 33, N-acetylglucosamine-6-phosphate deacetylase; 34, glutamine:Fru6P aminotransferase; 35, glucosamine-6-phosphate acetylase; 36, pyruvate phosphate dikinase; 37, NADH-dependent fumarate reductase; 38, glutamine synthetase; 39, FAD-dependent glycerol-3-phosphate dehydrogenase; 41, glyoxalase I; 42, glyoxalase II.

Recently, hexosamine uptake by amastigote was shown to be important, since parasites in which the enzyme responsible for the conversion of glucosamine to fructose-6-phosphate was deleted showed an attenuated virulence phenotype in mice. This study also suggests that hexosamine sugars may be more abundant in the host cell in the earlier stages of infection, while later other sugars will constitute the major source[297], probably due to an active gluconeogenesis pathway[298]. However, amastigotes are able to accumulate a unique intracellular carbohydrate reserve material named mannogen, despite living in a sugar poor niche. Mannogen is composed of short chains of β1-2 linked mannose, accumulates exclusively in the cytosol and is degraded under sugar-limiting conditions, suggesting that due to this reserve of de novo synthesis or uptake of sugars not to be limiting for amastigotes growth[299]. In *L. mexicana* promastigotes was detected the incorporation of glucose into mannogen at a similar rate as into the glycolytic intermediates, suggesting that excess of glucose/fructose-6-phosphate is converted to mannose-6-phosphate and GDP-Man[300].

The end-products of glucose catabolism in insect forms of trypanosomatids include succinate, pyruvate, acetate, alanine, ammonia, urea and lactate[269, 301-303]. Recently, a study using gas chromatography-mass spectrometry and ^{13}C-NMR has shown that glucose is rapidly catabolized to CO_2, partially oxidized to succinate, acetate, alanine and also a low level of glutamate, consistent with the operation of a succinate fermentation pathway, the conversion of acetyl-CoA to acetate and substantial flux of glycolytic end-products into the TCA cycle[300]. Acetate is produced by the mitochondrial enzyme acetate:succinyl-CoA transferase[304, 305] and alanine results of pyruvate transamination. Lactate is a metabolic end product of methylglyoxal, a toxic by-product of glycolysis

detoxified via glyoxalase pathway; this pathway is composed of two enzymes that use $T(SH)_2$ as cofactor in contrast with the GSH-dependent enzymes present in mammalian cells[306, 307]. Succinate production occurs through the succinate fermentation pathway, in which succinate is produced from phosphoenolpyruvate (PEP) involving two glycosomal NADH-dependent oxidoreductases, malate dehydrogenase and fumarate reductase, providing a means for the re-oxidation of NADH produced in the glycosome by the glycolytic glyceraldehyde-3-phosphate dehydrogenase (GADPH), resulting in the synthesis of one ATP and two molecules of NAD^+ for each PEP imported. Other pathways for regeneration of glycosomal ATP and NAD^+ have been described including a glycerol-3-phosphate/dihydroxyacetone shuttle and reactions catalyzed by a glycerol-3-phosphate kinase, glycosomal isoforms of 3 phosphoglycerate kinase and/or a pyruvate dikinase[20]. In *T. brucei* procyclic stages, succinate fermentation appears to be the major pathway for regenerating glycosomal pools of ATP/NAD^+, being responsible for a tightly balanced consumption and production of NADH within the glycosomes necessary to maintain the organellar redox (NAD^+/NADH) balance, while the other pathways are only activated in the case of succinate fermentation inhibition[308]. In contrast with *T. brucei*, *Leishmania* succinate fermentation may not be only essential to maintain the glycosome redox balance but also have an important role in TCA cycle anaplerosis (replenishment of TCA cycle intermediates). The majority of the C4 dicarboxylic acids, such as malate and fumarate, generated during glycosomal succinate fermentation are subsequently used for TCA cycle anaplerosis, suggesting that metabolic fluxes in the glycosome and mitochondria are intimately linked[300]. These findings are supported by previous observations that hexose uptake and catabolism is essential for amastigote survival in the mammalian host, despite the relatively high levels of amino acids in the phagolysosome, which can be used as the carbon source. Thus the hexose uptake may be needed to replenish the TCA cycle intermediates in order to sustain the synthesis of glutamate and related amino acids, such as proline and glutamine. Indeed, TCA cycle activity may increase markedly in the amastigote stages, likely exposed to low levels of glucose but relatively high levels of amino acids and lipids[296]. Furthermore, TCA cycle enzymes activity is up-regulated during differentiation, likely a consequence of up-regulation in β-oxidation, already reported *in vivo* as *Leishmania* starts to use fatty acids as carbon source [292], which leads to an increase production of acetyl-CoA units handled by TCA cycle in the mitochondria and then the generated reducing equivalents oxidized by the mitochondrial respiratory chain[245]. Mitochondrial function seems to be essential for *Leishmania* amastigote viability, as deletion of both alleles of the gene encoding a mitochondrial protein, named MIX was not achieved and just the deletion of one allele induced abnormalities in cell morphology, mitochondrial segregation and loss of virulence

in mice[309]; a similar phenotype was observed when MIX gene in *T. brucei* was targeted by RNAi[310]. Another *Leishmania* mitochondrial protein (*Ld*p27) was shown to be important as gene deleted parasites have less cytochrome c oxidase activity and ATP synthesis and were less virulent both in human macrophages and in BALB/c mice[311].

Besides glycolysis, glucose is also metabolized via PPP, which is found in most cell types and provides the major source of NADPH for anabolic reactions and regeneration of antioxidant systems. The pathway also provides phosphorylated carbohydrate intermediates including ribulose-5-phosphate that is incorporated into nucleotides for biosynthesis of nucleic acids and nucleotide cofactors[312, 313]. PPP is also active in *Leishmania* species containing all enzymes of the classical pathway in promastigotes[314]; the oxidative branch of PPP is compartmentalized inside glycosomes. Sugars such as ribose and erythrose are formed from glucose-6-phosphate via glucose-6-phosphate dehydrogenase and 6-phosphogluconate dehydrogenase[315]. It's noteworthy to mention that ^{13}C-glucose incorporation into the PPP intermediates has shown slower kinetics than the glycolytic intermediates, indicating a reduced flux into this pathway, but a simultaneous rapid labeling of several nucleotides supporting the crucial role of PPP pathway for nucleotide biosynthesis[300]. The major product of the pathway is ribose-5-phosphate (R5P), however PPP is not the only source of R5P as this metabolite can also be produced from free ribose activated by phosphorylation with ribokinase or released from nucleosides through the action of nucleoside hydrolase[314], that has been shown to accumulate via a specific carrier-protein in *Leishmania*[316]. PPP has an important role in defense against oxidative stress as shown by the fact that *L. infantum* mutants adapted to nitric oxide expressed high levels of the PPP enzyme 6-phosphogluconate dehydrogenase[317]. Also a higher PPP oxidative branch enzymatic activity was detected in *L. mexicana* promastigotes when compared with insect forms of *T. brucei* proposed to be due to a higher demand of NADPH to counteract the oxidative stress suffered by *Leishmania* promastigotes in the initial phase of infection[314].

Proteomic and biochemical studies have suggested that *Leishmania* intracellular forms are able to use lipids as a carbon source for energy generation through the β-oxidation of fatty acids. The higher activity of enzymes that catalyze β-oxidation of fatty acids in *L. mexicana* amastigotes[292] and protein up-regulation in this pathway during late differentiation of *L. donovani* parasites with simultaneously down-regulation of glycolysis[245], support the change in carbon sources as the parasite differentiate and colonize niches with different nutrient composition suggesting a more important role for fatty acid as a carbon source in intracellular amastigotes. *Leishmania*, as well as other

intracellular pathogens, can use fatty acids derived from complex host lipids, such as lipoproteins internalized by infected macrophages[318, 319]; lipid exchange between amastigote plasma membrane and the PV membrane may also occur, in a way that the host glycosphingolipids become intercalated into the amastigote membrane[283, 320, 321]. *Leishmania* can also a in defined medium lacking lipid moieties, since it is able to synthesize fatty acids de novo. Indeed, as observed in *T. brucei* and in *T.cruzi*, *L. major* encodes a type II FA synthase, however this does not seem to be the major pathway for fatty acid de novo synthesis. Trypanosomatids use a new mechanism involving endoplasmic reticulum-based elongases (ELOs) to make the bulk of their fatty acids, while other organisms use ELOs to make long chain fatty acids even longer[318].

Phospholipids (PLs) account for ~70% of total cellular lipids in *Leishmania* and are classified according to the "head group" as phosphatidylcholine (PC), phosphatidylethanolamine (PE), phosphatidyinositol (PI) and phosphatidylserine (PS). *Leishmania* parasites also synthesize low levels of phosphatidyglycerol (PG), cardiolipin and phosphatidic acid. The most abundant PL in *Leishmania* is PC with unusually long and unsaturated fatty acid species[322]. PC function is not yet known, but their polyunsaturated fatty acid chains could modulate membrane physiology by reducing the melting point and confer resistance to host derived oxidants[323]. PI is found in the anchors of surface glycoconjugates including glycosylinositolphospholipids (GIPLs), glycosylphosphatidylinositol (GPI)-containing membrane proteins and lipophosphoglycan (LPG)[324, 325]. In *Leishmania* it is not yet known if PS is synthesized by the parasite or acquired from the host, despite the presence of putative enzymes involved in PS metabolism. PS exposure on the outer surface of cells may trigger the removal of apoptotic cells by phagocytes[326, 327]. *Leishmania* has been reported to mimic such PS exposure acting as a "deactivating" signal for host cells, used as a strategy of silent entry into the macrophage[165, 328, 329]. PLs as the major components of *Leishmania* membranes are likely to be determinant in membrane permeability, fluidity and also have a profound impact in vesicular trafficking, nutrients acquisition through endocytosis and cell differentiation, which involves an extensive membrane remodeling. Furthermore, the fact that PLs diversity between *Leishmania* and mammals is quite different has been explored as a drug target by the use of lysophospholipid analogs including miltefosine, edelfosine and ilmofosine[330, 331]. Miltefosine effects described in *L. donovani* promastigotes include perturbations on lipid metabolism, specifically phospholipid content, fatty acid and sterol content[332]. Recently mitochondria and specifically the cytochrome c oxidase have been implicated as targets of miltefosine in *L. donovani* promastigotes[333].

The majority of spingolipids **(**SLs) in *Leishmania* belong to unglycosylated inositolphosphorylceramide (IPC) and ceramide. IPC are abundant, constituting nearly 10% of the total membrane phospholipids and are generated by the transfer of a phosphorylinositol headgroup from PI to ceramide, a process catalyzed by the IPC synthase, demonstrating that a functional SL pathway is present in these parasites[334]. SLs are not required for growth of *Leishmania*, since parasites that completely lack SLs grew normally in logarithmic phase and were still able to make “lipid rafts”. However, deletion of *SPT2,* the gene that encodes the key de novo biosynthetic enzyme serine palmitoyltransferase subunit 2, resulted in parasites deficient in de novo SLs synthesis that once in the stationary phase were not able to differentiate into metacyclic forms[335]. SLs are considered essential membrane components in all eukaryotes, mediating many signaling pathways including those key for apoptosis, growth and differentiation [336]. However, in *Leishmania* the primary role of SLs appears to be the provision of ethanolamine, as ethanolamine supplementation was able to overcome the phenotype observed in the SL-deficient mutant parasites[337]. Ethanolamine and choline are essential nutrients, and when available exogenously they can be salvaged by *Leishmania* via membrane transporters[338, 339]. Thus the significance of SL biosynthesis is likely to be stage-specific, being important in those stages in the sand fly that cannot rely upon salvaged ethanolamine. Indeed, amastigotes deficient in de novo SLs synthesis recovered from a mammalian host showed normal levels of IPC and thus amastigotes seems to be able to perform SLs salvage or use host lipids as precursors for synthesis of IPC[340]. Interesting is also the fact that SLs may play an important role in the modulation of host responses, given that the increase in ceramide levels detected in *Leishmania*-infected macrophages *in vitro* leads to the suppression of NF-kB activation in host macrophages[341].

Besides PLs and SLs *Leishmania* lipid composition also includes sterols that play an important role in the structure and function of cellular membranes and are essential for parasite growth and viability, revealed by the effect of antifungal compounds which inhibit the reactions of sterol biosynthesis[342]. In contrast with mammalian cells, *Leishmania* parasites synthesize ergosterol instead of cholesterol[100, 343], being able to incorporate cholesterol either from an infected host or culture medium; cholesterol uptake was observed in miltefosine resistant parasites[115]. Sterol biosynthesis in *Leishmania* parasites has received much attention as it may constitute a good drug target, due to the fact that parasites synthesize ergosterol derivatives instead of cholesterol as in mammalian cells. There are already some drugs reported to interfere with sterol biosynthesis, such as amphotericin B[344], atavaquone[345], synthetic quinuclidines[346, 347] and chalcones[348].

Moreover, sterols probably play a significant role in miltefosine action against the parasite, since membrane sterol depletion led to a decrease in drug susceptibility, suggesting that sterols can serve as a reservoir for miltefosine providing a constant supply to the respective transporter[112]. Drug effectiveness is mainly dependent on the interaction with the *Leishmania* membrane, thus it is clear that the ability of the parasite to change the lipid membrane composition inherent to its life cycle should be taken into consideration in the finding of new formulations.

Leishmania ability to synthesize amino acids is limited to nonessential ones plus threonine and methionine[269]. Cysteine can be produced either by de novo synthesis from serine or from homocysteine by the trans-sulfuration pathway[349]; aspartate and asparagine can be formed from oxaloacetate, while glycine can be formed from serine and alanine via transamination of pyruvate[289]. Methionine can be salvaged or synthesized by methionine synthase, which uses methyl- tetrahydrobiopterin (H_4F) and homocysteine to produce methionine and H_4F; methionine plays a crucial role as an essential amino acid and for formation of S-adenosylmethionine (SAM), which is required for methylation reactions and the synthesis of polyamines. Aromatic amino acids (phenylalanine, tyrosine or tryptophan), the branched amino acids (leucine, isoleucine or valine), lysine and histidine cannot be synthesized by *Leishmania*[269]. On the other hand, the *Leishmania* encodes several putative amino acid permeases. A high affinity arginine-specific transporter, named *Ld*AAP3 was the first permease to be identified in *L. donovani*[350]. Arginine is an essential amino acid in *Leishmania* parasites and must be taken up from the host as it is used not only for protein synthesis as well as the precursor for synthesis of polyamines[269, 351]. Arginine starvation resulted in the increase of both mRNA and *Ld*AAP3 protein levels, which were abrogated by supplementing amino acid-starved parasites with arginine. *Ld*AAP3 expression and activity increased whenever the cellular level of arginine decreased, suggesting that the parasites sense the intracellular level of arginine and adjust the transport to maintain homeostasis[352]. Recently, a lysine-specific transporter in *L. donovani* (*Ld*AAP7) was also identified and shown to be essential given the impossibility to delete the gene, suggesting that this is the only lysine transporter in *L. donovani*[353]. *Leishmania* parasites also contain several peptidases that are likely to play an important role in degrading proteins taken up from the environment, some of them being up-regulated in the amastigote stage. Moreover, cysteine proteinases *L. mexicana* mutants are attenuated *in vivo*, consistent with a role in parasite nutrition[9]. The fact that amino acid uptake was shown to be increased in *L. mexicana* amastigotes[292] and also the up-regulation of enzymes such as branched chain aminotransferase, alanine aminotransferase, glutamate dehydrogenase isoenzymes involved in the catabolism of certain amino acids (isoleucine, valine, alanine, glutamate, glycine) during

differentiation[245], give good indications of amino acid use as a carbon source, however there is no direct evidence for a dependency of amastigotes on amino acid catabolism *in vivo*, similar to the essential requirement for hexoses[295, 296]. Besides the use in protein biosynthesis, proline and glutamate may serve as important energy substrate for *Leishmania*. Proline is oxidized to glutamate, which will be incorporated into the TCA cycle[269], while leucine metabolized through 3-hydroxy-3-methylglutaryl-CoA (HMG-CoA) can be incorporated directly into *Leishmania's* sterol biosynthetic pathway[354]. A recent study by Saunders and co-workers using *L. mexicana* promastigotes has shown that only a limited number of amino acids such as aspartate and alanine were used as carbon sources, during *in vitro* culture. Also, several pathways of amino acid synthesis were repressed in the presence of exogenous amino acids, revealing that key enzymes involved in the amino acid biosynthesis are constitutively expressed but under tight control to ensure that exogenous nutrients are used first[300]. Moreover, glutamate identified as the most abundant amino acid in promastigotes stages is internalized at a low rate under standard culture conditions, a fact that may be explained by the high rate of glutamate synthesis through the incorporation of aspartate and alanine into the TCA cycle, where major anabolic function is likely to be the synthesis of glutamate[300].

Purines and pyrimidines are essential to all living organisms, performing many vital functions such as nucleic acids (DNA and RNA) synthesis and ATP which serves as the major energy source within the cell to drive a number of biological processes. *Leishmania* parasites, like other trypanosomatids, need to acquire purines from the medium, as they are incapable of de novo purine synthesis. Thus, the parasite has evolved a number of unique purine salvage enzymes that enables it to scavange host purines by interconversion and metabolism to phosphorylated nucleotides[355]. The parasites only present one of the 10 enzymes, adenylosuccinate, required to make inosine monophosphate (IMP) from phosphoribosyl pyrophosphate that participates in purine salvage by converting IMP to adenine monophosphate (AMP)[289, 356]. Purines, such as hypoxanthine and xanthine are essential for parasite growth and hence the need to add those to *in vitro* cultures; purine withdrawal from *L. donovani* promastigotes culture led to a dramatic and rapid increase of endogenous purine transport proteins and purine salvage componentes as well as to changes in the parasite morphology[357, 358]. It was established that *L. donovani* salvages purines primarily through hypoxanthine-guanine phosphoribosyltransferase (HGPRT) and xanthine phosphoribosyltransferase (XPRT)[359], genetic disruption of individual transporters had little impact on intracellular growth, suggesting a significant redundancy in the purine salvage; only deletion of both HGPRT and XPRT in the same cell line resulted in severely attenuated parasites *in vivo*. It is

noteworthy to mention, that a marked amplification and over-expression of the adenine phosphoribosyltransferase (APRT) gene was observed in the null mutant parasites recovered from animals, implying that APRT was capable of phosphoribosylating hypoxanthine and promote cell growth[360], despite being previously reported that it exclusively recognize adenine as a substrate[361, 362]. On the other hand, *Leishmania* is able to synthesize pyrimidines de novo from glutamine, bicarbonate and aspartate[289].

Other *Leishmania* metabolic requirements include, polyamines, such as putrescine, essential for *Leishmania* growth and survival as a precursor of spermidine that together with glutathione is the substrate for synthesis of $T(SH)_2$[363], an essential thiol that constitutes with trypanothine reductase the unique antioxidant system present in these parasites[364]. Polyamine production is dependent on arginine, an essential amino acid that the parasite is not able to synthesize[269]; disruption of the gene that encodes arginase, the initial enzyme in arginine catabolism led to severely restricted growth of intracellular amastigotes and growth of promastigotes only possible in the presence of ornithine, putrescine or spermidine, showing that amastigotes are dependent on the de novo polyamine biosynthesis as well as on the salvage of polyamines from the phagolysosome[365]. A polyamine transporter with high affinity for putrescine and spermidine has been identified in *L. major*[366] and pentamidine, a drug used in the treatment of leishmaniasis, was shown to inhibit putrecine and spermidine transport[367]. Moreover, deletion of the ornithine decarboxylase (ODC) gene in *L. donovani*, which encodes the enzyme that catalyzes the reaction of ornithine to putrescine, resulted in the generation of cells that can only survive in the presence of putrescine or spermidine and were not able to scavenge polyamines from the host in sufficient amounts to sustain an infection, confirming the essential role of polyamine biosynthesis[368, 369]. Thus, ODC has been validated as a drug target and the anti-*Leishmania* activity of DL-α-difluoromethylornithine (DFMO), a drug that irreversible inactivates the *T. brucei* enzyme, was also shown to be effective in killing *Leishmania* parasites[370].

Leishmania parasites are auxotrophic for both folate and unconjugated pteridins and thus need to salvage these metabolites from the host[371]; folates are acquired via active transport[372, 373]. DHFR-TS is a bifunctional enzyme that catalyzes the reduction of folate and biopterin to tetrahydroderivatives. The inability to delete DHFR-TS gene in *L. major*, led to the consideration that it as an essential gene and a potential good drug target[252]. However, PTR1, an enzyme that can reduce both folates and unconjugated pterins can act as a metabolic bypass of DHFR-TS inhibition leading to the antifolate drugs inefficacy[260, 374]. PTR1 seems also to be essential to the parasite[375]. *Leishmania* seems

well adapted to the lack of folate de novo synthesis as the parasites possess a reduced number of folate-dependent metabolic reactions, although the loss of several folate metabolic pathways results in attenuation or loss of virulence[371].

Leishmania are also haem auxotrophs and need to obtain these molecules or precursors directly from the host[376]. The *Leishmania* genome possess homologues for the three last enzymes of haem pathway likely to be functional, since these parasites can grow in medium in which hemin is replaced by protoporphyrin IX[377-379]. Haem is present in trypanosomatids hemoproteins such as peroxidases, cytochromes P450, which are involved in the oxidative stress response, detoxification, synthesis of polyunsaturated fatty acids and sterol biosynthesis[380-385]. Also, the presence of a fully functional mitochondria in these parasites[315], require haem for oxidative phosphorylation and other cellular processes[382, 383, 386].

Overall, *Leishmania* parasites have been able to survive due to the nutritional complex environment that encounter in the different hosts, which seems to fulfill the parasite metabolic requirements. In order to efficiently use the potential carbon sources and essential nutrients available, the parasite has evolved numerous mechanisms for salvage and conversion of host molecules.

CHAPTER 3

LEISHMANIA: THIOL METABOLISM AND ANTIOXIDANT DEFENSE

3.1 Thiol metabolism and antioxidant defense

During metabolic activity of organisms, the imbalance between the production of reactive oxygen species (ROS)/reactive nitrogen species (RNS) and antioxidants will lead to oxidative stress. To protect against it, cells have developed both enzymatic and non-enzymatic antioxidant defenses. Non-enzymatic defenses include ascorbate, glutathione (GSH) and polyamines among others, while catalase, superoxide dismutase, glutathione peroxidase belong to the enzymatic mechanisms that protect by directly scavenging toxic species converting them to less reactive species[387].

Contrary to other organisms, trypanosomatids lack genes for glutathione reductase (GR) and thioredoxin reductase (TR) as well as catalase and selenocysteine-containing glutathione peroxidases[364]. Instead, these parasites possess a redox metabolism that is based on the low molecular mass dithiol trypanothione (N^1,N^8-bis(glutathionyl)spermidine, $T(SH)_2$) and trypanothione reductase (TryR)[388]. The unique $T(SH)_2$/TryR system is responsible for the maintenance of the intracellular thiol redox homeostasis similar to the GSH/GR and thioredoxin(Trx)/TR systems in eukaryotic cells[364]. Besides kinetoplastids, $T(SH)_2$ and/or TryR also occur in some other protists[389-391]. Trypanosomatids can cope successfully with the oxidative burst during host infection due to the well organized and complex $T(SH)_2$/TryR system, involved at least in three important biological functions: hydroperoxide detoxification, regulation of replication and DNA synthesis[392-394].

In addition to $T(SH)_2$, trypanosomatids contain three other major low molecular mass thiols: GSH, mono-glutathionylspermidine (Gsp) and ovothiol (OvSH); $T(SH)_2$ can spontaneously reduce GSH and OvSH[395, 396]. A significant amount of GSH is present as $T(SH)_2$, formed by the conjugation of two GSH molecules linked by the polyamine spermidine in a two step reaction catalyzed by trypanothione synthetase (TryS)[397-399]. Another enzyme thought to be involved in $T(SH)_2$ biosynthesis, glutathionylspermidine synthetase (GspS) was identified but proven not necessary. GspS as well as TryS has amidase activity, being able to cleave $T(SH)_2$[398, 400], leading to the hypothesis that this activity may contribute to maintain a balance between GSH, Gsp, $T(SH)_2$ and spermidine[364]. However, TryS amidase activity was shown not to be required for parasite viability while the synthetase activity is essential since *T. brucei* TryS conditional double knockout lost the ability to produce $T(SH)_2$ with simultaneous accumulation of GSH and were unable to infect mice, validating TryS as a drug target[401]. Despite a quite similar redox potential, at a physiological pH $T(SH)_2$ it is more reactive than GSH[396]. Both the dithiol character of $T(SH)_2$, which favors its ability as a reductant of intramolecular

disulfides[402] and lower pK values in $T(SH)_2$ compared to GSH coinciding with the intracellular pH of the parasites[403] are responsible for the unique properties of $T(SH)_2$. It's still not understood why $T(SH)_2$ has evolved in trypanosomatids, however recently was shown that $T(SH)_2$ has a much higher capacity to neutralize toxic NO as it is able to sequester NO and iron in a free harmless dinitrosyl-iron complex, that in other organisms is found to be associated with glutathione S-transferases (GST)[404]. TryR, a flavoprotein oxidoreductase, plays an important role in the parasite redox state as it is responsible for keeping $T(SH)_2$ in the reduced form. As trypanosomatids lack GR, TryR is the only enzyme that connects the NADPH- and the thiol-based redox systems in these parasites. TryR is an essential enzyme as deletion of one allele was easily achieved but disruption of the second one was not possible or a genomic re-arrangement occurred to maintain a copy of the gene[254, 405]. Also down-regulation of TryR activity to 15% led to a significant impairment of parasite ability to regenerate $T(SH)_2$, but cells kept the capacity to metabolize H_2O_2. Although, parasites were not able to survive inside the activated macrophage[406]. Thus TryR, already characterized in *L. donovani*, *L. infantum* and *T. cruzi*[407-409], is a promising target for *Leishmania*-specific drug design. Indeed, recent studies are an example of the efforts being made to obtain TryR inhibitors[410, 411].

The reducing capacity of $T(SH)_2$ is strongly enhanced in the presence of tryparedoxins (TXNs), small dithiol redox proteins functional similar to glutaredoxins (Grxs) and Trxs. TXNs are oxidoreductases that in analogy with Grxs, are reduced by a low molecular mass thiol ($T(SH)_2$) and can reduce glutathione-mixed disulfides[386]. Indeed $T(SH)_2$ and TXN have a central role in the thiol metabolism of trypanosomes taking part in parasite-specific cascades (Figure 3.1) that catalyze the reduction of hydroperoxides and ribonucleotides[392, 393, 412].

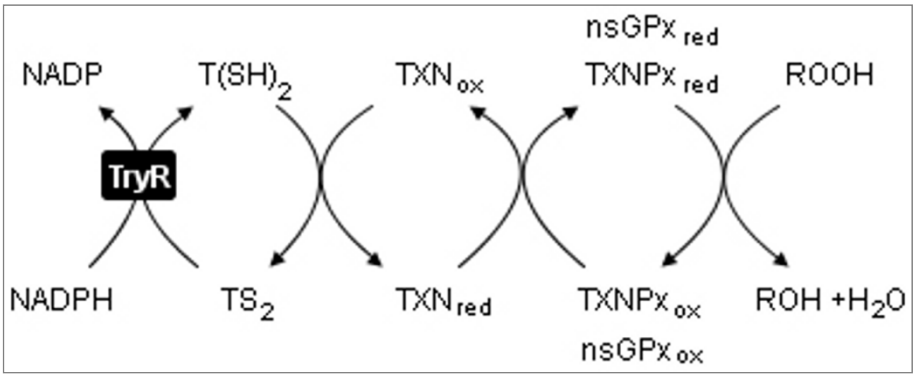

Figure 3.1 Trypanothione-mediated detoxification of hydroperoxides in trypanosomatids. Trypanothione reductase (TryR) regenerates trypanothione disulfide (TS_2) to trypanothione ($T(SH)_2$), which will reduce tryparedoxin (TXN). TXN will deliver

electrons to tryparedoxin peroxidase (TXNPx) or non-selenium glutathione peroxidase like enzymes (nsGPx), which will then metabolize hydroperoxides (ROOH) to an alcohol (ROH). The subscripts red and ox refer to the redox state of the proteins, dithiol and disulfide, respectively (adapted from Krauth-Siegel *et al.*[364]).

TXNs are specifically reduced by $T(SH)_2$. The reducing equivalents obtained from $T(SH)_2$ are transferred by TXNs to tryparedoxin peroxidases (TXNPxs) and also non-selenium glutathione peroxidase like enzymes (nsGPxs)[413-416]. Reduced TXN also delivers electrons to the ribonucleotide reductase (RR)[392], the universal minicircle sequence binding protein (UMSBP) involved in the initial step of replication of the kinetoplast[417] and to a monothiol GRx (1-Cys Grx)[418, 419]. Cytosolic TXN knock down in *T. brucei* resulted in impaired viability and increased sensitivity to hydroperoxides, demonstrating the essential role of cytosolic TXN and its pivotal function in the parasite defense against oxidative stress[420], while mitochondrial TXNs do not seem to be important for both *T. brucei* and *L. infantum*[421, 422]. TXNPxs are 2-Cys peroxiredoxins that primarily detoxify H_2O_2 and a wide range of organic hydroperoxides. These enzymes are highly conserved and present in various *Leishmania* species[394, 423, 424], with distinct subcellular localization, cytosolic and mitochondrial[425]. Cytosolic TXNPx was demonstrated to be essential in *T. brucei* and *L. infantum*, while deletion of mitochondrial TXNPx in *L. infantum* yields a less virulent parasite but no obvious phenothype detected in *T. brucei*[386, 422, 426]. The nsGPxs differ from the selenoenzymes found in mammals and some other organisms as the active site selenocysteine has been replaced by a cysteine residue being fuctionally similar to TXNPxs[413, 414, 427]. Besides, 2-Cys peroxiredoxins and nsGPxs the parasites possess a third family of enzymes involved in hydroperoxide detoxification, the ascorbate peroxidase (APx)[386]. APx is a heme containing peroxidase first identified in *L. major* that localizes in the intermembrane of the mitochondrial inner membrane of the parasite[428]. APx expression is up-regulated in the presence of increasing concentrations of H_2O_2 and deletion of the APx gene in *L. major* rendered the cells more sensitive to ROS *in vitro*, demonstrating the important role of APx in H_2O_2 detoxification[428, 429]. However, the parasite seems to be able in part to compensate for the effect of APx deletion by increasing the expression of nsGPx and also TXNPx, suggestting a high degree of redundancy in ROS detoxifying mechanisms in *Leishmania.* On the other hand, the null mutant cells exhibit hyper virulence after infection with macrophages as well as inoculation into BALB/c mice, which may be explained by the higher numbers of metacyclics, suggesting a role of APx in the control of parasite differentiation and survival in macrophages[429].

Overall, cellular redox homeostasis is maintained by biosynthesis of $T(SH)_2$, which is kept reduced by TryR, the enzyme that represents the only connection between the NADPH- and the thiol-based redox metabolism. Figure 3.2 gives an overview of parasite thiol metabolism and antioxidant defense. Contrary to other organisms no role has been attributed to GSH besides precursor of $T(SH)_2$ and thus remains the doubt about the importance of the free GSH presence in cells that do not possess GR. Given this, it is crucial to understand the possible role of proteins such as TDR1, which contain motifs characteristics of Trx and GST families.

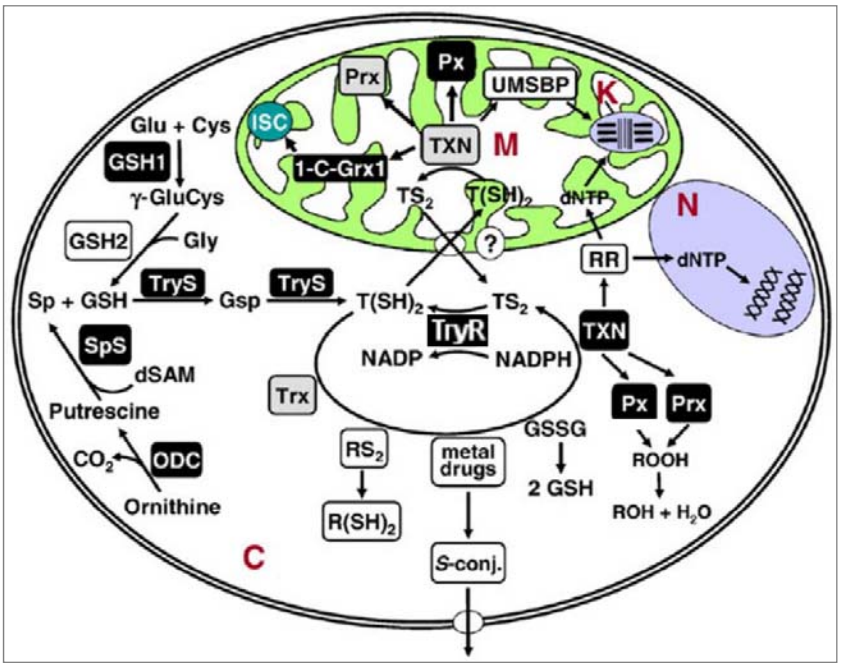

Figure 3.2 Thiol metabolism in trypanosomatids.

1-C-Grx1, a monothiol glutaredoxin; dSAM, decarboxylated S-adenosyl-L-methionine; dNTP, GSH1, γ-glutamylcysteine; GSH2, glutathione synthetase; GSSG, glutathione disulfide; GSH, glutathione; ODC, ornithine descarboxylase; Prx, 2-Cys-peroxiredoxins (also named TXNPX) ; Px, glutathione-peroxidase-type enzymes (also named nsGPx); RS_2, disulfide proteins; ROOH, hydroperoxides; ROH, alcohol; RR, ribonucleotide reductase Sp, spermidine; SpS, spermidine synthase; TryS, trypanothione synthetase, Trx, thioredoxin; TXN, tryparedoxin; TyrR, trypanothione reductase; $T(SH)_2$, trypanothione; TS_2, trypanothione disulfide; UMSBP, universal minicircle sequence binding protein; ISC, iron sulfur clusters; C, cytosol; K, kinetoplast; M, mitochondrion; N, nucleus. Proteins that were experimentally shown to be essential and dispensable for *T. brucei* are highlighted with black and light grey background, respectively (adapted from Krauth-Siegel *et al.*[364]).

3.2 Glutathione S-transferases

GSTs catalyze nucleophilic attack by reduced glutathione on non polar compounds that contain an electrophilic carbon, nitrogen or sulphur atom. GSTs are versatile enzymes able to inactivate a wide range of exogenous toxic molecules, including naturally occurring compounds, industrial chemicals, drugs, herbicides, and pesticides; these phase II detoxification reactions produce generally less reactive and more polar compounds, which can be actively extruded from the cytosol[430, 431]. In addition, GSTs are also important in the detoxification of endogenous reactive species produced during oxidative stress, such as lipid hydroperoxides[432] or reactive aldehydes[433]. In addition, GSTs can also serve as peroxidases, isomerases, thiol transferases or have a role in signalling processes. Therefore, GSTs are not solely detoxification enzymes and are also involved in other pathways such as leukotriene and prostaglandin biosynthesis and the catabolism of aromatic amino acids[434]. On the other hand, GSTs have been reported to be involved in the development of drug resistance towards chemotherapy agents, insecticides, herbicides, and microbial antibiotics, likely related to detoxification abilities[431, 435]. GSTs have been purified from a wide range of organisms and are classified into 3 major families according to their cellular localization: cytosolic, mitochondrial and microsomal (microsomal GSTs are also referred to as membrane associated proteins in eicosanoid and glutathione metabolism). All 3 families contain members that catalyze the conjugation of GSH with 1-chloro-2,4-dinitrobenzene (CDNB) and exhibit glutathione peroxidase activity towards cumene hydroperoxide[431]. Cytosolic GSTs are, generally, biologically active as dimers of subunits of 23-30 kDa and an average length of 200–250 aminoacids[434]. There are seven classes of cytosolic GSTs recognized in mammalian species: alpha, mu, pi (GSTPi), sigma, theta, omega (GSTO) and zeta[431]. Other classes such as lambda and tau have been identified in other organisms[436]. Each monomer in GSTs has a catalytic active site with two domains: G-site, responsible for GSH binding and H-site, which binds hydrophobic substrates. The H-site or substrate binding site is more variable in structure and is largely formed from residues at the C-terminal; the G-site is highly conserved and composed of amino acid residues found in the N-terminal domain; different amino acids (tyrosine, serine or cysteine) according to the class allow conjugation or thiol transfer[431]. The tyrosine or serine hydroxyl group acts as a hydrogen bond donor to the thiol group of GSH, promoting the formation and stabilization of the highly reactive thiolate anion which is the target for nucleophilic attack of an electrophilic substrate. By site directed mutagenesis, the serine or tyrosine residues have proven catalytically essential in GSTs of different organisms[434]. GSTOs, unlike other GSTs, have a cysteine residue in their active site, which promotes the formation of mixed disulphides

with glutathione rather than the formation of the thiolate anion. Therefore, GSTOs catalyze a range of thiol transferase and reduction reactions that are not catalyzed by members of other GSTs classes[437, 438]. This feature is also common to beta and lambda GSTs, dehydroascorbate reductases (DHARs), Grxs and chloride intracellular channel proteins. GSTOs have glutathione-dependent thiol transferase activity and can also catalyze dehydroascorbate (DHA) reduction, activities characteristics of Grxs[437]. Besides the detoxification of exogenous compounds through the conjugation with GSH, GSTs are also responsible for the detoxification of products of oxidative stress. ROS such as superoxide radical ($O_2^{\bullet -}$), hydrogen peroxide (H_2O_2), hydroxyl radical ($OH^{\bullet}$) and RNS such as nitric oxide ($NO^{\bullet}$) and peroxynitrite ($ONOO^-$) radicals are extremely reactive being inevitably associated with toxicity, causing damage in various biological molecules: lipids (causing lipid peroxidation and membrane damage), DNA (causing DNA breaks), and proteins (oxidation of various amino acids and inactivation of essential enzymes)[387]. In several organisms, GSTs are up-regulated by exposure to *pro-oxidants* indicating that induction of GSTs is an evolutionarily conserved response of cells to oxidative stress[439-445]. GST activity has been detected in parasitic nematodes, trematodes, ticks and malarial parasites and the identified GSTs assigned to the classes identified in mammalian cells based on the substrate specificity (in particular with the universal substrate CDNB) or sensitivity to inhibitors, such as bromosulphthalein, 1,2-dichloro-4-nitrobenzene, ethacrynic acid and cumene hydroperoxide among others[438, 446-452]. In helminths GSTs represent the major phase II detoxification system required for the parasite survival in the host, since these parasites contain very low levels of other detoxification enzymes such as catalase, superoxide dismutase and cytochrome P450, GST may provide the primary defense against electrophilic and oxidative damage[453]. Therefore helminth GSTs have been proposed as a potential drug target or for a vaccine candidate's development, as the enzyme differs in its primary amino acid sequence and gene structure from the host GST[454]. GST activity has also been detected in all *Plasmodium* species studied so far as well as in all intraerythrocytic stages of the parasite[446, 455-458]. *Plasmodium falciparum* GST may be essential for parasite survival by protecting the parasite against oxidative stress and/or acting as a buffer for detoxification of heme-binding compounds *in vivo*[446, 455]. Moreover, *P. falciparum* possesses only one GST, which is highly abundant and its activity is increased in parasites resistant to chloroquine, an anti-malarial drug[456, 458]. Thus inhibition of *P. falciparum* GST, whose structure presents features distinctive of human GSTs, is expected to impair detoxification processes, enhance levels of cytotoxic peroxides among other effects, being considered as a highly promising target for anti-malarial drug development[459, 460]. No GST activity has been reported in *Trypanosoma* or *Leishmania* parasites, apart from TDR1 that contain domains of the GSTO and uses GSH

as the reductant[90]. Although, in *L. major* a protein named eEF1B, with trypanothione *S*-transferase activity, was able to catalyze the aromatic nucleophilic substitution reactions between $T(SH)_2$ and CDNB[461], in agreement with the redox system used by trypanosomatids, based on $T(SH)_2$ and TR[364].

3.3 Thioredoxins and Glutaredoxins

The thioredoxins (Trxs) family is defined by a structural motif named the Trx fold, common to a variety of functionally different proteins as thiol-disulfide oxidoreductases, disulfide isomerases, glutathione S-transferases, thiol dependent peroxidases and chloride intracellular channels[462]. The family of proteins with a Trx fold includes Trxs and Grxs, small ubiquitous proteins with conserved CysXXCys/Ser (CXXC/S) active sites, where X represents various amino acids. Both are able to regulate several processes through reduction of disulfide bridges in target proteins in a reaction taking place in two steps: the N-terminal thiol of the CXXC motif attacks the disulfide bridge of the target protein, releasing a free thiol and forming a disulfide bridge with the second Cys of the target. Then the C terminal thiol of the CXXC motif breaks the Trx-target disulfide bridge, releasing the reduced target and oxidized redoxin protein[463]. The midpoint redox potential differs between Trxs and Grxs, being close to -300mV for Trx and -200mV for Grx. In the cytosol and mitochondria, Trxs are reduced via NADPH and an NADPH-dependent thioredoxin reductase (TR) and Grxs via NADPH-dependent GR and GSH as shown in Figure 3.3[464].

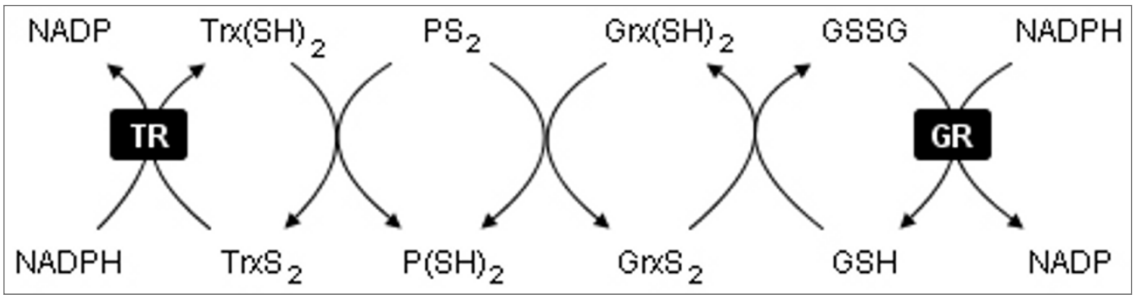

Figure 3.3 Thioredoxin and Glutaredoxin systems. Thioredoxin (Trx) and glutaredoxin (Grx) are reduced by NADPH-dependent enzymes, thioredoxin reductase (TR) and glutathione reductase (GR) respectively. Both Trx and Grx can serve as electron donors for metabolic enzymes, represented by P, being $P(SH)_2$ a reduced form and PS_2 an oxidized form (adapted from Ghezzi *et al.*[465])

The first Trx was originally discovered in *Escherichia coli* as an electron donor for RR, an enzyme required for DNA synthesis and later the identification of a glutathione dependent reductase able to restore the growth of *E. coli* in a mutant lacking Trx led to the discovery of Grx[466, 467]. Trxs are ubiquitous proteins, with molecular weight around 10-12 kDa, present in all forms of life. Mammalian cells contain two Trxs, one cytosolic (Trx1) and another localized in the mitochondria (Trx2); *E. coli* and yeast also contain two Trxs each and plants contain a variety of Trxs with highly specialized functions[468-471]. For example, *Arabidopsis thaliana* possesses multiple Trxs isoforms, and *in vitro* experiments have shown that some of them exhibit substrate specificity, suggesting that multiple Trxs may serve as a backup measure to cope with redox stress, it being likely that some cellular processes use preferentially one Trx[472]. Trxs are essential cofactors for DNA synthesis, sulfur assimilation and several antioxidant enzymes, such as peroxiredoxins, arsenate reductases and methionine sulfoxide reductase[463]. Trxs regulate the activity of several transcription factors, such as NF-κB in mammals[473] and OxyR in *E.coli*[474], and enzymes involved in different metabolic pathways[475, 476]. Grxs, also called thiol transferases, are small, GSH-dependent oxidoreductases with low molecular weights ranging from 9-15 kDa, which play a crucial role in biological processes such as regulation of transcription factors, protecting cells from oxidative stress and catalyzing reversible protein S-glutathionylation[462]. Based on the active site sequence, Grxs are divided into two categories: dithiol and monothiol. Dithiol Grxs have the characteristic Cys-Pro-Tyr-Cys active site motif, while monothiol Grxs lack the C-terminal active site thiol in its Cys-Gly-Phe-Ser active site but contains all structural and functional elements to bind and utilize GSH as a substrate[462, 477]. Dithiol glutaredoxins catalyze GSH-dependent reduction of disulfide bonds using either a monothiol or dithiol mechanism. Protein disulfides are reduced by a dithiol mechanism requiring both active cysteines while mixed disulfides between GSH and proteins or low molecular mass thiols are mainly reduced by a monothiol mechanism that involves only the more N-terminal redox active Cys[478]. Versatility of Grxs includes the reduction of a compound devoid of thiol groups, DHA, which results from the oxidation of ascorbate. Ascorbate can be regenerated by a variety of oxidoreductases including Grxs, protein disulfide isomerase, but not Trxs, through mechanisms similar to the monothiol and dithiol reactions[479, 480]. All organisms have an individual set of Grxs isoforms that occur in the cytosol, mitochondria, or nucleus of different cells. For example, *E.coli* contains four Grxs, two dithiols (Grx1, Grx2 and Grx3) and one monothiol (Grx4) Grxs. In *Sacharomyces cerevisiae* were descrided seven Grxs and human cells contain four Grxs. In plants, Grxs constitute a rapidly growing family at least when the identification is based on sequence similarity; in *Arabidopsis* there are about 50 genes encoding Grxs or Grx-like proteins, suggesting considerable functional

Grxs diversity in these organisms[481]. *E. coli* Grx1 can serve as electron donors for metabolic enzymes such as RR and phosphoadenylsulfate reductase (PAPS) and is also active in monothiol mechanism reactions. Despite structural similarity to Grx1, Grx3, the most abundant in the cell, is not efficient in the reduction of the same substrates; although genetic mutations in Grx3 led to an increase in the reduction activity thought to be due to an improved affinity for RR[482]. Grx2 is an unusual dithiol Grx as it is structural similar to GSTs family of proteins and lacks activity as hydrogen donors for RR[483]. The monothiol Grx4 does not exhibit classical Grx activity, but can be reduced by TR[484]. In mammalians Grx1, which is localized in the cytosol with small amounts in the nucleus, is a functional homologue of *E. coli* Grx1, while a modification in the active site of mammalian Grx2 enables the protein to receive electrons from GR[485]. Moreover, Grx2 is also able to coordinate an iron sulfur cluster and may play a role in iron–sulfur cluster assembly/biogenesis, activity also detected in chloroplastic Grxs[486-489]. Grxs are highly conserved in all organisms, although in malaria parasites besides the presence of a classical Grx and a glutaredoxin-like protein, which shares similarities with PICOT-HD-containing proteins[490], was also identified a novel functional redox active protein, named Plasmoredoxin (Plrx). Plrx was found exclusively in malaria parasites and is a member of the thioredoxin superfamily able to provide electrons for RR, an activity detected both in Trxs and Grxs[491].

All trypanosomatids organisms lack GR and thioredoxin reductase, as their redox metabolism is based on $T(SH)_2$ and TR[364]. The $T(SH)_2$ system has been shown to deliver the reducing equivalents for the synthesis of DNA percursores by RR[392] as well as the detoxification of hydroperoxides catalyzed by 2-Cys-peroxiredoxins and the glutathione peroxidase-type enzymes, which in these parasites act as trypanothione-dependent tryparedoxin peroxidases[394, 413, 414, 416, 420, 427, 492]. Despite the absence of TR, trypanosomes encode a thioredoxin gene, which results in very low protein levels and thus it may be compensated by tryparedoxins, present in the cell in much higher concentrations[493, 494]. *Trypanosoma brucei* possesses three genes for monothiol Grxs and two genes for dithiol Grxs. The three monothiol Grxs occur in both life stages, with the highest levels found in the stationary phase and distinct cellular functions. One of the monothiol Grxs, named 1-C-Grx1 is an abundant protein with a mitochondrial localization, able to form an iron-sulfur center using GSH as the non protein-ligand and thus may play an essential role in the iron and redox homeostasis of the parasite[418, 495]; the dithiol Grx1 also coordinates iron-sulfur clusters[496], as shown for other Grxs, human Grx2 and poplar Grx1C1[489, 497]. *T. brucei* Grx1 is a cytosolic protein that efficiently catalyzes the reduction of protein-GSH mixed disulfides; Grx1 can supply electrons for reduction of RR, while

Grx2 was able to reduce insulin disulfide, indicating that the two oxidoreductases have a high specificity toward distinct protein disulfides. On the other hand, Grx2 occurs in the mitochondrial intermembrane space and seems to be essential for procyclic parasites, as RNA interference against Grx2 resulted in growth retardation[496]. *T. brucei* Grx1 and Grx2 were able to catalyze the reduction of GSSH by $T(SH)_2$, suggesting a participation of those in the trypanothione metabolism. Thus besides a $T(SH)_2$ percursor GSH, in the absence of a GR, it may be involved in protein glutathionylation or as a reducing agent of Grxs. Indeed, recently was also identified a dithiol Grx in *T.cruzi*, which showed a typical thioltransferase activity and *in vitro* assays suggested a possible role in reduction of glutathione disulfide as well as in deglutathionylation of target proteins[498]. *L. infantum*, *L. mexicana* and *L. braziliensis* genomes revealed the presence of genes encoding two putative monothiol Grx, 1 putative Grx and one putative Grx-like protein; in *L. major* was detected an extra gene encoding for a putative monothiol Grx. However, none of those was yet characterized. TDR1 is the only protein characterized in *Leishmania* that contains an active site characteristic of Grxs and the thioltransferase activity typical of this family of proteins[90].

3.4 Protein S-glutathionylation as a mechanism of regulation in various cellular processes

All living organisms are exposed to various oxidants, resulting from their own metabolism or generated under oxidative stress. The levels of ROS and RNS in a cell are normally tightly regulated by antioxidant defense mechanisms. In a situation of oxidative stress, when ROS and/or RNS concentrations exceed the antioxidant capacity of the cell, cellular homeostasis is affected leading to disruption of redox signaling and/or molecular damage. ROS and/or RNS can cause specific, reversible or irreversible oxidative modifications on sensitive proteins, which may interfere with function of the oxidized protein[387].

Proteins can undergo different types of oxidation including carbonylation (introduction of a carbonyl group into proteins by oxidation of amino acid side chains such as lysine, arginine, histidine), oxidation of aromatic amino acids to various hydroxy derivatives and oxidation of methionine and cysteine to sulfoxides or sulfones. Methionine and cysteine residues are particularly sensitive to oxidation by almost all forms of ROS[499]. The thiol groups of Cys residues within the proteins act as redox-sensitive switches, as they are particularly susceptible to oxidative modifications and undergo various reversible and irreversible redox alterations as shown in Figure 3.4[500]. The vast majority of Cys residues,

in a reducing environment, remain almost completely protonated at a physiological pH and unlikely to be reactive with ROS/RNS. The Cys residues present in redox-sensitive proteins exist as thiolate anions at neutral pH, due to a lower pKa value that results from charge interactions with neighboring positively charged amino acids, therefore being more vulnerable to oxidation[501]. Thus the thiolate anion of redox-sensitive Cys residues can undergo a diverse spectrum of oxidative modifications. Sequential oxidation of Cys thiols yields sulfenic (–SOH), sulfinic (–SO_2H), or sulfonic (–SO_3H) acid derivatives. Reaction of protein thiols with low-molecular weight thiols such as GSH can yield mixed disulfides. Alternatively, oxidation by ROS and RNS can result in a disulfide bridge forming between two thiols either within a protein chain or between protein chains[502].

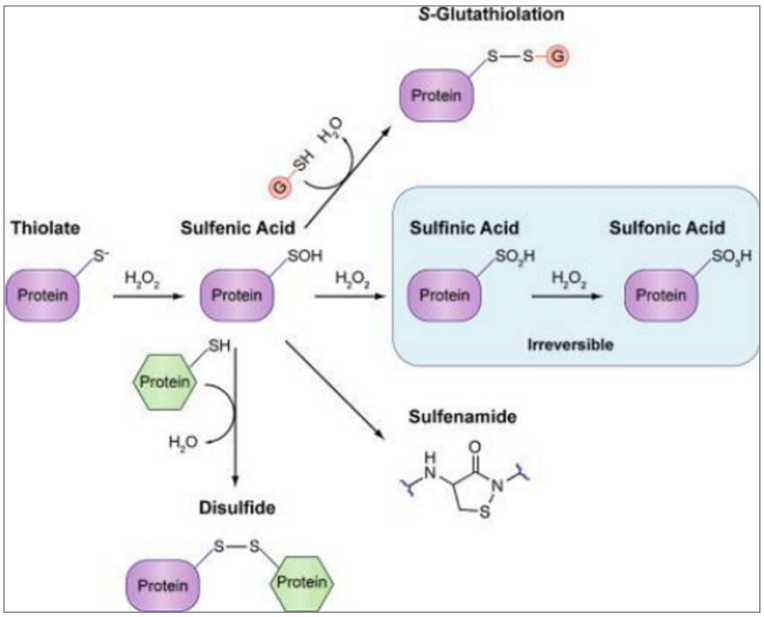

Figure 3.4 Oxidation fates of protein cysteines. Protein thiols, particularly low pKa cysteines, upon reaction with H_2O_2 form a sulfenic acid (SOH), which can react with a second cysteine resulting in intramolecular or intermolecular protein disulfide. SOH can also react with GSH (pink circle) to form a disulfide (S-glutathionylation). The irreversible sulfinic (SO_2H) and sulfonic (SO_3H) acids result from further reactions of SOH with H_2O_2**.** In the absence of a second cysteine or GSH, the amide nitrogen of the neighbouring residue can attack the SOH to form a sulfonamide (adapted from Paulsen *et al.*[500]).

Oxidation to sulfinic and sulfonic acid are irreversible and thus other means of oxidation named S-thiolation, such as the formation of mixed disulfides may prevent thiols over-oxidation and either protects and/or also modulates protein function. It's noteworthy that the Cys residue does not necessarily need to be part of the active site of the protein to alter its function, since modification of thiols may also cause conformational changes that

alter protein activity or even interaction with other proteins[501]. As GSH represents the major thiol in almost all organisms, with the exception of Trypanosomatids[364], protein S-glutathionylation (the covalent addition of glutathione to cysteine residues on target proteins) represents the most abundant form of reversible thiol modification; S-cysteinylation also occurs but the availability of free cysteine in the cell is much lower than GSH and thus this type of modification occurs at a lower rate than S-glutathionylation[503]. The reversible nature of S-glutathionylation and the fact that it occurs during oxidative stress but also under physiological conditions make it an important regulatory mechanism of biological processes[504]. In addition, S-glutathionylation may also serve as a storage form of GSH, which otherwise would be rapidly extruded from the cell under oxidative conditions[505]. S-glutathionylation is a dynamic process that can occur through several reactions (Figure 3.5): direct interaction between partially oxidized (activated) protein sulfhydryls (thiyl radical, sulfenic acid or protein S-nitrosothiol) and GSH; thiol/disulfide exchange reactions between protein thiols and GSSG or S-glutathionylated proteins; reaction between protein thiols and intermediate S-nitrosothiols such as S-nitrosoglutathione (GSNO), which is able to modify protein sulfhydryl groups by both protein S-nitrosation and S-glutathionylation and direct interaction between a free protein cysteinyl residue and GSH triggered by oxidants[506]. Also, glutathionylated proteins can result from the reaction catalyzed by Grx between the thiyl radical of GSH (formed by reaction with hydroxyl radicals) and proteins. Indeed, intracellular GSSG concentrations would need to change 100-fold, due to the redox potential of most cysteine residues, to induce S-glutathionylation through thiol exchange mechanism and thus unlikely to occur intracellularly[464]. However, the role of Grx seems to be primarily in the catalysis of protein deglutathionylation (S-glutathionylation reverse reaction). Human GSTPi was reported to catalyse S-glutathionylation reactions, for which contribute the high expression levels detected in many drug resistant tumours, not related to detoxification as GSTPi has a modest activity with of a number of identified substrates, particularly anticancer drugs[507].

To consider protein glutathionylation as a regulatory mechanism it was proposed that S-glutathionylation must change the protein activity and function in the cell, occur in intact cells in response to a physiological stimulus, occur at physiological GSH:GSSG ratios, and exhibit rapid and efficient mechanisms of specificity towards certain cysteine residues, and reversibility of protein-SSG[508].

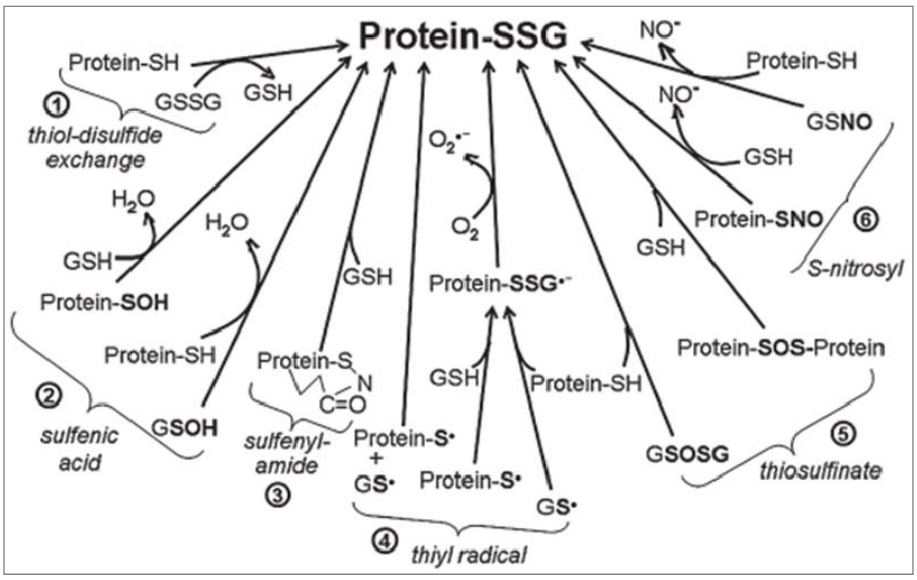

Figure 3.5 Potential mechanisms of protein S-glutathionylation. Modification of cysteine residues to protein–SSG mixed disulide can occur through several mechanisms: (1) thiol-disulfide exchange; (2) sulfenic acid intermediates; (3) sulfenylamide intermediates; (4) thiyl radical intermediates; (5) thiosulfinate intermediates; (6) S-nitrosyl intermediates (adapted from Mieyal *et al.*[506]).

Many proteins involved in a wide range of biological processes have been identified as potentially regulated by reversible S-glutathionylation, either inhibited or activated. However, the exact mechanism or importance of this type of modification *in vivo* remains unclear. Detection of S-glutathionylation targets have been reported in a wide range of organisms including animals, plants, fungi, and bacteria, through the analysis of purified proteins *in vitro* or large-scale proteomic studies. Two major strategies have been used to detect glutathionylated proteins: labeled GSH, which allows the detection of GSH adducts on S-thiolated proteins and anti-GSH antibodies or thiol alkylation after deglutathionylation by Grxs[509]. Other approach have been the identification of Trx- or Grx-interacting proteins through the use of mutant Trx or Grx immobilized in a resin that are able to catch target proteins as a mixed disulfide intermediate[510-512]. The putative target proteins are involved in many processes, including redox homeostasis, nitrogen, sulfur and carbon metabolisms, protein biosynthesis and protein folding[476, 502, 511-519]. Several metabolic enzymes were reported has susceptible to S-glutathionylation. The glycolitic enzyme, glyceraldehyde-3-phosphate dehydrogenase (GAPDH), which plays a primary role in energy production, is inactivated by S-gluathionylation[520-522]. Other enzymes such as ketoglutarate dehydrogenase[523], aldolase and triose phosphate isomerase can undergo S-glutathionylation both in human cells and plants[516, 524] suggesting an important role for this oxidative modification in the modulation of energy production. In *E.coli,* cobalamin-

independent methionine synthase, the enzyme that catalyses the final step of methionine biosynthesis is also inactivated by S-glutationylation during oxidative stress[525]. S-glutathionylation also plays a role in cell signaling, being involved in the regulation of the kinase activity of protein tyrosine phosphatase 1B (PTPB1) in response to oxidative stress[526, 527], among others; interferon regulatory factor 3 (IRF3) is an example of the crucial role of S-glutathionylation in the control of cell signaling pathways. IRF3 is an essential transcriptional regulator of the interferon genes and is S-glutathionylated in non infected cells, but after viral infection IRF3 undergoes deglutathionylation necessary for transcriptional activation of the interferon genes[528]. Activation of the NF-kB pathway is also dependent on the redox state of the cell as the transcription factor NF-kB is a target for oxidative inactivation by S-glutathionylation[529]. S-glutathionylation also plays a role in the regulation of redox homeostasis as shown by the inhibition of human and plants Trxs. In chloroplasts only f-type of Trxs (Trxfs) are required for activation of Calvin-cycle enzymes. Thus inactivation of Trxf will affect the activity of other enzymes such as NADP-malate dehydrogenase and GAPDH, which is strongly decreased when Trxfs are glutathionylated. As Trxfs are involved in the regulation of carbon-fixation enzymes by light, S-glutathionylation may constitute a mechanism of regulation of photosynthetic metabolism under oxidative stress[530]. Also, S-glutathionylation of human Trx abolished its enzymatic activity as insulin disulfide reductase in the presence of NADPH and TR suggesting that the redox state of the cell can regulate Trx functions reversibly through thiol-disulfide exchange reactions[531]. Concerning the detection of glutathionylated proteins in parasites, the malaria parasite *P. falciparum* has also been reported to have proteins redox regulated through S-glutathionylation being targeted by Trx, Grx and Plrx[511, 532, 533]. Proteins involved in antioxidant defense (peroxiredoxins) were identified specifically as potential Trx targets and proteins involved in carbohydrate metabolism were also found to interact with Trx, Grx and Plrx proteins[511]. Among the identified targets of protein S-glutathionylation in *P. falciparum*, as observed in other organisms, both GADPH and pyruvate kinase were reversible inhibited by S-glutathionylation and not only Grx1 but also Trx1 and Plrx were able to efficiently catalyze protein deglutathionylation[532]. In the case of trypanosomatids, there are no reports of glutathionylation of *Leishmania* proteins, although the related organism *Trypanosoma* uses GSH for the glutathionylation of thiol redox proteins as shown by the specific and reversible glutathionylation of Grx1, Trx and glutathione peroxidase type tryparedoxin peroxidase III of *T. brucei*[419]. In addition in *T.cruzi* was also identified a dithiol Grx with typical thioltransferase activity that may be involved in the reduction of glutathione disulfide as well as in deglutathionylation of target proteins[498]. These data suggest that free GSH in these parasites that do not possess a

GR may have other roles beside being a trypanothione precursor, such as protein glutathionylation and deglutathionylation or as a reducing agent of Grxs[364].
Interesting is the fact that S-glutathionylation occurs not only in response to oxidative stress but was demonstrated through the detection of glutathionylated proteins under physiological conditions[517, 534]. For example, constitutive S-glutathionylation has been shown in hemoglobin in red blood cells[535, 536] and actin in human fibroblasts and epidermal cells[537, 538]. Another example is *P. falciparum* GAPDH protein glutathionylation which occurs in the presence of low concentration of GSH, likely to reflect physiological conditions[419, 532].

The reverse reaction called deglutathionylation consists of the removal of the GSH moiety from protein mixed disulfides and can be efficiently catalyzed by Grx or Trx via a dithiol exchange mechanism, once the intracellular redox balance has been restored[470, 539-541]. Human sulfiredoxin has also been reported to catalyze deglutathionylation of a number of distinct proteins in response to oxidative and/or nitrosative stress, such as actin and PTP1B[542]. It has been shown that Grxs are very efficient glutathionyl mixed disulfide reductases, whereas Trxs are more specific for reduction of protein disulfide bonds and much less efficient than Grxs to catalyze deglutathionylation reactions[543, 544]. *C. reinhardtii* isocitrate lyase can be inactivated by glutathionylation and reactivated by Grx, while Trx does not appear to regulate protein activity[541]. Identification of S-glutathionylated proteins is based on the enzymatic reduction of S-glutathionylated proteins by Grx. Grx activity is often measured using the artificial substrate 2-hydroxyethyldisulphide (HEDS) or through deglutathionylation of radiolabeled protein-GSH mixed disulfides[545, 546]. More recently was developed a new real-time fluorescence-based method for measuring the deglutathionylation activity of Grxs using a glutathionylated peptide as a substrate, which measures the formation of the deglutathionylated product rather than indirectly the consumption of NADPH as in the classical HEDS assay[547].

3.5 Thiol Dependent Reductase 1

TDR1 is a parasite-specific enzyme, first identified in *L. major,* with an unusual two domain nature, where the N-terminal domain contains a CXXC motif characteristic of Grxs and Trxs, while the C-terminal active site is characteristic of GSTO; the protein is functional as a trimer[90]. TDR1 possesses thioltransferase and DHAR enzymatic activities, shown by the ability of using GSH as an electron donor to reduce HEDS (Figure 3.6) and DHA, respectively, with specific activities significantly higher than those reported for the

human GSTO[90]. Although, the conjugation of GSH with the generic GST substrate CDNB occurred at a low rate and no activities were detected with other GST substrates[90]. CDNB is a good substrate for all other classes of GSTs, which are able to catalyze the conjugation of free radicals, metals and other electrophilic compounds with GSH and play a major role in the detoxification of many reactive metabolites. Human GSTO instead has activities similar to Grxs, with thioltransferase activity being the most prominent[437].

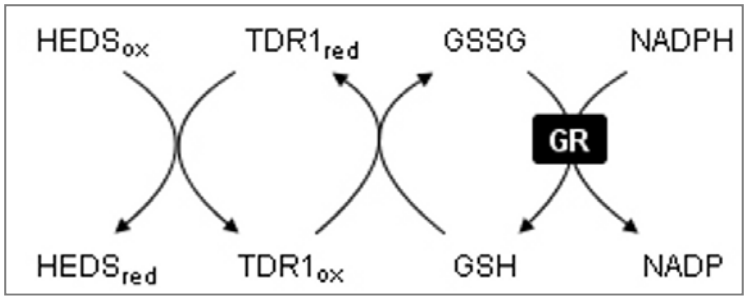

Figure 3.6 HEDS reduction by TDR1. Reactions involved in the thioltransferase *in vitro* assay using the artificial substrate HEDS. TDR1 is able to transfer electrons to 2-hydroxyethyldisulphide HEDS after glutathione (GSH) oxidation. Glutathione reductase (GR) is used to regenerate glutathione disulfide (GSSG) to GSH. The subscripts "red" and "ox" refer to the redox state of the proteins, dithiol and disulfide, respectively.

In addition, TDR1 is able to reduce the antileishmanial drug pentavalent antimonial (Sb^{V}) to a trivalent form (Sb^{III}), the active form against *Leishmania* intracellular amastigotes. Spontaneous conversion of pentavalent antimonials in the presence of GSH has been reported to occur *in vitro*[548, 549], however the rate of the reaction is much lower than when catalyzed by TDR1, suggesting a role for the enzyme in the anti-leishmanial activity of antimonial drugs[90]. Although, generally accepted that amastigotes are the susceptible form of the parasite to antimonials[550, 551], it is not yet known if activation occurs within the parasite or outside, leading to the question whether the TDR1 role in drug activation is biologically relevant. The fact that TDR1 levels of expression are 10-fold higher in the amastigotes[90] plus the observation that the conditions found within the phagolysosome, in which *Leishmania* resides (acidic pH and elevated temperature), favour this conversion support the hypothesis of a role in the activation of antimonials; however it can also, instead, play a part in the detoxification of the drug[90], consistent with the finding of several products of stibogluconate in *L. donovani* amastigotes[552]. Besides antimonial reduction, it has also been suggested that TDR1 may play a role in the detoxification of arsenic, due to its similarity with the arsenate reductases[90]. As observed for Sb^{V}, arsenate (As^{V}) can also be reduced to arsenite (As^{III}) nonenzymatically, although the process is too slow to be physiologically significant and, so organisms use enzymes that catalyze As^{V} reduction[553].

Arsenical resistant *Leishmania* strains are frequently cross-resistant to antimonials, justified by the fact that these compounds are related metalloids. This is supported by the identification and characterization of a an arsenate reductase in *L. major*, namely ACR2, capable of reducing Sb^{V} to Sb^{III}, that when over-expressed leads to an increase in susceptibility to sodium stibogluconate (SSG)[91].

TDR1 is conserved among *Leishmania* spp. and have also been characterized in *L. donovani* and *L. infantum*, with 100% homology between this two species and levels of thiol trasferase activity similar to those obtained with *L. major* enzyme (Silva et al, unpublished results). Moreover, a protein similar to TDR1 was identified on the related parasite *T.cruzi*, named Tc52, with an overall identity of 45.7%; the putative active-site residues of the two proteins are identical in the N-terminal domains (CPFC) but differ in the C-terminal domain, which contains the CPF motif similar to GSTO in TDR1 but in Tc52 the cysteine residue is replaced by a serine. Both possess thioltransferase activity and DHAR activity[90, 554]. In *Leishmania*, GST activity was not detectable, but a related trypanothione *S*-transferase activity was observed, *L. major* eEF1B was able to catalyze the aromatic nucleophilic substitution reactions between $T(SH)_2$ and CDNB[461], which correlates with the fact that *Leishmania* parasites rely on the $T(SH)_2$/TR system and lack GR and thioredoxin reductase[364]. Thus, given the data available on TDR1, Denton and co-workers have suggested the possibility that the two domains of TDR1 could function together as electron donor and reductase, providing Grx-like activities for *Leishmania*[90].

CHAPTER 4

OBJECTIVES AND RESULTS

4.1 Objectives

The identification and characterization of a parasite-specific enzyme, named TDR1, *in L. major* by Denton *et al.*[90] with interesting similarity to an enzyme known as Tc52 of the related parasite *T. cruzi* which had previously been reported as an important factor in the modulation of the host immune reponse to infection with *T. cruzi* [554-557], prompted this study. It had as main aims the objectives of determining whether TDR1 has a similar effect during *Leishmania* infection as Tc52 does during infection with *T. cruzi* and assessing the potential of the protein in vaccination approaches. An additional interesting aspect of TDR1 is that it possesses an intriguing two domain nature, with motifs characteristic of Grx and GSTO proteins[90]. This feature, added to the fact that TDR1 shows high conservation within the different *Leishmania* species and has the ability to catalyze the reduction of pentavalent antimonials which is necessary for effective action of the drug against the parasite, suggested an interesting and important role for the enzyme in the parasite. In order to provide insights into the role of TDR1 in visceral *Leishmania* species (*L. infantum* and *L. donovani*), we investigated the essentiality of the gene for parasite survival and virulence through the generation and characterization, including the use of untargeted metabolomics analysis, of *TDR1* null mutants.

The experimental results obtained in this study are organized in 6 sections within this thesis as follows:

4.2 Characterization of TDR1 expression, localization of TDR1 in *L. infantum*, and evaluation of the immune response induced by recombinant TDR1 in the context of *L. infantum* infection using a murine model;

4.3 Generation of a *TDR1* null mutant in *L. infantum*;

4.4 Elucidation of the role of TDR1 in *L. donovani,* through the generation of a null mutant and characterization of the generated cell lines in the context of oxidative stress, drug resistance and redox regulation;

4.5 Determination of the structure of *L. donovani* TDR1;

4.6 Analysis of the changes that occur at the metabolome level during *L. donovani* wild-type promastigote growth from logarithmic to stationary phase of *in vitro* culture, using an untargeted metabolomics approach;

4.7 Evaluation of potential differences between visceral (*L. donovani)* and cutaneous (*L. major) Leishmania* species through an untargeted metabolomics analysis.

4.2 Immunological role of *Leishmania infantum* Thiol Dependent Reductase 1

The need to develop an effective vaccine against leishmaniasis to prevent the 2 million new cases each year led to the search for antigens able to elicit protection against infection with *Leishmania*.

In this study we have evaluated the immune response induced by a recombinant parasite-specific protein of *L. infantum*, Thiol dependent reductase 1 (rTDR1) as well as the ability of this antigen to protect against experimental challenge using a murine model. rTDR1 immunization led to an expansion of CD8-T cell population and a decrease in IL-10 production. However, immunization with rTDR1 did not elicit high levels of protection, despite the maintenance of a significant decrease in IL-10 production. Nevertheless, immunization with rTDR1 induced an increase in CD8-T cell number during the chronic phase of infection, suggesting the generation of memory CD8-T cells. Indeed, analysis of CD8-T cells from rTDR1 immunized mice showed an increase in cells with characteristics of central memory T cells, while no differences were observed in the CD4-T cells from the same animals. Thus, the expansion of CD8-T cell induced by immunization with rTDR1 although insufficient to protect Balb/c mice, highlighted the potential importance of these cells in a vaccination strategy.

Under revision for publication in Parasite Immumology

Immunological role of *Leishmania infantum* Thiol Dependent Reductase 1

Ana Marta Silva[a,b,c], Joana Tavares[a,b], Ricardo Silvestre[a], Ali Ouaissi[d], Graham H Coombs[c] and Anabela Cordeiro-da-Silva[a,b*]

[a] IBMC – Instituto de Biologia Molecular e Celular, Universidade do Porto, Rua do Campo Alegre, 823, 4150-180 Porto, Portugal; [b] Laboratório de Ciências Biológicas, Faculdade de Farmácia da Universidade do Porto, R. Aníbal Cunha n.º 164, 4050-047 Porto, Portugal; [c] Strathclyde Institute of Pharmacy and Biomedical Sciences, University of Strathclyde, 161 Cathedral Street, Glasgow G4 0RE, UK; [d] INSERM, UMR CNRS 5235, Université de Montpellier 2, Bât 24 - CC 107, Pl. Eugène Bataillon, 34095 Montpellier Cx 5, France

[*] Corresponding author. Mailing address: Instituto de Biologia Molecular e Celular, Universidade do Porto, Rua do Campo Alegre, 823, 4150-180 Porto, Portugal. Phone: +351 226 074 900. Fax: +351 226 099 157. E-mail: cordeiro@ibmc.up.pt

Short title: TDR1 of *Leishmania* infantum

Keywords: Visceral leishmaniasis, *Leishmania infantum,* TDR1, CD8-T cells, memory T-cells

Summary

The need to develop an effective vaccine against leishmaniasis to prevent the 2 million new cases each year led to the search for antigens able to elicit protection against infection with *Leishmania*.

In this study we have evaluated the immune response induced by a recombinant parasite-specific protein of *L. infantum*, Thiol dependent reductase 1 (rTDR1) as well as the ability of this antigen to protect against experimental challenge using a murine model. rTDR1 immunization led to an expansion of CD8-T cell population and a decrease in IL-10 production. However, immunization with rTDR1 did not elicit high levels of protection,

despite the maintenance of a significant decrease in IL-10 production. Nevertheless, immunization with rTDR1 induced an increase in CD8-T cell number during the chronic phase of infection, suggesting the generation of memory CD8-T cells. Indeed, analysis of CD8-T cells from rTDR1 immunized mice showed an increase in cells with characteristics of central memory T cells, while no differences were observed in the CD4-T cells from the same animals. Thus, the expansion of CD8-T cell induced by immunization with rTDR1 although insufficient to protect Balb/c mice, highlighted the potential importance of these cells in a vaccination strategy.

1. Introduction

The leishmaniases remain a major public health problem with 350 million people at risk worldwide and 2 million estimated new cases every year in 88 countries. Clinical manifestations of *Leishmania* infection range from self-healing cutaneous (CL) and mucocutaneous (MCL) forms to visceral leishmaniasis (VL) which, if left untreated, is fatal[1]. Leishmaniasis is also found as an opportunistic disease associated with human immunodeficiency virus (HIV). HIV infection increases the risk of developing active VL by between 100 and 2320 times[2]. Unfortunately, there is no effective vaccine against this parasite, thus control of disease relies on chemotherapy. However, there are limitations in the use of available drugs due to high cost, toxicity, long courses of treatment and, in particular, the emergence of drug resistance[3]. The clinical outcome of infection is determined by a combination of several factors including parasite pathogenicity, determined by the *Leishmania* species, and the host's immune status[4].

In order to discover new therapeutic or preventative measures to control the disease, it is necessary to dissect the factors involved in the parasite-host interactions. *Leishmania* is able to modulate the immune response, facilitating the invasion and establishment of infection[5]. Recently, Silverman and co-workers described a new exosome-based mechanism for the release of *Leishmania* proteins into the host's cytoplasm[6]. Previously, a wide range of *Leishmania* proteins including GP63[7], A2[8], cysteine proteinases[9] and CRK3[10] have been implicated in the survival of the parasite in the mammalian host and consequently considered virulence factors[11]. Recombinant proteins of *Leishmania* such as LACK[12], HASPB1[13] and LeIF[14] have been assayed for their immunogenicity and protective potential in murine models; they elicited different degrees of protection. So far, despite many antigens being identified as vaccine candidates only the LEISH-F1+MPL-SE polyprotein vaccine seems promising; this was considered safe and immunogenic against

CL when administered alone[15] or in conjugation with antimonials in human clinical trials[16, 17]. Protection against challenge with *L. infantum* in Leish-F1+MPL-SE-immunized animals appears to be associated with a Th1-type immune response[18]. Moreover, Leish-F1+MPL-SE protective effect against *L. major* is also associated with memory cells that are capable of antigen-specific restimulation for at least 6 months[19].

An ideal vaccine against leishmaniasis should be able to elicit long-lasting immunity[20]. This involves the generation of CD4-T and CD8-T effector and memory T cells, which depends on the strength and duration of antigenic stimulation. CD4-T cells mediate their effector functions through the production of IFN-γ and IL-4, while CD8-T cells response involve both cytokine production and cytolytic mechanisms[21, 22]. Moreover, expansion of T cell populations in the context of infection will lead to an increase of antigen-specific T cells that ultimately result in the formation of T cell memory[23]. Maintenance of protective T cell memory against leishmaniasis has been difficult to achieve, despite different vaccination strategies being used including live attenuated parasites, recombinant antigens and DNA vaccines[1, 20]. Zaph et al. established that CD4- memory T cells provide effective and long-lasting protection against *L. major* infection, involving two population's of effector and central memory T cells. This study also showed that central memory T cells do not require the presence of the parasite to maintain the pool of memory cells[24]. $CD4^-$T cells are critical for the development of CD8-T-cell memory[25]. Host protection against *Leishmania* infection has been reported to be associated with CD8-T cells[26-29]. CD8-T cells are required for resistance to re-infection, as shown by the enhanced levels of IFN-γ released during a memory response to *L. major* by antigen-specific CD8-T cells from the lymph nodes and spleen cells of immune re-infected mice[30].

The current study was undertaken to investigate the role of *L. infantum* Thiol dependent reductase 1 (TDR1) in the parasite-host interaction. TDR1 was first identified in *L. major* as a parasite-specific enzyme by Denton and co-workers[31]. This enzyme has some similarities to human omega-GST, including its thiol transferase and dehydroascorbate reductase activities[31]. This is an interesting feature given the fact that *Leishmania* parasites do not possess the classical redox system based on glutathione and rely on the trypanothione system for protection against oxidant damage and toxic heavy metals[32]. Alignment of the predicted amino acid sequences also revealed a considerable identity (45.7%) between TDR1 and a *T. cruzi* protein named *Tc*52 and very high identity (95%) with *L. infantum*, which could suggest an important and conserved role for this protein[31]. *Tc*52 is an excreted/secreted protein of *T. cruzi* which has been reported to be important in modulation of the mammalian host's immune response by the suppression of T cell

proliferation[33]. Moreover, *Tc*52 targeted gene deletion gave evidence for a crucial importance of this protein in the survival and virulence of *T. cruzi*[34]. Similarly to TDR1, *Tc*52 also possesses thiol transferase and dehydroascorbate reductase enzymatic activity[35]. Thus, in this study we have evaluated the immune response induced by recombinant TDR1 when administered to Balb/c mice as well as the ability to induce protection against challenge with virulent *L. infantum* promastigotes. The data showed that recombinant TDR1 of *L. infantum* only elicited partial protection against chronic *Leishmania* infection, despite a decrease in IL-10 production and expansion in CD8-T cells with characteristics of central memory T cells.

2. Materials and Methods

2.1. *Leishmania* parasites

Leishmania infantum (clone MHOM/MA/67/ITMAP263) promastigotes were grown at 27ºC in RPMI complete medium (RPMI 1640, BioWhittaker) supplemented with 10% (v/v) heat inactivated fetal bovine serum (FBS, Gibco), 2 mM L-glutamine (Sigma), 20 mM Hepes (Gibco), 100 U/ml penicillin and 100 mg/ml streptomycin (BioWhittaker). Cultures were set up initially at a concentration of 1 x10^6 parasites/ml and sub-passaged every 5 days.

To obtain promastigotes in the different phases of growth, parasites were first synchronized by five daily passages of 1x10^6 parasites/ml and then harvested at days 1 (early log phase), 2 (late log phase) and 6 (stationary phase). Axenic amastigotes were grown at 37ºC with 5% CO_2 in MAA/20 medium. MAA/20 consists of modified medium 199 (GIBCO) with Hank's balanced salt supplemented with 0.5% trypto-casein (Oxoid), 15 mM D-glucose (Sigma), 5 mM L-glutamine, 4 mM $NaHCO_3$ (Sigma), 0.023 mM bovine hemin (Fluka), and 25 mM Hepes to a final pH of 5.8 and supplemented with 20% (v/v) FBS[36]. The differentiation process was initiated by incubation of stationary phase promastigotes in MAA/20 medium at 37°C with 5% CO_2. Parasites were harvested after 1, 3, 5, 10, 24, 48 and 72 h of incubation.

2.2. Cloning and purification of TDR1

The *L. infantum TDR1* was PCR amplified using *L. infantum* genomic DNA as template and the following forward (5'-GCCATATGGCCGCCCGCGCGCTAAAGCTATACGTG-3') and reverse (5'-GATCTAGATTACCCGCTCTGGGCCCTCCGTTGACGC-3') primers containing *NdeI* and *XbaI* restriction sites (underlined), respectively. Amplification conditions were as follows: 94ºC, 2 min; 30 cycles of 94ºC, 15 sec; 55ºC, 30 sec; 72ºC, 90

sec and 72ºC, 10 min. The PCR product (1349bp) was cloned into pGEM-T Easy vector (Promega). All the transformants were identified by restriction analysis and one of the clones chosen to be confirmed by sequencing (Eurofins MWG Operon). The insert was excised by digestion with *NdeI-XbaI* (New England Biolabs) and sub-cloned into the *Escherichia coli* expression vector pET28a$^+$ in frame with an amino-terminal six-histidine tag (pET28a$^+$ *TDR1*). Briefly, 500 ml cultures of recombinant *E. coli* BL21 (DE3) were induced to express TDR1 by the addition of 2 mM of isopropyl β D-thiogalactoside (IPTG), overnight at 15ºC. The induced culture was harvested and resuspended in 20 mM Tris/500 mM NaCl, pH 7.9 (Buffer A) containing 10 mM imidazole. The cells were lysed by sonication and the resulting suspension was centrifuged at 15000 x g for 30 min at 4 °C to remove cell debris. The clear supernatant containing soluble protein was applied on to a pre-equilibrated nickel-nitrilotriacetic acid (Ni-NTA) column (Qiagen). The column was washed with Buffer A containing 60 mM imidazole to remove the non-binding proteins and the His-tagged recombinant protein was eluted with Buffer A containing 250 mM of imidazole. After purification, the eluted fractions were pooled and buffer-exchanged into 20 mM Tris, 250 mM NaCl, pH 7.9 using a PD10 desalting column (GE Healthcare) and stored at -80ºC. The recombinant protein was designated rTDR1. To eliminate endotoxins, the recombinant protein was passed through an EndoTrap®red column (Profos, Germany) following manufacturer's instructions. Polyclonal antiserum against TDR1 was generated in mice by intraperitoneal (i.p.) injection of recombinant protein in incomplete Freund's adjuvant.

2.3. Immunofluorescence analysis of sub-cellular location of TDR1

L. infantum promastigotes and axenic amastigotes were pelleted by centrifugation at 1500 x g for 10 min, washed with phosphate buffered saline (PBS) and fixed to slides in a PBS solution containing 4% paraformaldehyde, for 20 min at room temperature. Fixed parasites were permeabilised with 0.1% (v/v) Triton X-100 in PBS. Slides were washed several times with PBS and blocked in PBS containing 1% bovine serum albumin (PBS-BSA) for 30 min at room temperature. Incubation with the anti-TDR1 mouse serum (1:100 in PBS-BSA) was made in a humid chamber, for 1 h at room temperature. After several washes in PBS, slides were blocked once more in PBS-BSA for 15 min at room temperature. Alexa Fluor® 488 goat anti-mouse IgG (Molecular Probes) diluted 1:100 in PBS-BSA was used as secondary antibody. Washed parasites were mounted in Vectashield (Vector Laboratories) and analyzed with a fluorescent microscope (Axioskop-Carl Zeiss, Germany) at 1000x magnification. A negative control with parasites treated only with secondary antibody was used.

2.4. Digitonin fractionation

Promastigote fractionation was done according to Häusler et al.[37]. Aliquots of $5x10^7$ cells (~100 µg of total protein), resuspended in 1.125 ml of 25 mM Tris pH 7.5, 0.6 M sucrose, 1 mM DTT, 1 mM EDTA and a cocktail of protease inhibitors, were permeabilized with 125 µl of pre-diluted digitonin (Calbiochem) to final concentrations of 0-10 mg of digitonin per mg of cellular protein. Upon incubation at 37ºC for 2 min, the samples were mixed in a vortex and centrifuged at 12000 x g at 4ºC for 10 min. Protein in the supernatants were concentrated by trichloroacetic acid precipitation and supernatant and pellet fractions corresponding to 1.125 x 10^7 ml promastigotes were run in SDS-PAGE and analyzed by Western Blot.

2.5. SDS-PAGE and Western Blot analysis

Lysates of *L. infantum* promastigotes and amastigotes were prepared by freeze-thaw lysis of parasite pellets. Insoluble cellular debris was removed by centrifugation at 12000 x g for 20 min at 4ºC, the proteins separated by SDS-PAGE (12%) and blotted to nitrocellulose for Western Blot analysis. Western blots were probed with a polyclonal mouse anti-TDR1 and goat anti-mouse IgG peroxidase-conjugated (SouthernBiotech) used as the secondary antibody. Antibodies raised against *L. infantum* cTXNPx and mTXNPx sera were used as control. Development was performed with an ECL detection system (Amersham).

2.6. Immunization and challenge infection

Balb/c mice were obtained from Charles River (Spain) and maintained at the animal facilities of the Instituto de Biologia Molecular e Celular (IBMC, Porto, Portugal). Mice were kept six per cage and allowed food and water ad libitum.

Balb/c mice (3 animals per group) were inoculated three times i.p. at 1 week intervals either with 25 µg of rTDR1 or just PBS. Two weeks after the last immunization, spleen and sera were collected. Additional groups were immunized following the scheme described above and two weeks after the last boost challenged i.p. with 10^8 *L. infantum* promastigotes in PBS. Mice were bled and sacrificed at 2, 5, 7 and 9 weeks post-infection and spleen, liver and sera were collected. The spleen from each individual mouse was gently dissected to obtain single cell suspensions for cell population and cytokine production analysis. Splenocytes were washed and resuspended in RPMI complete medium to a concentration of 10^7 cells/ml. Mice groups were designated as follows: TDR1, immunized with rTDR1; PBS, injected with PBS; TDR1 INF, immunized with TDR1 and infected; INF, injected with PBS and infected.

2.7. Assessment of parasite load

Parasite quantification in the spleen and liver was performed by limiting dilution as previously described[38]. Briefly, organs were removed, homogenised and resuspended in RPMI medium. Two-fold serial dilutions were prepared in flat bottom 96-well microtiter plates (Immune Plate Maxisorp; Nunc). After incubation for 15 days at 27ºC, plates were examined and the positive (presence of motile parasites) and negative (absence of motile parasites) wells were determined using an inverted microscope. The number of parasites per gram of organ (parasite load) was calculated as follows: parasite load = [(geometric mean of reciprocal titer from each quadruplicate cell culture/weight of homogenized organ) x reciprocal fraction of the homogenized organ inoculated into the first well].

2.8. Flow cytometry analysis

A total of 10^6 splenocytes resuspended in PBS supplemented with 10% (v/v) FBS were distributed into a 96-well microtiter culture plate and washed with PBS-2% FBS. For spleen cell population determinations, cells were incubated with saturating concentrations of fluorescein isothiocyanate (FITC)-conjugated rat anti-mouse CD8 (Ly-2) monoclonal antibody, FITC-conjugated rat anti-mouse CD4 (L3T4) from BD Pharmingen or FITC-conjugated goat anti-mouse IgM from Southern Biotechnology. After 30 min incubation on ice, the cells were washed three times with PBS-2% FBS and examined in a FACSCalibur (Becton Dickinson) using propidium iodide 0.25 μg/ml (BD Pharmingen) for cell death exclusion. For phenotypic characterization of spleen cells, CD8 and CD4 subsets were double stained with phycoerythrin (PE)-conjugated rat anti-mouse CD44 (clone IM7, BD Pharmingen) and APC-conjugated rat anti-mouse CD62L (clone MEL-14, BD Pharmingen). Data files were analyzed using FlowJo software (Tree Star, Inc.).

2.9. Cytokine ELISAs

Spleen cells were seeded at a density of 2×10^5 cells/well in the presence of rTDR1 (10 μg/ml), concanavaline A (Con A, 6 μg/ml) or medium alone. Plates were incubated for 24h (for detection of IL-2), 48 h (for detection of IL-10 and IL-4) or 72 h (for detection of IFN-γ) at 37ºC in 5% CO_2. The IFN-γ, IL-10 and IL-4 production in supernatants of splenocyte cultures was measured by two-site sandwich enzyme-linked immunosorbent assay (ELISA), as previously described[39]

2.10. Detection of specific rTDR1 antibodies

Serum samples from animals immunized with rTDR1 were analyzed by ELISA for specific IgG and IgG1, IgG2a, IgG2b subclasses to rTDR1 2 weeks after the last boost and also 2, 5, 7 and 9 weeks post-infection, as previously described[40].

2.11. Statistical analysis

Statistical analysis was performed using Student's T test. A *p* value smaller than 0.05 ($p<0.05$) was considered significant. GraphPad Prism 4 was used for plotting the graphs.

The *L. infantum* TDR1 sequence was submitted to the NCBI sequence database under the accession number JF767498.

3. Results

3.1. Molecular cloning, expression and purification of *L. infantum* TDR1

L. infantum TDR1 is predicted to encode a protein with a theoretical molecular weight of 49.9 kDa. Fig. 1 shows the *Li*TDR1 amino acid sequence and compares it with *Lm*TDR1 and *Tc*52. The sequence analysis revealed that *Li*TDR1 shares a high identity with *Lm*TDR1 (95.8%), as predicted by Denton and co-workers[31]. Moreover, *Li*TDR1 shares with *Tc*52 the putative active site positioned in the N-terminal region while the CPF motif, characteristic of omega GSTs, occurring in the C-terminal region of the *Leishmania* proteins is absent from *Tc*52. The CXXC sequence, where X represent any amino acid, is also characteristic of glutaredoxins[41].

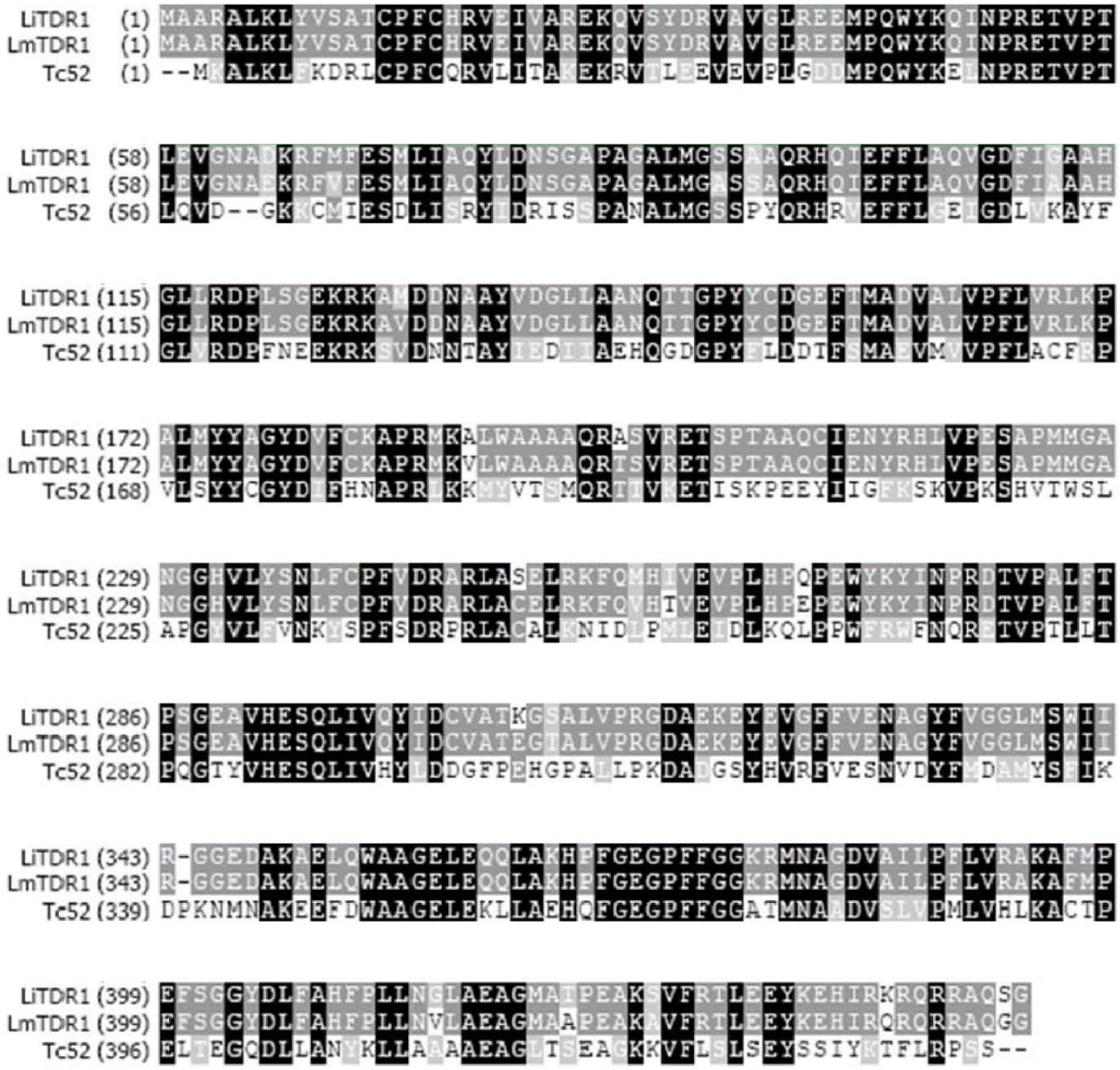

Figure 1. Amino acid alignment of *L. infantum* TDR1, *L. major* TDR1 and *T. cruzi Tc*52. The amino acid sequences of *L. infantum* TDR1 and *L. major* TDR1 (EBI accession no.AJ582069) were aligned and compared with *T. cruzi Tc*52 (EBI accession no. Q26950). Alignment was performed with AlignX (VectorNTI, Invitrogen). Identical amino acids in all sequences are shaded in black, identical amino acids in the *Leishmania* sequences are shaded in dark grey and light grey indicates similarity between amino acids. The putative active-sites are underlined.

In order to obtain TDR1 as a recombinant protein, *TDR1* was cloned into pET28a^{+} and expressed in *E. coli* with a N-terminal 6x Histidine-tag. As shown in Fig. 2, rTDR1 is a highly soluble recombinant protein with a yield of approximately 20 mg per liter of *E. coli* culture.

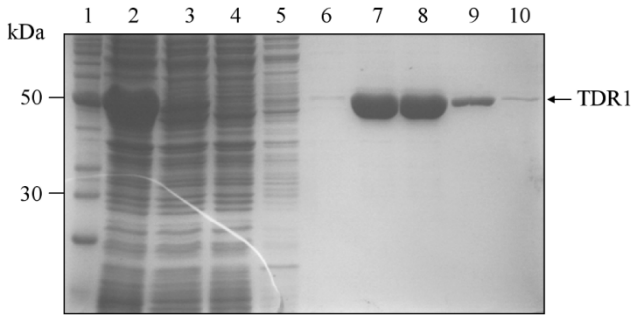

Figure 2. Expression and purification of *L. infantum* TDR1 in *E. coli*. Protein *samples* were separated in *12%* SDS-PAGE gel followed by Coomassie staining. Molecular mass standards (lane 1), lysate (lane 2) and supernatant (lane 3) of *E. coli* expressing recombinant protein; flow-through (lane 4); washes with Buffer A 60 mM imidazole (lanes 5 and 6) and purified recombinant protein eluted with Buffer A 250 mM imidazole (lanes 7 - 10). Estimated molecular masses and recombinant protein (arrowed) are indicated on the left and right, respectively

3.2. L. infantum TDR1 is constitutively expressed and is present in the cytosol of both parasite stages

To analyze the protein expression throughout the life cycle of *L. infantum*, promastigotes were synchronized to obtain the cells in different developmental stages (early log, late log and stationary phase of *in vitro* cultures), as well as differentiated into amastigotes. As shown in Fig. 3A, TDR1 expression is up-regulated in the axenic amastigote form and kept constant during exponential growth of promastigote stage.

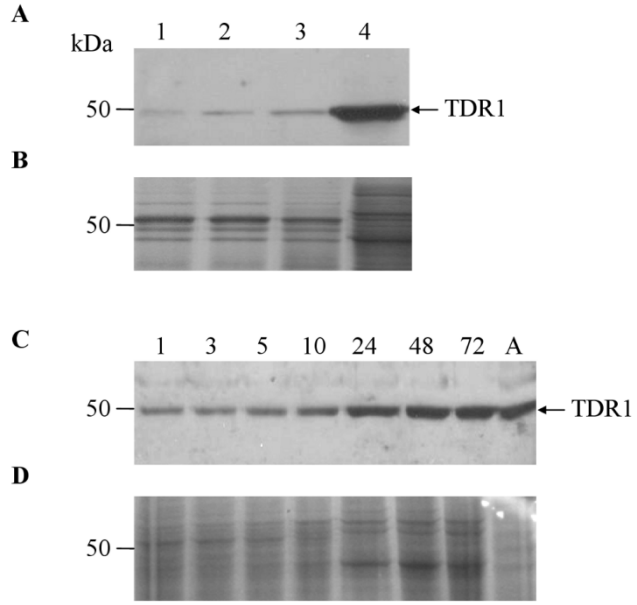

Figure 3. Expression of TDR1 throughout *L. infantum* development. (A) Western Blot analysis of TDR1 expression in total protein extracts from early log (lane 1), late log (lane

2) and stationary phase (lane 3) promastigotes and from axenic amastigotes (lane 4) using anti-TDR1 polyclonal antibody. (C) Western Blot analysis of TDR1 expression in total protein extracts resulting from differentiation of promastigotes into amastigotes. Expression was analyzed, using anti-TDR1 polyclonal antibody, 1, 3, 5, 10, 24, 48 and 72 h after initiation of incubation of promastigotes in MAA/20 medium at 37ºC. Coomassie blue staining of identical gel run in parallel (B, D) is shown as a loading control. Estimated molecular masses and TDR1 protein (arrowed) are indicated on the left and right, respectively.

This result was also confirmed by FACS analysis (Fig. S1 in supporting information). Furthermore, TDR1 expression increased in response to the temperature elevation and acidic pH in MAA/20 medium (Fig. 3C). The protein expression increased continuously until full differentiation to the amastigote form (Fig. 3C).

In order to gain insight into the localization of TDR1 in *L. infantum*, an immunofluorescence assay was performed with both promastigote and axenic amastigote forms (Fig. 4A). Immunostaining revealed a cytosolic localization with a punctate morphology. Cell fractionation by digitonin titration was carried out to further check the protein localization. Increasing concentrations of digitonin will permeabilise the different cellular membranes with the release of the proteins present in each cellular compartment[37]. Release of mitochondrial and cytosolic contents was monitored using a mitochondrial (*Li*mTXNPx) and cytosolic (*Lic*TXNPx) tryparedoxin peroxidases, respectively. As shown in Fig. 4B, TDR1 was released at very low concentrations of digitonin (0.1-0.5 mg digitonin/mg protein) in agreement with a cytosolic localization observed by immunofluorescence.

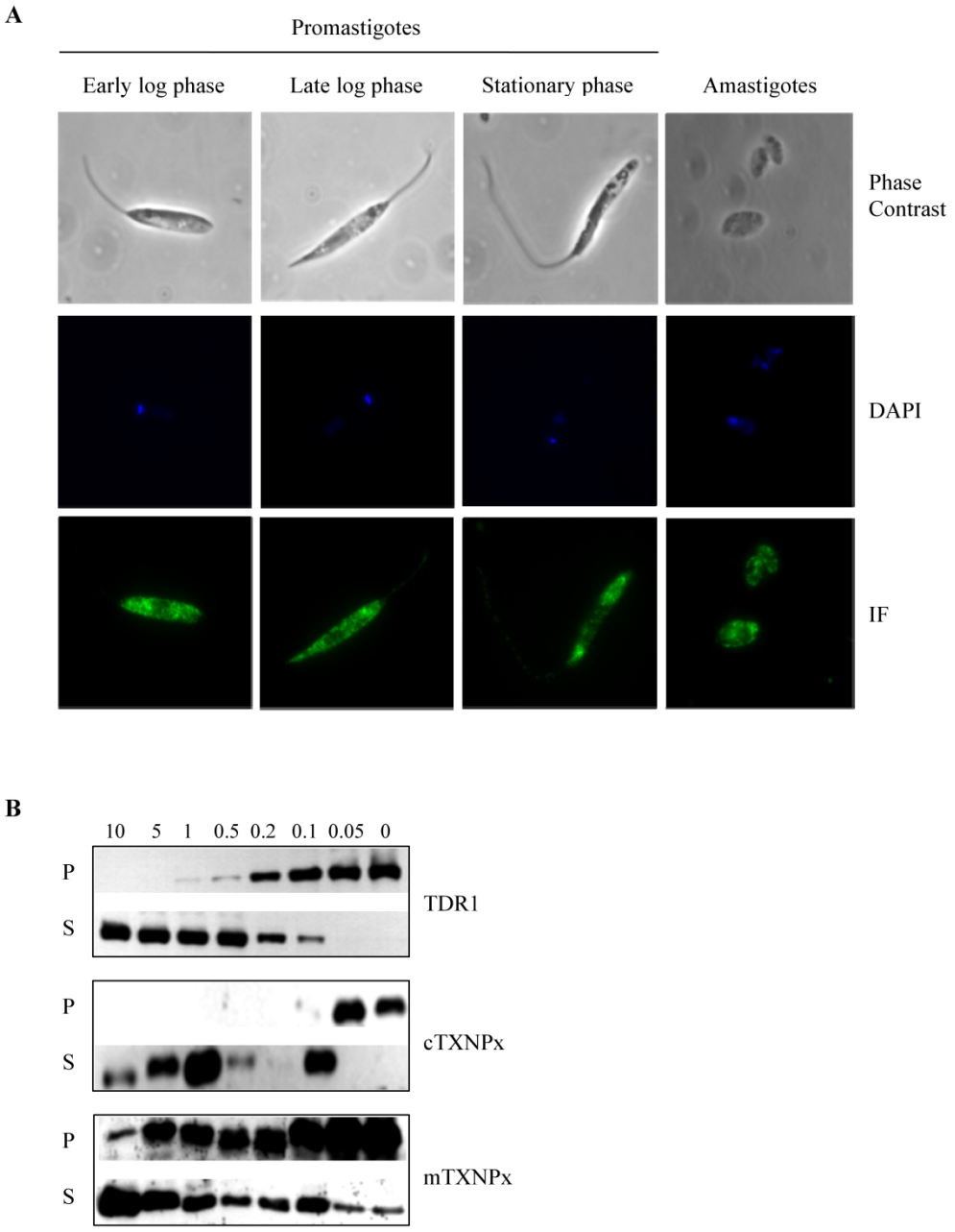

Figure 4. Sub-cellular localization of TDR1 in *L. infantum* promastigotes and axenic amastigotes. (A) Early log, late log, stationary phase promastigotes and axenic amastigotes were stained by immunofluorescence with mouse anti-TDR1 polyclonal antibody. A second antibody Alexa Fluor-488 goat anti-mouse IgG was used to detect the immune complex. Parasites were analyzed under a fluorescent microscope (Axioskop-Carl Zeiss, Germany) at 1000× magnification. (B) Western blot analysis, using anti-TDR1 polyclonal antibody, of supernatant (S) and pellet (P) fractions resulting from promastigotes permeabilisation with increasing concentrations of digitonin. Anti-cTXNPx and anti-mTXNPx were used as cytosolic and mitochondrial markers, respectively.

Given the fact that TDR1 has high homology with *Tc*52, an excreted/secreted protein from *T. cruzi*[33], we assessed the possibility of *L. infantum* TDR1 belong to the group of excreted/secreted molecules. TDR1 secretion was evaluated by immunoprecipitation of [^{35}S] methionine-labelled *L. infantum* promastigotes and axenic amastigotes antigens after pulse chase experiments, using anti-TDR1 antibodies. We found that the protein is released by promastigotes and axenic amastigotes into the culture medium at low levels (Fig. S2 in supporting information). Moreover, TDR1 was detected in vesicles purified from spent medium of *L. infantum* promastigote cultures, revealing the possible release of the protein by an exosome-based mechanism (N. Santarém et al., unpublished data).

3.3. TDR1 immunization leads to an increase in B and CD8-T cell numbers and a marked increase in specific IgG1 production

The effect of TDR1 on the immune response was investigated in Balb/c mice after administration of rTDR1. Two weeks after the last immunization, spleen cells were used to analyze the humoral and cellular responses. As shown in Fig. 5A, immunization with rTDR1 led to a significant increase in the total number of B cells (p=0.006) and CD8-T cells (p=0.0009). As a control Balb/c mice were immunized with two other *Leishmania* recombinant proteins, namely tryparedoxin 1 (TXN1) and mTXNPx, which were produced following the same procedure used to obtain rTDR1. Both TXN1 and mTXNPx are involved in *Leishmania* hydroperoxide metabolism[42] and TXN1 has been reported to up-regulate IL-10 secretion through activation of B cells[43]. There were no differences in the numbers of CD8-T cell population between mice only injected with PBS and mice immunized with rTXN1 or rmTXNPx (Fig. S3 in supporting information), suggesting that TDR1 induces specifically CD8-T cells expansion in vivo. Increase in B cell numbers induced both by rTDR1 and mTXNPx immunization could be related with polyclonal B cell activation reported to occur in response to *Leishmania* infection, although analysis of polyclonal antibodies against for example whale skeletal muscle type II myoglobulin (Myo) and native double-stranded DNA (DNA) in the sera of TDR1- or rmTXNPx-immunized Balb/c mice did not confirm it as were detected very low levels similar to the ones observed in the control animals. *In vitro* experiments showed no significant increase in CD69 surface expression, an early activation marker, by B or T cells in response to treatment with rTDR1. The latter suggest that TDR1 may need to be processed and presented *in vivo* to have an effect on the immune response.

In order to examine the *in vivo* effect of TDR1 on the cytokine production, splenocytes of rTDR1-immunized or PBS-injected Balb/c mice were stimulated with rTDR1 or Con A. Cell supernatants were collected and production of IFN-γ (Fig. 5B), IL-10 (Fig. 5C), IL-2 and

IL-4 (Fig. S4 in supporting information) were measured by ELISA. No significant differences were observed in the cytokines production from cells cultured in the presence or absence of rTDR1. However, spleen cells from TDR1 immunized mice stimulated with Con A showed a significant decrease in the IL-10 production (p=0.0073) when compared with cells from PBS-injected mice. This resulted in an increase in the IFN-γ/IL-10 ratio in the rTDR1 immunized mice (52) when compared with PBS-injected mice (39). Immunization of Balb/c mice with rTXN1 used as control did not induce any significant change in IL-10 production by spleen cells stimulated ex-vivo with Con A (data not shown).

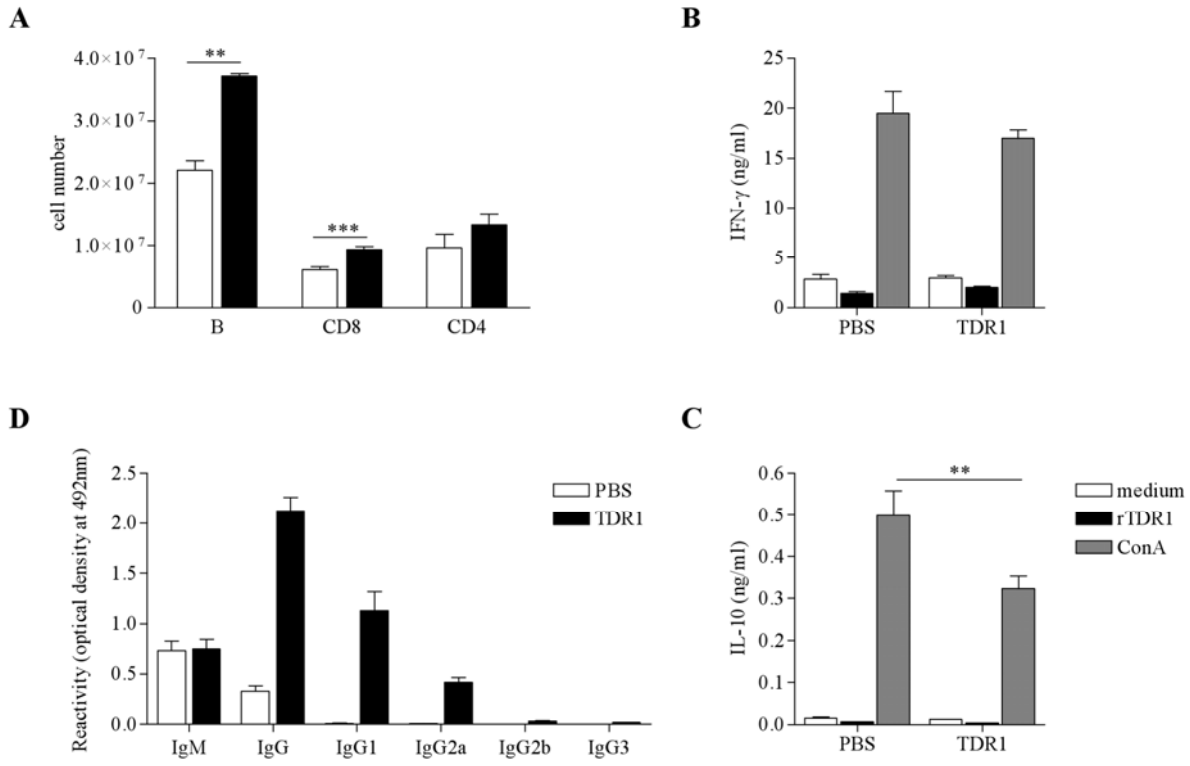

Figure 5. Cellular and humoral immune responses induced by immunization with rTDR1. Balb/c mice were immunized i.p. with 25 µg of rTDR1 three times with an interval of one week between each injection. The control group received PBS injections. Two weeks after the last immunization, the mice were sacrificed and spleens recovered. (A) Spleen cells were analyzed by flow cytometry to determine the percentage of B cells, CD4- and CD8-T cells. The number of each cell subpopulation was calculated based on the total viable cells determined by trypan blue exclusion and the percentage of cell bound to the specific cell marker (anti-CD4, anti-CD8, anti-µ). Cytokine production was quantified in the supernatant of spleen cells cultures by ELISA. Spleen cells ($2.5x10^5$) were stimulated with rTDR1 protein (10 µg/ml) or Con A (6 µg/ml) for 48 and 72 h for

quantification of IL-10 (C) and INF-γ (B) production, respectively. (D) Sera obtained from PBS- or TDR1-immunized mice were used to determine the levels of TDR1-specific IgM, IgG, IgG1, IgG2a, IgG2b and IgG3 by ELISA. The sera were diluted 1/100 in PBS-1% gelatin. The data represent the mean and standard deviations of three animals analyzed individually and are representative of three experiments carried out independently. Statistically significant differences between TDR1 and PBS groups are indicated ** $p<0.01$, *** $p<0.001$.

To evaluate the humoral response induced by TDR1 immunization, the levels of TDR1-specific isotypes in the sera of rTDR1 or PBS immunized mice were determined by ELISA. Fig. 5D shows that sera from rTDR1 immunized mice contained elevated levels of TDR1-specific IgG, with predominant IgG1 antibody isotype. Previously the IgG2a/IgG1 ratio has been used as a predictive measure for Th1 and Th2 responses since IgG2a levels are dependent on IFN-γ and IgG1 levels correlate with IL-4[44]. Based on the humoral response, rTDR1 immunization induced high levels of IgG1 compared with IgG2a revealing a tendency toward Th2 response, with a TDR1-specific IgG2a/IgG1 ratio of 0.37.

3.4. Expansion of CD8-T cells and decrease in IL-10 production elicited by rTDR1 immunization was insufficient to protect Balb/c mice against *L. infantum* infection

In order to investigate the effect of rTDR1 immunization to elicit protection against leishmaniasis, rTDR1 immunized mice were challenged with *L. infantum* promastigotes. The parasite load in the spleen and liver was evaluated by limiting dilution at 2, 5, 7 and 9 weeks post-infection. Fig. 6A shows that animals immunized with rTDR1 presented a lower parasite load in the spleen compared with PBS immunized animals during experimental infection, except for 2 weeks after infection. Significant differences were observed at 7 (p=0.023) and 9 weeks (p=0.002) post-infection. No significant differences were detected in the liver parasite load between the groups used in this study (Fig. 6B). An attempt to improve the protection levels induced by rTDR1 immunization using CpG as an adjuvant or protein delivery as a DNA vaccine proved unsuccessful (data not shown).

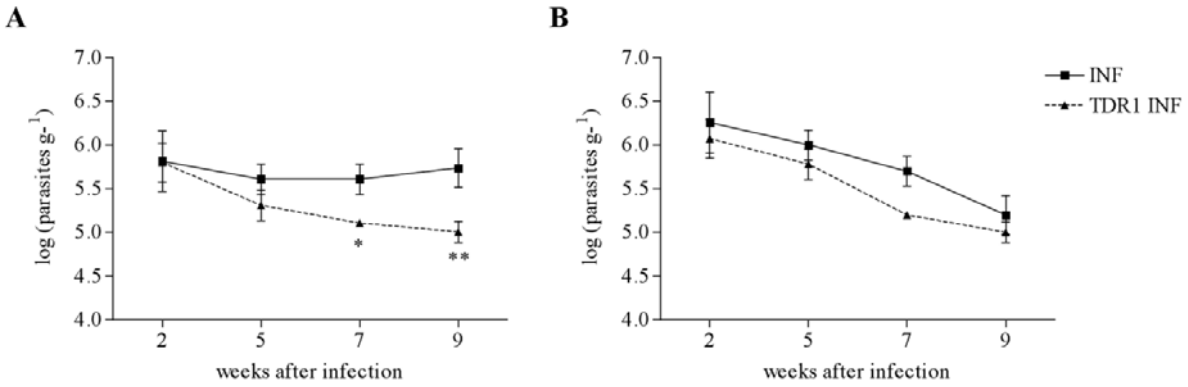

Figure 6. Parasite load in the spleen (A) and liver (B) of Balb/c mice immunized with rTDR1 after challenge with *L. infantum* promastigotes. Groups of mice were immunized i.p. with 25 µg rTDR1 (TDR1) or with PBS and challenged with 1x10^8 *L. infantum* promastigotes and groups designated as TDR1 INF (immunized and infected) and INF (infected). Limiting dilution analysis was performed 2, 5, 7 and 9 weeks after infection on the cells isolated from the spleen and liver of each individual mouse and cultured in quadruplicate for 2 weeks at 27º C. The cultures were then assessed microscopically for *L. infantum* viable parasites. The data represent the mean and standard deviations of three animals analyzed individually and are representative of three experiments carried out independently. Statistically significant differences between TDR1 INF and INF groups are indicated * p<0.05, ** p<0.01

Analysis of rTDR1-specific IgG isotypes in the sera of rTDR1 immunized mice during the course of experimental infection (Fig. 7) revealed the maintenance of high levels of specific IgG1 over IgG2a, as observed when analysing the humoral response after immunization with rTDR1. Sera from animals receiving PBS were essentially negative for TDR1-specific immunoglobulins.

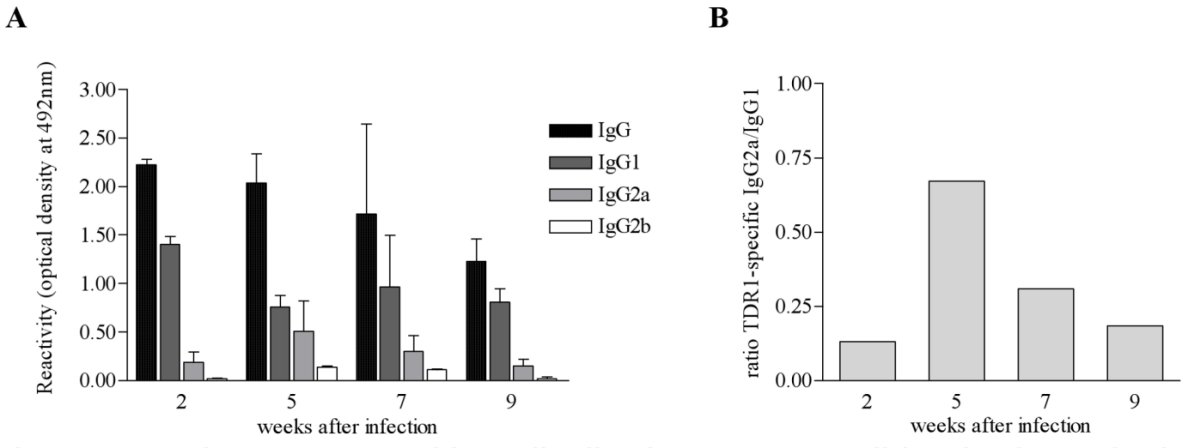

Figure 7. Levels of TDR1-specific antibodies in sera from Balb/c mice immunized with rTDR1 and infected with *L. infantum* promastigotes. (A) Levels of TDR1-specific

IgG, IgG1, IgG2a and IgG2b were determined by ELISA during *L. infantum* infection (2, 5, 7, and 9 weeks) in sera from Balb/c mice immunized with rTDR1. The sera were diluted 1/100 in PBS-1% gelatin. (B) Ratio between TDR1-specific IgG2a and IgG1 levels at 2, 5, 7 and 9 weeks post-infection. The data represent the mean and standard deviations of three animals analyzed individually and are representative of three experiments carried out independently.

Although rTDR1 immunization was only able to induce a small degree of protection, the cellular response of immunized and infected mice was assessed to determine whether the protection levels achieved resulted from a cell-mediated process. Production of IFN-γ, IL-10 and IL-4 was determined by ELISA after *ex-vivo* stimulation of spleen cells with rTDR1 or Con A. There was no significant difference in the profiles of IFN-γ and IL-4 production between rTDR1 immunized and infected mice and control group during the course of *Leishmania* infection (Fig. 8A and 8C).

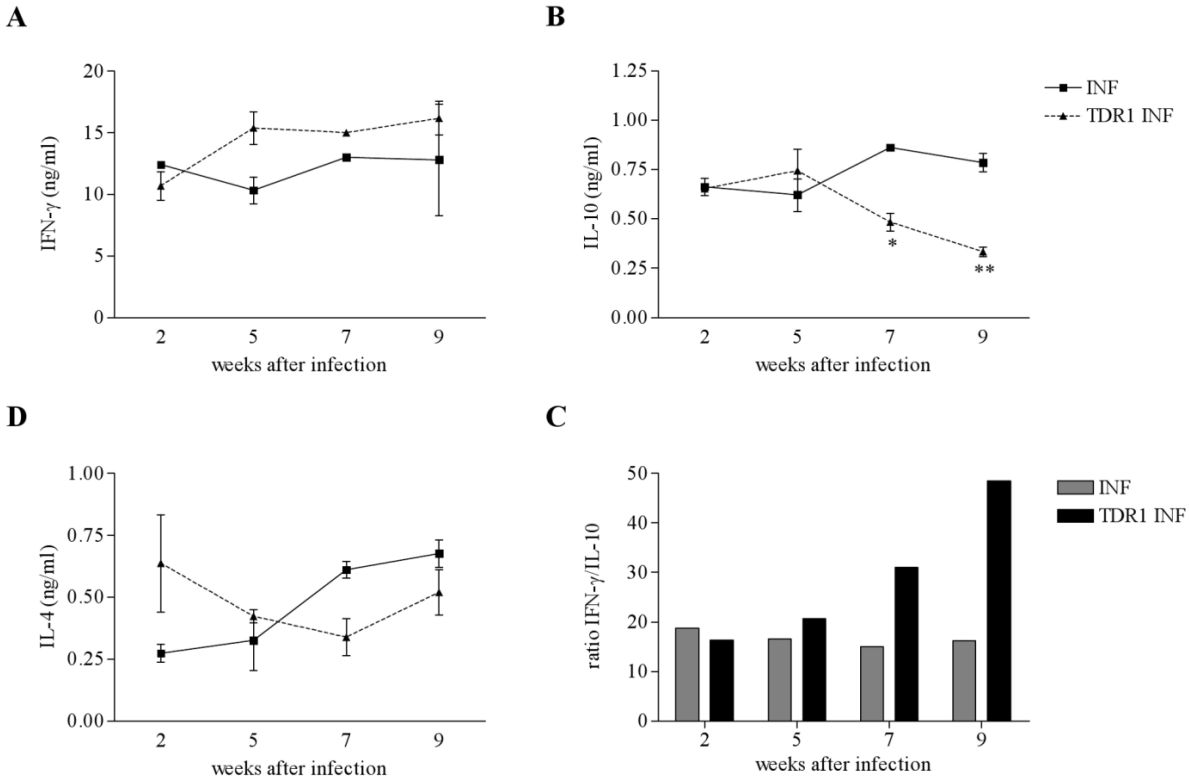

Figure 8. Cytokine production by spleen lymphocytes from Balb/c mice immunized with rTDR1 and challenged with *L. infantum* promastigotes. Spleen cells from Balb/c mice immunized with rTDR1 (TDR1) or PBS and challenged with 1x10^8 *L. infantum* promastigotes (groups designated as TDR1 INF (immunized and infected) and INF (infected)), were recovered at 2, 5, 7 and 9 weeks post-infection. Cells were stimulated

with 6 µg/ml of Con A for 72 h to determine INF-γ production (A) and for 48 h to determine IL-10 (B) and IL-4 (C) production by ELISA. (D) Ratio of INF-γ/IL-10 production by spleen cells stimulated with 6 µg/ml of Con A at 2, 5, 7 and 9 post-infection. The data represent the mean and standard deviations of three animals analyzed individually and are representative of three experiments carried out independently. Statistically significant differences between TDR1 INF and INF groups are indicated * $p<0.05$, ** $p<0.01$.

In contrast, a significant decrease in the production of IL-10 was observed in the case of spleen cells from rTDR1-immunized and infected mice at 7 (p=0.038) and 9 (p=0.0056) weeks post-infection upon their ex-vivo stimulation with Con A compared with the controls (Fig. 8B). This fact contributes to the increase in the ratio of IFN-γ/IL-10 in the rTDR1 immunized mice at 7 (30) and 9 weeks (48) post-infection while in the PBS immunized mice it remains at comparable levels (15 at 7 weeks and 16 at 9 weeks) during the course of infection (Fig. 8D). In *Leishmania* infection, IL-10 limits the magnitude of the immune response by inhibiting APC functions, such as IFN-γ secretion, which are essential for the parasite clearance[45]. Moreover, IL-10 produced by T regulatory cells has been shown to play an important role in disease chronicity [46], thus the decrease in IL-10 production may contribute to the reduction in the parasite load observed at 7 and 9 weeks post-infection in Balb/c immunized with rTDR1 but was not enough to induce high levels of protection.

As reported above, rTDR1 immunization induced an increase of splenic B cells and CD8-T cells. To investigate if the same occur in the context of *Leishmania* infection, spleen cell populations obtained from immunized mice challenged with *L. infantum* promastigotes were analyzed by flow cytometry. As shown in Table 1, two weeks post-infection spleens from mice immunized with rTDR1 show a significant increase in the number of CD8-T cells (p=0.003) when compared with the control. This is also observed at 9 weeks after infection (p=0.008), confirming the maintenance of an increase in the CD8-T cell population even in the context of *Leishmania* infection.

CD8-T cells upon antigenic stimulation up-regulate the expression of granzymes, perforin, IFN-γ secretion and become cytolytic, leading to the death of infected cells[47]. Thus, we tested the cytolytic capacity of spleen cells from mice immunized with rTDR1 or PBS and challenged with *L. infantum.* Spleen cells were stimulated *ex-vivo* with rTDR1 or *Leishmania* antigens and then put in contact with macrophage infected cells to determine the percentage of death induced in the infected population. No differences were observed between the control and the immunized mice, therefore the CD8-T cells number increase in the mice immunized with TDR1 do not seem to be involved in the death of infected cells

by a cytotoxic mechanism (Fig. S5 in supporting information). The maintenance of increase numbers of CD8-T cells in mice immunized with rTDR1 even in a chronic phase of the disease led us to hypothesize the generation of T cell memory induced by rTDR1 immunization.

Table 1. Analysis of spleen cell populations from Balb/c mice immunized with rTDR1 and challenged with *L. infantum* promastigotes

week	TDR1 treatment	Cell number (x10^7)		
		CD4	CD8	B
2	-	1.732 ± 0.063	0.684 ± 0.033	3.392 ± 0.028
	+	2.327 ± 0.039	1.008 ± 0.043**	3.772 ± 0.114
5	-	2.397 ± 0.028	1.220 ± 0.055	3.303 ± 0.218
	+	2.388 ± 0.099	1.267 ± 0.039	3.998 ± 0.316
7	-	1.920 ± 0.097	0.777 ± 0.101	4.307 ± 0.496
	+	2.017 ± 0.034	1.146 ± 0.170	4.012 ± 0.106
9	-	2.944 ± 0.420	0.990 ± 0.060	4.224 ± 0.541
	+	2.942 ± 0.590	1.422 ± 0.023**	5.287 ± 0.118

The percentage of B cells, CD4- and CD8-T cells were determined by flow cytometry analysis in the spleen of Balb/c mice immunized with rTDR1 (TDR1) or with PBS 2, 5, 7 and 9 weeks post-infection The number of each cell subpopulation was calculated based on the total viable cells determined by trypan blue exclusion and the percentage of cell bound to the specific cell marker (anti-CD4, anti-CD8, anti-μ). The data represent the mean and standard deviation of three animals analyzed individually and are representative of three experiments carried out independently. Statistically significant differences between TDR1 and PBS groups are indicated ** $P<0.01$.

In order to characterize T cells after immunization and challenge with *L. infantum*, spleen cells were labeled with antibodies that recognized T cell expression markers - allowing the distinction of different subsets of memory T cells. CD44, a surface protein required for lymphocyte extravasation to inflammatory sites[48], and CD62L, a lymph node homing receptor[49], were used since up-regulation of these markers is a hallmark of memory T cells. The combination of surface staining for CD44 and CD62L separates between two functionally distinct memory cell subsets, central memory T cells ($CD44^{high}$ and $CD62L^{high}$) and effector memory T cells ($CD44^{high}$ and $CD62L^{low}$). The stained splenocytes were analyzed by flow cytometry, and only CD8-T or CD4-T cells are shown in the analyses

(Fig. 9A). Analysis of spleen cells from TDR1-immunized mice 9 weeks post-infection revealed a significant difference in the $CD8^+$ central memory subset with an increase in the percentage of $CD8^+CD44^{high}CD62L^{high}$ cells (p=0.0085) when compared with splenocytes from PBS-immunized mice (Fig. 9B). CD4-T cells did not show any changes in the percentage of cells in the central memory subset when comparing the 2 groups analyzed (Fig. 9C).

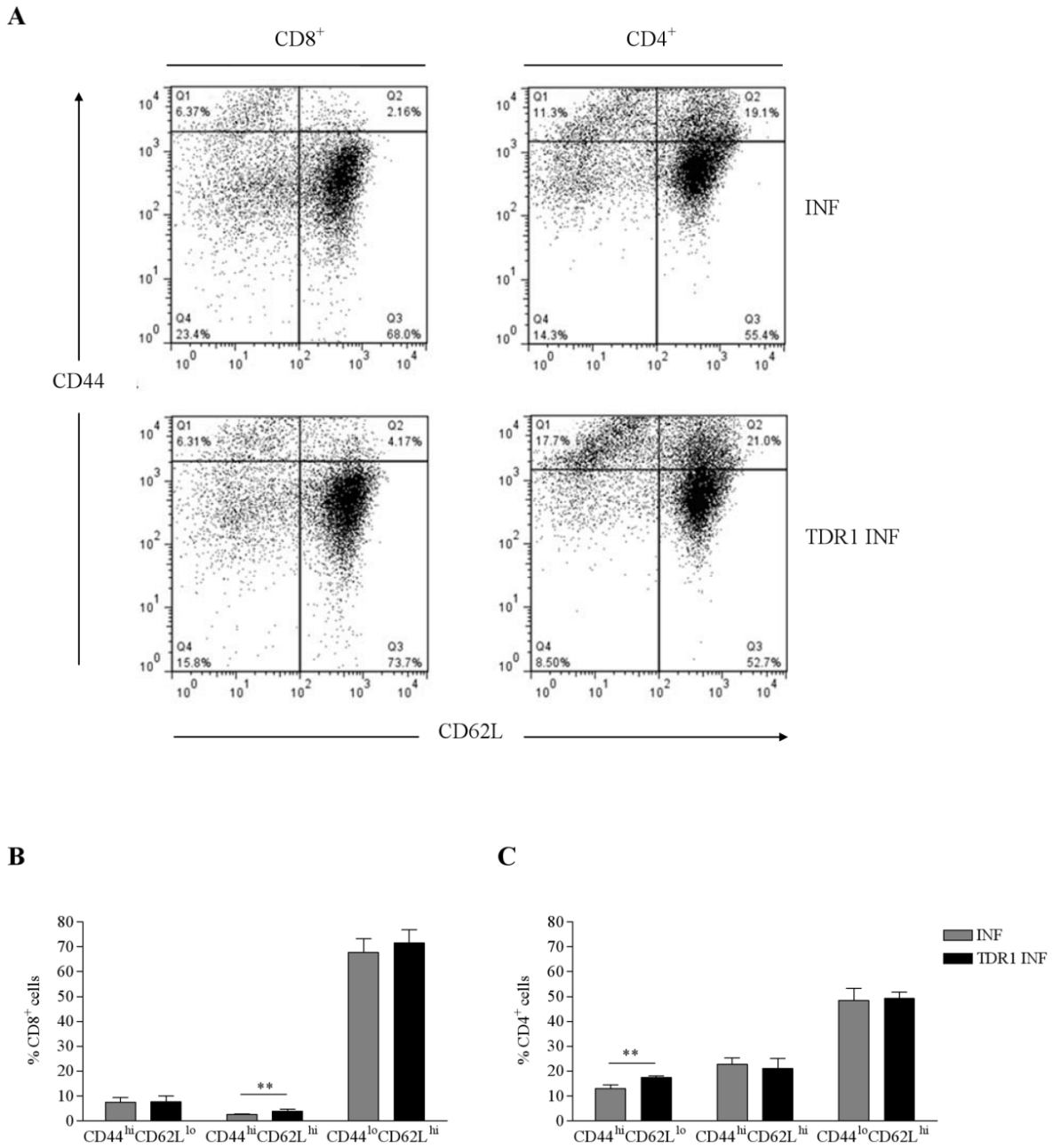

Figure 9. Representative three-color FACS contour plots of splenocytes. $CD4^+$ and $CD8^+$-gated cells were analyzed for CD44 and CD62L expression and the percentages for each subset are shown (A). Percentages of total spleen CD8- (B) and CD4- (C) T cells were obtained for $CD44^{high}CD62L^{low}$, $CD44^{high}CD62L^{high}$, $CD44^{low}CD62L^{high}$ subsets as

defined in (A). Spleens from rTDR1- or PBS-immunized Balb/c mice were harvested 9 weeks post-infection (groups designated as TDR1 INF (immunized and infected) and INF (infected)). and splenocytes stained with CD8 or CD4 monoclonal antibodies plus CD44 and CD62L. Results shown are representative of two experiments carried out independently. Statistically significant differences between TDR1 INF and INF groups are indicated * $p<0.05$, ** $p<0.01$.

Memory cell phenotype was checked during the course of infection with *L. infantum* based in the expression of high levels of CD62L on $CD44^{high}CD8^{+}$ and CD62L on $CD44^{high}CD4^{+}$ as shown in Table 2. Spleen cells from TDR1-immunized mice showed a significant increase in the percentage of $CD62L^{high}$ on $CD44^{high}CD8^{+}$ cells (p=0.005), the central memory subset, only at 9 weeks post-infection. Altogether, these observations suggest that generation of central memory T cells may be induced by TDR1 in the context of *Leishmania* infection, however not in a significant magnitude which could result in higher levels of protection against *Leishmania* infection.

Table 2. Expression of memory markers on splenic $CD8^{+}$ and $CD4^{+}$ T cells before and after challenge of rTDR1-immunized Balb/c mice with *L. infantum* promastigotes

		% $CD62L^{hi}$	
week	treatment	$CD44^{hi}CD8^{+}$	$CD44^{hi}CD4^{+}$
0	PBS	53.61 ± 3.62	47.48 ± 4.09
	TDR1	49.67 ± 7.75	51.48 ± 0.72
1	PBS	52.27 ± 7.50	42.39 ± 3.77
	TDR1 INF	54.83 ± 1.59	44.56 ± 5.75
7	INF	48.02 ± 3.27	44.09 ± 5.2
	TDR1 INF	47.33 ± 7.08	45.69 ± 8.0
9	INF	49.06 ± 3.5	58.89 ± 7.5
	TDR1 INF	60.27 ± 2.38**	61.22 ± 1.6

The results shown are percentage ± standard deviation of CD62Lhigh on CD44highCD8+ and CD62Lhigh on $CD44highCD4^{+}$ cells. Spleen cell suspensions from each mouse harvested before (0) or 1, 7 and 9 weeks post-infection were individually stained with CD8 or CD4 monoclonal antibodies plus CD44 and CD62L. Groups used were named as follow: TDR1-immunized mice before (TDR1) and after infection (TDR1 INF) and PBS-immunized before (PBS) and after infection (INF). Results shown are representative of two experiments carried out independently. Statistically significant differences between TDR1 INF and INF groups are indicated ** $p<0.01$.

4. Discussion

Leishmania have efficiently developed measures to survive in the sand fly and also inside the mammalian host, where the conditions are hostile. Among the different mechanisms is the secretion/excretion or release of molecules important in the initial steps of infection as well as in the manipulation of the hosts' immune responses. The search for parasite antigens able to induce a protective immune response in the mammalian host has lead to the identification of proteins that may constitute putative vaccine candidates[7-10, 13, 14]. The characterization of proteins involved in the parasite-host interactions has also contributed to understanding the biology of the parasite and its metabolic needs inside its hosts.

In this study, we characterized the immune response to a *L. infantum* recombinant protein named Thiol Dependent Reductase 1 (TDR1). The interesting feature of this protein that prompted our study was the observation of a high identity between *L. major* TDR1 and *Tc*52[31]. *Tc*52 has been previously demonstrated to be a virulence factor of *T. cruzi* and disruption of one allele of the gene encoding Tc52 resulted in a mutant which gave attenuated disease in mice[34]. We confirmed that TDR1 is highly conserved between *Leishmania* species and that *L. infantum* TDR1 is highly homologous with TDR1 of *L. major*. This observation was not unexpected as previous studies have shown a highly conserved gene content and synteny across the *Leishmania* genus[50]. The expression profile of TDR1 in *L. infantum* showed an increase expression in the amastigote stage, suggesting a role of TDR1 in adaptation to the mammalian host. Immunostaining analysis revealed that TDR1 is cytosolic in both stages of *Leishmania* parasites. However, we detected TDR1 in the spent medium of both promatigote and amastigote cultures and this could be relevant to the protein role in the parasite-host interaction. TDR1 protein lacks an N-terminal signal sequence that could facilitate secretion but it is known that the parasite has alternative pathways of secretion or release of molecules important for a successful infection[6, 51]. Such exosomes may explain the presence of many proteins with known intracellular functions in the spent medium of *Leishmania* cells, a finding reported through applying a proteomic analysis[52, 53].

Several *Leishmania* antigens have been used as vaccine candidates, with considerable differences in the parasite load reduction obtained. The outcome of leishmaniasis is dependent on the type of immune response generated. In visceral leishmaniasis, caused by *L. infantum* or *L. donovani* species, the Th1/Th2 dichotomy is not as important to the outcome of the disease in murine models as it is for *L. major* infection. Th1 responses are suppressed by IL-10 and TGF-β, contrary to what is described in the case of *L. major*

where infection is promoted by the expansion of Th2 cells producing IL-4, IL-10 and IL-13[54].

In this study, the ability of rTDR1 to induce protection against challenge with *L. infantum* in susceptible Balb/c mice was evaluated. Partial protection in the spleen was observed in mice immunized with rTDR1 whereas no difference was detected in the liver parasite load. Despite the partial protection obtained with rTDR1 immunization, two significant differences should be highlighted: the decrease in IL-10 and increase in CD8-T cell population with characteristics of central memory cells observed in a chronic phase of the disease. IL-10 decrease after *ex-vivo* stimulation of spleen cells with Con A was observed after immunization with rTDR1 but also in the context of rTDR1 immunization and infection with *L. infantum.* IL-10 is a regulatory cytokine that in visceral leishmaniasis has been described as a key factor in immunosupression. This was shown by the enhanced resistance to *L. donovani* infection observed in IL-10 deficient mice[55]. Increase in IFN-γ/IL-10 ratio in the context of *L. infantum* infection has been shown to allow an effective clearance of the parasite[40]. Also, *Leishmania* chronic infection is associated with expansion or accumulation of IL-10 producing regulatory T cells (Tregs). In cutaneous leishmaniasis naturally, Tregs modulate the development of effector responses and prevent complete elimination of the parasite. Nevertheless, in active cases of human visceral leishmaniasis Tregs did not accumulate at the site of infection, being disease progression-associated with IL-10 production by splenic $CD4^{+}CD25^{-}$ (Tr1 cells)[46]. Tr1 cells are a second type of regulatory T cells that are generated following exposure to antigen[45]. In the case of TDR1 immunization, the decrease in IL-10 only occurs in a chronic phase of the disease and is not accompanied by an IFN-γ increase that could account for enhancing the protection levels, since IFN-γ is required for protection against visceral leishmaniasis. It is possible to hypothesize that in Balb/c mice immunized with rTDR1 the decrease in IL-10 was due to a decrease in Tregs or Tr1 cells accumulation. CD8-T cells can be responsible for the suppression of regulatory CD4-T cells detrimental effects. Martin and co-workers have shown that CD8-T cells can work as contra-Treg, however these CD8-T cells are susceptible to IL-10-induced apoptosis and were unable to keep Treg in check 21 days after infection with *L. donovani*[56]. Therefore, this last observation does not support our data since the IL-10 decrease was observed in a later stage of infection. On the other hand, rTDR1 immunization induced an increase in CD8-T cells, to which we could attribute the contra-Treg role, however these did not show an increase ability to kill infected cells through cytotoxic mechanisms *in vitro* when compared with control cells.

Although, immunization with rTDR1 did not induce high levels of protection, the decrease in parasite load observed in a chronic phase of *L. infantum* infection after Balb/c can be

due to CD8-T cells, in particular to the generation or maintenance of memory T cells. After exposure to *Leishmania* antigens, there is a strong clonal expansion of antigen-specific CD8-T cells needed to control the infection and that will determine the magnitude of the memory response. However, *Leishmania* is able to evade the attack from CD8-T cells by suppressing their expansion and effector function inducing functional exhaustion and cell death. This was confirmed when i*n vivo* B7-H1 blockade during chronic *L. donovani* infection increased survival of dysfunctional CD8-T cell leading to a significant reduction in the splenic parasite burden[26]. The rTDR1 immunization that led to an increase in $CD8^+$ central memory T cells 9 weeks post-infection may be due to the ability of TDR1 to induce a greater CD8-T cells expansion to generate memory cells or to maintain the memory T cell population. This possibility should be further explored by determination of cytokines, such as IL-7 and IL-15, which are essential for long term-maintenance of CD8-T cell population and also through adoptive transfer of CD8-T cell population into naive recipient mice to evaluate the levels of protection induced.

The role of antibodies during *Leishmania* infection has been controversial, however recent work have shown that IgG1 can be detrimental to an infected host contributing to disease progression. Mice lacking IgG1 are more resistant to *L. mexicana*, developing earlier and stronger IgG2a and IgG3 responses[57]. The inability to obtain higher protection levels when using rTDR1 immunization in the context of *L. infantum* infection may be related with the high levels of TDR1-specific IgG1 detected in all experiments performed.

In summary, our study with rTDR1 from *L. infantum* has shown the ability of this antigen to induce expansion of CD8-T cells, decrease in IL-10 production, although not enough to confer high levels of protection against infection in Balb/c mice. Nevertheless, the induction of CD8-T cells with characteristics of central memory T cells highlights the importance of these cells in a vaccination strategy against leishmaniasis.

Acknowledgements

This work was supported by Fundação para a Ciência e Tecnologia (FCT) project number PTDC/CVT/65047/2006 and AMS is supported by FCT grant SFRH/BD/28316/2006. RS is supported by Programa Ciência 2008 from FCT. The authors have no competing interests.

References

1. Kedzierski L. Leishmaniasis Vaccine: Where are We Today? J Glob Infect Dis. 2010 May;2(2):177-85.

2. Alvar J, Aparicio P, Aseffa A, Den Boer M, Canavate C, Dedet JP, et al. The relationship between leishmaniasis and AIDS: the second 10 years. Clin Microbiol Rev. 2008 Apr;21(2):334-59.

3. Croft SL, Sundar S, Fairlamb AH. Drug resistance in leishmaniasis. Clin Microbiol Rev. 2006 Jan;19(1):111-26.

4. Gangneux JP, Sulahian A, Honore S, Meneceur P, Derouin F, Garin YJ. Evidence for determining parasitic factors in addition to host genetics and immune status in the outcome of murine *Leishmania infantum* visceral leishmaniasis. Parasite Immunol. 2000 Oct;22(10):515-9.

5. Santarem N, Silvestre R, Tavares J, Silva M, Cabral S, Maciel J, et al. Immune response regulation by *Leishmania* secreted and nonsecreted antigens. J Biomed Biotechnol. 2007;2007(6):85154.

6. Silverman JM, Clos J, de'Oliveira CC, Shirvani O, Fang Y, Wang C, et al. An exosome-based secretion pathway is responsible for protein export from *Leishmania* and communication with macrophages. J Cell Sci. 2010 Mar 15;123(Pt 6):842-52.

7. Yao C, Donelson JE, Wilson ME. The major surface protease (MSP or GP63) of *Leishmania sp*. Biosynthesis, regulation of expression, and function. Mol Biochem Parasitol. 2003 Nov;132(1):1-16.

8. Zhang WW, Matlashewski G. Loss of virulence in *Leishmania donovani* deficient in an amastigote-specific protein, A2. Proc Natl Acad Sci USA. 1997 Aug 5;94(16):8807-11.

9. Mottram JC, Brooks DR, Coombs GH. Roles of cysteine proteinases of trypanosomes and *Leishmania* in host-parasite interactions. Curr Opin Microbiol. 1998 Aug;1(4):455-60.

10. Hassan P, Fergusson D, Grant KM, Mottram JC. The CRK3 protein kinase is essential for cell cycle progression of *Leishmania mexicana*. Mol Biochem Parasitol. 2001 Apr 6;113(2):189-98.

11. Kubar J, Fragaki K. Leishmania proteins derived from recombinant DNA: current status and next steps. Trends Parasitol. 2006 Mar;22(3):111-6.

12. Mougneau E, Altare F, Wakil AE, Zheng S, Coppola T, Wang ZE, et al. Expression cloning of a protective *Leishmania* antigen. Science. 1995 Apr 28;268(5210):563-6.

13. Stager S, Smith DF, Kaye PM. Immunization with a recombinant stage-regulated surface protein from *Leishmania donovani* induces protection against visceral leishmaniasis. J Immunol. 2000 Dec 15;165(12):7064-71.

14. Skeiky YA, Kennedy M, Kaufman D, Borges MM, Guderian JA, Scholler JK, et al. LeIF: a recombinant *Leishmania* protein that induces an IL-12-mediated Th1 cytokine profile. J Immunol. 1998 Dec 1;161(11):6171-9.

15. Velez ID, Gilchrist K, Martinez S, Ramirez-Pineda JR, Ashman JA, Alves FP, et al. Safety and immunogenicity of a defined vaccine for the prevention of cutaneous leishmaniasis. Vaccine. 2009 Dec 11;28(2):329-37.

16. Nascimento E, Fernandes DF, Vieira EP, Campos-Neto A, Ashman JA, Alves FP, et al. A clinical trial to evaluate the safety and immunogenicity of the LEISH-F1+MPL-SE vaccine when used in combination with meglumine antimoniate for the treatment of cutaneous leishmaniasis. Vaccine. 2010 Sep 14;28(40):6581-7.

17. Llanos-Cuentas A, Calderon W, Cruz M, Ashman JA, Alves FP, Coler RN, et al. A clinical trial to evaluate the safety and immunogenicity of the LEISH-F1+MPL-SE vaccine when used in combination with sodium stibogluconate for the treatment of mucosal leishmaniasis. Vaccine. 2010 Oct 28;28(46):7427-35.

18. Coler RN, Goto Y, Bogatzki L, Raman V, Reed SG. Leish-111f, a recombinant polyprotein vaccine that protects against visceral Leishmaniasis by elicitation of CD4+ T cells. Infect Immun. 2007 Sep;75(9):4648-54.

19. Coler RN, Skeiky YA, Bernards K, Greeson K, Carter D, Cornellison CD, et al. Immunization with a polyprotein vaccine consisting of the T-Cell antigens thiol-specific antioxidant, *Leishmania major* stress-inducible protein 1, and *Leishmania* elongation initiation factor protects against leishmaniasis. Infect Immun. 2002 Aug;70(8):4215-25.

20. Kedzierski L, Zhu Y, Handman E. *Leishmania* vaccines: progress and problems. Parasitology. 2006;133 Suppl:S87-112.

21. Seder RA, Ahmed R. Similarities and differences in $CD4^+$ and $CD8^+$ effector and memory T cell generation. Nat Immunol. 2003 Sep;4(9):835-42.

22. Jordan KA, Hunter CA. Regulation of $CD8^+$ T cell responses to infection with parasitic protozoa. Exp Parasitol. 2010 Nov;126(3):318-25.

23. Tan JT, Surh CD. T cell memory. Curr Top Microbiol Immunol. 2006;311:85-115.

24. Zaph C, Uzonna J, Beverley SM, Scott P. Central memory T cells mediate long-term immunity to *Leishmania major* in the absence of persistent parasites. Nat Med. 2004 Oct;10(10):1104-10.

25. Shedlock DJ, Shen H. Requirement for CD4 T cell help in generating functional CD8 T cell memory. Science. 2003 Apr 11;300(5617):337-9.

26. Joshi T, Rodriguez S, Perovic V, Cockburn IA, Stager S. B7-H1 blockade increases survival of dysfunctional CD8(+) T cells and confers protection against *Leishmania donovani* infections. PLoS Pathog. 2009 May;5(5):e1000431.

27. Basu R, Bhaumik S, Haldar AK, Naskar K, De T, Dana SK, et al. Hybrid cell vaccination resolves *Leishmania* donovani infection by eliciting a strong CD8+ cytotoxic T-lymphocyte response with concomitant suppression of interleukin-10 (IL-10) but not IL-4 or IL-13. Infect Immun. 2007 Dec;75(12):5956-66.

28. Polley R, Stager S, Prickett S, Maroof A, Zubairi S, Smith DF, et al. Adoptive immunotherapy against experimental visceral leishmaniasis with CD8+ T cells requires the presence of cognate antigen. Infect Immun. 2006 Jan;74(1):773-6.

29. Belkaid Y, Von Stebut E, Mendez S, Lira R, Caler E, Bertholet S, et al. $CD8^+$ T cells are required for primary immunity in C57BL/6 mice following low-dose, intradermal challenge with *Leishmania major*. J Immunol. 2002 Apr 15;168(8):3992-4000.

30. Muller I, Kropf P, Louis JA, Milon G. Expansion of gamma interferon-producing $CD8^+$ T cells following secondary infection of mice immune to *Leishmania major*. Infect Immun. 1994 Jun;62(6):2575-81.

31. Denton H, McGregor JC, Coombs GH. Reduction of anti-leishmanial pentavalent antimonial drugs by a parasite-specific thiol-dependent reductase, TDR1. Biochem J. 2004 Jul 15;381(Pt 2):405-12.

32. Muller S, Liebau E, Walter RD, Krauth-Siegel RL. Thiol-based redox metabolism of protozoan parasites. Trends Parasitol. 2003 Jul;19(7):320-8.

33. Ouaissi A, Guevara-Espinoza A, Chabe F, Gomez-Corvera R, Taibi A. A novel and basic mechanism of immunosuppression in Chagas' disease: *Trypanosoma cruzi* releases *in vitro* and *in vivo* a protein which induces T cell unresponsiveness through specific interaction with cysteine and glutathione. Immunol Lett. 1995 Dec;48(3):221-4.

34. Garzon E, Borges MC, Cordeiro-da-Silva A, Nacife V, Meirelles Mde N, Guilvard E, et al. *Trypanosoma cruzi* carrying a targeted deletion of a Tc52 protein-encoding allele elicits attenuated Chagas' disease in mice. Immunol Lett. 2003 Oct 9;89(1):67-80.

35. Moutiez M, Quemeneur E, Sergheraert C, Lucas V, Tartar A, Davioud-Charvet E. Glutathione-dependent activities of *Trypanosoma cruzi* p52 makes it a new member of the thiol:disulphide oxidoreductase family. Biochem J. 1997 Feb 15;322 43-8.

36. Sereno D, Lemesre JL. Axenically cultured amastigote forms as an *in vitro* model for investigation of antileishmanial agents. Antimicrob Agents Chemother. 1997 May;41(5):972-6.

37. Hausler T, Stierhof YD, Wirtz E, Clayton C. Import of a DHFR hybrid protein into glycosomes in vivo is not inhibited by the folate-analogue aminopterin. J Cell Biol. 1996 Feb;132(3):311-24.

38. Buffet PA, Sulahian A, Garin YJ, Nassar N, Derouin F. Culture microtitration: a sensitive method for quantifying *Leishmania infantum* in tissues of infected mice. Antimicrob Agents Chemother. 1995 Sep;39(9):2167-8.

39. Cordeiro-Da-Silva A, Borges MC, Guilvard E, Ouaissi A. Dual role of the *Leishmania major* ribosomal protein S3a homologue in regulation of T- and B-cell activation. Infect Immun. 2001 Nov;69(11):6588-96.

40. Silvestre R, Cordeiro-Da-Silva A, Santarem N, Vergnes B, Sereno D, Ouaissi A. SIR2-deficient *Leishmania infantum* induces a defined IFN-gamma/IL-10 pattern that correlates with protection. J Immunol. 2007 Sep 1;179(5):3161-70.

41. Pan JL, Bardwell JC. The origami of thioredoxin-like folds. Protein Sci. 2006 Oct;15(10):2217-27.

42. Castro H, Tomas AM. Peroxidases of trypanosomatids. Antioxid Redox Signal. 2008 Sep;10(9):1593-606.

43. Cabral SM, Silvestre RL, Santarem NM, Tavares JC, Silva AF, Cordeiro-da-Silva A. A *Leishmania infantum* cytosolic tryparedoxin activates B cells to secrete interleukin-10 and specific immunoglobulin. Immunology. 2008 Apr;123(4):555-65.

44. Stober CB, Lange UG, Roberts MT, Alcami A, Blackwell JM. IL-10 from regulatory T cells determines vaccine efficacy in murine *Leishmania major* infection. J Immunol. 2005 Aug 15;175(4):2517-24.

45. Peters N, Sacks D. Immune privilege in sites of chronic infection: *Leishmania* and regulatory T cells. Immunol Rev. 2006 Oct;213:159-79.

46. Nylen S, Sacks D. Interleukin-10 and the pathogenesis of human visceral leishmaniasis. Trends Immunol. 2007 Sep;28(9):378-84.

47. Kaech SM, Wherry EJ, Ahmed R. Effector and memory T-cell differentiation: implications for vaccine development. Nat Rev Immunol. 2002 Apr;2(4):251-62.

48. DeGrendele HC, Estess P, Siegelman MH. Requirement for CD44 in activated T cell extravasation into an inflammatory site. Science. 1997 Oct 24;278(5338):672-5.

49. Jung TM, Gallatin WM, Weissman IL, Dailey MO. Down-regulation of homing receptors after T cell activation. J Immunol. 1988 Dec 15;141(12):4110-7.

50. Ivens AC, Peacock CS, Worthey EA, Murphy L, Aggarwal G, Berriman M, et al. The genome of the kinetoplastid parasite, *Leishmania major*. Science. 2005 Jul 15;309(5733):436-42.

51. McConville MJ, Mullin KA, Ilgoutz SC, Teasdale RD. Secretory pathway of trypanosomatid parasites. Microbiol Mol Biol Rev. 2002 Mar;66(1):122-54.

52. Cuervo P, De Jesus JB, Saboia-Vahia L, Mendonca-Lima L, Domont GB, Cupolillo E. Proteomic characterization of the released/secreted proteins of *Leishmania (Viannia) braziliensis* promastigotes. J Proteomics. 2009 Nov 2;73(1):79-92.

53. Silverman JM, Chan SK, Robinson DP, Dwyer DM, Nandan D, Foster LJ, et al. Proteomic analysis of the secretome of *Leishmania donovani*. Genome Biol. 2008;9(2):R35.

54. Wilson ME, Jeronimo SM, Pearson RD. Immunopathogenesis of infection with the visceralizing *Leishmania* species. Microb Pathog. 2005 Apr;38(4):147-60.

55. Murphy ML, Wille U, Villegas EN, Hunter CA, Farrell JP. IL-10 mediates susceptibility to *Leishmania donovani* infection. Eur J Immunol. 2001 Oct;31(10):2848-56.

56. Martin S, Pahari S, Sudan R, Saha B. CD40 signaling in $CD8^{+}CD40^{+}$ T cells turns on contra-T regulatory cell functions. J Immunol. 2010 May 15;184(10):5510-8.

57. Chu N, Thomas BN, Patel SR, Buxbaum LU. IgG1 is pathogenic in *Leishmania mexicana* infection. J Immunol. 2010 Dec 1;185(11):6939-46.

Supporting Information

Material and Methods

Flow cytometry determinations

L. infantum promastigotes and axenic amastigotes were washed twice in PBS-BSA and permeabilized before incubation for 30 min at 4ºC with mouse anti-*Li*TDR1 serum. After two washes with PBS–BSA, the parasites were incubated for 30 min at 4ºC with Alexa Fluor®-488 goat anti-mouse IgG (Molecular Probes). Labelled parasites were washed twice and resuspended in PBS–BSA followed by analysis in a FACSCalibur (Becton Dickinson).

Immunoprecipitation

L. infantum promastigotes and axenic amastigotes were incubated in methionine-free medium (Sigma) at 27ºC or 37ºC, respectively. After 1h, the parasites were washed twice at 2000 x g for 5min and resuspendend in medium containing 6.25µl of 500 µCi [^{35}S] methionine (Amersham) per ml. After 1h incubation as above, the parasites were washed two times and resuspended in RPMI complete medium or MAA/20 medium. Aliquots of 1mL were harvested by centrifugation at 3 or 6h, the pellet was subjected to lysis for 1h at 4ºC and the supernatant incubated for 3 h at 4ºC with serum against TDR1 or pre-immune serum. The immunocomplexes were captured by the addition of 100 µl protein G sepharose (Sigma), overnight at 4°C. After incubation the protein G sepharose was collected by centrifugation, washed, resuspended in 2x SDS sample buffer and incubated 1h at 56ºC. The beads were collected by centrifugation and supernatant subjected to SDS-PAGE analysis. After running, the gel was fixed, dried and exposed to X-ray film for 2 days at -80ºC.

In vitro cytotoxicity assays

In vitro cytotoxicity assay was performed by flow cytometry using a LIVE/DEAD cell-mediated cytotoxicity kit (Molecular Probes) according to the manufacturer's protocol. Spleen cells were stimulated with 50µg/ml of soluble *Leishmania* antigens (SLA) for 7 days (effector cells); as target cells were used J774 macrophages infected with *L. infantum*. Briefly, effector cells were incubated for 4h with 3,3-dioctadecylloxacarbocyanine ($DIOC_{18}$) target cells at different effector/target (E/T) cell ratios (5:1, 20:1 and 50:1) in the presence of propidium iodide. Cells were analyzed in a FACSCalibur (Becton Dickinson). The percentage of specific lysis was calculated as follows: [(dead target cells/all target cells)$_{+\ effectors}$ – (dead target cells/all target cells)$_{-effectors}$] x 100.

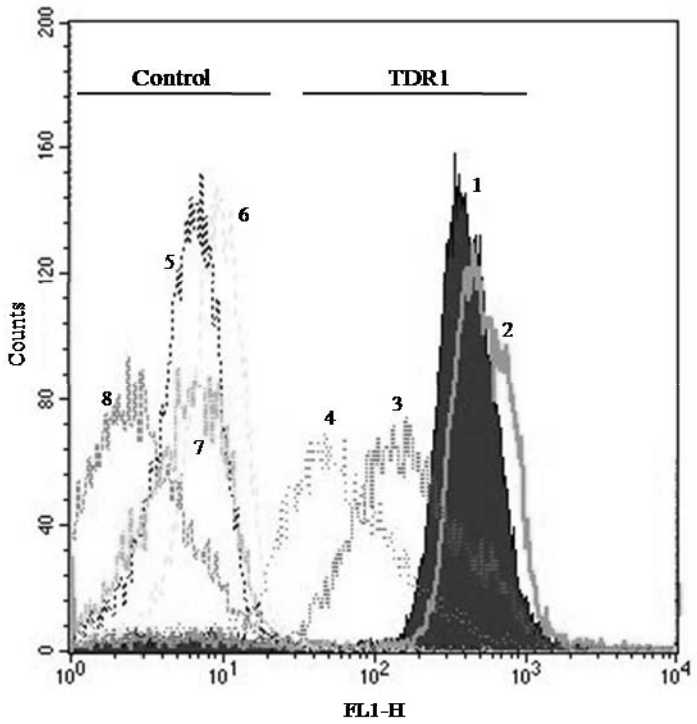

Figure S1. Flow cytometry analysis of TDR1 expression in *L. infantum* promastigotes and axenic amastigotes. *L. infantum* parasites were incubated with mouse anti-TDR1 polyclonal antibody and Alexa Fluor®-488 goat anti-mouse IgG was used as secondary antibody (TDR1). Parasites labeled just with secondary antibody were used as control (Control). TDR1 labelled parasites: early log phase promastigotes (1), late log phase promastigotes (2), stationary phase promastigotes (3) and axenic amastigotes (4); Control labelled parasites: early log phase promastigotes (5), late log phase promastigotes (6), stationary phase promastigotes (7) and axenic amastigotes (8). The results are representative of two experiments carried out independently.

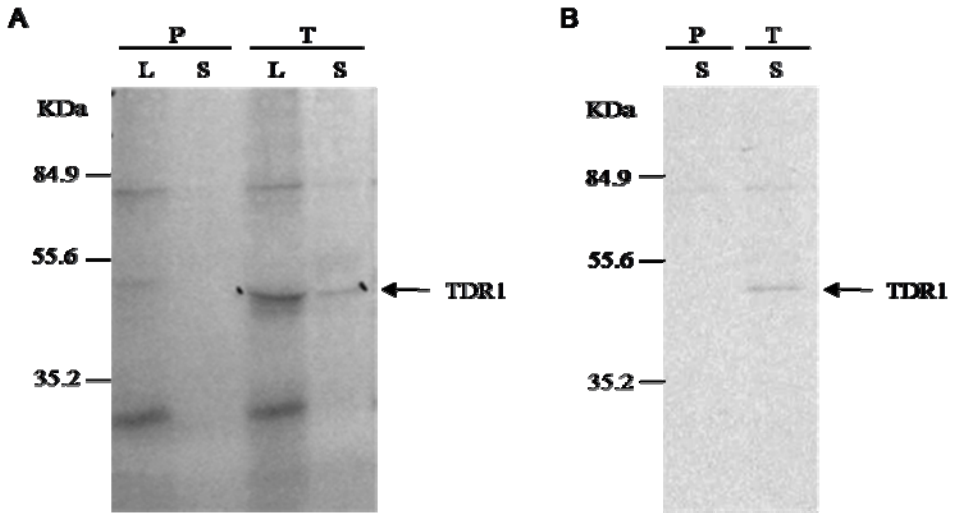

Figure S2. Identification of *L. infantum* TDR1 as an excreted/secreted antigen. *L. infantum* promastigotes (A) or axenic amastigotes (B) were metabolically labelled with [^{35}S] methionine for 3h and 6h, respectively. TDR1 protein from parasite lysate (L) or supernatant (S) was immunoprecipitated with a specific antibody (T) and the immunocomplexes were analyzed by 10% SDS-PAGE, followed by autoradiography of the dried gels. A pre-immune serum (P) was used as control. Estimated molecular masses and TDR1 protein (arrowed) are indicated on the left and right, respectively.

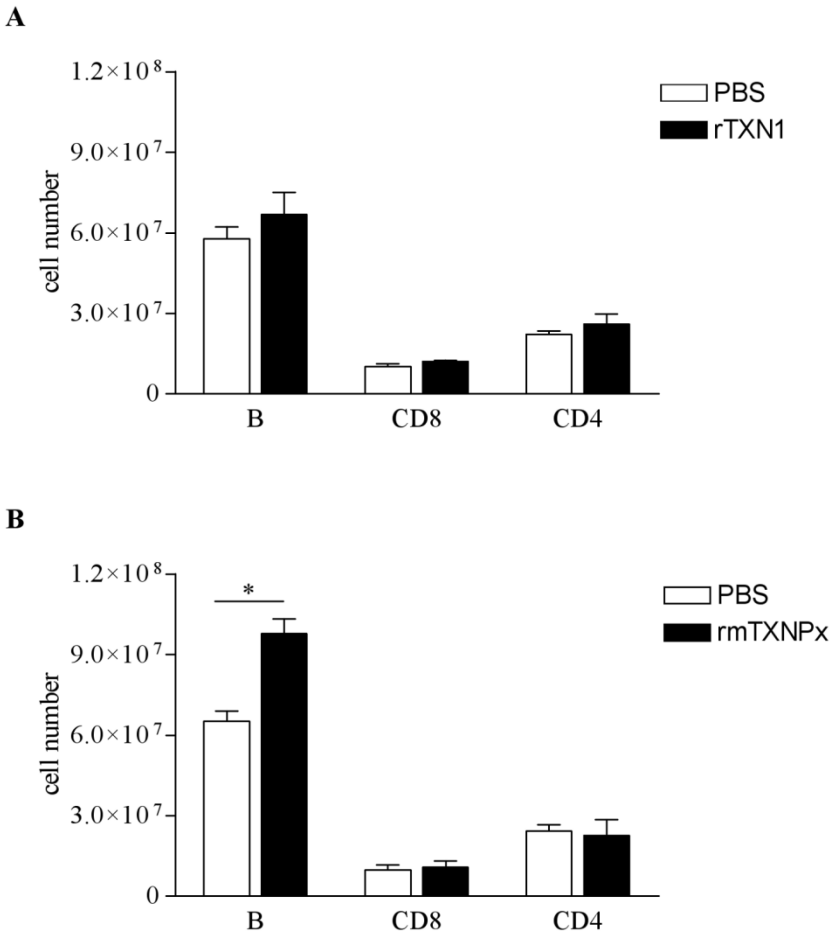

Figure S3. Splenic cell populations in Balb/c mice immunized either with (A) rTXN or (B) rmTXNPx. Balb/c mice were immunized i.p. with rTXN1 or rTXNPx three times with an interval of one week between each injection. The control group received PBS injections. Two weeks after the last immunization, the mice were sacrificed and spleens recovered. Spleen cells were analyzed by flow cytometry to determine the percentage of B cells, CD4- and CD8-T cells. The number of each cell subpopulation was calculated based on the total viable cells determined by trypan blue exclusion and the percentage of cell bound to the specific cell marker (anti-CD4, anti-CD8, anti-μ). The data represent the mean and standard deviations of three animals analyzed individually. Statistically significant differences between TDR1 and PBS groups are indicated * $p<0.05$.

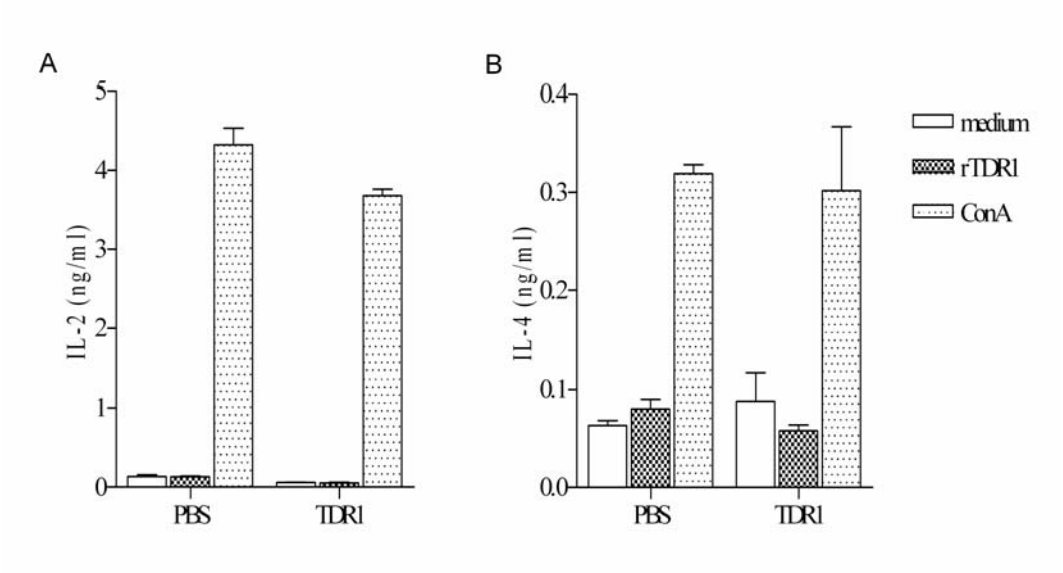

Figure S4. IL-2 and IL-4 cytokine production induced by immunization with rTDR1. Balb/c mice were immunized i.p. with 25µg of rTDR1 three times with an interval of one week between each injection. The control group received PBS injections. Two weeks after the last immunization the mice were sacrificed and spleen recovered. Cytokine production was quantified in the supernatant of spleen cells cultures by ELISA. Spleen cells ($2.5x10^5$) were stimulated with rTDR1 protein (10µg/ml) or ConA (6µg/ml) during 24 and 48h for quantification of IL-2 (A) and IL-4 (B) production, respectively. The data represent the mean and standard deviations of three animals analyzed individually and are representative of three experiments carried out independently.

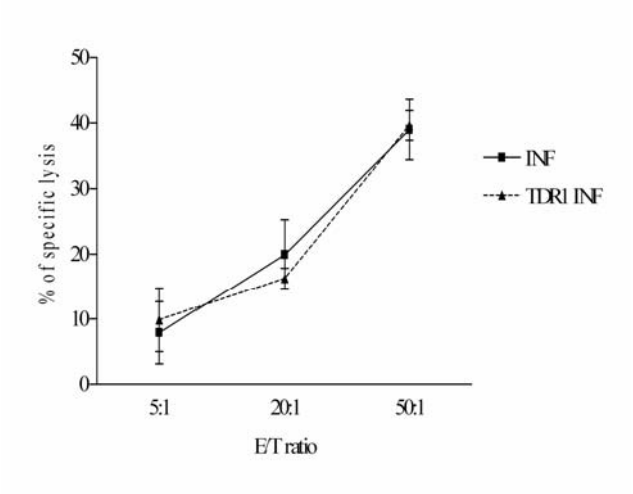

Figure S5. *In vitro* cytotoxicity of spleen cells from *L. infantum* rTDR1 immunized and infected mice. Lysis of *L. infantum*-infected J774 macrophages (target cells) by SLA stimulated splenocytes (effector cells) isolated from infected (INF) or rTDR1-immunnized infected (TDR1 INF) Balb/c mice 9 weeks post-infection with *L. infantum.* Effector cells were incubated with target cells at different effector/ target cells ratio (E/T) - 5:1, 20:1 and 50:1. The data represent the mean and standard deviations of three animals analyzed individually.

DNA vaccine encoding TDR1 do not protect Balb/c mice from infection with *Leishmania infantum*

Abstract

Parasitic protozoa, such as *Leishmania spp*., are responsible for several medically important tropical diseases, like visceral leishmaniasis, considered an important health problem that affects millions of people worldwide. Due to drug inefficacy and increase resistance is urgent to develop new vaccine candidates. DNA vaccination seems to be a promising tool and may offer a new alternative for the control of infectious diseases, once it is able to induce a complete immune response against the encoded antigen. Previously, we have shown that a *Leishmania* enzyme named Thiol Dependent Reductase 1 (TDR1) in the context of infection could induce some protection, through the increase of CD8-T cells population and decrease in IL-10 production, despite the high production of specific IgG1 that correlates with a Th2 profile. In order to enhance the levels of protection induced by TDR1, particularly the cellular response, we have produced a DNA vaccine encoding TDR1 protein (pVAX1-*TDR1*). Intramuscular immunization of Balb/c mice with pVAX1-*TDR1* was able to induce a high production of specific IgG2a that was maintained 2, 5 and 9 weeks after infection with *L. infantum* promastigotes. However, no protection was observed in mice immunized with the DNA vaccine. Prime-boost vaccination with the recombinant protein led to a lower IgG2a/IgG1 ratio due to an increase in IgG1 specific production and didn't induce protection at 5 and 9 weeks after *L. infantum* infection, lacking as before the induction of a cellular response. Delivery of TDR1 as a DNA vaccine did not improve the protection observed after administration of the recombinant protein. This highlights the fact that not all DNA vaccines will lead to successful results, due to several factors such as the encoding gene, the plasmid backbone and the route of delivery necessary to obtain the activation of the immune response and consequent protection.

Unpublished results

Introduction

Leishmaniasis is a disease caused by the protozoan parasites of the genus Leishmania. More than 20 species of *Leishmania* are responsible for complex clinical manifestations, which range from self-healing cutaneous ulcers to fatal visceral disease (22). The clinical outcome depends mainly on the infecting specie: cutaneous leishmaniasis (CL) is caused by infection with *L. major*, *L. braziliensis* among others whereas visceral leishmaniasis (VL) caused by infection with species from the *L. donovani* complex (8, 34). Leishmaniasis remains a major public health problem making part of the neglected tropical diseases (14), with 350 million people at risk worldwide and 2 million estimated new cases every year in 88 countries (22). CL predominates in Latin America, central Asia and north Africa (34) while 90% of the world's VL occurs in India, Bangladesh, Nepal, Sudan and Brazil (8). Moreover, leishmaniasis is complicated by human immunodeficiency virus (HIV) co-infection, which increases the risk of developing active VL by between 100 and 2320 times (1). There is still no effective vaccine for use in humans against leishmaniasis and the drugs available (36) are costly, toxic, limited and increase in drug resistance has been reported (11). Currently, a licensed vaccine, named Leishmune, based on fucose-mannose ligand antigen, present on the surface of the parasite throughout parasite life cycle, plus a saponin adjuvant is being used against canine visceral leishmaniasis. This vaccine is considered a transmission blocking vaccine since antibodies raised against Leishmume are able to block the parasite development in the sand fly rendering the vector non-infectious (4, 35).

Studies on antileishmanial vaccine candidates have increased remarkably in the recent years, largely due to a better understanding of the mechanisms necessary to induce immunity and the availability of *Leishmania* genome sequences. Several vaccine formulations provided partial protection, however there is no fully effective vaccine against leishmaniasis. An ideal vaccine should meet several attributes such as safety, low cost, be effective against species causing CL and VL, induce CD8-T and CD4-T cell responses and long-term immunological memory (23). In addition, an effective vaccine should efficiently stimulate dendritic cells (DC) as they play a key role in inducing both humoral and cellular responses (47). In the search for a vaccine against leishmaniasis have been used different strategies, including killed, live attenuated parasites, recombinant proteins or DNA vaccination among others (reviewed in (29)).

Live attenuated vaccines are considered a good strategy as the use of parasites that are infectious but not pathogenic closely mimics a natural infection (38), which may lead to parasite persistence that seems to be important for an effective protective response (21,

31). Examples of two successful live attenuated vaccines in murine models are *L. infantum* Sir2-deficient (40) and *L. donovani* centrin null mutants (37) parasites, protection correlated with an increase in the IFN-γ/IL-10 ratio. However, vaccination with genetically modified parasites should be used carefully because the attenuated parasites may revert back to a virulent form.

Several *Leishmania* antigens have been tested as possible vaccine candidates, chosen based in the protein expression, localization and involvement in parasite survival. These include LACK (27), HASPB1 (41), PSA-2 (18) among many others, administered alone or with adjuvants (reviewed in (29)) such as CpG (20, 46) , IL-12 (16, 41) or encapsulated in liposomes (2, 3, 28). Vaccination with recombinant proteins led to a variety of protection levels through the induction of a Th1 response involving the generation of specific INF-γ producing CD4-T and CD8-T cells. Although necessary for protection the Th1 response may not be sufficient to induce protection against *Leishmania* challenge. Leish-F1+MPL-SE consists of three recombinant *Leishmania* proteins (TSA, LmSTI1 and LeIF), together with the adjuvant monophosphoryl lipid and squalene in a stable emulsion (MPL-SE) (10). Leish-F1+MPL-SE was considered safe and immunogenic against CL when administered alone (48) or in conjugation with antimonials in human clinical trials (25, 30). In recent study was reported that LEISH-F1 + MPL-SE vaccine is safe and immunogenic in healthy subjects with and without history of previous infection with *L. donovani* (7).

DNA vaccines are an attractive alternative to conventional methods of vaccination due to several features that include the ability to elicit humoral and cellular immune responses, which can be modulated by the addition of adjuvants such as cytokines or CpG (28, 39). Prime boosting strategies that involve priming with DNA and boosting with the respective recombinant protein or other antigen delivery systems have also been used (12, 26, 33, 45), since heterologous prime-boost leads to a synergistic enhancement of immunity to the target antigen (49). DNA compared to recombinant protein vaccines present some advantages, largely due to stability and low cost of production. Moreover DNA vaccines may provide better protection as they can induce the expression of *Leishmania* antigens folded in its native conformation and normal posttranslational modifications to occur similar to natural infection and potentially with unaltered antigenecity (39). Induction of both humoral and cellular immune responses by DNA vaccines is due to the ability of DC to present the encoded antigen in the context of MHC class I and MHC class II (known as cross-priming) as they can be directly transfected with the plasmid or take up soluble proteins and debris from apoptotic transfected cells (47). Moreover has been suggested that this form of antigen delivery induces longer lasting immune responses (15). There are many reports involving vaccination with DNA encoding *Leishmania* antigens, some of

them tested previously as recombinant proteins, including GP63 (50), LACK (16, 43), LmST11 and TSA (6), cysteine proteinases (32), ORFF (44) among others with a wide range of success rate (13, 29).

In this study we have evaluated the potential of TDR1 to protect Balb/c mice against leishmaniasis when delivered as a DNA vaccine or used in a heterologous prime-boost strategy. Previously we have shown that mice immunized with recombinant TDR1 were partial protected against infection with *L. infantum* promastigotes (Silva et al, unpublished data). Thus, in order to enhance the protection levels induced by recombinant protein against *Leishmania* infection, Balb/c mice were immunized with a plasmid DNA encoding TDR1. Despite, the induction of high levels of specific IgG's neither DNA vaccination alone or combined with the recombinant protein were able to protect Balb/c mice against *Leishmania* infection.

Material and Methods

Leishmania parasites

Leishmania infantum (clone MHOM/MA/67/ITMAP263) promastigotes were grown at 27ºC in RPMI medium (BioWhittaker) supplemented with 10% (v/v) heat inactivated fetal bovine serum (FBS, Gibco), 2 mM L-glutamine (Sigma), 20 mM Hepes (Gibco), 100 U/ml penicillin and 100 mg/ml streptomycin (BioWhittaker). Cultures were set up initially at a concentration of 1 x10^6 parasites/ml and sub-passaged every 5 days.

Plasmid constructs and DNA preparation

The *L. infantum* TDR1 gene was PCR amplified using *L. infantum* genomic DNA as template and the following forward (5'-CGAAGCTTAATATGGCCGCCCGCGCGCT AAAGCTATACGTC-3') and reverse (5'-GATCTAGATTACCCGCTCTGGGCCCTC CGTTGACGC-3') primers containing *HindIII* and *XbaI* restriction sites (underlined), respectively. Cycling conditions were as follows: 94ºC, 2 min; 30 cycles of 94ºC, 15 sec; 55ºC, 30 sec; 72ºC, 90 sec and 72ºC, 10 min. The PCR product (1368 bp) was cloned into pGEM-Teasy vector (Promega). All the transformants were identified by restriction analysis and one of the clones chosen to be confirmed by sequencing (Eurofins MWG Operon). The insert was excised by digestion with *HindIII-XbaI* (New England Biolabs) and sub-cloned into pVAX1 vector, resulting the construct pVAX1-*TDR1*, under the control of CMV promoter, inserted downstream of a kozak consensus sequence and in frame with an initiation codon. The DH5α *E. coli* strain was used as a host during cloning experiments and to propagate the plasmid. All the transformants were identified by

restriction analysis. Plasmid DNA was purified using Endofree Plasmid Megakit (Quiagen) according to the commercial protocol. DNA concentration was estimated in a Qubit fluorometer with Quant-IT DNA Assay Kit (Invitrogen).

***In vitro* expression of pVAX1-*TDR1* in L929 cells**

L929 cells were transfected with 5 µg of pVAX1-*TDR1* or with the empty plasmid (pVAX1) using the TransFast Transfection reagent (Promega) according to the manufacturer's protocol. Briefly, 2.5 x 10^5 cells were seeded on 6-well plates in RPMI medium (BioWhittaker) supplemented with 10% FBS (Gibco), 2 mM L-glutamine (Sigma) and 20 mM Hepes (Gibco), the DNA/TransFast reagent mixture added and cells incubated at 37ºC, 5% CO_2. Seventy two hours after transfection the cells were washed with phosphate buffered saline (PBS) and fixed in a PBS solution containing 4% paraformaldehyde, for 20 min at room temperature. After permeabilisation with 0.1% (v/v) Triton X-100 in PBS, cells were washed several times with PBS and blocked in PBS containing 1% bovine serum albumin (PBS-BSA) for 30 min at room temperature. Incubation with a polyclonal mouse anti-TDR1 (1:100 in PBS-BSA) was made in a humid chamber, for 1 h at room temperature. After several washes in PBS, cells were incubated with a secondary antibody, Alexa Fluor® 488 goat anti-mouse IgG (Molecular Probes) diluted 1:100 in PBS-BSA. Washed cells were mounted in Vectashield (Vector Laboratories) and analyzed with a fluorescent microscope (Axioskop-Carl Zeiss, Germany) at 1000x magnification.

For detection of TDR1 expression by western blot, seventy two hours after transfection L929 cells were harvested, washed two times with ice-cold PBS and lysed by the addition of 50 mM Tris/HCl pH 8.0, 0.25% (v/v) Triton X-100, 20% (v/v) glycerol, 2 mM EDTA, 10 µM E-64, 400 µM 1,10-phenanthroline, 2 µM pepstatin A and 1 mM PMSF. Insoluble cellular debris was removed by centrifugation at 12000 x g for 20 min at 4ºC, proteins separated by SDS-PAGE (12%) and blotted to nitrocellulose for Western Blot analysis. Western blots were probed with a polyclonal mouse anti-TDR1 and goat anti-mouse IgG peroxidase-conjugated (Southern Biotech) used as the secondary antibody. Development was performed with an ECL detection system (Amersham).

Cloning, expression and purification of recombinant TDR1

The *L. infantum TDR1* was PCR amplified using *L. infantum* genomic DNA as template and the following forward (5'GCCATATGGCCGCCCGCGCGCTAAAGCTATACGT
G-3') and reverse (5'-GATCTAGATTACCCGCTCTGGGCCCTCCGTTGACGC-3') primers containing *NdeI* and *XbaI* restriction sites (underlined), respectively. Amplification conditions were as follows: 94ºC, 2 min; 30 cycles of 94ºC, 15 sec; 55ºC, 30 sec; 72ºC, 90 sec and 72ºC, 10 min. The PCR product (1349bp) was cloned into pGEM-T Easy vector

(Promega). All the transformants were identified by restriction analysis and one of the clones chosen to be confirmed by sequencing (Eurofins MWG Operon). The insert was excised by digestion with *NdeI-XbaI* (New England Biolabs) and sub-cloned into the *Escherichia coli* expression vector pET28a+ in frame with an amino-terminal six-histidine tag (pET28a^{+} *TDR1*). Briefly, 500 ml cultures of recombinant *E. coli* BL21 (DE3) were induced to express TDR1 by the addition of 2 mM of isopropyl β D-thiogalactoside (IPTG), overnight at 15ºC. The induced culture was harvested and resuspended in 20 mM Tris/500 mM NaCl, pH 7.9 (Buffer A) containing 10 mM imidazole. The cells were lysed by sonication and the resulting suspension was centrifuged at 15000 x g for 30 min at 4 °C to remove cell debris. The clear supernatant containing soluble protein was applied on to a pre-equilibrated nickel-nitrilotriacetic acid (Ni-NTA) column (Qiagen). The column was washed with Buffer A containing 60 mM imidazole to remove the non-binding proteins and the His-tagged recombinant protein was eluted with Buffer A containing 250 mM of imidazole. After purification, the eluted fractions were pooled and buffer-exchanged into 20 mM Tris, 250 mM NaCl, pH 7.9 using a PD10 desalting column (GE Healthcare) and stored at -80ºC. The recombinant protein was designated rTDR1. To eliminate endotoxins, the recombinant protein was passed through an EndoTrap®red column (Profos, Germany) following manufacturer's instructions. Polyclonal antiserum against TDR1 was generated in mice by intraperitoneal (i.p.) injection of recombinant protein in incomplete Freund's adjuvant.

Immunization of mice and parasite challenge

Balb/c mice were obtained from Charles River (Spain) and maintained at the animal facilities of the Instituto de Biologia Molecular e Celular (IBMC, Porto, Portugal). Mice were kept six per cage and allowed food and water ad libitum.

Balb/c mice (8 or 9 animals/group and in the case of mock control 3 animals/group) were immunized with DNA or DNA plus rTDR1 as follow: a) three times intramuscularly (i.m.) at 2 weeks intervals with 100 µg of pVAX1-*TDR1* or pVAX1 (mock control); b) two times intramuscularly (i.m.) at 2 weeks intervals with 100 µg of pVAX1-TDR1 or pVAX1; c) two times intramuscularly (i.m.) at 2 weeks intervals with 100 µg of pVAX1-*TDR1* or pVAX1 plus 25 µg of rTDR1 2 weeks after the last DNA boost. Two weeks after the last immunization, mice were challenged i.p. with 10^8 *L. infantum* promastigotes in PBS. Mice immunized as described in a) were bled and sacrificed 2 weeks post infection and mice immunized as described in b) and c) were bled and sacrificed at 5 and 9 weeks post-infection; spleen, liver and sera were collected. The spleen from each individual mouse was gently dissected to obtain single cell suspensions for cell population and cytokine

production analysis. Splenocytes were washed and resuspended in RPMI complete medium to a concentration of 10^7 cells/ml.

Evaluation of parasite burden

Parasite quantification in the spleen and liver was performed by limiting dilution as previously described (5). Briefly, organs were removed, homogenised and resuspended in RPMI medium. Two-fold serial dilutions were prepared in flat bottom 96-well microtiter plates (Immune Plate Maxisorp; Nunc). After incubation for 15 days at 27ºC, plates were examined and the positive (presence of motile parasites) and negative (absence of motile parasites) wells were determined using an inverted microscope. The number of parasites per gram of organ (parasite load) was calculated as follows: parasite load = [(geometric mean of reciprocal titer from each quadruplicate cell culture/weight of homogenized organ) x reciprocal fraction of the homogenized organ inoculated into the first well].

Flow cytometry analysis

A total of 10^6 splenocytes resuspended in PBS supplemented with 10% (v/v) FBS were distributed into a 96-well microtiter culture plate and washed with PBS-2% FBS. For spleen cell population determinations, cells were incubated with saturating concentrations of fluorescein isothiocyanate (FITC)-conjugated rat anti-mouse CD8 (Ly-2) monoclonal antibody, FITC-conjugated rat anti-mouse CD4 (L3T4) from BD Pharmingen, FITC-conjugated goat anti-mouse IgM from Southern Biotechnology and phycoerythrin (PE)-conjugated rat anti-mouse MAC-1. After 30 min incubation on ice, the cells were washed three times with PBS-2% FBS and examined in a FACSCalibur (Becton Dickinson) using propidium iodide 0.25 μg/ml (BD Pharmingen) for cell death exclusion.

Cytokine ELISAs

Spleen cells were seeded at a density of 2×10^5 cells/well in the presence of rTDR1 (10 μg/ml), concanavalin A (Con A, 6 μg/ml) or medium alone. Plates were incubated for 48 h (for detection of IL-10 and IL-4) or 72 h (for detection of INF-γ) at 37ºC in 5% CO_2. The IFN-γ, IL-12p40 and IL-10 production in supernatants of splenocyte cultures was measured by two-site sandwich enzyme-linked immunosorbent assay (ELISA). Immunosorbent ninety-six-well flat-bottom microtiter plates (Immune Plate Maxisorp, Nunc) were coated overnight at 4º C with unlabeled rat antibodies to the cytokines: IFN-γ (R4-6A2 cell line), IL-12p40 (BVD4-1D11 cell line) and IL-10 (JES5-2A5 cell line) in carbonate buffer (pH 8.2). The plates were washed with PBS containing 0.1% Tween 20 (PBS-T) and blocked with PBS–1% BSA (200 μl/well) for 2 h at room temperature. The plates were incubated with serial dilutions of each supernatant for 2 h at room

temperature. After being washed with PBS-T, the plates were incubated for 1 h at room temperature with biotinylated rat antibodies (BD Pharmingen) to the following cytokines: IFN-γ (XMG1.2 cell line), IL-12p40 (JES6- 5H4 cell line) and IL-10 (SXC-1 cell line). After a subsequent wash with PBS-T, the plates were incubated for 1 h at room temperature with streptavidin-peroxidase (Sigma) and developed with o-phenylenediamine (OPD, Sigma) in citrate buffer (0.1 M citrate acid and 0.2 M Na_2HPO_4, pH 5.4) The optical densities were recorded at 450 nm. The concentration of specific interleukins was determined by comparison with a standard curve generated with different recombinant interleukins: rIFN-γ; rIL-12; and rIL10 (R&D Systems).

Detection of specific rTDR1 antibody response

Serum samples from animals immunized with pVAX1-*TDR1* or pVAX1-*TDR1* plus rTDR1 were analyzed by ELISA for TDR1-specific IgG, IgG1 and IgG2a subclasses before each immunization or challenge with *L. infantum* promastigotes and 2, 5, and 9 weeks post-infection. Ninety-six-well flat-bottom microtiter plates (microtiter immunoplates, Greiner Bioscience) were coated with rTDR1 (5 µg/ml) in carbonate buffer (pH 8.5) and incubated overnight at 4º C. The plates were washed with PBS-T and blocked with PBS-1% gelatin (200 µl/well) for 1 h at room temperature. The plates were incubated with 1/100 dilutions of each serum sample in triplicate for 1 h at 37ºC. After being washed with PBS-T, the plates were incubated for 30 min at room temperature with peroxidase-labeled goat anti-mouse immunoglobulin isotypes (anti-IgG, anti-IgG1, anti-IgG2a and anti-IgG2b) and developed with OPD (Sigma) in citrate buffer. Reactions were stopped with 3 M HCl and the absorbance was measured at 492 nm in an automatic ELISA reader.

Statistical analysis

Statistical analysis was performed using Student's T test. A p value smaller than 0.05 (p<0.05) was considered significant. GraphPad Prism 4 was used for plotting the graphs.

Results

Construction of DNA vaccine and transient expression in L929 cells

We have already shown that *Leishmania* TDR1 recombinant protein is able to induce partial protection in Balb/c mice challenged with *L. infantum* (Silva et al, unpublished data). In order to improve the protection levels we tested the administration of TDR1 in a DNA format, as an alternative mean of antigen delivery. *TDR1* gene was sub-cloned into

the eukaryotic expression vector pVAX1 for expression under the control of a strong cytomegalovirus (CMV) promoter (Fig. 1). To assess the expression of TDR1 in mammalian cells, L929 cells were transiently transfected with pVAX1-*TDR1* or with the empty vector (pVAX1) as a control and after 72h protein expression was evaluated by immunofluorescence (Fig. 2) and western blot (data not shown). Despite a low transfection efficacy was possible to detect L929 cells expressing TDR1, which shows that the plasmid leads to the correct expression of the protein in mammalian cells.

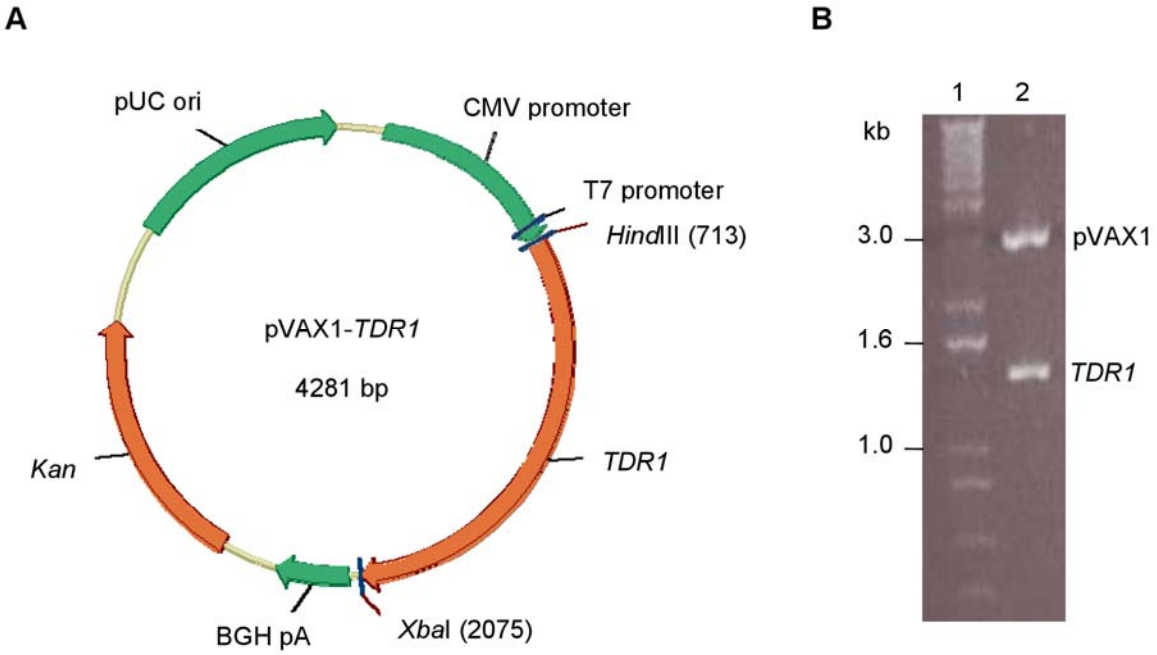

Figure 1. DNA vaccine construction. (A) Schematic representation of pVAX1-*TDR1* plasmid. The restriction sites used to sub-clone *TDR1* gene into pVAX1 were *Hind*III and *Xba*I. DNA vaccine transcription unit comprises of a CMV promoter (human cytomegalovirus immediate-early promoter), *TDR1* gene and a polyadenylation signal sequence (BGH pA, bovine growth hormone polyadenylation signal). A bacterial origin of replication (pUC ori) and an antibiotic resistance gene (Kan, kanamycin) are also incorporated in the vector backbone to allow growth and selection of the plasmid in bacteria (15). (B) pVAX1-*TDR1* plasmid analysis by double digest with *Hind*III and *Xba*I The samples were analysed in a 0.8% agarose gel and stained with ethidium bromide: 1Kb plus DNA ladder (lane 1) and pVAX1-*TDR1* plasmid (lane 2). DNA fragment identity and size (in kilobase pairs) are indicated on the right and left, respectively.

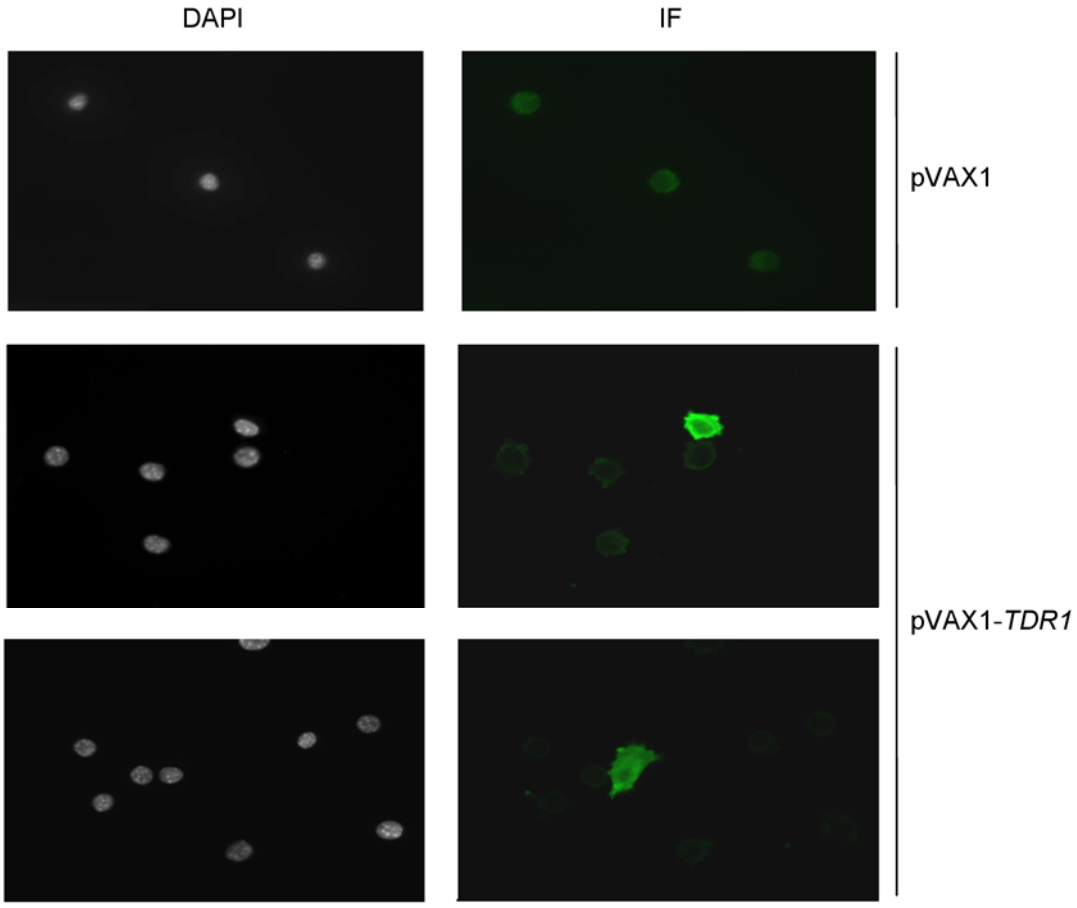

Figure 2. Transient expression of *TDR1* gene in L929 cells.
L929 cells transiently transfected with 5 µg of pVAX1-*TDR1* or with empty vector (pVAX1) were stained by immunofluorescence with anti-TDR1 polyclonal antibody. A second antibody Alexa-Fluor-488 goat anti-mouse IgG was used to detect the immune complex. Parasites were analyzed under a fluorescent microscope (Axioskop-Carl Zeiss, Germany) at 1000x magnification.

Humoral response induced by DNA vaccination before and after challenge with *L. infantum* promastigotes.

Antigen-specific immune response induced by DNA vaccination was used as a measure to monitorize the immunization efficacy, thus humoral responses were examined during immunization and after infection**.** First, we choose to immunize intramuscularly Balb/c mice three times with DNA before challenge (Fig. 3A), to evaluate if the third boost was necessary to induce a strong immune response, as in previous studies different protocols of immunization were used varying also the route of administration and the interval between the immunizations. Serum samples to evaluate the response induced by the 1st,

2nd and 3rd immunizations with DNA were collected and TDR1-specific IgG, IgG1 and IgG2a antibodies levels determined for each animal by ELISA. Fig. 3B-E shows the isotype profile obtained during immunization and also 2 weeks after infection. It is particular relevant the fact that for some animals after the second immunization was not detected the production of TDR1-specific antibodies (Fig. 3B-C) and in the case of animal 1 that was just detected after infection (Fig. 3D-E). This variability can be linked with the route and protocol of administration that can result in low and variable expression of the injected gene and influence the vaccination outcome, despite the high amount of DNA used to immunize mice. After the 2nd DNA immunization, 3 mice out of 6 showed high levels of TDR1-specific antibodies, with a high predominance of IgG2a levels, which suggests the induction of a Th1 response normally judged by the IgG2a/IgG1 ratio. IgG2a/IgG1 ratio has been used as a predictive measure for Th1 and Th2 responses since IgG2a levels are dependent on IFN-γ and IgG1 levels correlate with IL-4 (42)**.** Induction of high levels of IgG2a is not unexpected since DNA vaccines have an intrinsic adjuvant effect because of the presence of immune stimulatory CpG motifs**.** Unmethylated CpG dinucleotides in bacterial DNA or synthetic oligonucleotides (ODNs) cause B cell proliferation and preferentially elicit a Th1 type immune response by stimulating production of IL-12 and IFN-γ (17, 24).

The humoral response induced after the 3rd immunization was similar to the levels obtained after the 2nd boost, at least in the animals that already showed high levels of antibodies, suggesting that 2 immunizations with DNA should be enough to trigger an immune response due to TDR1 production. Accordingly to the humoral response observed during immunization in the analysis of further experiments mice were grouped into responders (R) and non-responders (NR), NR being mice for which is not detected the production of TDR1-specific antibodies. Infection with *L. infantum* leads to a switch in the specific-IgG production, since IgG2a predominance fades out in sera collected from mice 2 weeks after infection, while a large increase in the levels of IgG1 specific antibodies is detected leading to a decrease in IgG2a/IgG1 to levels near 1(Table 1)**.**

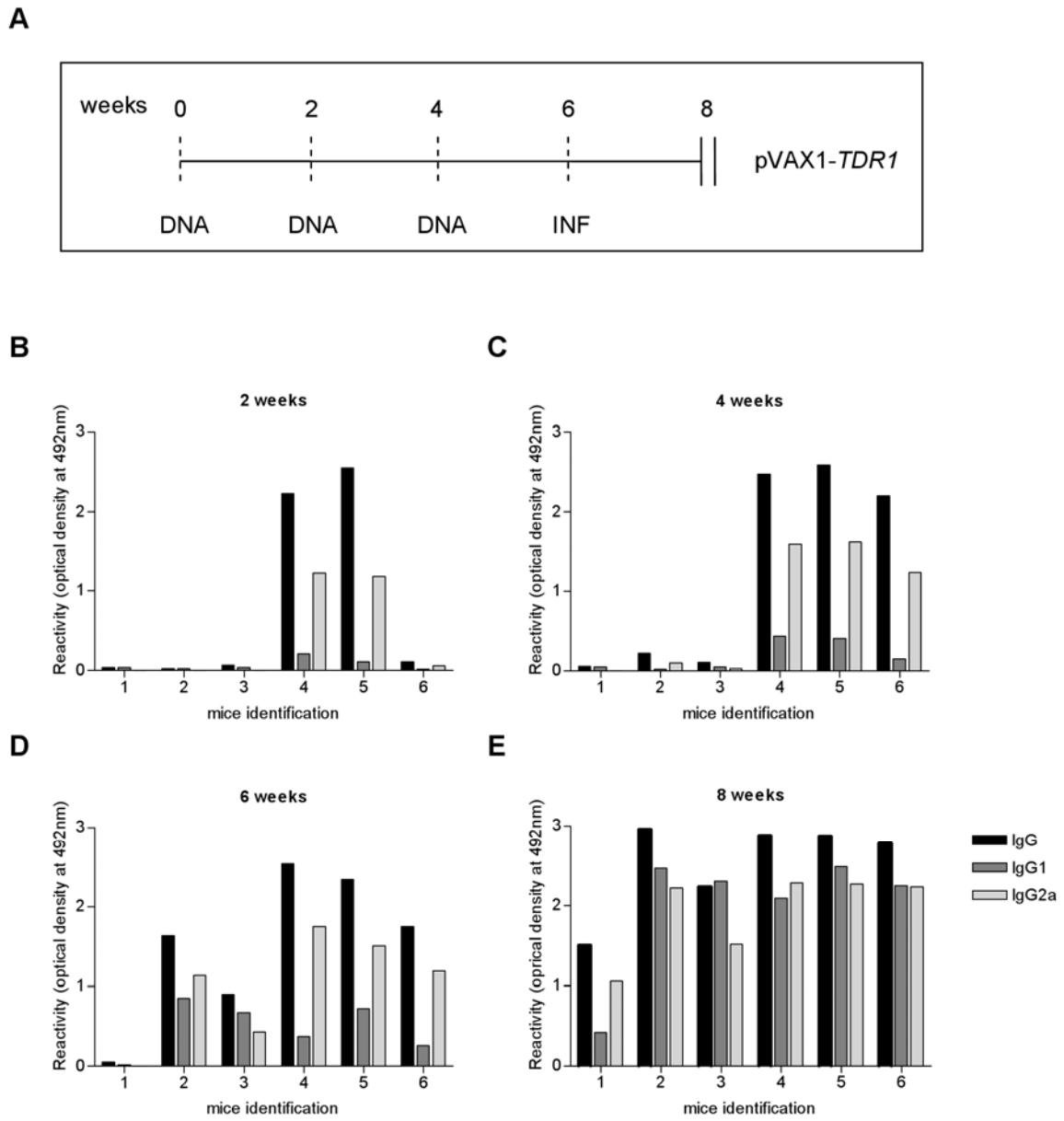

Figure 3. Analysis of specific humoral response induced by pVAX1-*TDR1* immunization in Balb/c mice before and after challenge with *L. infantum* promastigotes. (A) pVAX1-*TDR1* vaccination scheme. Mice were immunized 3 times intramuscularly (i. m.) with 100 µg of pVAX1-*TDR1* and control groups with the 100 µg of pVAX1 or with the correspondent volume of PBS. Mice were bled 2 weeks after first (B), second (C), third (D) immunizations and challenge with $1x10^8$ *L. infantum* promastigotes (E). A serum from each mouse immunized with pVAX1-*TDR1* (1-6) was tested individually at each time point by ELISA for IgG, IgG1 and IgG2a specific TDR1 antibodies production; sera from control groups showed no reactivity (data not shown).

Table 1 – Specific IgG2a and IgG1 responses in immunized mice before and after challenge

	IgG2a/IgG1			
	weeks after immunization			weeks after infection
Mice identification	2	4	6	2
1	0	0	0	2.5
2	0	3	1.3	0.9
3	0	0.6	0.6	0.7
4	5.8	3.7	4.7	1.1
5	10.7	3.9	2.1	0.9
6	3	8.2	4.6	1.0

Mice were immunized as described in Material and Methods. IgG2a/IgG1 levels represent the ratio of the absorbance at 490nm of specific antibodies for each animal (1-6) 2 weeks after the 1st, 2nd, 3rd DNA immunization and after infection with *L. infantum* promastigotes.

DNA vaccination failed to confer protection against *L. infantum* infection

To test the ability of immunization with a plasmid encoding TDR1 to protect Balb/c mice against *Leishmania* infection, mice were immunized with pVAX1-*TDR1* and challenged two weeks after the last boost. No differences were detected both in splenic and hepatic parasite load between vaccinated animals and control groups (pVAX1 or PBS) (Fig. 4).

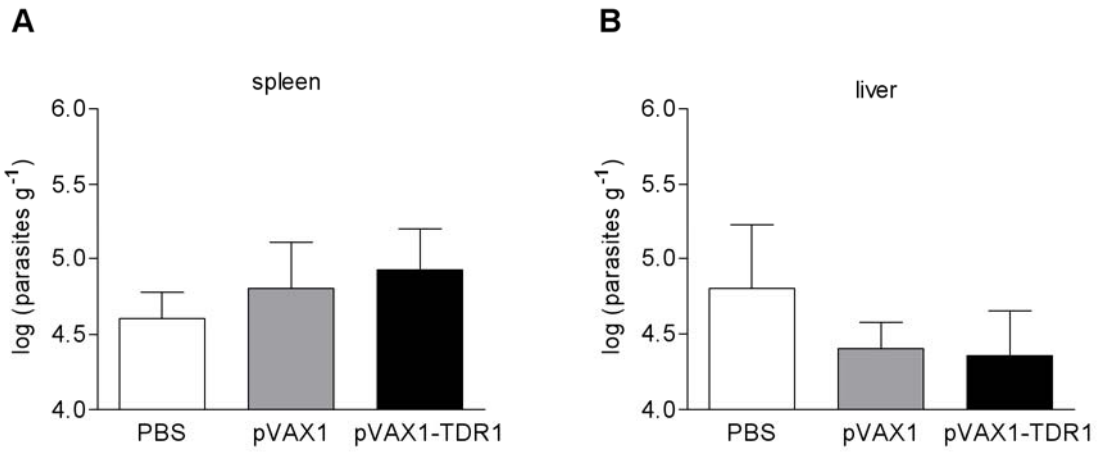

Figure 4. Parasite load in the spleen and liver of Balb/c mice immunized with pVAX1-*TDR1* determined 2 weeks after challenge with *L. infantum* promastigotes. Mice were immunized 3 times intramuscularly (i. m.) with 100 µg of pVAX1-*TDR1* and

control groups with 100 µg of pVAX1 or with the correspondent volume of PBS followed by challenge with $1x10^8$ *L. infantum* promastigotes. Limiting dilution analysis was performed 2 weeks after infection on the cells isolated from the spleen and liver of each individual mouse and cultured in quadruplicate for 2 weeks at 27º C. The cultures were then assessed microscopically for *L. infantum* viable parasites.

Nevertheless, we have reported before that rTDR1 protein is able to elicit partial protection in a chronic stage of *Leishmania* infection (Silva et al, submitted), thus we have assessed the ability of DNA vaccination to induce protection after longer periods of infection, 5 and 9 weeks after challenge with *L. infantum* promastigotes. Prime-boost vaccination regimens which includes the immunization with the DNA plasmid and boost with the recombinant protein are usually used to improve DNA vaccine immunogenicity, as DNA vaccination induces a strong Th1 immune response and thus is attractive as a priming strategy (19). In our study, we have performed in parallel the immunization with DNA and also the prime-boost vaccination, in which after two immunizations with the DNA vaccine, Balb/c mice were boosted with rTDR1 protein (Fig. 5A). However, 5 weeks post-infection, both vaccination regimens pVAX1-*TDR1* (Fig. 5B) or pVAX1-*TDR1*+rTDR1 (Fig.5C) failed to protect Balb/c mice against *L. infantum* infection, as there was no differences in splenic and hepatic parasite load between vaccinated and control groups, with exception of one animal from the DNA vaccine group (NR) that presents a considerable decrease in splenic parasite load and no parasites were detected in the liver.

Analysis of humoral response during immunization and after challenge (Fig. 6) reveals that as in the first experiment (Fig. 3) there are animals that do not produce TDR1-specific antibodies (Fig. 6A-B, E-F) and two weeks after the first DNA immunization was just detected the production of IgG2a specific antibodies, which increase in the second boost (Fig. 6B). Again, before infection the IgG2a/IgG1 ratio is higher than 5 weeks after the challenge (Fig. 6D), showing that infection with *Leishmania* leads to a change in the immunoglobulins profile, with a large increase in IgG1, thought to be detrimental for the infection resolution (9). In the case of animal 11 from the group vaccinated only with pVAX1-*TDR1* that showed a high level of protection, production of specific antibodies was only detected after infection, with IgG2a/IgG1 ratio levels near 1. However, other animals considered also as non-responders (animals 8, 9 and 10) even after infection did not produce TDR1-specific antibodies. Animals from the prime-boost regimen showed also high levels of IgG2a during immunization, sustained after the boost with the recombinant protein (Fig. 6F); nevertheless, immunization with rTDR1 led to an increase in IgG1 production to similar or higher levels than those observed for IgG2a (Fig. 6E). Figs. 6C

and 6G show the levels of TDR1-specific antibodies after infection induced by both vaccinations regimens. It is noteworthy to mention that one immunization with rTDR1 was enough to induce production of specific antibodies, since in animals considered as non-responders (animals 4, 8, 10 and 12) was only detected the production of specific antibodies after rTDR1 immunization and just 1 animal out of 4 presented higher levels of IgG2a than IgG1. In fact, we have already reported that immunization of Balb/c mice with rTDR1 induces preferentially the production of IgG1 with low levels of IgG2a specific antibodies (Silva et al, submitted).

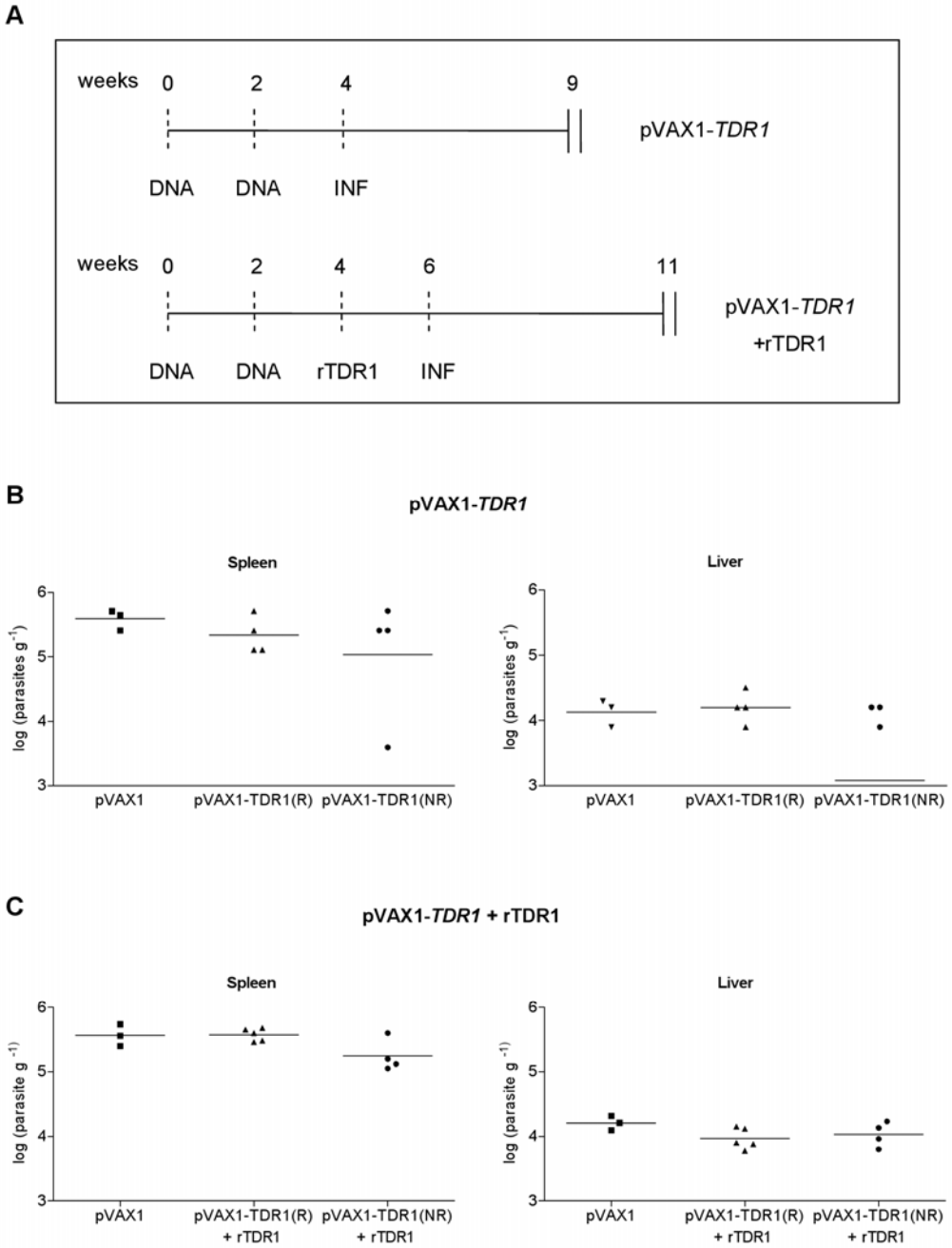

Figure 5. DNA vaccination or prime-boost regimens with pVAX1-*TDR1* do not protect Balb/c mice against *L. infantum* at 5 weeks post-infection. (A) DNA (pVAX1-

TDR1) and prime-boost (pVAX1-*TDR1*+rTDR1) vaccination schemes**.** Mice were immunized i.m. twice with 100 µg of plasmid DNA followed by challenge with $1x10^8$ *L. infantum* promastigotes or after the second DNA immunization boosted with 25µg of rTDR1 and 2 weeks later challenged with *L. infantum* promastigotes. Mice were grouped into non-responders (NR) or responders (R) taking into account the specific-TDR1 response produced during DNA immunization. Spleen and liver parasite load of immunized pVAX1-*TDR1* (B) or pVAX1-*TDR1*+rTDR1 (C) Balb/c mice 5 weeks after infection with *L. infantum* was determined by limiting dilution asssay. Limiting dilution analysis was performed on cells isolated from the spleen and liver of each individual mouse and cultured in quadruplicate for 2 weeks at 27º C. The cultures were then assessed microscopically for *L. infantum* viable parasites.
Indeed, a high level of IgG2a specific antibodies per se do not necessarily correlates with protection as animals with higher levels of IgG2a/IgG1 ratio than animal 11 were not protected. The differences observed could be potentially explained by the cellular immune response. Analysis of splenic cell populations (CD8- and CD4-Tcells, B cells and macrophages) did not reveal any differences in cell number (Table 2).

Spleen cells from vaccinated animals, either with pVAX1-*TDR1* or pVAX1-*TDR1*+rTDR1, included in the responders group, stimulated *ex-vivo* with rTDR1 produced higher amounts of IFN-γ than animals immunized with the empty vector (Fig. 7A-B). IL-10 levels were very low or undetectable although, in the case of pVAX1-*TDR1* immunization spleen cells from the control group when stimulated with rTDR1 produced higher levels of IL-10 than those from the vaccinated groups (Fig. 7C); no differences were observed in the IL-10 levels in the groups from the prime-boost regimen, except when cells were stimulated with ConA (Fig. 7D) and a similar profile among the different groups was observed in the levels of IL-12 with higher production by cells stimulated with rTDR1 than with SLA (Fig. 7E-F). Analysis of splenic parasite load 9 weeks post challenge with *Leishmania*, using the same immunization strategies described above (Fig. 8A) showed that DNA vaccination was not effective in protecting Balb/c mice from infection. Neverthless, DNA vaccination strategy seems slightly better that the prime boost regimen (Fig. 8B), although it is evident a high variability among the animals in the pVAX1-TDR1(R); there was no differences in liver parasite load. The immunoglobulins profile 9 weeks after infection was similar to the one observed in the earlier time point of infection analyzed, with IgG2a/IgG1 ratio around 1 in the prime boost regimen but higher in the DNA vaccination alone (Fig. 9); once again were detected animals that did not produce TDR1 antibodies, suggesting lower or no protein production at all. Given the fact that the protection was not achieved, parameters such as the cytokine production were not determined.

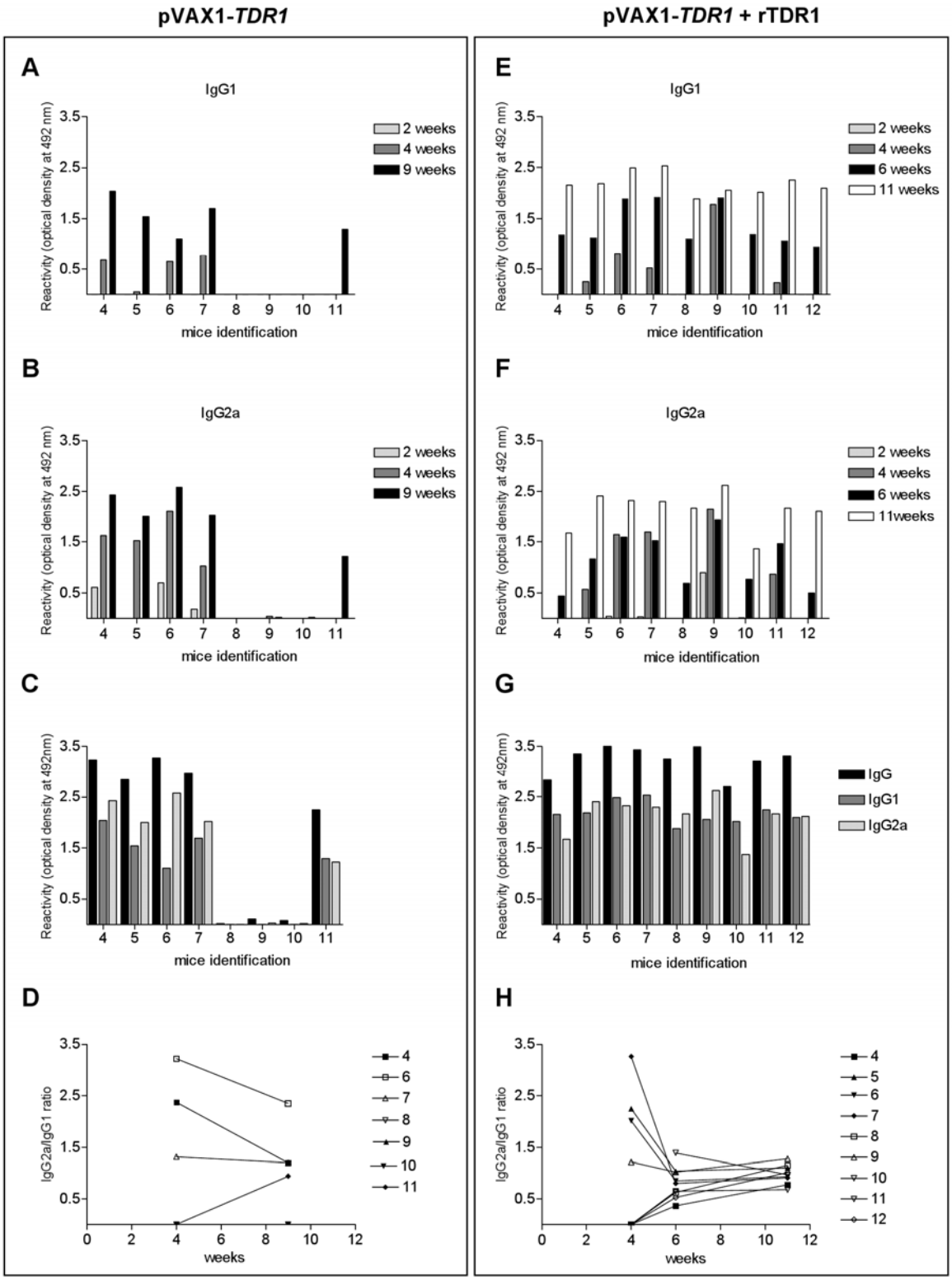

Figure 6. DNA vaccine elicits higher levels of IgG2a-specific TDR1 antibodies which decrease after rTDR1 immunization or *Leishmania* infection. Kinetics of specific isotype profile of antibody induced by immunization with pVAX1-*TDR1* (left panel) or pVAX1-*TDR1*+rTDR1 (right panel) after first (2 weeks) and second (4 weeks) immunizations, rTDR1 boost (6 weeks) and 5 weeks after challenge with *L. infantum* (9 or

11 weeks after first DNA immunization for the DNA vaccination or prime boost regimen, respectively). Left panel: animals 4, 5, 6 and 7 were included in pVAX1-*TDR1*(R) group and 8, 9, 10 and 11 in pVAX1-*TDR1*(NR) group; right panel: animals 5, 6, 7, 9 and 11 were included in pVAX1-TDR1(R) group and 4, 8, 10 and 12 in pVAX1-TDR1(NR) group. The sera from each individually mice collected during vaccination was used to monitorize the production of TDR1 specific IgG1 (A,E) and IgG2a (B,F) antibodies and 5 weeks after challenge (C, G). Ratio between TDR1-specific IgG2a and IgG1 levels during vaccination and 5 weeks post-infection (D, H).

Table 2- Analysis of immunized Balb/c mice spleen cell populations 5 weeks post-infection with *L. infantum* promastigotes

	Cell number ± SD (x10^7)			
	CD4	**CD8**	**B**	**MAC**
pVAX1-TDR1				
pVAX1	2.85 ± 0.304	1.03 ± 0.052	5.13 ± 0.358	0.309 ± 0.030
pVAX1-TDR1(R)	2.56 ± 0.314	1.02 ± 0.156	5.11 ± 0.548	0.328 ± 0.044
pVAX1-TDR1(NR)	2.28 ± 0.494	1.03 ± 0.250	4.94 ± 0.648	0.266 ± 0.029
pVAX1-TDR1 + rTDR1				
pVAX1 + rTDR1	2.17 ± 0.150	0.779 ± 0.032	3.71 ± 0.260	0.376 ± 0.022
pVAX1-TDR1(R) + rTDR1	2.08 ± 0.227	0.809 ± 0.091	4.12 ± 0.247	0.497 ± 0.056
pVAX1-TDR1(NR) + rTDR1	1.88 ± 0.139	0.751 ± 0.011	3.40 ± 0.574	0.372 ± 0.055

Mice were immunized as described in Material and Methods. Five weeks after infection with *L. infantum* promastigotes, spleens from Balb/c mice immunized with pVAX1-TDR1, pVAX1-TDR1 plus rTDR1 or pVAX1 were removed and single cell suspensions of each stained with monoclonal antibodies and analyzed on a FACScalibur flow cytometer. SD, standard deviation.

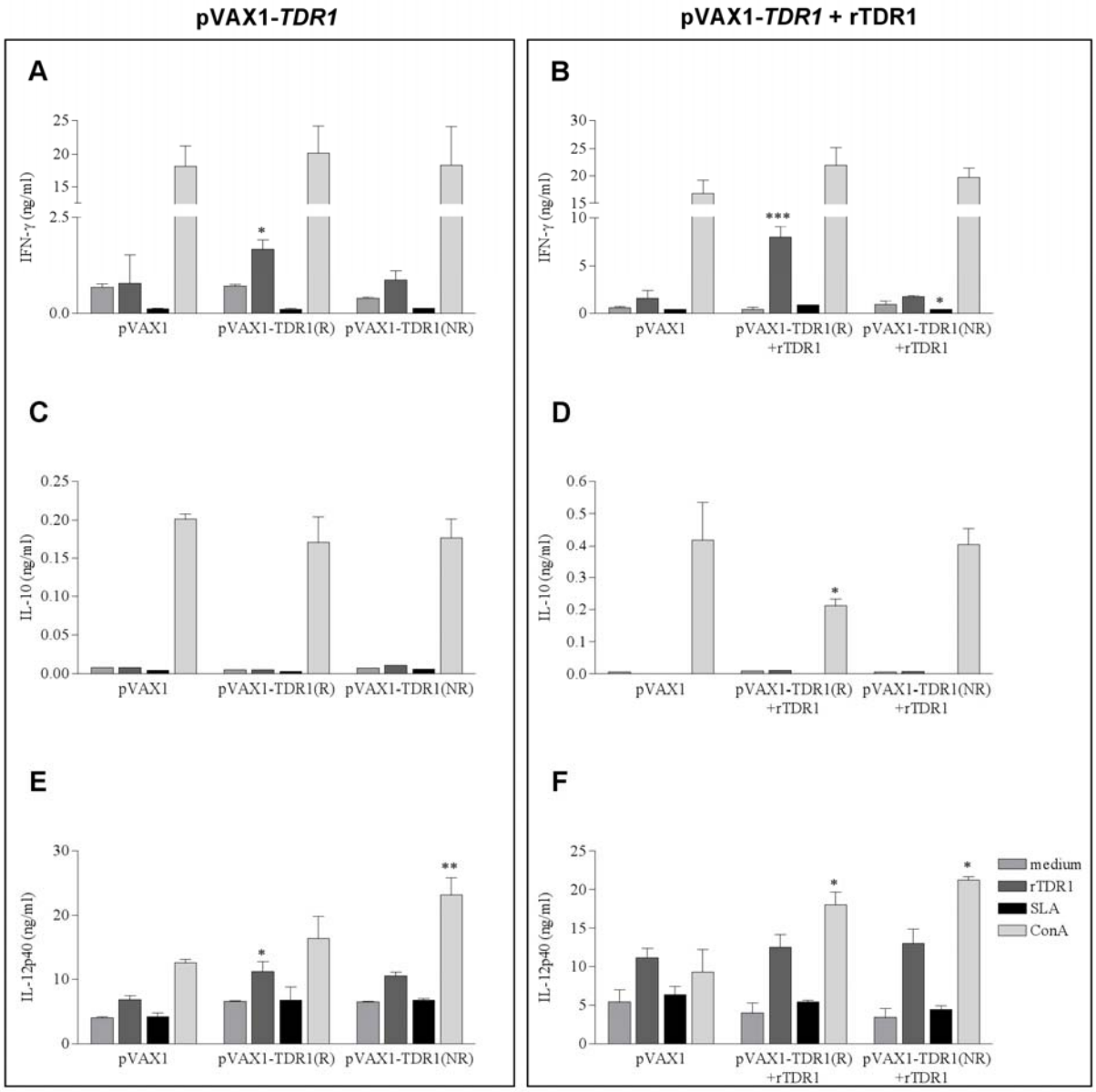

Figure 7. Cytokine production by spleen cells from Balb/c mice immunized with pVAX1-*TDR1* (left panel) or pVAX1-*TDR1*+rTDR1 (right panel) 5 weeks after infection with *L. infantum*. Mice were immunized i.m. twice with 100 µg of plasmid DNA followed by challenge with $1x10^8$ *L. infantum* promastigotes or after the second DNA immunization boosted with 25µg of rTDR1 and 2 weeks later challenged with *L. infantum* promastigotes. Five weeks post-infection mice were sacrificed and cells isolated from each individual mouse were stimulated with ConA (6µg/ml), rTDR1 (10µg/ml) and soluble *Leishmania* antigens (SLA) (10µg/ml) for quantification of INF-γ (A, B) production during 72 h, and for 48 h for quantification of IL-10 (C, D) and IL-12p40 (E, F) production. The data represent the mean ± SD of triplicate samples of three mice analyzed independently. Statistically significant differences between pVAX1-*TDR1* or pVAX1-*TDR1*+rTDR1 and pVAX1 groups are * $p<0.05$, ** $p<0.01$, *** $p<0.001$.

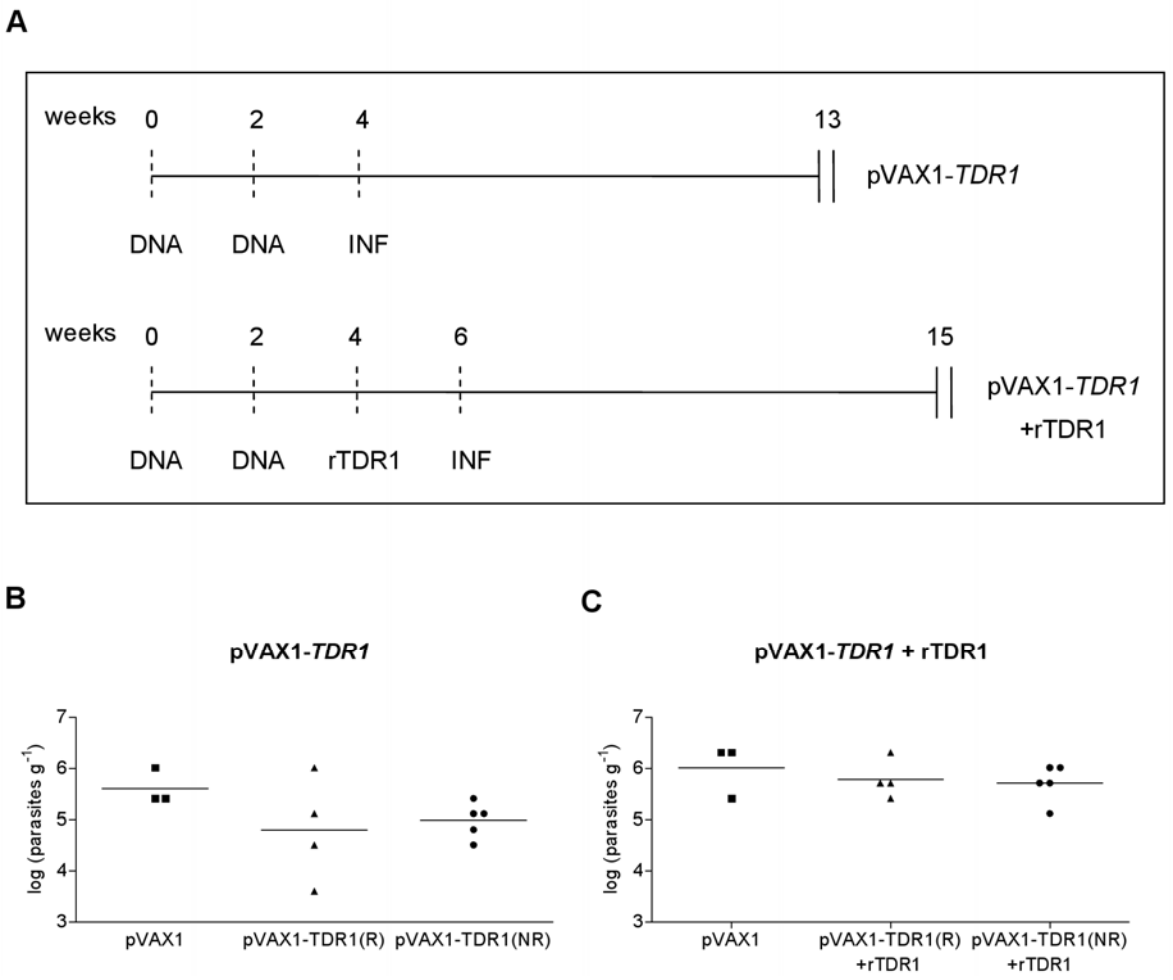

Figure 8. Parasite load in the spleen and liver of Balb/c mice immunized with pVAX1-*TDR1* determined 9 weeks after challenge with *L. infantum* promastigotes. (A) DNA (pVAX1-*TDR1*) and prime-boost (pVAX1-*TDR1*+rTDR1) vaccination schemes**.** Mice were immunized i.m. twice with 100 µg of pVAX1-*TDR1* and control groups with 100 µg of pVAX1 followed by challenge with $1x10^8$ *L. infantum* promastigotes. Spleen parasite load of immunized pVAX1-*TDR1* (B) or pVAX1-*TDR1*+rTDR1 (C) Balb/c mice 9 weeks after infection with *L. infantum* was determined by limiting dilution asssay. Mice were grouped into non-responders (NR) or responders (R) taking into account the specific-TDR1 response produced during DNA immunization. Limiting dilution analysis was performed on cells isolated from the spleen of each individual mouse and cultured in quadruplicate for 2 weeks at 27º C. The cultures were then assessed microscopically for *L. infantum* viable parasites.

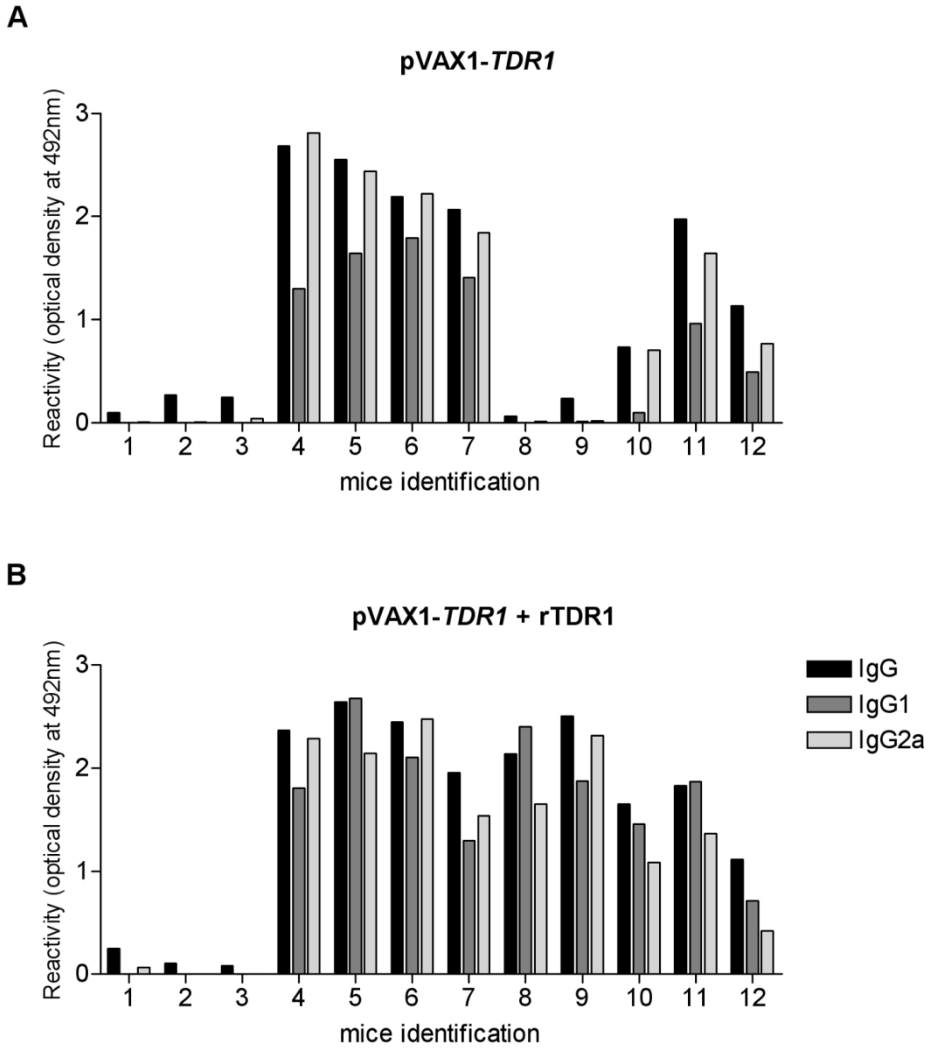

Figure 9. TDR1 specific immunoglobulin's profile of Balb/c mice immunized with pVAX1-*TDR1* or pVAX1-*TDR1*+rTDR1 9 weeks after infection with *L. infantum* promastigotes. Mice were immunized i.m. twice with 100 µg of pVAX1-*TDR1* (A), 100 µg of pVAX1-*TDR1*+rTDR1 (B) or pVAX1 (control group) followed by challenge with $1x10^8$ *L. infantum* promastigotes. Sera from each individually mice (1-3, control group; 4-12, vaccinated group (4-7, R and 8-12, NR)) collected 9 weeks after challenge was tested individually for IgG, IgG1 and IgG2a specific TDR1 antibodies production.

Conclusion

In this study, we have evaluated the ability of a TDR1 based DNA vaccine to elicit protection against *Leishmania* infection. Previously, we have shown that recombinant TDR1 is able to induce partial protection. The results presented here clearly show that the immunization with a DNA vaccine encoding TDR1 does not confer protection against challenge with *L. infantum* promastigotes, an unexpected outcome since many studies using this strategy have proven to be successful (reviewed in (29)). This demonstrates that different strategies based on the same antigen leads to different results, although DNA vaccines due to its characteristics are generally accepted to give better results. DNA vaccination failure may be attributed to other factors rather than the potency of the encoded antigen such as number of immunizations, immunization route and low levels of DNA uptake and/or *in vivo* transfection.

References

1. **Alvar, J., P. Aparicio, A. Aseffa, M. Den Boer, C. Canavate, J. P. Dedet, L. Gradoni, R. Ter Horst, R. Lopez-Velez, and J. Moreno.** 2008. The relationship between leishmaniasis and AIDS: the second 10 years. Clin Microbiol Rev **21:**334-359, table of contents.
2. **Badiee, A., M. R. Jaafari, and A. Khamesipour.** 2007. *Leishmania major*: immune response in BALB/c mice immunized with stress-inducible protein 1 encapsulated in liposomes. Exp Parasitol **115:**127-134.
3. **Bhowmick, S., R. Ravindran, and N. Ali.** 2008. gp63 in stable cationic liposomes confers sustained vaccine immunity to susceptible BALB/c mice infected with *Leishmania donovani*. Infect Immun **76:**1003-1015.
4. **Borja-Cabrera, G. P., A. Cruz Mendes, E. Paraguai de Souza, L. Y. Hashimoto Okada, A. T. F. A. de, J. K. Kawasaki, A. C. Costa, A. B. Reis, O. Genaro, L. M. Batista, M. Palatnik, and C. B. Palatnik-de-Sousa.** 2004. Effective immunotherapy against canine visceral leishmaniasis with the FML-vaccine. Vaccine **22:**2234-2243.
5. **Buffet, P. A., A. Sulahian, Y. J. Garin, N. Nassar, and F. Derouin.** 1995. Culture microtitration: a sensitive method for quantifying *Leishmania infantum* in tissues of infected mice. Antimicrob Agents Chemother **39:**2167-2168.
6. **Campos-Neto, A., J. R. Webb, K. Greeson, R. N. Coler, Y. A. Skeiky, and S. G. Reed.** 2002. Vaccination with plasmid DNA encoding TSA/LmSTI1 leishmanial fusion proteins confers protection against *Leishmania major* infection in susceptible BALB/c mice. Infect Immun **70:**2828-2836.

7. **Chakravarty, J., S. Kumar, S. Trivedi, V. K. Rai, A. Singh, J. A. Ashman, E. M. Laughlin, R. N. Coler, S. J. Kahn, A. M. Beckmann, K. D. Cowgill, S. G. Reed, S. Sundar, and F. M. Piazza.** A clinical trial to evaluate the safety and immunogenicity of the LEISH-F1+MPL-SE vaccine for use in the prevention of visceral leishmaniasis. Vaccine **29:**3531-3537.

8. **Chappuis, F., S. Sundar, A. Hailu, H. Ghalib, S. Rijal, R. W. Peeling, J. Alvar, and M. Boelaert.** 2007. Visceral leishmaniasis: what are the needs for diagnosis, treatment and control? Nat Rev Microbiol **5:**873-882.

9. **Chu, N., B. N. Thomas, S. R. Patel, and L. U. Buxbaum.** IgG1 is pathogenic in *Leishmania mexicana* infection. J Immunol **185:**6939-6946.

10. **Coler, R. N., Y. Goto, L. Bogatzki, V. Raman, and S. G. Reed.** 2007. Leish-111f, a recombinant polyprotein vaccine that protects against visceral Leishmaniasis by elicitation of CD4+ T cells. Infect Immun **75:**4648-4654.

11. **Croft, S. L., S. Sundar, and A. H. Fairlamb.** 2006. Drug resistance in leishmaniasis. Clin Microbiol Rev **19:**111-126.

12. **Dondji, B., E. Perez-Jimenez, K. Goldsmith-Pestana, M. Esteban, and D. McMahon-Pratt.** 2005. Heterologous prime-boost vaccination with the LACK antigen protects against murine visceral leishmaniasis. Infect Immun **73:**5286-5289.

13. **Dumonteil, E.** 2007. DNA Vaccines against Protozoan Parasites: Advances and Challenges. J Biomed Biotechnol **2007:**90520.

14. **Feasey, N., M. Wansbrough-Jones, D. C. Mabey, and A. W. Solomon.** 2009. Neglected tropical diseases. Br Med Bull **93:**179-200.

15. **Gurunathan, S., D. M. Klinman, and R. A. Seder.** 2000. DNA vaccines: immunology, application, and optimization. Annu Rev Immunol **18:**927-974.

16. **Gurunathan, S., L. Stobie, C. Prussin, D. L. Sacks, N. Glaichenhaus, A. Iwasaki, D. J. Fowell, R. M. Locksley, J. T. Chang, C. Y. Wu, and R. A. Seder.** 2000. Requirements for the maintenance of Th1 immunity in vivo following DNA vaccination: a potential immunoregulatory role for CD8+ T cells. J Immunol **165:**915-924.

17. **Halpern, M. D., R. J. Kurlander, and D. S. Pisetsky.** 1996. Bacterial DNA induces murine interferon-gamma production by stimulation of interleukin-12 and tumor necrosis factor-alpha. Cell Immunol **167:**72-78.

18. **Handman, E., F. M. Symons, T. M. Baldwin, J. M. Curtis, and J. P. Scheerlinck.** 1995. Protective vaccination with promastigote surface antigen 2 from *Leishmania major* is mediated by a TH1 type of immune response. Infect Immun **63:**4261-4267.

19. **Huygen, K.** 2005. Plasmid DNA vaccination. Microbes Infect **7:**932-938.

20. **Iborra, S., N. Parody, D. R. Abanades, P. Bonay, D. Prates, F. O. Novais, M. Barral-Netto, C. Alonso, and M. Soto.** 2008. Vaccination with the *Leishmania major* ribosomal proteins plus CpG oligodeoxynucleotides induces protection against experimental cutaneous leishmaniasis in mice. Microbes Infect **10:**1133-1141.

21. **Kebaier, C., J. E. Uzonna, S. M. Beverley, and P. Scott.** 2006. Immunization with persistent attenuated Delta lpg2 *Leishmania major* parasites requires adjuvant to provide protective immunity in C57BL/6 mice. Infect Immun **74:**777-780.

22. **Kedzierski, L.** 2010. Leishmaniasis Vaccine: Where are We Today? J Glob Infect Dis **2:**177-185.

23. **Kedzierski, L., Y. Zhu, and E. Handman.** 2006. *Leishmania* vaccines: progress and problems. Parasitology **133 Suppl:**S87-112.

24. **Klinman, D. M., A. K. Yi, S. L. Beaucage, J. Conover, and A. M. Krieg.** 1996. CpG motifs present in bacteria DNA rapidly induce lymphocytes to secrete interleukin 6, interleukin 12, and interferon gamma. Proc Natl Acad Sci U S A **93:**2879-2883.

25. **Llanos-Cuentas, A., W. Calderon, M. Cruz, J. A. Ashman, F. P. Alves, R. N. Coler, L. Y. Bogatzki, S. Bertholet, E. M. Laughlin, S. J. Kahn, A. M. Beckmann, K. D. Cowgill, S. G. Reed, and F. M. Piazza.** 2010. A clinical trial to evaluate the safety and immunogenicity of the LEISH-F1+MPL-SE vaccine when used in combination with sodium stibogluconate for the treatment of mucosal leishmaniasis. Vaccine **28:**7427-7435.

26. **Mazumder, S., M. Maji, A. Das, and N. Ali.** Potency, efficacy and durability of DNA/DNA, DNA/protein and protein/protein based vaccination using gp63 against *Leishmania donovani* in BALB/c mice. PLoS One **6:**e14644.

27. **Mougneau, E., F. Altare, A. E. Wakil, S. Zheng, T. Coppola, Z. E. Wang, R. Waldmann, R. M. Locksley, and N. Glaichenhaus.** 1995. Expression cloning of a protective *Leishmania* antigen. Science **268:**563-566.

28. **Mutiso, J. M., and J. C. Macharia.** 2010. A review of adjuvants for *Leishmania* vaccine candidates. Journal of Biomedical Research**:**16-25.

29. **Nagill, R., and S. Kaur.** 2011. Vaccine candidates for leishmaniasis: A review. Int Immunopharmacol.

30. **Nascimento, E., D. F. Fernandes, E. P. Vieira, A. Campos-Neto, J. A. Ashman, F. P. Alves, R. N. Coler, L. Y. Bogatzki, S. J. Kahn, A. M. Beckmann, S. O. Pine, K. D. Cowgill, S. G. Reed, and F. M. Piazza.** A clinical trial to evaluate the safety and immunogenicity of the LEISH-F1+MPL-SE vaccine when used in

combination with meglumine antimoniate for the treatment of cutaneous leishmaniasis. Vaccine **28:**6581-6587.

31. **Okwor, I., and J. Uzonna.** 2008. Persistent parasites and immunologic memory in cutaneous leishmaniasis: implications for vaccine designs and vaccination strategies. Immunol Res **41:**123-136.
32. **Rafati, S., A. H. Salmanian, T. Taheri, M. Vafa, and N. Fasel.** 2001. A protective cocktail vaccine against murine cutaneous leishmaniasis with DNA encoding cysteine proteinases of *Leishmania major*. Vaccine **19:**3369-3375.
33. **Rafati, S., F. Zahedifard, and F. Nazgouee.** 2006. Prime-boost vaccination using cysteine proteinases type I and II of *Leishmania infantum* confers protective immunity in murine visceral leishmaniasis. Vaccine **24:**2169-2175.
34. **Reithinger, R., J. C. Dujardin, H. Louzir, C. Pirmez, B. Alexander, and S. Brooker.** 2007. Cutaneous leishmaniasis. Lancet Infect Dis **7:**581-596.
35. **Saraiva, E. M., A. de Figueiredo Barbosa, F. N. Santos, G. P. Borja-Cabrera, D. Nico, L. O. Souza, C. de Oliveira Mendes-Aguiar, E. P. de Souza, P. Fampa, L. E. Parra, I. Menz, J. G. Dias, Jr., S. M. de Oliveira, and C. B. Palatnik-de-Sousa.** 2006. The FML-vaccine (Leishmune) against canine visceral leishmaniasis: a transmission blocking vaccine. Vaccine **24:**2423-2431.
36. **Seifert, K.** 2011. Structures, targets and recent approaches in anti-leishmanial drug discovery and development. Open Med Chem J **5:**31-39.
37. **Selvapandiyan, A., R. Dey, S. Nylen, R. Duncan, D. Sacks, and H. L. Nakhasi.** 2009. Intracellular replication-deficient *Leishmania donovani* induces long lasting protective immunity against visceral leishmaniasis. J Immunol **183:**1813-1820.
38. **Selvapandiyan, A., R. Duncan, A. Debrabant, N. Lee, G. Sreenivas, P. Salotra, and H. L. Nakhasi.** 2006. Genetically modified live attenuated parasites as vaccines for leishmaniasis. Indian J Med Res **123:**455-466.
39. **Shedlock, D. J., and D. B. Weiner.** 2000. DNA vaccination: antigen presentation and the induction of immunity. J Leukoc Biol **68:**793-806.
40. **Silvestre, R., A. Cordeiro-Da-Silva, N. Santarem, B. Vergnes, D. Sereno, and A. Ouaissi.** 2007. SIR2-deficient *Leishmania infantum* induces a defined IFN-gamma/IL-10 pattern that correlates with protection. J Immunol **179:**3161-3170.
41. **Stager, S., D. F. Smith, and P. M. Kaye.** 2000. Immunization with a recombinant stage-regulated surface protein from *Leishmania donovani* induces protection against visceral leishmaniasis. J Immunol **165:**7064-7071.
42. **Stober, C. B., U. G. Lange, M. T. Roberts, A. Alcami, and J. M. Blackwell.** 2005. IL-10 from regulatory T cells determines vaccine efficacy in murine *Leishmania major* infection. J Immunol **175:**2517-2524.

43. **Stobie, L., S. Gurunathan, C. Prussin, D. L. Sacks, N. Glaichenhaus, C. Y. Wu, and R. A. Seder.** 2000. The role of antigen and IL-12 in sustaining Th1 memory cells in vivo: IL-12 is required to maintain memory/effector Th1 cells sufficient to mediate protection to an infectious parasite challenge. Proc Natl Acad Sci U S A **97:**8427-8432.

44. **Sukumaran, B., P. Tewary, S. Saxena, and R. Madhubala.** 2003. Vaccination with DNA encoding ORFF antigen confers protective immunity in mice infected with *Leishmania donovani*. Vaccine **21:**1292-1299.

45. **Tewary, P., M. Jain, M. H. Sahani, S. Saxena, and R. Madhubala.** 2005. A heterologous prime-boost vaccination regimen using ORFF DNA and recombinant ORFF protein confers protective immunity against experimental visceral leishmaniasis. J Infect Dis **191:**2130-2137.

46. **Tewary, P., B. Sukumaran, S. Saxena, and R. Madhubala.** 2004. Immunostimulatory oligodeoxynucleotides are potent enhancers of protective immunity in mice immunized with recombinant ORFF leishmanial antigen. Vaccine **22:**3053-3060.

47. **Vanloubbeeck, Y., and D. E. Jones.** 2004. The immunology of *Leishmania* infection and the implications for vaccine development. Ann N Y Acad Sci **1026:**267-272.

48. **Velez, I. D., K. Gilchrist, S. Martinez, J. R. Ramirez-Pineda, J. A. Ashman, F. P. Alves, R. N. Coler, L. Y. Bogatzki, S. J. Kahn, A. M. Beckmann, K. D. Cowgill, S. G. Reed, and F. M. Piazza.** 2009. Safety and immunogenicity of a defined vaccine for the prevention of cutaneous leishmaniasis. Vaccine **28:**329-337.

49. **Woodland, D. L.** 2004. Jump-starting the immune system: prime-boosting comes of age. Trends Immunol **25:**98-104.

50. **Xu, D., and F. Y. Liew.** 1995. Protection against leishmaniasis by injection of DNA encoding a major surface glycoprotein, gp63, of *L. major.* Immunology **84:**173-176.

4.3 Deletion of the *TDR1* gene provides evidence of variable ploidy in *Leishmania infantum*

The occurrence of aneuploidy in *Leishmania* has been widely documented as a response to attempts to delete essential genes or overcome drug pressure, but naturally occurring and variable ('mosaic') aneuploidy has been realized only recently. Here we show that the *TDR1* gene of *L. infantum*, of which there is just one in the haploid genome, occurs in variable copy number suggestive of both diploid and tetraploid cells within the same cloned population. Two rounds of transfection were sufficient to generate a null mutant for *TDR1* but other cloned transfectants required four rounds of transfection to achieve the same. This clear demonstration of variation of gene copy number within a cloned line has implications for understanding the biology of *Leishmania*.

Submitted for publication to FEMS Microbiology Letters

Deletion of the *TDR1* gene provides evidence of variable ploidy in *Leishmania infantum*

Ana Marta Silva[1,2,3], Anabela Cordeiro-da-Silva[2,3] and Graham H. Coombs[1*]

[1]Strathclyde Institute of Pharmacy and Biomedical Sciences, University of Strathclyde, 161 Cathedral Street, Glasgow G4 0RE, UK
[2]Instituto de Biologia Molecular e Celular, Universidade do Porto, Rua do Campo Alegre, 823, 4150-180 Porto, Portugal
[3]Laboratório de Ciências Biológicas, Faculdade de Farmácia da Universidade do Porto, R. Aníbal Cunha n.º 164, 4050-047 Porto, Portugal

*Corresponding author: E-mail: graham.coombs@strath.ac.uk; Tel. +44 141 548 2155; Fax +44 141 552 2562

Running title: *Leishmania infantum* TDR1 aneuploidy.

Keywords: *Leishmania infantum*, variable ploidy, tetraploidy.

Abstract

The occurrence of aneuploidy in *Leishmania* has been widely documented as a response to attempts to delete essential genes or overcome drug pressure, but naturally occurring and variable ('mosaic') aneuploidy has been realized only recently. Here we show that the *TDR1* gene of *L. infantum*, of which there is just one in the haploid genome, occurs in variable copy number suggestive of both diploid and tetraploid cells within the same cloned population. Two rounds of transfection were sufficient to generate a null mutant for *TDR1* but other cloned transfectants required four rounds of transfection to achieve the same. This clear demonstration of variation of gene copy number within a cloned line has implications for understanding the biology of *Leishmania*.

Introduction

Leishmaniasis is still one of the world's most neglected diseases and novel therapies are urgently required (WHO, 2010). One avenue in drug discovery is the identification of essential genes encoding 'druggable' target proteins (Handman*, et al.*, 2008). A mechanism for demonstrating gene essentiality is targeted gene replacement, an extremely powerful method that allows investigation of the role of a gene and its encoded protein by a loss of function strategy (Beverley, 2003). *Leishmania* have in the past been considered to be diploid organisms generally (Cruz & Beverley, 1990), although aneuploidy has been known to occur naturally, established examples being chromosome 1 trisomy (Sunkin*, et al.*, 2000) and chromosome 31 tetrasomy (Akopyants*, et al.*, 2009) in *L. major*, and has frequently arisen during attempts to delete essential genes and been interpreted as chromosome reorganization occurring to ensure retention of the gene (Cruz*, et al.*, 1993, Mottram*, et al.*, 1996, Ilgoutz*, et al.*, 1999, Dubessay*, et al.*, 2002, Martinez-Calvillo*, et al.*, 2005, Vergnes*, et al.*, 2005, Mukherjee*, et al.*, 2009, Murta*, et al.*, 2009, Romao*, et al.*, 2009). In these cases, additional evidence for gene essentiality can be provided through the generation of a 'conditional' null mutant in the presence of an extrachromosomal (also known as episomal) copy of the gene (Cruz*, et al.*, 1993, Mottram*, et al.*, 1996, Ilgoutz*, et al.*, 1999, Vergnes*, et al.*, 2005, Mukherjee*, et al.*, 2009, Murta*, et al.*, 2009, Romao*, et al.*, 2009), which is used to prove that under these circumstances the endogenous locus can be deleted and so is not refractory to genetic manipulation. Recently, however, it was reported that the ploidy of *Leishmania* was less constant with the concept of mosaicism, with cells in a population having different ploidy, being postulated (Sterkers*, et al.*, 2010). Moreover, detailed genome analyses using the latest technologies have revealed that the ploidy of different lines of *Leishmania* species are not the same, with individual chromosomes being apparently diploid in one line and triploid or tetraploid in others (Downing*, et al.*, 2011, Rogers*, et al.*, 2011).

We report here variation in ploidy between cells in a population of *L. infantum*. The overall study aimed to define the precise role of an enzyme called thiol dependent reductase 1 (TDR1), which is trypanosomatid-specific and first identified in *L. major* (Denton*, et al.*, 2004). Our approach was to investigate the function of TDR1 in *L. infantum* via generation of null mutants for the gene encoding it (*TDR1*). We have been able to generate a null mutant with just two rounds of transfection, but also have isolated clones that required four rounds of transfection to achieve deletion of all gene alleles. Thus this approach has shown that within a cloned line there can be variable ploidy in a gene, even one that is

non-essential, but also that the ploidy cannot be super-variable in that gene deletions using differing numbers of allele deletions were possible.

Materials and methods

Leishmania parasites

Leishmania infantum promastigotes (clone MHOM/MA/67/ITMAP-263) were grown at 26ºC in RPMI 1640 (PAA Laboratories) supplemented with 20 mM Hepes, 2 mM L-glutamine, 100U mL^{-1} penicillin, 100 mg mL^{-1} streptomycin (PAA Laboratories) and 10% (v/v) heat inactivated fetal calf serum (FCS, PAA Laboratories). Cultures were set up initially at 2.5 x 10^5 parasite mL^{-1} and sub-passaged every 6 days.

Transfection constructs

To generate the constructs for deletion of *L. infantum TDR1* by homologous recombination, the 3'and 5' untranslated regions (UTR) of *TDR1* were PCR amplified using the primers P1 and P2 or P3 and P4, respectively, (Table 1) and *L. infantum* genomic DNA as template, which was isolated from *L. infantum* promastigotes as described previously (Medina-Acosta & Cross, 1993). Each resulting PCR product (1.0Kb) was cloned directly at the T/A cloning site of pGEM-T Easy (Promega). The 5'UTR was digested with *Hind*III and *Sal*I and cloned into the corresponding sites of plmcpb-hyg (Mottram*, et al.*, 1996), yielding pldtdr1-hyg5', followed by the 3'UTR ligated to the *Sma*I and *Bgl*II sites of pldtdr1-hyg5' to give pldtdr1-hyg5'3' (construct 1). The hygromycin phosphotransferase resistance gene (*HYG*) was replaced either with bleomycin (*BLE*) , streptothricin acetyltransferase (*SAT*), blasticidin deaminase (*BLA*) resistance genes by digestion with *Spe*I-*BamH*I and ligation to the *Spe*I and *BamH*I sites of pldtdr1-hyg5'3' yielding construct 2, 3 and 4, , respectively. Before transfection, constructs 1-4 were linearised with *Hind*III and Bgl*II* restriction enzymes.

For complementation studies, the *TDR1* open reading frame (ORF) was cloned into the pRIB vector for chromosomal integration (Misslitz*, et al.*, 2000) or into pXG, an episomal vector (Ha*, et al.*, 1996). The *TDR1* ORF was PCR amplified using P5 and P6 or P7 and P8, respectively (Table 1) and *L. infantum* genomic DNA as template*.* The resulting PCR products were sub-cloned into pGEM-T Easy (Promega) and confirmed by sequencing analysis before cloning into *Cla*I- and *Age*I-digested pRIB or *Bam*HI- and *Sma*I-digested pXG. The integration cassette from the pRIB plasmid containing the *TDR1* ORF was released by digestion with *Pac*I and *Pme*I before transfection.

Table 1 – Primers used in this study

P1	3'UTR *TDR1*	5' -CCCGGGAGGCTCGTCGAGGGGATCGACGTG- 3'
P2	3'UTR *TDR1*	5' -AGATCTGGGGAGGGAGGGAATGTAGTAGTCCTCTGTGCCTGT- 3'
P3	5'UTR *TDR1*	5' -AAGCTTTGTGCAGCGTTTCTTAGTACCGCTGTGCAGTTTTG- 3'
P4	5'UTR *TDR1*	5' - GTCGACCCTCGACGCCAGGCACGCAGTGGCTTAGTT- 3'
P5	*TDR1*	5' - GATCCATATGGCCGCCCGCGCGCTAAAGCTATAC- 3'
P6	*TDR1*	5' -CTACCGGTTTACCCGCTCTGGGCCCTCCGTTG- 3'
P7	*TDR1*	5' -GACCCGGGATGGCCGCCCGCGCGCTAAAGCTATAC- 3'
P8	*TDR1*	5' -CTGGATCCTTACCCGCTCTGGGCCCTCCGTTG- 3'

For each oligonucleotide the restriction sites included are underlined; UTR, untranslated region.

Transfection and selection of *L. infantum* promastigotes

Late logarithmic phase promastigotes were resuspended at 5 x 10^7 cells mL^{-1} in nucleofector solution (Amaxa nucleofector kit, Lonza). 100 µl of cell suspension was either mixed with 10 µg of linearised or circular DNA or 10 µl of water as control and electroporated in a disposable cuvette using an Amaxa electroporation device (Lonza). Cells were immediately transferred to RPMI medium supplemented with 20% (v/v) FCS and 24 h later the antibiotic required for transfectant selection added as follows: hygromycin B (Sigma) at 50 µg mL^{-1}; phleomycin (Jena Bioscience) at 40 µg mL^{-1}; nourseothricin (Jena Bioscience) at 50 µg mL^{-1}; neomycin (G418, Sigma) at 50 µg mL^{-1} and puromycin (Calbiochem) at 100 µg mL^{-1}.

Southern blot analyses

To verify the correct integration events, genomic DNA from wild type (WT) and mutant *L. infantum* promastigotes was analyzed by Southern blot. Briefly, 2 µg DNA were digested with *Xho*I, *Sal*I or *Not*I, electrophoresed through a 0.7% or 0.8% agarose gel and blotted onto Hybond-N+ membrane (Amersham Bioscience). The 3´UTR of *TDR1* generated from genomic DNA by PCR with primers P1 and P2 was labelled with the AlkPhos Direct Labelling kit (Amersham Bioscience) and used to probe the blot. After overnight hybridization at 55ºC, the blot was washed, drained and developed using CDP-Star Detection reagent and Hyperfilm ECL (Amersham Biosciences) according to the manufacturer's instructions.

Western blot analyses

L. infantum promastigotes were lysed by the addition of 0.25 M sucrose, 0.25% (v/v) Triton X-100, 10 mM EDTA, 10 µM E-64, 2 mM 1,10-phenanthroline, 4 µM pepstatin A and 1 mM PMSF. Insoluble cellular debris was removed by centrifugation at 12000 x g for 20 min at 4ºC, proteins separated by SDS-PAGE (12%) and blotted to nitrocellulose for Western blot analysis. Western blots were probed with polyclonal sheep anti-TDR1 serum or, as a loading control, rabbit anti-CS (cysteine synthase) and rabbit anti-sheep or goat anti-rabbit secondary antibodies coupled to peroxidase (Pierce) followed by chemiluminescence using ECL detection system (Pierce).

Results and Discussion

In order to elucidate the role of TDR1 in *L. infantum*, we attempted to generate null mutants for *TDR1*, a single copy gene, using homologous gene replacement. Most gene deletions reported previously with *Leishmania* species required just two rounds of gene replacement, which is consistent with the organism being diploid, although aneuploidy has been reported (Sunkin*, et al.*, 2000, Akopyants*, et al.*, 2009).

Southern blot analysis of Xho*I*-digested genomic DNA of selected clones after the first round of transfection confirmed the successful deletion of a first allele of *TDR1* and integration of the *HYG* selectable marker (to give *TDR1*/*tdr1*). The two hybridizing bands detected (1.71 and 4.27 kb) with the 3'UTR *TDR1* probe represented, respectively, the endogenous *TDR1* (WT) gene and the correct integration of the *HYG* replacement cassette (Fig. 1B, lanes 1 and 2). The *TDR1*/*tdr1* clone was then transfected with either construct 2 or 3 (Fig. 1A) with the aim of deleting the remaining WT allele.

Deletion of the second and remaining allele of the *TDR1* gene was confirmed by Southern blot analysis, the hybridizing band of 3.60 kb corresponding to the replacement of the remaining WT allele of the gene by the *BLE* cassette, showing that a null mutant (∆*tdr1*) had been obtained (Fig. 1B, lane 3). Western blot analysis confirmed the deletion of the gene by the absence of TDR1 protein expression in ∆*tdr1* (Fig. 2A, lane 1). To be able to have definitive evidence that any phenotypic differences between the WT parasite and the ∆*tdr1* null mutant were directly related to the gene deletion, ∆*tdr1* was complemented either with a ribosomal or an episomal *Leishmania* expression vector containing the *TDR1* ORF. Analysis of both generated lines by western blot showed successful re-expression of TDR1 in the null mutant (Fig. 2A). We selected two clones resulting from independent

transfections in the case of Δ*tdr1*[pXG*TDR1*] (Fig. 2A, lanes 5 and 6) and independent selection post-transfection in the case of Δ*tdr1*::P_{RRNA}*TDR1* clones (Fig. 2A, lanes 8 and 9); each have similar levels of TDR1 expression.

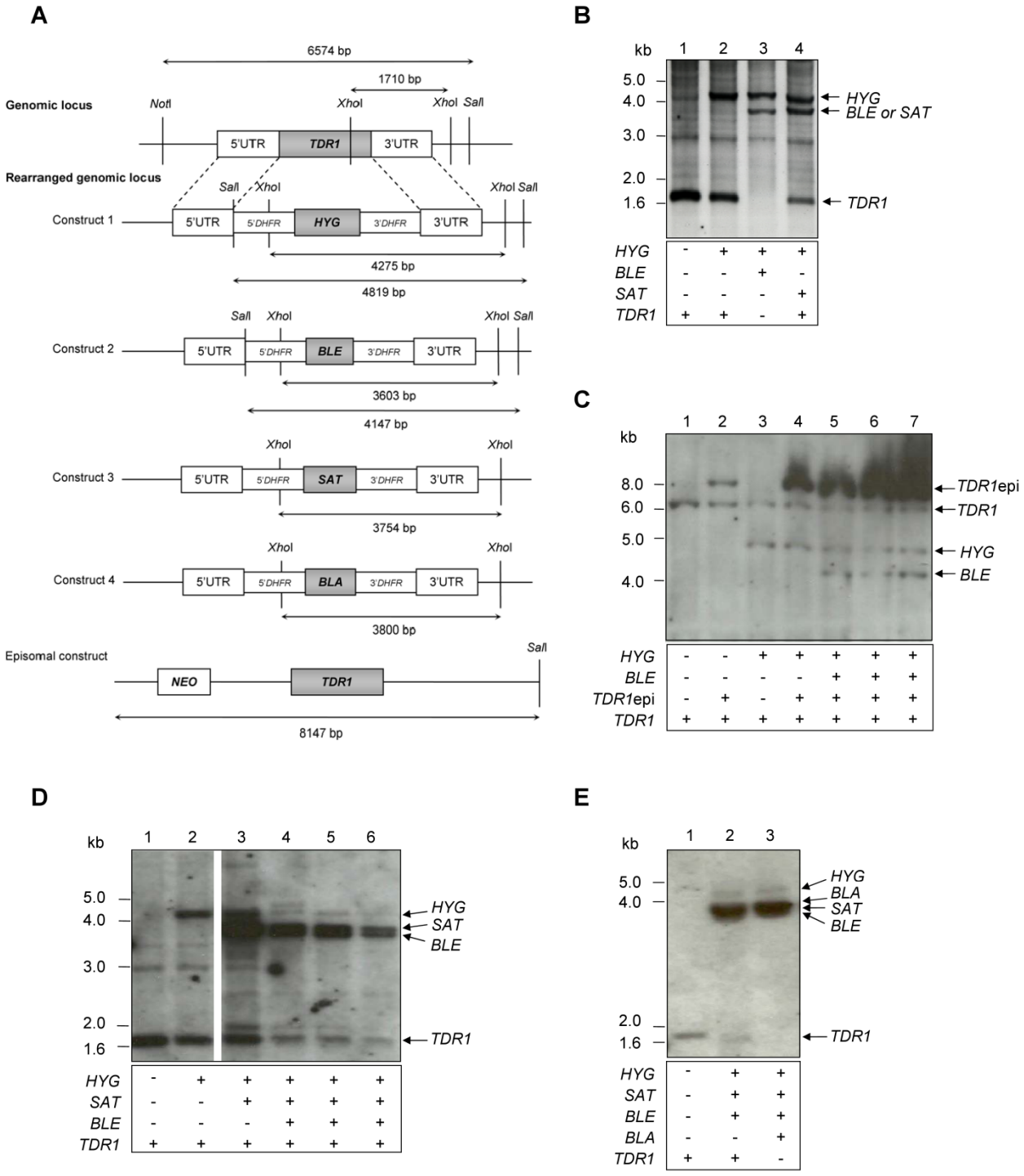

Figure 1 – Targeted replacement of the *TDR1* gene of *L. infantum* reveals variable ploidy (A) Schematic representation of the *TDR1* locus and the constructs used to replace the gene alleles and to provide episomal expression of TDR1. Expected sizes of the *Xho*I, *Sal*I and *Not*I fragments revealed by Southern blot analysis are shown. UTR,

untranslated region; *DHFR*, dihydrofolate reductase gene; *HYG*, hygromycin phosphotransferase gene; *BLE*, bleomycin acetyltransferase gene; *SAT*, streptothricin acetyltransferase gene; *BLA*, blasticidin deaminase gene; *NEO*, neomycin phosphotransferase gene. (B) Southern blot analysis of genomic DNA digested with *Xho*I, separated on a 0.8% agarose gel and blotted onto a nylon membrane. DNA from the wild type *L. infantum* (WT, lane 1), a single allele replacement clone (*TDR1/tdr1*, lane 2), the *TDR1* null mutant (∆*tdr1*, lane 3) and a double allele replacement clone that still has present the WT gene (*TDR1*/*tdr1*/*tdr1*, lane 4). (C) Southern blot analysis of genomic DNA digested with *Not*I and *Sal*I, separated on a 0.7% agarose gel and blotted onto a nylon membrane. DNA from the WT (lane 1), WT[pXG *TDR1*] (to allow the distinction of the gene in the episome from the other expected bands, lane 2), *TDR1*/*tdr1* (lane 3), a single allele replacement clone transfected with episomal construct (*TDR1*/*tdr1*[pXG *TDR1*], lane 4), clones that resulted from transfection of *TDR1*/*tdr1* [pXG *TDR1*] with construct 2, in which the WT gene is still present (*TDR1*/*tdr1*/*tdr1* [pXG *TDR1*], lanes 5, 6 and 7). (D) Southern blot analysis of genomic DNA digested with *Xho*I, separated on a 0.8% agarose gel and blotted onto a nylon membrane. DNA from the WT (lane 1), *TDR1/tdr1* (lane 2), *TDR1*/*tdr1*/*tdr1* (lane 3); a triple allele replacement clone, that resulted from transfection of *TDR1*/*tdr1*/*tdr1* with construct 2, in which the WT gene is still present (*TDR1*/*tdr1*/*tdr1*/*tdr1*, lanes 4, 5 and 6). (E) Southern blot analysis of genomic DNA digested with *Xho*I, separated on a 0.8% agarose gel and blotted onto a nylon membrane. DNA from the WT (lane 1), *TDR1/tdr1/tdr1/tdr1* (lane 2) and the ∆*tdr1* obtained after 4 rounds of transfection (lane 3). Membranes were hybridized with an alkaline phosphatase-labeled DNA probe comprising the 3'UTR of the *TDR1* gene. The positions of the molecular size markers (kb) and identity of the bands are shown on the left and on the right, respectively. The box below summarizes which genes are present. *TDR1*epi refers to the gene present in the episomal construct.

Although we were able to generate a *TDR1* null mutant as detailed above, we did obtain just the one null mutant clone. In this, the *TDR1* alleles were replaced by the *HYG* and *BLE* resistance genes. All of the clones resistant to hygromycin and nourseothricin still had the WT gene present in the genome, despite the correct integration of *SAT* and *HYG* replacement cassettes (Fig. 1B, lane 4). The successful replacement of two alleles of the endogenous gene by resistance markers being accompanied by retention of a copy of the WT gene has been reported on multiple occasions in attempts to target essential genes in *Leishmania*, the mechanisms involved in retaining the WT gene are uncertain although changes in chromosome ploidy, translocation of a chromosomal segment to another chromosome, and intrachromosomal tandem duplication have been reported (Cruz*, et al.*,

1993, Mottram*, et al.*, 1996, Dumas*, et al.*, 1997, Martinez-Calvillo*, et al.*, 2005, Mukherjee*, et al.*, 2011). As we wished to have more than one null mutant clone, and as a further approach to obtaining null mutants to cover the possibility that the gene may be hard to delete due to its importance, we transfected *TDR1*/*tdr1* with a plasmid carrying *TDR1* for episomal expression (Fig. 1A, episomal construct) before the second round of transfection aimed at endogenous gene replacement using the *BLE* construct (Fig. 1A, construct 2). This strategy has been commonly applied successfully when attempting to delete essential genes, with the second allele of the endogenous gene being easily deleted after such complementation with an extrachromosomal gene copy (Cruz*, et al.*, 1993, Mottram*, et al.*, 1996, Ilgoutz*, et al.*, 1999, Vergnes*, et al.*, 2005, Mukherjee*, et al.*, 2009, Murta*, et al.*, 2009, Romao*, et al.*, 2009). Southern blot analysis of *Sal*I and *Not*I-digested genomic DNA of clones subsequently selected resulted in detection of the episomal construct itself (8.14 kb) and a new hybridizing band of 3.60 kb, corresponding to the integration of the *BLE* cassette (Fig. 1C, lanes 5, 6 and 7). This confirmed the successful replacement of the second endogenous *TDR1* allele. However, the selected clones still had the WT gene as well as the episomal copy and western blot analysis confirmed the overexpression of TDR1 by the episomal plasmid in the generated lines (Fig. 2B, lanes 4 and 5). This result was an indication that *TDR1* is a potential case of aneuploidy and clearly raised the possibility of variable ploidy within the *L. infantum* cloned population.

Occurrence of aneuploidy in *Leishmania* has frequently been reported, but it has usually emerged as described above in response to attempts to knockout essential genes (Cruz*, et al.*, 1993, Mottram*, et al.*, 1996, Ilgoutz*, et al.*, 1999, Vergnes*, et al.*, 2005, Mukherjee*, et al.*, 2009, Murta*, et al.*, 2009, Romao*, et al.*, 2009) or to drug pressure (Grondin*, et al.*, 1996, Ubeda*, et al.*, 2008, Leprohon*, et al.*, 2009). However, the fact that we had generated a *TDR1* null mutant in *L. infantum* after just two rounds of transfection, albeit getting just a single clone, and the findings that *TDR1* null mutants of *L. major* were obtained after just two rounds of transfection (J. McGregor and G.H. Coombs, unpublished data) whereas the *TDR1* gene in *L. donovani* required three rounds of transfection to generate null mutant clones (which are viable although they show a phenotype, A.M. Silva, G.D. Westrop, S. Müller, A. Cordeiro-da-Silva and G.H. Coombs, submitted), made us consider that *TDR1* was unlikely to be essential for *L. infantum*. The recent reports of naturally occurring aneuploidy in *Leishmania*, especially *L. donovani*, suggested to us that aneuploidy at the *TDR1* locus may be a natural genomic feature of the *L. infantum* line used in this study. Moreover, Sterkers and co-workers had recently reported that every chromosome was observed in at least two ploidy stages in a

population and that chromosome ploidy distribution was variable among clones and strains; a phenomenon that they named mosaicism and postulated could might explain the genomic plasticity observed in *Leishmania* (Sterkers*, et al.*, 2010). Thus in order to determine whether this was the case in the *L. infantum* line used in this study, we attempted to delete the remaining *TDR1* allele(s) in one of the clones obtained after two rounds of transfection with constructs 1 and 3 that still had a WT *TDR1* allele present. In a third round of transfection we found that *TDR1* gene replacement by the *BLE* cassette was effected, as clearly shown in hybridization studies with the 3'UTR *TDR1* probe, but an endogenous *TDR1* allele also remained intact as the 1.7 kb genomic *Xho*I fragment was still present in the triple targeted mutants (Fig. 1D, lanes 4, 5 and 6). Western blot analysis of the clones generated after three rounds of transfection confirmed the presence of the gene by protein expression (Fig. 2B, lanes 7 and 8). This suggested the presence of more than three copies of the *TDR1* gene.

With the concept that this inability to generate a *TDR1* null mutant in *L. infantum* after 3 rounds of transfection was due to the presence of a fourth allele of the gene, construct 4, containing *BLA* (Fig. 1A), was used to transfect the clone in which three *TDR1* alleles have been replaced by *HYG*, *SAT* and *BLE* cassettes (Fig. 1D). Of the multiple clones selected and analyzed by PCR, just two were negative for *TDR1* and subsequent Southern blot analysis of one of these revealed the correct integration of *BLA* replacement cassette and the successful deletion of a fourth and final *TDR1* allele (Fig. 1E, lane 3), also confirmed by the absence of TDR1 expression (Fig. 2C, lane 3), and so confirmation of null mutant status.

Phenotypic analyses of promastigotes of the two ∆*tdr1* null mutants, one generated after two rounds of transfection and one after four, revealed no substantive differences from the WT, confirming that *TDR1* is not essential to *L. infantum* promastigotes (data not shown). We have recently shown that TDR1 apparently plays a part in redox regulation through glutathionylation/deglutathionylation of key enzymes of *L. donovani* (A.M. Silva, G.D. Westrop, S. Müller, A. Cordeiro-da-Silva and G.H. Coombs, submitted), it remains for investigation whether TDR1 plays the same role in *L. infantum*. All of the data for *L. infantum*, *L. donovani* and *L. major*, however, confirm that *TDR1* is not essential to promastigotes.

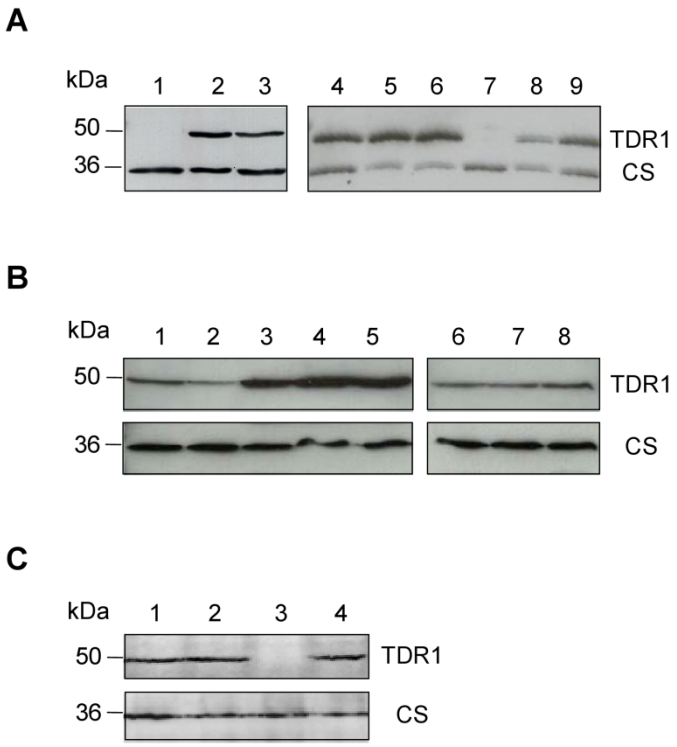

Figure 2 – TDR1 expression in the cell lines generated after targeted gene replacement. Western blot analysis of cell lysate from stationary phase promastigotes of (A) Δ*tdr1* generated after two rounds of tranfection (lanes 1 and 7), WT (lanes 2 and 4), *TDR1/tdr1* (lane 3), the episomal add-back (Δ*tdr1*[pXG*TDR1*], lanes 5 and 6) and the ribosomal add-back (Δ*tdr1*::P_{RRNA}*TDR1,* lanes 8 and 9); (B) WT (lane 1), *TDR1/tdr1* (lane 2), *TDR1*/*tdr1*[pXG*TDR1*] (lane 3), *TDR1/tdr1*/*tdr1*[pXG*TDR1*] (lanes 4 and 5), *TDR1*/*tdr1*/*tdr1* (lane 6) and *TDR1/tdr1*/*tdr1*/*tdr1* (lanes 7 and 8). (C) WT (lane 1), *TDR1/tdr1/tdr1/tdr1* (lane 2), Δ*tdr1* generated after four rounds of transfection (lane 3), the episomal add-back (Δ*tdr1*[pXG*TDR1*], lane 4). Cell extracts were separated using 12% SDS-PAGE and immunoblotted with polyclonal sheep anti-TDR1 serum. Anti-serum raised in rabbit against cysteine synthase (CS) was used to confirm equivalent protein loading; molecular masses are indicated on the left (kDa) and identity of the bands is shown on the right.

Thus our results show that we generated *TDR1* null mutant parasites from cells with different ploidy at the *TDR1* locus even though they were in the same *L. infantum* cloned population. This leads us to conclude the *TDR1* locus in *L. infantum* is diploid in at least some cells but tetraploid in others. These findings of the existence of supernumerary *TDR1* allelles in *L. infantum* and apparent variable ploidy within the same population are consistent with the finding of mosaic ploidy in *L. major* using FISH analysis (Sterkers*, et al.*, 2010) and the data arising from the analyses, just reported, of the genome structures

of different *Leishmania* species and lines; the application of new sequence technology that allows read depth coverage across all the *Leishmania* chromosomes revealed ploidy variation (Downing*, et al.*, 2011, Rogers*, et al.*, 2011). These recent studies report the existence of supernumerary chromosomes in *Leishmania*, differences in chromosome copy number variations between species and strains, and also that the variation is chromosome specific with stable disomy, stable tetrasomy or variable ploidy. In addition, Rogers and co-workers were able to validate the chromosome copy number through the generation of LinJ.36.0640 and LinJ.31.3030 null mutants, genes which reside in disomic and tetrasomic chromosomes, respectively (Rogers*, et al.*, 2011). These findings together point to chromosome copy number variations as a major source of genomic diversity (Downing*, et al.*, 2011, Rogers*, et al.*, 2011). Interestingly, Rogers and co-workers have also found chromosomes with "intermediate" read depth, being neither disomic or trisomic in *L. mexicana*, *L. braziliensis* and *L. donovani*, potentially due to a mixture of individual cells within a population with monosomic, disomic and trisomic chromosomes. This situation is similar to the chromosome copy number mosaicism in a population as previous described for *L. major* by (Sterkers*, et al.*, 2010). In these studies, all *L. donovani* lines and *L. infantum* JPCM5 (MCAN/ES/98/LLM-887), a different line from the one used in this study, had chromosome 33, on which *TDR1* resides, among the supernumerary chromosomes. The data that we have generated with *L. donovani* (MHOM/NP/03/BPK206/0clone10) (A.M. Silva, G.D. Westrop, S. Müller, A. Cordeiro-da-Silva and G.H. Coombs, submitted) and now with *L. infantum* in this study provide additional evidence for the variability between species and lines, but also, importantly, within a population of *L. infantum*. Our findings are consistent with aneuploidy of *TDR1* being due to variation in chromosome copy number. Although genes can reside on extrachromosomal DNA in *Leishmania*, this seems to occur as a mechanism of maintaining essential genes (Mottram*, et al.*, 1996, Genest*, et al.*, 2005), which is clearly not the case with *TDR1* as we were able to delete it.

The findings in this study reiterate the occurrence of natural genomic plasticity in *Leishmania* species and importantly have shown that there is variation even within a cloned population. This includes non-essential genes such as *TDR1*. Our findings support the concept of mosaic aneuploidy as described by Sterkers *et al.* (2010), but also show that the ploidy cannot be super-variable within cells because in that case gene deletions such as we have achieved would not be possible. Clearly *Leishmania* cope well with aneuploidy, and it seems likely that it provides a mechanism to generate the diversity that allows the parasite to survive and take advantage of the different host environments. It also has implications for many experimental studies on the parasites and, in particular, in

deciding upon essentiality of genes and so their suitability for inclusion in drug discovery programmes.

Acknowledgements

The study was supported by Fundação para a Ciência e Tecnologia (FCT) project number PTDC/CVT/65047/2006 and AMS is supported by FCT grant SFRH/BD/28316/2006. We thank Gareth Westrop and Roderick Williams (Strathclyde) for helpful technical suggestions and discussions.

References

Akopyants NS, Kimblin N, Secundino N, Patrick R, Peters N, Lawyer P, Dobson DE, Beverley SM & Sacks DL (2009) Demonstration of genetic exchange during cyclical development of *Leishmania* in the sand fly vector. *Science* **324**: 265-268.

Beverley SM (2003) Protozomics: trypanosomatid parasite genetics comes of age. *Nat Rev Genet* **4**: 11-19.

Cruz A & Beverley SM (1990) Gene replacement in parasitic protozoa. *Nature* **348**: 171-173.

Cruz AK, Titus R & Beverley SM (1993) Plasticity in chromosome number and testing of essential genes in *Leishmania* by targeting. *Proc Natl Acad Sci U S A* **90**: 1599-1603.

Denton H, McGregor JC & Coombs GH (2004) Reduction of anti-leishmanial pentavalent antimonial drugs by a parasite-specific thiol-dependent reductase, TDR1. *Biochem J* **381**: 405-412.

Downing T, Imamura H, Decuypere S*, et al.* (2011) Whole genome sequencing of multiple *Leishmania donovani* clinical lines provides insights into population structure and mechanisms of drug resistance. *Genome Research* **21**: 2143-2156.

Dubessay P, Ravel C, Bastien P, Crobu L, Dedet J, Pagès M & Blaineau C (2002) The switch region on *Leishmania major* chromosome 1 is not required for mitotic stability or gene expression, but appears to be essential. *Nucleic Acids Res* **30**: 3692-3697.

Dumas C, Ouellette M, Tovar J, Cunningham ML, Fairlamb AH, Tamar S, Olivier M & Papadopoulou B (1997) Disruption of the trypanothione reductase gene of *Leishmania* decreases its ability to survive oxidative stress in macrophages. *EMBO J* **16**: 2590-2598.

Genest PA, ter Riet B, Dumas C, Papadopoulou B, van Luenen HG & Borst P (2005) Formation of linear inverted repeat amplicons following targeting of an essential gene in *Leishmania*. *Nucleic Acids Res* **33**: 1699-1709.

Grondin K, Roy G & Ouellette M (1996) Formation of extrachromosomal circular amplicons with direct or inverted duplications in drug-resistant *Leishmania tarentaloae*. *Mol Cell Biol* **16**: 3587-3595.

Ha DS, Schwarz JK, Turco SJ & Beverley SM (1996) Use of the green fluorescent protein as a marker in transfected *Leishmania*. *Mol Biochem Parasitol* **77**: 57-64.

Handman E, Kedzierski L, Uboldi AD & Goding JW (2008) Fishing for anti-*leishmania* drugs: principles and problems. *Adv Exp Med Biol* **625**: 48-60.

Ilgoutz SC, Zawadzki JL, Ralton JE & McConville MJ (1999) Evidence that free GPI glycolipids are essential for growth of *Leishmania mexicana*. *EMBO J* **18**: 2746-2755.

Leprohon P, Legare D, Raymond F, Madore E, Hardiman G, Corbeil J & Ouellette M (2009) Gene expression modulation is associated with gene amplification, supernumerary chromosomes and chromosome loss in antimony-resistant *Leishmania infantum*. *Nucleic Acids Res* **37**: 1387-1399.

Martinez-Calvillo S, Stuart K & Myler PJ (2005) Ploidy changes associated with disruption of two adjacent genes on *Leishmania major* chromosome 1. *Int J Parasitol* **35**: 419-429.

Medina-Acosta E & Cross GA (1993) Rapid isolation of DNA from trypanosomatid protozoa using a simple 'mini-prep' procedure. *Mol Biochem Parasitol* **59**: 327-329.

Misslitz A, Mottram JC, Overath P & Aebischer T (2000) Targeted integration into a rRNA locus results in uniform and high level expression of transgenes in *Leishmania* amastigotes. *Mol Biochem Parasitol* **107**: 251-261.

Mottram JC, McCready BP, Brown KG & Grant KM (1996) Gene disruptions indicate an essential function for the LmmCRK1 cdc2-related kinase of *Leishmania mexicana*. *Mol Microbiol* **22**: 573-583.

Mottram JC, Souza AE, Hutchison JE, Carter R, Frame MJ & Coombs GH (1996) Evidence from disruption of the lmcpb gene array of *Leishmania mexicana* that cysteine proteinases are virulence factors. *Proc Natl Acad Sci U S A* **93**: 6008-6013.

Mukherjee A, Langston LD & Ouellette M (2011) Intrachromosomal tandem duplication and repeat expansion during attempts to inactivate the subtelomeric essential gene GSH1 in *Leishmania*. *Nucleic Acids Res* **39**: 7499-7511.

Mukherjee A, Roy G, Guimond C & Ouellette M (2009) The gamma-glutamylcysteine synthetase gene of *Leishmania* is essential and involved in response to oxidants. *Mol Microbiol* **74**: 914-927.

Murta SM, Vickers TJ, Scott DA & Beverley SM (2009) Methylene tetrahydrofolate dehydrogenase/cyclohydrolase and the synthesis of 10-CHO-THF are essential in *Leishmania major. Mol Microbiol* **71**: 1386-1401.

Rogers MB, Hilley JD, Dickens NJ*, et al.* (2011) Chromosome and gene copy number variation allow major structural change between species and strains of *Leishmania*. *Genome Research* **21**: 2129-2142.

Romao S, Castro H, Sousa C, Carvalho S & Tomas AM (2009) The cytosolic tryparedoxin of *Leishmania infantum* is essential for parasite survival. *Int J Parasitol* **39**: 703-711.

Sterkers Y, Lachaud L, Crobu L, Bastien P & Pages M (2010) FISH analysis reveals aneuploidy and continual generation of chromosomal mosaicism in *Leishmania major*. *Cell Microbiol* **13**: 274-283.

Sunkin SM, Kiser P, Myler PJ & Stuart K (2000) The size difference between *Leishmania major* Friedlin chromosome one homologues is localized to sub-telomeric repeats at one chromosomal end. *Mol Biochem Parasitol* **109**: 1-15.

Ubeda JM, Legare D, Raymond F*, et al.* (2008) Modulation of gene expression in drug resistant *Leishmania* is associated with gene amplification, gene deletion and chromosome aneuploidy. *Genome Biol* **9**: R115.

Vergnes B, Sereno D, Tavares J, Cordeiro-da-Silva A, Vanhille L, Madjidian-Sereno N, Depoix D, Monte-Alegre A & Ouaissi A (2005) Targeted disruption of cytosolic SIR2 deacetylase discloses its essential role in *Leishmania* survival and proliferation. *Gene* **363**: 85-96.

WHO (2010) Control of the leishmaniases. *World Health Organ Tech Rep Ser* pp. 1-186.

4.4 Thiol Dependent Reductase 1 of *Leishmania* is implicated in the regulation of central metabolism via deglutathionylation

Thiol Dependent Reductase 1 (TDR1) of *Leishmania donovani* is a parasite-specific enzyme with a two domain structure, comprising glutaredoxin and omega-glutathione-S-transferase motifs, that has thiol transferase and dehydroascorbate reductase activities *in vitro*. In order to provide insight into the role of TDR1 in *Leishmania* parasites, a *TDR1* null mutant (Δ*tdr1*) was generated. Three rounds of transfection were required, revealing that the gene locus is triploid; providing more evidence that the genome of *L. donovani* has plasticity in terms of ploidy. *Leishmania* virulence or susceptibility to oxidative/nitrosative stress was little affected by *TDR1* deletion, although an increased sensitivity to trivalent antimony and trivalent arsenite was observed. Analysis of parasite's metabolome revealed few but striking differences between Δ*tdr1* and the wild type parent line, notably in the levels of metabolites related to energy and amino acid metabolism (glycerol-3-phosphate, proline, argininosuccinic acid and S-adenosylhomocysteine). This metabolic re-configuration in Δ*tdr1* implicates TDR1 in regulation through S-glutathionylation of key enzymes, an hypothesis supported by the demonstration that recombinant TDR1 has deglutathionylation activity towards protein and peptide substrates. The data also confirm that metabolic profiling of gene-deletion mutants is a method that allows detailed dissection of a protein's function.

Submitted for publication to Free Radical Biology & Medicine

Thiol Dependent Reductase 1 of *Leishmania* is Implicated in the Regulation of Central Metabolism via Deglutathionylation

Ana Marta Silva[1,2,3], Gareth D. Westrop[1], Sylke Müller[4], Anabela Cordeiro-da-Silva[2,3] and Graham H. Coombs[1*]

[1]Strathclyde Institute of Pharmacy and Biomedical Sciences, University of Strathclyde, 161 Cathedral Street, Glasgow G4 0RE, UK; E-mails: graham.coombs@strath.ac.uk; gareth.westrop@strath.ac.uk; amsilva@ibmc.up.pt

[2]Instituto de Biologia Molecular e Celular, Universidade do Porto, Rua do Campo Alegre, 823, 4150-180 Porto, Portugal; E-mail: cordeiro@ibmc.up.pt

[3]Laboratório de Ciências Biológicas, Faculdade de Farmácia da Universidade do Porto, R. Aníbal Cunha n.º 164, 4050-047 Porto, Portugal;

[4]Wellcome Trust Centre for Molecular Parasitology, Institute of Infection, Immunity and Inflammation, College of Medical, Veterinary and Life Sciences, University of Glasgow, Glasgow, G12 8TA, UK. E-mail: sylke.muller@glasgow.ac.uk

*Corresponding author: E-mail: graham.coombs@strath.ac.uk ; Tel. +44 141 548 2155; Fax +44 141 552 2562

Abbreviations: Grx, glutaredoxin; GSH, glutathione; GST, glutathione-S-transferases; GSTO, omega class GST; HEDS, 2-hydroxyethyl disulfide; HPLC, high performance liquid chromatography; LC-MS, liquid chromatography mass spectrometry; $^{\cdot}NO$, nitric oxide; $O_2^{\cdot -}$, superoxide radical; $ONOO^-$, peroxynitrite; ORF, open reading frame; PBS, phosphate buffered saline; ppm, parts per million; RNS, reactive nitrogen species; ROS, reactive oxygen species; Sb^{III}, trivalent antimonial; Sb^{V}, pentavalent antimonial; SIN-1, 3-morpholinosydnonimine·HCL; SD, standard deviation; SDS, sodium dodecyl sulfate; SNAP, S-nitroso-N-acetylpenicillamine; SSG, sodium stibogluconate; TDR1, thiol dependent reductase 1; Trx, thioredoxin; ($T(SH)_2$), trypanothione; UTR, untranslated region.

Abstract

Thiol Dependent Reductase 1 (TDR1) of *Leishmania donovani* is a parasite-specific enzyme with a two domain structure, comprising glutaredoxin and omega-glutathione-S-transferase motifs, that has thiol transferase and dehydroascorbate reductase activities *in vitro*. In order to provide insight into the role of TDR1 in *Leishmania* parasites, a *TDR1* null mutant (Δ*tdr1*) was generated. Three rounds of transfection were required, revealing that the gene locus is triploid; providing more evidence that the genome of *L. donovani* has plasticity in terms of ploidy. *Leishmania* virulence or susceptibility to oxidative/nitrosative stress was little affected by *TDR1* deletion, although an increased sensitivity to trivalent antimony and trivalent arsenite was observed. Analysis of parasite's metabolome revealed few but striking differences between Δ*tdr1* and the wild type parent line, notably in the levels of metabolites related to energy and amino acid metabolism (glycerol-3-phosphate, proline, argininosuccinic acid and S-adenosylhomocysteine). This metabolic re-configuration in Δ*tdr1* implicates TDR1 in regulation through S-glutathionylation of key enzymes, an hypothesis supported by the demonstration that recombinant TDR1 has deglutathionylation activity towards protein and peptide substrates. The data also confirm that metabolic profiling of gene-deletion mutants is a method that allows detailed dissection of a protein's function.

Keywords: parasite, *Leishmania*, promastigote, thiol dependent reductase, glutaredoxin, glutathione S-transferase, deglutathionylation, redox regulation.

Introduction

Leishmania is a protozoan parasite that encounters a variety of different environments during its life cycle involving sand fly and mammalian hosts, living within macrophages in the latter. It is thus exposed to a series of variations in temperature and pH, reactive oxygen (ROS) and nitrogen species (RNS), and the availability of nutrients and oxygen [1]. To survive and multiply *Leishmania* has evolved multiple strategies, including adopting various morphological forms which are also, at least in part, metabolically distinct [2-4] and contain a variety of antioxidant proteins [5-8]. Rather little is known on how these changes are regulated, although clearly this is of vital importance to the parasite. Thus we undertook this study with the aim of determining whether thiol dependent reductase 1 (TDR1), an unusual trypanosomatid-specific enzyme with similarities to glutaredoxins and glutathione S-transferases, has roles both in countering redox stresses and in the molecular mechanisms of metabolic regulation in *Leishmania*. We anticipated that the

insights obtained could underpin the development of future improved therapies against infections caused by *Leishmania*.

TDR1, a trypanosomatid-specific enzyme first identified in *L. major* [9], possesses thiol transferase and dehydroascorbate reductase enzymatic activities and is present in both promastigotes and amastigotes of *Leishmania*. The enzyme is functional as a trimer of a protein with an intriguing two domain nature, with the N-terminal domain containing a CysXXCys (CXXC) motif characteristic of glutaredoxin (Grx) and thioredoxin (Trx), while the C-terminal active site is characteristic of omega glutathione-S-transferase (GSTO) [9]. TDR1 is able to reduce pentavalent antimonials such as sodium stibogluconate (SSG) to a trivalent form *in vitro*, suggesting that it may play a part in the antileishmanial activity of antimonial drugs and could account for the parasite-specificity of these drugs [9]. Although, the physiological function of TDR1 is unclear, its very unusual structure suggests some specific role.

Glutaredoxins (Grxs), members of the Trx superfamily, are small molecular mass, glutathione (GSH)-dependent oxidoreductases that play an important part in a cell's defense against oxidative stress and maintenance of redox homeostasis [10]; most cells have a specialized set of glutaredoxin isoforms located in various cellular compartments and with distinct roles [11-14]. Grxs can have either one or two active site cysteines - being classified as dithiol (with a CXXC motif) and monothiol (CXXS) Grxs, respectively. Grxs reduce both low molecular weight and protein disulfides using a dithiol mechanism, while the reduction of mixed disulfides and glutathionylated proteins occur by a monothiol mechanism [15]. However, all the dithiol Grxs known are also able to catalyze monothiol reactions - showing the versatility of these proteins, based on the affinity for the GSH moiety [15]. Grxs have been implicated in a wide range of biological processes, including the reversible S-glutathionylation of proteins [10]. S-glutathionylation can be promoted by oxidative stress and through the protection of sensitive thiols of proteins is a means of avoiding irreversible modification of a protein's function; it may also serve as a storage mechanism for GSH, which otherwise would be extruded from the cell [16]. However, S-glutathionylation also occurs under physiological conditions as a mechanism of regulating the activity of proteins [16-18]. It can lead to inhibition or activation of an enzyme's activity and the so-called redox regulation of many proteins is achieved via this post-translational modification. Deglutathionylation, removing the GSH moiety from the protein mixed disulfide, reverses the change [16]. We hypothesized that TDR1, with its Grx-like domain, may be responsible for S-glutathionylation or/and deglutathionylation of enzymes in *Leishmania* and so have an important role in regulating metabolism. *Leishmania* rely on

the trypanothione ($T(SH)_2$)/trypanothione reductase system unique to trypanosomatids and lack glutathione reductase and thioredoxin reductase [19], which has prompted the suggestion that GSH may have little function in the organism apart from as a precursor of trypanothione [19]. Our hypothesis, if correct, would mean that there is indeed at least one specific role for GSH per se.

The C-terminal domain of TDR1 has an active site more similar to that present in GSTO [9]. The omega class of GSTs is functionally distinct from the other classes of GST despite maintenance of the characteristic GST fold. Human GSTO has very low activity with 1-chloro-2,4-dinitrobenzene (CDNB)[20]. This is a good substrate for all other classes of GSTs, which are able to catalyze the conjugation of free radicals, metals and other electrophilic compounds with GSH and play a major role in the detoxification of many reactive metabolites. Human GSTO instead has activities similar to Grxs, with thiol transferase activity being the most prominent [20]. TDR1 has similarities to human GSTO in its activity profile, although the thioltransferase activity is greater and the glutathione-S-transferase activity with CDNB is lower [9]. Interestingly, there is a report of a GSTO being able to carry out deglutathionylation [21] and also another class of GST (GST-P) having glutathionylation activity [22]. Thus our hypothesis incorporates the likelihood that the two domains of TDR1 complement each other in providing Grx-like activities for *Leishmania*, but the unique two domain arrangement and trimeric functional protein suggests some adaptation specific for functions in the parasite. A protein similar to TDR1 occurs in another trypanosomatid, *Trypanosoma cruzi*. This has an activity profile very similar to TDR1, although it has substitutions in the active site in the C-terminal domain [23].

To test our hypothesis on the function of TDR1 in *Leishmania*, we applied a gene knockout strategy that allows analysis of the effect of a deletion of the gene of interest on the biology of parasite, including its virulence to its host. As a key part of our analyses of the phenotype of the null mutant parasite, we have applied a metabolomics approach to dissect the effect of the *TDR1* gene deletion at a metabolic level. The study of the metabolome is an emerging field, mainly due to the fact that better procedures for obtaining reliable high resolution data now are available [24-31]. This technology has great potential in highlighting phenotypic differences between lines and so the possibility of identifying biomarkers for diagnosis and drug therapy [32]. This current study has confirmed the potential of metabolomics technologies in such analyses and has provided data that support our hypothesis that TDR1 plays a role in regulating the activity of enzymes in *Leishmania*. This idea has been further supported by our demonstration that TDR1 catalyses the deglutathionylation of protein-GSH mixed disulfides *in vitro*. Thus

deglutathionylation involving TDR1 may be an important mechanism of enzyme regulation in *Leishmania*.

Material and methods

Leishmania parasites

Leishmania donovani (MHOM/NP/03/BPK206/0clone10) promastigotes had been cloned from an isolate from a visceral leishmaniasis patient sensitive to pentavalent antimonials in Nepal, as described by Rijal and co-workers [33]. Promastigotes were grown on modified Eagle's medium (designated HOMEM medium, Invitrogen) supplemented with 20% (v/v) heat inactivated fetal calf serum (FCS, PAA Laboratories) at 26°C. Cultures were set up initially at a density of 2.5 x 10^5 parasites/ml and sub-passaged every 6 days.

Plasmid constructs for targeted gene replacement

Genomic DNA was isolated from *L. donovani* promastigotes as described previously [34]. The 5'untranslated region (5'UTR) of *LdTDR1* (LdBPK_330260.1) (hereafter designated as *TDR1*) was PCR amplified using the following forward (P1) and reverse (P2) primers and *L. donovani* genomic DNA as template. P1 (5'-AAGCTTTGTGCAGCGTTTCTTAGTA CCGCTGTGCAGTTTTG-3') contains a *Hind*III restriction site (underlined). P2 (5'-GTCGACCCTCGACGCCAGGCACGCAGTGGCTTATT-3') contains a *Sal*I restriction site (underlined).The design of the primers was based on the *L. infantum* genome sequence available (http://www.genedb.org). The resulting PCR product (1.0 kb) was cloned directly at the T/A cloning site of pGEM-T Easy (Promega). The 5'UTR was digested with *Hind*III and *Sal*I and cloned into the corresponding sites of plmcpb-hyg [35], yielding pldtdr1-hyg5'. The 3'untranslated region (3'UTR) of *TDR1* (1.0 kb) was obtained by the same procedure used for the 5'UTR with the following forward (P3) and reverse (P4) primers. P3 (5'-CCCGGGAGGCTCGTCGAGGGGATCGACGTG-3') contains a *Sma*I restriction site (underlined). P4 (5'-AGATCTGGGGAGGGAGGGAATGTAGTAGTCCTCTGTGCCTG T-3') contains a *Bgl*II restriction site (underlined). The 3'UTR was excised from pGEM-T Easy after digestion with *Sal*I-*Hind*III and ligated to the *SalI* and *Hind*III sites of pldtdr1-hyg5' to give pldtdr1-hyg5'3' (construct 1). The hygromycin phosphotransferase resistance gene (*HYG*) was replaced either with bleomycin (*BLE*) or streptothricin acetyltransferase (*SAT*) resistance genes by digestion with *Spe*I-*BamH*I and ligated to the *Spe*I and *BamH*I sites of pldtdr1-hyg5'3' yielding pldtdr1-bleo5'3' (construct 2) and pldtdr1-sat5'3' (construct 3), respectively. The *HYG*-, *BLE*- and *SAT*-containing *TDR1* gene replacement cassettes were excised from the plasmids by *Hind*III-Bgl*II* digestion prior to transfection. For the re-

expression experiments, the *TDR1* ORF was cloned into the pRIB vector for chromosomal integration into a ribosomal RNA locus, where the gene is expressed under the control of the rRNA promoter [36]. In addition, TDR1 was expressed from the episomal vector pXG [37]. The *TDR1* ORF was PCR-amplified using the primers P5 (5'-GACCCGGGATGGCCGCCCGCGCGCTAAAGCTATAC-3') and P6 (5'-CTGGATCCTTAC CCGCTCTGGGCCCTCCGTTG-3') (for the episomal add-back) or the primers P7 (5'-GATCCATATGGCCGCCCGCGCGCTAAAGCTATAC-3') and P8 (5'-CTACCGGTTTACC CGCTCTGGGCCCTCCGTTG-3') (for the ribosomal add-back) and *L. donovani* genomic DNA as template (restrictions sites for *Sma*I, *BamH*I, *Cla*I and *Age*I, respectively, are underlined). The PCR products were cloned into pGEM-T Easy before excising fragments for subcloning into expression vectors. The episomal add-back plasmid was constructed by cloning the *Sma*I-*BamH*II-cut *TDR1* ORF into pXG [37] and the ribosomal add-back plasmid was obtained by cloning the *Cla*I-*Age*I-cut *TDR1* ORF into pRIB [36], yielding pXG-*TDR1* and pRIB-*TDR1*, respectively. The integration cassette from pRIB-*TDR1* was excised by digestion with *Pac*I and *Pme*I before transfection. All PCR-generated products were verified by sequencing (Eurofins MWG Operon) and correct orientation of the cloned fragments was checked by restriction enzyme digests.

Transfection and selection of L. donovani promastigotes

For transfection, late logarithmic phase promastigotes were resuspended at 5 x 10^7 cells/ml in nucleofector solution (Amaxa nucleofector kit, Lonza). 100 µl of cell suspension was either mixed with 10 µg of DNA or 10 µl of water as control and electroporated in a disposable cuvette using an Amaxa electroporation device (Lonza). Cells were immediately transferred to HOMEM medium supplemented with 20% (v/v) FCS and 24 h later the antibiotic required for transfectant selection added as follows: hygromycin B (Sigma) at 50 µg/ml; phleomycin (Jena Bioscience) at 20 µg/ml; nourseothricin (Jena Bioscience) at 50 µg/ml; neomycin (G418, Sigma) at 50 µg/ml and puromycin (Calbiochem) at 100 µg/ml. The *TDR1* null mutant was constructed by sequential removal of *TDR1* alleles by homologous recombination using the three gene replacement cassettes (Fig. 1A). Transfection with construct 1 or 3 was performed as described above and recombinants were cloned by serial dilution in 96-well plates in medium containing 50 µg/ml of hygromycin B or 50 µg/ml of nourseothricin. Genomic DNA isolated from these cloned parasites was used in Southern blot analyses to confirm the loss of one allele of *TDR1* and replacement by the hygromycin phosphotransferase or streptothricin acetyltransferase resistance cassettes. One clone with the hygromycin phosphotransferase resistance gene was subjected to transfection with construct 2, selected with 50 µg/ml of hygromycin B plus 20 µg/ml of phleomycin and checked for the

replacement of the second allele by the bleomycin resistance cassette. Construct 3 was used to replace the third allele of the *TDR1* gene and clones resulting from the third round of transfection were selected in 50 µg/ml of hygromycin B, 20 µg/ml of phleomycin and 50 µg/ml of nourseothricin. The clones (designated ∆*tdr1*) were analyzed for the complete removal of *TDR1* by Southern blot analysis. Complementation of one Δ*tdr1* clone was achieved by transfection of parasites either with pXG-*TDR1* (episomal add-back) or pRIB-*TDR1* (ribosomal add-back) constructs, selected with 50 µg/ml of G418 or 100 µg/ml of puromycin, respectively, and protein expression assessed by western blot analysis.

Southern blot analysis

To verify the correct integration events, genomic DNA from wild type and mutant *L. donovani* promastigotes was analyzed by Southern blot. Briefly, 2 µg DNA were digested with *Xho*I*,* electrophoresed through a 0.8% agarose gel and blotted onto Hybond-N+ membrane (Amersham Bioscience). The 3´UTR of *TDR1* generated from genomic DNA by PCR with primers P3 and P4 was labelled with the AlkPhos Direct Labelling kit (Amersham Bioscience) and used to probe the blot. After overnight hybridization at 55ºC, the blot was washed, drained and developed using CDP-Star Detection reagent and Hyperfilm ECL (Amersham Biosciences) according to the manufacturer's instructions.

Western blot analysis

L. donovani promastigotes were lysed by the addition of 0.25 M sucrose, 0.25% (v/v) Triton X-100, 10 mM EDTA, 10 µM E-64, 2 mM 1,10-phenanthroline, 4 µM pepstatin A and 1 mM PMSF. Insoluble cellular debris was removed by centrifugation at 12000 x g for 20 min at 4ºC, proteins separated by SDS-PAGE (12%) and blotted to nitrocellulose for Western blot analysis. Western blots were probed with polyclonal sheep anti-TDR1 serum or, as a loading control, rabbit anti-*Ld*CS (*L. donovani* cysteine synthase) and rabbit anti-sheep or goat anti-rabbit secondary antibodies coupled to peroxidase (Pierce) followed by chemiluminescence using ECL detection system (Pierce).

In vitro promastigote susceptibility assays

The susceptibility of *L. donovani* promastigotes to oxidative/nitrosative stress and metals was assessed by an Alamar Blue assay, as previously described [38] with slight modifications. Briefly, promastigotes were diluted in medium to 2 x 10^6 parasites/ml and 100 µl of suspension was incubated with 100 µl of S-Nitroso-N-acetylpenicillamine (SNAP, Biomol; up to 2000 µM), hydrogen peroxide (H_2O_2, Sigma; up to 4000 µM), potassium antimonyl tartrate (Sb^{III}, Sigma; up to 1000 µg/ml), sodium arsenite (As^{III}, Sigma; up to 5 mM), cadmium chloride (Cd^{II}, Sigma; up to 5 mM), copper sulfate (Cu^{IV}, Fisher Scientific;

up to 5 mM) or 3-morpholinosydnonimine·HCL (SIN-1, Biomol; up to 20 mM), dispensed in quadriplicate into 96-well flat-bottom plates at 26°C, and incubated for 72 h (or, with SIN-1, 1 h). After incubation, 20 µl of sterile resazurin solution (0.0125% resazurin salt (Sigma) in phosphate buffered saline) was added to each well and plates were further incubated for 18 h. The fluorescence was then measured using 550 nm excitation and 595 nm emission wavelengths. IC_{50} values were determined using GraFit 5 data analysis software (Erithacus Software).

Intracellular thiol measurement by HPLC

The quantification of thiols was carried out as previously described [39] using an HPLC method involving the conversion of thiols to fluorescent derivatives by reaction with monobromobimane, a fluorescent dye.

In vitro macrophage infections

Peritoneal macrophages obtained from BALB/c mice were cultured in RPMI medium with 20% (v/v) FCS at 2 x 10^4 cells/well in 24-well plates. After overnight incubation at 37ºC with 5% CO_2, non-adherent cells were removed and macrophages were incubated with stationary phase *L. donovani* promastigotes at a parasite/macrophage ratio of 5:1. After 2 h of infection, non-internalized parasites were washed off, replaced with fresh RPMI medium with 20% (v/v) FCS and incubated at 37ºC with 5% CO_2 for up to 3 days. Cells were fixed with 100% methanol, stained with Giemsa stain (VWR BDH Prolabo) and the parasite infections of the macrophages were assessed at 0, 24 and 72 h post-infection. Sensitivity of the intracellular parasites to sodium stibogluconate (SSG) was determined using peritoneal macrophages infected with *L. donovani* promastigotes using a promastigote/macrophage ratio of 10:1 (to maximize infection rates). After 24 h of incubation at 37ºC with 5% CO_2, non-internalized parasites were washed off and the medium replaced with fresh RPMI medium with 20% (v/v) FCS containing varying concentrations of SSG: 0, 9.5, 19, 38, 75 and 150 µg/ml. After 3 days of incubation at 37ºC with 5% CO_2, cells were fixed with 100% methanol, stained with Giemsa stain and the percentage of infected macrophages was determined. Results were normalized, taking as 100% the infection rate in the absence of SSG treatment. All assays were performed in triplicate for each time point or condition tested.

In vivo infections and assessment of parasite load

Age-matched female BALB/c mice in-house bred at University of Strathclyde and commercially obtained Golden Syrian hamsters (*Mesocricetusauratus*; Harlan Laboratories, U.K.) were used in this study. All animal procedures were undertaken in

adherence to experimental guidelines and procedures approved by The Home Office of the UK government. All work was covered by Home Office Project Licence PPL60/3929 entitled 'Mechanism of control of parasite infection'. All animal protocols received ethical approval from the University of Strathclyde Ethics Committee.

BALB/c mice (3 animals per group) were infected by intravenous injection (tail vein) with 2 x 10^7 *L. donovani* promastigotes in 200 µl of PBS. Two and six weeks post-infection, spleen and liver were removed and each organ was gently homogenised and resuspended in RPMI medium to obtain single cell suspensions for parasite load assessment. Golden Syrian hamsters were infected by intravenous injection (tongue vein) with 2 x 10^7 *L. donovani* promastigotes in 200 µl of PBS and sacrificed 3 months later. The spleen from each individual hamster was gently homogenized and resuspended in RPMI medium to obtain single cell suspensions for parasite load assessment.

Quantification of the parasite load in the spleens and livers was performed by limiting dilution as previously described [40]. Two-fold serial dilutions of the parasite suspensions were prepared in flat-bottomed 96-well microtiter plates. After incubation for 15 days at 26ºC, plates were examined and the positive (presence of motile parasites) and negative (absence of motile parasites) wells were determined using an inverted microscope. The number of parasites per gram of organ (parasite load) was calculated as follows: parasite load = [(geometric mean of reciprocal titer from each quadruplicate cell culture/weight of homogenized organ) x reciprocal fraction of the homogenized organ inoculated into the first well].

Leishmania extracts for metabolite analysis

L. donovani promastigote cultures were initiated at 2.5 x 10^5 cells/ml in four replicate 10 ml cultures in order to obtain cell samples from four independently growing cultures (biological replicates). Promastigotes from each culture were harvested at days 5 and 6 for protein estimation (for normalizing the metabolite data) and metabolite extraction. The metabolite extraction was performed as previously described [28]. Briefly, promastigotes quenching was performed in a dry ice/ethanol bath with rapid temperature decrease to 2ºC and then immediate transfer to ice. Two aliquots of 4 x 10^7 cells were taken from each culture flask (technical replicates). After centrifugation at 12000 g for 10 min at 4ºC, the supernatant (designated the spent medium) was removed and stored on ice. Cell pellets were washed three times in 1 ml of PBS at 4ºC by centrifugation at 12000 g for 10 min at 4ºC. For cell disruption and metabolite extraction, cell pellets were resuspended in 200 µl cold chloroform/methanol/water (20/60/20, v/v/v) and incubated 1 h in a

Thermomixer(1400 rpm, 4ºC). After centrifugation at 12000 g for 10 min at 4ºC, the supernatant containing the extracted metabolites was recovered and stored at -70ºC until analysed. To 75 µl of spent medium was added 300 µl of cold chloroform/methanol (20/60, v/v) followed by incubation for 1 h on ice. After centrifugation at 12000 g for 10 min at 4ºC, the supernatant was recovered and stored at -70ºC until analysed.

Liquid chromatography mass spectrometry (LC-MS) analysis and data processing

LC-MS analysis and data processing was carried out generally as described by t'Kindt and co-workers [28, 29] also applying subsequently improved analysis software [41]. Provisional identification of metabolites was carried out using a mass accuracy difference of up to 2 ppm (parts per million) and taking into account retention times. The identity of metabolites of interest was confirmed by co-elution with pure standards. The standards used to confirm identities of metabolites in this study are listed in Table S1. Intensity level ratios were used to compare the different cell lines, with the following criteria being applied for differences to be considered of interest and potentially due to *TDR1* gene deletion: (i) there was at least a 2-fold difference between the WT and Δ*tdr1*; (ii) there was at least a 2-fold difference between the Δ*tdr1* and the episomal add-back line; (iii) there was a statistically significant difference ($p<0.01$) between the cell lines being compared. The data are expressed as intensity per 25 µg cell protein.

Recombinant protein expression and purification

The *L. donovani* TDR1 (*Ld*TDR1) and the *L. infantum* dithiol glutaredoxin (*Li*GRX1) genes were amplified from genomic DNA by PCR and cloned into the vector pET15b (Novagen) which was modified to incorporate a tobacco etch virus protease site in place of the thrombin site in the N-terminal His-Tag [42]. Forward (5'-GCCATATGGCCGCCCGCGCG CTAAAGCTATACGTG-3') and reverse primers (5'-CTGGATCCTTACCCGCTCTGGGCC CTCCGTTG-3') containing *Nde*I and *BamH*I restriction sites (underlined), respectively, were used to clone *Ld*TDR1 and primers (5'-GCCATATGCTCTCCAGCCGTTTTCTCTAT CG-3' and 5'-ATCCTCGAGTTACGCAAGCTTCGCAGCCAG-3') containing *Nde*I and *Xho*I restriction sites (underlined) were used to clone *Li*GRX1. Nucleotide sequencing confirmed that the *Ld*TDR1 is identical to the *L. infantum* TDR1 (LinJ.33.0260), making suitable the comparison between *Ld*TDR1 and *Li*GRX1 recombinant proteins. The *Li*GRX1 (LinJ.27.0670) is homologous to the *T. brucei* GRX1 (Tb11.47.0012) characterized previously by Ceylan and co-workers [11]. Both *Ld*TDR1 and *Li*GRX1 were expressed in *E. coli* strain BL21/DE3 for 16 h at 15ºC, following induction with 1 mM isopropyl-β-D-thiogalactopyranoside. The recombinant proteins (hereafter designated TDR1 and GRX1) from 250 ml cultures were purified to more than 90% homogeneity

using nickel nitrilotriacetate (Ni-NTA) agarose (QIAGEN) columns. Cells were harvested by centrifugation and resuspended in 5 ml of buffer A (50 mM sodium phosphate buffer, 300 mM NaCl, pH 8.0) containing 10 mM imidazole. Cell lysates were prepared by sonication and cleared by centrifugation at 13,000 x g for 30 minutes at 4ºC. The soluble fraction was applied to a 1 ml Ni-NTA column equilibrated with buffer A containing 10 mM imidazole. After washing with 10 ml of buffer A containing 20 mM imidazole, the N-terminally His-tagged protein was eluted with 250 mM imidazole in buffer A. Fractions containing TDR1 were pooled and buffer exchanged against 25 mM Tris HCl pH 8.0 containing 250 mM NaCl using a PD-10 column (GE Healthcare) and stored at -80^{o}C, whereas GRX1 fractions were stored at 4ºC without further treatment for up to 1 month. 20 mg of TDR1 and 7 mg of GRX1 were obtained from 250 ml cultures.

Assays for determining deglutathionylation activity

Deglutathionylation activities of *Ld*TDR1 and *Li*GRX1 were measured using glutathionylated bovine serum albumin (BSA-SG) and a synthetic glutathionylated peptide (Peptide-SG) as substrates.

To prepare BSA-SG, the BSA (Sigma) was reduced, denatured and then glutathionylated by incubation with GSH in the presence of an oxidizing agent as previously described by Cheng *et al*.[43]. Briefly, BSA (10 mg/ml) in 50 mM Tris-HCl, 200 mM NaCl, pH 7.5 containing 0.1 % (v/v) SDS and 5 mM DTT was heated for 2 min at 100ºC; the SDS and DTT were removed using a PD-10 column (GE Healthcare) equilibrated with 50 mM Tris-HCl, 200 mM NaCl, pH 7.5. The reduced and denatured BSA was then mixed with 1 mM GSH and 100 mM H_2O_2 and incubated for 15 min at 30^{o}C before passing through a PD-10 column as described above. The protein concentration was determined by measuring the absorbance at 280 nm and the total thiol content was quantified using a 5,5'-dithiobis 2-nitrobenzoic acid assay [44]. The reduced and denatured BSA typically contained 7 cysteine thiols per molecule whereas only 0.4 thiols were detected after oxidation. This shows that the BSA-SG contains a maximum of 7 or 8 glutathionylated cysteine residues per molecule but other types of cysteine oxidation are also possible including disulfide bond formation. Reduction or deglutathionylation of the BSA-SG was assayed in 200 µl of 50 mM Tris-HCL, 5 mM EDTA, pH 7.0 containing 200 µM NADPH, 2 U/ml glutathione reductase (GR), 1 mM GSH and 120 nM TDR1 or 1.7 µM GRX1. The assay mixture was pre-incubated for 5 min at 30ºC before starting the reaction by addition of 30 µM of BSA-SG. Deglutathionylation activity was quantified by measuring the decrease in absorbance at 340 nm due to NADPH oxidation. Specific activities were expressed as µmol/min/mg protein and represent the means ± standard deviation of three independent experiments.

A peptide with a sequence SQLWCLSN with a GSH residue linked to the cysteine residue by a disulfide bond, as used previously in deglutathionylation assays [45, 46], was obtained from Peptide Protein Research Ltd. The glutathionylated peptide (Peptide-SG) was used to quantify deglutathionylation in a coupled assay with GR as described by Bonilla *et al.* [46]. The assay was carried out in 200 µl of 50 mM Tris-HCl, pH 7.0 containing 5 mM EDTA, 200 µM NADPH, 2 U/ml GR, 250 µM GSH and 100 nM TDR1 or 50 nM GRX1. The assay components were incubated for 5 min at 30ºC before starting the reaction by addition of Peptide-SG to a final concentration of 100 µM. Deglutathionylation activity was quantified by measuring the decrease in absorbance at 340 nm due to NADPH oxidation. The K_m of TDR1 for Peptide-SG was determined with a fixed concentration of GSH (250µM) and 50-600 µM Peptide-SG. The K_m of GRX1 was determined with 250 µM GSH and 2.5-200 µM Peptide-SG.

Statistical analyses

Statistical analysis was performed using Student's T test: a *p* value smaller than 0.05 ($p<0.05$) was considered significant; SPSS Statistics software (IBM) was used to perform principal component analysis; GraphPad Prism 4 was used for plotting the graphs and VisuMap software (VisuMap Technologies Inc.) was used to visualize the data as heatmaps.

Results

Generation of mutants lacking TDR1

To investigate the role of TDR1 in *L. donovani*, we created a null mutant (designated ∆*tdr1*) by homologous gene replacement. Targeted gene replacement is a powerful method that has enabled the deletion of many *Leishmania* genes after two rounds of knockout as most *Leishmania* species are predominantly diploid [47], although recent findings have revealed quite extensive aneuploidy especially in *L. donovani* [48, 49]. Fig. 1A shows the constructs used to replace the *TDR1* alleles in *L. donovani* by the hygromycin phosphotransferase (*HYG*), bleomycin acetyltransferase (*BLE*) or streptothricin acetyltransferase (*SAT*) genes flanked at the 5' and 3' ends with the 5' and 3' UTRs of the *TDR1* gene. After two rounds of transfection, two alleles of the *TDR1* gene had been replaced by the selection constructs. However, Southern blot analysis, using the 3' UTR of *TDR1* as the probe, showed that the wild type (WT) gene was still present in the genome of these parasite clones (Fig. 1B, lane 3) - which were thus designated *TDR1/tdr1/tdr1*. Several attempts to obtain a null mutant after two rounds of transfection

were made, but in all cases they resulted in the generation of parasites in which the WT gene remained. *TDR1* null mutants of *L. major* had been obtained after just two rounds of transfection, showing that the gene is not essential for this related species (J.C. McGregor and G.H. Coombs, unpublished results). We reasoned, therefore, that, as *L. major* and *L. donovani* are relatively closely related, *TDR1* is unlikely to be essential for *L. donovani*. Thus, we hypothesized that the impossibility of deleting the *TDR1* gene from *L. donovani* after two rounds of transfection was due to triploidy of the *TDR1* gene. After a third round of transfection using the *SAT* construct, we obtained parasites able to grow in the presence of all three of the selection drugs and Southern blot analysis confirmed the deletion of a third copy of the *TDR1* gene (Fig. 1B, lane 4) and so the generation of a null mutant (Δ*tdr1*).

Loss of TDR1 expression in Δ*tdr1* was confirmed by western blot analysis using anti-TDR1 antibody (Fig. 1C, lane 3). To aid in the identification of phenotypic differences between the WT parasite and the Δ*tdr1* null mutant that directly related to loss of the gene, the null mutant was complemented either with an episomal or a ribosomal *Leishmania* expression vector containing *TDR1* and these complemented (add-back) lines were termed Δ*tdr1*[pXG*TDR1*] and Δ*tdr1*::P_{RRNA}*TDR1*, respectively. Analysis of both lines by western blot showed successful re-expression of TDR1 in the null mutant (Fig. 1C, lanes 4 and 5). These findings on the generation of the *TDR1* null mutant of *L. donovani* provide strong evidence that this isolate of *L. donovani* is triploid at the *TDR1* locus. Deletion of *TDR1* did not affect the growth of promastigotes *in vitro,* as the growth rates of the WT parasites and the various mutants generated were all similar (Fig. 1D). Thus *TDR1* is not essential for viability of *L. donovani* promastigotes.

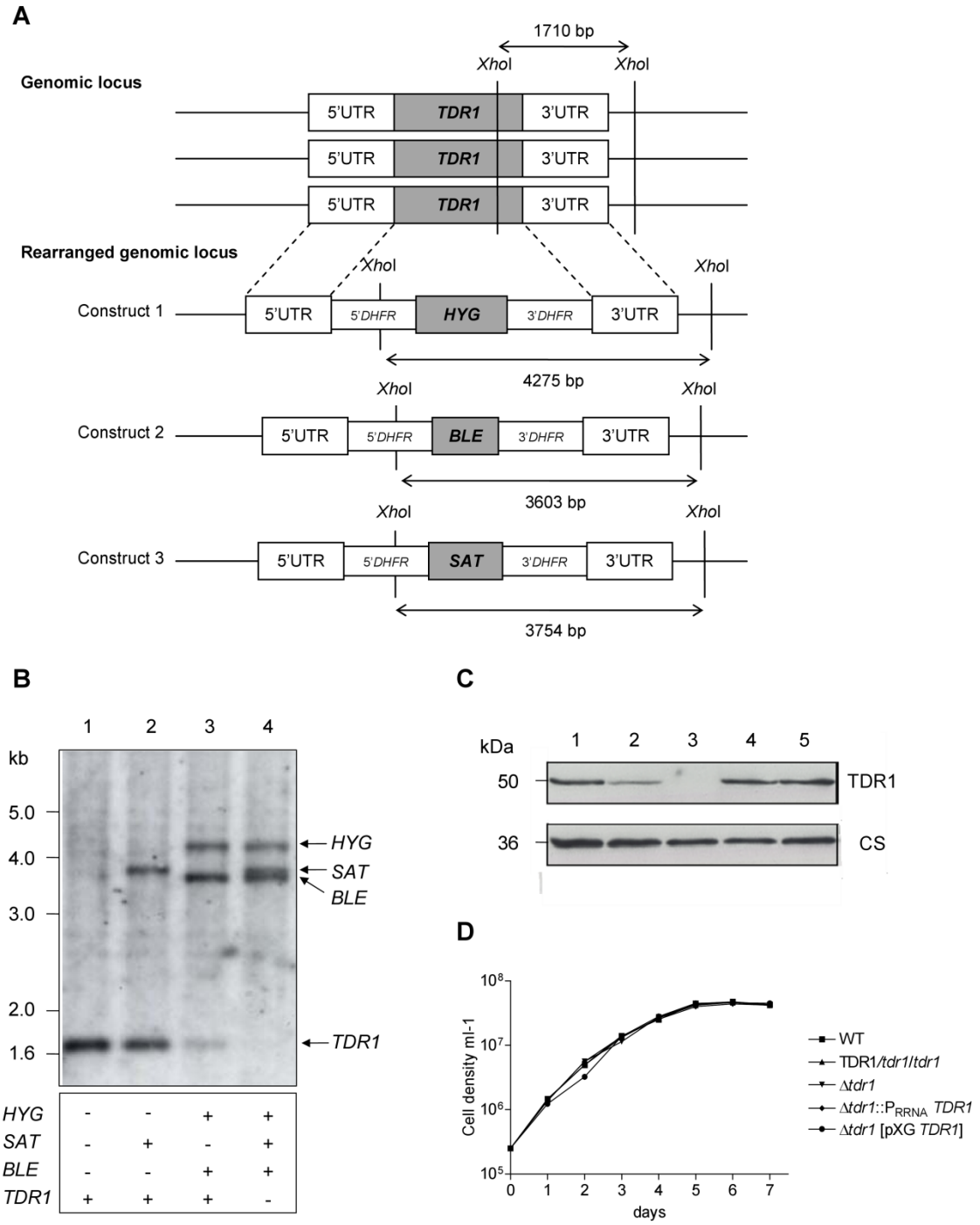

Figure 1. Targeted replacement of the *TDR1* gene of *L. donovani*. (A) Schematic representation of the *TDR1* locus and the constructs used to replace the gene copies. Expected sizes of the *Xho*I fragments revealed by Southern blot analysis are shown. UTR, untranslated region; *DHFR*, dihydrofolate reductase gene; *HYG*, hygromycin phosphotransferase gene; *BLE*, bleomycin acetyltransferase gene; *SAT*, streptothricin acetyltransferase gene. (B) Southern blot analysis of genomic DNA digested with *Xho*I, separated on a 0.8% agarose gel and blotted onto a nylon membrane. The membrane was hybridized with an alkaline phosphatase-labeled DNA probe comprising the 3'UTR of

the *TDR1* gene. DNA was from the wild type *L. donovani* (WT, lane 1), a single allele replacement clone (*TDR1/TDR1/tdr1*, lane 2; a clone with the *SAT* replacement is shown to clarify the genes in Δ*tdr1*, lane 4), a two allele replacement clone (*TDR1/tdr1/tdr1*, lane 3) and the *TDR1* null mutant (Δ*tdr1*, lane 4); the positions of the molecular size markers (kb) and identity of the bands are shown on the left and on the right, respectively. The box below summarizes which genes are present. (C) Western blot analysis of cell lysate from stationary phase promastigotes of WT (lane 1), *TDR1/tdr1/tdr1* (lane 2), Δ*tdr1* (lane 3), ribosomal add-back line (Δ*tdr1*::P_{RRNA}*TDR1,* lane 4) and episomal add-back line (Δ*tdr1*[pXG *TDR1*], lane 5). Cell extracts were separated using 12% SDS-PAGE and immunoblotted with polyclonal sheep anti-TDR1 serum. Anti-serum raised in rabbit against cysteine synthase (CS) was used to confirm equivalent protein loading; molecular masses are indicated on the left (kDa) and identity of the bands is shown on the right. (D) The effect of *TDR1* disruption on the *in vitro* growth as promastigotes of *L. donovani* WT, *TDR1/tdr1/tdr1*, Δ*tdr1*, Δ*tdr1*::P_{RRNA}*TDR1* and Δ*tdr1*[pXG *TDR1*]. Cultures were seeded at 2.5 x 10^5 parasites/ml and counted daily. Log base 10-transformed cell density is shown. Δ*tdr1*[pXG *TDR1*] were grown in the presence of 50 μg/ml G418.

Deletion of TDR1 renders L. donovani promastigotes more sensitive to trivalent arsenite and trivalent antimony but not reactive oxygen and nitrogen species

Leishmania parasites are exposed to a variety of reactive oxygen and nitrogen species (ROS and RNS) - from their own metabolism and from the oxidative burst generated during phagocytosis by their host macrophage that includes superoxide ($O_2^{\cdot -}$), H_2O_2, hydroxyl radical ($^{\cdot}OH$), nitric oxide ($^{\cdot}NO$) and peroxynitrite ($ONOO^-$) (reviewed in [8]). *Leishmania* rely on an antioxidant defense system mainly based on trypanothione [19], which is able to suppress macrophage responses [50]. To investigate whether TDR1 may also play a role in protection against oxidative and nitrosative stress, we used H_2O_2, SNAP and SIN-1 as reagents that induce stress of a different nature and potentially mimic those to which *Leishmania* is naturally exposed. SNAP releases $^{\cdot}NO$ under physiological conditions while SIN-1 induces mixed oxidative/nitrosative stress by the generation of both $O_2^{\cdot -}$ and $^{\cdot}NO$ that spontaneously form $ONOO^-$. Promastigotes were exposed to different concentrations of H_2O_2, SNAP or SIN-1 and their viability assessed by an Alamar Blue assay. The data generated (Table 1) show all of the lines were similarly susceptible to the oxidative/nitrosative stresses induced.

Table 1. Susceptibility of *L. donovani* promastigotes to oxidative/nitrosative stresses

	IC_{50} ± SD (μM)		
Parasite line	H_2O_2	SNAP	SIN-1
WT	477 ± 62	68 ± 12	871± 182
TDR1/tdr1/tdr1	468 ± 76	41 ± 4	878 ± 183
Δ*tdr1*	446 ± 42	46 ± 13	904 ± 170
Δ*tdr1*::P_{RRNA}*TDR1*	482 ± 110	47 ± 9	899 ± 154
Δ*tdr1*[pXG *TDR1*]	601 ± 73	42 ± 7	837 ± 137

IC_{50} represents the concentration of hydrogen peroxide (H_20_2), S-Nitroso-N-acetylpenicillamine (SNAP) or 3-morpholinosydnonimine·HCl (SIN-1) that inhibited by 50% the growth of the wild type (WT), *TDR1* null mutant (Δ*tdr1*), ribosomal add-back (Δ*tdr1*::P_{RRNA}*TDR1)* and episomal add-back (Δ*tdr1*[pXG *TDR1*]) lines. Each value is a mean ± standard deviation (SD) of three independent experiments. GraFit 5 software was used to calculate the IC_{50} values.

The susceptibility of the *L. donovani* promastigotes to metal compounds that can have a direct effect through the induction of DNA damage, GSH depletion, and binding to protein sulphydryl groups or an indirect one by the generation of ROS and RNS [51] was also tested (Table 2). Statistically significant differences were observed between the susceptibility of WT parasites and Δ*tdr1* to Sb^{III} or As^{III}, but not to Cd^{II} or Cu^{IV}. It is noteworthy that the episomal add-back returned the susceptibility to WT levels, whereas the ribosomal add-back line was similarly susceptible as Δ*tdr1* itself.

The activity of TDR1 involves the use of glutathione as a reducing agent [9] and so it appeared possible that the greater susceptibility of the null mutant to metal compounds could reflect an interference with the mechanisms for thiol homeostasis. In order to evaluate the effect of *TDR1* deletion on the parasite's thiol pool, GSH, $T[SH]_2$ and cysteine levels were measured by HPLC for WT, Δ*tdr1* and Δ*tdr1*[pXG*TDR1*] promastigotes from different days of growth *in vitro*. No significant differences between lines were observed on any of days 4-6 of growth (data not shown).

Table 2. TDR1 null mutants display increased susceptibility to trivalent antimony and trivalent arsenite

Parasite line	IC_{50} ± SD (µg/ml)			
	Sb^{III}	As^{III}	Cd^{II}	Cu^{IV}
WT	70 ± 8	234 ± 15	239 ± 37	194 ± 41
TDR1/tdr1/tdr1	79 ± 7	198 ± 22	218 ± 24	153 ± 20
Δ*tdr1*	37 ± 9**	169 ± 5*	161 ± 54	121 ± 3
Δ*tdr1*::P_{RRNA}*TDR1*	45 ± 7*	136 ± 75	140 ± 50	120 ± 24
Δ*tdr1*[pXG *TDR1*]	77 ± 14	366 ± 78	228 ± 12	154 ± 26

IC_{50} represents the concentration of potassium antimonyl tartrate (SbIII), sodium arsenite (As^{III}), cadmium chloride (Cd^{II}) or copper sulfate (Cu^{IV}) that inhibited by 50% the growth of the wild type (WT), *TDR1* null mutant (Δ*tdr1*), ribosomal add-back (Δ*tdr1*::P_{RRNA}*TDR1)* and episomal add-back (Δ*tdr1*[pXG *TDR1*]) lines. Each value is a mean ± standard deviation (SD) of three independent experiments. GraFit 5 software was used to calculate the IC_{50} values. Statistically significant differences between WT and Δ*tdr1* or WT and Δ*tdr1*::P_{RRNA}*TDR1* lines are indicated: * p<0.05, ** p<0.01.

TDR1 deletion does not affect virulence to macrophages in vitro and to mice

Stationary phase promastigotes of the different cell lines were assessed for their ability to infect and survive in peritoneal macrophages *in vitro*. The extent of macrophage infection was determined at 0, 24 and 72 h post exposure to promastigotes (Fig. 2A). There was a decrease in the number of macrophages infected by the null mutant by 72 h, although this was not statistically significant when compared with the WT (p = 0.064), and there was no difference in the number of parasites per infected macrophage (data not shown).

The ability of promastigotes of the various lines to cause infection in BALB/c mice and in hamsters was investigated. All infected, and no differences were observed for the parasite loads in the spleen and liver between the WT and null mutant parasites in either host (data not shown).

TDR1 does not seem to be involved in susceptibility to pentavalent antimonials

Pentavalent antimonials (Sb^{V}) are pro-drugs that need to be reduced to trivalent antimonials (Sb^{III}) in order to be toxic to *Leishmania*. TDR1 is able to reduce Sb^{V} to Sb^{III} *in vitro* [9] and therefore it was postulated to have a role in susceptibility of the parasites to

Sb^V. The reduction of Sb^V could, however, also work in favor of the parasite, as the Sb^{III} form of the drug is readily extruded from the cell when conjugated with thiols [52]. Thus TDR1 could potentially have a role in drug susceptibility or drug resistance. In order to investigate whether TDR1 plays a part in determining the susceptibility of *Leishmania* to Sb^V, the relative susceptibility of the WT, Δ*tdr1* and the episomal add-back line in macrophages to Sb^V was analysed (Fig. 2B). No statistically significant differences between the Δ*tdr1* and WT lines were observed. Interestingly, the add-back line appeared slightly less susceptible to Sb^V, although there was no statistically significant difference compared with WT.

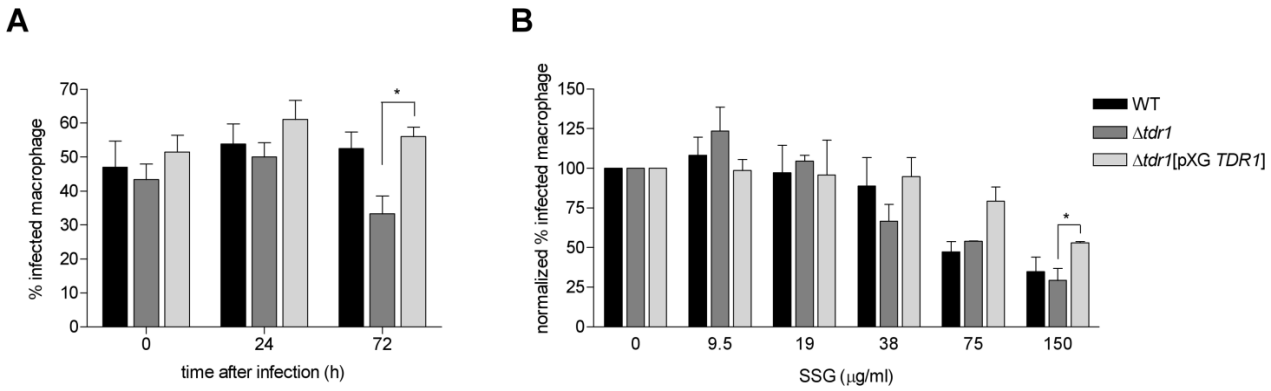

Figure 2. Infectivity to macrophages *in vitro* of *L. donovani* Δ*tdr1* promastigotes and susceptibility to sodium stibogluconate. (A) *L. donovani* WT, Δ*tdr1* and Δ*tdr1*[pXG*TDR1*] stationary phase promastigotes were used to infect peritoneal macrophages at a ratio of 5:1. After 2 h of infection, non-internalized parasites were washed off, replaced with fresh medium and incubated at 37ºC. Macrophage infection was determined at 0, 24 and 72 h post-infection. Each value is a mean ± standard deviation from three replicates and is representative of two independent experiments. (B) Stationary phase promastigotes were used to infect peritoneal macrophages at a ratio of 10:1 and incubated for 24 h. Non-internalized parasites were then washed off and replaced with fresh medium containing varying concentrations of sodium stibogluconate (SSG): 0, 9.5, 19, 38, 75 and 150 μg/ml. After 3 days of incubation, the percentage of infected macrophages was determined and the results normalized - taking as 100% the number of infected macrophages in the cultures not treated with SSG. Each value is a mean ± standard deviation from three replicates. Statistically significant differences between Δ*tdr1* and Δ*tdr1*[pXG *TDR1*] groups are indicated: * $p<0.05$.

Analyses of the effect of TDR1 deletion on the parasite's metabolome

To obtain insights into the role of TDR1 in the metabolism of *L. donovani*, we adopted a global metabolomics approach to identify differences between the metabolomes of WT and ∆*tdr1* promastigotes. We applied stringent conditions in experimental design, in selecting metabolite differences and confirming the identity of metabolites of interest (see methods section), including the requirement that differences between WT and Δ*tdr1* needed to be complemented in an add-back line.

As a means of ensuring that observed phenotypic changes between WT and Δ*tdr1* are the result of the gene deletion alone, we generated two add-back cell lines with the re-expression of TDR1 being from different loci (as described in the methods). Presence of the appropriate protein as analysed by western blot is usually taken as successful complementation of gene deletion, although the literature indicates that full complementation of phenotypic differences is not always observed [53-56]. In this study, we compared the metabolic profile of each add-back cell line with the metabolomes of the WT and Δ*tdr1* lines to analyse the effectiveness of the two methods of complementation to recover the WT metabolome phenotype. The ribosomal add-back (Δ*tdr1*::P_{RRNA}*TDR1)* did not result in reversion of metabolites to levels observed in the WT line as shown in Fig. 3. Principal component analysis (PCA) is an unsupervised clustering technique that allows the reduction of the data into two dimensions (principal component 1 and principal component 2), which capture and enable visualization of data variability [57]. The PCA analysis shows that replicates samples from Δ*tdr1*::P_{RRNA}*TDR1* and Δ*tdr1* cluster closely together, indicating a very similar metabolic profile, but removed from the WT which clearly demonstrates the separation between these two mutant cell lines and the WT line. In contrast, the episomal add-back (Δ*tdr1*[pXG*TDR1*]) did result in recovery to the WT levels for most metabolites (being very similar with respect to principal component 1 which accounts for 57.1% of total variance), with there only being variation in the second principal component which accounts for just 17.3% of the total variance. Thus surprisingly, as expression of TDR1 was similar in both add-backs as determined by western blot analysis (Fig. 1C), the ribosomal add-back did not recover any of the metabolite levels that differed by 2-fold between Δ*tdr1* and WT promastigotes, whereas the episomal add-back was effective in all except 18% of the metabolites (Table S2). The ribosomal add-back, as an integrative construct, is generally expected to lead to stable and consistent expression of the protein and so be more reliable than complementation using episomal expression, but our data show unambiguously that this is not the case with our mutant lines. Given these results, we only used the episomal add-back line in the remainder of the analyses (as indicated in the datasets themselves).

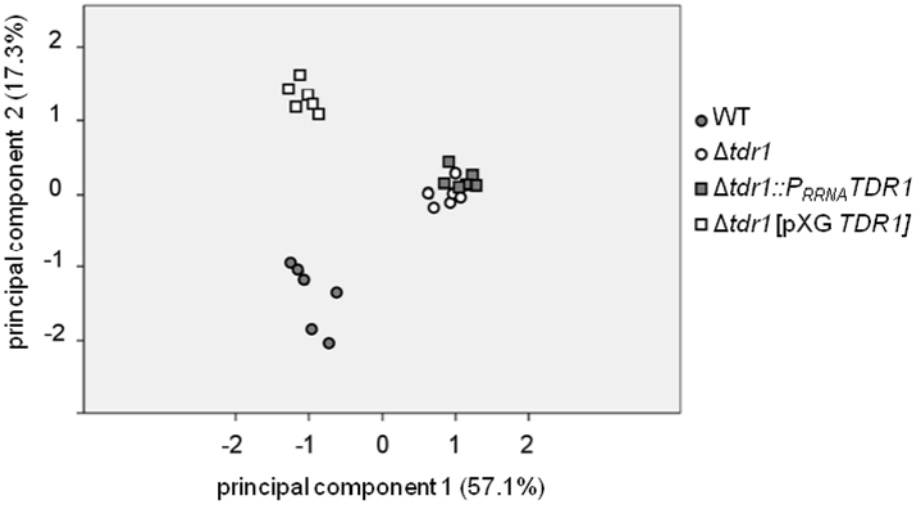

Figure 3. Episomal complementation of Δ*tdr1* is more effective than with an integrative construct. Principal component analysis of all metabolites identified by LC-MS in cell extracts from *L. donovani* WT, Δ*tdr1*, Δ*tdr1*::P_{RRNA}*TDR1* and Δ*tdr1*[pXG *TDR1*] promastigotes on day 5 of growth *in vitro*. Principal component 1 and principal component 2 explain 57.1% and 17.3% of the total variance, respectively.

In order to obtain meaningful data, it is important to have an indication of the relative intracellular concentrations of metabolites in the different lines. Thus it is necessary to take into account changes in cell size that occur during the life cycle of *Leishmania* (such as between different forms of promastigotes that occur in the *in vitro* cultures – procyclic promastigotes and metacyclic promastigotes) and also any changes induced by the genetic manipulations. A simple approximate correlate of cell size is protein content and we have shown in a previous study that a significant decrease in protein content occurs as *L. donovani* WT promastigotes progress into stationary phase [4]; this correlates with metacyclogenesis being initiated in late log phase and resulting in the metacyclic promastigotes that are characterized by a smaller body size [58]. To ensure that differences in the sizes of WT and Δ*tdr1* would not have an impact in the metabolome analysis and comparison, we checked for differences in protein content between these cell lines after 5 and 6 days in culture. As expected and observed previously [4] there was a decrease in protein content between the two time points, however there were no significant differences between the protein content of the WT and Δ*tdr1* promastigotes. To enable comparison of the metabolomes of promastigotes on days 5 and 6 of *in vitro* culture, we have expressed the data on metabolite levels per cell protein (rather than cell number), as we have reported previously [4].

In order to obtain an extensive metabolic profile of each cell line, promastigote cultures of *L. donovani* WT, Δ*tdr1* and Δ*tdr1*[pXG*TDR1*] were set up and harvested at 5 days, which corresponds to the transition between logarithmic and stationary phases of growth, and at stationary phase (6 days) when the number of mammal-infective metacyclic promastigotes are high. The experiments were performed based on four biological replicates per cell line to obtain representative data; also during the cell processing from each culture two samples (designated technical replicates) were taken to control for variation due to technical factors. Analysis of the data for identification of metabolites was carried out using a mass accuracy difference of up to 2 part per million (ppm). The initial identification of the metabolites was carried out based on the database of metabolites detailed by t'Kindt and co-workers [28, 29]. After manual verification of the metabolites initially identified by the software using LeishCyc database [59], we had a total of 363 and 378 putative metabolites for the day 5 and day 6 samples, respectively. The main comparison between WT and Δ*tdr1* cell extracts was performed based on the ratio of the signal intensity for each metabolite identified with the LeishCyc database. The intensities of the majority of metabolites identified were unaffected by *TDR1* gene deletion, with only about 10% of metabolites differing at least by 2-fold between the WT and Δ*tdr1* (Fig. 4). The putative compounds identified belong to a wide range of metabolic pathways, with lipids and amino acids and their derivatives being those identified in highest numbers (Fig. 5). A general overview of the metabolites within central metabolic pathways that were putatively detected is shown in Fig. S1. The full list of putatively identified metabolites at days 5 and 6 are detailed in Tables S3 and S4 of Supplementary Material. A comparative analysis of the levels of the metabolites identified in WT, Δ*tdr1* and Δ*tdr1*[pXG*TDR1*] promastigotes on days 5 and 6 of *in vitro* growth is shown in Fig. 5. This highlights that there were more differences between Δ*tdr1* and WT promastigotes on day 5 as some of the most prominent differences observed between the extracts on day 5 were not present by day 6. It is noteworthy that, in agreement with the PCA data (Fig. 3), there was a very good complementation of the metabolite levels by the episomal add-back, as verified by the values obtained for the ratio (WT/Δ*tdr1*[pXG*TDR1*]) being between 0.5 and 2 for almost all putatively identified metabolites (Tables S3 and S4).

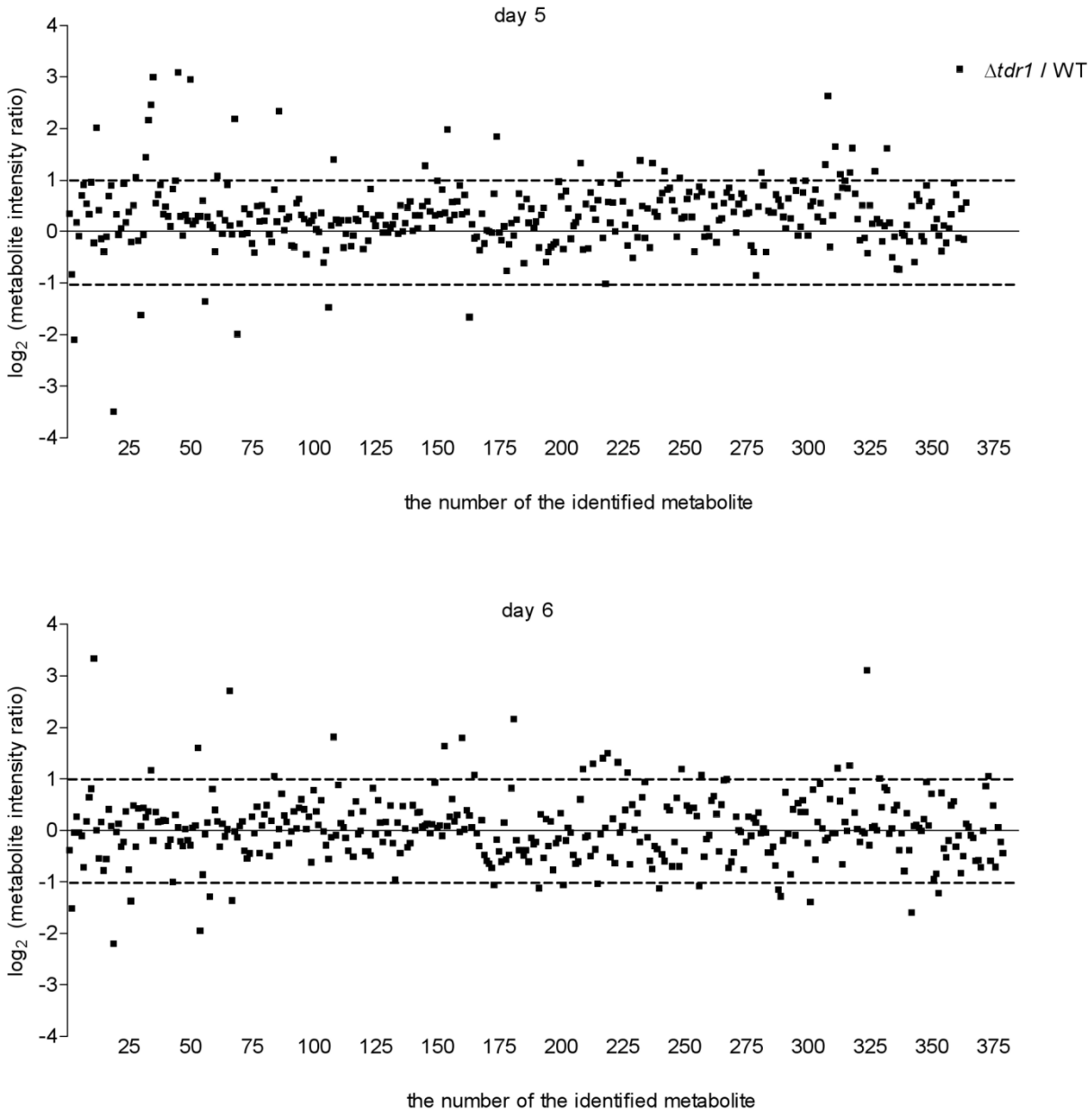

Figure 4. TDR1 deletion leads to few changes at a metabolic level. Differences detected between the levels of intracellular metabolites in *L. donovani* WT and Δ*tdr1* on days 5 (A) and 6 (B). Following a logarithmic transformation (base 2) the average signal intensity ratios of Δ*tdr1*/WT for all identified metabolites are plotted. The dotted lines represent the fold-change cut-off used in this study for a given metabolite profile being considered to be different between WT and Δ*tdr1*: $\log_2$ (metabolite intensity ratio) below -1 or above 1 indicates a 2-fold difference between the cell lines compared. The metabolites differing in intensity by at least 2-fold between WT and Δ*tdr1* on days 5 and 6 represented 10.4% and 10.5%, respectively, of all metabolites identified.

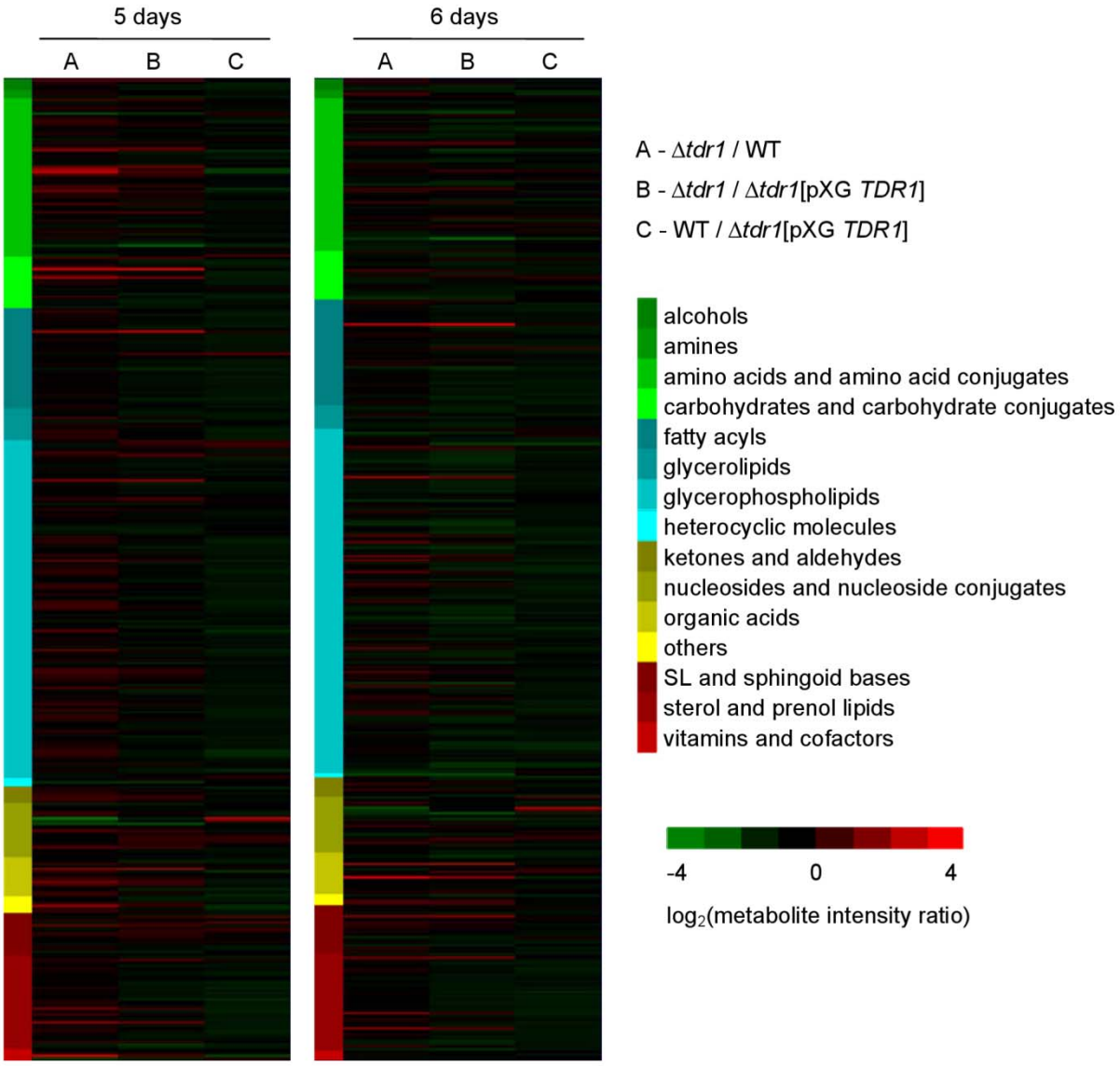

Figure 5. Comparative levels of all intracellular metabolites identified in *L. donovani* WT, Δ*tdr1* and Δ*tdr1*[pXG*TDR1*] promastigotes. The heatmap was generated using log base 2-transformed fold-changes determined by the average signal intensity ratios of Δ*tdr1*/WT (A), Δ*tdr1*/Δ*tdr1*[pXG *TDR1*] (B) and WT/Δ*tdr1*[pXG *TDR1*] (C) for all metabolites detected. Metabolites are ordered by compound category shown on the left and log values of measurements are color coded as indicated in the scale on the right of the heatmap, from green to red.

The criteria that we have used in this study to define whether detected differences in intensity levels of a metabolite between the cells lines is of interest are that both ratios Δ*tdr1*/WT and Δ*tdr1*/Δ*tdr1*[pXG*TDR1*] show greater than 2-fold differences and that these are statistical significant (p<0.01); thus we have concentrated on the metabolite changes for which recovery by the episomal add-back was achieved. Moreover, we have only

included in the following analysis metabolites whose identity has been confirmed by using standards. Metabolites identified in the data for days 5 and 6 of growth that fulfilled these conditions are shown in Fig. 6. Proline, 2-ketoisocaproate, indolelactate, deoxycytidine, argininosuccinic acid and CDP-choline were significantly different on both days. Some metabolites differed only on one day: histidine, glycerol-3-phosphate and S-adenosylhomocysteine are metabolites for which the fold change between the Δ*tdr1* mutant and WT became lower than 2 on day 6, whilst mevalonate is not shown on day 5 because the ratio Δ*tdr1*/Δ*tdr1*[pXG*TDR1*] is lower than 2 - thus that recovery by the episomal add-back was not to the level required for inclusion. The identity of metabolites in Fig. 6 was confirmed by co-elution with standards. Some metabolites fulfilling the criteria of being >2-fold and significantly different between the WT and Δ*tdr1* were excluded from Fig. 6 as we have been unable to confirm their putative identification by co-elution with standards. These include proline betaine, 10-pentadecenal, valerylglycine, 8-amino-7-oxo-nonanoic acid, and 4alpha,14alpha-dimethyl-24-methylene-cholest-7,(11)-dien-3beta-ol.

We also investigated the metabolite changes in the culture medium, as metabolite uptake and release are part of the overall metabolic events occurring. Just a few metabolite levels differed significantly between the spent media for WT and ∆*tdr1* parasites after 6 days of growth *in vitro* (Fig. 7 and Table S5). Only a few met the criteria applied for being meaningfully different between the ∆*tdr1* and WT lines (Fig. 7C). Interestingly, the extracellular proline levels were decreased with ∆*tdr1* compared with the WT, as were the intracellular levels (Fig. 6). Also, 2-ketoisocaproate levels were increased in the null mutant spent medium relatively to the WT spent medium; the concentrations also increased intracellularly. The other significant differences (aspartic acid and glutamic acid) were not mirrored by intracellular changes that fulfilled our criteria for inclusion as being significant.

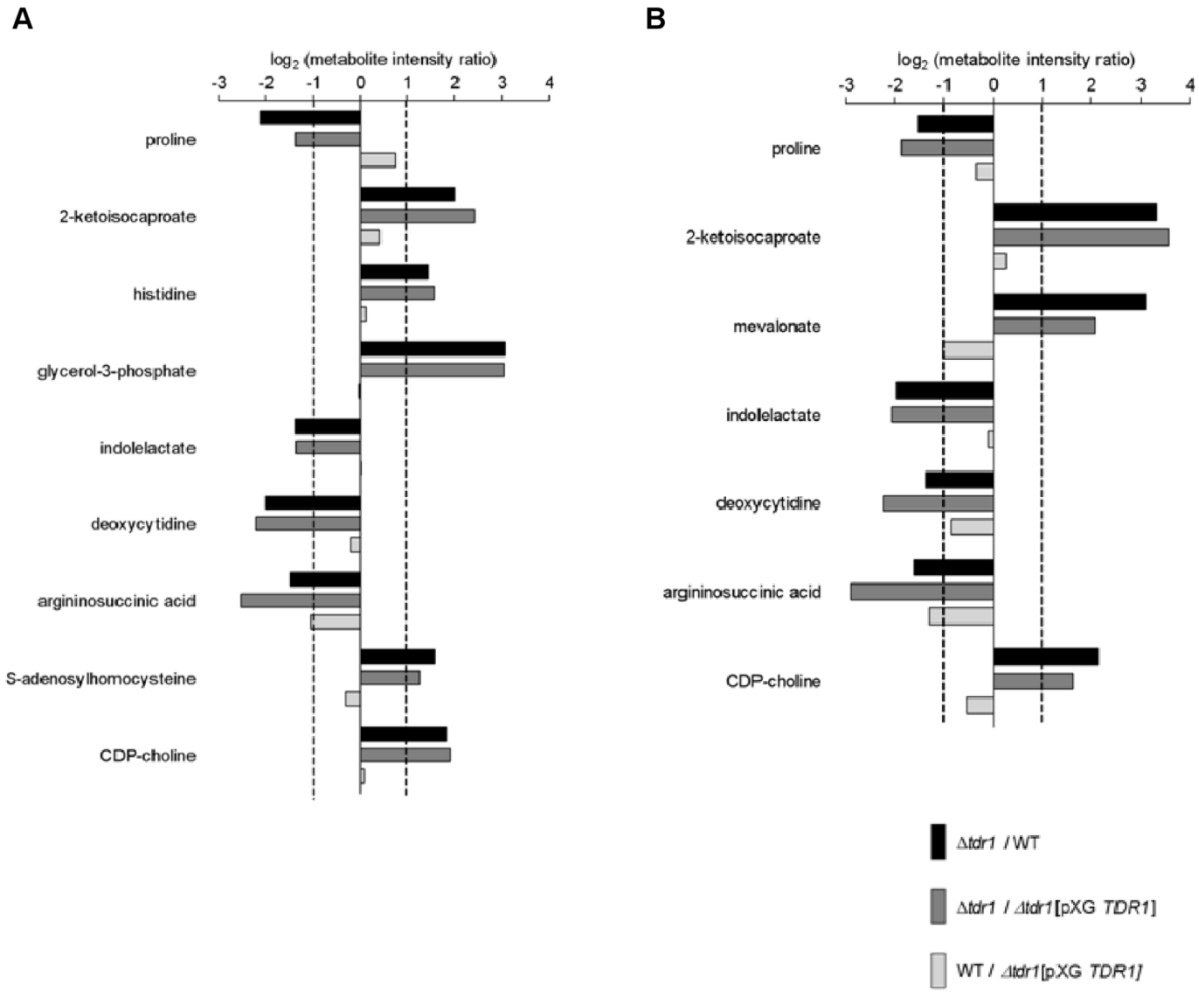

Figure 6. Intracellular metabolites at different levels in *L. donovani* WT and Δ*tdr1* promastigotes. *L. donovani* WT, Δ*tdr1* and Δ*tdr1*[pXG *TDR1*] were harvested after 5 and 6 days of growth *in vitro* and cell extracts analyzed by LC-MS. Following a logarithmic transformation (base 2), the average signal intensity ratios of Δ*tdr1*/WT, Δ*tdr1*/Δ*tdr1*[pXG *TDR1*] and WT/Δ*tdr1*[pXG *TDR1*] for metabolites at interestingly different levels identified on day 5 (A) and day 6 (B) were plotted. Dotted lines represent the adopted cut-off for significant changes in a given metabolite profile: $\log_2$ (metabolite intensity ratio) below -1 or above 1 indicates a 2-fold difference between the cell lines compared. All metabolites shown were statistically significant different between Δ*tdr1* and WT or Δ*tdr1*[pXG *TDR1*] and their identities were confirmed by co-elution with the respective standard. The metabolites are ordered according to mass.

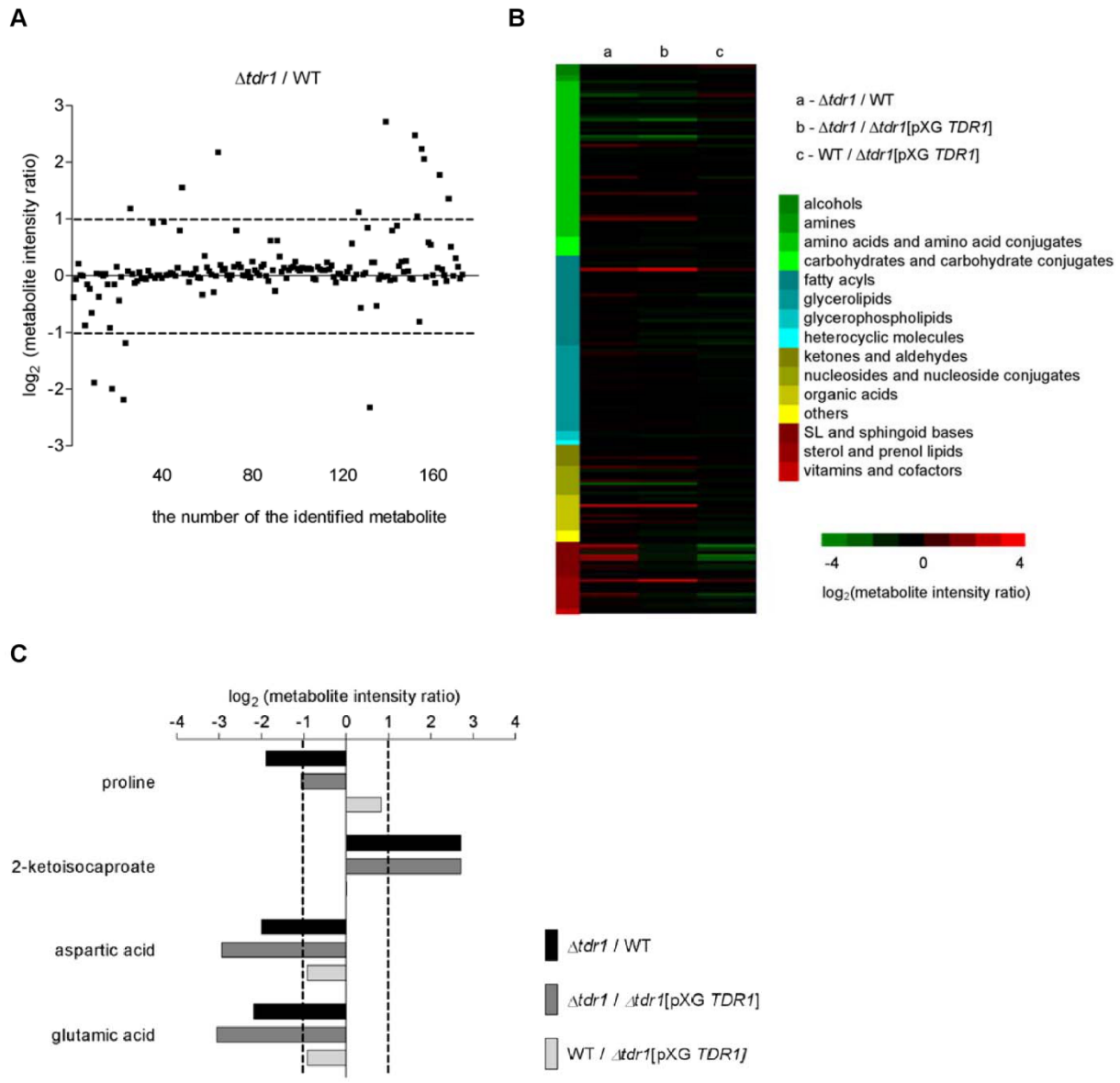

Figure 7. Changes in extracellular metabolite profile due to *TDR1* gene deletion. (A) Differences detected between the levels of all metabolites identified in the spent culture media of *L. donovani* WT and Δ*tdr1* promastigotes on day 6 of growth *in vitro*. Following a logarithmic transformation (base 2), the average signal intensity ratios of Δ*tdr1*/WT for all metabolites was plotted. The metabolites differing at least by 2-fold between the WT and Δ*tdr1* on day 6 represented 9.3% of the all of the metabolites identified. (B) Comparison of levels of all extracellular metabolites detected in the spent media of *L.donovani* WT, Δ*tdr1* and Δ*tdr1*[pXG *TDR1*] promastigotes on day 6 of growth *in vitro*. The heatmap was generated using log base 2-transformed average signal intensity ratios of Δ*tdr1*/WT (a), Δ*tdr1*/Δ*tdr1*[pXG *TDR1*] (b) and WT/Δ*tdr1*[pXG *TDR1*] (c) for all metabolites identified using 2 ppm cut-off. Metabolites are ordered by compound category shown on the left and log values of measurements are color-coded as indicated in the scale on the right of the

heatmap, from green to red. (C) Metabolites identified at significant different levels in the spent media of WT and Δ*tdr1* on day 6. Following a logarithmic transformation (base 2), the average signal intensity ratios of Δ*tdr1*/WT, Δ*tdr1*/Δ*tdr1*[pXG *TDR1*] and WT/Δ*tdr1*[pXG *TDR1*] were plotted. Dotted lines in A and C represent the adopted cut-off for significant changes in a given metabolite profile: $\log_2$ (metabolite intensity ratio) below -1 or above 1 indicates a 2-fold difference between the cell lines compared. All metabolites shown in C were statistically significant different between Δ*tdr1* and WT or Δ*tdr1*[pXG *TDR1*] and their identities were confirmed by co-elution with the respective standard. The metabolites are ordered according to mass.

Recombinant TDR1 has deglutathionylation activity towards protein and peptide substrates

In order to investigate whether the changes observed in Δ*tdr1* parasites at a metabolome level could reflect TDR1 having a role in regulation of enzymes via glutathionylation, we evaluated the ability of TDR1 to catalyze protein deglutathionylation. TDR1 and GRX1 were purified as recombinant N-terminally His-tagged proteins and confirmed to catalyse the deglutathionylation of a small molecule mixed-disulfide in the 2-hydroxyethyl disulfide (HEDS) assay (data not shown) with specific activities that were comparable to those reported for *L. major* TDR1 [9] and *T. brucei* GRX1 [11]. To determine whether TDR1 and GRX1 can also use protein-GSH mixed disulfides as a substrate, BSA was glutathionylated chemically by reduction and denaturation followed oxidation in the presence of GSH. The specific activity of TDR1 in reducing the glutathionylated BSA (BSA-SG) was 3.1 ± 0.7 µmol/min/mg, which was similar to that obtained with GRX1 (1.6 ± 0.4 µmol/min/mg). Kinetic analysis of the protein deglutathionylation reaction was performed using a peptide with the sequence SQLWCLSN, synthesised with a GSH linked to the cysteine residue by a disulfide bond (Peptide-SG). Peltoniemi and co-workers used this glutathionylated peptide in a fluorescence assay, exploiting the observation that the disulfide bond quenches the fluorescence of the adjacent tryptophan residue [45]. However, in this study it was more convenient to measure peptide deglutathionylation in a coupled assay with GR as described by [46]. Table 3 shows a comparison of the kinetic parameters obtained with TDR1 and GRX1 in this study, as well as published data for the *E. coli* GRX1 with the same substrate (Peptide-SG) [45] and for *T. brucei* Grxs (GRX1 and GRX2) with glutathionylated tryparedoxin-dependent peroxiredoxin protein (TXNPx-SG) as a substrate [11]. The K_m for the Peptide-SG was 40-fold higher for TDR1 than for GRX1, but the turnover of the glutathionylated peptide by TDR1 was also higher. Interestingly, similar differences in these kinetic parameters were observed when *T. brucei* GRX1 and GRX2 were compared [11]. The k_{cat} value obtained with TDR1 in the peptide

deglutathionylation was comparable to published values for different glutaredoxins with gluthionylated proteins or peptides as substrates [11, 45, 60]. The catalytic efficiency (k_{cat} /K_m) of GRX1 in reducing peptide-SG is similar to that of its homolog *T. brucei* GRX1 with TXNPx-SG as a substrate, whereas the catalytic efficiency of TDR1 in this assay is more similar to that of *T. brucei* GRX2.

Table 3. Kinetic analysis of peptide deglutathionylation catalysed by TDR1

Enzyme	Substrate	k_{cat} (s^{-1})	K_m (μM)	k_{cat}/K_m ($M^{-1}s^{-1}$)	Ref.
*Ld*TDR1	Peptide-SG	6.5 ± 1.7	433 ± 175	1.5 x 10^4	this study
*Li*GRX1	Peptide-SG	1.0 ± 0.1	7.6 ± 0.2	1.3 x 10^5	this study
*Eco*GRX1	Peptide-SG	4.4	7.8	5.1 x 10^5	[45]
*Tb*GRX1	TXNPx-SG	1.5	21	6.9 x 10^4	[11]
*Tb*GRX2	TXNPx-SG	1.0	269	3.8 x 10^3	[11]

Results for *L. donovani* TDR1 (*Ld*TDR1) and *L. infantum* GRX1 (*Li*GRX1) are the means of 2 independent experiments (± 0.5 range). Enzymes: *Eco*GRX1, *E. coli* glutaredoxin type 1; *Tb*GRX1, *T. brucei* glutaredoxin type 1; *Tb*GRX2, *T. brucei* glutaredoxin type 2. *T .brucei* GRX1 is the homolog of *Li*GRX1. *Tb*GRX2 has the active site motif CQFC and only 25% amino acid identity with *Tb*GRX1 [11]. The *Leishmania* homolog of GRX2 has only one cysteine in the active site (CQFS). Substrates: Peptide-SG, SQLWCLSN with GSH linked to the cysteine by a disulfide bond; TXNPx-SG, glutathionylated *T. brucei* tryparedoxin-dependent peroxiredoxin.

Discussion

In order to gain insights into the role of TDR1 in *Leishmania*, we have generated a *TDR1* null mutant using *L. donovani* promastigotes. To obtain the null mutant it was necessary to perform three rounds of transfection, because of the presence of three copies of the gene. Although an unexpected finding, recently published studies using new and refined methods to sequence *Leishmania* genomes from different species have shown that chromosome copy number variation seems to be widespread and a potential contributor for *Leishmania* genetic plasticity and diversity [48, 49]. *Leishmania* has been considered to be predominantly diploid [47], with the exception of chromosome 1 trisomy [61] and

chromosome 31 tetrasomy in *L. major* [62]. Many previous reports of the emergence of aneuploid parasites have been associated with attempts to knockout essential genes [63-65] or in response to drug pressure [66]. Thus our finding of aneuploidy that was not brought about by genetic manipulation or drug pressure but is a genomic feature of the *L. donovani* strain used is unusual but may reflect a situation occurring more commonly than reported to date, certainly our finding supports the recently published genome sequencing data [48, 49]. It is important to note that the aneuploidy is not a feature of the whole genome in this line – we were able to generate a null mutant for cysteine synthase, after just two rounds of transfection (L. McCaig, G.H. Coombs and S. Müller, unpublished results); thus triploidy and diploidy can clearly occur simultaneously in one cell. Sterkers and co-workers [67] described a mechanism that might explain the genomic plasticity observed in *Leishmania.* Their data suggested that every chromosome was observed in at least two ploidy stages and also chromosome ploidy distribution was variable among clones and strains. This phenomenon, named chromosomal mosaicism, appeared to be constitutive and potentially responsible for the generation of phenotypic variability from genomic plasticity. Such mosaicism would raise many questions and have implications for the methodology that could be used to study *Leishmania*, as it would make it difficult to predict the variability in chromosome copy number. The subsequent findings from genome sequencing [48, 49] provide clear evidence of aneuploidy, especially in *L. donovani*. However, the fact that gene null mutants can be obtained, albeit in this study requiring three gene deletion events, suggests that the genome is not very variable within a population; if it was one would expect there always to remain parasites with an endogenous copy of the gene. Thus the data available show convincingly that gene copy number varies, but the frequency and rate of change remains to be determined. Such gene dose fluctuation may provide significant adaptive advantage to the parasite in coping with different environments, including drug pressure, and may be crucial in facilitating the development of resistance to antiparasite drugs.

The two domain structure of TDR1, with motifs characteristics of Grxs and GSTO, and the ability of the recombinant protein to use GSH as an electron donor to reduce dehydroascorbate (DHA) and HEDS, an artificial substrate generally used to measure deglutathionylation activity of Grx [9], suggested a possible role of TDR1 in regulation of redox-sensitive proteins within the parasite and so an active part in antioxidant defense during the parasite's multi-environment life cycle. Thus, we challenged the *TDR1* null mutant (Δ*tdr1*) to different compounds known to induce oxidative and nitrosative stress. No evidence was obtained for the greater susceptibility of the mutant than WT to these stressers, which does not support the suggestion that TDR1 has an involvement in

protection of the parasite against this type of stress. Importantly, however, several other *Leishmania* proteins, including ascorbate peroxidase [6] and peroxiredoxins [5], have been reported to be central players in the regulation of ROS content in the parasite. For instance, recently Wyllie and co-workers demonstrated that *L. donovani* antimony-resistant field isolates have higher levels of tryparedoxin and tryparedoxin peroxidase than antimony-sensitive isolates, which could comprise an enhanced antioxidant defense to protect the parasite from the oxidative stress induced by exposure to the antimonial drug [7]. Thus as many enzymes appear to be involved in protecting *Leishmania* from oxidative/nitrosative stress during its life cycle (reviewed in [8]), those stresses generated in the different environments and also due to drug pressure, there is probably significant redundancy between them. Therefore although the deletion of *TDR1* did not lead to a change in the overall susceptibility of the living parasite to such stressers, this should not be interpreted as confirmation that the enzyme plays no part in protection against oxidative/nitrosative stress – it may play a part together with others. Analyses of the parasite's intracellular thiols also showed that these were not significantly affected by deletion of *TDR1*, which is consistent with the parasites being able to cope without TDR1 in combating many challenges. This conclusion was reiterated by the finding that *TDR1* null mutant promastigotes were able to infect macrophages *in vitro* and animals as well as the WT line. These results show that TDR1 is not vital for these processes and that, whatever role it does play, TDR1 clearly it is not essential.

The null mutant promastigotes were more susceptible than WT parasites to trivalent antimony and arsenite (Table 2). This is consistent with TDR1 having a role in drug detoxification, which has been implicated in drug resistance [52, 68]. Resistance to antimonial drugs is thought to be multifactorial but one of the key factors is the concentration of active drug (the trivalent form Sb^{III}) within the parasite, which can be modulated by decreased uptake and increased inactivation of the drug by the parasite. Inactivation can be achieved by the conjugation of Sb^{III} with glutathione or trypanothione, leading to extrusion of the drug out of the cell [52]. On the other hand, Sb^{III} leads to an imbalance in thiol homeostasis and a consequent accumulation of reactive oxygen species [69, 70]. As our evidence is that the presence of TDR1 is not essential for protecting the cell against oxidative stress, at least in the conditions tested, it is possible that the greater sensitivity of the *TDR1* null mutant parasites to trivalent antimonials could be explained by TDR1 being involved in the extrusion of the toxic metal out of the cell. TDR1 is able to convert the clinically used pentavalent antimonial drugs (Sb^{V}) to a trivalent form (Sb^{III}) *in vitro* [9], a reduction that is necessary for the effective action of the drug against *Leishmania* as Sb^{III} is the form that is toxic to the cells. This conversion of

Sb^{V} to Sb^{III} is thought to occur only in amastigotes, which explains why promastigotes are not susceptible to Sb^{V} [71]. It is important to note that Sb^{V} reduction has also been shown to be effected non-enzymatically by thiols, however the reduction is much faster when catalyzed by TDR1 [9]. However, neither of these possibilities, that TDR1 could be involved in antimonial activation or resistance to the compounds, were supported by the finding that there was no change in susceptibility to Sb^{V} of the TDR1 null mutant compared with the wild type line when they were intracellular in macrophages (Fig. 2B). Thus the sensitivity of Δ*tdr1* promastigotes to the metals suggests that the trivalent metals mediate their toxicity in a way different from SSG and one which is countered by TDR1.

These data confirmed that the absence of TDR1 had some impact upon the parasite and thus we used a metabolomics approach in further attempts to elucidate the physiological role of TDR1 in *Leishmania*. The differences that we have detected between the metabolic status of Δ*tdr1* and the WT parasite have allowed the construction of a novel hypothesis on the involvement of TDR1 in *Leishmania* and provided some evidence to support it. Metabolomics is a developing technology that has not yet been applied extensively to *Leishmania* or other parasites although this is now happening [4, 25, 29, 31]. We based our procedures upon published protocols [28, 41] that have been validated and used strict criteria for inclusion of data, as detailed in the Materials and Methods and Results sections. This approach yielded data consistent with there being relatively few large differences between the metabolomes of the null mutant and wild type lines (Fig. 4) and it is those metabolites that differed greatly and for which we confirmed their identity with standards on which we have concentrated in developing ideas on the role of TDR1.

One incidental finding from our study may be of widespread significance for all studies involving gene deletion approaches. This was that the two add-back lines generated as controls gave very different results. Only the episomal add-back line complemented to a large extent the changes observed between the null mutant and WT lines, the integrated add-back failing to do so. This finding was surprising, as both add-back approaches generated lines expressing a level of TDR1 protein, as analysed by western blot (Fig. 1C), similar to that in the WT parent. Our interpretation of these results is that the TDR1 in the integrated complementation line is not appropriately active. The generally accepted criteria for a satisfactorily complemented line is the presence of a protein band, we suggest that this should reconsidered and that the presence of such a band is insufficient information on which to judge success of complementation. Comparing the metabolome would seem to be far more informative and a reliable analytical method. The literature contains many examples of complementation (as judged by protein presence) not

restoring well phenotypic changes resulting from gene deletion [53-56]; our data offer an explanation for this.

TDR1 gene deletion led to changes in the levels of putative metabolites known to participate in a variety of metabolic pathways, many of these are shown in Fig. S1 of Supplementary Material. This pictorial representation reiterates that the levels of many putative metabolites were not greatly affected, even when in a pathway in which some detected metabolites did differ. This is a reflection that the fluxes through pathways are controlled at various key steps. The figure also serves as reminder that many metabolites were not detected in our analysis. Nevertheless, some distinct differences in confirmed metabolite levels were discovered (Fig. 6). The variety of changes resulting from *TDR1* deletion could reflect the involvement of TDR1 in multiple processes in the cell, but it could also be indicative of a primary effect and then several secondary effects resulting from the primary change. The main challenge in analyzing metabolomics data is to integrate all the changes found from a biological point of view.

Several of the metabolites which changed greatly, both within the cells (Fig. 6) and also in some cases in the spent medium (Fig. 7), were in the area of amino acid and energy metabolism. *Leishmania* are known to be able to use amino acids, especially proline, as energy substrates, although sugar oxidation via glycolysis is also important [3, 30, 72] as is hexosamine use [73]. Thus the decreased levels of proline, aspartic acid and glutamic acid in the medium and proline intracellularly in the mutant with the concomitant increase in intracellular levels of glycerol-3-phosphate could be interpreted as a switch from glycolysis to amino acid utilization as energy source. How could TDR1 deletion lead to such metabolic re-configuration? These changes in levels of metabolites related with energy metabolism, which can be read as a consequence of a change in the carbon source used to generate energy, cannot be interpreted as an adaptation in response to availability as the *TDR1* null mutant and wild type promastigotes were both grown in medium rich in sugars and amino acids. However, they could reflect a blockage in the pathway responsible for the use of a given energy source; thus the build up of glycerol-3-phosphate could result from a block towards the final steps in the glycolytic pathway, glycerol-3-phosphate being generated as a means of maintaining redox balance.

Regulation of energy metabolism in other organisms involves protein modification, including S-glutathionylation in which GSH combines reversibly with a specific protein cysteinyl group to form a mixed disulfide [16, 17, 74, 75]. S-glutathionylation can occur in the presence of ROS and RNS and is mediated by the formation of reactive thiol

derivatives of GSH and the protein cysteinyl group such as sulfenates, thiyl radicals and nitrosothiols [15]. This modification results in protein-specific functional changes, that can protect a protein's sensitive thiol from irreversible oxidation during oxidative stress but can also occur under physiological conditions as a regulatory mechanism of enzyme activities [16] S-glutathionylation is reversed and therefore regulated by deglutathionylation catalysed by Grxs [15]. Many enzymes have been identified as being susceptible to this type of modification which can lead to activation or inhibition [76] and this so called 'redox regulation' is increasingly being implicated as an important mechanism of regulation of metabolism.

Metabolic re-configuration occurs in many organisms as a response to oxidative stress, often through redirection of metabolic flux from glycolysis to the pentose phosphate pathway generating NADPH [77]. Oxygen tension has also been implicated in the regulation of intermediary metabolism in *L. major*, with an increase in glycerol formation and decrease in glucose consumption being associated with anaerobic conditions [78]. Post-translational modification of proteins in *Leishmania* certainly occurs [79]. *Leishmania* has the enzyme capacity to use S-glutathionylation for redox regulation, encoding two glutaredoxins and other thiol-disulfide oxidoreductases including Trx and tryparedoxin [19]. Like the Grxs, TDR1 uses GSH as a substrate for the reduction of the mixed disulfide formed between GSH and HEDS [9, 11]. Moreover, we found that recombinant TDR1 is able to reduce glutathionylated protein and peptide substrates *in vitro* (Table 3). The BSA-SG was prepared by an established method [43] and although the structure of the substrate was not determined experimentally, BSA-SG is a known substrate of the *T. brucei* GRX1 and other glutaredoxins [11, 60]. The activity of TDR1 detected with BSA-SG is therefore likely to represent deglutathionylation of a protein mixed disulfide rather than the reduction of a protein disulfide. This is further supported by the observation that TDR1 has no protein disulfide reductase activity with insulin as a substrate (G.D. Westrop and G.H. Coombs, unpublished results). The k_{cat}/K_m of TDR1 with the peptide substrate was found to be 10-fold lower than that obtained with recombinant *Leishmania* GRX1. However, turnover by TDR1 was 5-fold higher, indicating that TDR1 can efficiently catalyse deglutathionylation but has a low affinity for binding this particular peptide. These results provide proof in-principle that TDR1 could function as a deglutathionylating enzyme and its apparent increase in substrate specificity compared with *Leishmania* glutaredoxin is consistent with a regulatory role for the protein. The *T. brucei* glutaredoxin*s,* GRX1 and GRX2, were similarly reported to have different specificities for a glutathionylated peroxiredoxin protein [11]. Also GRX1 and GRX2 from *Chlamydomonas reinhardtii* have been shown to catalyze deglutathionylation at different rates depending

on the protein substrate [14], suggesting a certain degree of substrate specificity among Grxs that may be crucial for the regulation of cellular processes. There are no previous reports on glutathionylation of *Leishmania* proteins, although the related organism *Trypanosoma* uses glutathione for the glutathionylation of thiol redox proteins [80]. The malaria parasite *Plasmodium falciparum* has also been reported to have proteins redox regulated through being targeted by Trx and Grx [81, 82]. Proteins involved in antioxidant defense (peroxiredoxins) were identified specifically as potential Trx targets and proteins involved in carbohydrate metabolism were also found to interact with Trx, Grx and plasmoredoxin (Plrx) proteins [82]. However, TDR1 reduction of other proteins such as Trx or tryparedoxin seems unlikely as TDR1 is unable to act as an electron donor for tryparedoxin in an insulin reduction assay (G.D. Westrop and G.H. Coombs, unpublished results). Thus we interpret our findings to indicate that TDR1 has a regulatory role through deglutathionylating key target enzymes, the identity of these, for which TDR1 presumably has a relatively high affinity and specificity, remain to be elucidated.

Could such an action of TDR1 explain the data obtained in this study? Most of the enzymes involved in glycolysis are sulfhydryl proteins sensitive to redox regulation and have been reported, through proteomic approaches in bacteria, plants and mammalian cells, as Trx and/or Grx targets [75, 76, 82-87]. S-glutathionylation leads to the inhibition of several glycolytic enzymes, notably glyceraldehyde-3-phosphate dehydrogenase (GAPDH) [74] and triose phosphate isomerase [17]. Our findings are consistent with TDR1 playing a role in maintaining the activity of glycolytic enzymes towards the end of glycolysis. Pyruvate kinase is known to be glutathionylated in the presence of high concentrations of GSSG and the enzyme of *Plasmodium falciparum* can be enzymatically deglutathionylated by *Pf*Trx1, *Pf*Grx1, and *Pf*Plrx. The same was also observed with *Pf*GAPDH [81, 82]. Fig. 8 outlines the hypothesis arising from this study and other reports; it shows enzymes potentially under regulation through glutathionylation and the levels of metabolites in some of the pathways in the WT, Δ*tdr1* and add-back line.

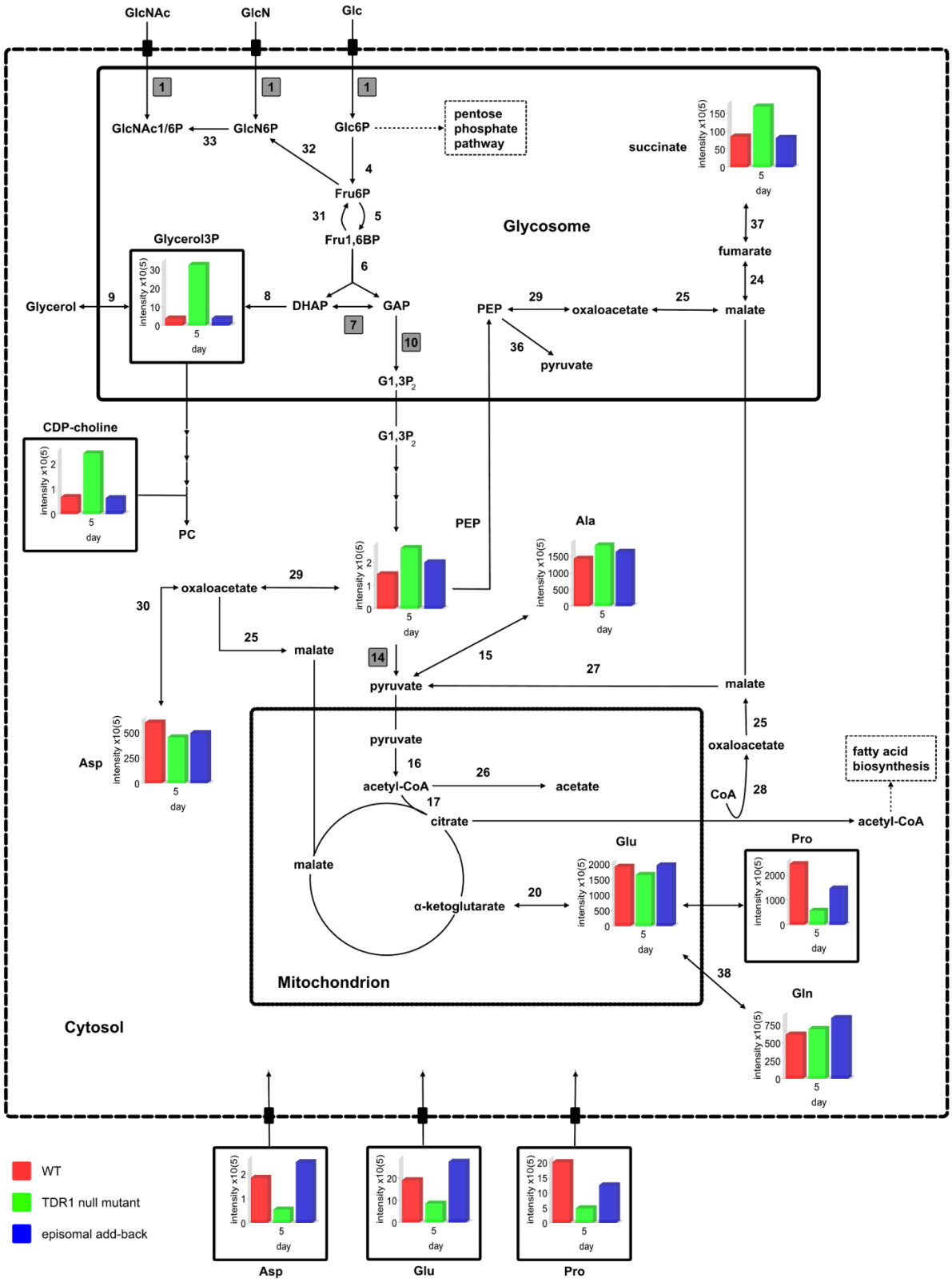

Figure 8. Schematic representation of central carbon metabolism in *Leishmania* promastigotes. Intensity/25 µg cell protein levels (x 10^5) are shown for intracellular metabolites identified in WT, Δ*tdr1* and Δ*tdr1*[pXG*TDR1*] promastigotes on day 5 of culture *in vitro* and culture medium from the same day (the latter shown outside the large dotted box); metabolites within solid boxes represent metabolites for which at least a 2-

fold difference between WT and Δ*tdr1* was observed. Grey boxes represent enzymes putatively or experimentally identified in other parasites as targets of S-glutathionylation modification; dashed arrows represent multiple enzymatic steps; dashed boxes represent pathways linked with the ones described. Abbreviations: Glc, glucose; Fru, fructose; Fru1,6BP, fructose-1,6-bisphosphate; GlcN, glucosamine; GlcNAc, N-acetyl-glucosamine; DHAP, dihydroxyacetone phosphate; GAP, glyceraldehyde-3-phosphate; G1,3P_2, 1,3-biphosphoglycerate; PGA, phosphoglycerate; PEP, phosphoenolpyruvate; Ala, alanine; Glu, glutamic acid; Gln, glutamine; Asp, aspartic acid; Pro, proline. Enzymes: 1, hexokinase; 2, phosphoglucose isomerase; 3, phosphofructokinase; 4, fructose biphosphate aldolase; 5, triosephosphate isomerase; 6, glycerol-3-phosphate dehydrogenase; 7, glycerol kinase; 8, glyceraldehyde-3-phosphate dehydrogenase; 9, pyruvate kinase; 10, alanine aminotransferase; 11, pyruvate dehydrogenase; 12, acetate-succinate CoA transferase; 13, glutamate dehydrogenase; 14, glutamine synthetase; 15, acetyl-CoA synthethase; 16, malate dehydrogenase; 17, malic enzyme; 18, phosphoenolpyruvate carboxykinase; 19, aspartate aminotransferase; 20, pyruvate phosphate dikinase; 21, fumarate hydratase; 22, NADH-dependent fumarate reductase; 23, fructose-1,6-bis-phosphatase; 24, glucosamine-6-phosphate deaminase; 25, N-acetylglucosamine-6-phosphate deacetylase.

A similar involvement in regulating enzyme activity through S-glutathionylation/deglutathionylation could also explain some of the other metabolic changes observed. Argininosuccinic acid is synthesized from citrulline and aspartic acid as part of the urea cycle in mammals. Despite the presence of several genes for enzymes of the urea cycle, *Leishmania* do not seem to have a functional cycle since it lacks the genes coding for ornithine carbamoyl transferase and argininosuccinate lyase [88]. Argininosuccinate synthase, the enzyme that catalyzes the synthesis of argininosuccinic acid from citrulline and aspartic acid, has been reported to be regulated by Trx or/and Grx in photosynthetic organisms [85-87]. Inactivation or inhibition of argininosuccinate synthase due to lack of deglutathionylation in Δ*tdr1* could explain the decrease in argininosuccinic acid levels observed in the *TDR1* null mutant. Such control would suggest some important as yet undiscovered role for argininosuccinic acid in *Leishmania* metabolism. An alternative possibility is that the greater use of amino acids due to the purposed metabolic re-configuration in Δ*tdr1* would lead to less availability of aspartic acid for this reaction, and consequent decrease in argininosuccinic acid levels.

Another interesting change in the TDR1 null mutant was the increase in the intracellular levels of S-adenosylhomocysteine (SAH). This is converted to homocysteine and

adenosine by S-adenosylhomocysteine hydrolase (SAHH), a crucial enzyme of S-adenosylmethionine (SAM) metabolism as it prevents the accumulation of this toxic metabolite. SAHH is tightly regulated and is, similarly to methionine synthase and SAM synthase (two other enzymes involved in SAM metabolism), susceptible to redox regulation in, for example, plants and algae [85, 87, 89]. In *P. falciparum*, SAHH has been shown to interact with Grx and Trx [82]. Thus S-glutathionylation is a potential mechanism of SAHH regulation, and the increase in the levels of SAH that we found in ∆*tdr1* could reflect a lack of deglutathionylation of SAHH by TDR1.

Other of the changes found with the *TDR1* null mutant could also be rationalized in a similar way, through TDR1 being involved, directly or indirectly, in regulating enzyme activities via deglutathionylation, although further analyses are required to understand fully the mechanisms involved.

Conclusions

This study has revealed new insights into how metabolism in *Leishmania* may be regulated via glutathionylation and how TDR1 appears to play a key role in this through its deglutathionylation activity. Deletion of TDR1 resulted in specific changes in central energy metabolism and also amino acid metabolism. The null mutant lines were also more sensitive to metal-induced stress. The unusual structure and parasite-specificity of TDR1 suggests that it has particular roles and investigating these further is likely to yield new detailed information on mechanisms by which metabolism is regulated in *Leishmania*, which could be a determinant in the search for better drugs or even be targeted in drug discovery.

Acknowledgements

We thank: Lesley McCaig (Glasgow) for generating the mutant with two *TDR1* gene alleles deleted and for obtaining the sheep anti-*Ld*TDR1 and rabbit anti-*Ld*CS sera; Malcolm McConville and colleagues (Melbourne) for excellent guidance on the methods of sample preparation for the metabolomics analyses; Ruben t'Kindt (ITM, Antwerp, and Strathclyde) for assistance with the sample preparation method for the metabolomics analyses; Dave G Watson and Alex Zhang (Strathclyde) for help with the LC-MS technology; and Chris Carter (Strathclyde) for carrying out the animal experiments. The

study was supported by Fundação para a Ciência e Tecnologia (FCT) project number PTDC/CVT/65047/2006 and AMS is supported by FCT grant SFRH/BD/28316/2006. This work was supported by the Wellcome Trust [WT061173MA-SM]. The Wellcome Trust Centre for Molecular Parasitology is supported by core funding from the Wellcome Trust [085349].

References

[1] Burchmore, R. J.; Barrett, M. P. Life in vacuoles--nutrient acquisition by *Leishmania* amastigotes. *Int J Parasitol* **31:**1311-1320; 2001.

[2] McConville, M. J.; de Souza, D.; Saunders, E.; Likic, V. A.; Naderer, T. Living in a phagolysosome; metabolism of *Leishmania* amastigotes. *Trends Parasitol* **23:**368-375; 2007.

[3] Opperdoes, F. R.; Coombs, G. H. Metabolism of *Leishmania*: proven and predicted. *Trends Parasitol* **23:**149-158; 2007.

[4] Silva, A. M.; Cordeiro-da-Silva, A.; Coombs, G. H. Metabolic variation during development in culture of *Leishmania donovani* promastigotes *PLoS Negl Trop Dis* **In press**; 2011.

[5] Castro, H.; Sousa, C.; Santos, M.; Cordeiro-da-Silva, A.; Flohe, L.; Tomas, A. M. Complementary antioxidant defense by cytoplasmic and mitochondrial peroxiredoxins in *Leishmania infantum*. *Free Radic Biol Med* **33:**1552-1562; 2002.

[6] Dolai, S.; Yadav, R. K.; Pal, S.; Adak, S. *Leishmania major* ascorbate peroxidase overexpression protects cells against reactive oxygen species-mediated cardiolipin oxidation. *Free Radic Biol Med* **45:**1520-1529; 2008.

[7] Wyllie, S.; Mandal, G.; Singh, N.; Sundar, S.; Fairlamb, A. H.; Chatterjee, M. Elevated levels of tryparedoxin peroxidase in antimony unresponsive *Leishmania* donovani field isolates. *Mol Biochem Parasitol* **173:**162-164; 2010.

[8] Van Assche, T.; Deschacht, M.; da Luz, R. A.; Maes, L.; Cos, P. *Leishmania*-macrophage interactions: insights into the redox biology. *Free Radic Biol Med* **51:**337-351; 2011.

[9] Denton, H.; McGregor, J. C.; Coombs, G. H. Reduction of anti-leishmanial pentavalent antimonial drugs by a parasite-specific thiol-dependent reductase, TDR1. *Biochem J* **381:**405-412; 2004.

[10] Lillig, C. H.; Berndt, C.; Holmgren, A. Glutaredoxin systems. *Biochim Biophys Acta* **1780:**1304-1317; 2008.

[11] Ceylan, S.; Seidel, V.; Ziebart, N.; Berndt, C.; Dirdjaja, N.; Krauth-Siegel, R. L. The dithiol glutaredoxins of african trypanosomes have distinct roles and are closely linked to the unique trypanothione metabolism. *J Biol Chem* **285:**35224-35237; 2010.

[12] Hashemy, S. I.; Johansson, C.; Berndt, C.; Lillig, C. H.; Holmgren, A. Oxidation and S-nitrosylation of cysteines in human cytosolic and mitochondrial glutaredoxins: effects on structure and activity. *J Biol Chem* **282:**14428-14436; 2007.

[13] Li, W. F.; Yu, J.; Ma, X. X.; Teng, Y. B.; Luo, M.; Tang, Y. J.; Zhou, C. Z. Structural basis for the different activities of yeast Grx1 and Grx2. *Biochim Biophys Acta* **1804:**1542-1547; 2010.

[14] Gao, X. H.; Zaffagnini, M.; Bedhomme, M.; Michelet, L.; Cassier-Chauvat, C.; Decottignies, P.; Lemaire, S. D. Biochemical characterization of glutaredoxins from *Chlamydomonas reinhardtii*: kinetics and specificity in deglutathionylation reactions. *FEBS Lett* **584:**2242-2248; 2010.

[15] Gallogly, M. M.; Starke, D. W.; Mieyal, J. J. Mechanistic and kinetic details of catalysis of thiol-disulfide exchange by glutaredoxins and potential mechanisms of regulation. *Antioxid Redox Signal* **11:**1059-1081; 2009.

[16] Dalle-Donne, I.; Rossi, R.; Colombo, G.; Giustarini, D.; Milzani, A. Protein S-glutathionylation: a regulatory device from bacteria to humans. *Trends Biochem Sci* **34:**85-96; 2009.

[17] Ito, H.; Iwabuchi, M.; Ogawa, K. The sugar-metabolic enzymes aldolase and triose-phosphate isomerase are targets of glutathionylation in *Arabidopsis thaliana*: detection using biotinylated glutathione. *Plant Cell Physiol* **44:**655-660; 2003.

[18] Michelet, L.; Zaffagnini, M.; Marchand, C.; Collin, V.; Decottignies, P.; Tsan, P.; Lancelin, J. M.; Trost, P.; Miginiac-Maslow, M.; Noctor, G.; Lemaire, S. D. Glutathionylation of chloroplast thioredoxin f is a redox signaling mechanism in plants. *Proc Natl Acad Sci U S A* **102:**16478-16483; 2005.

[19] Krauth-Siegel, R. L.; Comini, M. A. Redox control in trypanosomatids, parasitic protozoa with trypanothione-based thiol metabolism. *Biochim Biophys Acta* **1780:**1236-1248; 2008.

[20] Board, P. G.; Coggan, M.; Chelvanayagam, G.; Easteal, S.; Jermiin, L. S.; Schulte, G. K.; Danley, D. E.; Hoth, L. R.; Griffor, M. C.; Kamath, A. V.; Rosner, M. H.; Chrunyk, B. A.; Perregaux, D. E.; Gabel, C. A.; Geoghegan, K. F.; Pandit, J. Identification, characterization, and crystal structure of the Omega class glutathione transferases. *J Biol Chem* **275:**24798-24806; 2000.

[21] Meux, E.; Prosper, P.; Ngadin, A.; Didierjean, C.; Morel, M.; Dumarcay, S.; Lamant, T.; Jacquot, J. P.; Favier, F.; Gelhaye, E. Glutathione transferases of

Phanerochaete chrysosporium: S-glutathionyl-p-hydroquinone reductase belongs to a new structural class. *J Biol Chem* **286:**9162-9173; 2010.

[22] Tew, K. D.; Manevich, Y.; Grek, C.; Xiong, Y.; Uys, J.; Townsend, D. M. The role of glutathione S-transferase P in signaling pathways and S-glutathionylation in cancer. *Free Radic Biol Med* **51:**299-313; 2011.

[23] Moutiez, M.; Quemeneur, E.; Sergheraert, C.; Lucas, V.; Tartar, A.; Davioud-Charvet, E. Glutathione-dependent activities of *Trypanosoma cruzi* p52 makes it a new member of the thiol:disulphide oxidoreductase family. *Biochem J* **322 (Pt 1):**43-48; 1997.

[24] de Carvalho, L. P.; Fischer, S. M.; Marrero, J.; Nathan, C.; Ehrt, S.; Rhee, K. Y. Metabolomics of *Mycobacterium tuberculosis* reveals compartmentalized co-catabolism of carbon substrates. *Chem Biol* **17:**1122-1131; 2010.

[25] De Souza, D. P.; Saunders, E. C.; McConville, M. J.; Likic, V. A. Progressive peak clustering in GC-MS Metabolomic experiments applied to *Leishmania* parasites. *Bioinformatics* **22:**1391-1396; 2006.

[26] Olszewski, K. L.; Mather, M. W.; Morrisey, J. M.; Garcia, B. A.; Vaidya, A. B.; Rabinowitz, J. D.; Llinas, M. Branched tricarboxylic acid metabolism in *Plasmodium falciparum*. *Nature* **466:**774-778; 2010.

[27] Olszewski, K. L.; Morrisey, J. M.; Wilinski, D.; Burns, J. M.; Vaidya, A. B.; Rabinowitz, J. D.; Llinas, M. Host-parasite interactions revealed by *Plasmodium falciparum* metabolomics. *Cell Host Microbe* **5:**191-199; 2009.

[28] t'Kindt, R.; Jankevics, A.; Scheltema, R. A.; Zheng, L.; Watson, D. G.; Dujardin, J. C.; Breitling, R.; Coombs, G. H.; Decuypere, S. Towards an unbiased metabolic profiling of protozoan parasites: optimisation of a *Leishmania* sampling protocol for HILIC-orbitrap analysis. *Anal Bioanal Chem* **398:**2059-2069; 2010.

[29] t'Kindt, R.; Scheltema, R. A.; Jankevics, A.; Brunker, K.; Rijal, S.; Dujardin, J. C.; Breitling, R.; Watson, D. G.; Coombs, G. H.; Decuypere, S. Metabolomics to unveil and understand phenotypic diversity between pathogen populations. *PLoS Negl Trop Dis* **4:**e904; 2010.

[30] Saunders, E. C.; Ng, W. W.; Chamber, J. M.; Ng, M.; Naderer, T.; Kroemer, J. O.; Likic, V. A.; McConville, M. J. Isoptopomer profiling of *Leishmania mexicana* promastigotes reveals important roles for succinate fermentation and aspartate uptake in TCA cycle anaplerosis, glutamate synthesis and growth. *J Biol Chem*; 2011.

[31] Creek, D. J.; Anderson, J.; McConville, M. J.; Barrett, M. P. Metabolomic analysis of trypanosomatid protozoa. *Mol Biochem Parasitol*; 2011.

[32] Kaddurah-Daouk, R.; Kristal, B. S.; Weinshilboum, R. M. Metabolomics: a global biochemical approach to drug response and disease. *Annu Rev Pharmacol Toxicol* **48:**653-683; 2008.

[33] Rijal, S.; Yardley, V.; Chappuis, F.; Decuypere, S.; Khanal, B.; Singh, R.; Boelaert, M.; De Doncker, S.; Croft, S.; Dujardin, J. C. Antimonial treatment of visceral leishmaniasis: are current *in vitro* susceptibility assays adequate for prognosis of *in vivo* therapy outcome? *Microbes Infect* **9:**529-535; 2007.

[34] Medina-Acosta, E.; Cross, G. A. Rapid isolation of DNA from trypanosomatid protozoa using a simple 'mini-prep' procedure. *Mol Biochem Parasitol* **59:**327-329; 1993.

[35] Mottram, J. C.; Souza, A. E.; Hutchison, J. E.; Carter, R.; Frame, M. J.; Coombs, G. H. Evidence from disruption of the lmcpb gene array of *Leishmania mexicana* that cysteine proteinases are virulence factors. *Proc Natl Acad Sci U S A* **93:**6008-6013; 1996.

[36] Misslitz, A.; Mottram, J. C.; Overath, P.; Aebischer, T. Targeted integration into a rRNA locus results in uniform and high level expression of transgenes in *Leishmania* amastigotes. *Mol Biochem Parasitol* **107:**251-261; 2000.

[37] Ha, D. S.; Schwarz, J. K.; Turco, S. J.; Beverley, S. M. Use of the green fluorescent protein as a marker in transfected *Leishmania*. *Mol Biochem Parasitol* **77:**57-64; 1996.

[38] Mikus, J.; Steverding, D. A simple colorimetric method to screen drug cytotoxicity against *Leishmania* using the dye Alamar Blue. *Parasitol Int* **48:**265-269; 2000.

[39] Williams, R. A.; Westrop, G. D.; Coombs, G. H. Two pathways for cysteine biosynthesis in *Leishmania major*. *Biochem J* **420:**451-462; 2009.

[40] Buffet, P. A.; Sulahian, A.; Garin, Y. J.; Nassar, N.; Derouin, F. Culture microtitration: a sensitive method for quantifying *Leishmania infantum* in tissues of infected mice. *Antimicrob Agents Chemother* **39:**2167-2168; 1995.

[41] Creek, D. J.; Jankevics, A.; Breitling, R.; Watson, D. G.; Barrett, M. P.; Burgess, K. E. Toward global metabolomics analysis with hydrophilic interaction liquid chromatography-mass spectrometry: improved metabolite identification by retention time prediction. *Anal Chem* **83:**8703-8710; 2011.

[42] Fyfe, P. K.; Dawson, A.; Hutchison, M.; Cameron, S.; Hunter, W. N. Structure of *Staphylococcus aureus* adenylsuccinate lyase (PurB) and assessment of its potential as a target for structure-based inhibitor discovery. *Acta Crystallogr D Biol Crystallogr* **66:**881-888; 2010.

[43] Cheng, G.; Ikeda, Y.; Iuchi, Y.; Fujii, J. Detection of S-glutathionylated proteins by glutathione S-transferase overlay. *Arch Biochem Biophys* **435:**42-49; 2005.

[44] Ellman, G. Tissue sulfhydryl groups. *Arch Biochem Biophys* **82:**70-77; 1959.

[45] Peltoniemi, M. J.; Karala, A. R.; Jurvansuu, J. K.; Kinnula, V. L.; Ruddock, L. W. Insights into deglutathionylation reactions. Different intermediates in the glutaredoxin and protein disulfide isomerase catalyzed reactions are defined by the gamma-linkage present in glutathione. *J Biol Chem* **281:**33107-33114; 2006.

[46] Bonilla, M.; Denicola, A.; Marino, S. M.; Gladyshev, V. N.; Salinas, G. Linked thioredoxin-glutathione systems in platyhelminth parasites: alternative pathways for glutathione reduction and deglutathionylation. *J Biol Chem* **286:**4959-4967; 2011.

[47] Cruz, A.; Beverley, S. M. Gene replacement in parasitic protozoa. *Nature* **348:**171-173; 1990.

[48] Downing, T.; Imamura, H.; Decuypere, S.; Clark, T. G.; Coombs, G. H.; Cotton, J. A.; Hilley, J. D.; de Doncker, S.; Maes, I.; Mottram, J. C.; Quail, M. A.; Rijal, S.; Sanders, M.; Schonian, G.; Stark, O.; Sundar, S.; Vanaerschot, M.; Hertz-Fowler, C.; Dujardin, J. C.; Berriman, M. Whole genome sequencing of multiple *Leishmania donovani* clinical isolates provides insights into population structure and mechanisms of drug resistance. *Genome Res*; 2011.

[49] Rogers, M. B.; Hilley, J. D.; Dickens, N. J.; Wilkes, J.; Bates, P. A.; Depledge, D. P.; Harris, D.; Her, Y.; Herzyk, P.; Imamura, H.; Otto, T. D.; Sanders, M.; Seeger, K.; Dujardin, J. C.; Berriman, M.; Smith, D. F.; Hertz-Fowler, C.; Mottram, J. C. Chromosome and gene copy number variation allow major structural change between species and strains of *Leishmania*. *Genome Res*; 2011.

[50] Murray, H. W.; Nathan, C. F. Macrophage microbicidal mechanisms *in vivo*: reactive nitrogen versus oxygen intermediates in the killing of intracellular visceral *Leishmania donovani*. *J Exp Med* **189:**741-746; 1999.

[51] Valko, M.; Morris, H.; Cronin, M. T. Metals, toxicity and oxidative stress. *Curr Med Chem* **12:**1161-1208; 2005.

[52] Mukhopadhyay, R.; Dey, S.; Xu, N.; Gage, D.; Lightbody, J.; Ouellette, M.; Rosen, B. P. Trypanothione overproduction and resistance to antimonials and arsenicals in Leishmania. *Proc Natl Acad Sci U S A* **93:**10383-10387; 1996.

[53] Garami, A.; Ilg, T. Disruption of mannose activation in *Leishmania mexicana*: GDP-mannose pyrophosphorylase is required for virulence, but not for viability. *EMBO J* **20:**3657-3666; 2001.

[54] Besteiro, S.; Coombs, G. H.; Mottram, J. C. A potential role for ICP, a Leishmanial inhibitor of cysteine peptidases, in the interaction between host and parasite. *Mol Microbiol* **54:**1224-1236; 2004.

[55] Folgueira, C.; Carrion, J.; Moreno, J.; Saugar, J. M.; Canavate, C.; Requena, J. M. Effects of the disruption of the HSP70-II gene on the growth, morphology, and virulence of *Leishmania infantum* promastigotes. *Int Microbiol* **11:**81-89; 2008.

[56] Denise, H.; Poot, J.; Jimenez, M.; Ambit, A.; Herrmann, D. C.; Vermeulen, A. N.; Coombs, G. H.; Mottram, J. C. Studies on the CPA cysteine peptidase in the *Leishmania infantum* genome strain JPCM5. *BMC Mol Biol* **7:**42; 2006.

[57] Wishart, D. S. Computational approaches to metabolomics. *Methods Mol Biol* **593:**283-313; 2010.

[58] Rogers, M. E.; Chance, M. L.; Bates, P. A. The role of promastigote secretory gel in the origin and transmission of the infective stage of Leishmania mexicana by the sandfly *Lutzomyia longipalpis*. *Parasitology* **124:**495-507; 2002.

[59] Doyle, M. A.; MacRae, J. I.; De Souza, D. P.; Saunders, E. C.; McConville, M. J.; Likic, V. A. LeishCyc: a biochemical pathways database for *Leishmania major*. *BMC Syst Biol* **3:**57; 2009.

[60] Johansson, C.; Lillig, C. H.; Holmgren, A. Human mitochondrial glutaredoxin reduces S-glutathionylated proteins with high affinity accepting electrons from either glutathione or thioredoxin reductase. *J Biol Chem* **279:**7537-7543; 2004.

[61] Sunkin, S. M.; Kiser, P.; Myler, P. J.; Stuart, K. The size difference between *Leishmania major* friedlin chromosome one homologues is localized to sub-telomeric repeats at one chromosomal end. *Mol Biochem Parasitol* **109:**1-15; 2000.

[62] Akopyants, N. S.; Kimblin, N.; Secundino, N.; Patrick, R.; Peters, N.; Lawyer, P.; Dobson, D. E.; Beverley, S. M.; Sacks, D. L. Demonstration of genetic exchange during cyclical development of Leishmania in the sand fly vector. *Science* **324:**265-268; 2009.

[63] Cruz, A. K.; Titus, R.; Beverley, S. M. Plasticity in chromosome number and testing of essential genes in *Leishmania* by targeting. *Proc Natl Acad Sci U S A* **90:**1599-1603; 1993.

[64] Dumas, C.; Ouellette, M.; Tovar, J.; Cunningham, M. L.; Fairlamb, A. H.; Tamar, S.; Olivier, M.; Papadopoulou, B. Disruption of the trypanothione reductase gene of Leishmania decreases its ability to survive oxidative stress in macrophages. *EMBO J* **16:**2590-2598; 1997.

[65] Mottram, J. C.; McCready, B. P.; Brown, K. G.; Grant, K. M. Gene disruptions indicate an essential function for the LmmCRK1 cdc2-related kinase of *Leishmania mexicana*. *Mol Microbiol* **22:**573-583; 1996.

[66] Leprohon, P.; Legare, D.; Raymond, F.; Madore, E.; Hardiman, G.; Corbeil, J.; Ouellette, M. Gene expression modulation is associated with gene amplification, supernumerary chromosomes and chromosome loss in antimony-resistant *Leishmania infantum*. *Nucleic Acids Res* **37:**1387-1399; 2009.

[67] Sterkers, Y.; Lachaud, L.; Crobu, L.; Bastien, P.; Pages, M. FISH analysis reveals aneuploidy and continual generation of chromosomal mosaicism in *Leishmania major*. *Cell Microbiol* **13:**274-283; 2010.

[68] Dey, S.; Ouellette, M.; Lightbody, J.; Papadopoulou, B.; Rosen, B. P. An ATP-dependent As(III)-glutathione transport system in membrane vesicles of *Leishmania tarentolae*. *Proc Natl Acad Sci U S A* **93:**2192-2197; 1996.

[69] Wyllie, S.; Cunningham, M. L.; Fairlamb, A. H. Dual action of antimonial drugs on thiol redox metabolism in the human pathogen *Leishmania donovani*. *J Biol Chem* **279:**39925-39932; 2004.

[70] Mandal, G.; Wyllie, S.; Singh, N.; Sundar, S.; Fairlamb, A. H.; Chatterjee, M. Increased levels of thiols protect antimony unresponsive *Leishmania donovani* field isolates against reactive oxygen species generated by trivalent antimony. *Parasitology* **134:**1679-1687; 2007.

[71] Roberts, W. L.; Berman, J. D.; Rainey, P. M. *In vitro* antileishmanial properties of tri- and pentavalent antimonial preparations. *Antimicrob Agents Chemother* **39:**1234-1239; 1995.

[72] Naderer, T.; Ellis, M. A.; Sernee, M. F.; De Souza, D. P.; Curtis, J.; Handman, E.; McConville, M. J. Virulence of *Leishmania major* in macrophages and mice requires the gluconeogenic enzyme fructose-1,6-bisphosphatase. *Proc Natl Acad Sci U S A* **103:**5502-5507; 2006.

[73] Naderer, T.; Heng, J.; McConville, M. J. Evidence that intracellular stages of *Leishmania major* utilize amino sugars as a major carbon source. *PLoS Pathog* **6:**e1001245; 2010.

[74] Zaffagnini, M.; Michelet, L.; Marchand, C.; Sparla, F.; Decottignies, P.; Le Marechal, P.; Miginiac-Maslow, M.; Noctor, G.; Trost, P.; Lemaire, S. D. The thioredoxin-independent isoform of chloroplastic glyceraldehyde-3-phosphate dehydrogenase is selectively regulated by glutathionylation. *FEBS J* **274:**212-226; 2007.

[75] Fratelli, M.; Demol, H.; Puype, M.; Casagrande, S.; Eberini, I.; Salmona, M.; Bonetto, V.; Mengozzi, M.; Duffieux, F.; Miclet, E.; Bachi, A.; Vandekerckhove, J.; Gianazza, E.; Ghezzi, P. Identification by redox proteomics of glutathionylated proteins in oxidatively stressed human T lymphocytes. *Proc Natl Acad Sci U S A* **99:**3505-3510; 2002.

[76] Townsend, D. M. S-glutathionylation: indicator of cell stress and regulator of the unfolded protein response. *Mol Interv* **7:**313-324; 2007.

[77] Ralser, M.; Wamelink, M. M.; Kowald, A.; Gerisch, B.; Heeren, G.; Struys, E. A.; Klipp, E.; Jakobs, C.; Breitenbach, M.; Lehrach, H.; Krobitsch, S. Dynamic rerouting of the carbohydrate flux is key to counteracting oxidative stress. *J Biol* **6:**10; 2007.

[78] Keegan, F.; Blum, J. J. Effects of oxygen concentration on the intermediary metabolism of *Leishmania major* promastigotes. *Mol Biochem Parasitol* **39:**235-245; 1990.

[79] Rosenzweig, D.; Smith, D.; Myler, P. J.; Olafson, R. W.; Zilberstein, D. Post-translational modification of cellular proteins during *Leishmania donovani* differentiation. *Proteomics* **8:**1843-1850; 2008.

[80] Melchers, J.; Dirdjaja, N.; Ruppert, T.; Krauth-Siegel, R. L. Glutathionylation of trypanosomal thiol redox proteins. *J Biol Chem* **282:**8678-8694; 2007.

[81] Kehr, S.; Jortzik, E.; Delahunty, C.; Yates Iii, J. R.; Rahlfs, S.; Becker, K. Protein S-glutathionylation in malaria parasites. *Antioxid Redox Signal*; 2011.

[82] Sturm, N.; Jortzik, E.; Mailu, B. M.; Koncarevic, S.; Deponte, M.; Forchhammer, K.; Rahlfs, S.; Becker, K. Identification of proteins targeted by the thioredoxin superfamily in *Plasmodium falciparum*. *PLoS Pathog* **5:**e1000383; 2009.

[83] Fu, C.; Wu, C.; Liu, T.; Ago, T.; Zhai, P.; Sadoshima, J.; Li, H. Elucidation of thioredoxin target protein networks in mouse. *Mol Cell Proteomics* **8:**1674-1687; 2009.

[84] Gao, X. H.; Bedhomme, M.; Veyel, D.; Zaffagnini, M.; Lemaire, S. D. Methods for analysis of protein glutathionylation and their application to photosynthetic organisms. *Mol Plant* **2:**218-235; 2009.

[85] Lemaire, S. D.; Guillon, B.; Le Marechal, P.; Keryer, E.; Miginiac-Maslow, M.; Decottignies, P. New thioredoxin targets in the unicellular photosynthetic eukaryote *Chlamydomonas reinhardtii*. *Proc Natl Acad Sci U S A* **101:**7475-7480; 2004.

[86] Li, M.; Yang, Q.; Zhang, L.; Li, H.; Cui, Y.; Wu, Q. Identification of novel targets of cyanobacterial glutaredoxin. *Arch Biochem Biophys* **458:**220-228; 2007.

[87] Dixon, D. P.; Skipsey, M.; Grundy, N. M.; Edwards, R. Stress-induced protein S-glutathionylation in *Arabidopsis*. *Plant Physiol* **138:**2233-2244; 2005.

[88] Myler, P. J.; Fasel, N. *Leishmania*: After the Genome. *Caister Academic Press***:**306; 2008.

[89] Rouhier, N.; Villarejo, A.; Srivastava, M.; Gelhaye, E.; Keech, O.; Droux, M.; Finkemeier, I.; Samuelsson, G.; Dietz, K. J.; Jacquot, J. P.; Wingsle, G. Identification of plant glutaredoxin targets. *Antioxid Redox Signal* **7:**919-929; 2005.

Supplementary Material

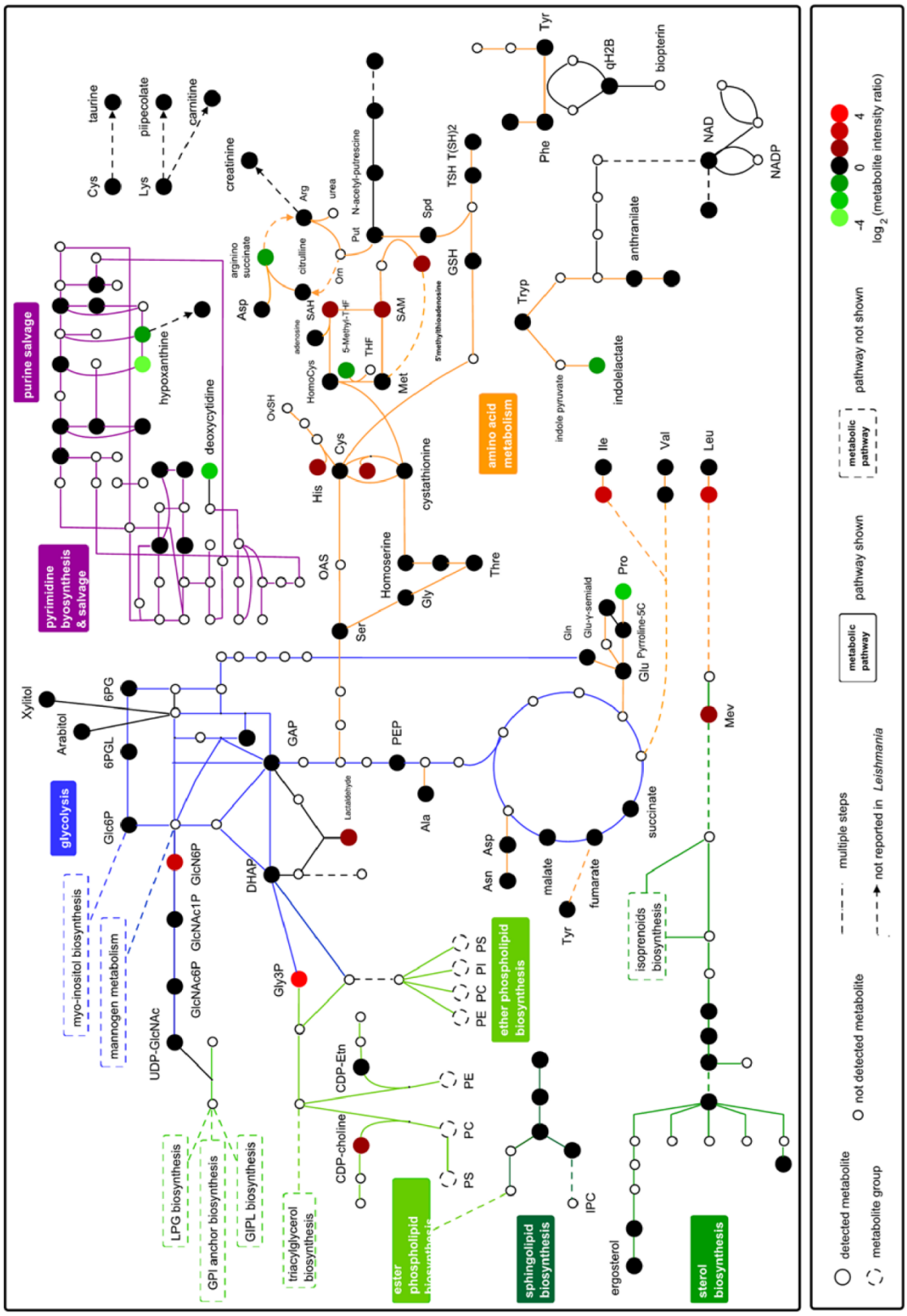

Figure S1. Schematic representation of the changes in metabolite levels resulting from *TDR1* deletion in *L. donovani*. 100 of the metabolites putatively identified in day 5

cell lysates are represented; each is color-coded indicating whether the level differed between WT and Δ*tdr1* promastigotes (green lower in Δ*tdr1*, red higher in Δ*tdr1*).

Table S1. The standards used to verify the identity of metabolites in this study. The identity of all of the listed metabolites was confirmed for the extracts of *L. donovani* analysed in this study.

Table S2. Comparison of metabolic profiles resulting from different complementation strategies. Metabolites identified below 1 ppm in day 5 samples of each of *L. donovani* WT, Δ*tdr1*, Δ*tdr1*::P_{RRNA}*TDR1* and Δ*tdr1*[pXG*TDR1*] are listed in mass order. For each metabolite the following information is shown: ionisation mode; detected mass; retention time (min); putative metabolite identification; ppm deviation between detected mass and theoretical mass of the putative metabolite identified; signal intensity in each sample; average signal in each cell line; standard deviation in each cell line; ratio of average signal intensity between the different cell lines; Student's T test Δtdr1 versus WT, Δ*tdr1* versus Δ*tdr1*::P_{RRNA}*TDR1*, Δ*tdr1* versus Δ*tdr1*[pXG*TDR1*]; p value < 0.01 Δ*tdr1* versus WT, Δ*tdr1* versus Δ*tdr1*::P_{RRNA}*TDR1*, Δ*tdr1* versus Δ*tdr1*[pXG*TDR1*] indicating whether or not there was a statistically significant difference; decision on whether or not the compound was significantly changed in level based on a two-fold or higher average difference in signal intensity and statistical significant (p<0.01) between Δ*tdr1*/WT, Δ*tdr1*/Δtdr1::P_{RRNA}*TDR1*, Δ*tdr1*/Δ*tdr1*[pXG*TDR1*]; compound category.

Table S3. Metabolites identified in day 5 samples of *L. donovani* WT, Δ*tdr1* and Δ*tdr1*[pXG*TDR1*]. For each compound the following information is shown: ionisation mode; detected mass; retention time (min); putative metabolite identification; ppm deviation between detected mass and theoretical mass of the putative metabolite identified; signal intensity in each sample; average signal in each cell line; standard deviation in each cell line; ratio of average signal intensity between the different cell lines; Student's T test Δ*tdr1* versus WT, Δ*tdr1* versus Δ*tdr1*[pXG*TDR1*]; p value < 0.01 Δtdr1 versus WT, Δ*tdr1* versus Δ*tdr1*[pXG*TDR1*] indicating whether or not there was a statistically significant difference; decision on whether or not the compound was significantly changed in level based on a two-fold or higher average difference in signal intensity and statistical significant (p<0.01) between Δ*tdr1*/WT, Δ*tdr1*/Δ*tdr1*[pXG*TDR1*]; compound category.

Table S4. Metabolites identified in day 6 samples of *L. donovani* WT, Δ*tdr1* and Δ*tdr1*[pXG*TDR1*]. The data presented are as described for Table S2.

Table S5. Metabolites identified in day 6 samples of spent media from cultures of *L. donovani* WT, Δ*tdr1* and Δ*tdr1*[pXG *TDR1*]. The data presented are as described for Table S2.

Tables S1 to S5 are available in the electronic version of the thesis.

4.5 *Leishmania donovani* TDR1, a unique trimeric glutathione transferase evolved by gene duplication then fusion

Thiol-dependent reductase 1 (TDR1) occurs only in the trypanosomatid parasites *Trypanosoma cruzi* and *Leishmania* and is thought to contribute to activation of antimonial pro-drugs used to treat leishmaniasis. Our structure of *L. donovani* TDR1 reveals a unique trimer of subunits each containing two glutathione-S-transferase (GST) domains. The similarities of individual domains, and comparisons with GST classes, suggest that TDR1 evolved by gene duplication, diversification and gene fusion; an event unknown until now in the GST protein superfamily.

To be submitted

Leishmania donovani TDR1, a unique trimeric glutathione transferase evolved by gene duplication then fusion

Paul K. Fyfe, Gareth D. Westrop[#], Ana Marta Silva[#], Graham H. Coombs[#] and William N. Hunter*

Division of Biological Chemistry and Drug Discovery, College of Life Sciences, University of Dundee, DD1 5EH, United Kingdom and [#]Strathclyde Institute of Pharmacy and Biomedical Sciences, University of Strathclyde, Glasgow, G4 0RE, United Kingdom.

*****Correspondence e-mail: w.n.hunter@dundee.ac.uk

Abstract

Thiol-dependent reductase 1 (TDR1) occurs only in the trypanosomatid parasites *Trypanosoma cruzi* and *Leishmania* and is thought to contribute to activation of antimonial pro-drugs used to treat leishmaniasis. Our structure of *L. donovani* TDR1 reveals a unique trimer of subunits each containing two glutathione-S-transferase (GST) domains. The similarities of individual domains, and comparisons with GST classes, suggest that TDR1 evolved by gene duplication, diversification and gene fusion; an event unknown until now in the GST protein superfamily.

The kinetoplastida parasites *Leishmania sp*. and *Trypanosoma cruzi* proliferate intracellularly within humans and cause the widespread neglected tropical diseases leishmaniasis and Chagas Disease. Each parasite is characterized by the presence of a trimeric thiol reductase protein known as TDR1 (the *T. cruzi* enzyme has been called Tc52), apparently involved, in the case of *Leishmania*, in redox regulation and perhaps mediating the parasite's susceptibility to the antimonial pro-drugs Pentostam and Glucantime (Denton et al., 2004; Silva AM, Westrop GW, Müller S, Cordeiro-da-Silva A and Coombs GH, submitted). Therapeutic activity depends on reduction of the relatively inert pentavalent metalloid to the more toxic trivalent species. This reduction occurs slowly in the presence of low molecular mass thiols such as glutathione (GSH) or the

trypanosomatid specific polyamine conjugate of GSH called trypanothione *in vitro*, especially at low pH such as found in the parasitophorous vacuole in which *Leishmania* resides (Ferreira *et al.*, 2003; Yan *et al.*, 2003). TDR1 catalyses this reduction by acting on a metalloid glutathione complex and it has been postulated that it thus mediates the key activation of the pro-drug (Denton et al., 2004). The reaction might be considered as a de-glutathionylation of an Sb(V)-glutathione adduct during which reduction to Sb(III) occurs and thus is a side-activity of the TDR1's perceived main intracellular function of redox regulation via de-glutathionylation of target enzymes (Silva AM, Westrop GW, Müller S, Cordeiro-da-Silva A and Coombs GH, submitted).

The structure of the enzyme from *L.donovani* (*Ld*TDR1), determined by single-wavelength anomalous dispersion on a SeMet derivative and refined to 2.3 Å resolution (Supp. material, Table 1), reveals a new class of trimeric GST. The asymmetric unit consists of a homotrimer with D_3 symmetry, total mass approximately 150 kDa (Figure 1A). A few residues, 1-3 in subunit A, 1-4 and 445-450 in subunit B, C1-2 in subunit C are omitted from the model due to poor electron density. A high degree of non-crystallographic symmetry is evident (r.m.s.d. of subunit A with B, 0.24 Å; B with C, 0.30 Å; A with C, 0.29 Å) therefore subunit A is detailed, unless stated otherwise.

The TDR1 subunit contains two similar domains (domain I residues 1-219 and domain II 231-450; Figure 1B & C), linked by a short section of ten residues. The domains share a sequence identity of 30% and 199 Cα positions overlay with an r.m.s.d of 1.8 Å. Both TDR1 domains are closely related to the Ω and τ class glutathione-S-transferases (Board *et al.*, 2000; Thom *et al.*, 2002; Axarli *et al.*, 2009). The interface between the domains is primarily hydrophobic and of some 680 $Å^2$, or ~6 % of the surface area of each domain.

Cytosolic GST subunits consist of an N-terminal thioredoxin-like sub-domain and a C-terminal α-helical sub-domain (Figure 1C). Superimposition of the thioredoxin-like domains (residues 6-78 and 232-301) from a subunit reveals a sequence identity of 39 % and r.m.s.d. 0.95 Å. A larger divergence is noted between the α-helical sub-domains with an additional short helix (α4) present in the N-terminal domain. Superimposing the core of these sub-domains (residues 95-209 with 319-434) reveals a sequence identity of about 25% and r.m.s.d. on Cα atoms of almost 2 Å. This value is strongly influenced by differences in α5-α6 of domain I compared to the related α16-αι7 of domain II. The short link between α5-α6 in domain I contributes to the interface between the two domains in a

subunit; the same region in domain II is, however, exposed to solvent far removed from any domain:domain interactions.

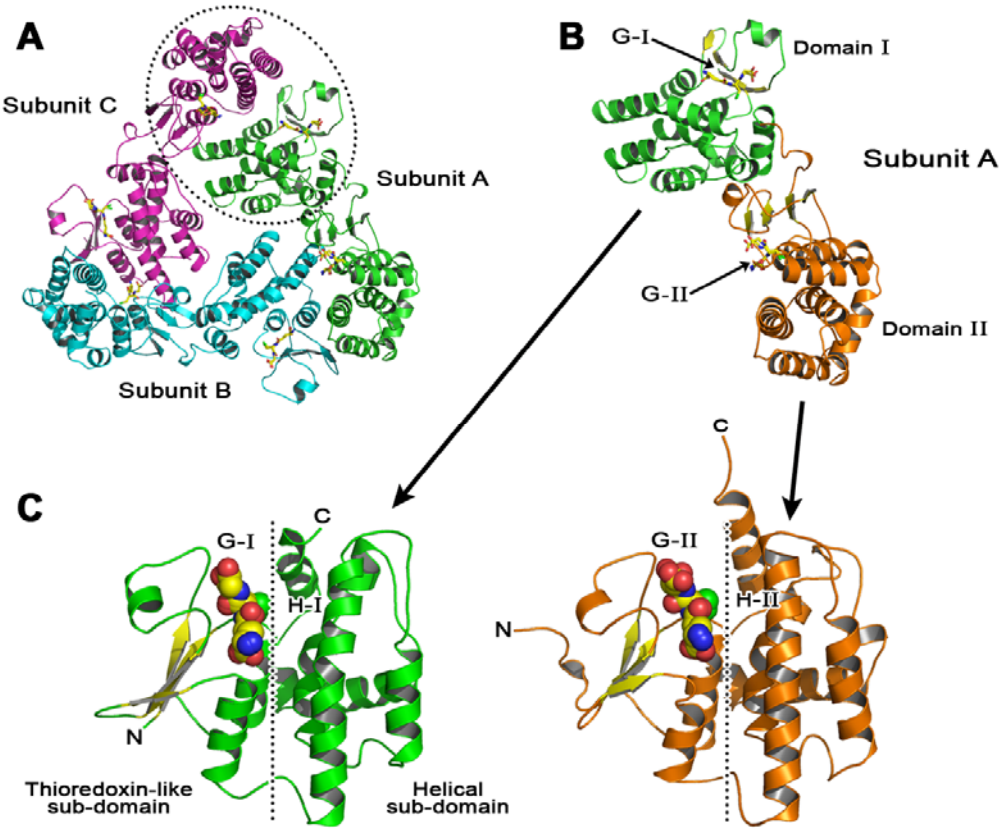

Figure 1. The structure of *Ld*TDR1. A. The trimer with glutathione shown in stick format. The position of one of the GST-like dimers is indicated by the dotted circle; **B**. TDR1 subunit A, coloured by domain; **C**. Domain I and domain II separated and presented in the same orientation. The thioredoxin-like and helical sub-domains are indicated. Glutathione is depicted as VDW spheres colour coded: C yellow, N blue, O red, S green. The position of the G- and H-sites are labeled.

The trimeric quaternary structure of TDR1 differs from the dimeric cytosolic GST enzymes (Oakley, 2005). Each *Ld*TDR1 subunit is constructed from two GST-like domains (Figure 1). The closest structurally related molecule is τ-GST from *Glycine max* (Protein Data Bank (PDB) code 3FHS, Axarli *et al.*, 2007). Comparison of the *Ld*TDR1 trimer against the 3FHS model reveals a typical GST-dimeric structure is formed, with each subunit contributing one domain to form a dimer with the alternate GST-domain from the neighboring subunit (Figure 1A). The trimer presents three GST-like dimers generated through inter- rather than intra-subunit interactions.

The domain I – II subunit interface regions have an average surface accessible area (ASA) of 1030 Å^2, or ~5 % of the total ASA of a subunit. This is towards the lower end of the range (~1000 Å^2 to ~1700 Å^2) found in GSTs. Hydrogen bonds are made between the side chain of Lys189 to the backbone carbonyls of Ala141 and Ala142; Tyr321 OH and the backbone amide of Phe69, the Asn329 and Arg52 side chains and there are also salt bridges involving Glu322 - Arg66 and Glu358 - Arg52.

TDR1 lacks the N-terminal extension widely observed in τ and Ω GST classes (Board *et al*, 2000). However, one τ and Ω class specific feature (Thom *et al.*, 2002) present in TDR1 is a F-F-G-G motif in the α17 – α18 loop on domain II. In domain I the phenylalanine residues are replaced by tyrosines and the glycines are replaced by a cysteine aspartate combination. This is the case in all three *Leishmania* TDR1 sequences as well as Tc52 from *T. cruzi*. In domain I this loop is solvent exposed on the surface of a subunit whereas in domain II it contributes significantly to the subunit:subunit interface.

Each subunit contains two glutathione binding or G-sites (Suppl. Figure S1) and nearby, about 10 Å distant, ligand or substrate binding sites that in GSTs are predominantly hydrophobic and usually termed the H-site (Figure 1C). The sites are designated G-I/H-I and G-II/H-II within TDR1 domains I and II, respectively. G-I and G-II binding sites contain four distinctive, highly conserved GST family features related to substrate binding. Firstly, a *cis*-proline (Pro56, Pro281) occurs in an α – β loop and supports the formation of a hydrogen bond from the backbone of the neighboring valine (Val55, Val280) to the cysteinyl moiety of glutathione (Dirr, *et al.*, 1994). Secondly, Ramachandran outliers Glu70 and Glu293 form hydrogen bonds to bind the glutathione γ-glutamyl moiety. Mutation of this highly conserved glutamate has a profoundly deleterious effect on activity and stability of GSTs (Allocati *et al.,* 2002; Winayanuwattikun & Ketterman, 2004). The active site cysteines (Cys14, Cys240) at the N-terminus of an α-helix interact with the glutathione thiol and the helix dipole is expected to enhance cysteine nucleophilicity (Kortemme & Creighton, 1995). Finally the phenylalanine in the C-P-F-C active site motif stacks over the aliphatic backbone of the glutamyl moiety of GSH. A large hydrophobic residue always occupies this position, contributing van der Waals interactions to stabilize the complex.

Although the G-I and G-II sites and interactions formed with glutathione are highly conserved, there are distinctive features (Suppl. Figure S2, S3). In both substrate binding sites the cysteinyl moiety forms mixed thiol-disulfide species with the active site cysteines

(Cys14 in G-I; Cys240 in G-II). The C-P-F-C motif in G-I mirrors that found in glutaredoxin and thioredoxin, with the proline crucial to ensure the proper alignment of three thiols from GSH, Cys14 and Cys17, such that the latter is available to stabilize the Cys14 thiolate. In subunit B, there is a mixed thiol-disulfide formed between Cys14 and Cys17 but in the other subunits the sulfur atoms of Cys14 and Cys17 are 3.4 Å and 3.6 Å apart. In G-II Cys17 is replaced by Val243 so the mixed disulfide configuration is not possible.

In the G-I site, hydrogen bonds occur between glutathione and Val55, Glu70, Arg39 and Ser71. Similar associations are noted in the G-II site involving Val280, Glu293 Ser294. Other than the cysteine to valine change in the G-II site compared to G-I, the alterations are restricted to the region in the pocket responsible for binding the glycyl moiety of glutathione. Here a hydrogen bond with the main chain of an arginine (Arg39) in G-I is replaced by a hydrogen bond to Gln267 NE2 in G-II. The position of Arg39 in G-I corresponds to His265 in G-II, while the position of Gln267 important in G-II is Glu41 in G-I.

In most GSTs the glutathione binding site is a relatively open cleft but in TDR1, as in Ω and τ-GSTs, the presence of an α-helix (α12 results in a smaller, partially occluded H-site the entrance of which is about 6.5 Å in diameter (Suppl. Figure S4). The pocket is partially formed by the almost ubiquitous Pro-Phe (often Tyr) motif following on from the active site cysteine. The H-I pocket is reduced in size due to the presence of His114 and Tyr215 at the base of the cleft, the side chains of which are linked by a hydrogen bond (data not shown).

In the H-II pocket, Met338 and Ile440 replace His114 and Tyr215, respectively, resulting in a different shape and the loss of a hydrogen bond linking two helical sections together may allow α20 to adopt a configuration giving rise to a more open cavity (Suppl. Figure S5). The H-II site, which is guarded by Pro241, Met338, Ile342, Arg443 and His439, extends 6 Å in one direction, nearly 10Å in another with a depth of some 14 Å away from the GSH thiol. Neither H-I nor H-II fit the hydrophobic descriptor, due to the presence of basic residues (His, Arg). The electrostatic properties of the pocket suggest that the natural substrates of TDR1 are acidic rather than hydrophobic.

The C-terminal domain G-II site, carries the dehydroascorbate reductase (DHAR) activity and treatment with iodoacetamide confirms that cysteine is important for the DHAR activity (Denton *et al.*, 2004). However, treatment of TDR1 with sodium arsenite or potassium antimonyl tartrate does not reduce DHAR activity – these reagents would be

expected to block the two cysteines found in the C-P-F-C motif of G-I, but not the C-P-F-V motif of G-II. The C-terminal domain was also cloned and expressed, and shown to carry DHAR activity.

The *Ld*TDR1 domains were treated as a single GST for sequence comparisons, large-scale alignments and tree calculations (Figure 2B). The introduction of *L. mexicana* and *L. infantum* TDR1 sequences along with Tc52 indicates two new branches in the GST phylogenetic tree, which correspond to a separation of domain I from domain II. That these two groupings are then more closely related to one another suggests the origin of TDR1/Tc52 is a gene duplication followed by a gene fusion event. Diversification has likely occurred after gene duplication leading to C-X-X-C motif in one domain and a C-X-X-S motif in the other. There is no other example where such a combination of events has occurred in a GST. Multiplication of the gene encoding GSTs has frequently occurred but not allied to a fusion. A fortuitous consequence of *Ld*TDR1 evolution is the presence of an activating agent that supports the successful deployment of antimonial pro-drugs.

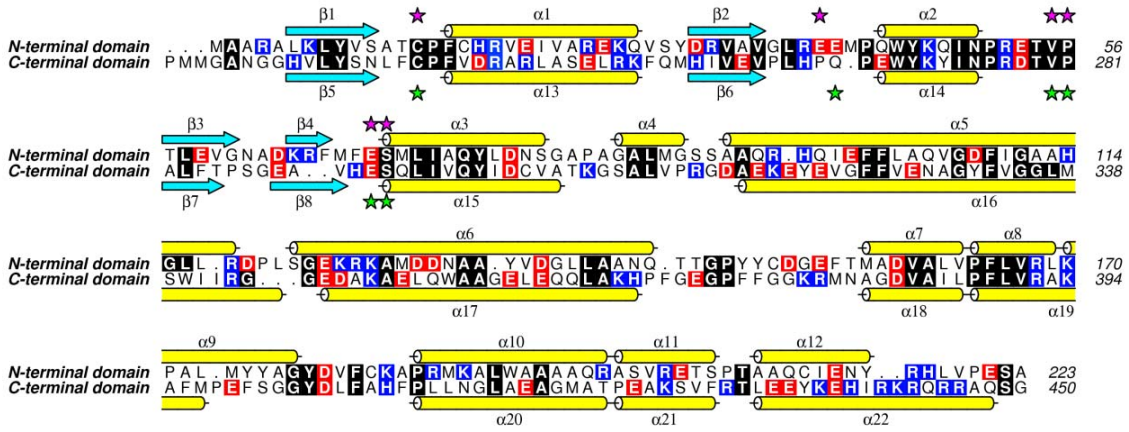

Figure 2A. Sequence alignment of domain I and domain II from *L. donovani* TDR1. Secondary structure elements are identified by cyan arrows for β-strands and yellow cylinders for α-helices, and labeled. Selected residues involved in binding glutathione are indicated by purple, for domain I, and green, for domain II, stars. Strictly conserved residues are encased in black, acidic residues in red and basic in blue. The alignment was performed using MUSCLE[15] and the figure produced with ALINE.[16] The purple and green stars mark residues from domain I and II respectively that interact with glutathione.

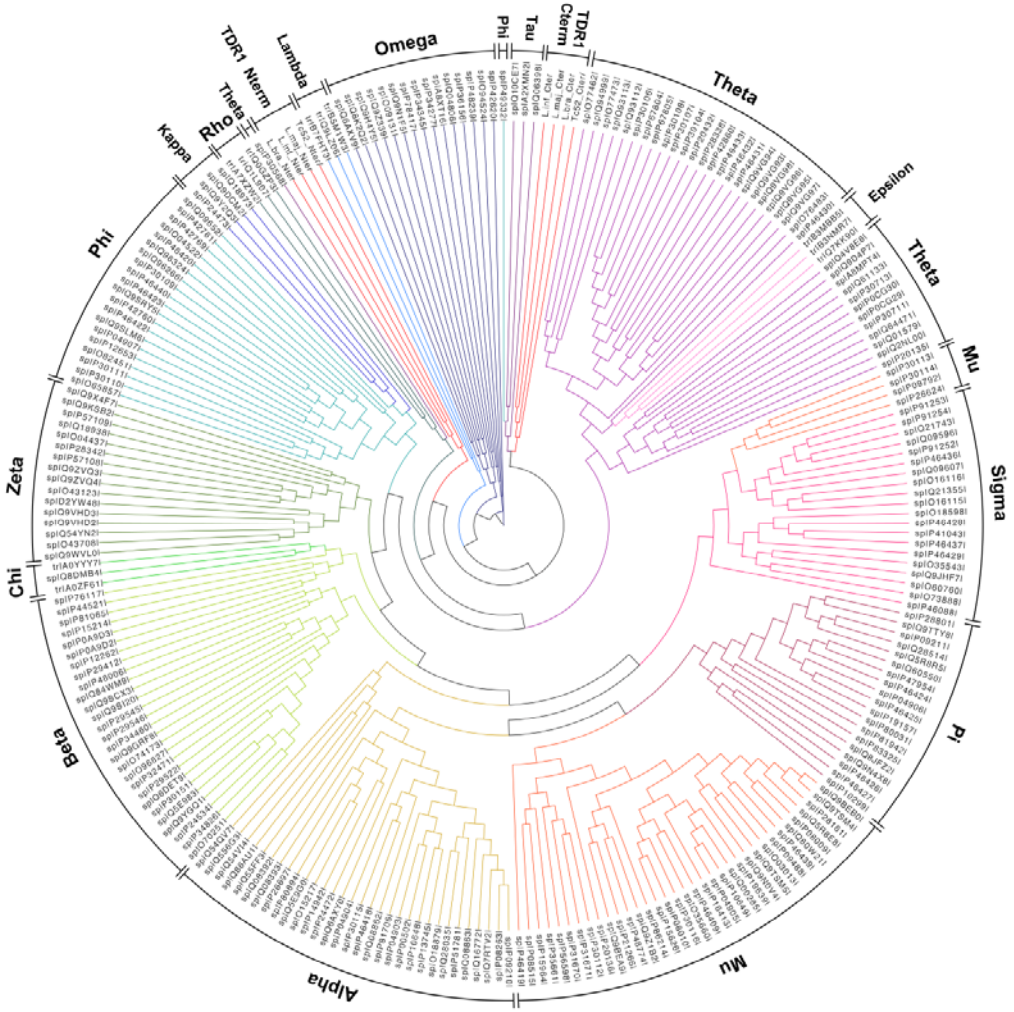

Figure 2B. Circular cladogram of GST family members. All marked assignments taken from database entries. TDR1 and Tc52 are considered as domains I and II for the analysis. Alignments were prepared using MUSCLE and the tree calculated through average distance using BLOSUM62 in Jalview.[17] The branch carrying TDR1 and Tc52 is coloured red.

Acknowledgements

Funded by The Wellcome trust (grants 083481 and 082596) and with support from the Diamond Light Source synchrotron. AMS is supported by Fundação para a Ciência e Tecnologia (FCT) grant SFRH/BD/28316/2006 (project number PTDC/CVT/65047/2006). We thank Tom Eadsforth for discussions.

References

Axarli, I., Dhavala, P. , Papageorgiou, A.C. & Labrou, N.E. (2009) Crystal structure of *Glycine max* glutathione transferase in complex with glutathione: investigation of the mechanism operating by the Tau class glutathione transferases. *Biochem. J.*, **422**, 247-256.

Allocati, N., Masulli, M., Casalone, E., Santucci, S., Favaloro, B., Parker, M.W., Di Ilio, C. (2002) Glutamic acid-65 is an essential residue for catalysis in *Proteus mirabilis* glutathione S-transferase B1-1. *Biochem. J.*, **363**, 189-193.

Board, P.G., Coggan, M., Chelvanayagam, G., Easteal, S., Jermiin, L.S., Schulte, G.K., Danley, D.E., Hoth, L.R., Griffor, M.C., Kamath, A.V., Rosner, M.H., Chrunyk, B.A., Perregaux, D.E., Gabel, C.A., Geoghegan, K.F. & Pandit, J. (2000) Identification, characterization, and crystal structure of the Ω class glutathione transferases. *J. Biol. Chem.*, **275**, 24798-24806.

Bond, C.S. and Schüttelkopf, A.W. (2009) ALINE: a WYSIWYG protein-sequence alignment editor for publication-quality alignments. *Acta cryst.*, **D65**, 510-512.

Denton, H., McGregor, J.C. & Coombs, G.H. (2004) Reduction of anti-leishmanial pentavalent animonial drugs by a parasite-specific thiol-dependant reductase, TDR1. *Biochem. J.*, **381**, 405-412.

Dirr, H., Reinemer, P. & Huber, R. (1994) X-ray crystal structures of cytosolic glutathione S-transferases. Implications for protein architecture, substrate recognition and catalytic function. *Eur. J. Biochem.*, **220**, 645-661.

Dixon DP, Skipsey M, Edwards R. Roles for glutathione transferases in plant secondary metabolism. Phytochemistry. 2010 Mar;71(4):338-50.

Edgar, R.C. (2004) MUSCLE: multiple sequence alignment with high accuracy and high throughput. *Nuc. Acid. Res.*, **32**, 1792-1797.

Ephros, M., Waldman, E. & Zilberstein (1997) Pentostam induces resistance to antimony and the preservative chlorocresol in *Leishmani donovani* promastigotes and axenically grown amastigotes. *Antimicrob. Agents. Chemother.*, **41**, 1064-1068.

Ferreira, C.d.S., Martins, P.S., Demicheli, C., Brochu, C., Ouelette, M. & Frezard, F. (2003) Thiol-induced reduction of antimony (V) into antimony (III): A comparitive study with trypanothione, cysteinyl-glycine, cysteine and glutathione. *Biometals*, **16**, 441-446

Frova, C. (2006) Glutathione transferases in the genomics era: new insights and perspectives. Biomolecular Engineering 23, 149-169.

Kortemme, T. & Creighton, T.E. (1995) Ionisation of cysteine residues at the termini of model α-helical peptides. relevance to unusual thiol pK_a values in proteins of the thioredoxin Family. *J. Mol. Biol.*, **253**, 799-812.

Meux, E. Propser, P., Ngadin, A., Didierjean, C., Morel, M., Dumarcy, S., Lamant, T., Jacquot, J-P., Favier, F. & Gelhaye, E. (2011) Glutathione Transferases of *Phanerochaete chrysosporium*: S-Glutathionyl-p-hydroquinone reductase belongs to a new structural class. *J. Biol. Chem.*, **286**, 9162-9173.

Murta, S.M.F., Nogueira, F.B., Dos Santos, P.F., Campos, F.M.F., Volpe, C., Liarte, D.B., Nirdé, P., Probst, C.M., Krieger, M.A., Goldenberg, S. & Romanha, A.J. (2008) Differential gene expression in *Trypanosoma cruzi* populations susceptible and resistant to benznidazole. *Acta* Tropica, **107**, 59-65.

Oakley, A.J., (2005) Glutathione transferases: new functions. **15**, 716-723.

Shaked-Mishan, P., Ulrich, N., Ephros, M. and Zilberstein, D. (2001) Novel intracellular SbV reducing activity correlates with antimony susceptibility in *Leishmania donovani*. *J. Biol. Chem.*, **276**, 3971–3976.

Tew KD, Townsend DM. Regulatory functions of glutathione S-transferase P1-1 unrelated to detoxification. Drug Metab Rev. 2011 May;43(2):179-93.

Thom, R., Cummins, I., Dixon, D.P., Edwards, R., Cole, D.J. & Lapthorn, A.J. (2002). Structure of a tau class glutathione S-transferase from wheat active in herbicide detoxification. *Biochemistry*, **41**, 7008-7020.

Tripathi, T., Rahlfs, S., Becker, K. & Bhakuni, V. (2007) Glutathione mediated regulation of oligomeric structure and functional activity of *Plasmodium falciparum* glutathione S-transferase. *BMC Structural Biology*, **7**, 67-76.

Waterhouse, A.M., Procter, J.B., Martin, D.M.A., Clamp, M. & Barton, G.J. (2009), Jalview version 2: A Multiple Sequence Alignment and Analysis Workbench, *Bioinformatics*, **25**, 1189-1191.

Winayanuwattikun, P. & Ketterman, A.J. (2004) Catalytic and structural contributions for glutathione-binding residues in a Delta class glutathione S-transferase. *Biochem. J.*, **382**, 751-757.

Yan, S., Li, F., Ding, K., Sun, H. (2003) Reduction of pentavalent antimony by trypanothione and formation of a binary and ternary complex of antimony (III) and trypanothione. *J. Biol. Inorg. Chem.*, **8**, 689-697.

Supplemental Material

Materials and Methods

Sample preparation and crystallization

The *L. donovani TDR1* gene was cloned into pET15bTEV to add a tobacco etch virus (TEV) protease cleavable histidine tag as an aid for purification of the recombinant protein (*Ld*TDR1). A selenomethionine (SeMet) derivative was prepared in the methionine auxotroph *Escherichia coli* strain B834 (DE3), using selenomethionine medium (Molecular Dimensions, UK), supplemented with 40 mg mL^{-1} selenomethionine. A purification protocol commonly used in our laboratory was applied (Dawson *et al.*, 2008). In summary, the first stage involved nickel affinity chromatography with a 5 mL Ni-NTA column (Qiagen). A linear concentration gradient was applied to elute the product, which was then incubated for two hours with His-tagged TEV protease at 30 °C, before dialysis at room temperature against 20 mM Tris-HCl, pH 7.8, 150 mM for one hour. The resulting mixture was applied to the Ni-NTA column, which bound the cleaved His-tag, the protease and uncleaved *Ld*TDR1. The *Ld*TDR1, from which the His-tag had been cleaved, was in the flow-through. Fractions were analyzed using sodium dodecyl sulfate polyacrylamide gel electrophoresis (SDS-PAGE) and those containing *Ld*TDR1 were pooled. The protein was further purified by size exclusion chromatography using a calibrated Superdex 200 26/60 column (GE Healthcare) equilibrated with 20 mM Tris-HCl, 150 mM NaCl pH 7.8. This final purification stage also indicated that *Ld*TDR1 formed a stable trimer in solution (data not shown). The high level of *Ld*TDR1 purity was confirmed by SDS-PAGE and matrix-assisted laser desorption/ionization-time-of-flight mass spectrometry. The latter technique also confirmed full incorporation of SeMet. The sample was dialyzed into 10 mM HEPES pH 7.8, 50 mM NaCl then concentrated using a Vivaspin 20 (Sartorius) to provide a stock solution for crystallization. A theoretical extinction coefficient of 56185 M^{-1} cm^{-1} at 280 nm, was used to estimate protein concentration (*PROTPARAM*, Gasteiger *et al.,* 2005); the theoretical mass of one subunit of the SeMet derivative is 50872 Da.

*Ld*TDR1 was crystallized at 20 °C by the hanging drop vapor diffusion method using 0.75 µL of protein solution at a concentration of 5 mg mL^{-1} containing 1 mM glutathione, mixed with 0.75 µL of reservoir containing 12 % polyethylene glycol (PEG) 8000, 0.1 M HEPES buffer pH 7.0, 8 % (v/v) ethylene glycol. Monoclinc rods, with approximate dimensions of 1.0 x 0.2 x 0.2 mm, grew over 1-2 days. The concentration of PEG 8000 and ethylene

glycol in the mother liquor provided sufficient cryo-protection that crystals could be placed in a stream of cold N_2 gas directly and characterized in-house using a Rigaku HF007 rotating anode X-ray generator coupled to an RAXIS IV^{++} image plate detector. The crystals were monoclinic in space group *C*2 with unit cell lengths *a* = 197.5, *b* = 58.4, *c* = 160.4 Å with β = 111.8°. Crystals were stored in liquid N_2 for data collection at a synchrotron. Attempts to obtain crystals of the apo-form, and of complexes with glutathionylspermidine or trypanothione were unsuccessful.

X-ray data collection, processing, structure solution and refinement

Single-wavelength anomalous diffraction (SAD) data were measured from a SeMet derivative on beam line I02 of the Diamond Light Source using an ADSC Q315 CCD detector. Data were indexed and integrated using *MOSFLM* (Leslie, 2006) and scaled using SCALA (Evans, 2006). The SAD data were collected near the Se K-absorption edge *f*" maximum, determined using X-ray Absorption Near Edge Structure spectroscopy. Initial phases were obtained by SAD-phasing within the CCP4 pipeline CRANK (Ness *et al.*, 2004; Pannu *et al.*, 2011). Substructure detection and refinement were performed using AFRO (Pannu, *unpublished*), CRUNCH2 (de Graff *et al.*, 2001) and BP3 (Pannu *et al.*, 2003), and identified the positions of all 39 selenium atoms present. The initial figure-of-merit was 0.49. Hand determination followed by density modification was performed using SOLOMON (Abrahams & Leslie, 1996) with an estimated solvent content of 55 %, and this improved the figure-of-merit to 0.71. Automated map interpretation with BUCCANEER (Cowtan, 2006) produced a partial model consisting of 1335 residues in 15 polypeptide chains giving an R_{work} and R_{free} values of 33.5 % and 36.9 % respectively. The model was then extended in COOT (Emsley & Cowtan, 2004).

Refinement was performed in REFMAC5 (Murshudov *et al.*, 1997) utilizing Translation/Libration/Screw refinement (Winn *et al.*, 2000), and alternated with rounds of electron and difference density map inspection and model manipulation together with ligand incorporation using COOT. Non-crystallographic symmetry (NCS) restraints were not employed. MOLPROBITY (Chen *et. al.*, 2010) was used to investigate model geometry in combination with the validation tools provided in COOT. Crystallographic statistics are presented in Table 1. Analyses of surface areas and interactions were made using the PISA server (Krissinel & Henrick, 2007) and figures were prepared with PyMOL (DeLano, 2002). Amino acid sequence alignments were carried out using the program MUSCLE (Edgar, 2004) and structural superimposition performed with SSM (Krissinel & Henrick, 2004). The PDBeFold server (http://www.ebi.ac.uk/msd-srv/ssm; Krissinel & Henrick (2004)) was used to performing a search of the protein structural database.

Table S1. Crystallographic statistics

Data Collection	
Space group	$C2$
Wavelength	0.9795 Å
Unit cell parameters	
a, *b*, *c*, (Å)	197.5, 58.4, 160.4 111.8
β (°)	
Resolution Range (Å)	29.8 – 2.3
Unique reflections	74,464
Completeness (%)[a]	97.9 (98.7)
<I/s(I)>	12.6 (3.9)
Multiplicity	4.0 (4.2)
R_{merge} (%)[b]	5.9 (25.9)
Refinement	
Resolution Range (Å)	30.0 – 2.3
No. of used reflections	70,625
R_{work}[c], R_{free}	14.9, 20.8
Protein atoms	11,011
Glutathione / ethylene glycol / water	6, 15, 1165
R.m.s. deviations from ideal geometry	
bond lengths (Å)	0.015
bond angles (°)	1.418
Thermal parameters (Å^2)	
Wilson *B*	42.9
Mean *B*	
subunit A, B, C	55.2 / 60.5 / 55.9
GSH, water, ethylene glycol	46.8 / 60.2 / 72.7
Ramachandran plot (%)	98.3 / 1.2 / 0.5
favoured/allowed	

a. Values in parentheses refer to the highest resolution bin of width approx. 0.1 Å; **b.** R_{merge} = $\sum h \sum i ||(h,i) - \langle I(h) \rangle \sum h \sum i\ I(h,i)$; **c.** R_{work} = $\sum hkl ||F_o|-|F_c|| / \sum |F_o|$, where F_o is the observed structure factor and F_c the calculated structure factor; **d.** R_{free} is the same as R-work except calculated using 5% of the data that are not included in any refinement calculations.

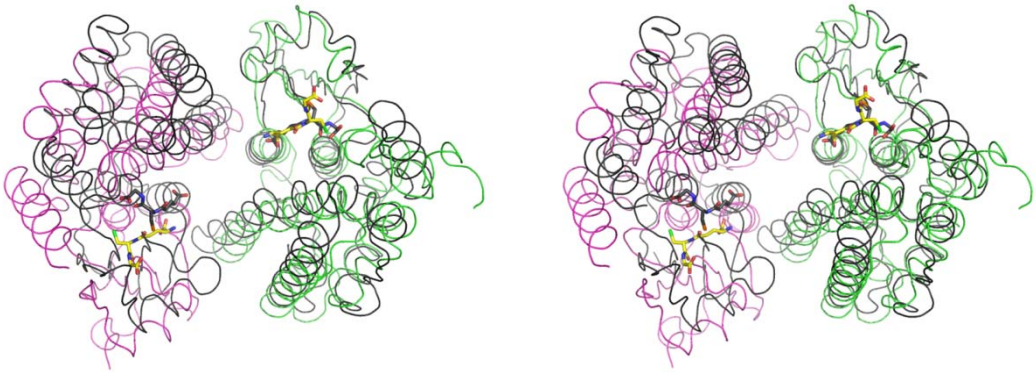

Figure S1. Stereoview comparison of TDR1 inter-subunit (A-C) dimer with the dimer formed by the closest structurally related tau class GST dimer (PDB code: 3FHS[21]). The polypeptide trace of 3FHS is shown in dark grey, superimposed on domain I from subunit A (purple) and domain II from subunit C (green), which generate the TDR1 GST-like dimer. The bound glutathione molecules are depicted sticks colored with yellow C atoms for the TDR1 model, grey for the 3FHS model.

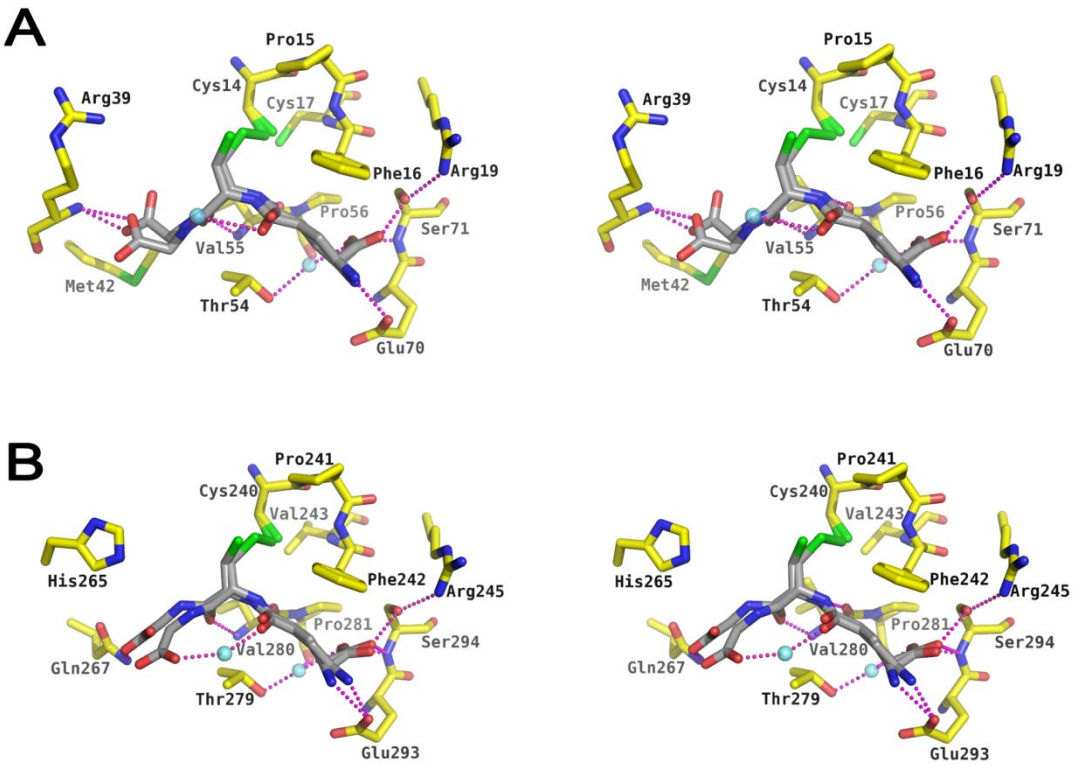

Figure S2. Stereoview images of the two glutathione binding sites within subunit A. **A.** G-I - the domain I glutathione binding site; **B.** G-II - the domain II binding site. Atomic positions are color coded: N blue, O red, S green, C grey for the ligands and yellow for the protein. Water molecules are shown as cyan spheres. Dotted lines represent potential hydrogen bonding interactions. Glutathione has been modeled as a 50:50 mixture of reduced and oxidized forms.

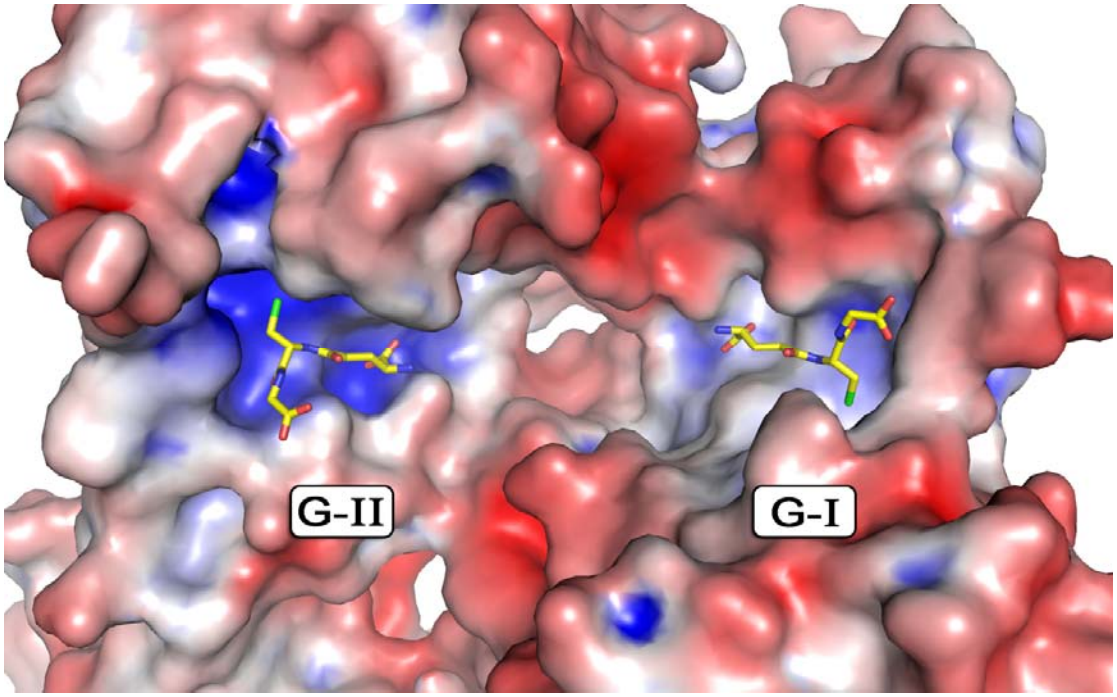

Figure S3. The electrostatic properties of the G-I and G-II binding sites. TDR1 is depicted as van der Waals surface colored with blue representing positive charge, red negative and grey neutral. Although many structural features are conserved between the two glutathione binding sites are distinct with G-II displaying a much greater basic character than G-I.

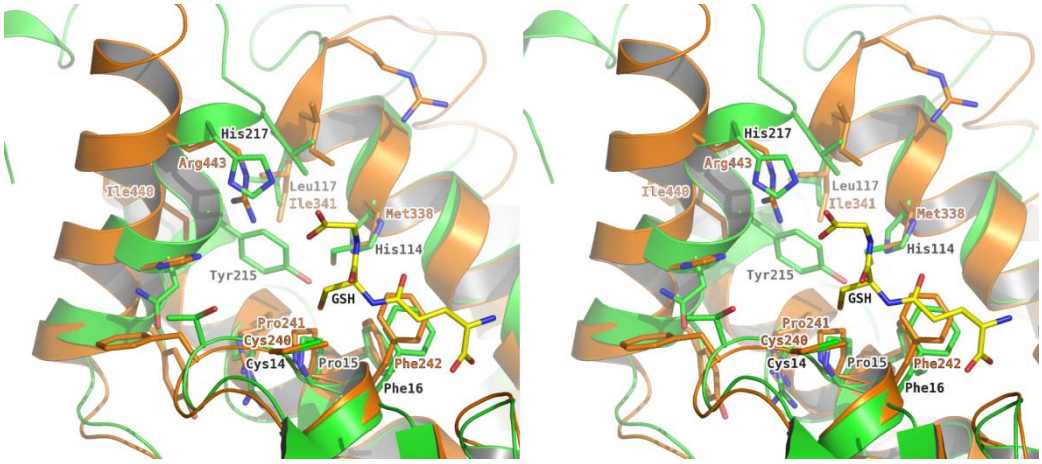

Figure S4. Stereoimage showing an overlay of the hydrophobic (H-sites) from domain I (H-I, green) and domain II (H-II, orange) from subunit A. The Cys-Pro-Phe motif is conserved in both near the GSH binding site, but there is conservation in the H-site itself. The H-I pocket is restricted by the positioning of Tyr215 and His114 and with the movement of α12 to narrow the pocket.

Supplemental References

Abrahams, J. P. & Leslie A. G. W. (1996). Methods used in the structure determination of bovine mitochondrial F1 ATPase. *Acta Cryst.* **D52**, 30-42.

Chen, V.B., Arendall III, W.B., Headd, J.J., Keedy, D.A., Immormino, R.M., Kapral, G.J., Murray, L.W., Richardson, J.S. & Richardson, D.C. (2010) MolProbity: all-atom structure validation for macromolecular crystallography. *Acta Cryst.,* **D66**, 12-21.

Cowtan, K. (2006) The Buccaneer software for automated model building *Acta Cryst.,* **D62**, 1002-1011.

Dawson, A., Fyfe, P.K. & Hunter, W.N. (2008) Specificity and reactivity in menaquinone biosynthesis; the structure of *Escherichia coli* MenD [2-succinyl-5-enolpyruvyl-6-hydroxy-3-cyclohexadiene-1-carboxylate synthase]. *J. Mol. Biol.* **384,** 1353-1368.

DeLano, W.L. (2002). The PyMOL Molecular Graphics System, http://www.pymol.org

Denton, H., McGregor, J.C. & Coombs, G.H. (2004) Reduction of anti-leishmanial pentavalent animonial drugs by a parasite-specific thiol-dependant reductase, TDR1. *Biochem. J.*, **381**, 405-412.

Edgar, R.C. (2004) MUSCLE: multiple sequence alignment with high accuracy and high throughput. *Nuc. Acid. Res.*, **32**, 1792-1797.

Emsley, P. & Cowtan K. (2004). Coot: Model building tools for molecular graphics. *Acta Cryst.* **D60**, 2126-2132.

Evans, P. (2006). Scaling and assessment of data quality. *Acta. Cryst.* **D62**, 72-82.

de Graaff, R. A. G., Hilge, M., van der Plas, J. L. & Abrahams, J. P. (2001). Matrix methods for solving protein substructures of chlorine and sulfur from anomalous data. *Acta Cryst*. **D57**, 1857-1862.

Krissinel, E. & Henrick, K. (2004) Secondary-structure matching (SSM), a new tool for fast protein structure alignment in three dimensions. *Acta Cryst.,* **D60**, 2256-2268.

Krissinel, E. & Henrick, K. (2007). Inference of Macromolecular Assemblies from Crystalline State *J. Mol. Biol.* **372**, 774-797.

Leslie, A.G.W. (2006). The integration of macromolecular diffraction data. *Acta Cryst.* ***D*62,** 48-57.

McCoy, A.J., Grosse-Kunstleve, R.W., Adams, P.D., Winn, M.D., Storoni, L.C. & Read, R.J. (2007). *Phaser* crystallographic software. *J. Appl. Cryst.*, **40**, 658-674.

Murshudov, G.N., Vagin, A.A. & Dodson, E.J. (1997) Refinement of Macromolecular Structures by the Maximum-Likelihood Method. *Acta Cryst.*, **D53**, 240-255.

Ness, S.R., de Graff, A.G., Abrahams, J.P. & Pannu, N.S. (2004) CRANK: New methods for automated macromolecular crystal structure solution. *Structure*, **12**, 1753-1761.

Pannu, N. S., McCoy A. J. & Read, R. J. (2003). Application of the complex multivariate normal distribution to crystallographic methods with insights into multiple isomorphous replacement phasing. *Acta Cryst.,* **D59**, 1801-1808.

Pannu, N.S. & Read, R.J. (2004) The application of multivariate statistical techniques improves single-wavelength anomalous diffraction phasing. *Acta Cryst.*, **D60**, 22-27.

Pannu, N.S., Wattereus, W.J., Skubák, P., Sikharulidze, I., Abrahams, J.P. & de Graaff, R.A.G. (2011) Recent advances in the CRANK software suite for experimental phasing. *Acta Cryst.*, **D67**, 331-337.

Winn, M., Isupov, M. and Murshudov, G.N. (2000) Use of TLS parameters to model anisotropic displacements in macromolecular refinement. *Acta Cryst.*, **D57**, 122-1

4.6 Metabolic variation during development in culture of *Leishmania donovani* promastigotes

The genome sequencing of several *Leishmania* species has provided immense amounts of data and allowed the prediction of the metabolic pathways potentially operating. Subsequent genetic and proteomic studies have identified stage-specific proteins and putative virulence factors but many aspects of the metabolic adaptations of *Leishmania* remain to be elucidated. In this study, we have used an untargeted metabolomics approach to analyze changes in the metabolite profile as promastigotes of *L. donovani* develop during *in vitro* cultures from logarithmic to stationary phase. The results show that the metabolomes of promastigotes on days 3-6 of culture differ significantly from each other, consistent with there being distinct developmental changes. Most notable were the structural changes in glycerophospholipids and increase in the abundance of sphingolipids and glycerolipids as cells progress from logarithmic to stationary phase.

Reprinted from PLoS Neglected Tropical Disease 2011 Dec 5 (12):e1451.

OPEN ACCESS Freely available online

PLoS NEGLECTED TROPICAL DISEASES

Metabolic Variation during Development in Culture of *Leishmania donovani* Promastigotes

Ana Marta Silva[1,2,3], Anabela Cordeiro-da-Silva[2,3], Graham H. Coombs[1]*

1 Strathclyde Institute of Pharmacy and Biomedical Sciences, University of Strathclyde, Glasgow, United Kingdom, **2** Instituto de Biologia Molecular e Celular, Universidade do Porto, Porto, Portugal, **3** Laboratório de Ciências Biológicas, Faculdade de Farmácia da Universidade do Porto, Porto, Portugal

Abstract

The genome sequencing of several *Leishmania* species has provided immense amounts of data and allowed the prediction of the metabolic pathways potentially operating. Subsequent genetic and proteomic studies have identified stage-specific proteins and putative virulence factors but many aspects of the metabolic adaptations of *Leishmania* remain to be elucidated. In this study, we have used an untargeted metabolomics approach to analyze changes in the metabolite profile as promastigotes of *L. donovani* develop during *in vitro* cultures from logarithmic to stationary phase. The results show that the metabolomes of promastigotes on days 3–6 of culture differ significantly from each other, consistent with there being distinct developmental changes. Most notable were the structural changes in glycerophospholipids and increase in the abundance of sphingolipids and glycerolipids as cells progress from logarithmic to stationary phase.

Citation: Silva AM, Cordeiro-da-Silva A, Coombs GH (2011) Metabolic Variation during Development in Culture of *Leishmania donovani* Promastigotes. PLoS Negl Trop Dis 5(12): e1451. doi:10.1371/journal.pntd.0001451

Editor: Genevieve Milon, Institut Pasteur, France

Received August 31, 2011; **Accepted** November 10, 2011; **Published** December 20, 2011

Funding: The study was supported by Fundação para a Ciência e Tecnologia (FCT) project number PTDC/CVT/65047/2006 and AMS is supported by FCT grant SFRH/BD/28316/2006. The funders had no role in study design, data collection and analysis, decision to publish, or preparation of the manuscript.

Competing Interests: The authors have declared that no competing interests exist.

* E-mail: graham.coombs@strath.ac.uk

Introduction

Leishmaniasis remains one of the major infectious diseases with 350 million people at risk in 88 countries worldwide and 2 million estimated new cases every year [1]. The lack of effective chemotherapy and emergence of drug resistance (reviewed in [2]) highlights the need for an improved knowledge of the parasite's cell biology to discover peculiarities that could potentially be explored as drug targets.

The *Leishmania* life cycle involves several developmental stages and alternates between sand fly and mammalian hosts. A major developmental difference is the occurrence as intracellular amastigotes in mammalian macrophages and as extracellular promastigotes in the sand fly. However, multiple forms of promastigotes have been identified based on morphology, location, infectivity, growth rate, ability to divide, and specific features such as expression of surface molecules [3–8]. It is believed that the parasite's occurrence in different developmental forms is a mechanism whereby it adapts to survive and persist in the various environmental conditions in which it is confronted with variations in temperature, pH, nutrient and oxygen availability and exposure to reactive oxygen (ROS) and nitrogen species (RNS) [9]. Despite the extensive investigations on various features of *Leishmania* over many years and the recent pioneering application of metabolomics technologies to studies on the parasite [10–13], particularly the elucidation of ways in which amastigotes differ from promastigotes [13–16], currently relatively little is known about the detail of the metabolic variation that happens during this developmental sequence in the sand fly.

The developmental sequence in the sand fly vector, which terminates in transformation to the metacyclic form infective to a mammalian host, appears to be mimicked, at least in part, during growth axenically in vitro; this comprises multiplication of procyclic promastigote forms and then differentiation to the metacyclic form, a process known as metacyclogenesis which is accompanied by morphological changes, including reduction in size of the cell body and a relatively longer flagellum, and some known biochemical changes such as lipophosphoglycan (LPG) and surface protein expression [5–7,17–20]. Thus the in vitro system provides an opportunity to investigate the metabolome changes that accompany and perhaps underpin the developmental sequence of the promastigote. In the present study, we have applied state-of-the-art metabolomics approaches to analyse the changes in the metabolome of promastigotes of *Leishmania donovani* during culture in vitro. The results show that there is distinct variation in the metabolome, especially in the lipid composition.

Methods

Leishmania parasites

Leishmania donovani (MHOM/NP/03/BPK206/0clone10) promastigotes had been cloned from an isolate from a visceral leishmaniasis patient sensitive to pentavalent antimonials in Nepal, as described by Rijal and co-workers [21]. Promastigotes were grown on modified Eagle's medium (designated HOMEM medium, Invitrogen) supplemented with 20% (v/v) heat inactivated fetal calf serum (FCS, PAA Laboratories) at 26°C. Cultures were set up initially at a density of 2.5×10^5 parasites/ml and sub-passaged every 6 days.

Leishmania extracts for metabolite analysis

L. donovani promastigote cultures were initiated at 2.5×10^5 cells/ml in 16×10 ml cultures in order to obtain cell samples from four

Author Summary

Leishmania infections are considered neglected tropical diseases as the parasites affect millions of people worldwide but there are limited research efforts aimed at obtaining vaccines and new drugs. *Leishmania* has a digenetic life cycle alternating between promastigote forms, which develop in the sand-fly, the vector of the disease, and an amastigote form, which grows in mammals after being bitten by an infected sand-fly. *In vitro* studies with the promastigote forms are routinely used to gain insights about the parasite's cell biology. Little is known about how the different promastigotes forms are metabolically adapted to their particular micro-environment in the host or how they are pre-adapted metabolically for infecting a mammal, thus we have undertaken a study of the metabolite profile of *L. donovani* promastigotes in order to gain an understanding of the changes that occur during promastigote development. The analysis has revealed that the changes in promastigotes' metabolome between days 3 and 6 take place in a progressive manner; however major differences were observed when comparing the promastigotes on days 3 and 6. An increase in lipid abundance as promastigote development occurred was notable and is likely to reflect remodelling of the parasite's surface in readiness for infecting a mammal.

independently growing cultures (biological replicates) on each day. Promastigotes from each culture were harvested at days 3, 4, 5 and 6 for metabolite extraction. The metabolite extraction was performed as previously described [11]. Briefly, promastigotes quenching was performed in a dry ice/ethanol bath with rapid temperature decrease to 2°C and then immediate transfer to ice. Two aliquots of 4×10^7 cells were taken from each culture flask (technical replicates). Cell pellets were obtained by centrifugation at 12000 g for 10 min at 4°C, and washed 3 times in 1 ml of PBS. For cell disruption and metabolite extraction, cell pellets were resuspended in 200 µl cold chloroform/methanol/water (20/60/20, v/v/v) and incubated for 1 h in a Thermomixer (1400 rpm, 4°C). After centrifugation at 12000 g for 10 min at 4°C, the supernatant containing the extracted metabolites was recovered and stored at −70°C until analysed.

Liquid chromatography mass spectrometry (LC-MS) analysis and data processing

LC-MS analysis and data processing was done as described by t'Kindt and co-workers [11,12]. Metabolite level comparisons between the time points analyzed (after 3, 4, 5 and 6 days of in vitro growth) were performed based on the ratio between the intensity on each day and the mean intensity level for the 4 day period, that is $x/\overline{X}_{3-6}$. The following criteria were applied to assign differences in metabolite levels among the time points analyzed as being potentially interesting and so worthy of inclusion in the full analysis: (i) there was at least a 2-fold difference between at least one of the time points when compared with the mean intensity level; and (ii) there was a statistically significant difference ($p<0.05$) between the time points being compared. The data are expressed as intensity per 25 µg cell protein.

Statistical analysis

Statistical analysis was performed using Analysis of Variance (ANOVA), which allowed the simultaneous comparison of all time point analyzed: a p value smaller than 0.05 ($p<0.05$) was considered significant; SPSS Statistics software (IBM) was used to perform principal component analysis; GraphPad Prism 4 was used for plotting the graphs and VisuMap software (VisuMap Technologies Inc.) was used to visualise the data as heatmaps.

Results

In order to obtain detailed information about the metabolic changes that occur during the development of promastigotes under defined conditions in vitro, we have applied an untargeted metabolomics approach. Promastigotes were collected after 3, 4, 5 and 6 days of in vitro growth (thus including different proportions of various promastigote forms, including procyclic promastigotes which dominate during logarithmic growth and the non-dividing metacyclic forms that start to be formed at late stages of logarithmic phase) and analyzed by LC-MS. We used four parallel cultures (designated biological replicates) to obtain representative data and during the cell processing from each culture two samples were taken (designated technical replicates) to control for variation due to technical factors. Analysis of a parasite's metabolome needs to take into account the changes in cell volume that occur during development and growth. Measurement of the protein content of the cells showed that transformation to the metacyclic form at late logarithmic phase of growth was accompanied by a decrease in protein content, which is thought to correlate with the decrease in cell size (Figure 1). There was a great difference in protein content between the cells on days 3 and 6 ($p<0.0028$) but also a significant difference between the cells on days 3 and 4 ($p<0.025$) and days 5 and 6 ($p<0.034$). To assure that the metabolome analysis of the parasite would reflect the changes observed in cell size, we have expressed the data as intensity per cell protein (rather than per cell number), thus facilitating meaningful comparison of the metabolite levels in cells of differing volume. This method of normalization had significant effects, for instance the general decreases in metabolite intensity when expressed per cell number that were observed between promastigotes on day 3 and day 6 were almost abolished when data were expressed as intensity/mg cell protein. Indeed the summed total of the metabolite intensities normalized

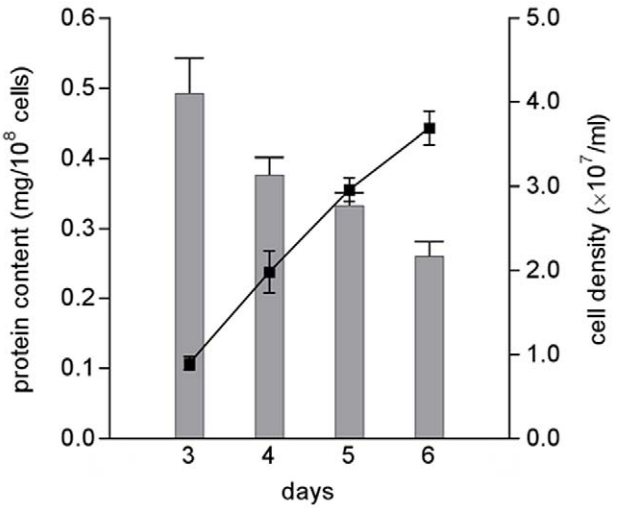

Figure 1. Relantionship between protein content and cell density during *in vitro* growth of *L. donovani* promastigotes. *L. donovani* promastigotes were seeded at 2.5×10^5 parasites/ml, counted daily and harvested at days 3, 4, 5 and 6. Protein content was determined by the Lowry method. Each value is a mean ± standard deviation from four cultures. Statistically significant differences observed between the days evaluated: days 3 and 4, $p<0.05$; days 5 and 6, $p<0.05$; days 4 and 6, $p<0.05$; days 3 and 6, $p<0.01$.
doi:10.1371/journal.pntd.0001451.g001

to cell protein were relatively constant over the four days whereas when expressed as intensity/cell number it declined 33% on day 6. We believe that this method of taking into account the changes in cell size during growth is currently optimal and provides a means of generating data that are meaningful and can be interpreted with confidence.

In order to understand better the metabolic fluctuations as the promastigotes developed over the four days, we compared the profiles of metabolites levels (Figures 2A and 3). The analysis shown in Figure 2A (in which the metabolite intensity level on each day is compared with the mean level over the 4 day period) highlights that, of the total metabolites identified, the levels of the majority remained rather similar throughout although 26.9% differed by at least 2-fold on one of the days when compared with the mean. The day 3 levels were the most different from the others (22% being at least 2-fold different from the centered-mean for the period analyzed) and with just some metabolites differing greatly at other times. This is consistent with there being a progressive change in many metabolite levels over the four day period. However, comparison between the metabolite intensities on days 3 and 6 revealed that 48.4% of all the metabolites identified differed by more than 2-fold (Figure 2B), suggesting a significant difference in metabolic profile between promastigote populations in logarithmic (mainly procyclic promastigotes) and stationary phases (containing many metacyclic promastigotes).

The metabolic profile was also analysed by principal component analysis (PCA). PCA is an unsupervised clustering technique that allows the reduction of the data into two dimensions (principal component 1 [PC1] and principal component 2 [PC2]), which capture and enable visualization of data variability; this method is generally applied to large sets of data, such as those resulting from microarray or metabolomic analyses, as a way of obtaining a summary or overview of all samples, to find clusters and trends, and to identify the outliers. It is recommended as a starting point for analysis of multivariate data [22]. The PCA score plots (Figure 4) of the LC-MS data show clearly the identification of four distinct clusters, each one corresponding to one of the groups of samples analyzed on a particular day of growth. PC1 and PC2 account for more than 81% of the variables which shows the clear metabolic differences between the samples. Moreover, the tight clustering within each group indicates good reproducibility. The data in Figure 4 show that promastigotes on days 4 and 5 are aligned closely with each other indicating that they have a similar metabolic profile that is clearly distinguished from those on days 3 and 6 (which explains 59.0% of total variance given by the second principal component). These data are consistent with there being metabolic changes as the promastigotes develop from procyclic promastigotes to metacyclic promastigotes, and the relatively large number of metabolites that differ in levels significantly between days 3 and 6.

The identity of the metabolites was carried out based on the databases detailed by t'Kindt and co-workers [11,12]. We were able to identify 368 putative metabolites (267 at <1 parts per million [ppm] deviation and 101 at the 1–2 ppm deviation level). The compounds identified belong to a wide range of metabolic pathways and include amino acids, nucleosides, carbohydrates, fatty acyls, sterols and glycerophospholipids among others, as shown in Figure 3. The full list of putatively identified metabolites at days 3, 4, 5 and 6 at below 1 ppm and between 1–2 ppm deviation are provided in Tables S1 and S2 of supplementary data, respectively. The majority of the metabolites remained at a relatively constant level. Indeed, the overall sum of intensities of the identified metabolites in the samples from the different days show that there is little apparent variation in the total metabolome identified, with the only difference being between day 3 and day 4 (Figure S1); clearly, however, such data have to be used with caution as not all of the parasite's metabolites are included in the dataset and the method is not fully quantitative. There were, however, some apparent variations within each group of metabolites (Figure S2). Lipids, in general, increased substantially from day 3 to day 6. Carbohydrates and nucleosides similarly apparently increase in abundance, whereas other groups of metabolites including amino acids and derivatives, organic acids and alcohols remain at relatively constant levels.

All metabolites that differed from the mean for the 4-day period by at least a 2-fold on one or more days and were statistically different between the time points analyzed ($p<0.05$) are represented in heatmap format to visualize the main changes that occur during transformation of promastigotes in logarithmic phase to those in stationary phase (Figure 5) and the intensity levels are provided on Table S3. This group (97 in total, 26% of the total number of metabolites putatively identified) includes metabolites representative of all of the compound categories shown in Figure 3 with the exception of organic acids and alcohols. It was possible to distinguish five general patterns by which metabolites fluctuated during the 4-day period analyzed (Figure S3 and Table S3). The levels of some metabolites continually increased from day 3 to day 6 (pattern 1, 74% of the 97 varying metabolites), while the opposite happened with others (pattern 3, 9%). Other metabolites showed peak levels on days 4 or 5 which then declined (pattern 2, 9%), while others decreased from day 3 to day 4 and then increased (pattern 4, 2%). Some metabolites had a fluctuating profile showing an increase followed by a decrease and then another increase (pattern 5, 6%).

A more detailed analysis of each of the categories of metabolites suggests specific variation potentially related with the cell stage. For instance, analysis of structural properties of the fatty acyl side chains of phosphatidylethanolamine (PE) and phosphatidylcholine (PC) lipids revealed that there was an increased abundance of the PC lipids with lower unsaturated fatty acyl chains as the promastigotes developed from day 3 to day 6 (Figure 6 and S4 in supplementary data); this seems also to happen in PE lipids, but less so than with PC lipids. These data suggest that there are changes in the composition of membranes with development from procyclic to metacyclic promastigotes. Another class of metabolites showing striking differences depending on the cell stage were the sphingolipids (SLs). In *Leishmania*, SLs are not essential for growth but they are for differentiation, probably due to the high demand in vesicular trafficking required for parasite remodeling [23]. The abundance of these metabolites in general increased on day 5 and greatly on day 6, such that for some of the SLs identified, such as N-(eicosanoyl)-sphinganine, N-(hexadecanoyl)-sphinganine and heptadecasphinganine, the day 6 intensity amounted to more than 70% of the total amount detected over the four days (Figure 7A). A similar situation was seen with some of the identified glycerolipids, with the diacylglycerol putatively identified as DAG(42:3) being especially increased on day 6 (Figure 7B). The abundance of sterols, prenol lipids and fatty acyl metabolites generally increased during growth and thus were more abundant on days 5 and 6, although there were exceptions such as N-(11Z-eicosaenoyl)-ethanolamine and N-(11Z,14Z-eicosaenoyl)-ethanolamine (Figures S5 and S6).

In contrast to the lipids, amino acids and derivatives in general did not differ greatly during the four day period, although some were less abundant on day 6 (proline, glutamate-semialdehyde, homocysteine, carnitine and cystathionine among others) while others were increased (for example N-butyrylglycine, lysine,

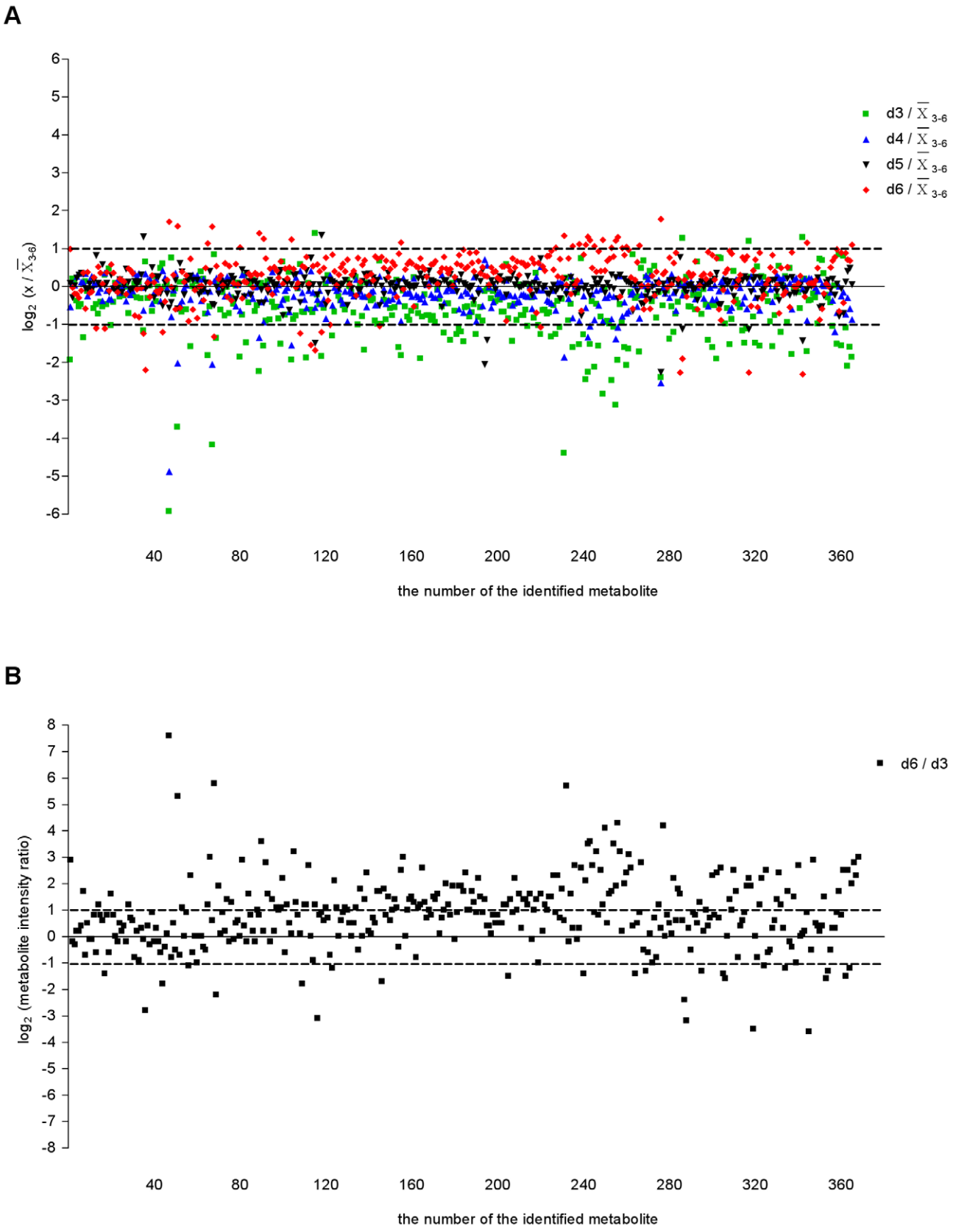

Figure 2. Overview of intracellular metabolite levels in *L. donovani* promastigotes during *in vitro* growth. (A) Relative levels of intracellular metabolites in *L. donovani* promastigotes detected from day 3 to day 6. Metabolite intensity levels on each day were compared with the mean level over the 4-day period. Following a logarithmic transformation (base 2), the relative level of each metabolite was plotted. Dotted lines

represent the fold-change cut-off considered as significantly different between the day analyzed and the mean level of the 4-day period: $\log_2$ (dx/$\overline{X}_{3-6}$) below or above 1 indicates a 2-fold change; dx, time point analyzed (day 3, 4, 5 or 6). The metabolites differing at least by 2-fold on one of the days when compared with the mean were 26.9% of the all of the metabolites identified. (B) Comparison between day 6 (d6) and day 3 (d3) intensity ratios for each identified metabolite. All metabolites within the 2 ppm cut-off are included and following a logarithmic transformation (base 2) the average signal intensity ratios of d6/d3 for all metabolites were plotted. Dotted lines represent the fold-change cut-off in this study for a given metabolite profile being considered to be significantly different between day 6 and day 3: $\log_2$ (metabolite intensity ratio) below −1 or above 1 indicates a 2-fold change between time points compared. The metabolites differing at least by 2-fold between day 6 and day 3 were 48.4% of the total number of metabolites identified.
doi:10.1371/journal.pntd.0001451.g002

valerylglycine, acetyl-lysine, and N-acetyl-arginine) (Table S3 and Figure S7). A higher abundance of carbohydrates, such as maltohexose among others, was observed as cells reach stationary phase (Table S3 and Figure S8). The intensity variation for hypoxanthine and xanthine over the 4 days had a clearly distinct pattern from the other nucleosides or nucleoside conjugates, with a large increase in the abundance of these metabolites on day 6, while, for example, cytosine and deoxycytidine decreased in abundance on day 6 (Table S3 and Figure S9). The great increase in the abundance of hypoxanthine and xanthine at day 6 is responsible for the large change observed in the overall abundance of all metabolites included in this group (Figure S2); the overall abundance of this group was relatively unchanged over the 4 day period of analysis if these two metabolites were not included. None of the metabolites included in the organic acids group accomplish the criteria defined, despite, for example, the statistically significant difference observed in the levels of mevalonate on day 6 (Figure S10). A marked decrease in abundance on day 6 was also observed for 5-methyl-THF, dihydrobiopterin and N-acetylputrescine (Table S3 and Figure S11).

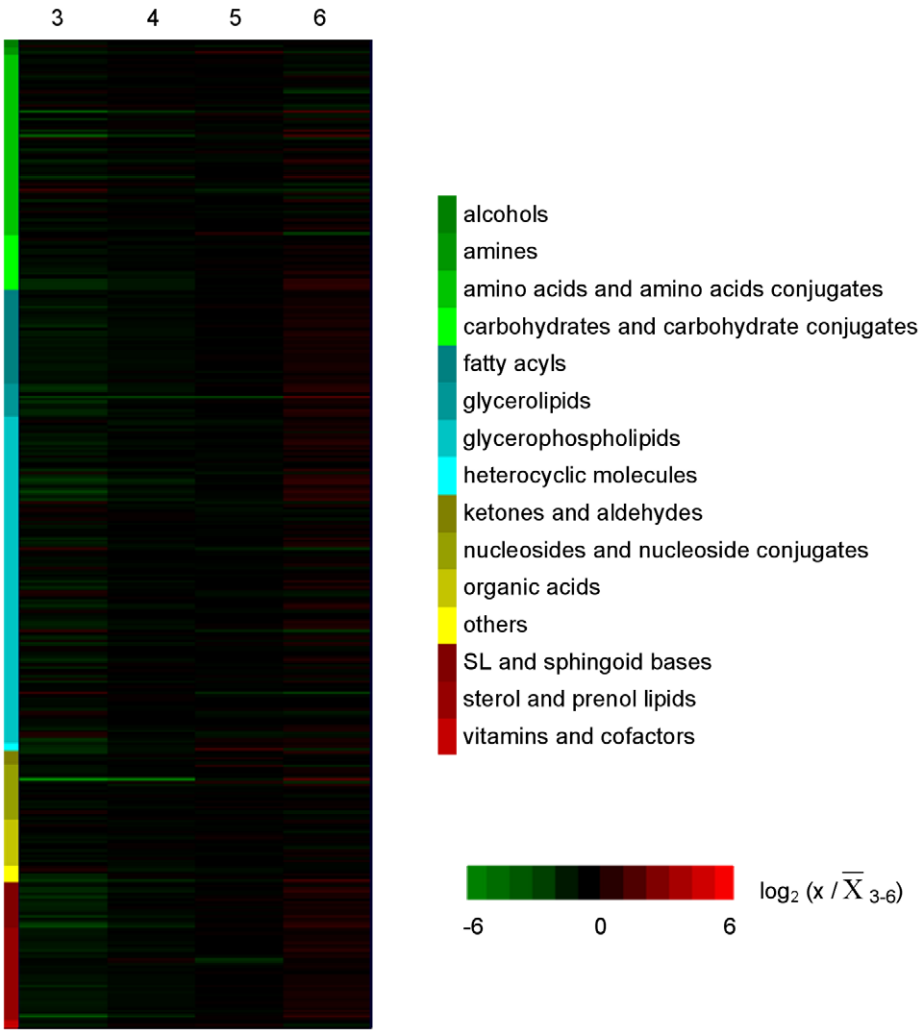

Figure 3. Intracellular metabolic fluctuations during *in vitro* development of *L. donovani* promastigotes. Profiles of all intracellular metabolites identified below 2 ppm deviation in relative levels. Metabolite levels on each day were compared with the mean level over the 4-day period. Following a logarithmic transformation (base 2), the relative level of each metabolite is shown; $\log_2$ (x/$\overline{X}_{3-6}$) below −1 or above 1 indicates a 2-fold change; x, time point analyzed (day 3, 4, 5 or 6). Metabolite profiles are ordered by compound category shown on the left and log values of measurements are color-coded as indicated in the scale on the right of the heat map, from green to red.
doi:10.1371/journal.pntd.0001451.g003

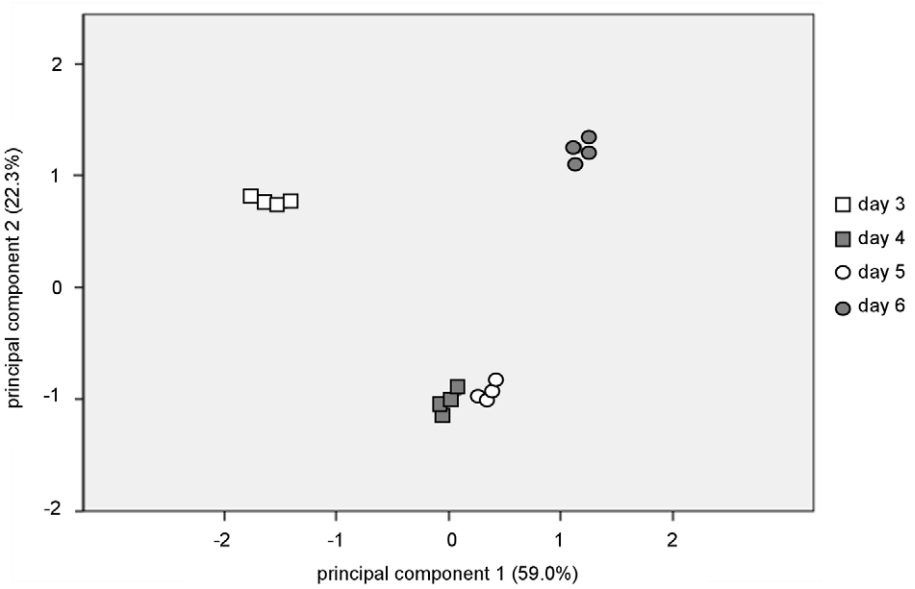

Figure 4. *L. donovani* promastigote development is accompanied by significant changes in the metabolome. Principal component analysis of all metabolites identified by LC-MS in cell extracts from *L. donovani* promastigotes harvested on days 3, 4, 5 and 6 of in vitro growth; each datapoint corresponds to the analysis of one biological replicate. Principal component 1 and principal component 2 explain 59.0% and 22.3% of the total variance, respectively.
doi:10.1371/journal.pntd.0001451.g004

Discussion

Leishmania promastigotes development in the sand fly includes a wide range of modifications in order to prepare the parasite for transmission to a mammalian host. The number of distinct developmental stages that occur is uncertain for although many have been named and identified based on morphology [3,4] most have not been sufficiently characterized to be certain that they are truly distinct developmental stages. As expected, in vitro we were able to observe various morphological forms of *L. donovani* promastigotes but the major clear difference was the appearance of small morphs as the culture reached stationary phase, when metacyclic forms are predominant. This reflects the remodeling of cell shape during life cycle transitions and involved a decrease in protein content (Figure 1). This was taken into consideration in analyzing the metabolite dataset and indeed the data were normalized to protein content as a means of taking into account changes in cell size.

Analysis of metabolome during in vitro growth of promastigotes revealed that whereas the overall metabolite abundance remained relatively constant there were variations in the levels of individual metabolites, suggesting that parasite differentiation from procyclic to metacyclic forms takes place in a progressive manner and involves changes in certain individual or groups of metabolites. This study reinforces the idea that there are multiple forms of promastigotes that are adapted differently at the metabolic level, presumably reflecting the differing challenges that they face naturally in the sand fly. It has been postulated previously from studies on morphology of *Leishmania* promastigotes in sand flies and in vitro cultures that the parasite undergoes similar developmental transitions in vitro as occur in the sand fly host [24], despite the absence of the host pressure. This has been interpreted as the parasite being genetically pre-adapted to survive in the sand fly. The biochemical changes that accompany these morphological/developmental changes are not fully known, although some characteristics of the metacyclic promastigote of *L. major* have been reported. Differentiation to the infective metacyclic promastigote form involves modifications in LPG structure [6,25], which have been shown to occur both in in vitro culture and during in vivo development in the sand fly [26]. HASPB and SHERP are stage-specific proteins present in the infective stages, with SHERP being exclusively present in the metacyclic forms; the stage-specific expression of both has been observed in vitro as well as during the development in the vector [8]. Other surface molecules, including the metallopeptidase GP63, also undergo changes in expression pattern as the promastigotes development progresses [27]. The LPG modifications are essential for parasite infectivity and occur in vitro and in vivo demonstrating that in the absence of the host this essential processes still occurs; these findings are suggestive that other changes similarly also occur in vitro and the data of our current study show that indeed this is the case.

Metacyclogenesis is marked by a great increase in membrane trafficking and remodeling [28] and previous studies have shown that the organization of *Leishmania* membrane differs between procyclic and metacyclic promastigotes, in part due to the distribution of LPG into lipid rafts during differentiation [29]. Phospholipids (PLs) account for ~70% of total cellular lipids in *Leishmania*, with PC, the most abundant glycerophospholipid, predominantly present in a diacyl form [30] with unusually long and unsaturated fatty acid species [31]. These properties, the acyl length and degree of unsaturation, may play an important role in the fluidity of *Leishmania* membrane, thus they are likely to be regulated throughout parasite development in its hosts. Indeed, our data show that promastigote phospholipid composition changed remarkably in terms of the unsaturation levels observed in the fatty acid chains, in particular of PC lipids. Promastigotes in stationary phase (day 6) presented a higher abundance of PC lipids with lower levels of unsaturation than those observed on day 3 (Figure 6), revealing a shift towards lower unsaturation of PC lipids and consequently a decrease in membrane fluidity with metacyclic promastigote generation. These observed changes in membrane

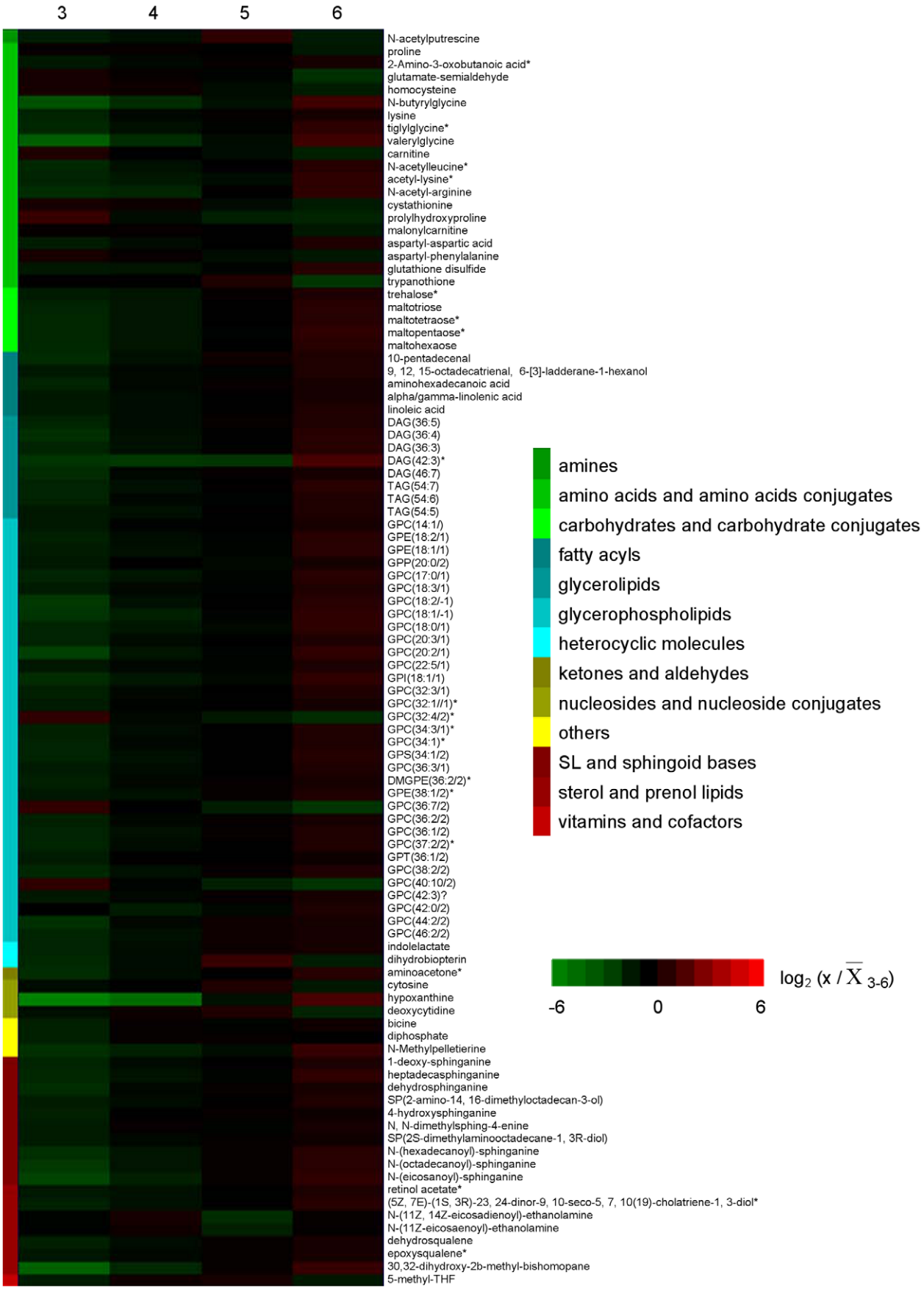
3
4
5
6
N-acetylputrescine
proline
2-Amino-3-oxobutanoic acid*
glutamate-semialdehyde
homocysteine
N-butyrylglycine
lysine
tiglylglycine*
valerylglycine
carnitine
N-acetylleucine*
acetyl-lysine*
N-acetyl-arginine
cystathionine
prolylhydroxyproline
malonylcarnitine
aspartyl-aspartic acid
aspartyl-phenylalanine
glutathione disulfide
trypanothione
trehalose*
maltotriose
maltotetraose*
maltopentaose*
maltohexaose
10-pentadecenal
9, 12, 15-octadecatrienal, 6-[3]-ladderane-1-hexanol
aminohexadecanoic acid
alpha/gamma-linolenic acid
linoleic acid
DAG(36:5)
DAG(36:4)
DAG(36:3)
DAG(42:3)*
DAG(46:7)
TAG(54:7)
TAG(54:6)
TAG(54:5)
GPC(14:1/)
GPE(18:2/1)
GPE(18:1/1)
GPP(20:0/2)
GPC(17:0/1)
GPC(18:3/1)
GPC(18:2/-1)
GPC(18:1/-1)
GPC(18:0/1)
GPC(20:3/1)
GPC(20:2/1)
GPC(22:5/1)
GPI(18:1/1)
GPC(32:3/1)
GPC(32:1//1)*
GPC(32:4/2)*
GPC(34:3/1)*
GPC(34:1)*
GPS(34:1/2)
GPC(36:3/1)
DMGPE(36:2/2)*
GPE(38:1/2)*
GPC(36:7/2)
GPC(36:2/2)
GPC(36:1/2)
GPC(37:2/2)*
GPT(36:1/2)
GPC(38:2/2)
GPC(40:10/2)
GPC(42:3)?
GPC(42:0/2)
GPC(44:2/2)
GPC(46:2/2)
indolelactate
dihydrobiopterin
aminoacetone*
cytosine
hypoxanthine
deoxycytidine
bicine
diphosphate
N-Methylpelletierine
1-deoxy-sphinganine
heptadecasphinganine
dehydrosphinganine
SP(2-amino-14, 16-dimethyloctadecan-3-ol)
4-hydroxysphinganine
N, N-dimethylsphing-4-enine
SP(2S-dimethylaminooctadecane-1, 3R-diol)
N-(hexadecanoyl)-sphinganine
N-(octadecanoyl)-sphinganine
N-(eicosanoyl)-sphinganine
retinol acetate*
(5Z, 7E)-(1S, 3R)-23, 24-dinor-9, 10-seco-5, 7, 10(19)-cholatriene-1, 3-diol*
N-(11Z, 14Z-eicosadienoyl)-ethanolamine
N-(11Z-eicosaenoyl)-ethanolamine
dehydrosqualene
epoxysqualene*
30,32-dihydroxy-2b-methyl-bishomopane
5-methyl-THF
amines
amino acids and amino acids conjugates
carbohydrates and carbohydrate conjugates
fatty acyls
glycerolipids
glycerophospholipids
heterocyclic molecules
ketones and aldehydes
nucleosides and nucleoside conjugates
others
SL and sphingoid bases
sterol and prenol lipids
vitamins and cofactors
-6
0
6
log2 (x / X 3-6)

Figure 5. Heatmap depicting significant fluctuations in *L. donovani* promastigotes intracellular metabolome during *in vitro* development. Profiles over 4 days of intracellular metabolites that differed at least by 2-fold from the mean levels in at least one of the time points analyzed. Metabolite intensity levels on each day were compared with the mean level over the 4 day period. Following a logarithmic transformation (base 2), the relative level of each metabolite is shown; $\log_2 (x/\overline{X}_{3-6})$ below −1 or above 1 indicates a 2-fold change; x, time point analyzed (day 3, 4, 5 or 6). Metabolites labelled with * represent peaks with multiple potential identifications, for which just one is shown in this figure but the full list is given in the Supporting Information; metabolite profiles are ordered by compound category shown on the left and log values of ratios are color-coded as indicated in the scale on the right of the heat map, from green to red.
doi:10.1371/journal.pntd.0001451.g005

fluidity may be a mechanism whereby the parasite becomes pre-adapted for survival upon infecting a mammalian host, at which time it is confronted by a dramatic increase in temperature. Thus perhaps the change in membrane composition enables the parasite to maintain an appropriate membrane fluidity even at the higher temperature encountered. It is well known that the well-being of organisms is dependent upon the maintenance of optimal level of membrane fluidity [32]. In yeast, changes in the degree of unsaturation of fatty acids has been reported as a response to changes in the environmental temperature and complements other mechanisms such as modifications in fatty acid chain length, branching and cellular fatty acid content [33]. A recent study by Turk and co-workers [34] have related membrane fluidity to the adaptation level of different yeast to environmental stresses and to their growth temperature range, demonstrating that plasma-membrane fluidity can be used as an indicator of fitness for survival in extreme environments [34]. Changes in membrane fluidity in plants was also suggested to be crucial in sensing and influencing gene expression during temperatures fluctuations [35]. Alterations in membrane fluidity have been associated with the occurrence of drug resistance in *Leishmania*; it is thought that membrane lipid composition may influence drug-membrane interactions and interfere with drug uptake by the amastigotes residing in the mammalian host [36–38]. Indeed, comparison of promastigotes derived from clinical *L. donovani* isolates with different antimonial sensitivity has shown a shift towards higher unsaturation of PC lipids in drug-resistant clones, suggesting an increase in membrane fluidity that may be related to the changes in uptake ability observed in the drug-resistant cell lines [12].

Another group of lipids that notably increased in abundance during *L. donovani* promastigotes development in vitro were the SLs (Figure 7A). SLs are not required for growth of *Leishmania*, since parasites that completely lack SLs grew normally in logarithmic phase and were still able to make "lipid rafts". However, deletion of *spt2-*, the gene that encodes the key de novo biosynthetic enzyme serine palmitoyltransferase subunit 2, resulted in parasites deficient in de novo SLs synthesis that once in the stationary phase were not able to differentiate into metacyclic forms [23]. The increase in SLs during stationary phase we have found in this study is consistent with the requirement of these metabolites for differentiation to metacyclic froms. SLs are considered essential membrane components in all eukaryotes, mediating many signaling pathways including those key for apoptosis, growth and differentiation [39]. However, in *Leishmania* the primary role of SLs appears to be the provision of ethanolamine, as ethanolamine supplementation was able to overcome the phenotype observed in the SL-deficient mutant parasites [40]. Ethanolamine and choline are essential nutrients, and when available exogenously they can be salvaged by *Leishmania* via membrane transporters [41,42]. Thus the significance of SL biosynthesis is likely to be stage-specific, being important in those stages in the sand fly that cannot rely upon salvaged ethanolamine. Indeed, amastigotes deficient in de novo SLs synthesis recovered from a mammalian host showed normal levels of inositolphosphoryl ceramide (IPC) and thus amastigotes seems to be able to perform SLs salvage [43].

Glycerolipids, represented by diacylglycerols (DAG) and triacylglycerols (TAG), also increased in abundance as *L. donovani* promastigote development progressed (Figure 7B). PC and PE lipids are synthesized by conjugation of a lipid anchor such as DAG with either CDP-choline or CDP-ethanolamine, the last step of the in de novo biosynthesis of phospholipids (the Kennedy pathway) (reviewed in [44]). Thus the observed increase in neutral lipids correlates well with the changes observed in *Leishmania* membrane lipid composition during promastigote development.

Sterol and prenol lipids also increased with time in culture, although the changes during *L. donovani* promastigotes development were not so accentuated as for SLs and glycerolipids. Sterols are the target of the important antileishmanial drug amphotericin B [36] and they may also play a significant role in the activity of miltefosine against the parasite, as sterol depletion led to a decrease in susceptibility [45]. Effectiveness of these drugs is mainly dependent on their interaction with the *Leishmania* membrane, thus it is clear that the ability of the parasite to change its lipid membrane composition, which occurs inherent during its life cycle, should be taken into consideration when considering new drug formulations.

Leishmania parasites are auxotrophic for many amino acids and must scavenge essential amino acids from their hosts. Besides the use in protein biosynthesis, some amino acids, notably proline, can be used as major energy sources [46]. Recently, Saunders and co-workers have reported that aspartate, alanine and glutamate are internalized by *L. mexicana* promastigotes and incorporated into the TCA cycle, revealing the importance of this pathway in glutamate, glutamine and proline synthesis and demonstrating that the TCA cycle in *Leishmania* is not only a catabolic pathway [47]. One notable feature in the levels of amino acids and amino acid conjugates during growth of promastigotes in vitro was a large increase in metabolites of fatty acids named acyl glycines (valerylglycine, tiglyglycine, N-butyrylglycine). Increases in levels of acyl glycines in higher eukaryotes is associated with mitochondrial energy metabolism disorders, indeed the measurement of these metabolites is used as a diagnostic tool. Glycine conjugation is considered to be an important detoxification system, preventing the accumulation of acyl-CoA esters in several inherited metabolic disorders of humans [48]. Moreover, valerylglycine was found to be increased in urine of *Plasmodium vivax*-infected individuals, which indicates an alteration in the fatty acid metabolism during infection [49]. These changes in acylglycines abundance during promastigote development could reflect changes in mitochondrial metabolism, but caution needs to be exercised as increased levels of this group of compounds was also found in drug-resistant parasites [12] and also in genetically manipulated mutants (A.M. Silva et al., unpublished results) – which indicates that the levels of these metabolites may be disturbed in a variety of situations.

Leishmania also take up from their environment other essential nutrients, such as purines and growth factors. Biopterin and folate uptake has been shown to decrease when promastigote have entered stationary phase [50], which is consistent with our findings that there was a decrease in abundance of 5-methyl-THF and dihydrobiopterin in *L. donovani* promastigotes at day 6 of in vitro growth. Indeed, low levels of tetrahydrobiopterin were associated

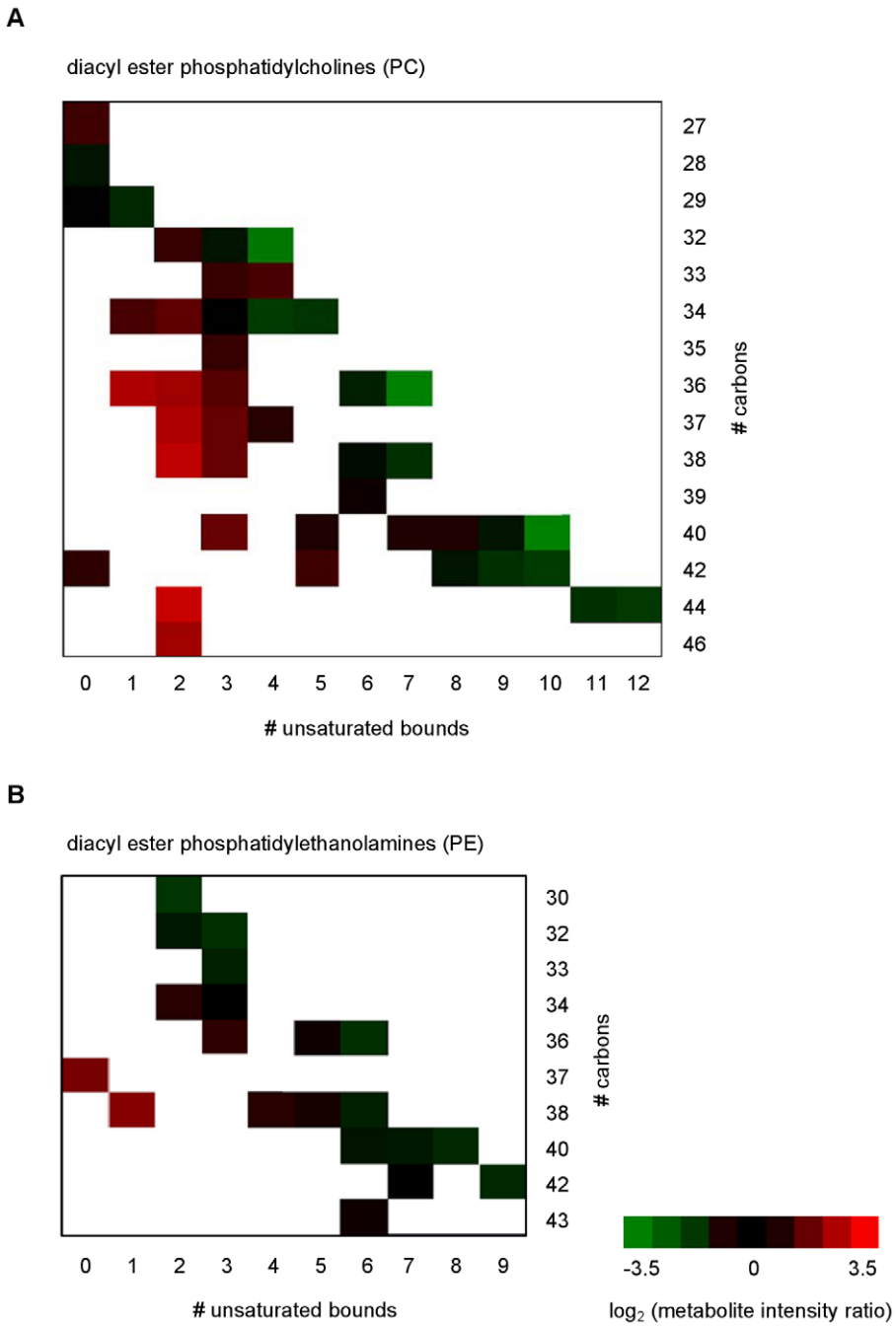

Figure 6. Comparative analysis of phosphatidylcholines and phosphatidylethanolamines in *L. donovani* promastigotes on days 3 and 6. Fatty acyl structure properties in (A) phosphatidylcholines (PC) and (B) phosphatidylethanolamines (PE) for each phospholipid detected on day 6 and day 3. The x-axis shows the total number of unsaturated bonds present in the 2 fatty acyl chains, while the y-axis shows the length of the fatty acyl chains in total number of carbon units. Data are shown as ratios of signal intensity, day 6/day 3, after a logarithmic transformation (base 2) and represented by a color code as indicated in the scale on the right of the heat map, from green to red, where green represents a decrease and a red an increase in abundance of the given phospholipid on day 6.
doi:10.1371/journal.pntd.0001451.g006

with increased differentiation of *L. major* into the infective metacyclic form and thus postulated to be an important factor controlling this process [51]. *Leishmania* parasites are not able to synthesize purines de novo and need to acquire either nucleosides or nucleobases [52]. Hypoxanthine uptake by *L. major* promastigotes is greatly reduced in stationary phase compared with logarithmic growth phase. This was shown to correlate with down-regulation of expression of the NT3 permease as promastigotes reach stationary phase [53] and it was reasoned that these changes reflected the fact that at this stage the population is mainly composed by non-dividing cells, the metacyclic promastigotes, that do not require purines for mitosis. Our findings of an increase in the levels of hypoxanthine and xanthine at day 6 of *L. donovani* promastigotes in vitro growth

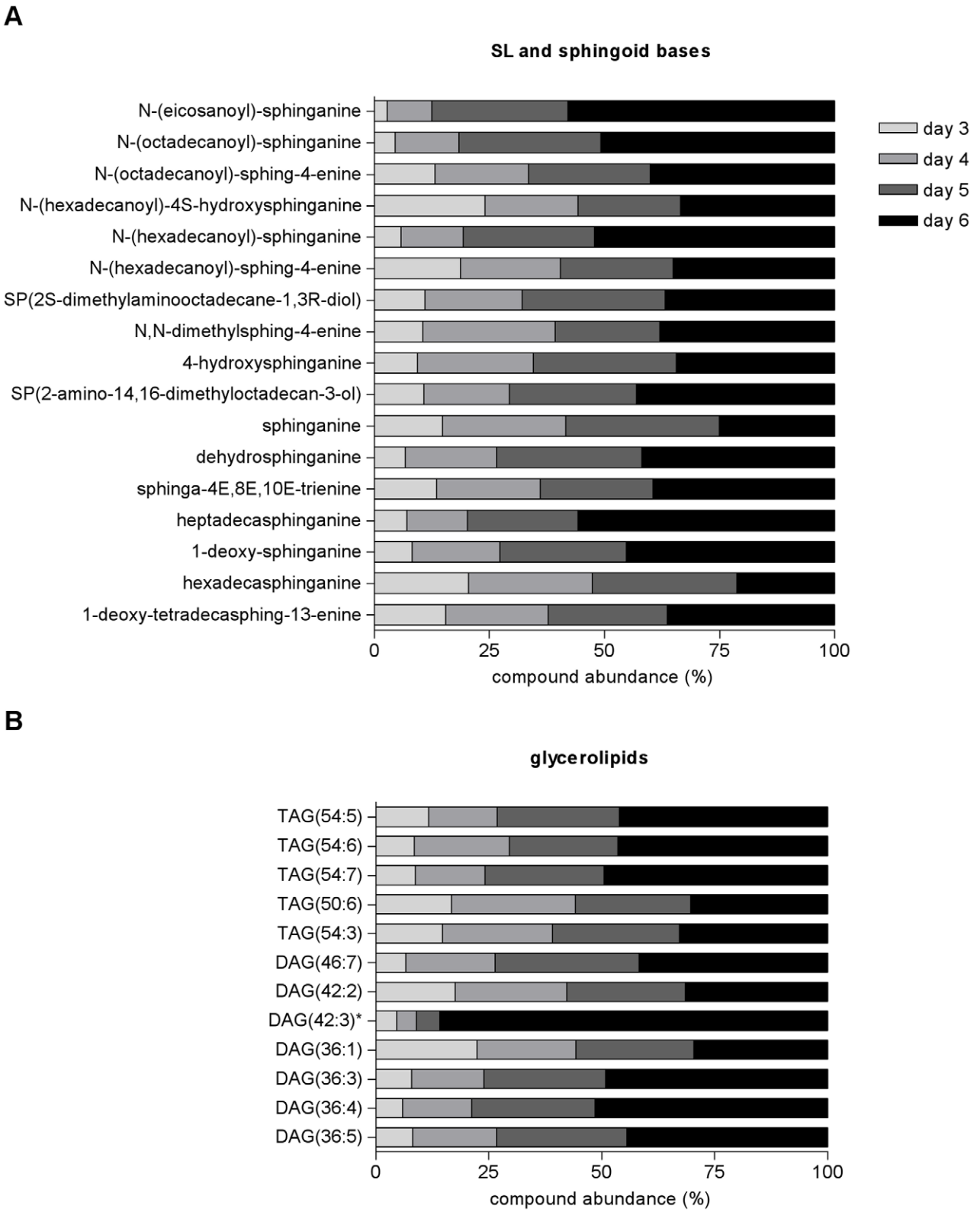

Figure 7. Stage specific increase of sphingolipids and glycerolipids abundance during *L. donovani* promastigotes development *in vitro*. (A) Sphingolipids and sphingoid base and (B) glycerolipid metabolites abundance is represented for each day as a percentage of the total abundance detected, which comprises the sum of the total metabolite intensity on each of the 4 days analysed. Metabolites labelled with * represent peaks with multiple potential identifications, for which just one is shown in this figure but the full list is given in the Supporting Information. DAG, diacylglycerol; TAG, triacylglycerol.
doi:10.1371/journal.pntd.0001451.g007

explain why less uptake is required at this stage. Moreover, one can speculate that these higher levels in the metacyclic forms are beneficial in enabling the subsequent differentiation events after infection of a mammal, a transition phase that occurs in the parasitophorous vacuole of a macrophage where availability of some nutrients may be limiting [54,55].

Overall the results of this study have provided convincing data that promastigotes of *Leishmania* at different stages of culture in vitro differ from each other significantly in terms of the composition of their metabolome, whereas the total metabolite abundance appears to remain relatively constant as the promastigotes develop from day 3 to day 6. The study has provided insights into the overall changes that occur, which adds to the many previous reports on changes in individual metabolites, groups of metabolites and enzymatic reactions involved in metabolite production (see, for example, [16,46,56–58]). Our data are consistent in particular with previous findings obtained using other approaches, such as changes observed in the content of sphingolipids and other lipids that may contribute to successful parasite survival in the mammalian host [23,57]. These changes observed undoubtedly reflect adaptations to differing conditions that *Leishmania* encounters in its two hosts, but the full understanding of how these adaptations function require additional data on the environments themselves (the detailed content of the parasitophorous vacuole in a macrophage and the intestinal tract of the sand fly, and how these change with time, are largely unknown) as well as more complete analyses of metabolism of individual promastigote forms and if possible integration of the generated data with those arising from other –omics approaches. However, understanding the variation in metabolism of promastigotes will be informative in elucidating more fully the metabolic capabilities of *Leishmania* and hopefully highlight unusual features that can be exploited in novel approaches to designing therapies.

Supporting Information

Figure S1 Overall metabolite levels remain similar during *L. donovani* promastigotes development *in vitro*. Sum of total metabolite intensities from *L. donovani* promastigotes identified by LC-MS analysis at days 3, 4, 5 or 6 of in vitro growth.
(PDF)

Figure S2 Overall metabolite levels for each compound category during *L. donovani* promastigotes development *in vitro*. Sum of total metabolite intensities from *L. donovani* promastigotes identified by LC-MS analysis at days 3, 4, 5 or 6 of in vitro growth grouped by compound categories.
(PDF)

Figure S3 Patterns of metabolite variation in level during *L. donovani* promastigote *in vitro* growth from day 3 to day 6. Analysis of *L. donovani* promastigotes metabolome at day 3, 4, 5 and 6 allowed the distinction of 5 patterns (1–5) based on the metabolic profile for each metabolite that differed in intensity by 2-fold or more from the mean levels in at least one of the time points analyzed (a total of 97 metabolites). The relative level of each metabolite is shown, following logarithmic transformation (base 2); $\log_2 (x/\overline{X}_{3-6})$ below −1 or above 1 indicates a 2-fold change; x, time point analyzed (day 3, 4, 5 or 6). (A) Pattern 1 (74% of all metabolites considered) and (C) pattern 3 (9%) include metabolites that increased or decreased, respectively, continuously during all the whole period analyzed; (B) pattern 2 (9%) include metabolites which had peak levels on days 4 or 5 but which then declined; (D) pattern 4 (2%) metabolite levels decreased from day 3 to day 4 and then increased and (E) pattern 5 (6%) include metabolites that showed an increase followed by a decrease and then another increase.
(PDF)

Figure S4 Glycerophospholipids abundance during *L. donovani* promastigotes development *in vitro*. Glycerophospholipids abundance is represented for each metabolite on each day as a percentage of the total abundance detected, which comprises the sum of the total metabolite intensity during the 4-day period of analysis.
(PDF)

Figure S5 Sterol and prenol lipids abundance during *L. donovani* promastigotes development *in vitro*. Sterol and prenol lipids abundance is represented for each metabolite on each day as a percentage of the total abundance detected, which comprises the sum of the total metabolite intensity during the 4-day period of analysis. Metabolites labelled with * represent peaks with multiple potential identifications, for which just one is shown in this figure but the full list is given in Tables S1 and S2.
(PDF)

Figure S6 Fatty acyls abundance during *L. donovani* promastigotes development *in vitro*. Fatty acyls abundance is represented for each metabolite on each day as a percentage of the total abundance detected, which comprises the sum of the total metabolite intensity during the 4-day period of analysis. Metabolites labelled with * represent peaks with multiple potential identifications, for which just one is shown in this figure but the full list is given in Tables S1 and S2.
(PDF)

Figure S7 Amino acids and amino acids conjugates abundance during *L. donovani* promastigotes development *in vitro*. Amino acids and amino acids conjugates abundance is represented for each metabolite on each day as a percentage of the total abundance detected, which comprises the sum of the total metabolite intensity during the 4-day period of analysis. Metabolites labelled with * represent peaks with multiple potential identifications, for which just one is shown in this figure but the full list is given in Tables S1 and S2.
(PDF)

Figure S8 Carbohydrates and carbohydrate conjugates abundance during *L. donovani* promastigotes development *in vitro*. Carbohydrates and carbohydrate conjugates abundance is represented for each metabolite on each day as a percentage of the total abundance detected, which comprises the sum of the total metabolite intensity during the 4-day period of analysis. Metabolites labelled with * represent peaks with multiple potential identifications, for which just one is shown in this figure but the full list is given in Tables S1 and S2.
(PDF)

Figure S9 Nucleosides and nucleoside conjugates abundance during *L. donovani* promastigotes development *in vitro*. Nucleosides and nucleoside conjugate metabolites abundance is represented for each metabolite on each day as a percentage of the total abundance detected, which comprises the sum of the total metabolite intensity during the 4-day period of analysis. Metabolites labelled with * represent peaks with multiple potential identifications, for which just one is shown in this figure but the full list is given in Tables S1 and S2.
(PDF)

Figure S10 Organic acids abundance during *L. donovani* promastigotes development *in vitro*. Organic acids abundance is represented for each metabolite on each day as a

percentage of the total abundance detected, which comprises the sum of the total metabolite intensity during the 4-day period of analysis. Metabolites labelled with * represent peaks with multiple potential identifications, for which just one is shown in this figure but the full list is given in Tables S1 and S2.
(PDF)

Figure S11 Vitamins and cofactors, ketones and aldehydes, heterocyclic molecules, amines and alcohols abundance during *L. donovani* promastigotes development *in vitro*. Vitamins and cofactors, ketones and aldehydes, heterocyclic molecules, amines and alcohols abundance is represented for each metabolite on each day as a percentage of the total abundance detected, which comprises the sum of the total metabolite intensity during the 4-day period of analysis. Metabolites labelled with * represent peaks with multiple potential identifications, for which just one is shown in this figure but the full list is given in Tables S1 and S2.
(PDF)

Table S1 Metabolites identified below 1 ppm deviation in samples of *L. donovani* promastigotes from day 3 to day 6 of *in vitro* growth. For each compound the following information is shown: ionisation (ESI) mode; detected mass; retention time (min); putative metabolite identification; ppm deviation between detected mass and theoretical mass of the putative metabolite identified; intensity per 25 μg cell protein for each sample; average intensity per 25 μg cell protein in each time-point analyzed (3D, 4D, 5D or 6D); standard deviation in each time point analyzed; log base 2 of ratio of the average signal intensity in each time point against the mean intensity level during the 4 day period; F test statistics and p values obtained by analysis of variance (ANOVA), indicating whether or not there was a statistically significant difference between the time points analyzed; decision on whether or not the compound was significantly changed in level based on a two-fold or higher average difference in signal intensity in at least one of the time points analyzed and statistical significance ($p<0.05$); compound category.
(XLS)

Table S2 Metabolites identified between 1–2 ppm deviation in samples of *L. donovani* promastigotes from day 3 to day 6 of *in vitro* growth. The data presented are as described for Table S1.
(XLS)

Table S3 Intensity levels of metabolites that differ significantly during *L. donovani* promastigote development *in vitro*. Metabolites are ordered by compound category; for each metabolite is shown the average intensity per 25 μg cell protein at days 3, 4, 5 and 6 and the respective metabolic profile pattern (analysis shown in Figure S2). Metabolites labelled with * represent peaks with multiple potential identifications, for which just one is shown in this figure but the full list is given in Table S1 and S2.
(PDF)

Acknowledgments

We thank: Malcolm McConville and colleagues (Melbourne) for excellent guidance on the methods of sample preparation for the metabolomics analyses; Ruben t'Kindt (ITM, Antwerp, and Strathclyde) for assistance with the sample preparation method for the metabolomics analyses; Dave G. Watson and Alex Zhang (Strathclyde) for help with the LC-MS technology.

Author Contributions

Conceived and designed the experiments: AMS AC GHC. Performed the experiments: AMS. Analyzed the data: AMS GHC. Wrote the paper: AMS AC GHC.

References

1. Kedzierski L (2010) Leishmaniasis Vaccine: Where are We Today? J Glob Infect Dis 2: 177–185.
2. Croft SL, Sundar S, Fairlamb AH (2006) Drug resistance in leishmaniasis. Clin Microbiol Rev 19: 111–126.
3. Gossage SM, Rogers ME, Bates PA (2003) Two separate growth phases during the development of Leishmania in sand flies: implications for understanding the life cycle. Int J Parasitol 33: 1027–1034.
4. Kamhawi S (2006) Phlebotomine sand flies and Leishmania parasites: friends or foes? Trends Parasitol 22: 439–445.
5. McConville MJ, Blackwell JM (1991) Developmental changes in the glycosylated phosphatidylinositols of Leishmania donovani. Characterization of the promastigote and amastigote glycolipids. J Biol Chem 266: 15170–15179.
6. McConville MJ, Turco SJ, Ferguson MA, Sacks DL (1992) Developmental modification of lipophosphoglycan during the differentiation of Leishmania major promastigotes to an infectious stage. EMBO J 11: 3593–3600.
7. Sacks DL, Pimenta PF, McConville MJ, Schneider P, Turco SJ (1995) Stage-specific binding of Leishmania donovani to the sand fly vector midgut is regulated by conformational changes in the abundant surface lipophosphoglycan. J Exp Med 181: 685–697.
8. Sadlova J, Price HP, Smith BA, Votypka J, Volf P, et al. (2010) The stage-regulated HASPB and SHERP proteins are essential for differentiation of the protozoan parasite Leishmania major in its sand fly vector, Phlebotomus papatasi. Cell Microbiol 12: 1765–1779.
9. Burchmore RJ, Barrett MP (2001) Life in vacuoles–nutrient acquisition by Leishmania amastigotes. Int J Parasitol 31: 1311–1320.
10. De Souza DP, Saunders EC, McConville MJ, Likic VA (2006) Progressive peak clustering in GC-MS Metabolomic experiments applied to Leishmania parasites. Bioinformatics 22: 1391–1396.
11. t'Kindt R, Jankevics A, Scheltema RA, Zheng L, Watson DG, et al. (2010) Towards an unbiased metabolic profiling of protozoan parasites: optimisation of a Leishmania sampling protocol for HILIC-orbitrap analysis. Anal Bioanal Chem 398: 2059–2069.
12. t'Kindt R, Scheltema RA, Jankevics A, Brunker K, Rijal S, et al. (2010) Metabolomics to unveil and understand phenotypic diversity between pathogen populations. PLoS Negl Trop Dis 4: e904.
13. Saunders EC, Ng WW, Chamber JM, Ng M, Naderer T, et al. (2011) Isoptopomer profiling of Leishmania mexicana promastigotes reveals important roles for succinate fermentation and aspartate uptake in TCA cycle anaplerosis, glutamate synthesis and growth. J Biol Chem.
14. Naderer T, Heng J. McConville MJ Evidence that intracellular stages of Leishmania major utilize amino sugars as a major carbon source. PLoS Pathog 6: e1001245.
15. McConville MJ, Naderer T (2011) Metabolic Pathways Required for the Intracellular Survival of Leishmania. Annu Rev Microbiol.
16. Saunders EC, DP DES, Naderer T, Sernee MF, Ralton JE, et al. Central carbon metabolism of Leishmania parasites. Parasitology 137: 1303–1313.
17. Rogers ME, Chance ML, Bates PA (2002) The role of promastigote secretory gel in the origin and transmission of the infective stage of Leishmania mexicana by the sandfly Lutzomyia longipalpis. Parasitology 124: 495–507.
18. Davies CR, Cooper AM, Peacock C, Lane RP, Blackwell JM (1990) Expression of LPG and GP63 by different developmental stages of Leishmania major in the sandfly Phlebotomus papatasi. Parasitology 101 Pt 3: 337–343.
19. Schneider P, Rosat JP, Bouvier J, Louis J, Bordier C (1992) Leishmania major: differential regulation of the surface metalloprotease in amastigote and promastigote stages. Exp Parasitol 75: 196–206.
20. Pimenta PF, Saraiva EM, Sacks DL (1991) The comparative fine structure and surface glycoconjugate expression of three life stages of Leishmania major. Exp Parasitol 72: 191–204.
21. Rijal S, Yardley V, Chappuis F, Decuypere S, Khanal B, et al. (2007) Antimonial treatment of visceral leishmaniasis: are current in vitro susceptibility assays adequate for prognosis of in vivo therapy outcome? Microbes Infect 9: 529–535.
22. Wishart DS (2010) Computational approaches to metabolomics. Methods Mol Biol 593: 283–313.
23. Zhang K, Showalter M, Revollo J, Hsu FF, Turk J, et al. (2003) Sphingolipids are essential for differentiation but not growth in Leishmania. EMBO J 22: 6016–6026.
24. Bates PA, Rogers ME (2004) New insights into the developmental biology and transmission mechanisms of Leishmania. Curr Mol Med 4: 601–609.
25. Sacks DL, Brodin TN, Turco SJ (1990) Developmental modification of the lipophosphoglycan from Leishmania major promastigotes during metacyclogenesis. Mol Biochem Parasitol 42: 225–233.

26. Saraiva EM, Pimenta PF, Brodin TN, Rowton E, Modi GB, et al. (1995) Changes in lipophosphoglycan and gene expression associated with the development of Leishmania major in Phlebotomus papatasi. Parasitology 111(Pt 3): 275–287.
27. Yao C, Donelson JE, Wilson ME (2003) The major surface protease (MSP or GP63) of Leishmania sp. Biosynthesis, regulation of expression, and function. Mol Biochem Parasitol 132: 1–16.
28. Besteiro S, Williams RA, Morrison LS, Coombs GH, Mottram JC (2006) Endosome sorting and autophagy are essential for differentiation and virulence of Leishmania major. J Biol Chem 281: 11384–11396.
29. Denny PW, Smith DF (2004) Rafts and sphingolipid biosynthesis in the kinetoplastid parasitic protozoa. Mol Microbiol 53: 725–733.
30. Wassef MK, Fioretti TB, Dwyer DM (1985) Lipid analyses of isolated surface membranes of Leishmania donovani promastigotes. Lipids 20: 108–115.
31. Zufferey R, Allen S, Barron T, Sullivan DR, Denny PW, et al. (2003) Ether phospholipids and glycosylinositolphospholipids are not required for amastigote virulence or for inhibition of macrophage activation by Leishmania major. J Biol Chem 278: 44708–44718.
32. Beney L, Gervais P (2001) Influence of the fluidity of the membrane on the response of microorganisms to environmental stresses. Appl Microbiol Biotechnol 57: 34–42.
33. Suutari M, Liukkonen K, Laakso S (1990) Temperature adaptation in yeasts: the role of fatty acids. J Gen Microbiol 136: 1469–1474.
34. Turk M, Plemenitas A, Gunde-Cimerman N (2011) Extremophilic yeasts: plasma-membrane fluidity as determinant of stress tolerance. Fungal Biol 115: 950–958.
35. Wahid A, Gelani S, Ashraf M, Foolad MR (2007) Heat tolerance in plants: An overview. Environmental and Experimental Botan 61: 199–223.
36. Mbongo N, Loiseau PM, Billion MA, Robert-Gero M (1998) Mechanism of amphotericin B resistance in Leishmania donovani promastigotes. Antimicrob Agents Chemother 42: 352–357.
37. Cauchetier E, Loiseau PM, Lehman J, Rivollet D, Fleury J, et al. (2002) Characterisation of atovaquone resistance in Leishmania infantum promastigotes. Int J Parasitol 32: 1043–1051.
38. Rakotomanga M, Saint-Pierre-Chazalet M, Loiseau PM (2005) Alteration of fatty acid and sterol metabolism in miltefosine-resistant Leishmania donovani promastigotes and consequences for drug-membrane interactions. Antimicrob Agents Chemother 49: 2677–2686.
39. Hannun YA, Obeid LM (2008) Principles of bioactive lipid signalling: lessons from sphingolipids. Nat Rev Mol Cell Biol 9: 139–150.
40. Zhang K, Pompey JM, Hsu FF, Key P, Bandhuvula P, et al. (2007) Redirection of sphingolipid metabolism toward de novo synthesis of ethanolamine in Leishmania. EMBO J 26: 1094–1104.
41. Zufferey R, Mamoun CB (2002) Choline transport in Leishmania major promastigotes and its inhibition by choline and phosphocholine analogs. Mol Biochem Parasitol 125: 127–134.
42. Rifkin MR, Fairlamb AH (1985) Transport of ethanolamine and its incorporation into the variant surface glycoprotein of bloodstream forms of Trypanosoma brucei. Mol Biochem Parasitol 15: 245–256.
43. Zhang K, Hsu FF, Scott DA, Docampo R, Turk J, et al. (2005) Leishmania salvage and remodelling of host sphingolipids in amastigote survival and acidocalcisome biogenesis. Mol Microbiol 55: 1566–1578.
44. Gibellini F, Smith TK. The Kennedy pathway–De novo synthesis of phosphatidylethanolamine and phosphatidylcholine. IUBMB Life 62: 414–428.
45. Saint-Pierre-Chazalet M, Ben Brahim M, Le Moyec L, Bories C, Rakotomanga M, et al. (2009) Membrane sterol depletion impairs miltefosine action in wild-type and miltefosine-resistant Leishmania donovani promastigotes. J Antimicrob Chemother 64: 993–1001.
46. Opperdoes FR, Coombs GH (2007) Metabolism of Leishmania: proven and predicted. Trends Parasitol 23: 149–158.
47. Saunders EC, Ng WW, Chamber JM, Ng M, Naderer T, et al. Isoptopomer profiling of Leishmania mexicana promastigotes reveals important roles for succinate fermentation and aspartate uptake in TCA cycle anaplerosis, glutamate synthesis and growth. J Biol Chem.
48. Bonafe L, Troxler H, Kuster T, Heizmann CW, Chamoles NA, et al. (2000) Evaluation of urinary acylglycines by electrospray tandem mass spectrometry in mitochondrial energy metabolism defects and organic acidurias. Mol Genet Metab 69: 302–311.
49. Sengupta A (2010) A Urine IH NMR based Metabonomic Approach to Understand the Host Metabolic Response towards Plasmodium vivax Infection. Proceedings of 2010 International Conference on Systems in Medicine and Biology.
50. Cunningham ML, Beverley SM (2001) Pteridine salvage throughout the Leishmania infectious cycle: implications for antifolate chemotherapy. Mol Biochem Parasitol 113: 199–213.
51. Cunningham ML, Titus RG, Turco SJ, Beverley SM (2001) Regulation of differentiation to the infective stage of the protozoan parasite Leishmania major by tetrahydrobiopterin. Science 292: 285–287.
52. Landfear SM, Ullman B, Carter NS, Sanchez MA (2004) Nucleoside and nucleobase transporters in parasitic protozoa. Eukaryot Cell 3: 245–254.
53. Ortiz D, Sanchez MA, Pierce S, Herrmann T, Kimblin N, et al. (2007) Molecular genetic analysis of purine nucleobase transport in Leishmania major. Mol Microbiol 64: 1228–1243.
54. Naderer T, McConville MJ (2008) The Leishmania-macrophage interaction: a metabolic perspective. Cell Microbiol 10: 301–308.
55. McConville MJ, de Souza D, Saunders E, Likic VA, Naderer T (2007) Living in a phagolysosome; metabolism of Leishmania amastigotes. Trends Parasitol 23: 368–375.
56. Rosenzweig D, Smith D, Opperdoes F, Stern S, Olafson RW, et al. (2008) Retooling Leishmania metabolism: from sand fly gut to human macrophage. FASEB J 22: 590–602.
57. Zhang K, Beverley SM (2010) Phospholipid and sphingolipid metabolism in Leishmania. Mol Biochem Parasitol 170: 55–64.
58. Colotti G, Ilari A (2011) Polyamine metabolism in Leishmania: from arginine to trypanothione. Amino Acids 40: 269–285.

Supporting Information

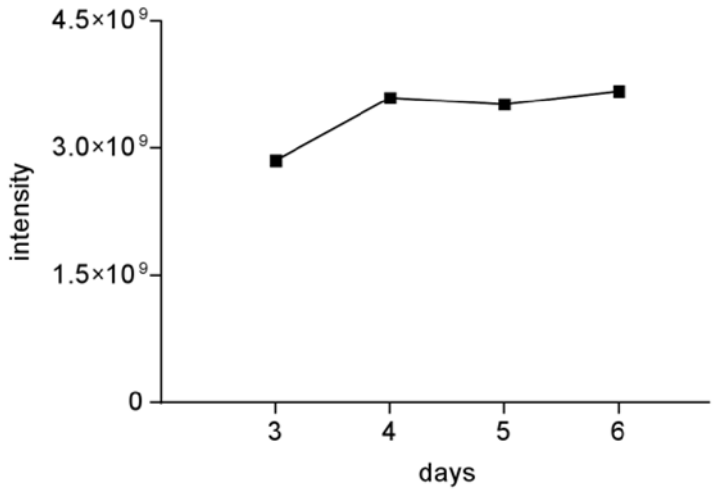

Figure S1. Overall metabolite levels remain similar during *L. donovani* promastigotes development *in vitro*. Sum of total metabolite intensities from *L. donovani* promastigotes identified by LC-MS analysis at days 3, 4, 5 or 6 of *in vitro* growth.

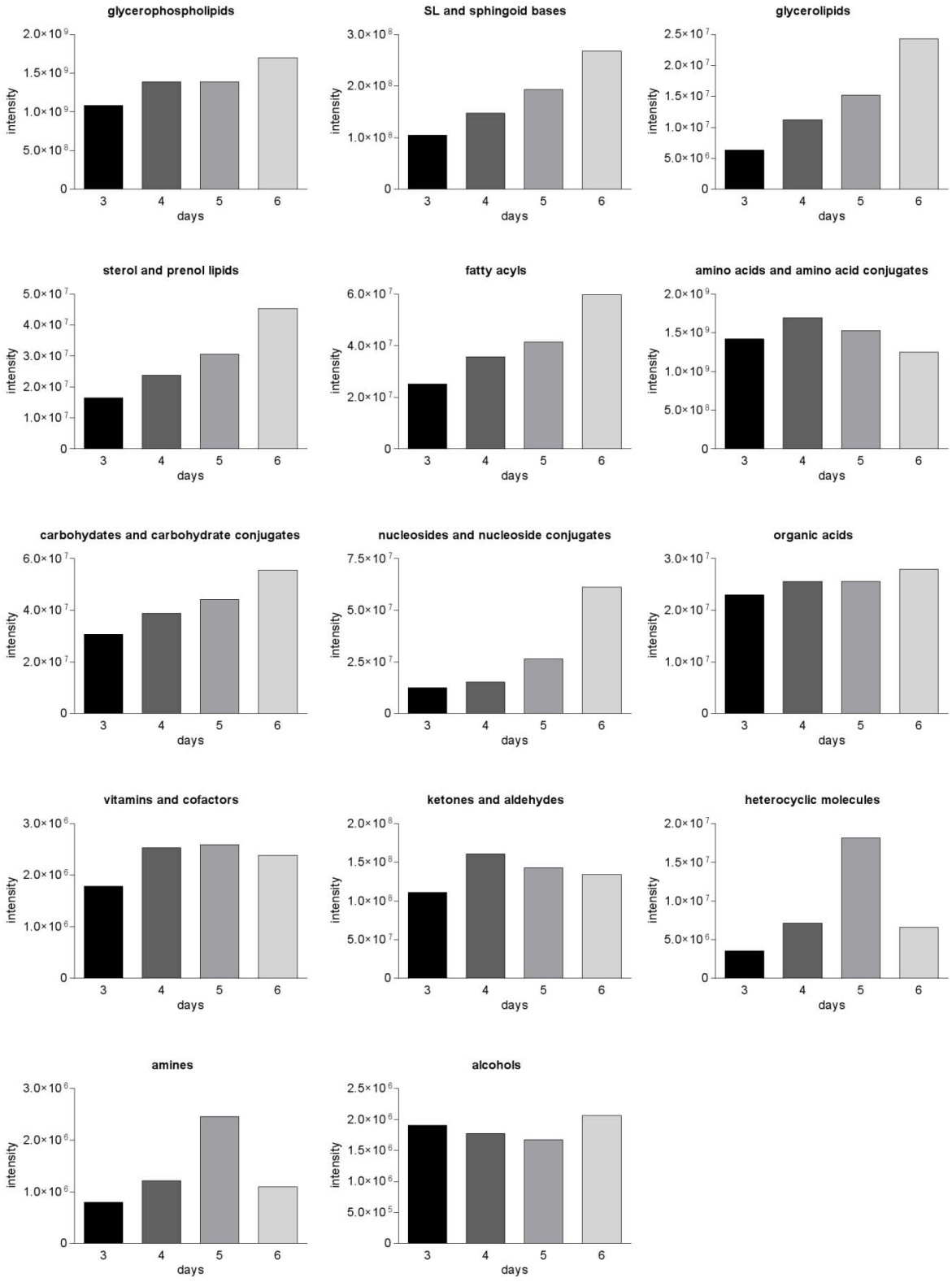

Figure S2. Overall metabolite levels for each compound category during *L. donovani* promastigotes development *in vitro*. Sum of total metabolite intensities from *L. donovani* promastigotes identified by LC-MS analysis at days 3, 4, 5 or 6 of *in vitro* growth grouped by compound categories.

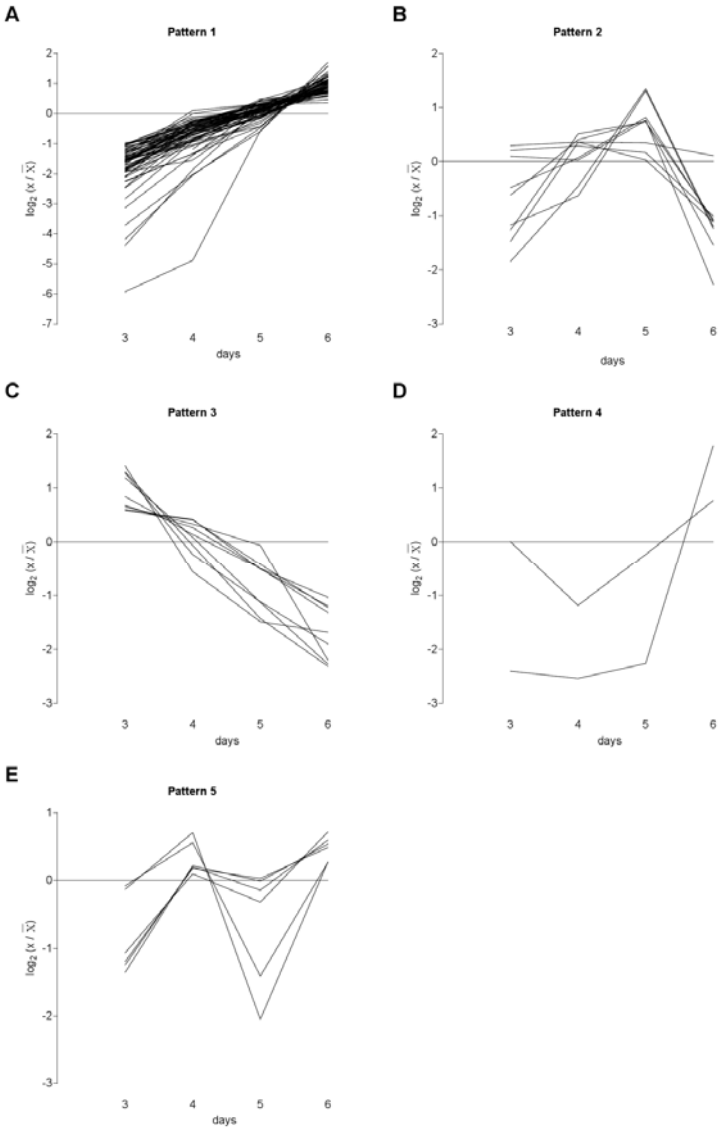

Figure S3. Patterns of metabolite variation in level during *L. donovani* promastigote *in vitro* growth from day 3 to day 6. Analysis of *L. donovani* promastigotes metabolome at day 3, 4, 5 and 6 allowed the distinction of 5 patterns (1-5) based on the metabolic profile for each metabolite that differed in intensity by 2-fold or more from the mean levels in at least one of the time points analyzed (a total of 97 metabolites). The relative level of each metabolite is shown, following logarithmic transformation (base 2); $\log_2 (x/\overline{X}_{3\text{-}6})$ below -1 or above 1 indicates a 2-fold change; x, time point analyzed (day 3, 4, 5 or 6). (A) Pattern 1 (74% of all metabolites considered) and (C) pattern 3 (9%) include metabolites that increased or decreased, respectively, continuously during all the whole period analyzed,; (B) pattern 2 (9%) include metabolites which had peak levels on days 4 or 5 but which then declined; (D) pattern 4 (2%) metabolite levels decreased from day 3 to day 4 and then increased and (E) pattern 5 (6%) include metabolites that showed an increase followed by a decrease and then another increase.

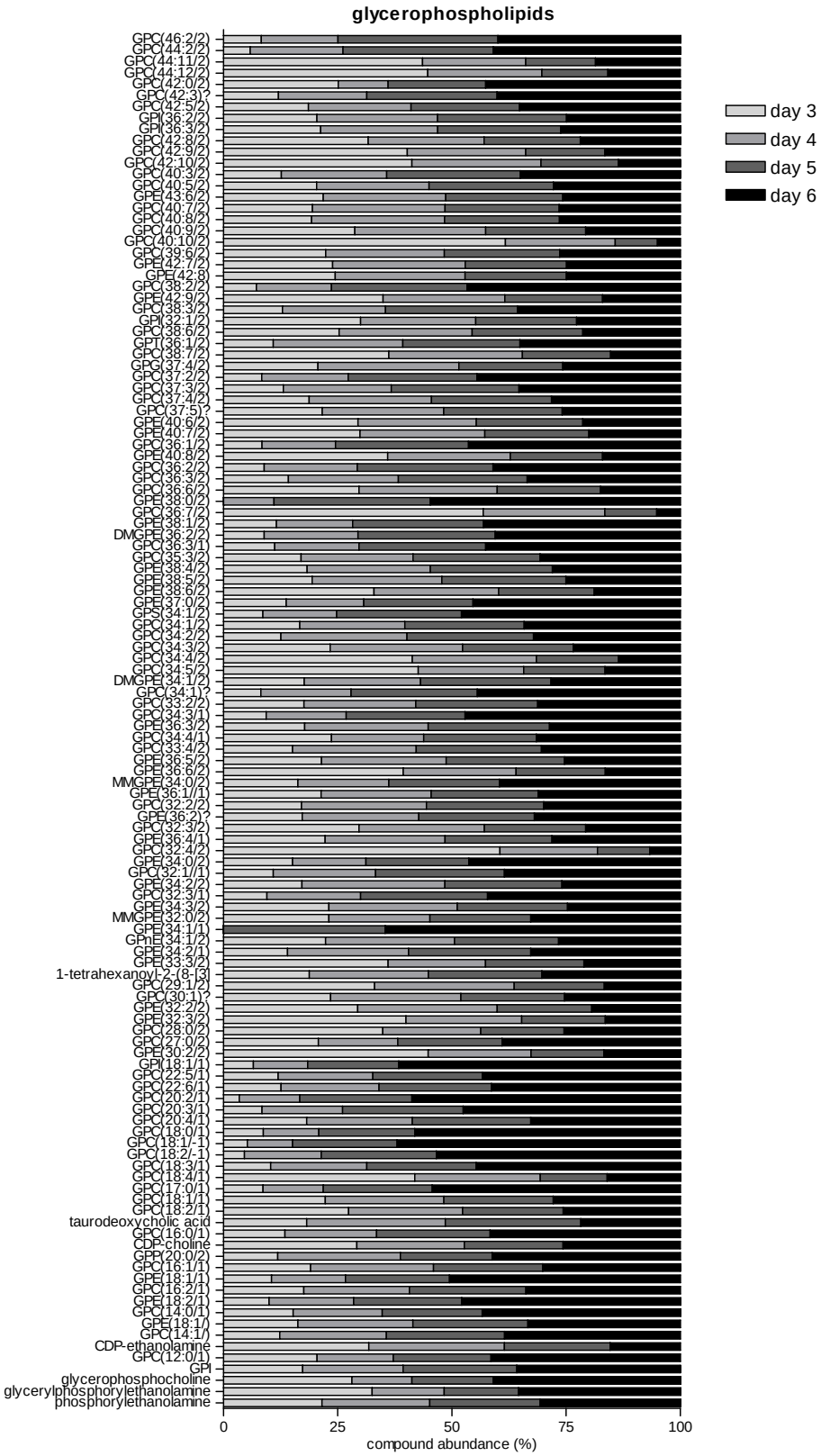

Figure S4. Glycerophospholipids abundance during *L. donovani* promastigotes development *in vitro*. Glycerophospholipids abundance is represented for each metabolite on each day as a percentage of the total abundance detected, which comprises the sum of the total metabolite intensity during the 4-day period of analysis.

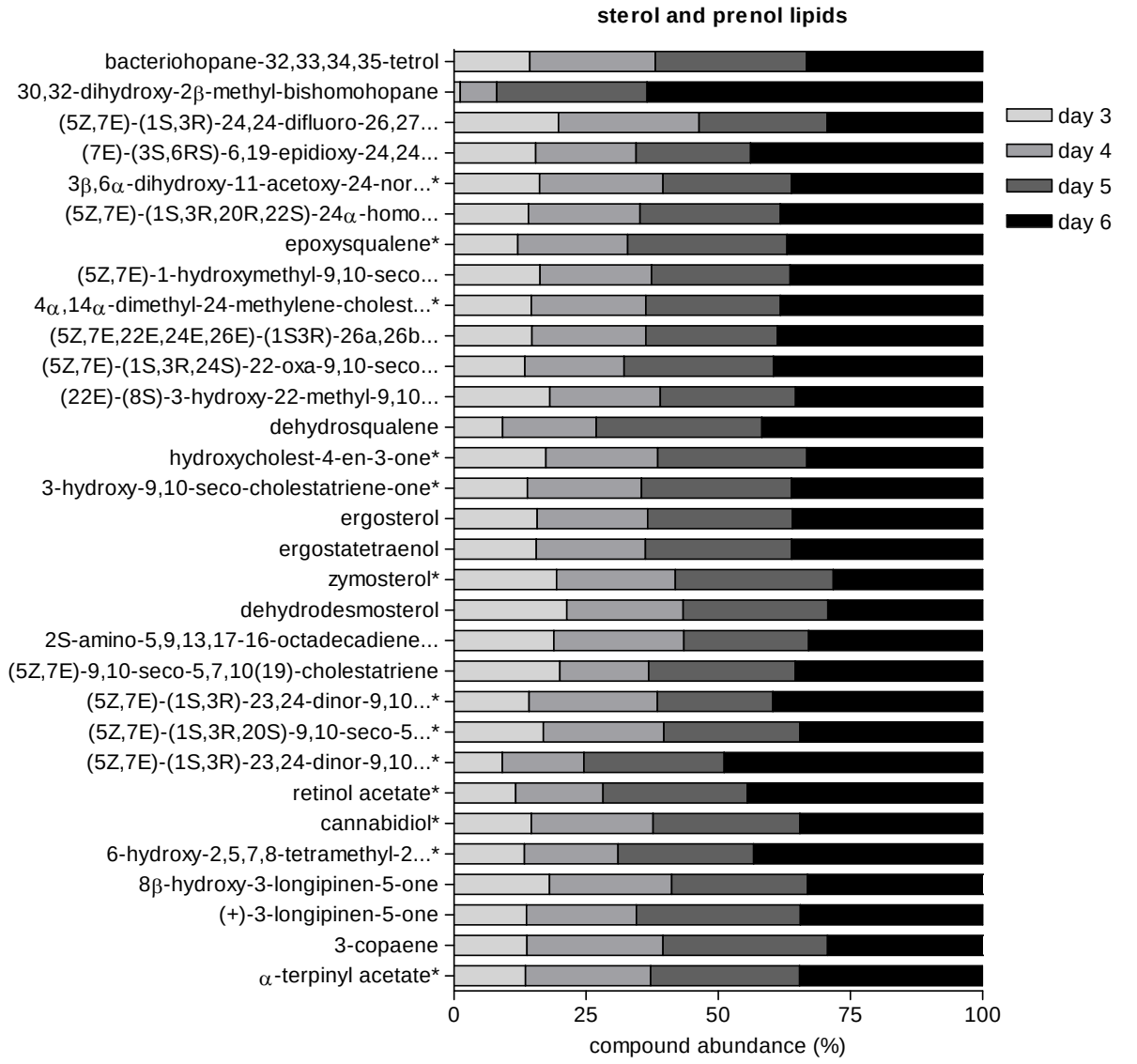

Figure S5. Sterol and prenol lipids abundance during *L. donovani* promastigotes development *in vitro*. Sterol and prenol lipids abundance is represented for each metabolite on each day as a percentage of the total abundance detected, which comprises the sum of the total metabolite intensity during the 4-day period of analysis. Metabolites labelled with * represent peaks with multiple potential identifications, for which just one is shown in this figure but the full list is given in Tables S1 and S2.

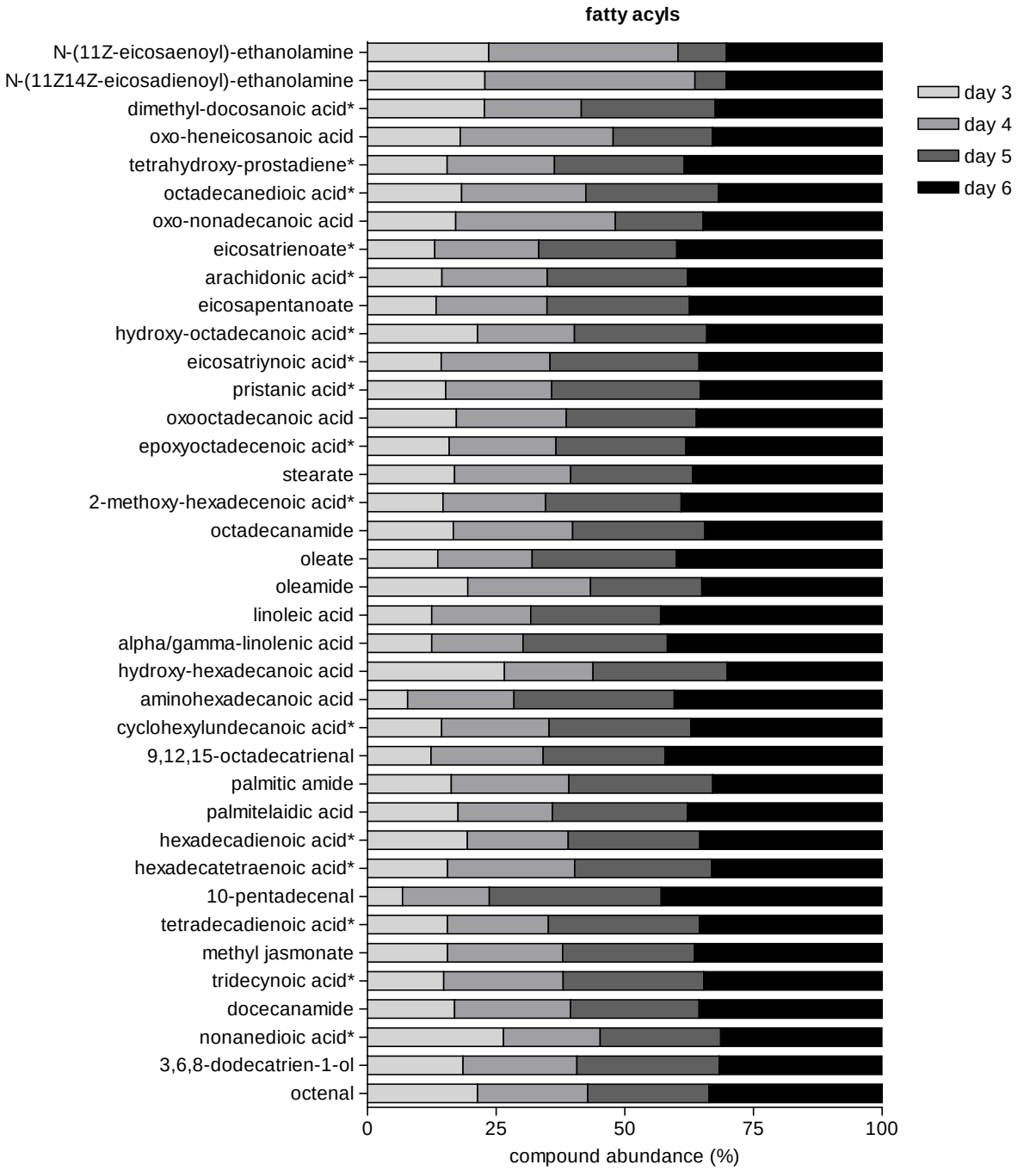

Figure S6. Fatty acyls abundance during *L. donovani* promastigotes development *in vitro*. Fatty acyls abundance is represented for each metabolite on each day as a percentage of the total abundance detected, which comprises the sum of the total metabolite intensity during the 4-day period of analysis. Metabolites labelled with * represent peaks with multiple potential identifications, for which just one is shown in this figure but the full list is given in Tables S1 and S2.

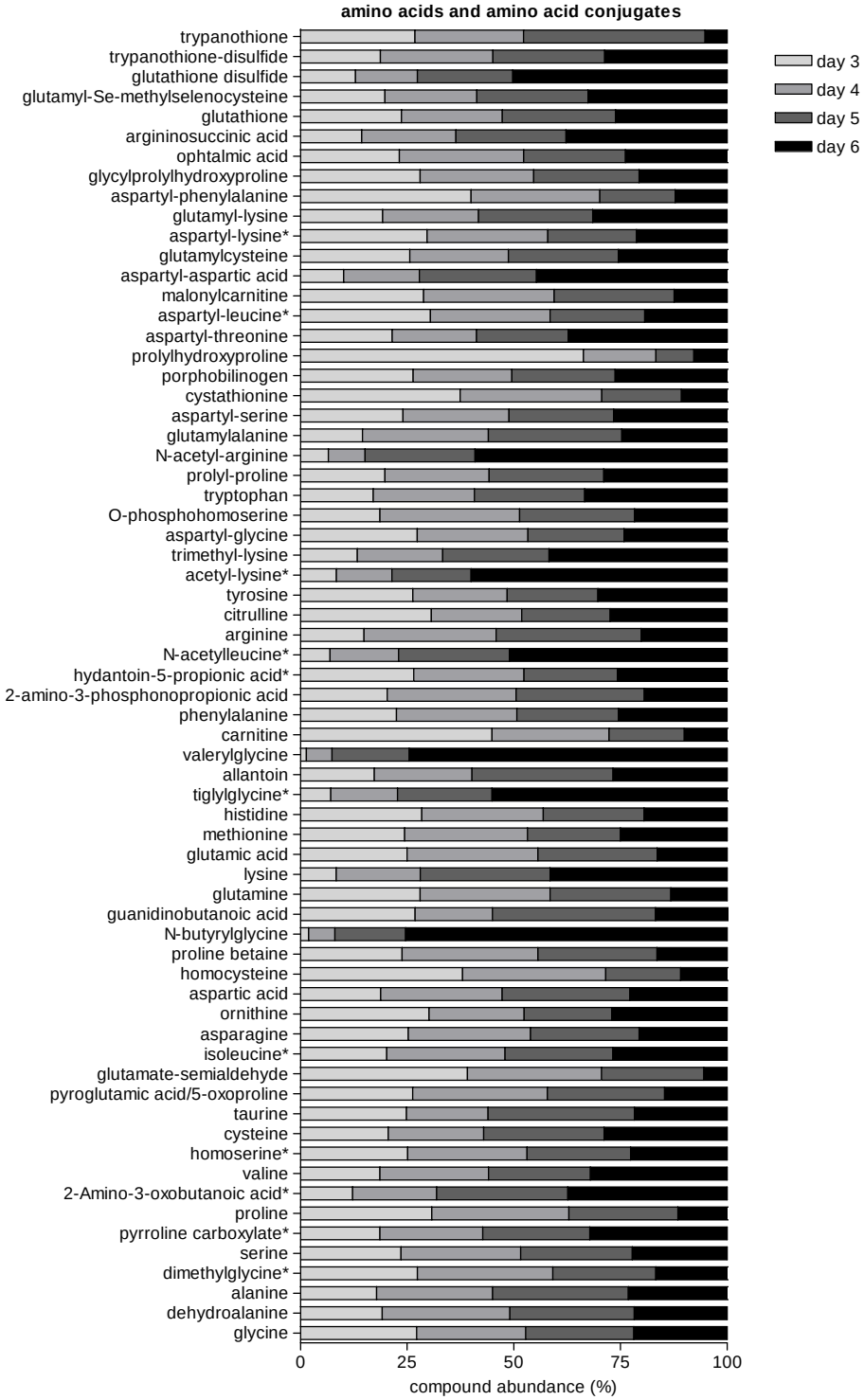

Figure S7. Amino acids and amino acids conjugates abundance during *L. donovani* promastigotes development *in vitro*. Amino acids and amino acids conjugates abundance is represented for each metabolite on each day as a percentage of the total abundance detected, which comprises the sum of the total metabolite intensity during the 4-day period of analysis. Metabolites labelled with * represent peaks with multiple potential identifications, for which just one is shown in this figure but the full list is given in Tables S1 and S2.

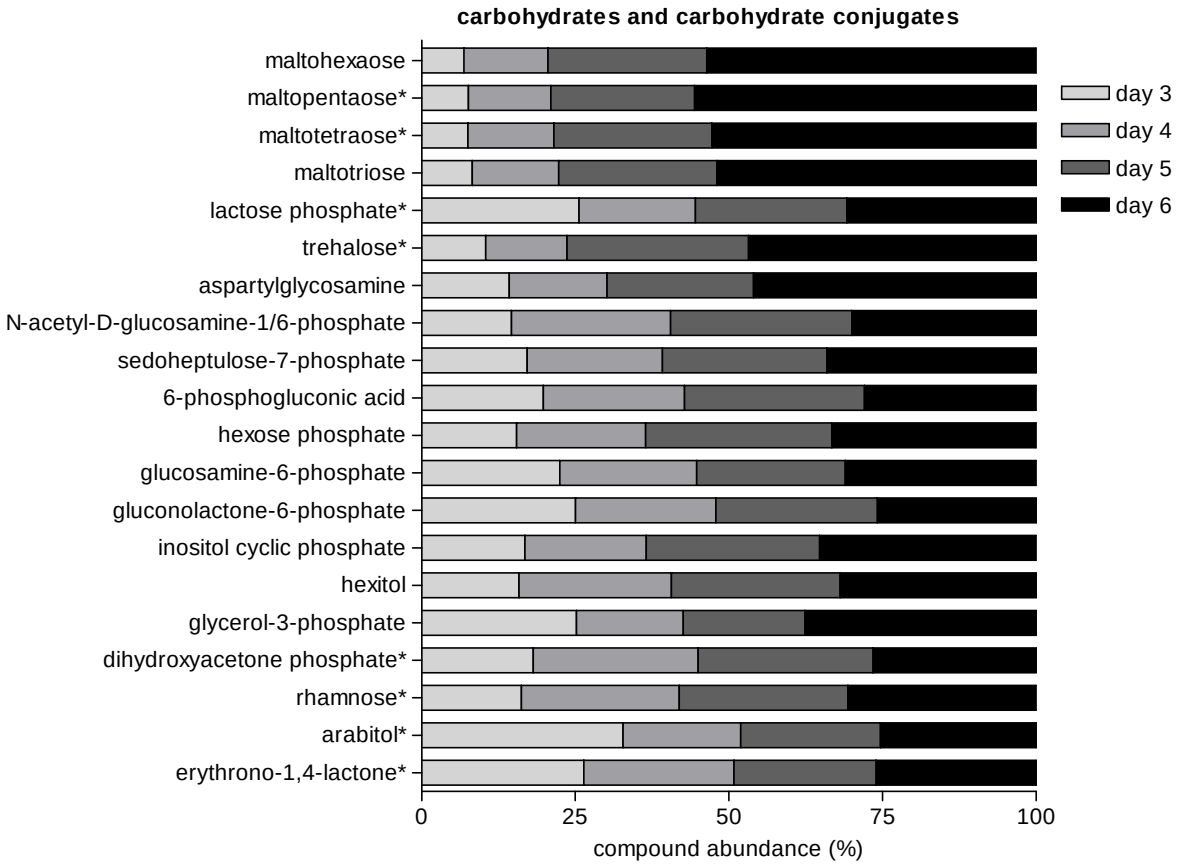

Figure S8. Carbohydrates and carbohydrate conjugates abundance during *L. donovani* promastigotes development *in vitro*. Carbohydrates and carbohydrate conjugates abundance is represented for each metabolite on each day as a percentage of the total abundance detected, which comprises the sum of the total metabolite intensity during the 4-day period of analysis. Metabolites labelled with * represent peaks with multiple potential identifications, for which just one is shown in this figure but the full list is given in Tables S1 and S2.

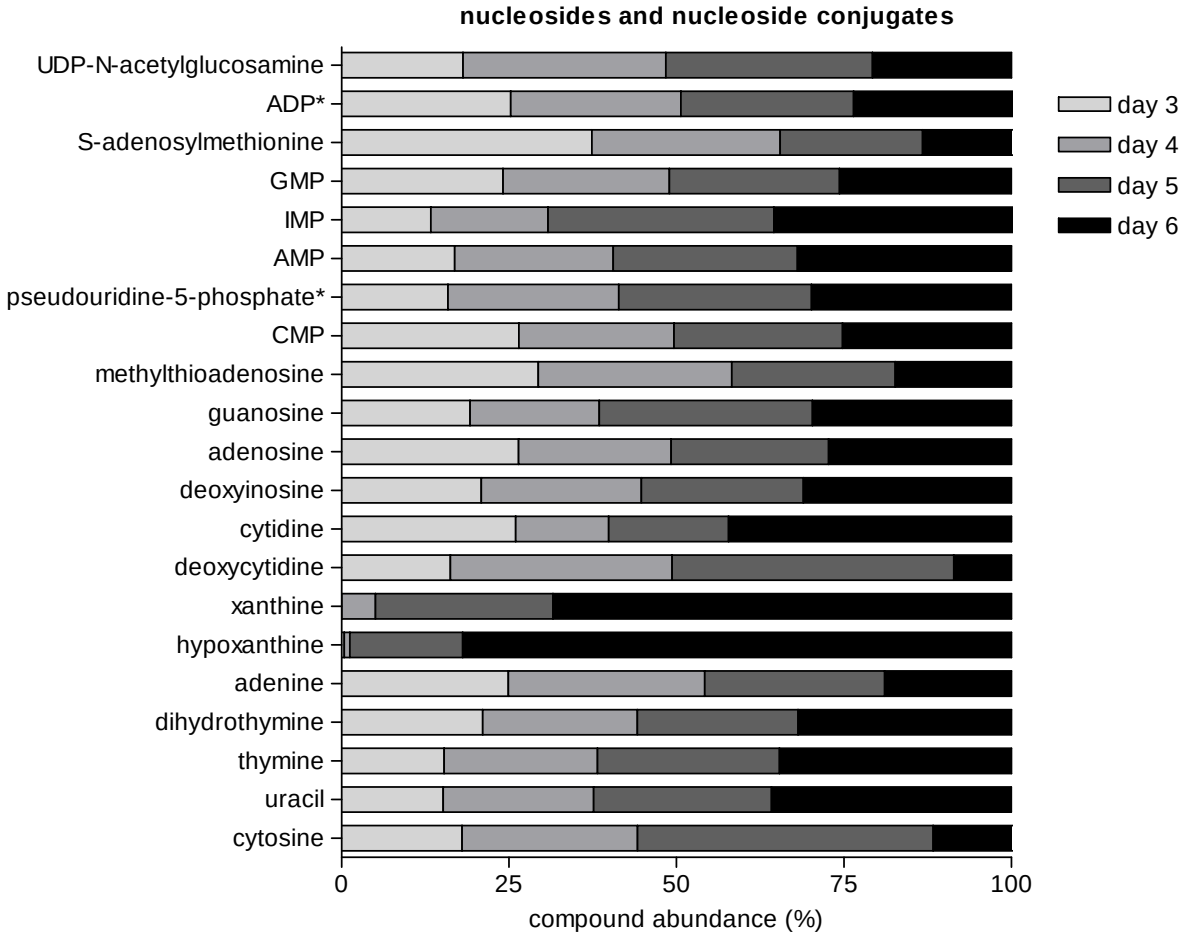

Figure S9. Nucleosides and nucleoside conjugates abundance during *L. donovani* promastigotes development *in vitro*. Nucleosides and nucleoside conjugate metabolites abundance is represented for each metabolite on each day as a percentage of the total abundance detected, which comprises the sum of the total metabolite intensity during the 4-day period of analysis. Metabolites labelled with * represent peaks with multiple potential identifications, for which just one is shown in this figure but the full list is given in Tables S1 and S2.

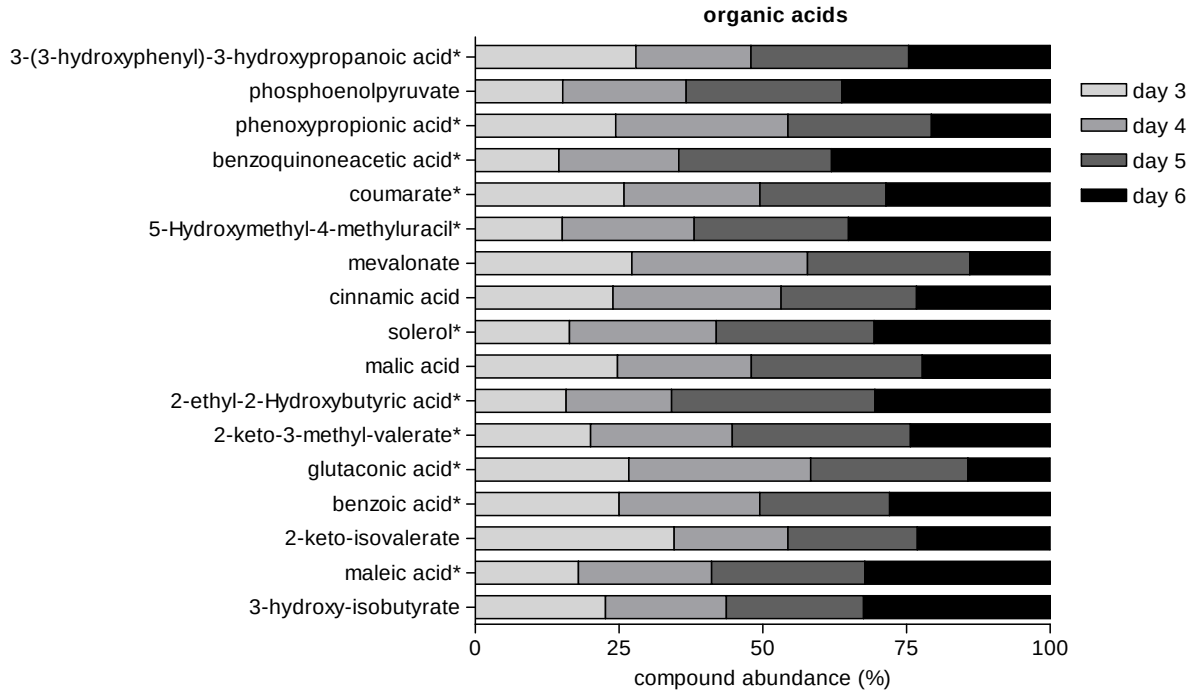

Figure S10. Organic acids abundance during *L. donovani* promastigotes development *in vitro*. Organic acids abundance is represented for each metabolite on each day as a percentage of the total abundance detected, which comprises the sum of the total metabolite intensity during the 4-day period of analysis. Metabolites labelled with * represent peaks with multiple potential identifications, for which just one is shown in this figure but the full list is given in Tables S1 and S2.

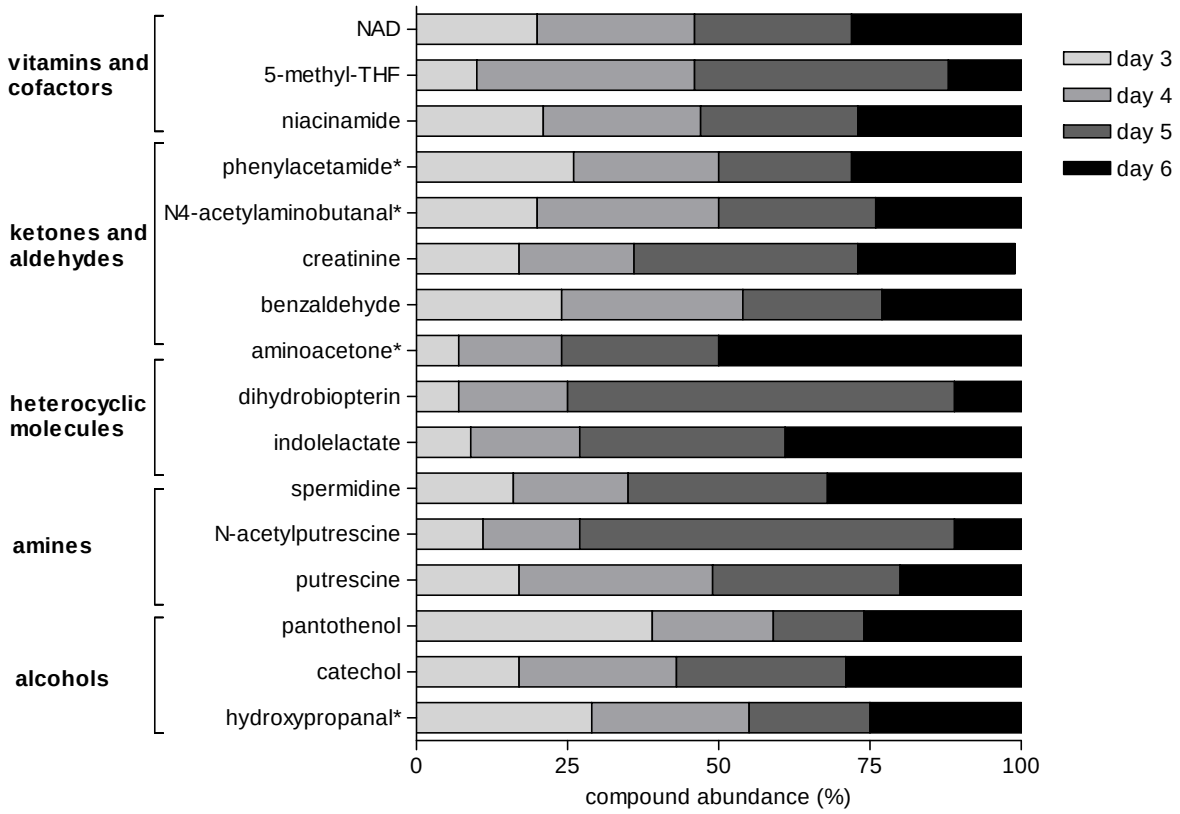

Figure S11. Vitamins and cofactors, ketones and aldehydes, heterocyclic molecules, amines and alcohols abundance during *L. donovani* promastigotes development *in vitro*. Vitamins and cofactors, ketones and aldehydes, heterocyclic molecules, amines and alcohols abundance is represented for each metabolite on each day as a percentage of the total abundance detected, which comprises the sum of the total metabolite intensity during the 4-day period of analysis. Metabolites labelled with * represent peaks with multiple potential identifications, for which just one is shown in this figure but the full list is given in Tables S1 and S2.

Table S1 – Metabolites identified below 1 ppm deviation in samples of *L. donovani* promastigotes from day 3 to day 6 of *in vitro* growth. For each compound the following information is shown: ionisation (ESI) mode; detected mass; retention time (min); putative metabolite identification; ppm deviation between detected mass and theoretical mass of the putative metabolite identified; intensity per 25 µg cell protein for each sample; average intensity per 25 µg cell protein in each time-point analyzed (3D, 4D, 5D or 6D); standard deviation in each time point analyzed; log base 2 of ratio of the average signal intensity in each time point against the mean intensity level during the 4 day period; F test statistics and p values obtained by analysis of variance (ANOVA), indicating whether or not there was a statistically significant difference between the time points analyzed; decision on whether or not the compound was significantly changed in level based on a two-fold or higher average difference in signal intensity in at least one of the time points analyzed and statistical significance (p<0.05); compound category.

Table S2 – Metabolites identified between 1-2 ppm deviation in samples of *L. donovani* promastigotes from day 3 to day 6 of *in vitro* growth. The data presented are as described for Table S1.

Tables S1 and S2 are available in the electronic version of the thesis.

Table S3 – Intensity levels of metabolites that differ significantly during *L. donovani* promastigote development *in vitro*

	Average intensity per 25µg cell protein				
	day 3	**day 4**	**day 5**	**day 6**	**pattern**
amines					
N-acetylputrescine	2.53E+05	3.69E+05	1.42E+06	2.42E+05	2
amino acids and amino acids conjugates					
proline	2.95E+08	3.07E+08	2.45E+08	1.10E+08	2
2-amino-3-oxobutanoic acid*	2.29E+05	3.69E+05	5.77E+05	6.99E+05	1
glutamate-semialdehyde	1.36E+07	1.09E+07	8.36E+06	1.89E+06	3
homocysteine	2.56E+05	2.26E+05	1.18E+05	7.34E+04	3
N-butyrylglycine	1.28E+05	4.13E+05	1.11E+06	5.04E+06	1
lysine	5.54E+06	1.31E+07	2.01E+07	2.75E+07	1
tiglylglycine*	7.76E+04	1.70E+05	2.41E+05	6.00E+05	1
valerylglycine	1.64E+05	7.21E+05	2.16E+06	8.90E+06	1
carnitine	1.89E+06	1.16E+06	7.44E+05	4.24E+05	3
N-acetylleucine*	8.48E+04	1.97E+05	3.19E+05	6.26E+05	1
acetyl-lysine*	1.37E+05	2.11E+05	3.01E+05	9.75E+05	1
N-acetyl-arginine	7.16E+04	9.36E+04	2.82E+05	6.45E+05	1
cystathionine	7.54E+07	6.69E+07	3.76E+07	2.15E+07	3
prolylhydroxyproline	3.64E+06	9.33E+05	4.89E+05	4.28E+05	3
malonylcarnitine	3.10E+05	3.29E+05	3.02E+05	1.33E+05	2
aspartyl-aspartic acid	2.44E+05	4.27E+05	6.60E+05	1.08E+06	1
aspartyl-phenylalanine	1.20E+07	9.04E+06	5.29E+06	3.64E+06	3
glutathione disulfide	4.47E+04	5.03E+04	7.74E+04	1.74E+05	1
trypanothione	1.32E+06	1.25E+06	2.09E+06	2.55E+05	2
carbohydrates and carbohydrate conjugates					
trehalose*	4.18E+04	5.29E+04	1.18E+05	1.87E+05	1
maltotriose	1.30E+05	2.21E+05	4.06E+05	8.18E+05	1
maltotetraose*	2.15E+05	3.97E+05	7.31E+05	1.50E+06	1
maltopentaose*	5.27E+05	9.24E+05	1.61E+06	3.84E+06	1
maltohexaose	7.40E+04	1.46E+05	2.78E+05	5.75E+05	1
fatty acyls					
10-pentadecenal	8.05E+05	1.99E+06	3.95E+06	5.07E+06	1
9, 12, 15-octadecatrienal*	4.12E+05	7.24E+05	7.89E+05	1.40E+06	1
aminohexadecanoic acid	1.24E+06	3.28E+06	4.95E+06	6.42E+06	1
linoleic acid	4.13E+05	6.35E+05	8.33E+05	1.42E+06	1
N-(11Z, 14Z-eicosadienoyl)-ethanolamine	1.25E+06	2.24E+06	3.32E+05	1.66E+06	5
N-(11Z-eicosaenoyl)-ethanolamine	4.26E+05	6.65E+05	1.71E+05	5.46E+05	5
glycerolipids					
DAG(36:5)	2.75E+05	6.27E+05	9.69E+05	1.49E+06	1
DAG(36:4)	2.41E+05	6.16E+05	1.10E+06	2.08E+06	1
DAG(36:3)	2.01E+05	4.02E+05	6.79E+05	1.24E+06	1
DAG(42:3)*	2.07E+05	1.87E+05	2.28E+05	3.74E+06	4
DAG(46:7)	1.18E+06	3.49E+06	5.64E+06	7.39E+06	1
TAG(54:7)	9.96E+04	1.76E+05	2.99E+05	5.63E+05	1
TAG(54:6)	9.75E+04	2.42E+05	2.75E+05	5.33E+05	1
TAG(54:5)	1.05E+05	1.34E+05	2.41E+05	4.09E+05	1

	Average intensity per 25µg cell protein				
	day 3	**day 4**	**day 5**	**day 6**	**pattern**
glycerophospholipids					
GPC(14:1)	1.63E+05	3.07E+05	3.41E+05	5.07E+05	1
lysoPE(18:2/1)	5.44E+05	1.00E+06	1.29E+06	2.60E+06	1
GPE(18:1/1)	4.08E+05	6.25E+05	8.82E+05	1.96E+06	1
GPP(20:0/2)	1.08E+05	2.45E+05	1.83E+05	3.76E+05	5
GPC(17:0/1)	1.35E+05	2.05E+05	3.70E+05	8.45E+05	1
GPC(18:3/1)	1.80E+06	3.66E+06	4.16E+06	7.79E+06	1
GPC(18:2/-1)	2.57E+06	9.45E+06	1.41E+07	3.00E+07	1
GPC(18:1/-1)	1.03E+06	1.96E+06	4.49E+06	1.22E+07	1
GPC(18:0/1)	2.37E+06	3.32E+06	5.71E+06	1.58E+07	1
lysoPC(20:3/1)	4.60E+05	9.64E+05	1.44E+06	2.59E+06	1
lysoPC (20:2/1)	2.17E+05	8.20E+05	1.52E+06	3.65E+06	1
GPC(22:5/1)	1.60E+06	2.76E+06	3.20E+06	5.78E+06	1
GPI(18:1/1)	7.03E+05	1.28E+06	2.15E+06	6.64E+06	1
GPC(32:3/1)	5.42E+06	1.17E+07	1.58E+07	2.41E+07	1
GPC(32:1//1)*	7.21E+06	1.48E+07	1.86E+07	2.55E+07	1
GPC(32:4/2)*	7.73E+06	2.72E+06	1.47E+06	8.56E+05	3
GPC(34:3/1)*	1.94E+06	3.61E+06	5.38E+06	9.75E+06	1
GPC(34:1)*	1.81E+06	4.36E+06	6.10E+06	9.81E+06	1
GPS(34:1/2)	4.93E+04	9.19E+04	1.56E+05	2.73E+05	1
GPC(36:3/1)	8.31E+05	1.36E+06	2.05E+06	3.16E+06	1
DMGPE(36:2/2)*	3.04E+06	7.00E+06	1.02E+07	1.38E+07	1
GPE(38:1/2)*	7.82E+05	1.12E+06	1.93E+06	2.91E+06	1
GPC(36:7/2)	1.77E+07	8.26E+06	3.54E+06	1.61E+06	3
GPC(36:2/2)	3.92E+07	8.97E+07	1.31E+08	1.80E+08	1
GPC(36:1/2)	7.42E+06	1.42E+07	2.57E+07	4.08E+07	1
GPC(37:2/2)*	4.74E+05	1.07E+06	1.59E+06	2.52E+06	1
GPT(36:1/2)	1.11E+06	2.89E+06	2.61E+06	3.58E+06	5
GPC(38:2/2)	1.46E+06	3.34E+06	6.01E+06	9.48E+06	1
GPC(40:10/2)	1.61E+07	6.25E+06	2.41E+06	1.31E+06	3
GPC(42:3)	2.29E+05	3.68E+05	5.41E+05	7.63E+05	1
GPC(42:0/2)	1.61E+05	7.04E+04	1.37E+05	2.74E+05	4
GPC(44:2/2)	3.37E+05	1.17E+06	1.90E+06	2.36E+06	1
GPC(46:2/2)	8.51E+04	1.72E+05	3.58E+05	4.09E+05	1
heterocyclic molecules					
indolelactate	2.40E+05	4.93E+05	9.25E+05	1.08E+06	1
dihydrobiopterin	1.61E+06	4.21E+06	1.46E+07	2.49E+06	2
ketones and aldehydes					
aminoacetone*	6.33E+05	1.66E+06	2.54E+06	4.79E+06	1
nucleosides and nucleoside conjugates					
cytosine	4.23E+05	6.16E+05	1.04E+06	2.74E+05	2
hypoxanthine	1.97E+05	4.06E+05	8.04E+06	3.92E+07	1
deoxycytidine	2.58E+05	5.26E+05	6.69E+05	1.37E+05	2
others					
diphosphate	2.29E+05	8.11E+05	8.09E+05	6.86E+05	2
N-methylpelletierine	6.41E+04	1.19E+05	2.23E+05	8.01E+05	1

	Average intensity per 25µg cell protein				
	day 3	**day 4**	**day 5**	**day 6**	**pattern**
sphingolipids and sphingoid bases					
1-deoxy-sphinganine	7.66E+05	1.78E+06	2.56E+06	4.22E+06	1
heptadecasphinganine	2.03E+05	3.77E+05	6.85E+05	1.59E+06	1
dehydrosphinganine	5.47E+05	1.62E+06	2.57E+06	3.41E+06	1
SP(2-amino-14, 16-dimethyloctadecan-3-ol)	1.97E+05	3.43E+05	5.10E+05	7.92E+05	1
4-hydroxysphinganine	1.54E+05	4.09E+05	5.08E+05	5.61E+05	1
N, N-dimethylsphing-4-enine	1.66E+05	4.56E+05	3.60E+05	6.02E+05	5
SP(2S-dimethylaminooctadecane-1, 3R-diol)	9.15E+05	1.77E+06	2.59E+06	3.07E+06	1
N-(hexadecanoyl)-sphing-4-enine	4.60E+06	1.08E+07	2.28E+07	4.17E+07	1
N-(hexadecanoyl)-4S-hydroxysphinganine	1.99E+06	6.10E+06	1.36E+07	2.24E+07	1
N-(octadecanoyl)-sphing-4-enine	1.41E+05	4.74E+05	1.46E+06	2.87E+06	1
sterol and prenol lipids					
retinol acetate*	3.05E+05	4.31E+05	7.13E+05	1.16E+06	1
(5Z, 7E)-(1S, 3R)-23, 24-dinor-9, 10-seco…*	2.00E+05	3.37E+05	5.79E+05	1.07E+06	1
dehydrosqualene	4.84E+05	9.31E+05	1.65E+06	2.19E+06	1
epoxysqualene*	2.21E+05	3.80E+05	5.52E+05	6.77E+05	1
30,32-dihydroxy-2b-methyl-bishomohopane	1.40E+05	8.12E+05	3.36E+06	7.48E+06	1
vitamins and cofactors					
5-methyl-THF	1.31E+05	4.47E+05	5.24E+05	1.49E+05	2

Metabolites are ordered by compound category; for each metabolite is shown the average intensity per 25 µg cell protein at days 3, 4, 5 and 6 and the respective metabolic profile pattern (analysis shown in Figure S2). Metabolites labelled with * represent peaks with multiple potential identifications, for which just one is shown in this figure but the full list is given in Table S1 and S2.

4.7 Comparative metabolomic analyses of *Leishmania donovani* and *Leihmania major* reveal specificity in tryptophan metabolism

We have undertaken a comparative analysis of the metabolomes of promastigotes of *L. donovani* and *L. major*, species that cause visceral and cutaneous leishmaniasis, respectively. 30.7% of the identified metabolites differed between the two species, although the overall abundance of all identified metabolites was similar. Large differences were detected in some amino acids, peptides and amines, as well as with some lipids. A particularly notable finding was the differing utilization of tryptophan. The data provide clear evidence on the value of metabolomics in detecting species-specific metabolic features of *Leishmania*, thus application of this technology should aid in obtaining a better understanding of the parasite's cell biology and also contribute to novel drug and vaccine discovery.

Unpublished results

Comparative metabolomic analyses of *Leishmania donovani* and *Leishmania major* reveal specificity in tryptophan metabolism

Ana Marta Silva[1,2,3], Anabela Cordeiro-da-Silva[2,3] and Graham H. Coombs[1*]

[1]Strathclyde Institute of Pharmacy and Biomedical Sciences, University of Strathclyde, 161 Cathedral Street, Glasgow G4 0RE, UK;
[2]Instituto de Biologia Molecular e Celular, Universidade do Porto, Rua do Campo Alegre, 823, 4150-180 Porto, Portugal;
[3]Laboratório de Ciências Biológicas, Faculdade de Farmácia da Universidade do Porto, R. Aníbal Cunha n.º 164, 4050-047 Porto, Portugal;

*Corresponding author: E-mail: graham.coombs@strath.ac.uk

Short title: Metabolome of *Leishmania* species

Keywords: parasite, *Leishmania*, promastigote, metabolome, tryptophan

Abbreviations: SD, standard deviation; LC-MS, liquid chromatography mass spectrometry; ppm, parts per million, Sm, spent medium; Cm, culture medium;

Abstract

We have undertaken a comparative analysis of the metabolomes of promastigotes of *L. donovani* and *L. major*, species that cause visceral and cutaneous leishmaniasis, respectively. 30.7% of the identified metabolites differed between the two species, although the overall abundance of all identified metabolites was similar. Large differences were detected in some amino acids, peptides and amines, as well as with some lipids. A particularly notable finding was the differing utilization of tryptophan. The data provide clear evidence on the value of metabolomics in detecting species-specific metabolic features of *Leishmania*, thus application of this technology should aid in obtaining a better understanding of the parasite's cell biology and also contribute to novel drug and vaccine discovery.

Introduction

Leishmaniasis, caused by the protozoan parasite *Leishmania*, is an important global health problem with an estimated 2 million new cases annually and some 350 million people at risk worldwide [1]. More than 20 different *Leishmania* species can cause disease [2], which ranges from self-healing cutaneous lesions to fatal visceral infections [1]. The clinical outcome of *Leishmania* infection is mainly dependent on the infecting species, but other factors such as the host immune status also play a role [2-4]. Visceral leishmaniasis is caused by *L. donovani* complex parasites while species resulting in cutaneous leishmaniasis include *L. major*, *L. tropica* and *L. mexicana*; *L. braziliensis* and *L. panamensis* are examples of species that can cause the especially debilitating condition known as mucocutaneous leishmaniasis [5]. Although the characteristics of the various forms of leishmaniasis are well known, the mechanisms underlying the differing clinical outcomes resulting from infections with the various species are not well understood. The pathogenicity of *Leishmania* is thought to be mainly determined by the parasite species itself, thus understanding how species differ at the metabolic level should provide insights into not only the innate biological variation between species but also how each is adapted for its own niche within its host.

Comparative genomics analysis of different *Leishmania* species has revealed strong conservation of gene content and synteny, with relatively few species-specific genes among *L. major*, *L. braziliensis* and *L. infantum* [6] even though the species have clear biological differences. Recent new sequencing technology has greatly facilitated the analyses of the *L. donovani* and *L. mexicana* genomes [7,8]; simultaneously details of the reference genomes of *L. major*, *L. braziliensis* and *L. infantum* were also refined [8]. These new data confirm the very small number of species-specific genes [7,8], as described before [6]. It was anticipated that discovery of species-specific genes would provide a key understanding of the differing ability of species to infect and survive in different tissues and hosts and the differing pathogenicity. A2 is one example of a species-specific gene that is required for *L. donovani* visceral infection in mice [9] and which, upon introduction into *L. major* , did impart some properties with respect to tissue tropism [10]. However, the results so far suggest that the phenotypic differences between the various species must be brought about through differential regulation of gene expression and protein function rather than simply the possession of different genes. Whilst genomics has a major role to play in revealing differences between the genomes of *Leishmania* species, it is limited in providing contextual and integrative information that is necessary to decipher the mechanisms of cellular function. In contrast, metabolites are

key in linking together the web of complex interactions, cellular pathways, molecular participants and environmental stimuli. Thus studies on the metabolomes of the various species should aid greatly in gaining an understanding of the adaptations of the individual species. The advent of improved methods for detecting and identifying metabolites has meant that the technology of 'metabolomics' now allows the measurement at high resolution of a cell's metabolites. Thus it is being applied increasingly in drug discovery, disease diagnostics and treatment [11] and is now also beginning to be applied in research on parasites [12-15]. In this study, we have used an untargeted metabolomics approach to compare promastigotes of *L. donovani* and *L. major*. The data presented show that indeed there are some large differences in the levels of individual metabolites in the two species, whereas there is a high similarity between the two species in the overall metabolite profile.

Material and Methods

Leishmania parasites

L. donovani (MHOM/NP/03/BPK206/0clone10) and *L. major* (MHOM/IL/80/Friedlin) were used in this study. *L. donovani* promastigotes had been cloned from an isolate from a visceral leishmaniasis patient sensitive to pentavalent antimonials in Nepal, as described by Rijal and co-workers [16]. *L. donovani* and *L. major* promastigotes were grown in modified Eagle's medium (designated HOMEM medium, Invitrogen) supplemented with 20% or 10% (v/v) heat inactivated fetal calf serum (PAA Laboratories) and at 26°C or 27ºC, respectively. Cultures were set up initially at a concentration of 2.5 x 10^5 parasites/ml and *L. donovani* was sub-passaged every 6 days, while *L. major* was sub-passaged every 7 days.

Leishmania extracts for metabolite analysis

Promastigotes cultures were initiated at 2.5 x 10^5 cells/ml in 4 x 10 ml cultures in order to obtain cell samples from four independently growing cultures (biological replicates). Promastigotes from each culture were harvested at day 5 for metabolite extraction. The metabolite extraction was performed as previously described [12]. Briefly, promastigotes quenching was performed in a dry ice/ethanol bath with rapid temperature decrease to 2ºC and then immediate transfer to ice. Two aliquots of 4 x 10^7 cells were taken from each culture flask (technical replicates). After centrifugation at 12000 g for 10 min at 4ºC, the supernatant (designated the spent medium) was removed and stored on ice. Cell pellets were washed 3 times in 1 ml of PBS at 4ºC by centrifugation at 12000 g for 10 min at 4ºC.

For cell disruption and metabolite extraction, cell pellets were resuspended in 200 µl cold chloroform/methanol/water (20/60/20, v/v/v) and incubated 1 h in a Thermomixer (1400 rpm, 4ºC). After centrifugation at 12000 g for 10 min at 4ºC, the supernatant containing the extracted metabolites was recovered and stored at -70ºC until analysed. To 75 µl of spent medium was added 300 µl of cold chloroform/methanol (20/60, v/v) followed by incubation for 1 h on ice. After centrifugation at 12000 g for 10 min at 4ºC, the supernatant was recovered and stored at -70ºC until analysed.

Liquid chromatography mass spectrometry (LC-MS) analysis and data processing

LC-MS analysis and data processing was done as described by t'Kindt and co-workers [12,13] except that the intensity levels of each identified peak were normalized against the protein content of the cells used in order to take into account the differing cell volumes. Intensity level ratios were used to compare the different cell lines, with the following criteria being applied for differences to be considered of interest: (i) there was at least a 2-fold difference between the *L. donovani* and *L. major*; (ii) there was a statistically significant difference ($p<0.05$) between the cell lines being compared. The metabolite data are expressed as intensity per 25 µg cell protein.

Statistical analysis

Statistical analysis was performed using Student's T test: a *p* value smaller than 0.05 ($p<0.05$) was considered significant; GraphPad Prism 4 was used for plotting the graphs.

Results and Discussion

L. donovani and *L. major* cause leishmaniasis with different clinical manifestations, visceral and cutaneous, and associated pathology [4]. Some distinct differences between the two species are known, for instance the lipophosphoglycan on the surface of the promastigotes is species-specific and is thought to account for differences in the attachment to sand fly midgut and play a role in the transmission to the mammalian host [17,18]. However, genomic and transcriptomic analyses have not yet provided explanations for the distinct species-specific biology of the two species [6,19]. Thus we undertook this study in the anticipation that identification of differences between the metabolomes of the species would provide greater insights into the individual characteristics of each. The results have yielded some key details on metabolic differences between the species which start to provide a framework for understanding how each is adapted for its particular biological niche.

In analyzing the intracellular metabolites of *L. donovani* and *L. major* promastigotes after 5 days of *in vitro* culture, the metabolite intensity levels resulting from the LC-MS analysis were normalized against the protein content of the cells as this clearly differed between the two species (Table 1) reflecting differences in cell volumes.

Table 1 – Comparison between *L. major* and *L. donovani* protein content and cell density at day 5 of *in vitro* growth

	Cell density ($\times 10^7$/ml)	**Protein content** (mg/10^8 cells)
L. donovani	3.39 ± 0.138	0.371 ± 0.0023
L. major	3.94 ± 0.147 **	0.284 ± 0.0017 ***

L. donovani and *L. major* cell lines were seeded at 2.5 x 10^5 parasites/ml, counted daily and harvested at day 5. Protein content was determined by the Lowry method. Each value is a mean ± standard deviation from four cultures. Statistically significant differences between cell lines are indicated: ** $p<0.01$, *** $p<0.001$.

Analysis of the intracellular metabolites of *L. donovani* and *L. major* lead to the putative identification of 208 metabolites (147 at <1 ppm deviation and 61 at 1-2 ppm deviation), of which 9 were only detected in one species. Fig. 1 shows the comparative intensity ratio between *L. donovani* and *L. major* for each metabolite putatively identified; 68 metabolites (34.2% of the total number of metabolites identified in both species) differed in intensity at least 2-fold between *L. donovani* and *L. major,* although the overall intensities in the two species was similar (1.33 x 10^9 and 1.46 x10^9, respectively).

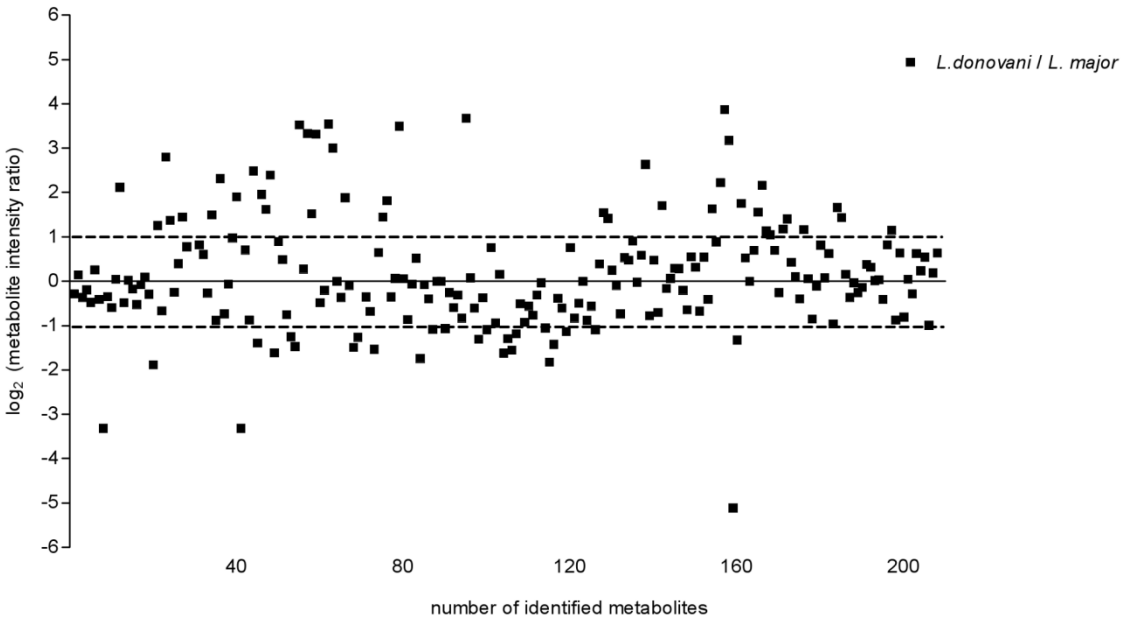

Figure 1. Overview of intracellular metabolite levels comparison between *L. donovani* and *L. major* promastigotes. *L. donovani* and *L. major* promastigotes were harvested after 5 days of *in vitro* growth and cell extracts analyzed by LC-MS. All metabolites within the 2 ppm cut-off are included and following a logarithmic transformation (base 2) the average signal intensity ratios of *L. donovani / L. major* for all metabolites were plotted. Dotted lines represent the fold-change cut-off in this study for a given metabolite profile being considered to be significantly different between *L. donovani* and *L. major*: $\log_2$ (metabolite intensity ratio) below -1 or above 1 indicates a 2-fold change between cell lines compared. The metabolites differing at least by 2-fold between *L. donovani* and *L. major* promastigotes were 34.2% of the metabolites identified.

Metabolites from a wide range of categories were detected, with glycerophospholipids and amino acids being the most represented, followed by sterols and prenol lipids, fatty acyls and carbohydrates (Fig. 2). Glycerolipids is the only group of compounds for which the overall intensity differs remarkably between *L. donovani* and *L. major* promastigotes (4-fold higher in *L. major*) (Fig. S1). The full list of putatively identified metabolites are provided in Tables S1 and S2.

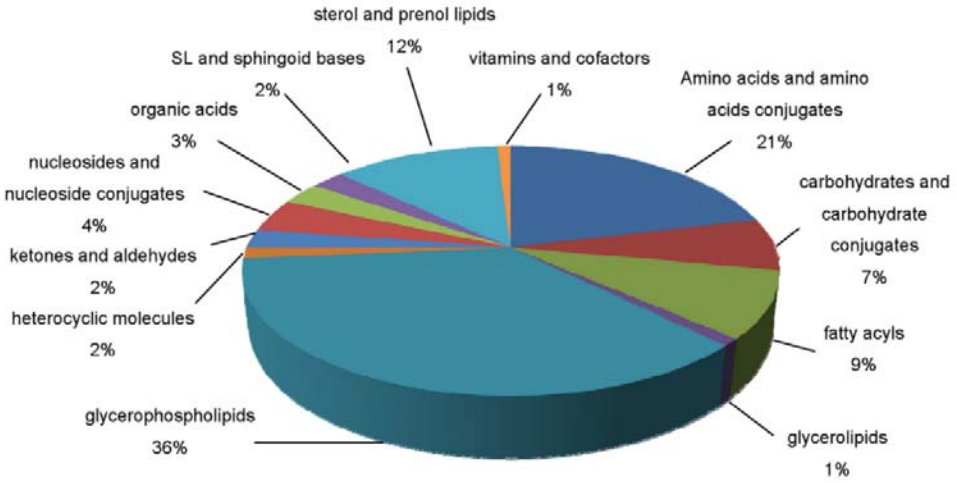

Figure 2. Distribution of the identified intracellular metabolites by compound category. *L. donovani* and *L. major* promastigotes were harvested after 5 days of *in vitro* growth and cell extracts analyzed by LC-MS. All identified intracellular metabolites were grouped by compound category. For each category compound is indicated the % of compounds identified.

In analyzing the differences between *L. donovani* and *L. major*, we concentrated upon the metabolites that differed by at least 2-fold between the two species and for which a statistical significant difference ($p<0.05$) was observed. From a total of 61 metabolites that met these criteria (30.7% of all the metabolites identified in both species), 67.2% were due to a higher abundance in *L. donovani*. The two categories of compounds most represented in this group of metabolites were glycerophospholipids and amino acids (Fig. 3).

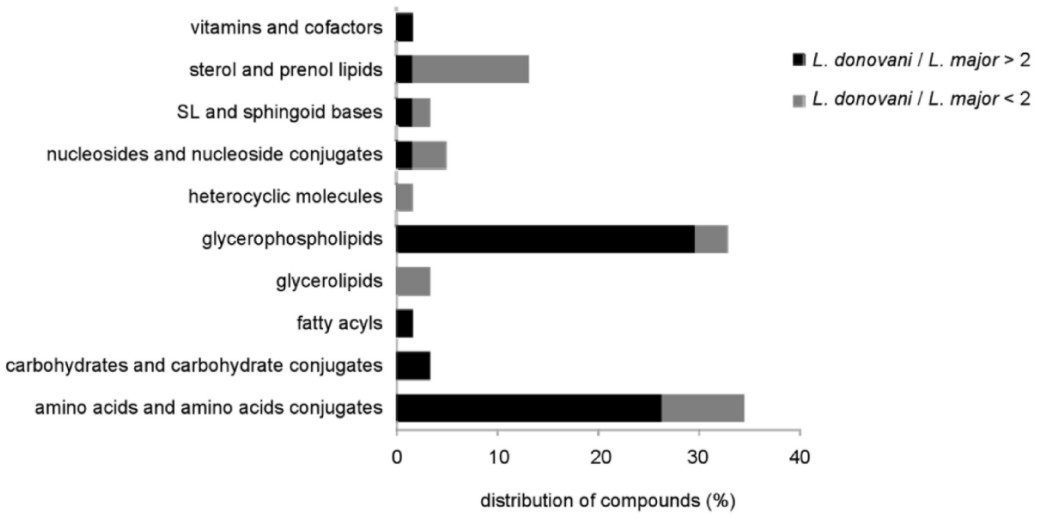

Figure 3. Metabolites significant different between *L. donovani* and *L. major*. *L. donovani* and *L. major* promastigotes were harvested after 5 days of *in vitro* growth and

cell extracts analyzed by LC-MS. Differences between *L. donovani* and *L. major* promastigotes were based on average intensity per 25 µg cell protein ratios between the two cell lines, with a 2-fold difference being required for inclusion in the dataset.

The significant differences observed between *L. donovani* and *L. major* are detailed in Fig. 4. Large differences were found between the two species in the abundance of some lipids, amino acids and derivatives. All glycerophospholipids identified as differing between the two species were present in higher levels in *L. donovani*, while the majority of significant metabolites identified as sterol or prenol lipids were detected in higher levels in *L. major.* Some of the most interesting differences detected concern amino acids and their metabolites. For example, proline, arginine and tryptophan were detected in higher levels in *L. major* than in *L. donovani* while homoserine, glutamine, aspartic acid and numerous aspartyl peptides were more abundant in *L. donovani*. Intracellular proline levels were higher in *L. major* than in *L. donovani,* the reverse being the case for glutamine; but there were no differences in the intracellular levels of glutamate (Fig. 4). Related to this, it was found that the levels of glutamic acid in the spent media were remarkably lower for *L. major* than for *L. donovani* (Table 2). Recent data for *L. mexicana* promastigotes suggest that glutamate uptake is minimal under standard *in vitro* culture conditions; the same study also suggested that the internalized glutamic acid is primary used for anabolic than catabolic functions as a precursor of other amino acids such as proline and glutamine [20]. Proline, however, can also be oxidized to glutamic acid and used as an energy substrates in *Leishmania* [21]. Thus our study has demonstrated clearly that there are some distinct species differences in amino acid metabolism and this suggests that further analysis should be undertaken to understand fully the subtlety of the species-specific metabolism of proline and glutamate. The higher levels of intracellular arginine and ornithine detected in *L. major* when compared to *L. donovani* (Fig. 4) may reflect differences in polyamines requirements and/or a higher rate of polyamines production in *L. major*. Arginine, as a polyamine biosynthesis precursor, is an essential amino acid [22] and *Leishmania* needs to acquire it from the medium. The finding that *L. major* promastigotes uptake more arginine from the culture medium than do *L. donovani* promastigotes (Table 2) is consistent with the higher intracellular levels of arginine and ornithine and also a potential difference in the production of polyamines and trypanothione.

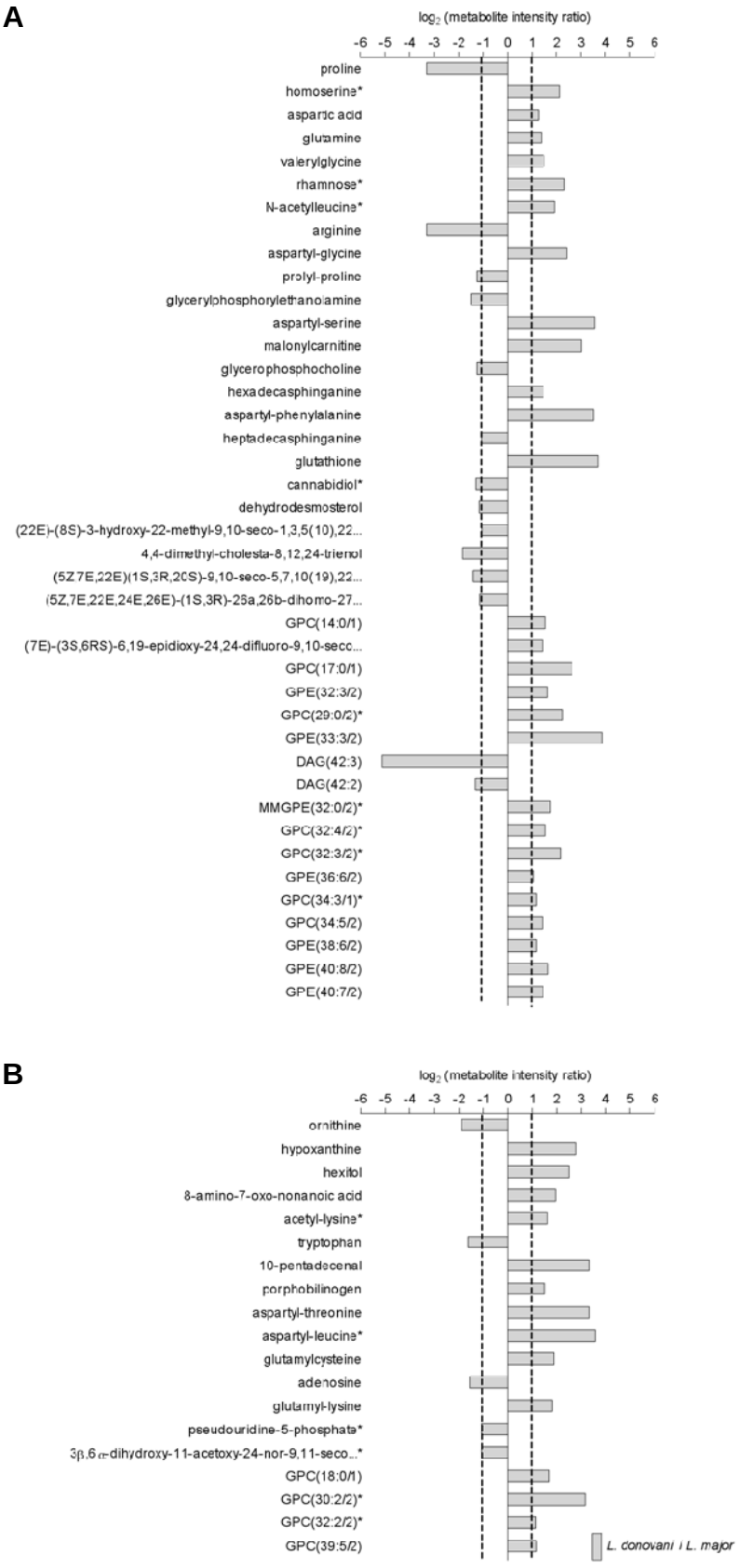

Figure 4. Intracellular metabolites with significantly different profiles between *L. donovani* and *L. major* promastigotes. The average signal intensity ratio of *L. donovani* / *L. major* for metabolites at significantly different levels identified using 1 ppm deviation

cut-off (A) or identified between 1 to 2 ppm deviation (B) were plotted following a logarithmic transformation (base 2). Metabolites labeled with * represent peaks with multiple potential identifications, for which just one is shown in this figure but the full list is given in the Supporting Information. Dotted lines represent the adopted cut-off for significant changes in a given metabolite profile: $\log_2$ (metabolite intensity ratio) below -1 or above 1 indicates a 2-fold change between the cell lines compared. All metabolites shown were statistically significant different between *L. donovani* and *L. major.*

Table 2 - Comparison of metabolites levels detected both in spent medium and culture medium of *L. donovani* and *L. major* promastigotes at day 5 of *in vitro* growth

	Average signal intensity					
	Cm		Sm		$\log_2$ (Sm / Cm)	
	L. donovani	***L. major***	***L. donovani***	***L. major***	***L. donovani***	***L.major***
glutamine	5.01E+06	5.34E+06	3.08E+06	3.73E+06	-0.70	-0.52
glutamic acid	2.62E+06	1.95E+06	7.45E+05	2.57E+04	-1.82	-6.24
arginine	8.99E+06	9.10E+06	6.66E+06	3.81E+06	-0.43	-1.26
tryptophan	4.51E+06	4.49E+06	3.44E+06	1.89E+04	-0.39	-7.90

L. donovani and *L. major* cell lines were seeded at $2.5x10^5$ parasites/ml and 5 days after *in vitro* growth spent culture medium (Sm) was harvested and analyzed by LC-MS. The data are the intensities obtained from the 5 µl samples of extracted supernant analyses as described in Material and Methods. Metabolite levels detected in Sm were compared with intensity levels detected in the initial culture medium (Cm); $\log_2$ (Sm/Cm) below -1 or above 1 indicates a 2-fold change between the samples compared.

Another interesting observation was the facts that *L. major* promastigotes had higher amounts of intracellular tryptophan and, remarkably, there was 180-fold lower level of this amino acid in the spent culture medium (Sm) of *L. major* compared with that of *L. donovani* (Table 2 and Fig. 5). Comparison with the culture medium (Cm) itself shows that tryptophan appears to be taken up extensively by *L. major* but not at all by *L. donovani*. Tryptophan is an essential amino acid in mammals but little is known about its metabolism in *Leishmania*. It was reported that it is not used as a carbon energy source by *L. donovani* but that it is catabolised to indole-3-lactate [23], the latter pathway was also predicted from the genome analysis of *L. major* [21]. Indole-3-lactate levels were, however, very similar in *L. major* and *L. donovani* and also in their Sm (Fig. 5). Another major catabolic route for tryptophan in some cells is via kynurenine to generate kynurenic

acid, anthranilate or NAD [24,25]. However, these metabolites also were at similar levels in the two species and their Sm. Indeed, a recent report has shown that *L. infantum* is a NAD^+ auxotroph and relies on the environmental supply of exogenous precursors to synthesize NAD^+ by a salvage pathway [26]. They showed that the parasite cannot perform de novo synthesis and that addition of exogenous tryptophan had no effect on the intracellular NAD^+ content [26]. Our data, however, showing different metabolic patterns for *L. donovani* and *L. major* (Table 2 and Fig. 5) reveal some marked differences in the uptake or release of the metabolites by the two species. Most dramatic is the finding that the tryptophan levels in the Sm of *L. major* were about 240-fold lower than in the initial culture medium, while no significant changes were detected for *L. donovani* (1.3-fold lower). Thus there was a remarkable uptake of tryptophan by *L. major* promastigotes. These two metabolites were also higher in *L. major* cell extracts compared with those of *L. donovani* (Fig. 4). Furthermore, differences between the lines were found for metabolites that potentially are produced from tryptophan (Fig. 5), suggesting possible differences in the route used by the parasites to metabolize this amino acid. Kynurenine and anthranilate were present in lower levels in *L. major* Sm while indole-3-lactate and kynurenic acid were at greater levels in *L. major* Sm (Fig. 5). These data strongly suggest that there are species differences in this area of metabolism with *L. major* having greater metabolic capacity than *L. donovani* or *L. infantum*, however further analysis is required to obtain a full understanding of this variation.

Overall the differences in the amino acids levels in *L. donovani* and *L. major* presumably reflect the differing metabolism of the species, but this also will be affected by the conditions. Snapshot data such as those obtained in this study always have to be interpreted carefully and the recent demonstration that de novo synthesis of serine, glycine and proline was repressed in the presence of exogenous amino acids provides a good example of the complex interplay that exists [20]. However, the data that we have generated so far provide a framework within which to conduct the further studies.

Another interesting difference detected between the two species in this analysis is the higher abundance of aspartyl dipeptides in *L. donovani* than in *L. major* (Fig. 4). The explanation for this is unclear, but it seems likely that they result from the activity of dipeptidases about which little is known currently but presumably they may be important components of the hydrolysis of proteins and the differing levels between the two species suggest that these are not identical in the two species.

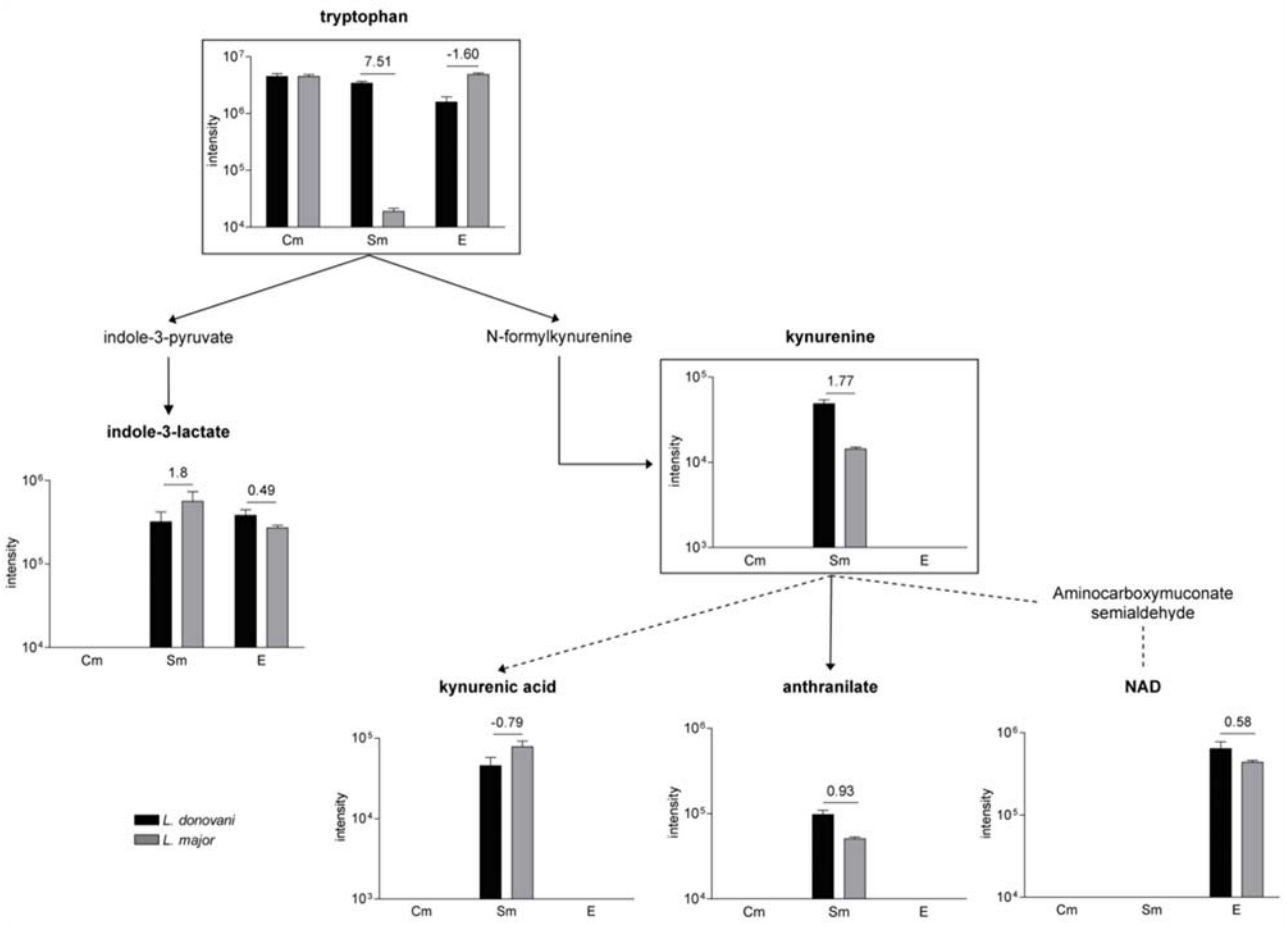

Figure 5. Comparison of tryptophan and derivative metabolite levels between *L. donovani* and *L. major* promastigotes. *L. donovani* and *L. major* promastigotes were harvested after 5 days of *in vitro* growth and cell extracts (E) or spent media (Sm) analyzed by LC-MS; initial culture medium (Cm) was also analyzed by LC-MS. Intensity levels of tryptophan and derivatives (indole-3-lactate, kynurenine, anthranilate, NAD, kynurenic acid) are shown. Graphs within boxes represent metabolites for which at least a 2-fold difference between *L. donovani* and *L. major* was observed. Key: dotted line, multiple steps; dotted arrow, not reported in *Leishmania*; values above the bars correspond to the average intensity ratio between *L. donovani* and *L. major* following logarithmic transformation (base 2) for E, Sm or Cm. Data are means from four biological replicates ± standard deviation.

Much of the current knowledge about *Leishmania* metabolic pathways has been inferred from the genome sequences and is based on what occurs in other organisms, so it is necessary to obtain experimental evidences to confirm the functioning of the described pathways or gain insights into possible new ones. This study is a step towards this goal

although further analyses, especially involving amastigotes, are required in order to discover all of the crucial components of each *Leishmania* species that lead to the distinctive clinical outcomes.

Acknowledgments

We thank: Malcolm McConville and colleagues (Melbourne) for excellent guidance on the methods of sample preparation for the metabolomics analyses; Ruben t'Kindt (ITM, Antwerp, and Strathclyde) for assistance with the sample preparation method for the metabolomics analyses; Dave G Watson and Alex Zhang (Strathclyde) for help with the LC-MS technology. The study was supported by Fundação para a Ciência e Tecnologia (FCT) project number PTDC/CVT/65047/2006 and AMS is supported by FCT grant SFRH/BD/28316/2006.

References

1. Kedzierski L (2010) Leishmaniasis Vaccine: Where are We Today? J Glob Infect Dis 2: 177-185.
2. Pearson RD, Sousa AQ (1996) Clinical spectrum of Leishmaniasis. Clin Infect Dis 22: 1-13.
3. Gangneux JP, Sulahian A, Honore S, Meneceur P, Derouin F, et al. (2000) Evidence for determining parasitic factors in addition to host genetics and immune status in the outcome of murine *Leishmania infantum* visceral leishmaniasis. Parasite Immunol 22: 515-519.
4. Wilson ME, Jeronimo SM, Pearson RD (2005) Immunopathogenesis of infection with the visceralizing *Leishmania* species. Microb Pathog 38: 147-160.
5. Lynn MA, McMaster WR (2008) *Leishmania*: conserved evolution--diverse diseases. Trends Parasitol 24: 103-105.
6. Peacock CS, Seeger K, Harris D, Murphy L, Ruiz JC, et al. (2007) Comparative genomic analysis of three *Leishmania* species that cause diverse human disease. Nat Genet 39: 839-847.
7. Downing T, Imamura H, Decuypere S, Clark TG, Coombs GH, et al. (2011) Whole genome sequencing of multiple *Leishmania donovani* clinical isolates provide insights into population structure and mechanisms of drug resistance. Genome Res 21:2143-2156.

8. Rogers MB, Hilley JD, Dickens NJ, Wilkes J, Bates PA, et al. (2011) Chromosome and gene copy number variation allow major structural change between species and strains of *Leishmania*. Genome Res 21: 2129-2142.

9. Zhang WW, Mendez S, Ghosh A, Myler P, Ivens A, et al. (2003) Comparison of the A2 gene locus in *Leishmania donovani* and *Leishmania major* and its control over cutaneous infection. J Biol Chem 278: 35508-35515.

10. Zhang WW, Matlashewski G Screening *Leishmania donovani*-specific genes required for visceral infection. Mol Microbiol 77: 505-517.

11. Kaddurah-Daouk R, Kristal BS, Weinshilboum RM (2008) Metabolomics: a global biochemical approach to drug response and disease. Annu Rev Pharmacol Toxicol 48: 653-683.

12. t'Kindt R, Jankevics A, Scheltema RA, Zheng L, Watson DG, et al. (2010) Towards an unbiased metabolic profiling of protozoan parasites: optimisation of a *Leishmania* sampling protocol for HILIC-orbitrap analysis. Anal Bioanal Chem 398: 2059-2069.

13. t'Kindt R, Scheltema RA, Jankevics A, Brunker K, Rijal S, et al. (2010) Metabolomics to unveil and understand phenotypic diversity between pathogen populations. PLoS Negl Trop Dis 4: e904.

14. Olszewski KL, Mather MW, Morrisey JM, Garcia BA, Vaidya AB, et al. (2010) Branched tricarboxylic acid metabolism in *Plasmodium falciparum*. Nature 466: 774-778.

15. Olszewski KL, Morrisey JM, Wilinski D, Burns JM, Vaidya AB, et al. (2009) Host-parasite interactions revealed by *Plasmodium falciparum* metabolomics. Cell Host Microbe 5: 191-199.

16. Rijal S, Yardley V, Chappuis F, Decuypere S, Khanal B, et al. (2007) Antimonial treatment of visceral leishmaniasis: are current *in vitro* susceptibility assays adequate for prognosis of *in vivo* therapy outcome? Microbes Infect 9: 529-535.

17. McConville MJ, Turco SJ, Ferguson MA, Sacks DL (1992) Developmental modification of lipophosphoglycan during the differentiation of *Leishmania major* promastigotes to an infectious stage. EMBO J 11: 3593-3600.

18. Sacks DL, Pimenta PF, McConville MJ, Schneider P, Turco SJ (1995) Stage-specific binding of *Leishmania donovani* to the sand fly vector midgut is regulated by conformational changes in the abundant surface lipophosphoglycan. J Exp Med 181: 685-697.

19. Depledge DP, Evans KJ, Ivens AC, Aziz N, Maroof A, et al. (2009) Comparative expression profiling of *Leishmania*: modulation in gene expression between species and in different host genetic backgrounds. PLoS Negl Trop Dis 3: e476.

20. Saunders EC, Ng WW, Chamber JM, Ng M, Naderer T, et al. (2011) Isoptopomer profiling of *Leishmania mexicana* promastigotes reveals important roles for succinate fermentation and aspartate uptake in TCA cycle anaplerosis, glutamate synthesis and growth. J Biol Chem.
21. Opperdoes FR, Coombs GH (2007) Metabolism of *Leishmania*: proven and predicted. Trends Parasitol 23: 149-158.
22. Colotti G, Ilari A (2011) Polyamine metabolism in *Leishmania*: from arginine to trypanothione. Amino Acids 40: 269-285.
23. Leelayoova S, Marbury D, Rainey PM, Mackenzie NE, Hall JE (1992) *In vitro* tryptophan catabolism by *Leishmania donovani* donovani promastigotes. J Protozool 39: 350-358.
24. Foster JW, Moat AG (1980) Nicotinamide adenine dinucleotide biosynthesis and pyridine nucleotide cycle metabolism in microbial systems. Microbiol Rev 44: 83-105.
25. Gazzaniga F, Stebbins R, Chang SZ, McPeek MA, Brenner C (2009) Microbial NAD metabolism: lessons from comparative genomics. Microbiol Mol Biol Rev 73: 529-541, Table of Contents.
26. Gazanion E, Garcia D, Silvestre R, Gerard C, Guichou JF, et al. (2011) The *Leishmania* nicotinamidase is essential for NAD(+) production and parasite proliferation. Mol Microbiol.

Supporting Information

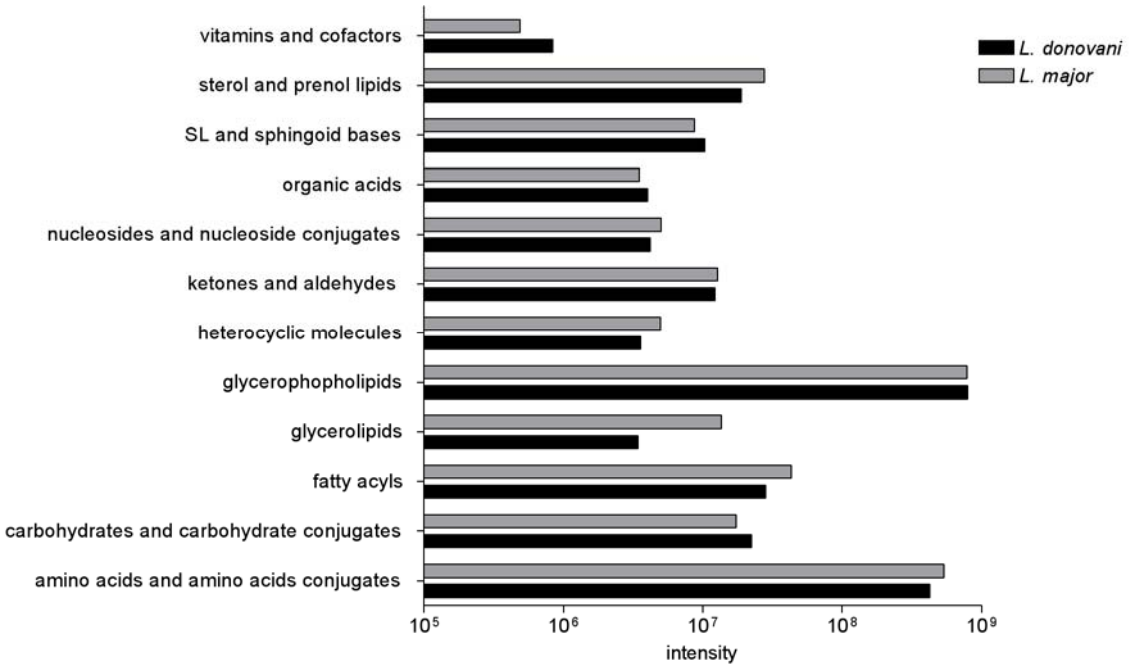

Figure S1. Overall intracellular metabolite levels for each compound category in *L. donovani* and *L. major* promastigotes. Sum of total intracellular metabolite intensities from *L. donovani* and *L. major* promastigotes identified by LC-MS analysis at day 5 of *in vitro* growth grouped by compound categories: vitamins and cofactors, sterol and prenol lipids, sphingolipids (SL) and sphingoid bases, organic acids, nucleosides and nucleoside conjugates, ketones and aldehydes, heterocyclic molecules, glycerophospholipids, glycerolipids, fatty acyls, carbohydrates and carbohydrate conjugates, amino acids and amino acid conjugates.

Table S1 – Metabolites identified below 1 ppm deviation in samples of *L. donovani* and *L. major* promastigotes at day 5 of *in vitro* growth. For each compound the following information is shown: ionisation (ESI) mode; detected mass; retention time (min); putative metabolite identification; ppm deviation between detected mass and theoretical mass of the putative metabolite identified; intensity per 25 µg cell protein for each sample; average intensity per 25 µg cell protein in each cell line ; standard deviation in each cell line; ratio of average intensity per 25 µg cell protein between the different cell lines; Student's T test *L. donovani* versus *L. major* indicating whether or not there was a statistically significant difference; decision on whether or not the compound was significantly changed in level based on a two-fold or higher average difference in signal intensity and statistical significant (p<0.05) between *L. donovani* and *L. major*; compound category.

Table S2 – Metabolites identified between 1-2 ppm deviation in samples of *L. donovani* and *L. major* promastigotes at day 5 of *in vitro* growth. The data presented are as described for Table S1.

Tables S1 and S2 are available in the electronic version of the thesis.

CHAPTER 5

DISCUSSION AND PERSPECTIVES

Leishmaniasis, a vector-borne parasitic disease that affects millions of people, mainly the world's poorest ones, is considered a neglected tropical disease, together with other infections such as Chagas disease and schistosomiasis. The fact that the number of annual deaths does not mirror the impact in the populations is the main reason why neglected tropical diseases have been neglected as important public health threats. Although, taking into account that this group of diseases elicits chronic morbidity without causing death, leading to millions of disabled people, the level of importance is equivalent to other diseases such as malaria or HIV/AIDS. The lack of economic opportunity offered by neglected tropical diseases to multinational pharmaceutical companies, as the diseases occur almost exclusively in developing countries, has contributed to the slow progress in the development of new diagnostic tools, drugs and vaccines that could lead ultimately to the eradication of the diseases[558]. Thus as an aid to tackling these devastating diseases, researchers have embarked on the study of the parasites' cell biology and evaluation of the strategies and requirements necessary for the parasites to invade successfully, survive and persist inside mammalian hosts.

In the recent years many progresses have been achieved in *Leishmania* research, both due to the annotation of the genome sequence of different *Leishmania* species[203, 204, 210] and the development of tools such as proteomics and metabolomics and the application of these to the study of the parasite[559, 560]. The primary goal underlying the comparison of *Leishmania* genomes has been the search for species-specific genes that could explain the differences in the clinical outcome induced by visceral and cutaneous species. Surprisingly, however, just a few species-specific genes were identified[202], highlighting the fact that *Leishmania* parasites possess other means such as regulation of protein expression by post-translational modifications that are crucial for adaptation to different environments during its life cycle[281, 282]. In addition, the recent genome analyses describe other ways by which *Leishmania* species can differ rather than by the absence or presence of certain genes. Variations in chromosome copy number or gene dosage are potential contributors for *Leishmania* genetic plasticity and diversity[203, 204]. *Leishmania* genome plasticity had been previosuly experienced during attempts to delete essential genes[252-254, 426, 561-564] or in drug resistance strains[255, 256], but aneuploidy was recently reported as a natural genomic feature in different *Leishmania* species[203, 204]. As the parasite regulates protein expression mainly at post-transcriptional levels, proteomics should provide insights into the mechanisms of differentiation, virulence and drug resistance. Indeed, proteomics analysis has been used to compare the protein expression profiles of different *Leishmania* developmental stages[221, 227, 242, 244, 245], to investigate protein secretion[565], to carry out serum protein profiling during visceral leishmaniasis[566], to

identify novel antigens for development of new diagnostic tools and vaccines and to investigate the changes in protein expression in attenuated or drug-resistant cell lines [567-569]. However, the methods need to be developed further since using the current ones results in membrane proteins being under represented and the lack of sensitivity leads to the over-representation of the most abundant proteins[560]. Metabolomics, now seen as an emergent area in the study of parasites, mainly due to the development of new methods and use of better technology[201, 206-209, 559, 570-572], has been quite extensively applied to study other diseases, such as cancer, with the aim of identifying disease biomarkers for establishing preventative or therapeutic approaches[205]. Since the interaction between metabolites and specific targets is dynamic, an integrated analysis of metabolomics and other -omics may provide an excellent opportunity to detect changes not possible to determine when studying just one component of the cell by itself. It is thought that metabolomics approaches will allow the detection of subtle changes in the cell biology of the parasite that are crucial for its adaptation and survival but that would not be detected by other means. Although, the challenges posed by an integrative analysis are enormous, mainly due to the high flux and rapid turnover of metabolites, the potential of this kind of approach for improving the understanding of *Leishmania* cell biology are also huge, since it is expected to provide a "real time picture" of "what is happening" in a cell under different situations.

On the other hand, recent advances in understanding the parasite-host interaction have elucidated the role of different cells and molecules of the immune system during the early phase of *Leishmania* infection, this is particularly important as the nature of the early parasite-host interactions will influence the parasite-specific adaptive immune responses and ultimately the outcome of the disease (reviewed by Kaye P. and Scott P.[573]). Furthermore, the generation of transgenic parasites expressing firefly luciferase and/or fluorescent proteins have expanded the capacity to detect and quantify the parasite in different experimental situations, in particularly the *in vivo* imaging of the transgenic parasites in a live host [574, 575], which can be used to screen potential chemotherapy drugs and vaccines. Vaccines formulations comprising the whole live, killed, attenuated or genetically modified parasites and also recombinant proteins have been evaluated, alone or in the presence of adjuvants and using different delivery systems. Even though considerable progresses in the understanding of the mechanisms involved in protective immunity have been made, the lack of correlation between vaccine efficacy in the mouse model and humans is still a major problem. Experimental vaccines have frequently failed to confer significant protection against natural exposure in people, suggesting that the parameters considered such as the generation of Th1 responses and the reduction of

lesion size and/or parasite number following mice infection may not necessarily mimic the requirements for protection against natural transmission in humans.

Advances in the understanding of *Leishmania* cell biology and the nature of the parasite-host interactions have been great in recent years, nevertheless there is no human vaccine currently available and chemotherapy is far from being satisfactory, with associated high costs and an alarming increase in drug resistance[84-86].

In this study were used different approaches to gain insights into the role of TDR1 in visceral species of *Leishmania*, *L. infantum* and *L. donovani*. TDR1, first identified in *L. major*, shows high conservation within the different *Leishmania* species, suggestive of an important role in the parasite. TDR1 possesses an unusual two domain nature with active sites characteristic of Grx and GSTO and is able to use GSH as the reductant to catalyze thiol transferase and dehydroascorbate reductase activities. The enzyme was implicated in the activation of pentavalent antimonials by its reduction to the toxic form, although this was not shown to occur *in vivo*[90]. Indeed, analysis of *TDR1* gene expression in *L. braziliensis* and *L. guanyensis* parasites isolated from patients with different antimonial treatment outcomes showed no differences in the expression levels[576], although this result should be interpreted with caution as mRNA levels often do not mirror protein expression in *Leishmania*. Another enzyme identified in *L. major*, an arsenate reductase known as ACR2, was reported to be involved also in pentavalent antimonial reduction and expression in *L. infantum* promastigotes led to an increase in the sensitivity of intracellular amastigotes to the drug[91]. The ability to reduce pentavalent antimonials clearly could only be a side-activity of TDR1's main role in the cell. There is high similarity between TDR1 and a *T. cruzi* enzyme named Tc52, which was previously reported as an excreted/secreted protein able to modulate the host's immune response to infection and consequently considered a virulence factor[555, 577]. Moreover, deletion of both *Tc52* alleles was not possible showing the essentiality of the gene for parasite survival[578]. These findings led us to investigate whether TDR1 could have a similar role in *Leishmania* parasites, through the evaluation of the immune response induced by the recombinant protein and its potential to elicit protection in Balb/c mice from infection *with L. infantum* promastigotes. In addition, in order to get definitive data on the role of TDR1 in visceral *Leishmania* species (*L. infantum* and *L. donovani*), we attempted to generate *TDR1* null mutants by homologous recombination, a strategy commonly used to delete *Leishmania* genes[249] to study their role. This is the most common approach with this parasite, as interference RNA (RNAi) does not operate in these parasites, apart from *L. braziliensis*, due to the lack of RNAi machinery[579].

As reported previously for *L. major*[90], TDR1 expression in *L. infantum* parasites is higher in the amastigote forms, which could indicate a specific role for the protein in the intracellular stage of the parasite [Chapter 4, section 4.2]. Moreover, we have detected TDR1 in *L. infantum* promastigotes and amastigotes spent medium, which could suggest a role for TDR1 in the interaction with the host. Recently was shown that *Leishmania* release exosomes which contain a surprisingly large number of proteins from a wide range of cellular pathways[279] and thus TDR1 may be included in these structures although it was not found in the study[279]. Balb/c immunization with rTDR1 led to an increase in CD8-T cell splenic population and a decrease in IL-10 production in the chronic phase of infection; however this was not sufficient to elicit high levels of protection. The high levels of IgG1 in the serum of rTDR1-immunized mice suggest a dominance of Th2 response, resulting in weak protection against infection, although the role of antibodies in *Leishmania* infection is still controversial. In many cases, purified antigens are weak immunogens and the immune response generated is not of a sufficient magnitude to confer immunity. We have attempted to enhance the levels of protection induced by TDR1 through the use of an adjuvant, CpG, and a DNA vaccine encoding the protein, which lead to the expression of *Leishmania* antigens folded in its native conformation, potentially with unaltered antigenicity, stimulating both cellular and humoral immune reponses due to the ability of DC to present the encoded antigen in the context of MHC class I and MHC class II[117, 147]. However, neither immunization of rTDR1 in the presence of CpG or delivery as a DNA vaccine improved the levels of protection obtained with the protein alone [Chapter 4, section 4.2]. Clearly TDR1 does not have a significant effect on the immune response to infection as that observed for *T.cruzi* Tc52, whose similarity led us to perform this study, showing that it has a different role in the parasite and host-parasite interaction.

The generation of viable *L. infantum* and *L. donovani TDR1* null mutants has shown that the gene is not essential in either species [Chapter 4, sections 4.3 and 4.4] and highlighted a “new reality” in the genomic plasticity and diversity of *Leishmania* parasites, which clearly demonstrates the existence of aneuploidy as a natural genomic feature more common than reported previously; indeed the *Leishmania* genome has been considered to be predominantly diploid. Deletion of *L. donovani TDR1* was only achieved after 3 rounds of transfection due to the presence of three copies of the gene, while *L. infantum TDR1* null mutants were obtained after 2 and 4 rounds, suggesting variable ploidy in the *L. infantum* population. Previous studies have reported aneuploidy during attempts to delete genes by homologous recombination, described as a strategy used by *Leishmania* parasites to maintain essential genes[252-254]; clearly not the case of *TDR1* gene; with exceptions of *L. major* chromosome 1 trisomy[250] and chromosome 31

tetraploidy[56]. *Leishmania* genomic plasticity through chromosome copy number variation as a natural genomic feature was not suggested until Sterkers and co-workers[264] described a phenomenon, named chromosomal moisacism, in which every chromosome was observed in at least 2 ploidy states. Subsequently, genome sequence analysis of *L. donovani* and *L. braziliensis* as well as new refined versions of *L. major*, *L. infantum* and *L. braziliensis* genomes, using improved technologies, allowed the detection of genomic features not described in the previous genome sequence analysis[202, 210] and provided evidence for natural aneuploidy[203, 204]. The consequences of chromosome and gene copy number variations are not yet fully understood, but this feature of the *Leishmania* genome shows that evolution is driven by large structural changes, which are generally detrimental for other organisms. Clearly this is not so for *Leishmania*, which copes well with aneuploidy and presumably takes advantage from it. This unusual variation is not only observed between species but also among strains and is likely to be important in the ability of *Leishmania* to cause disease and also be involved in drug resistance[203, 204].

Generation of the *L. donovani TDR1* null mutant and respective add-back cell lines, necessary to control for any phenotypic changes not due to the gene deletion, allowed the analysis of *L. donovani* phenotype in the absence of *TDR1* [Chapter 4, section 4.4]. Based on TDR1 *in vitro* activities and similarities to GSTO, a natural approach was to test the susceptibility of *TDR1* null mutant parasites to oxidative and nitrosative stress as well as to metal-related compounds. GSTs play a key role in the detoxification of a wide range of toxic molecules, including products resulting from oxidative stress as well as exogenous products such drugs, through the conjugation with GSH[431-433, 435]. In order to survive, *Leishmania* parasites need to cope with the macrophage oxidative burst, thus it could be predicted that an enzyme with such characteristics as TDR1 would play an important role in the parasite's survival against this. However, TDR1's similarity with GSTO lead us to predict that TDR1 may have another role in the cell, as this class of GSTs possess characteristics of Grxs[437]. Indeed, *TDR1* null mutants did not show an increase in susceptibility to oxidative and nitrosative stress, demonstrating that TDR1 is not involved in the parasite's defense against this kind of stresser. In fact this result was not unexpected since the parasite has a wide range of proteins, such as tryparedoxins, tryparedoxin peroxidase, trypanothione S-transferase, ascorbate peroxidase, and also low molecular mass thiols, which have a crucial role in the parasite antioxidant defense[364, 580]. Although, *TDR1* null mutants were more sensitivity to trivalent antimony and trivalent arsenite than the WT parent cell line, which could suggest an involvement of TDR1 in drug detoxification, no differences were detected in the susceptibility of *Leishmania* infected

macrophages to treatment with SSG and thus the results did not support the role of TDR1 in drug reduction and activation nor as a detoxifying enzyme.

The opportunity to evaluate the changes induced by *TDR1* deletion in *L. donovani* promastigotes through the use of an untargeted metabolomics approach facilitated the detection of changes that suggested TDR1's involvement in the redox regulation of enzymes. As mentioned above, untargeted metabolomics provides a "real time picture" of the cell and thus changes that would not be detect by other techniques or not considered as a hypothesis are likely to be identified. This is particularly relevant to situations in which major phenotypic differences are not observed after gene deletion due to the fact that the cell is able to cope with the subtle changes and the approach has a lot to offer in understanding how cells adapt to different challenges.

Analyses of the *TDR1* null mutant metabolome revealed few but specific changes in the levels of metabolites participating in *Leishmania* energy and amino acid metabolism, consistent with a possible role of TDR1 in enzyme redox regulation. In other organisms, metabolic reconfiguration has been attributed to the inactivation of enzymes through S-glutathionylation, a post-translational modification which is promoted and readily reversed by Grxs and GSTs[464, 507, 540, 581]. S-glutathionylation induces functional changes in target proteins, either activation or inhibition, leading to alteration of cellular pathways in response to oxidative stress. Moreover, S-glutathionylation can occur under physiological conditions as a redox-regulatory mechanism[502, 582, 583]. The use of protein post-translational modifications by *Leishmania* parasites fits well with the fact that the parasite seems genetically pre-adapted to the different life stages, supported by the high degree of genome conservation and synteny between the different *Leishmania* species and the identification of few species-specific genes despite the distinct clinical outcomes[202]. Rosenzweig and co-workers have reported the use of post-translational modifications such as phosphorylation and methylation during *L. donovani* differentiation[281]. Thus, it is seems entitrely feasible that the parasite uses S-glutathionylation to regulate the expression of certain enzymes, depending on the environmental conditions, as a mechanism to cope with changes in nutrient availability, temperature and pH among others, and to survive successfully in different hosts. Although S-glutathionylation has been extensively reported to occur in mammals[516, 517, 529, 584], plants[518, 524], yeast[585], green algaes[586] and also in *P. falciparum*[587] and *T. brucei*[419], the effect of *S*-glutathionylation on enzyme activity and subsequently cellular function *in vivo* remains to be elucidated and this type of modification has not yet been reported in *Leishmania.* Indeed, we were able to add experimental support to our metabolomics driven hypothesis, by the demonstration

that TDR1 is able to catalyse the reduction of glutathionylated protein and peptide substrates *in vitro*. Although, TDR1 can efficiently catalyze deglutathionylation, the low affinity for the peptide used in this study compared with *Leishmania* Grx1, suggests substrate specificity and thus the involvement of TDR1 in the regulation of specific enzymes, a characteristic already reported for *T. brucei* and *Chlamydomonas reinhardtii* Grxs. This may explain why many organisms have a specialized set of glutaredoxin isoforms located in various cellular compartments and with distinct roles[496, 540, 588, 589].

The fact that the *TDR1* null mutant was able to infect macrophages *in vitro* and mice as well as the WT parent line shows that the gene is not essential for parasite virulence and survival, even though changes at a metabolome level were detected. Indeed, the growth conditions used for the *L. donovani TDR1* null mutant (a rich medium, where both glucose and amino acids are abundant) may have masked the effect of gene deletion, and the metabolic re-configuration that we discovered as an adaptation mechanism for survival may not be possible in the natural *Leishmania* environment, when glucose or amino acids are scarce.

Throughout the development of the work presented in this thesis, metabolomics analysis applied to *Leishmania* parasites undertook an enormous evolution which involved improvements in the experimental protocols enabling the extraction of *Leishmania* promastigotes metabolites, together with the increase in sensitivity and resolution of LC-MS and also the development of software to help in the identification of *Leishmania* metabolites[201, 206, 207, 570]. Despite not initially being part of the thesis work plan, the opportunity to apply this new methodology to characterize the *TDR1* null mutants, as described above, brought clear advantages to the study. Thus, we have carried out the characterization of *L. donovani* WT promastigotes development *in vitro* [Chapter 4, section 4.6] as well as a comparison between a visceral (*L. donovani*) and a cutaneous (*L. major*) *Leishmania* species [Chapter 4, section 4.7] at a metabolome level, although the latter is still work in progress.

Analysis of *L. donovani* promastigotes during *in vitro* growth, particularly following the changes that occur as the parasite differentiates from procyclic (logarithimic phase) to metacyclic forms (stationary phase), should provide valuable information on the requirements for the development of *Leishmania* infective forms and consequently lead to a better understanding of the mechanisms underlying a successful differentiation into the intracellular amastigote forms. Indeed, we were able to show that the metabolome of *L. donovani* promastigotes undergo significant changes, supporting the existence of different

developmental promastigotes stages[590], related with adaptations to the nutrient availability and also metacyclogenesis, which includes some known biochemical changes such as lipophosphoglycan and surface protein expression, vital for a successful transmission to the mammalian host[7, 591-594]. Promastigotes in logarithmic phase were significantly distinct from stationary phase parasites reflecting, as expected, two different populations from active to non-dividing cells. Parasite remodelling was highlighted by the significant structural changes observed in glycerophospholipids and increase in sphingolipids, already shown to be essential for parasite differentiation[335]. Furthermore, it was possible to link some of metabolome data with previous results obtained either through genomic or proteomic analysis, increasing our knowledge about the changes underlying promastigotes development. The data that were obtained clearly support the concept of studying *Leishmania* and other parasites through the use of an -omics integrative approach.

Overall, the study detailed in this thesis has generated important information about the potential role of TDR1 *in vivo* and also the application of new metabolomes approaches to characterize *Leishmania* null mutants as well as different developmental stages of the parasite.

Following this work, further investigation should address the importance of TDR1 as a deglutathionylating enzyme *in vivo*, through the identification of TDR1-specific target proteins and the effect of TDR1 on the target proteins' activities. This will elucidate whether *Leishmania* employs *S*-glutathionylation for regulatory or protection purposes. This has not yet been reported for *Leishmania*, but has been reported to occur in a wide range of organisms including *P. falciparum* and *T. brucei* parasites. Such analyses would also be likely to prove a new role for the considerable levels of free glutathione that occur in trypanosomatids. These organisms differ form others in possessing trypanothione as their main low molecular weight thiol. This leads to the inevitable question, yet to be resolved, of whether trypanothione can form a mixed-disulfide bridge with an accessible free thiol on a protein, protecting specific cysteine residues from irreversible oxidation, or modulating protein activities.

Undoubtedly a better understanding of how the parasite regulates many cellular processes through the use of post-translational modifications such as S-glutathionylation will lead to a rethink of the ways in which we can challenge the parasite through exploiting new drug targets.

BIBLIOGRAPHY

1. Bari Au. Chronology of cutaneous Leishmaniasis: An overview of the history of the disease. Journal of Pakistan Association of Dermatologists 2006.

2. Sacks D, Kamhawi S. Molecular aspects of parasite-vector and vector-host interactions in Leishmaniasis. Annu Rev Microbiol 2001;55:453-83.

3. Pearson RD, Sousa AQ. Clinical spectrum of Leishmaniasis. Clin Infect Dis 1996 Jan;22(1):1-13.

4. Banuls AL, Hide M, Prugnolle F. *Leishmania* and the Leishmaniases: a parasite genetic update and advances in taxonomy, epidemiology and pathogenicity in humans. Adv Parasitol 2007;64:1-109.

5. Bates PA. Transmission of *Leishmania* metacyclic promastigotes by phlebotomine sand flies. Int J Parasitol 2007 Aug;37(10):1097-106.

6. WHO. Control of the Leishmanises:report of a meeting of the WHO Expert Committee on the Control of Leishmaniases. WHO Technical Report Series 2010 2010.

7. Kamhawi S. Phlebotomine sand flies and *Leishmania* parasites: friends or foes? Trends Parasitol 2006 Sep;22(9):439-45.

8. Waller RF, McConville MJ. Developmental changes in lysosome morphology and function *Leishmania* parasites. Int J Parasitol 2002 Nov;32(12):1435-45.

9. Besteiro S, Williams RA, Coombs GH, Mottram JC. Protein turnover and differentiation in *Leishmania*. Int J Parasitol 2007 Aug;37(10):1063-75.

10. Chang PC. The ultrastructure of *Leishmania donovani*. J Parasitol 1956 Apr;42(2):126-36.

11. Clayton C, Hausler T, Blattner J. Protein trafficking in kinetoplastid protozoa. Microbiol Rev 1995 Sep;59(3):325-44.

12. Landfear SM, Ignatushchenko M. The flagellum and flagellar pocket of trypanosomatids. Mol Biochem Parasitol 2001 Jun;115(1):1-17.

13. McConville MJ, Mullin KA, Ilgoutz SC, Teasdale RD. Secretory pathway of trypanosomatid parasites. Microbiol Mol Biol Rev 2002 Mar;66(1):122-54; table of contents.

14. Ginger ML, Portman N, McKean PG. Swimming with protists: perception, motility and flagellum assembly. Nat Rev Microbiol 2008 Nov;6(11):838-50.

15. Krishnamurthy G, Vikram R, Singh SB, Patel N, Agarwal S, Mukhopadhyay G, et al. Hemoglobin receptor in *Leishmania* is a hexokinase located in the flagellar pocket. J Biol Chem 2005 Feb 18;280(7):5884-91.

16. de Souza W. Special organelles of some pathogenic protozoa. Parasitol Res 2002 Dec;88(12):1013-25.

17. Liu B, Liu Y, Motyka SA, Agbo EE, Englund PT. Fellowship of the rings: the replication of kinetoplast DNA. Trends Parasitol 2005 Aug;21(8):363-9.

18. Liu Y, Englund PT. The rotational dynamics of kinetoplast DNA replication. Mol Microbiol 2007 May;64(3):676-90.

19. Stuart K, Panigrahi AK. RNA editing: complexity and complications. Mol Microbiol 2002 Aug;45(3):591-6.

20. Michels PA, Bringaud F, Herman M, Hannaert V. Metabolic functions of glycosomes in Trypanosomatids. Biochim Biophys Acta 2006 Dec;1763(12):1463-77.

21. Haanstra JR, van Tuijl A, Kessler P, Reijnders W, Michels PA, Westerhoff HV, et al. Compartmentation prevents a lethal turbo-explosion of glycolysis in Trypanosomes. Proc Natl Acad Sci U S A 2008 Nov 18;105(46):17718-23.

22. Alexander J, Satoskar AR, Russell DG. *Leishmania* species: models of intracellular parasitism. J Cell Sci 1999 Sep;112 Pt 18:2993-3002.

23. Bates PA, Rogers ME. New insights into the developmental biology and transmission mechanisms of *Leishmania*. Curr Mol Med 2004 Sep;4(6):601-9.

24. Kaye P, Scott P. Leishmaniasis: complexity at the host-pathogen interface. Nat Rev Microbiol 2011;9(8):604-15.

25. Bates PA. *Leishmania* sand fly interaction: progress and challenges. Curr Opin Microbiol 2008 Aug;11(4):340-4.

26. Killick-Kendrick R. The biology and control of phlebotomine sand flies. Clin Dermatol 1999 May-Jun;17(3):279-89.

27. Kato H, Gomez EA, Caceres AG, Uezato H, Mimori T, Hashiguchi Y. Molecular epidemiology for vector research on Leishmaniasis. Int J Environ Res Public Health 2010 Mar;7(3):814-26.

28. Murray HW, Berman JD, Davies CR, Saravia NG. Advances in Leishmaniasis. Lancet 2005 Oct 29-Nov 4;366(9496):1561-77.

29. Pimenta PF, Saraiva EM, Rowton E, Modi GB, Garraway LA, Beverley SM, et al. Evidence that the vectorial competence of phlebotomine sand flies for different species of *Leishmania* is controlled by structural polymorphisms in the surface lipophosphoglycan. Proc Natl Acad Sci U S A 1994 Sep 13;91(19):9155-9.

30. Rogers ME, Ilg T, Nikolaev AV, Ferguson MA, Bates PA. Transmission of cutaneous Leishmaniasis by sand flies is enhanced by regurgitation of fPPG. Nature 2004 Jul 22;430(6998):463-7.

31. Sadlova J, Hajmova M, Volf P. Phlebotomus (Adlerius) halepensis vector competence for *Leishmania major* and L. tropica. Med Vet Entomol 2003 Sep;17(3):244-50.

32. Kamhawi S, Modi GB, Pimenta PF, Rowton E, Sacks DL. The vectorial competence of Phlebotomus sergenti is specific for *Leishmania tropica* and is controlled

by species-specific, lipophosphoglycan-mediated midgut attachment. Parasitology 2000 Jul;121 (Pt 1):25-33.

33. Sacks DL. *Leishmania*-sand fly interactions controlling species-specific vector competence. Cell Microbiol 2001 Apr;3(4):189-96.

34. Sacks DL, Saraiva EM, Rowton E, Turco SJ, Pimenta PF. The role of the lipophosphoglycan of *Leishmania* in vector competence. Parasitology 1994;108 Suppl:S55-62.

35. Shao L, Serrano D, Mayer L. The role of epithelial cells in immune regulation in the gut. Semin Immunol 2001 Jun;13(3):163-76.

36. Rogers ME, Chance ML, Bates PA. The role of promastigote secretory gel in the origin and transmission of the infective stage of *Leishmania mexicana* by the sandfly Lutzomyia longipalpis. Parasitology 2002 May;124(Pt 5):495-507.

37. Kamhawi S, Ramalho-Ortigao M, Pham VM, Kumar S, Lawyer PG, Turco SJ, et al. A role for insect galectins in parasite survival. Cell 2004 Oct 29;119(3):329-41.

38. Dantas-Torres F. The role of dogs as reservoirs of *Leishmania* parasites, with emphasis on *Leishmania* (*Leishmania*) *infantum* and *Leishmania* (Viannia) braziliensis. Vet Parasitol 2007 Nov 10;149(3-4):139-46.

39. Ghawar W, Snoussi MA, Hamida NB, Boukthir AC, Yazidi R, Cha Bane S, et al. First Report of Natural Infection of Least Weasel (*Mustela nivalis Linnaeus*, 1776) with *Leishmania major* in Tunisia. Vector Borne Zoonotic Dis 2011 Nov;11(11):1507-9.

40. Ghawar W, Toumi A, Snoussi MA, Chlif S, Zaatour A, Boukthir A, et al. *Leishmania major* infection among psammomys obesus and meriones shawi: reservoirs of zoonotic cutaneous *Leishmania*sis in sidi bouzid (central Tunisia). Vector Borne Zoonotic Dis 2011 Dec;11(12):1561-8.

41. Azizi K, Moemenbellah-Fard MD, Fakoorziba MR, Fekri S. Gerbillus nanus (Rodentia: Muridae): a new reservoir host of *Leishmania major*. Ann Trop Med Parasitol 2011 Sep;105(6):431-7.

42. Quaresma PF, Rego FD, Botelho HA, da Silva SR, Moura Junior AJ, Teixeira Neto RG, et al. Wild, synanthropic and domestic hosts of *Leishmania* in an endemic area of cutaneous *Leishmania*sis in Minas Gerais State, Brazil. Trans R Soc Trop Med Hyg 2011 Oct;105(10):579-85.

43. Lukes J, Mauricio IL, Schonian G, Dujardin JC, Soteriadou K, Dedet JP, et al. Evolutionary and geographical history of the *Leishmania donovani* complex with a revision of current taxonomy. Proc Natl Acad Sci U S A 2007 May 29;104(22):9375-80.

44. Tibayrenc M, Ayala FJ. The clonal theory of parasitic protozoa: 12 years on. Trends Parasitol 2002 Sep;18(9):405-10.

45. Tibayrenc M. Clonality in *Leishmania*. Parasitol Today 1993 Feb;9(2):58.

46. Victoir K, Dujardin JC. How to succeed in parasitic life without sex? Asking *Leishmania*. Trends Parasitol 2002 Feb;18(2):81-5.

47. Tibayrenc M, Kjellberg F, Ayala FJ. A clonal theory of parasitic protozoa: the population structures of *Entamoeba, Giardia, Leishmania, Naegleria, Plasmodium, Trichomonas,* and *Trypanosoma* and their medical and taxonomical consequences. Proc Natl Acad Sci U S A 1990 Apr;87(7):2414-8.

48. Ravel C, Cortes S, Pratlong F, Morio F, Dedet JP, Campino L. First report of genetic hybrids between two very divergent *Leishmania* species: *Leishmania infantum* and *Leishmania major*. Int J Parasitol 2006 Nov;36(13):1383-8.

49. Banuls AL, Guerrini F, Le Pont F, Barrera C, Espinel I, Guderian R, et al. Evidence for hybridization by multilocus enzyme electrophoresis and random amplified polymorphic DNA between *Leishmania braziliensis* and *Leishmania* panamensis/guyanensis in Ecuador. J Eukaryot Microbiol 1997 Sep-Oct;44(5):408-11.

50. Dujardin JC, Banuls AL, Llanos-Cuentas A, Alvarez E, DeDoncker S, Jacquet D, et al. Putative *Leishmania* hybrids in the Eastern Andean valley of Huanuco, Peru. Acta Trop 1995 Aug;59(4):293-307.

51. Nolder D, Roncal N, Davies CR, Llanos-Cuentas A, Miles MA. Multiple hybrid genotypes of *Leishmania* (viannia) in a focus of mucocutaneous *Leishmania*sis. Am J Trop Med Hyg 2007 Mar;76(3):573-8.

52. Kelly JM, Law JM, Chapman CJ, Van Eys GJ, Evans DA. Evidence of genetic recombination in *Leishmania*. Mol Biochem Parasitol 1991 Jun;46(2):253-63.

53. Rougeron V, De Meeus T, Kako Ouraga S, Hide M, Banuls AL. "Everything you always wanted to know about sex (but were afraid to ask)" in *Leishmania* after two decades of laboratory and field analyses. PLoS Pathog 2010;6(8).

54. Bastien P, Blaineau C, Pages M. *Leishmania*: sex, lies and karyotype. Parasitol Today 1992 May;8(5):174-7.

55. Blaineau C, Bastien P, Pages M. Multiple forms of chromosome I, II and V in a restricted population of *Leishmania infantum* contrasting with monomorphism in individual strains suggest haploidy or automixy. Mol Biochem Parasitol 1992 Feb;50(2):197-204.

56. Akopyants NS, Kimblin N, Secundino N, Patrick R, Peters N, Lawyer P, et al. Demonstration of genetic exchange during cyclical development of *Leishmania* in the sand fly vector. Science 2009 Apr 10;324(5924):265-8.

57. Jenni L, Marti S, Schweizer J, Betschart B, Le Page RW, Wells JM, et al. Hybrid formation between African trypanosomes during cyclical transmission. Nature 1986 Jul 10-16;322(6075):173-5.

58. Gibson W, Peacock L, Ferris V, Williams K, Bailey M. The use of yellow fluorescent hybrids to indicate mating in *Trypanosoma brucei*. Parasit Vectors 2008;1(1):4.

59. Heitman J. Sexual reproduction and the evolution of microbial pathogens. Curr Biol 2006 Sep 5;16(17):R711-25.

60. Volf P, Sadlova J. Sex in *Leishmania*. Science 2009 Jun 26;324(5935):1644.

61. Gangneux JP, Sulahian A, Honore S, Meneceur P, Derouin F, Garin YJ. Evidence for determining parasitic factors in addition to host genetics and immune status in the outcome of murine *Leishmania infantum* visceral Leishmaniasis. Parasite Immunol 2000 Oct;22(10):515-9.

62. Chappuis F, Sundar S, Hailu A, Ghalib H, Rijal S, Peeling RW, et al. Visceral *Leishmania*sis: what are the needs for diagnosis, treatment and control? Nat Rev Microbiol 2007 Nov;5(11):873-82.

63. Reithinger R, Dujardin JC, Louzir H, Pirmez C, Alexander B, Brooker S. Cutaneous *Leishmania*sis. Lancet Infect Dis 2007 Sep;7(9):581-96.

64. Goto H, Lindoso JA. Current diagnosis and treatment of cutaneous and mucocutaneous Leishmaniasis. Expert Rev Anti Infect Ther 2010 Apr;8(4):419-33.

65. David CV, Craft N. Cutaneous and mucocutaneous *Leishmania*sis. Dermatol Ther 2009 Nov-Dec;22(6):491-502.

66. Duthie MS, Raman VS, Piazza FM, Reed SG. The development and clinical evaluation of second-generation Leishmaniasis vaccines. Vaccine 2011 Nov 12.

67. Sundar S, Rai M. Laboratory diagnosis of visceral Leishmaniasis. Clin Diagn Lab Immunol 2002 Sep;9(5):951-8.

68. Srivastava P, Dayama A, Mehrotra S, Sundar S. Diagnosis of visceral Leishmaniasis. Trans R Soc Trop Med Hyg 2010 Jan;105(1):1-6.

69. Zijlstra EE, Ali MS, el-Hassan AM, el-Toum IA, Satti M, Ghalib HW, et al. Kala-azar: a comparative study of parasitological methods and the direct agglutination test in diagnosis. Trans R Soc Trop Med Hyg 1992 Sep-Oct;86(5):505-7.

70. Babiker ZO, Davidson R, Mazinda C, Kipngetich S, Ritmeijer K. Utility of lymph node aspiration in the diagnosis of visceral Leishmaniasis in Sudan. Am J Trop Med Hyg 2007 Apr;76(4):689-93.

71. Spanakos G, Patsoula E, Kremastinou T, Saroglou G, Vakalis N. Development of a PCR-based method for diagnosis of *Leishmania* in blood samples. Mol Cell Probes 2002 Dec;16(6):415-20.

72. Fissore C, Delaunay P, Ferrua B, Rosenthal E, Del Giudice P, Aufeuvre JP, et al. Convenience of serum for visceral Leishmaniasis diagnosis by PCR. J Clin Microbiol 2004 Nov;42(11):5332-3.

73. Reithinger R, Dujardin JC. Molecular diagnosis of Leishmaniasis: current status and future applications. J Clin Microbiol 2007 Jan;45(1):21-5.

74. Herwaldt BL. Leishmaniasis. Lancet 1999 Oct 2;354(9185):1191-9.

75. Sundar S, Maurya R, Singh RK, Bharti K, Chakravarty J, Parekh A, et al. Rapid, noninvasive diagnosis of visceral Leishmaniasis in India: comparison of two immunochromatographic strip tests for detection of anti-K39 antibody. J Clin Microbiol 2006 Jan;44(1):251-3.

76. Sundar S, Singh RK, Maurya R, Kumar B, Chhabra A, Singh V, et al. Serological diagnosis of Indian visceral Leishmaniasis: direct agglutination test versus rK39 strip test. Trans R Soc Trop Med Hyg 2006 Jun;100(6):533-7.

77. Boelaert M, El-Safi S, Hailu A, Mukhtar M, Rijal S, Sundar S, et al. Diagnostic tests for kala-azar: a multi-centre study of the freeze-dried DAT, rK39 strip test and KAtex in East Africa and the Indian subcontinent. Trans R Soc Trop Med Hyg 2008 Jan;102(1):32-40.

78. Sundar S, Singh RK, Bimal SK, Gidwani K, Mishra A, Maurya R, et al. Comparative evaluation of parasitology and serological tests in the diagnosis of visceral Leishmaniasis in India: a phase III diagnostic accuracy study. Trop Med Int Health 2007 Feb;12(2):284-9.

79. Claborn DM. The biology and control of Leishmaniasis vectors. J Glob Infect Dis 2010 May;2(2):127-34.

80. Noli C, Auxilia ST. Treatment of canine Old World visceral Leishmaniasis: a systematic review. Vet Dermatol 2005 Aug;16(4):213-32.

81. Reithinger R, Coleman PG, Alexander B, Vieira EP, Assis G, Davies CR. Are insecticide-impregnated dog collars a feasible alternative to dog culling as a strategy for controlling canine visceral Leishmaniasis in Brazil? Int J Parasitol 2004 Jan;34(1):55-62.

82. Dantas-Torres F. Leishmune vaccine: the newest tool for prevention and control of canine visceral leishmaniosis and its potential as a transmission-blocking vaccine. Vet Parasitol 2006 Oct 10;141(1-2):1-8.

83. Palatnik-de-Sousa CB, Silva-Antunes I, Morgado Ade A, Menz I, Palatnik M, Lavor C. Decrease of the incidence of human and canine visceral Leishmaniasis after dog vaccination with Leishmune in Brazilian endemic areas. Vaccine 2009 Jun 2;27(27):3505-12.

84. Handman E, Kedzierski L, Uboldi AD, Goding JW. Fishing for anti-*Leishmania* drugs: principles and problems. Adv Exp Med Biol 2008;625:48-60.

85. Croft SL, Sundar S, Fairlamb AH. Drug resistance in Leishmaniasis. Clin Microbiol Rev 2006 Jan;19(1):111-26.

86. Kedzierski L. Leishmaniasis Vaccine: Where are We Today? J Glob Infect Dis 2010 May;2(2):177-85.

87. Sundar S, Sinha PK, Rai M, Verma DK, Nawin K, Alam S, et al. Comparison of short-course multidrug treatment with standard therapy for visceral Leishmaniasis in India: an open-label, non-inferiority, randomised controlled trial. Lancet 2011 Feb 5;377(9764):477-86.

88. Sundar S, Sinha PK, Verma DK, Kumar N, Alam S, Pandey K, et al. Ambisome plus miltefosine for Indian patients with kala-azar. Trans R Soc Trop Med Hyg 2011 Feb;105(2):115-7.

89. van Griensven J, Balasegaram M, Meheus F, Alvar J, Lynen L, Boelaert M. Combination therapy for visceral Leishmaniasis. Lancet Infect Dis 2010 Mar;10(3):184-94.

90. Denton H, McGregor JC, Coombs GH. Reduction of anti-*Leishmania*l pentavalent antimonial drugs by a parasite-specific thiol-dependent reductase, TDR1. Biochem J 2004 Jul 15;381(Pt 2):405-12.

91. Zhou Y, Messier N, Ouellette M, Rosen BP, Mukhopadhyay R. *Leishmania major* LmACR2 is a pentavalent antimony reductase that confers sensitivity to the drug pentostam. J Biol Chem 2004 Sep 3;279(36):37445-51.

92. Brochu C, Wang J, Roy G, Messier N, Wang XY, Saravia NG, et al. Antimony uptake systems in the protozoan parasite *Leishmania* and accumulation differences in antimony-resistant parasites. Antimicrob Agents Chemother 2003 Oct;47(10):3073-9.

93. Mukhopadhyay R, Dey S, Xu N, Gage D, Lightbody J, Ouellette M, et al. Trypanothione overproduction and resistance to antimonials and arsenicals in *Leishmania*. Proc Natl Acad Sci U S A 1996 Sep 17;93(19):10383-7.

94. Wyllie S, Mandal G, Singh N, Sundar S, Fairlamb AH, Chatterjee M. Elevated levels of tryparedoxin peroxidase in antimony unresponsive *Leishmania donovani* field isolates. Mol Biochem Parasitol 2010 Oct;173(2):162-4.

95. Wyllie S, Cunningham ML, Fairlamb AH. Dual action of antimonial drugs on thiol redox metabolism in the human pathogen *Leishmania donovani*. J Biol Chem 2004 Sep 17;279(38):39925-32.

96. Mandal G, Wyllie S, Singh N, Sundar S, Fairlamb AH, Chatterjee M. Increased levels of thiols protect antimony unresponsive *Leishmania donovani* field isolates against reactive oxygen species generated by trivalent antimony. Parasitology 2007 Nov;134(Pt 12):1679-87.

97. Murray HW. Clinical and experimental advances in treatment of visceral Leishmaniasis. Antimicrob Agents Chemother 2001 Aug;45(8):2185-97.

98. Pathak MK, Yi T. Sodium stibogluconate is a potent inhibitor of protein tyrosine phosphatases and augments cytokine responses in hemopoietic cell lines. J Immunol 2001 Sep 15;167(6):3391-7.

99. Muniz-Junqueira MI, de Paula-Coelho VN. Meglumine antimonate directly increases phagocytosis, superoxide anion and TNF-alpha production, but only via TNF-alpha it indirectly increases nitric oxide production by phagocytes of healthy individuals, in vitro. Int Immunopharmacol 2008 Dec 10;8(12):1633-8.

100. Goad LJ, Holz GG, Jr., Beach DH. Sterols of *Leishmania* species. Implications for biosynthesis. Mol Biochem Parasitol 1984 Feb;10(2):161-70.

101. Matlashewski G, Arana B, Kroeger A, Battacharya S, Sundar S, Das P, et al. Visceral Leishmaniasis: elimination with existing interventions. Lancet Infect Dis Apr;11(4):322-5.

102. de Souza W, Attias M, Rodrigues JC. Particularities of mitochondrial structure in parasitic protists (Apicomplexa and Kinetoplastida). Int J Biochem Cell Biol 2009 Oct;41(10):2069-80.

103. Mehta A, Shaha C. Apoptotic death in *Leishmania donovani* promastigotes in response to respiratory chain inhibition: complex II inhibition results in increased pentamidine cytotoxicity. J Biol Chem 2004 Mar 19;279(12):11798-813.

104. Mukherjee A, Padmanabhan PK, Sahani MH, Barrett MP, Madhubala R. Roles for mitochondria in pentamidine susceptibility and resistance in *Leishmania donovani*. Mol Biochem Parasitol 2006 Jan;145(1):1-10.

105. Amato VS, Tuon FF, Campos A, Bacha HA, Nicodemo AC, Amato Neto V, et al. Treatment of mucosal Leishmaniasis with a lipid formulation of amphotericin B. Clin Infect Dis 2007 Jan 15;44(2):311-2.

106. Maltezou HC. Drug resistance in visceral Leishmaniasis. J Biomed Biotechnol 2010;2010:617521.

107. Fernandez MM, Malchiodi EL, Algranati ID. Differential effects of paromomycin on ribosomes of *Leishmania mexicana* and mammalian cells. Antimicrob Agents Chemother 2011 Jan;55(1):86-93.

108. Jhingran A, Chawla B, Saxena S, Barrett MP, Madhubala R. Paromomycin: uptake and resistance in *Leishmania donovani*. Mol Biochem Parasitol 2009 Apr;164(2):111-7.

109. Paris C, Loiseau PM, Bories C, Breard J. Miltefosine induces apoptosis-like death in *Leishmania donovani* promastigotes. Antimicrob Agents Chemother 2004 Mar;48(3):852-9.

110. Verma NK, Dey CS. Possible mechanism of miltefosine-mediated death of *Leishmania donovani*. Antimicrob Agents Chemother 2004 Aug;48(8):3010-5.

111. Denny PW, Field MC, Smith DF. GPI-anchored proteins and glycoconjugates segregate into lipid rafts in Kinetoplastida. FEBS Lett 2001 Feb 23;491(1-2):148-53.

112. Saint-Pierre-Chazalet M, Ben Brahim M, Le Moyec L, Bories C, Rakotomanga M, Loiseau PM. Membrane sterol depletion impairs miltefosine action in wild-type and miltefosine-resistant *Leishmania donovani* promastigotes. J Antimicrob Chemother 2009 Nov;64(5):993-1001.

113. Perez-Victoria FJ, Sanchez-Canete MP, Seifert K, Croft SL, Sundar S, Castanys S, et al. Mechanisms of experimental resistance of *Leishmania* to miltefosine: Implications for clinical use. Drug Resist Updat 2006 Feb-Apr;9(1-2):26-39.

114. Seifert K, Perez-Victoria FJ, Stettler M, Sanchez-Canete MP, Castanys S, Gamarro F, et al. Inactivation of the miltefosine transporter, LdMT, causes miltefosine resistance that is conferred to the amastigote stage of *Leishmania donovani* and persists in vivo. Int J Antimicrob Agents 2007 Sep;30(3):229-35.

115. Rakotomanga M, Saint-Pierre-Chazalet M, Loiseau PM. Alteration of fatty acid and sterol metabolism in miltefosine-resistant *Leishmania donovani* promastigotes and consequences for drug-membrane interactions. Antimicrob Agents Chemother 2005 Jul;49(7):2677-86.

116. Kedzierski L, Zhu Y, Handman E. *Leishmania* vaccines: progress and problems. Parasitology 2006;133 Suppl:S87-112.

117. Vanloubbeeck Y, Jones DE. The immunology of *Leishmania* infection and the implications for vaccine development. Ann N Y Acad Sci 2004 Oct;1026:267-72.

118. Nagill R, Kaur S. Vaccine candidates for Leishmaniasis: a review. Int Immunopharmacol 2011 Oct;11(10):1464-88.

119. Noazin S, Khamesipour A, Moulton LH, Tanner M, Nasseri K, Modabber F, et al. Efficacy of killed whole-parasite vaccines in the prevention of Leishmaniasis: a meta-analysis. Vaccine 2009 Jul 30;27(35):4747-53.

120. Mayrink W, Botelho AC, Magalhaes PA, Batista SM, Lima Ade O, Genaro O, et al. Immunotherapy, immunochemotherapy and chemotherapy for American cutaneous Leishmaniasis treatment. Rev Soc Bras Med Trop 2006 Jan-Feb;39(1):14-21.

121. Titus RG, Gueiros-Filho FJ, de Freitas LA, Beverley SM. Development of a safe live *Leishmania* vaccine line by gene replacement. Proc Natl Acad Sci U S A 1995 Oct 24;92(22):10267-71.

122. Veras P, Brodskyn C, Balestieri F, Freitas L, Ramos A, Queiroz A, et al. A dhfr-ts-*Leishmania major* knockout mutant cross-protects against *Leishmania amazonensisi*. Mem Inst Oswaldo Cruz 1999 Jul-Aug;94(4):491-6.

123. Amaral VF, Teva A, Oliveira-Neto MP, Silva AJ, Pereira MS, Cupolillo E, et al. Study of the safety, immunogenicity and efficacy of attenuated and killed *Leishmania*

(Leishmania) major vaccines in a rhesus monkey (Macaca mulatta) model of the human disease. Mem Inst Oswaldo Cruz 2002 Oct;97(7):1041-8.

124. Uzonna JE, Spath GF, Beverley SM, Scott P. Vaccination with phosphoglycan-deficient *Leishmania major* protects highly susceptible mice from virulent challenge without inducing a strong Th1 response. J Immunol 2004 Mar 15;172(6):3793-7.

125. Kebaier C, Uzonna JE, Beverley SM, Scott P. Immunization with persistent attenuated Delta lpg2 *Leishmania major* parasites requires adjuvant to provide protective immunity in C57BL/6 mice. Infect Immun 2006 Jan;74(1):777-80.

126. Spath GF, Lye LF, Segawa H, Sacks DL, Turco SJ, Beverley SM. Persistence without pathology in phosphoglycan-deficient *Leishmania major*. Science 2003 Aug 29;301(5637):1241-3.

127. Silvestre R, Cordeiro-Da-Silva A, Santarem N, Vergnes B, Sereno D, Ouaissi A. SIR2-deficient *Leishmania infantum* induces a defined IFN-gamma/IL-10 pattern that correlates with protection. J Immunol 2007 Sep 1;179(5):3161-70.

128. Selvapandiyan A, Dey R, Nylen S, Duncan R, Sacks D, Nakhasi HL. Intracellular replication-deficient *Leishmania donovani* induces long lasting protective immunity against visceral *Leishmania*sis. J Immunol 2009 Aug 1;183(3):1813-20.

129. Silvestre R, Cordeiro-da-Silva A, Ouaissi A. Live attenuated *Leishmania* vaccines: a potential strategic alternative. Arch Immunol Ther Exp (Warsz) 2008 Mar-Apr;56(2):123-6.

130. Reed SG, Bertholet S, Coler RN, Friede M. New horizons in adjuvants for vaccine development. Trends Immunol 2009 Jan;30(1):23-32.

131. Duthie MS, Windish HP, Fox CB, Reed SG. Use of defined TLR ligands as adjuvants within human vaccines. Immunol Rev Jan;239(1):178-96.

132. Kaye PM, Aebischer T. Visceral Leishmaniasis: immunology and prospects for a vaccine. Clin Microbiol Infect 2011 Oct;17(10):1462-70.

133. Costa CH, Peters NC, Maruyama SR, de Brito EC, Jr., Santos IK. Vaccines for the *Leishmania*ses: proposals for a research agenda. PLoS Negl Trop Dis 2011;5(3):e943.

134. Melby PC, Yang J, Zhao W, Perez LE, Cheng J. *Leishmania donovani* p36(LACK) DNA vaccine is highly immunogenic but not protective against experimental visceral *Leishmania*sis. Infect Immun 2001 Aug;69(8):4719-25.

135. Nascimento E, Fernandes DF, Vieira EP, Campos-Neto A, Ashman JA, Alves FP, et al. A clinical trial to evaluate the safety and immunogenicity of the LEISH-F1+MPL-SE vaccine when used in combination with meglumine antimoniate for the treatment of cutaneous *Leishmania*sis. Vaccine 2011 Sep 14;28(40):6581-7.

136. Chakravarty J, Kumar S, Trivedi S, Rai VK, Singh A, Ashman JA, et al. A clinical trial to evaluate the safety and immunogenicity of the LEISH-F1+MPL-SE vaccine for use in the prevention of visceral Leishmaniasis. Vaccine 2011 Apr 27;29(19):3531-7.

137. Coler RN, Goto Y, Bogatzki L, Raman V, Reed SG. Leish-111f, a recombinant polyprotein vaccine that protects against visceral Leishmaniasis by elicitation of CD4+ T cells. Infect Immun 2007 Sep;75(9):4648-54.

138. Skeiky YA, Coler RN, Brannon M, Stromberg E, Greeson K, Crane RT, et al. Protective efficacy of a tandemly linked, multi-subunit recombinant *Leishmania*l vaccine (Leish-111f) formulated in MPL adjuvant. Vaccine 2002 Sep 10;20(27-28):3292-303.

139. Campos-Neto A, Porrozzi R, Greeson K, Coler RN, Webb JR, Seiky YA, et al. Protection against cutaneous Leishmaniasis induced by recombinant antigens in murine and nonhuman primate models of the human disease. Infect Immun 2001 Jun;69(6):4103-8.

140. Velez ID, Gilchrist K, Martinez S, Ramirez-Pineda JR, Ashman JA, Alves FP, et al. Safety and immunogenicity of a defined vaccine for the prevention of cutaneous *Leishmania*sis. Vaccine 2009 Dec 11;28(2):329-37.

141. Llanos-Cuentas A, Calderon W, Cruz M, Ashman JA, Alves FP, Coler RN, et al. A clinical trial to evaluate the safety and immunogenicity of the LEISH-F1+MPL-SE vaccine when used in combination with sodium stibogluconate for the treatment of mucosal Leishmaniasis. Vaccine Oct 28;28(46):7427-35.

142. Gradoni L, Foglia Manzillo V, Pagano A, Piantedosi D, De Luna R, Gramiccia M, et al. Failure of a multi-subunit recombinant Leishmanial vaccine (MML) to protect dogs from *Leishmania infantum* infection and to prevent disease progression in infected animals. Vaccine 2005 Nov 1;23(45):5245-51.

143. da Silva VO, Borja-Cabrera GP, Correia Pontes NN, de Souza EP, Luz KG, Palatnik M, et al. A phase III trial of efficacy of the FML-vaccine against canine kala-azar in an endemic area of Brazil (Sao Goncalo do Amaranto, RN). Vaccine 2000 Dec 8;19(9-10):1082-92.

144. Nogueira FS, Moreira MA, Borja-Cabrera GP, Santos FN, Menz I, Parra LE, et al. Leishmune vaccine blocks the transmission of canine visceral Leishmaniasis: absence of *Leishmania* parasites in blood, skin and lymph nodes of vaccinated exposed dogs. Vaccine 2005 Sep 23;23(40):4805-10.

145. Borja-Cabrera GP, Cruz Mendes A, Paraguai de Souza E, Hashimoto Okada LY, de ATFA, Kawasaki JK, et al. Effective immunotherapy against canine visceral Leishmaniasis with the FML-vaccine. Vaccine 2004 Jun 2;22(17-18):2234-43.

146. Saraiva EM, de Figueiredo Barbosa A, Santos FN, Borja-Cabrera GP, Nico D, Souza LO, et al. The FML-vaccine (Leishmune) against canine visceral *Leishmania*sis: a transmission blocking vaccine. Vaccine 2006 Mar 20;24(13):2423-31.

147. Shedlock DJ, Weiner DB. DNA vaccination: antigen presentation and the induction of immunity. J Leukoc Biol 2000 Dec;68(6):793-806.

148. Mutiso JM, Macharia JC. A review of adjuvants for *Leishmania* vaccine candidates. Journal of Biomedical Research 2010:16-25.

149. Tewary P, Jain M, Sahani MH, Saxena S, Madhubala R. A heterologous prime-boost vaccination regimen using ORFF DNA and recombinant ORFF protein confers protective immunity against experimental visceral *Leishmania*sis. J Infect Dis 2005 Jun 15;191(12):2130-7.

150. Dondji B, Perez-Jimenez E, Goldsmith-Pestana K, Esteban M, McMahon-Pratt D. Heterologous prime-boost vaccination with the LACK antigen protects against murine visceral Leishmaniasis. Infect Immun 2005 Aug;73(8):5286-9.

151. Mazumder S, Maji M, Das A, Ali N. Potency, efficacy and durability of DNA/DNA, DNA/protein and protein/protein based vaccination using gp63 against *Leishmania donovani* in BALB/c mice. PLoS One;6(2):e14644.

152. Rafati S, Zahedifard F, Nazgouee F. Prime-boost vaccination using cysteine proteinases type I and II of *Leishmania infantum* confers protective immunity in murine visceral *Leishmania*sis. Vaccine 2006 Mar 15;24(12):2169-75.

153. Woodland DL. Jump-starting the immune system: prime-boosting comes of age. Trends Immunol 2004 Feb;25(2):98-104.

154. Gurunathan S, Klinman DM, Seder RA. DNA vaccines: immunology, application, and optimization*. Annu Rev Immunol 2000;18:927-74.

155. Xu D, Liew FY. Protection against Leishmaniasis by injection of DNA encoding a major surface glycoprotein, gp63, of *L. major.* Immunology 1995 Feb;84(2):173-6.

156. Gurunathan S, Stobie L, Prussin C, Sacks DL, Glaichenhaus N, Iwasaki A, et al. Requirements for the maintenance of Th1 immunity in vivo following DNA vaccination: a potential immunoregulatory role for CD8+ T cells. J Immunol 2000 Jul 15;165(2):915-24.

157. Stobie L, Gurunathan S, Prussin C, Sacks DL, Glaichenhaus N, Wu CY, et al. The role of antigen and IL-12 in sustaining Th1 memory cells in vivo: IL-12 is required to maintain memory/effector Th1 cells sufficient to mediate protection to an infectious parasite challenge. Proc Natl Acad Sci U S A 2000 Jul 18;97(15):8427-32.

158. Campos-Neto A, Webb JR, Greeson K, Coler RN, Skeiky YA, Reed SG. Vaccination with plasmid DNA encoding TSA/LmSTI1 Leishmanial fusion proteins confers protection against *Leishmania major* infection in susceptible BALB/c mice. Infect Immun 2002 Jun;70(6):2828-36.

159. Rafati S, Salmanian AH, Taheri T, Vafa M, Fasel N. A protective cocktail vaccine against murine cutaneous Leishmaniasis with DNA encoding cysteine proteinases of *Leishmania major*. Vaccine 2001 May 14;19(25-26):3369-75.

160. Sukumaran B, Tewary P, Saxena S, Madhubala R. Vaccination with DNA encoding ORFF antigen confers protective immunity in mice infected with *Leishmania donovani*. Vaccine 2003 Mar 7;21(11-12):1292-9.

161. Nagill R, Kaur S. Vaccine candidates for Leishmaniasis: A review. Int Immunopharmacol 2011 May 25.

162. Dumonteil E. DNA Vaccines against Protozoan Parasites: Advances and Challenges. J Biomed Biotechnol 2007;2007(6):90520.

163. Sibley LD. Invasion and intracellular survival by protozoan parasites. Immunol Rev 2011 Mar;240(1):72-91.

164. Kimblin N, Peters N, Debrabant A, Secundino N, Egen J, Lawyer P, et al. Quantification of the infectious dose of *Leishmania major* transmitted to the skin by single sand flies. Proc Natl Acad Sci U S A 2008 Jul 22;105(29):10125-30.

165. van Zandbergen G, Bollinger A, Wenzel A, Kamhawi S, Voll R, Klinger M, et al. *Leishmania* disease development depends on the presence of apoptotic promastigotes in the virulent inoculum. Proc Natl Acad Sci U S A 2006 Sep 12;103(37):13837-42.

166. Dominguez M, Torano A. Immune adherence-mediated opsonophagocytosis: the mechanism of *Leishmania* infection. J Exp Med 1999 Jan 4;189(1):25-35.

167. Filardy AA, Pires DR, DosReis GA. Macrophages and neutrophils cooperate in immune responses to *Leishmania* infection. Cell Mol Life Sci 2011 Jun;68(11):1863-70.

168. Charmoy M, Auderset F, Allenbach C, Tacchini-Cottier F. The prominent role of neutrophils during the initial phase of infection by *Leishmania* parasites. J Biomed Biotechnol 2010;2010:719361.

169. Ritter U, Frischknecht F, van Zandbergen G. Are neutrophils important host cells for *Leishmania* parasites? Trends Parasitol 2009 Nov;25(11):505-10.

170. Novais FO, Santiago RC, Bafica A, Khouri R, Afonso L, Borges VM, et al. Neutrophils and macrophages cooperate in host resistance against *Leishmania braziliensis* infection. J Immunol 2009 Dec 15;183(12):8088-98.

171. Peters NC, Egen JG, Secundino N, Debrabant A, Kimblin N, Kamhawi S, et al. In vivo imaging reveals an essential role for neutrophils in Leishmaniasis transmitted by sand flies. Science 2008 Aug 15;321(5891):970-4.

172. McFarlane E, Perez C, Charmoy M, Allenbach C, Carter KC, Alexander J, et al. Neutrophils contribute to development of a protective immune response during onset of infection with *Leishmania donovani*. Infect Immun 2008 Feb;76(2):532-41.

173. Gueirard P, Laplante A, Rondeau C, Milon G, Desjardins M. Trafficking of *Leishmania donovani* promastigotes in non-lytic compartments in neutrophils enables the subsequent transfer of parasites to macrophages. Cell Microbiol 2008 Jan;10(1):100-11.

174. Laskay T, van Zandbergen G, Solbach W. Neutrophil granulocytes as host cells and transport vehicles for intracellular pathogens: apoptosis as infection-promoting factor. Immunobiology 2008;213(3-4):183-91.

175. van Zandbergen G, Klinger M, Mueller A, Dannenberg S, Gebert A, Solbach W, et al. Cutting edge: neutrophil granulocyte serves as a vector for *Leishmania* entry into macrophages. J Immunol 2004 Dec 1;173(11):6521-5.

176. Nathan C. Neutrophils and immunity: challenges and opportunities. Nat Rev Immunol 2006 Mar;6(3):173-82.

177. Laufs H, Muller K, Fleischer J, Reiling N, Jahnke N, Jensenius JC, et al. Intracellular survival of *Leishmania major* in neutrophil granulocytes after uptake in the absence of heat-labile serum factors. Infect Immun 2002 Feb;70(2):826-35.

178. van Zandbergen G, Hermann N, Laufs H, Solbach W, Laskay T. *Leishmania* promastigotes release a granulocyte chemotactic factor and induce interleukin-8 release but inhibit gamma interferon-inducible protein 10 production by neutrophil granulocytes. Infect Immun 2002 Aug;70(8):4177-84.

179. Teixeira MJ, Teixeira CR, Andrade BB, Barral-Netto M, Barral A. Chemokines in host-parasite interactions in Leishmaniasis. Trends Parasitol 2006 Jan;22(1):32-40.

180. Muller K, van Zandbergen G, Hansen B, Laufs H, Jahnke N, Solbach W, et al. Chemokines, natural killer cells and granulocytes in the early course of *Leishmania major* infection in mice. Med Microbiol Immunol 2001 Nov;190(1-2):73-6.

181. Oghumu S, Lezama-Davila CM, Isaac-Marquez AP, Satoskar AR. Role of chemokines in regulation of immunity against Leishmaniasis. Exp Parasitol 2010 Nov;126(3):389-96.

182. Xin L, Vargas-Inchaustegui DA, Raimer SS, Kelly BC, Hu J, Zhu L, et al. Type I IFN receptor regulates neutrophil functions and innate immunity to *Leishmania* parasites. J Immunol 2010 Jun 15;184(12):7047-56.

183. Lopez Kostka S, Dinges S, Griewank K, Iwakura Y, Udey MC, von Stebut E. IL-17 promotes progression of cutaneous Leishmaniasis in susceptible mice. J Immunol 2009 Mar 1;182(5):3039-46.

184. Wanderley JL, Barcinski MA. Apoptosis and apoptotic mimicry: the *Leishmania* connection. Cell Mol Life Sci 2010 May;67(10):1653-9.

185. Ribeiro-Gomes FL, Otero AC, Gomes NA, Moniz-De-Souza MC, Cysne-Finkelstein L, Arnholdt AC, et al. Macrophage interactions with neutrophils regulate *Leishmania major* infection. J Immunol 2004 Apr 1;172(7):4454-62.

186. Aga E, Katschinski DM, van Zandbergen G, Laufs H, Hansen B, Muller K, et al. Inhibition of the spontaneous apoptosis of neutrophil granulocytes by the intracellular parasite *Leishmania major*. J Immunol 2002 Jul 15;169(2):898-905.

187. Ribeiro-Gomes FL, Moniz-de-Souza MC, Alexandre-Moreira MS, Dias WB, Lopes MF, Nunes MP, et al. Neutrophils activate macrophages for intracellular killing of *Leishmania major* through recruitment of TLR4 by neutrophil elastase. J Immunol 2007 Sep 15;179(6):3988-94.

188. Brinkmann V, Reichard U, Goosmann C, Fauler B, Uhlemann Y, Weiss DS, et al. Neutrophil extracellular traps kill bacteria. Science 2004 Mar 5;303(5663):1532-5.

189. Guimaraes-Costa AB, Nascimento MT, Froment GS, Soares RP, Morgado FN, Conceicao-Silva F, et al. *Leishmania amazonensisi* promastigotes induce and are killed by neutrophil extracellular traps. Proc Natl Acad Sci U S A 2009 Apr 21;106(16):6748-53.

190. Gabriel C, McMaster WR, Girard D, Descoteaux A. *Leishmania donovani* promastigotes evade the antimicrobial activity of neutrophil extracellular traps. J Immunol 2010 Oct 1;185(7):4319-27.

191. Thalhofer CJ, Chen Y, Sudan B, Love-Homan L, Wilson ME. Leukocytes infiltrate the skin and draining lymph nodes in response to the protozoan *Leishmania infantum* chagasi. Infect Immun 2010 Jan;79(1):108-17.

192. Ehrchen JM, Roebrock K, Foell D, Nippe N, von Stebut E, Weiss JM, et al. Keratinocytes determine Th1 immunity during early experimental Leishmaniasis. PLoS Pathog 2010 Apr;6(4):e1000871.

193. Udey MC, von Stebut E, Mendez S, Sacks DL, Belkaid Y. Skin dendritic cells in murine cutaneous Leishmaniasis. Immunobiology 2001 Dec;204(5):590-4.

194. Antoine JC, Prina E, Courret N, Lang T. *Leishmania spp*.: on the interactions they establish with antigen-presenting cells of their mammalian hosts. Adv Parasitol 2004;58:1-68.

195. Von Stebut E. Immunology of cutaneous Leishmaniasis: the role of mast cells, phagocytes and dendritic cells for protective immunity. Eur J Dermatol 2007 Mar-Apr;17(2):115-22.

196. Ng LG, Hsu A, Mandell MA, Roediger B, Hoeller C, Mrass P, et al. Migratory dermal dendritic cells act as rapid sensors of protozoan parasites. PLoS Pathog 2008 Nov;4(11):e1000222.

197. Misslitz AC, Bonhagen K, Harbecke D, Lippuner C, Kamradt T, Aebischer T. Two waves of antigen-containing dendritic cells in vivo in experimental *Leishmania major* infection. Eur J Immunol 2004 Mar;34(3):715-25.

198. Mosser DM, Edelson PJ. The mouse macrophage receptor for C3bi (CR3) is a major mechanism in the phagocytosis of *Leishmania* promastigotes. J Immunol 1985 Oct;135(4):2785-9.

199. Brittingham A, Morrison CJ, McMaster WR, McGwire BS, Chang KP, Mosser DM. Role of the *Leishmania* surface protease gp63 in complement fixation, cell adhesion, and resistance to complement-mediated lysis. J Immunol 1995 Sep 15;155(6):3102-11.

200. Forestier CL, Machu C, Loussert C, Pescher P, Spath GF. Imaging host cell-*Leishmania* interaction dynamics implicates parasite motility, lysosome recruitment, and host cell wounding in the infection process. Cell Host Microbe 2011 Apr 21;9(4):319-30.

201. Scheltema RA, Decuypere S, T'Kindt R, Dujardin JC, Coombs GH, Breitling R. The potential of metabolomics for *Leishmania* research in the post-genomics era. Parasitology 2010 Aug;137(9):1291-302.

202. Peacock CS, Seeger K, Harris D, Murphy L, Ruiz JC, Quail MA, et al. Comparative genomic analysis of three *Leishmania* species that cause diverse human disease. Nat Genet 2007 Jul;39(7):839-47.

203. Downing T, Imamura H, Decuypere S, Clark TG, Coombs GH, Cotton JA, et al. Whole genome sequencing of multiple *Leishmania donovani* clinical isolates provides insights into population structure and mechanisms of drug resistance. Genome Res 2011 Dec;21(12):2143-56.

204. Rogers MB, Hilley JD, Dickens NJ, Wilkes J, Bates PA, Depledge DP, et al. Chromosome and gene copy number variation allow major structural change between species and strains of *Leishmania*. Genome Res 2011 Dec;21(12):2129-42.

205. Kaddurah-Daouk R, Kristal BS, Weinshilboum RM. Metabolomics: a global biochemical approach to drug response and disease. Annu Rev Pharmacol Toxicol 2008;48:653-83.

206. t'Kindt R, Jankevics A, Scheltema RA, Zheng L, Watson DG, Dujardin JC, et al. Towards an unbiased metabolic profiling of protozoan parasites: optimisation of a *Leishmania* sampling protocol for HILIC-orbitrap analysis. Anal Bioanal Chem 2010 Nov;398(5):2059-69.

207. t'Kindt R, Scheltema RA, Jankevics A, Brunker K, Rijal S, Dujardin JC, et al. Metabolomics to unveil and understand phenotypic diversity between pathogen populations. PLoS Negl Trop Dis 2010;4(11):e904.

208. Olszewski KL, Mather MW, Morrisey JM, Garcia BA, Vaidya AB, Rabinowitz JD, et al. Branched tricarboxylic acid metabolism in *Plasmodium falciparum*. Nature 2010 Aug 5;466(7307):774-8.

209. Olszewski KL, Morrisey JM, Wilinski D, Burns JM, Vaidya AB, Rabinowitz JD, et al. Host-parasite interactions revealed by *Plasmodium falciparum* metabolomics. Cell Host Microbe 2009 Feb 19;5(2):191-9.

210. Ivens AC, Peacock CS, Worthey EA, Murphy L, Aggarwal G, Berriman M, et al. The genome of the kinetoplastid parasite, *Leishmania major*. Science 2005 Jul 15;309(5733):436-42.

211. Martinez-Calvillo S, Yan S, Nguyen D, Fox M, Stuart K, Myler PJ. Transcription of *Leishmania major* Friedlin chromosome 1 initiates in both directions within a single region. Mol Cell 2003 May;11(5):1291-9.

212. Britto C, Ravel C, Bastien P, Blaineau C, Pages M, Dedet JP, et al. Conserved linkage groups associated with large-scale chromosomal rearrangements between Old World and New World *Leishmania* genomes. Gene 1998 Nov 5;222(1):107-17.

213. Zhang WW, Peacock CS, Matlashewski G. A genomic-based approach combining in vivo selection in mice to identify a novel virulence gene in *Leishmania*. PLoS Negl Trop Dis 2008;2(6):e248.

214. Zhang WW, Matlashewski G. Loss of virulence in *Leishmania donovani* deficient in an amastigote-specific protein, A2. Proc Natl Acad Sci U S A 1997 Aug 5;94(16):8807-11.

215. Zhang WW, Matlashewski G. Characterization of the A2-A2rel gene cluster in *Leishmania donovani*: involvement of A2 in visceralization during infection. Mol Microbiol 2001 Feb;39(4):935-48.

216. Zhang WW, Mendez S, Ghosh A, Myler P, Ivens A, Clos J, et al. Comparison of the A2 gene locus in *Leishmania donovani* and *Leishmania major* and its control over cutaneous infection. J Biol Chem 2003 Sep 12;278(37):35508-15.

217. Bankaitis VA, Malehorn DE, Emr SD, Greene R. The Saccharomyces cerevisiae SEC14 gene encodes a cytosolic factor that is required for transport of secretory proteins from the yeast Golgi complex. J Cell Biol 1989 Apr;108(4):1271-81.

218. Smith DF, Peacock CS, Cruz AK. Comparative genomics: from genotype to disease phenotype in the Leishmaniases. Int J Parasitol 2007 Sep;37(11):1173-86.

219. Eschenlauer SC, Coombs GH, Mottram JC. PFPI-like genes are expressed in *Leishmania major* but are pseudogenes in other *Leishmania* species. FEMS Microbiol Lett 2006 Jul;260(1):47-54.

220. Holzer TR, McMaster WR, Forney JD. Expression profiling by whole-genome interspecies microarray hybridization reveals differential gene expression in procyclic promastigotes, lesion-derived amastigotes, and axenic amastigotes in *Leishmania mexicana*. Mol Biochem Parasitol 2006 Apr;146(2):198-218.

221. Leifso K, Cohen-Freue G, Dogra N, Murray A, McMaster WR. Genomic and proteomic expression analysis of *Leishmania* promastigote and amastigote life stages: the

Leishmania genome is constitutively expressed. Mol Biochem Parasitol 2007 Mar;152(1):35-46.

222. Alcolea PJ, Alonso A, Gomez MJ, Moreno I, Dominguez M, Parro V, et al. Transcriptomics throughout the life cycle of *Leishmania infantum*: high down-regulation rate in the amastigote stage. Int J Parasitol 2010 Nov;40(13):1497-516.

223. Saxena A, Lahav T, Holland N, Aggarwal G, Anupama A, Huang Y, et al. Analysis of the *Leishmania donovani* transcriptome reveals an ordered progression of transient and permanent changes in gene expression during differentiation. Mol Biochem Parasitol 2007 Mar;152(1):53-65.

224. Depledge DP, Evans KJ, Ivens AC, Aziz N, Maroof A, Kaye PM, et al. Comparative expression profiling of *Leishmania*: modulation in gene expression between species and in different host genetic backgrounds. PLoS Negl Trop Dis 2009;3(7):e476.

225. Rochette A, Raymond F, Corbeil J, Ouellette M, Papadopoulou B. Whole-genome comparative RNA expression profiling of axenic and intracellular amastigote forms of *Leishmania infantum*. Mol Biochem Parasitol 2009 May;165(1):32-47.

226. Cohen-Freue G, Holzer TR, Forney JD, McMaster WR. Global gene expression in *Leishmania*. Int J Parasitol 2007 Aug;37(10):1077-86.

227. Pescher P, Blisnick T, Bastin P, Spath GF. Quantitative proteome profiling informs on phenotypic traits that adapt *Leishmania donovani* for axenic and intracellular proliferation. Cell Microbiol 2011 Jul;13(7):978-91.

228. Liang XH, Haritan A, Uliel S, Michaeli S. trans and cis splicing in trypanosomatids: mechanism, factors, and regulation. Eukaryot Cell 2003 Oct;2(5):830-40.

229. Quijada L, Soto M, Alonso C, Requena JM. Identification of a putative regulatory element in the 3'-untranslated region that controls expression of HSP70 in *Leishmania infantum*. Mol Biochem Parasitol 2000 Sep;110(1):79-91.

230. Charest H, Zhang WW, Matlashewski G. The developmental expression of *Leishmania donovani* A2 amastigote-specific genes is post-transcriptionally mediated and involves elements located in the 3'-untranslated region. J Biol Chem 1996 Jul 19;271(29):17081-90.

231. Zilka A, Garlapati S, Dahan E, Yaolsky V, Shapira M. Developmental regulation of heat shock protein 83 in *Leishmania*. 3' processing and mRNA stability control transcript abundance, and translation id directed by a determinant in the 3'-untranslated region. J Biol Chem 2001 Dec 21;276(51):47922-9.

232. Boucher N, Wu Y, Dumas C, Dube M, Sereno D, Breton M, et al. A common mechanism of stage-regulated gene expression in *Leishmania* mediated by a conserved 3'-untranslated region element. J Biol Chem 2002 May 31;277(22):19511-20.

233. McNicoll F, Muller M, Cloutier S, Boilard N, Rochette A, Dube M, et al. Distinct 3'-untranslated region elements regulate stage-specific mRNA accumulation and translation in *Leishmania*. J Biol Chem 2005 Oct 21;280(42):35238-46.

234. Wu Y, El Fakhry Y, Sereno D, Tamar S, Papadopoulou B. A new developmentally regulated gene family in *Leishmania* amastigotes encoding a homolog of amastin surface proteins. Mol Biochem Parasitol 2000 Oct;110(2):345-57.

235. Clayton C, Shapira M. Post-transcriptional regulation of gene expression in trypanosomes and *Leishmanias*. Mol Biochem Parasitol 2007 Dec;156(2):93-101.

236. Bringaud F, Muller M, Cerqueira GC, Smith M, Rochette A, El-Sayed NM, et al. Members of a large retroposon family are determinants of post-transcriptional gene expression in *Leishmania*. PLoS Pathog 2007 Sep 7;3(9):1291-307.

237. Haile S, Papadopoulou B. Developmental regulation of gene expression in trypanosomatid parasitic protozoa. Curr Opin Microbiol 2007 Dec;10(6):569-77.

238. Rochette A, McNicoll F, Girard J, Breton M, Leblanc E, Bergeron MG, et al. Characterization and developmental gene regulation of a large gene family encoding amastin surface proteins in *Leishmania* spp. Mol Biochem Parasitol 2005 Apr;140(2):205-20.

239. Gygi SP, Rochon Y, Franza BR, Aebersold R. Correlation between protein and mRNA abundance in yeast. Mol Cell Biol 1999 Mar;19(3):1720-30.

240. Mader U, Antelmann H, Buder T, Dahl MK, Hecker M, Homuth G. *Bacillus subtilis* functional genomics: genome-wide analysis of the DegS-DegU regulon by transcriptomics and proteomics. Mol Genet Genomics 2002 Dec;268(4):455-67.

241. Thompson DK, Beliaev AS, Giometti CS, Tollaksen SL, Khare T, Lies DP, et al. Transcriptional and proteomic analysis of a ferric uptake regulator (fur) mutant of *Shewanella oneidensis*: possible involvement of fur in energy metabolism, transcriptional regulation, and oxidative stress. Appl Environ Microbiol 2002 Feb;68(2):881-92.

242. McNicoll F, Drummelsmith J, Muller M, Madore E, Boilard N, Ouellette M, et al. A combined proteomic and transcriptomic approach to the study of stage differentiation in *Leishmania infantum*. Proteomics 2006 Jun;6(12):3567-81.

243. Bente M, Harder S, Wiesgigl M, Heukeshoven J, Gelhaus C, Krause E, et al. Developmentally induced changes of the proteome in the protozoan parasite *Leishmania donovani*. Proteomics 2003 Sep;3(9):1811-29.

244. Nugent PG, Karsani SA, Wait R, Tempero J, Smith DF. Proteomic analysis of *Leishmania mexicana* differentiation. Mol Biochem Parasitol 2004 Jul;136(1):51-62.

245. Rosenzweig D, Smith D, Opperdoes F, Stern S, Olafson RW, Zilberstein D. Retooling *Leishmania* metabolism: from sand fly gut to human macrophage. FASEB J 2008 Feb;22(2):590-602.

246. El Fakhry Y, Ouellette M, Papadopoulou B. A proteomic approach to identify developmentally regulated proteins in *Leishmania infantum*. Proteomics 2002 Aug;2(8):1007-17.

247. Walker J, Vasquez JJ, Gomez MA, Drummelsmith J, Burchmore R, Girard I, et al. Identification of developmentally-regulated proteins in *Leishmania* panamensis by proteome profiling of promastigotes and axenic amastigotes. Mol Biochem Parasitol 2006 May;147(1):64-73.

248. Alcolea PJ, Alonso A, Larraga V. Proteome profiling of *Leishmania infantum* promastigotes. J Eukaryot Microbiol 2011 Jul-Aug;58(4):352-8.

249. Cruz A, Beverley SM. Gene replacement in parasitic protozoa. Nature 1990 Nov 8;348(6297):171-3.

250. Sunkin SM, Kiser P, Myler PJ, Stuart K. The size difference between *Leishmania major* friedlin chromosome one homologues is localized to sub-telomeric repeats at one chromosomal end. Mol Biochem Parasitol 2000 Jun;109(1):1-15.

251. Dujardin JC. Structure, dynamics and function of *Leishmania* genome: resolving the puzzle of infection, genetics and evolution? Infect Genet Evol 2009 Mar;9(2):290-7.

252. Cruz AK, Titus R, Beverley SM. Plasticity in chromosome number and testing of essential genes in *Leishmania* by targeting. Proc Natl Acad Sci U S A 1993 Feb 15;90(4):1599-603.

253. Mottram JC, McCready BP, Brown KG, Grant KM. Gene disruptions indicate an essential function for the LmmCRK1 cdc2-related kinase of *Leishmania mexicana*. Mol Microbiol 1996 Nov;22(3):573-83.

254. Dumas C, Ouellette M, Tovar J, Cunningham ML, Fairlamb AH, Tamar S, et al. Disruption of the trypanothione reductase gene of *Leishmania* decreases its ability to survive oxidative stress in macrophages. EMBO J 1997 May 15;16(10):2590-8.

255. Leprohon P, Legare D, Raymond F, Madore E, Hardiman G, Corbeil J, et al. Gene expression modulation is associated with gene amplification, supernumerary chromosomes and chromosome loss in antimony-resistant *Leishmania infantum*. Nucleic Acids Res 2009 Apr;37(5):1387-99.

256. Ubeda JM, Legare D, Raymond F, Ouameur AA, Boisvert S, Rigault P, et al. Modulation of gene expression in drug resistant *Leishmania* is associated with gene amplification, gene deletion and chromosome aneuploidy. Genome Biol 2008;9(7):R115.

257. El Fadili K, Messier N, Leprohon P, Roy G, Guimond C, Trudel N, et al. Role of the ABC transporter MRPA (PGPA) in antimony resistance in *Leishmania infantum* axenic and intracellular amastigotes. Antimicrob Agents Chemother 2005 May;49(5):1988-93.

258. Guimond C, Trudel N, Brochu C, Marquis N, El Fadili A, Peytavi R, et al. Modulation of gene expression in *Leishmania* drug resistant mutants as determined by targeted DNA microarrays. Nucleic Acids Res 2003 Oct 15;31(20):5886-96.

259. Beverley SM, Coderre JA, Santi DV, Schimke RT. Unstable DNA amplifications in methotrexate-resistant *Leishmania* consist of extrachromosomal circles which relocalize during stabilization. Cell 1984 Sep;38(2):431-9.

260. Nare B, Hardy LW, Beverley SM. The roles of pteridine reductase 1 and dihydrofolate reductase-thymidylate synthase in pteridine metabolism in the protozoan parasite *Leishmania major*. J Biol Chem 1997 May 23;272(21):13883-91.

261. Selmecki A, Forche A, Berman J. Genomic plasticity of the human fungal pathogen Candida albicans. Eukaryot Cell 2010 Jul;9(7):991-1008.

262. Weaver BA, Silk AD, Montagna C, Verdier-Pinard P, Cleveland DW. Aneuploidy acts both oncogenically and as a tumor suppressor. Cancer Cell 2007 Jan;11(1):25-36.

263. Rajagopalan H, Lengauer C. Aneuploidy and cancer. Nature 2004 Nov 18;432(7015):338-41.

264. Sterkers Y, Lachaud L, Crobu L, Bastien P, Pages M. FISH analysis reveals aneuploidy and continual generation of chromosomal mosaicism in *Leishmania major*. Cell Microbiol 2010 Feb;13(2):274-83.

265. Wang DG, Fan JB, Siao CJ, Berno A, Young P, Sapolsky R, et al. Large-scale identification, mapping, and genotyping of single-nucleotide polymorphisms in the human genome. Science 1998 May 15;280(5366):1077-82.

266. Clayton CE. Life without transcriptional control? From fly to man and back again. EMBO J 2002 Apr 15;21(8):1881-8.

267. Young LY, Hull CM, Heitman J. Disruption of ergosterol biosynthesis confers resistance to amphotericin B in Candida lusitaniae. Antimicrob Agents Chemother 2003 Sep;47(9):2717-24.

268. Croft SL, Seifert K, Duchene M. Antiprotozoal activities of phospholipid analogues. Mol Biochem Parasitol 2003 Feb;126(2):165-72.

269. Opperdoes FR, Coombs GH. Metabolism of *Leishmania*: proven and predicted. Trends Parasitol 2007 Apr;23(4):149-58.

270. Chavali AK, Whittemore JD, Eddy JA, Williams KT, Papin JA. Systems analysis of metabolism in the pathogenic trypanosomatid *Leishmania major*. Mol Syst Biol 2008;4:177.

271. Doyle MA, MacRae JI, De Souza DP, Saunders EC, McConville MJ, Likic VA. LeishCyc: a biochemical pathways database for *Leishmania major*. BMC Syst Biol 2009;3:57.

272. Morales MA, Watanabe R, Laurent C, Lenormand P, Rousselle JC, Namane A, et al. Phosphoproteomic analysis of *Leishmania donovani* pro- and amastigote stages. Proteomics 2008 Jan;8(2):350-63.

273. Mojtahedi Z, Clos J, Kamali-Sarvestani E. *Leishmania major*: identification of developmentally regulated proteins in procyclic and metacyclic promastigotes. Exp Parasitol 2008 Jul;119(3):422-9.

274. Cuervo P, de Jesus JB, Junqueira M, Mendonca-Lima L, Gonzalez LJ, Betancourt L, et al. Proteome analysis of *Leishmania* (*Viannia) braziliensis* by two-dimensional gel electrophoresis and mass spectrometry. Mol Biochem Parasitol 2007 Jul;154(1):6-21.

275. Cuervo P, De Jesus JB, Saboia-Vahia L, Mendonca-Lima L, Domont GB, Cupolillo E. Proteomic characterization of the released/secreted proteins of *Leishmania* (*Viannia) braziliensis* promastigotes. J Proteomics 2009 Nov 2;73(1):79-92.

276. Paape D, Barrios-Llerena ME, Le Bihan T, Mackay L, Aebischer T. Gel free analysis of the proteome of intracellular *Leishmania mexicana*. Mol Biochem Parasitol 2010 Feb;169(2):108-14.

277. Gupta SK, Sisodia BS, Sinha S, Hajela K, Naik S, Shasany AK, et al. Proteomic approach for identification and characterization of novel immunostimulatory proteins from soluble antigens of *Leishmania donovani* promastigotes. Proteomics 2007 Mar;7(5):816-23.

278. Dea-Ayuela MA, Rama-Iniguez S, Bolas-Fernandez F. Proteomic analysis of antigens from *Leishmania infantum* promastigotes. Proteomics 2006 Jul;6(14):4187-94.

279. Silverman JM, Clos J, de'Oliveira CC, Shirvani O, Fang Y, Wang C, et al. An exosome-based secretion pathway is responsible for protein export from *Leishmania* and communication with macrophages. J Cell Sci 2010 Mar 15;123(Pt 6):842-52.

280. Jensen ON. Interpreting the protein language using proteomics. Nat Rev Mol Cell Biol 2006 Jun;7(6):391-403.

281. Rosenzweig D, Smith D, Myler PJ, Olafson RW, Zilberstein D. Post-translational modification of cellular proteins during *Leishmania donovani* differentiation. Proteomics 2008 May;8(9):1843-50.

282. Morales MA, Watanabe R, Dacher M, Chafey P, Osorio y Fortea J, Scott DA, et al. Phosphoproteome dynamics reveal heat-shock protein complexes specific to the *Leishmania donovani* infectious stage. Proc Natl Acad Sci U S A 2010 May 4;107(18):8381-6.

283. Naderer T, McConville MJ. The *Leishmania*-macrophage interaction: a metabolic perspective. Cell Microbiol 2008 Feb;10(2):301-8.

284. Vinayavekhin N, Homan EA, Saghatelian A. Exploring disease through metabolomics. ACS Chem Biol 2010 Jan 15;5(1):91-103.

285. Wang Y, Holmes E, Nicholson JK, Cloarec O, Chollet J, Tanner M, et al. Metabonomic investigations in mice infected with *Schistosoma mansoni*: an approach for biomarker identification. Proc Natl Acad Sci U S A 2004 Aug 24;101(34):12676-81.

286. Martin FP, Verdu EF, Wang Y, Dumas ME, Yap IK, Cloarec O, et al. Transgenomic metabolic interactions in a mouse disease model: interactions of *Trichinella spiralis* infection with dietary *Lactobacillus paracasei* supplementation. J Proteome Res 2006 Sep;5(9):2185-93.

287. Coustou V, Biran M, Breton M, Guegan F, Riviere L, Plazolles N, et al. Glucose-induced remodeling of intermediary and energy metabolism in procyclic *Trypanosoma brucei*. J Biol Chem 2008 Jun 13;283(24):16342-54.

288. McConville MJ, Naderer T. Metabolic Pathways Required for the Intracellular Survival of *Leishmania*. Annu Rev Microbiol 2011 Sep 28 *in press*

289. Opperdoes FR, Michels PAM. The metabolic repertoire of *Leishmania* and implications for drug discovery. 2008.

290. Opperdoes FR. The glycosome of Trypanosomatids. Microbiology Monographs 2010:285-98.

291. Saunders EC, DP DES, Naderer T, Sernee MF, Ralton JE, Doyle MA, et al. Central carbon metabolism of *Leishmania* parasites. Parasitology 2010 Aug;137(9):1303-13.

292. Hart DT, Coombs GH. *Leishmania mexicana*: energy metabolism of amastigotes and promastigotes. Exp Parasitol 1982 Dec;54(3):397-409.

293. Ilg T. Generation of myo-inositol-auxotrophic *Leishmania mexicana* mutants by targeted replacement of the myo-inositol-1-phosphate synthase gene. Mol Biochem Parasitol 2002 Mar;120(1):151-6.

294. Naderer T, Wee E, McConville MJ. Role of hexosamine biosynthesis in *Leishmania* growth and virulence. Mol Microbiol 2008 Aug;69(4):858-69.

295. Burchmore RJ, Rodriguez-Contreras D, McBride K, Merkel P, Barrett MP, Modi G, et al. Genetic characterization of glucose transporter function in *Leishmania mexicana*. Proc Natl Acad Sci U S A 2003 Apr 1;100(7):3901-6.

296. Naderer T, Ellis MA, Sernee MF, De Souza DP, Curtis J, Handman E, et al. Virulence of *Leishmania major* in macrophages and mice requires the gluconeogenic enzyme fructose-1,6-bisphosphatase. Proc Natl Acad Sci U S A 2006 Apr 4;103(14):5502-7.

297. Naderer T, Heng J, McConville MJ. Evidence that intracellular stages of *Leishmania major* utilize amino sugars as a major carbon source. PLoS Pathog 2010;6(12):e1001245.

298. Rodriguez-Contreras D, Landfear SM. Metabolic changes in glucose transporter-deficient *Leishmania mexicana* and parasite virulence. J Biol Chem 2006 Jul 21;281(29):20068-76.

299. Ralton JE, Naderer T, Piraino HL, Bashtannyk TA, Callaghan JM, McConville MJ. Evidence that intracellular beta1-2 mannan is a virulence factor in *Leishmania* parasites. J Biol Chem 2003 Oct 17;278(42):40757-63.

300. Saunders EC, Ng WW, Chambers JM, Ng M, Naderer T, Kromer JO, et al. Isotopomer profiling of *Leishmania mexicana* promastigotes reveals important roles for succinate fermentation and aspartate uptake in tricarboxylic acid cycle (TCA) anaplerosis, glutamate synthesis, and growth. J Biol Chem 2011 Aug 5;286(31):27706-17.

301. Bringaud F, Riviere L, Coustou V. Energy metabolism of trypanosomatids: adaptation to available carbon sources. Mol Biochem Parasitol 2006 Sep;149(1):1-9.

302. Tielens AG, van Hellemond JJ. Surprising variety in energy metabolism within Trypanosomatidae. Trends Parasitol 2009 Oct;25(10):482-90.

303. Darling TN, Davis DG, London RE, Blum JJ. Products of *Leishmania braziliensis* glucose catabolism: release of D-lactate and, under anaerobic conditions, glycerol. Proc Natl Acad Sci U S A 1987 Oct;84(20):7129-33.

304. Van Hellemond JJ, Opperdoes FR, Tielens AG. Trypanosomatidae produce acetate via a mitochondrial acetate:succinate CoA transferase. Proc Natl Acad Sci U S A 1998 Mar 17;95(6):3036-41.

305. Riviere L, van Weelden SW, Glass P, Vegh P, Coustou V, Biran M, et al. Acetyl:succinate CoA-transferase in procyclic *Trypanosoma brucei*. Gene identification and role in carbohydrate metabolism. J Biol Chem 2004 Oct 29;279(44):45337-46.

306. Vickers TJ, Greig N, Fairlamb AH. A trypanothione-dependent glyoxalase I with a prokaryotic ancestry in *Leishmania major*. Proc Natl Acad Sci U S A 2004 Sep 7;101(36):13186-91.

307. Wyllie S, Fairlamb AH. Methylglyoxal metabolism in *Trypanosomes* and *Leishmania*. Semin Cell Dev Biol 2011 May;22(3):271-7.

308. Ebikeme C, Hubert J, Biran M, Gouspillou G, Morand P, Plazolles N, et al. Ablation of succinate production from glucose metabolism in the procyclic trypanosomes induces metabolic switches to the glycerol 3-phosphate/dihydroxyacetone phosphate shuttle and to proline metabolism. J Biol Chem 2010 Oct 15;285(42):32312-24.

309. Uboldi AD, Lueder FB, Walsh P, Spurck T, McFadden GI, Curtis J, et al. A mitochondrial protein affects cell morphology, mitochondrial segregation and virulence in *Leishmania*. Int J Parasitol 2006 Dec;36(14):1499-514.

310. Zikova A, Panigrahi AK, Uboldi AD, Dalley RA, Handman E, Stuart K. Structural and functional association of *Trypanosoma brucei* MIX protein with cytochrome c oxidase complex. Eukaryot Cell 2008 Nov;7(11):1994-2003.

311. Dey R, Meneses C, Salotra P, Kamhawi S, Nakhasi HL, Duncan R. Characterization of a *Leishmania* stage-specific mitochondrial membrane protein that enhances the activity of cytochrome c oxidase and its role in virulence. Mol Microbiol 2010 Jul;77(2):399-414.

312. Wood T. Physiological functions of the pentose phosphate pathway. Cell Biochem Funct 1986 Oct;4(4):241-7.

313. Wood T. Distribution of the pentose phosphate pathway in living organisms. Cell Biochem Funct 1986 Oct;4(4):235-40.

314. Maugeri DA, Cazzulo JJ, Burchmore RJ, Barrett MP, Ogbunude PO. Pentose phosphate metabolism in *Leishmania mexicana*. Mol Biochem Parasitol 2003 Aug 31;130(2):117-25.

315. Hannaert V, Bringaud F, Opperdoes FR, Michels PA. Evolution of energy metabolism and its compartmentation in Kinetoplastida. Kinetoplastid Biol Dis 2003 Oct 28;2(1):11.

316. Pastakia KB, Dwyer DM. Identification and characterization of a ribose transport system in *Leishmania donovani* promastigotes. Mol Biochem Parasitol 1987 Nov;26(1-2):175-81.

317. Holzmuller P, Sereno D, Lemesre JL. Lower nitric oxide susceptibility of trivalent antimony-resistant amastigotes of *Leishmania infantum*. Antimicrob Agents Chemother 2005 Oct;49(10):4406-9.

318. Lee SH, Stephens JL, Englund PT. A fatty-acid synthesis mechanism specialized for parasitism. Nat Rev Microbiol 2007 Apr;5(4):287-97.

319. Samanovic M, Molina-Portela MP, Chessler AD, Burleigh BA, Raper J. *Trypanosome* lytic factor, an antimicrobial high-density lipoprotein, ameliorates *Leishmania* infection. PLoS Pathog 2009 Jan;5(1):e1000276.

320. McConville MJ, Blackwell JM. Developmental changes in the glycosylated phosphatidylinositols of *Leishmania donovani*. Characterization of the promastigote and amastigote glycolipids. J Biol Chem 1991 Aug 15;266(23):15170-9.

321. Winter G, Fuchs M, McConville MJ, Stierhof YD, Overath P. Surface antigens of *Leishmania mexicana* amastigotes: characterization of glycoinositol phospholipids and a macrophage-derived glycosphingolipid. J Cell Sci 1994 Sep;107 (Pt 9):2471-82.

322. Zufferey R, Allen S, Barron T, Sullivan DR, Denny PW, Almeida IC, et al. Ether phospholipids and glycosylinositolphospholipids are not required for amastigote virulence

or for inhibition of macrophage activation by *Leishmania major*. J Biol Chem 2003 Nov 7;278(45):44708-18.

323. Zhang K, Beverley SM. Phospholipid and sphingolipid metabolism in *Leishmania*. Mol Biochem Parasitol 2010 Apr;170(2):55-64.

324. Schneider P, Ferguson MA, McConville MJ, Mehlert A, Homans SW, Bordier C. Structure of the glycosyl-phosphatidylinositol membrane anchor of the *Leishmania major* promastigote surface protease. J Biol Chem 1990 Oct 5;265(28):16955-64.

325. McConville MJ, Ferguson MA. The structure, biosynthesis and function of glycosylated phosphatidylinositols in the parasitic protozoa and higher eukaryotes. Biochem J 1993 Sep 1;294 (Pt 2):305-24.

326. Vance JE, Steenbergen R. Metabolism and functions of phosphatidylserine. Prog Lipid Res 2005 Jul;44(4):207-34.

327. Balasubramanian K, Mirnikjoo B, Schroit AJ. Regulated externalization of phosphatidylserine at the cell surface: implications for apoptosis. J Biol Chem 2007 Jun 22;282(25):18357-64.

328. Nguewa PA, Fuertes MA, Valladares B, Alonso C, Perez JM. Programmed cell death in trypanosomatids: a way to maximize their biological fitness? Trends Parasitol 2004 Aug;20(8):375-80.

329. Wanderley JL, Pinto da Silva LH, Deolindo P, Soong L, Borges VM, Prates DB, et al. Cooperation between apoptotic and viable metacyclics enhances the pathogenesis of Leishmaniasis. PLoS One 2009;4(5):e5733.

330. Sindermann H, Croft SL, Engel KR, Bommer W, Eibl HJ, Unger C, et al. Miltefosine (Impavido): the first oral treatment against Leishmaniasis. Med Microbiol Immunol 2004 Nov;193(4):173-80.

331. Soto J, Arana BA, Toledo J, Rizzo N, Vega JC, Diaz A, et al. Miltefosine for new world cutaneous Leishmaniasis. Clin Infect Dis 2004 May 1;38(9):1266-72.

332. Rakotomanga M, Blanc S, Gaudin K, Chaminade P, Loiseau PM. Miltefosine affects lipid metabolism in *Leishmania donovani* promastigotes. Antimicrob Agents Chemother 2007 Apr;51(4):1425-30.

333. Luque-Ortega JR, Rivas L. Miltefosine (hexadecylphosphocholine) inhibits cytochrome c oxidase in *Leishmania donovani* promastigotes. Antimicrob Agents Chemother 2007 Apr;51(4):1327-32.

334. Zhang K, Bangs JD, Beverley SM. Sphingolipids in parasitic protozoa. Adv Exp Med Biol 2010;688:238-48.

335. Zhang K, Showalter M, Revollo J, Hsu FF, Turk J, Beverley SM. Sphingolipids are essential for differentiation but not growth in *Leishmania*. EMBO J 2003 Nov 17;22(22):6016-26.

336. Hannun YA, Obeid LM. Principles of bioactive lipid signalling: lessons from sphingolipids. Nat Rev Mol Cell Biol 2008 Feb;9(2):139-50.

337. Zhang K, Pompey JM, Hsu FF, Key P, Bandhuvula P, Saba JD, et al. Redirection of sphingolipid metabolism toward de novo synthesis of ethanolamine in *Leishmania*. EMBO J 2007 Feb 21;26(4):1094-104.

338. Rifkin MR, Fairlamb AH. Transport of ethanolamine and its incorporation into the variant surface glycoprotein of bloodstream forms of *Trypanosoma brucei.* Mol Biochem Parasitol 1985 Jun;15(3):245-56.

339. Zufferey R, Mamoun CB. Choline transport in *Leishmania major* promastigotes and its inhibition by choline and phosphocholine analogs. Mol Biochem Parasitol 2002 Nov-Dec;125(1-2):127-34.

340. Zhang K, Hsu FF, Scott DA, Docampo R, Turk J, Beverley SM. *Leishmania* salvage and remodelling of host sphingolipids in amastigote survival and acidocalcisome biogenesis. Mol Microbiol 2005 Mar;55(5):1566-78.

341. Ghosh S, Bhattacharyya S, Sirkar M, Sa GS, Das T, Majumdar D, et al. *Leishmania donovani* suppresses activated protein 1 and NF-kappaB activation in host macrophages via ceramide generation: involvement of extracellular signal-regulated kinase. Infect Immun 2002 Dec;70(12):6828-38.

342. Chance ML, Havercroft PR, Goad LJ. Observations on leucine incorporation into sterol by *Leishmania*, and its inhibition by terbinafine. Ann Trop Med Parasitol 1999 Mar;93(2):185-8.

343. Xu X, Bittman R, Duportail G, Heissler D, Vilcheze C, London E. Effect of the structure of natural sterols and sphingolipids on the formation of ordered sphingolipid/sterol domains (rafts). Comparison of cholesterol to plant, fungal, and disease-associated sterols and comparison of sphingomyelin, cerebrosides, and ceramide. J Biol Chem 2001 Sep 7;276(36):33540-6.

344. Mbongo N, Loiseau PM, Billion MA, Robert-Gero M. Mechanism of amphotericin B resistance in *Leishmania donovani* promastigotes. Antimicrob Agents Chemother 1998 Feb;42(2):352-7.

345. Cauchetier E, Loiseau PM, Lehman J, Rivollet D, Fleury J, Astier A, et al. Characterisation of atovaquone resistance in *Leishmania infantum* promastigotes. Int J Parasitol 2002 Jul;32(8):1043-51.

346. Granthon AC, Braga MV, Rodrigues JC, Cammerer S, Lorente SO, Gilbert IH, et al. Alterations on the growth and ultrastructure of *Leishmania* chagasi induced by squalene synthase inhibitors. Vet Parasitol 2007 May 15;146(1-2):25-34.

347. Rodrigues JC, Urbina JA, de Souza W. Antiproliferative and ultrastructural effects of BPQ-OH, a specific inhibitor of squalene synthase, on *Leishmania amazonensisi*. Exp Parasitol 2005 Dec;111(4):230-8.

348. Torres-Santos EC, Sampaio-Santos MI, Buckner FS, Yokoyama K, Gelb M, Urbina JA, et al. Altered sterol profile induced in *Leishmania amazonensisi* by a natural dihydroxymethoxylated chalcone. J Antimicrob Chemother 2009 Mar;63(3):469-72.

349. Williams RA, Westrop GD, Coombs GH. Two pathways for cysteine biosynthesis in *Leishmania major*. Biochem J 2009 Jun 15;420(3):451-62.

350. Shaked-Mishan P, Suter-Grotemeyer M, Yoel-Almagor T, Holland N, Zilberstein D, Rentsch D. A novel high-affinity arginine transporter from the human parasitic protozoan *Leishmania donovani*. Mol Microbiol 2006 Apr;60(1):30-8.

351. Roberts SC, Tancer MJ, Polinsky MR, Gibson KM, Heby O, Ullman B. Arginase plays a pivotal role in polyamine precursor metabolism in *Leishmania*. Characterization of gene deletion mutants. J Biol Chem 2004 May 28;279(22):23668-78.

352. Darlyuk I, Goldman A, Roberts SC, Ullman B, Rentsch D, Zilberstein D. Arginine homeostasis and transport in the human pathogen *Leishmania donovani*. J Biol Chem 2009 Jul 24;284(30):19800-7.

353. Inbar E, Canepa GE, Carrillo C, Glaser F, Suter Grotemeyer M, Rentsch D, et al. Lysine transporters in human trypanosomatid pathogens. Amino Acids 2010 Dec 18.

354. Ginger ML, Chance ML, Sadler IH, Goad LJ. The biosynthetic incorporation of the intact leucine skeleton into sterol by the trypanosomatid *Leishmania mexicana*. J Biol Chem 2001 Apr 13;276(15):11674-82.

355. Landfear SM, Ullman B, Carter NS, Sanchez MA. Nucleoside and nucleobase transporters in parasitic protozoa. Eukaryot Cell 2004 Apr;3(2):245-54.

356. Van den Berghe G, Vincent MF, Jaeken J. Inborn errors of the purine nucleotide cycle: adenylosuccinase deficiency. J Inherit Metab Dis 1997 Jun;20(2):193-202.

357. Carter NS, Yates PA, Gessford SK, Galagan SR, Landfear SM, Ullman B. Adaptive responses to purine starvation in *Leishmania donovani*. Mol Microbiol 2010 Oct;78(1):92-107.

358. Ortiz D, Valdes R, Sanchez MA, Hayenga J, Elya C, Detke S, et al. Purine restriction induces pronounced translational upregulation of the NT1 adenosine/pyrimidine nucleoside transporter in *Leishmania major*. Mol Microbiol 2010 Oct;78(1):108-18.

359. Boitz JM, Ullman B. A conditional mutant deficient in hypoxanthine-guanine phosphoribosyltransferase and xanthine phosphoribosyltransferase validates the purine salvage pathway of *Leishmania donovani*. J Biol Chem 2006 Jun 9;281(23):16084-9.

360. Boitz JM, Ullman B. Amplification of adenine phosphoribosyltransferase suppresses the conditionally lethal growth and virulence phenotype of *Leishmania*

donovani mutants lacking both hypoxanthine-guanine and xanthine phosphoribosyltransferases. J Biol Chem 2010 Jun 11;285(24):18555-64.

361. Allen T, Hwang HY, Wilson K, Hanson S, Jardim A, Ullman B. Cloning and expression of the adenine phosphoribosyltransferase gene from *Leishmania donovani*. Mol Biochem Parasitol 1995 Oct;74(1):99-103.

362. Allen TE, Hwang HY, Jardim A, Olafson R, Ullman B. Cloning and expression of the hypoxanthine-guanine phosphoribosyltransferase from *Leishmania donovani*. Mol Biochem Parasitol 1995 Jul;73(1-2):133-43.

363. Colotti G, Ilari A. Polyamine metabolism in *Leishmania*: from arginine to trypanothione. Amino Acids 2011 Feb;40(2):269-85.

364. Krauth-Siegel RL, Comini MA. Redox control in trypanosomatids, parasitic protozoa with trypanothione-based thiol metabolism. Biochim Biophys Acta 2008 Nov;1780(11):1236-48.

365. Gaur U, Roberts SC, Dalvi RP, Corraliza I, Ullman B, Wilson ME. An effect of parasite-encoded arginase on the outcome of murine cutaneous *Leishmania*sis. J Immunol 2007 Dec 15;179(12):8446-53.

366. Hasne MP, Ullman B. Identification and characterization of a polyamine permease from the protozoan parasite *Leishmania major*. J Biol Chem 2005 Apr 15;280(15):15188-94.

367. Basselin M, Coombs GH, Barrett MP. Putrescine and spermidine transport in *Leishmania*. Mol Biochem Parasitol 2000 Jun;109(1):37-46.

368. Boitz JM, Yates PA, Kline C, Gaur U, Wilson ME, Ullman B, et al. *Leishmania donovani* ornithine decarboxylase is indispensable for parasite survival in the mammalian host. Infect Immun 2009 Feb;77(2):756-63.

369. Jiang Y, Roberts SC, Jardim A, Carter NS, Shih S, Ariyanayagam M, et al. Ornithine decarboxylase gene deletion mutants of *Leishmania donovani*. J Biol Chem 1999 Feb 5;274(6):3781-8.

370. Mukhopadhyay R, Kapoor P, Madhubala R. Characterization of alpha-difluoromethylornithine resistant *Leishmania donovani* and its susceptibility to other inhibitors of the polyamine biosynthetic pathway. Pharmacol Res 1996 Jul-Aug;34(1-2):43-6.

371. Vickers TJ, Beverley SM. Folate metabolic pathways in *Leishmania*. Essays in Biochemistry 2011;51.

372. Ouellette M, Drummelsmith J, El-Fadili A, Kundig C, Richard D, Roy G. Pterin transport and metabolism in *Leishmania* and related trypanosomatid parasites. Int J Parasitol 2002 Apr;32(4):385-98.

373. Lemley C, Yan S, Dole VS, Madhubala R, Cunningham ML, Beverley SM, et al. The *Leishmania donovani* LD1 locus gene ORFG encodes a biopterin transporter (BT1). Mol Biochem Parasitol 1999 Oct 25;104(1):93-105.

374. Bello AR, Nare B, Freedman D, Hardy L, Beverley SM. PTR1: a reductase mediating salvage of oxidized pteridines and methotrexate resistance in the protozoan parasite *Leishmania major*. Proc Natl Acad Sci U S A 1994 Nov 22;91(24):11442-6.

375. Ong HB, Sienkiewicz N, Wyllie S, Fairlamb AH. Dissecting the metabolic roles of pteridine reductase 1 in *Trypanosoma brucei* and *Leishmania major*. J Biol Chem 2011 Mar 25;286(12):10429-38.

376. Koreny L, Lukes J, Obornik M. Evolution of the haem synthetic pathway in kinetoplastid flagellates: an essential pathway that is not essential after all? Int J Parasitol 2010 Feb;40(2):149-56.

377. Akilov OE, Kosaka S, O'Riordan K, Hasan T. Parasiticidal effect of delta-aminolevulinic acid-based photodynamic therapy for cutaneous Leishmaniasis is indirect and mediated through the killing of the host cells. Exp Dermatol 2007 Aug;16(8):651-60.

378. Sah JF, Ito H, Kolli BK, Peterson DA, Sassa S, Chang KP. Genetic rescue of *Leishmania* deficiency in porphyrin biosynthesis creates mutants suitable for analysis of cellular events in uroporphyria and for photodynamic therapy. J Biol Chem 2002 Apr 26;277(17):14902-9.

379. Srivastava P, Sharma GD, Kamboj KK, Rastogi AK, Pandey VC. Heme metabolism in promastigotes of *Leishmania donovani*. Mol Cell Biochem 1997 Jun;171(1-2):65-8.

380. Chen CK, Doyle PS, Yermalitskaya LV, Mackey ZB, Ang KK, McKerrow JH, et al. *Trypanosoma cruzi* CYP51 inhibitor derived from a *Mycobacterium tuberculosis* screen hit. PLoS Negl Trop Dis 2009;3(2):e372.

381. Wilkinson SR, Obado SO, Mauricio IL, Kelly JM. *Trypanosoma cruzi* expresses a plant-like ascorbate-dependent hemoperoxidase localized to the endoplasmic reticulum. Proc Natl Acad Sci U S A 2002 Oct 15;99(21):13453-8.

382. Lepesheva GI, Hargrove TY, Kleshchenko Y, Nes WD, Villalta F, Waterman MR. CYP51: A major drug target in the cytochrome P450 superfamily. Lipids 2008 Dec;43(12):1117-25.

383. Tripodi KE, Buttigliero LV, Altabe SG, Uttaro AD. Functional characterization of front-end desaturases from trypanosomatids depicts the first polyunsaturated fatty acid biosynthetic pathway from a parasitic protozoan. FEBS J 2006 Jan;273(2):271-80.

384. Bridges DJ, Pitt AR, Hanrahan O, Brennan K, Voorheis HP, Herzyk P, et al. Characterisation of the plasma membrane subproteome of bloodstream form *Trypanosoma brucei*. Proteomics 2008 Jan;8(1):83-99.

385. Verma S, Mehta A, Shaha C. CYP5122A1, a Novel Cytochrome P450 Is Essential for Survival of *Leishmania donovani*. PLoS One 2011;6(9):e25273.

386. Castro H, Tomas AM. Peroxidases of trypanosomatids. Antioxid Redox Signal 2008 Sep;10(9):1593-606.

387. Scandalios JG. Oxidative stress: molecular perception and transduction of signals triggering antioxidant gene defenses. Braz J Med Biol Res 2005 Jul;38(7):995-1014.

388. Fairlamb AH, Blackburn P, Ulrich P, Chait BT, Cerami A. Trypanothione: a novel bis(glutathionyl)spermidine cofactor for glutathione reductase in trypanosomatids. Science 1985 Mar 22;227(4693):1485-7.

389. Montrichard F, Le Guen F, Laval-Martin DL, Davioud-Charvet E. Evidence for the co-existence of glutathione reductase and trypanothione reductase in the non-trypanosomatid Euglenozoa: Euglena gracilis Z. FEBS Lett 1999 Jan 8;442(1):29-33.

390. Ondarza RN, Iturbe A, Hurtado G, Tamayo E, Ondarza M, Hernandez E. Entamoeba histolytica: a eukaryote with trypanothione metabolism instead of glutathione metabolism. Biotechnol Appl Biochem 1999 Aug;30 (Pt 1):47-52.

391. Ondarza RN, Hurtado G, Tamayo E, Iturbe A, Hernandez E. Naegleria fowleri: a free-living highly pathogenic amoeba contains trypanothione/trypanothione reductase and glutathione/glutathione reductase systems. Exp Parasitol 2006 Nov;114(3):141-6.

392. Dormeyer M, Reckenfelderbaumer N, Ludemann H, Krauth-Siegel RL. Trypanothione-dependent synthesis of deoxyribonucleotides by *Trypanosoma brucei*ribonucleotide reductase. J Biol Chem 2001 Apr 6;276(14):10602-6.

393. Nogoceke E, Gommel DU, Kiess M, Kalisz HM, Flohe L. A unique cascade of oxidoreductases catalyses trypanothione-mediated peroxide metabolism in *Crithidia fasciculata.* Biol Chem 1997 Aug;378(8):827-36.

394. Flohe L, Budde H, Bruns K, Castro H, Clos J, Hofmann B, et al. Tryparedoxin peroxidase of *Leishmania donovani*: molecular cloning, heterologous expression, specificity, and catalytic mechanism. Arch Biochem Biophys 2002 Jan 15;397(2):324-35.

395. Ariyanayagam MR, Fairlamb AH. Ovothiol and trypanothione as antioxidants in trypanosomatids. Mol Biochem Parasitol 2001 Jul;115(2):189-98.

396. Fairlamb AH, Cerami A. Metabolism and functions of trypanothione in the Kinetoplastida. Annu Rev Microbiol 1992;46:695-729.

397. Oza SL, Tetaud E, Ariyanayagam MR, Warnon SS, Fairlamb AH. A single enzyme catalyses formation of Trypanothione from glutathione and spermidine in *Trypanosoma cruzi*. J Biol Chem 2002 Sep 27;277(39):35853-61.

398. Fyfe PK, Oza SL, Fairlamb AH, Hunter WN. *Leishmania* trypanothione synthetase-amidase structure reveals a basis for regulation of conflicting synthetic and hydrolytic activities. J Biol Chem 2008 Jun 20;283(25):17672-80.

399. Comini M, Menge U, Flohe L. Biosynthesis of trypanothione in *Trypanosoma brucei*brucei. Biol Chem 2003 Apr;384(4):653-6.

400. Oza SL, Ariyanayagam MR, Fairlamb AH. Characterization of recombinant glutathionylspermidine synthetase/amidase from *Crithidia fasciculata.* Biochem J 2002 Jun 15;364(Pt 3):679-86.

401. Wyllie S, Oza SL, Patterson S, Spinks D, Thompson S, Fairlamb AH. Dissecting the essentiality of the bifunctional trypanothione synthetase-amidase in *Trypanosoma brucei*using chemical and genetic methods. Mol Microbiol 2009 Nov;74(3):529-40.

402. Gilbert HF. Molecular and cellular aspects of thiol-disulfide exchange. Adv Enzymol Relat Areas Mol Biol 1990;63:69-172.

403. Moutiez M, Meziane-Cherif D, Aumercier M, Sergheraert C, Tartar A. Compared reactivities of trypanothione and glutathione in conjugation reactions. Chem Pharm Bull 1994;42:2641-4.

404. Bocedi A, Dawood KF, Fabrini R, Federici G, Gradoni L, Pedersen JZ, et al. Trypanothione efficiently intercepts nitric oxide as a harmless iron complex in trypanosomatid parasites. FASEB J 2010 Apr;24(4):1035-42.

405. Tovar J, Wilkinson S, Mottram JC, Fairlamb AH. Evidence that trypanothione reductase is an essential enzyme in *Leishmania* by targeted replacement of the tryA gene locus. Mol Microbiol 1998 Jul;29(2):653-60.

406. Tovar J, Cunningham ML, Smith AC, Croft SL, Fairlamb AH. Down-regulation of *Leishmania donovani* trypanothione reductase by heterologous expression of a trans-dominant mutant homologue: effect on parasite intracellular survival. Proc Natl Acad Sci U S A 1998 Apr 28;95(9):5311-6.

407. Baiocco P, Franceschini S, Ilari A, Colotti G. Trypanothione reductase from *Leishmania infantum*: cloning, expression, purification, crystallization and preliminary X-ray data analysis. Protein Pept Lett 2009;16(2):196-200.

408. Cunningham ML, Fairlamb AH. Trypanothione reductase from *Leishmania donovani*. Purification, characterisation and inhibition by trivalent antimonials. Eur J Biochem 1995 Jun 1;230(2):460-8.

409. Krauth-Siegel RL, Enders B, Henderson GB, Fairlamb AH, Schirmer RH. Trypanothione reductase from *Trypanosoma cruzi*. Purification and characterization of the crystalline enzyme. Eur J Biochem 1987 Apr 1;164(1):123-8.

410. Eberle C, Lauber BS, Fankhauser D, Kaiser M, Brun R, Krauth-Siegel RL, et al. Improved inhibitors of trypanothione reductase by combination of motifs: synthesis, inhibitory potency, binding mode, and antiprotozoal activities. ChemMedChem 2011 Feb 7;6(2):292-301.

411. Walton JG, Jones DC, Kiuru P, Durie AJ, Westwood NJ, Fairlamb AH. Synthesis and evaluation of indatraline-based inhibitors for trypanothione reductase. ChemMedChem 2011 Feb 7;6(2):321-8.

412. Flohe L, Hecht HJ, Steinert P. Glutathione and trypanothione in parasitic hydroperoxide metabolism. Free Radic Biol Med 1999 Nov;27(9-10):966-84.

413. Wilkinson SR, Meyer DJ, Taylor MC, Bromley EV, Miles MA, Kelly JM. The *Trypanosoma cruzi* enzyme TcGPXI is a glycosomal peroxidase and can be linked to trypanothione reduction by glutathione or tryparedoxin. J Biol Chem 2002 May 10;277(19):17062-71.

414. Hillebrand H, Schmidt A, Krauth-Siegel RL. A second class of peroxidases linked to the trypanothione metabolism. J Biol Chem 2003 Feb 28;278(9):6809-15.

415. Konig J, Fairlamb AH. A comparative study of type I and type II tryparedoxin peroxidases in *Leishmania major*. FEBS J 2007 Nov;274(21):5643-58.

416. Gommel DU, Nogoceke E, Morr M, Kiess M, Kalisz HM, Flohe L. Catalytic characteristics of tryparedoxin. Eur J Biochem 1997 Sep 15;248(3):913-8.

417. Onn I, Milman-Shtepel N, Shlomai J. Redox potential regulates binding of universal minicircle sequence binding protein at the kinetoplast DNA replication origin. Eukaryot Cell 2004 Apr;3(2):277-87.

418. Filser M, Comini MA, Molina-Navarro MM, Dirdjaja N, Herrero E, Krauth-Siegel RL. Cloning, functional analysis, and mitochondrial localization of *Trypanosoma brucei*monothiol glutaredoxin-1. Biol Chem 2008 Jan;389(1):21-32.

419. Melchers J, Dirdjaja N, Ruppert T, Krauth-Siegel RL. Glutathionylation of trypanosomal thiol redox proteins. J Biol Chem 2007 Mar 23;282(12):8678-94.

420. Comini MA, Krauth-Siegel RL, Flohe L. Depletion of the thioredoxin homologue tryparedoxin impairs antioxidative defence in African trypanosomes. Biochem J 2007 Feb 15;402(1):43-9.

421. Castro H, Romao S, Carvalho S, Teixeira F, Sousa C, Tomas AM. Mitochondrial redox metabolism in trypanosomatids is independent of tryparedoxin activity. PLoS One 2010;5(9):e12607.

422. Wilkinson SR, Horn D, Prathalingam SR, Kelly JM. RNA interference identifies two hydroperoxide metabolizing enzymes that are essential to the bloodstream form of the african trypanosome. J Biol Chem 2003 Aug 22;278(34):31640-6.

423. Castro H, Budde H, Flohe L, Hofmann B, Lunsdorf H, Wissing J, et al. Specificity and kinetics of a mitochondrial peroxiredoxin of *Leishmania infantum*. Free Radic Biol Med 2002 Dec 1;33(11):1563-74.

424. Levick MP, Tetaud E, Fairlamb AH, Blackwell JM. Identification and characterisation of a functional peroxidoxin from *Leishmania major*. Mol Biochem Parasitol 1998 Oct 30;96(1-2):125-37.

425. Castro H, Sousa C, Santos M, Cordeiro-da-Silva A, Flohe L, Tomas AM. Complementary antioxidant defense by cytoplasmic and mitochondrial peroxiredoxins in *Leishmania infantum*. Free Radic Biol Med 2002 Dec 1;33(11):1552-62.

426. Romao S, Castro H, Sousa C, Carvalho S, Tomas AM. The cytosolic tryparedoxin of *Leishmania infantum* is essential for parasite survival. Int J Parasitol 2009 May;39(6):703-11.

427. Schlecker T, Schmidt A, Dirdjaja N, Voncken F, Clayton C, Krauth-Siegel RL. Substrate specificity, localization, and essential role of the glutathione peroxidase-type tryparedoxin peroxidases in *Trypanosoma brucei*. J Biol Chem 2005 Apr 15;280(15):14385-94.

428. Dolai S, Yadav RK, Pal S, Adak S. *Leishmania major* ascorbate peroxidase overexpression protects cells against reactive oxygen species-mediated cardiolipin oxidation. Free Radic Biol Med 2008 Dec 1;45(11):1520-9.

429. Pal S, Dolai S, Yadav RK, Adak S. Ascorbate peroxidase from *Leishmania major* controls the virulence of infective stage of promastigotes by regulating oxidative stress. PLoS One 2010;5(6):e11271.

430. Armstrong RN. Structure, catalytic mechanism, and evolution of the glutathione transferases. Chem Res Toxicol 1997 Jan;10(1):2-18.

431. Hayes JD, Flanagan JU, Jowsey IR. Glutathione transferases. Annu Rev Pharmacol Toxicol 2005;45:51-88.

432. Hurst R, Bao Y, Jemth P, Mannervik B, Williamson G. Phospholipid hydroperoxide glutathione peroxidase activity of human glutathione transferases. Biochem J 1998 May 15;332 (Pt 1):97-100.

433. Berhane K, Widersten M, Engstrom A, Kozarich JW, Mannervik B. Detoxication of base propenals and other alpha, beta-unsaturated aldehyde products of radical reactions and lipid peroxidation by human glutathione transferases. Proc Natl Acad Sci U S A 1994 Feb 15;91(4):1480-4.

434. Frova C. Glutathione transferases in the genomics era: new insights and perspectives. Biomol Eng 2006 Sep;23(4):149-69.

435. Townsend DM, Tew KD. The role of glutathione-S-transferase in anti-cancer drug resistance. Oncogene 2003 Oct 20;22(47):7369-75.

436. Dixon DP, Lapthorn A, Edwards R. Plant glutathione transferases. Genome Biol 2002;3(3):REVIEWS3004.

437. Board PG, Coggan M, Chelvanayagam G, Easteal S, Jermiin LS, Schulte GK, et al. Identification, characterization, and crystal structure of the Omega class glutathione transferases. J Biol Chem 2000 Aug 11;275(32):24798-806.

438. Girardini J, Amirante A, Zemzoumi K, Serra E. Characterization of an omega-class glutathione S-transferase from *Schistosoma mansoni* with glutaredoxin-like dehydroascorbate reductase and thiol transferase activities. Eur J Biochem 2002 Nov;269(22):5512-21.

439. Allocati N, Favaloro B, Masulli M, Alexeyev MF, Di Ilio C. *Proteus mirabilis* glutathione S-transferase B1-1 is involved in protective mechanisms against oxidative and chemical stresses. Biochem J 2003 Jul 1;373(Pt 1):305-11.

440. Burmeister C, Luersen K, Heinick A, Hussein A, Domagalski M, Walter RD, et al. Oxidative stress in *Caenorhabditis elegans*: protective effects of the Omega class glutathione transferase (GSTO-1). FASEB J 2008 Feb;22(2):343-54.

441. Dixon DP, Davis BG, Edwards R. Functional divergence in the glutathione transferase superfamily in plants. Identification of two classes with putative functions in redox homeostasis in Arabidopsis thaliana. J Biol Chem 2002 Aug 23;277(34):30859-69.

442. Kampkotter A, Volkmann TE, de Castro SH, Leiers B, Klotz LO, Johnson TE, et al. Functional analysis of the glutathione S-transferase 3 from *Onchocerca volvulus* (Ov-GST-3): a parasite GST confers increased resistance to oxidative stress in *Caenorhabditis elegans*. J Mol Biol 2003 Jan 3;325(1):25-37.

443. Veal EA, Toone WM, Jones N, Morgan BA. Distinct roles for glutathione S-transferases in the oxidative stress response in *Schizosaccharomyces pombe.* J Biol Chem 2002 Sep 20;277(38):35523-31.

444. Sharma R, Yang Y, Sharma A, Awasthi S, Awasthi YC. Antioxidant role of glutathione S-transferases: protection against oxidant toxicity and regulation of stress-mediated apoptosis. Antioxid Redox Signal 2004 Apr;6(2):289-300.

445. Zhao T, Singhal SS, Piper JT, Cheng J, Pandya U, Clark-Wronski J, et al. The role of human glutathione S-transferases hGSTA1-1 and hGSTA2-2 in protection against oxidative stress. Arch Biochem Biophys 1999 Jul 15;367(2):216-24.

446. Liebau E, Bergmann B, Campbell AM, Teesdale-Spittle P, Brophy PM, Luersen K, et al. The glutathione S-transferase from *Plasmodium falciparum*. Mol Biochem Parasitol 2002 Sep-Oct;124(1-2):85-90.

447. Liebau E, Eckelt VH, Wildenburg G, Teesdale-Spittle P, Brophy PM, Walter RD, et al. Structural and functional analysis of a glutathione S-transferase from *Ascaris suum.* Biochem J 1997 Jun 1;324 (Pt 2):659-66.

448. Liebau E, Muller V, Lucius R, Walter RD, Henkle-Duhrsen K. Molecular cloning, expression and characterization of a recombinant glutathione S-transferase from *Echinococcus multilocularis*. Mol Biochem Parasitol 1996 Apr;77(1):49-56.

449. Liebau E, Wildenburg G, Brophy PM, Walter RD, Henkle-Duhrsen K. Biochemical analysis, gene structure and localization of the 24 kDa glutathione S-transferase from *Onchocerca volvulus*. Mol Biochem Parasitol 1996 Sep;80(1):27-39.

450. Ahmad R, Srivastava AK, Walter RD. Purification and biochemical characterization of cytosolic glutathione-S-transferase from filarial worms *Setaria cervi*. Comp Biochem Physiol B Biochem Mol Biol 2008 Nov;151(3):237-45.

451. Rao UR, Salinas G, Mehta K, Klei TR. Identification and localization of glutathione S-transferase as a potential target enzyme in Brugia species. Parasitol Res 2000 Nov;86(11):908-15.

452. Torres-Rivera A, Landa A. Glutathione transferases from parasites: a biochemical view. Acta Trop 2008 Feb;105(2):99-112.

453. Brophy PM, Barrett J. Glutathione transferase in helminths. Parasitology 1990 Apr;100 Pt 2:345-9.

454. Brophy PM, Pritchard DI. Parasitic helminth glutathione S-transferases: an update on their potential as targets for immuno- and chemotherapy. Exp Parasitol 1994 Aug;79(1):89-96.

455. Harwaldt P, Rahlfs S, Becker K. Glutathione S-transferase of the malarial parasite *Plasmodium falciparum*: characterization of a potential drug target. Biol Chem 2002 May;383(5):821-30.

456. Dubois VL, Platel DF, Pauly G, Tribouley-Duret J. *Plasmodium berghei*: implication of intracellular glutathione and its related enzyme in chloroquine resistance in vivo. Exp Parasitol 1995 Aug;81(1):117-24.

457. Na BK, Kang JM, Kim TS, Sohn WM. *Plasmodium vivax:* molecular cloning, expression and characterization of glutathione S-transferase. Exp Parasitol 2007 Aug;116(4):414-8.

458. Srivastava P, Puri SK, Kamboj KK, Pandey VC. Glutathione-S-transferase activity in malarial parasites. Trop Med Int Health 1999 Apr;4(4):251-4.

459. Fritz-Wolf K, Becker A, Rahlfs S, Harwaldt P, Schirmer RH, Kabsch W, et al. X-ray structure of glutathione S-transferase from the malarial parasite *Plasmodium falciparum*. Proc Natl Acad Sci U S A 2003 Nov 25;100(24):13821-6.

460. Hiller N, Fritz-Wolf K, Deponte M, Wende W, Zimmermann H, Becker K. *Plasmodium falciparum* glutathione S-transferase--structural and mechanistic studies on ligand binding and enzyme inhibition. Protein Sci 2006 Feb;15(2):281-9.

461. Vickers TJ, Fairlamb AH. Trypanothione S-transferase activity in a trypanosomatid ribosomal elongation factor 1B. J Biol Chem 2004 Jun 25;279(26):27246-56.

462. Berndt C, Lillig CH, Holmgren A. Thioredoxins and glutaredoxins as facilitators of protein folding. Biochim Biophys Acta 2008 Apr;1783(4):641-50.

463. Meyer Y, Buchanan BB, Vignols F, Reichheld JP. Thioredoxins and glutaredoxins: unifying elements in redox biology. Annu Rev Genet 2009;43:335-67.

464. Starke DW, Chock PB, Mieyal JJ. Glutathione-thiyl radical scavenging and transferase properties of human glutaredoxin (thioltransferase). Potential role in redox signal transduction. J Biol Chem 2003 Apr 25;278(17):14607-13.

465. Ghezzi P, Di Simplicio P. Glutathionylation pathways in drug response. Curr Opin Pharmacol 2007 Aug;7(4):398-403.

466. Holmgren A. Hydrogen donor system for *Escherichia coli* ribonucleoside-diphosphate reductase dependent upon glutathione. Proc Natl Acad Sci U S A 1976 Jul;73(7):2275-9.

467. Holmgren A. Glutathione-dependent synthesis of deoxyribonucleotides. Purification and characterization of glutaredoxin from *Escherichia coli.* J Biol Chem 1979 May 10;254(9):3664-71.

468. Meyer Y, Reichheld JP, Vignols F. Thioredoxins in *Arabidopsis* and other plants. Photosynth Res 2005 Dec;86(3):419-33.

469. Lemaire SD, Michelet L, Zaffagnini M, Massot V, Issakidis-Bourguet E. Thioredoxins in chloroplasts. Curr Genet 2007 Jun;51(6):343-65.

470. Greetham D, Vickerstaff J, Shenton D, Perrone GG, Dawes IW, Grant CM. Thioredoxins function as deglutathionylase enzymes in the yeast *Saccharomyces cerevisiae*. BMC Biochem 2010;11:3.

471. Ortenberg R, Gon S, Porat A, Beckwith J. Interactions of glutaredoxins, ribonucleotide reductase, and components of the DNA replication system of *Escherichia coli*. Proc Natl Acad Sci U S A 2004 May 11;101(19):7439-44.

472. Collin V, Issakidis-Bourguet E, Marchand C, Hirasawa M, Lancelin JM, Knaff DB, et al. The Arabidopsis plastidial thioredoxins: new functions and new insights into specificity. J Biol Chem 2003 Jun 27;278(26):23747-52.

473. Matthews JR, Wakasugi N, Virelizier JL, Yodoi J, Hay RT. Thioredoxin regulates the DNA binding activity of NF-kappa B by reduction of a disulphide bond involving cysteine 62. Nucleic Acids Res 1992 Aug 11;20(15):3821-30.

474. Aslund F, Zheng M, Beckwith J, Storz G. Regulation of the OxyR transcription factor by hydrogen peroxide and the cellular thiol-disulfide status. Proc Natl Acad Sci U S A 1999 May 25;96(11):6161-5.

475. Montrichard F, Alkhalfioui F, Yano H, Vensel WH, Hurkman WJ, Buchanan BB. Thioredoxin targets in plants: the first 30 years. J Proteomics 2009 Apr 13;72(3):452-74.

476. Fu C, Wu C, Liu T, Ago T, Zhai P, Sadoshima J, et al. Elucidation of thioredoxin target protein networks in mouse. Mol Cell Proteomics 2009 Jul;8(7):1674-87.

477. Holmgren A, Johansson C, Berndt C, Lonn ME, Hudemann C, Lillig CH. Thiol redox control via thioredoxin and glutaredoxin systems. Biochem Soc Trans 2005 Dec;33(Pt 6):1375-7.

478. Lillig CH, Berndt C, Holmgren A. Glutaredoxin systems. Biochim Biophys Acta 2008 Nov;1780(11):1304-17.

479. Wells WW, Xu DP, Yang YF, Rocque PA. Mammalian thioltransferase (glutaredoxin) and protein disulfide isomerase have dehydroascorbate reductase activity. J Biol Chem 1990 Sep 15;265(26):15361-4.

480. Washburn MP, Wells WW. The catalytic mechanism of the glutathione-dependent dehydroascorbate reductase activity of thioltransferase (glutaredoxin). Biochemistry 1999 Jan 5;38(1):268-74.

481. Meyer Y, Siala W, Bashandy T, Riondet C, Vignols F, Reichheld JP. Glutaredoxins and thioredoxins in plants. Biochim Biophys Acta 2008 Apr;1783(4):589-600.

482. Porat A, Lillig CH, Johansson C, Fernandes AP, Nilsson L, Holmgren A, et al. The reducing activity of glutaredoxin 3 toward cytoplasmic substrate proteins is restricted by methionine 43. Biochemistry 2007 Mar 20;46(11):3366-77.

483. Vlamis-Gardikas A, Aslund F, Spyrou G, Bergman T, Holmgren A. Cloning, overexpression, and characterization of glutaredoxin 2, an atypical glutaredoxin from *Escherichia coli.* J Biol Chem 1997 Apr 25;272(17):11236-43.

484. Fernandes AP, Fladvad M, Berndt C, Andresen C, Lillig CH, Neubauer P, et al. A novel monothiol glutaredoxin (Grx4) from *Escherichia coli* can serve as a substrate for thioredoxin reductase. J Biol Chem 2005 Jul 1;280(26):24544-52.

485. Johansson C, Lillig CH, Holmgren A. Human mitochondrial glutaredoxin reduces S-glutathionylated proteins with high affinity accepting electrons from either glutathione or thioredoxin reductase. J Biol Chem 2004 Feb 27;279(9):7537-43.

486. Bandyopadhyay S, Gama F, Molina-Navarro MM, Gualberto JM, Claxton R, Naik SG, et al. Chloroplast monothiol glutaredoxins as scaffold proteins for the assembly and delivery of [2Fe-2S] clusters. EMBO J 2008 Apr 9;27(7):1122-33.

487. Johansson C, Kavanagh KL, Gileadi O, Oppermann U. Reversible sequestration of active site cysteines in a 2Fe-2S-bridged dimer provides a mechanism for glutaredoxin 2 regulation in human mitochondria. J Biol Chem 2007 Feb 2;282(5):3077-82.

488. Rouhier N, Couturier J, Johnson MK, Jacquot JP. Glutaredoxins: roles in iron homeostasis. Trends Biochem Sci 2010 Jan;35(1):43-52.

489. Lillig CH, Berndt C, Vergnolle O, Lonn ME, Hudemann C, Bill E, et al. Characterization of human glutaredoxin 2 as iron-sulfur protein: a possible role as redox sensor. Proc Natl Acad Sci U S A 2005 Jun 7;102(23):8168-73.

490. Rahlfs S, Fischer M, Becker K. *Plasmodium falciparum* possesses a classical glutaredoxin and a second, glutaredoxin-like protein with a PICOT homology domain. J Biol Chem 2001 Oct 5;276(40):37133-40.

491. Becker K, Kanzok SM, Iozef R, Fischer M, Schirmer RH, Rahlfs S. Plasmoredoxin, a novel redox-active protein unique for malarial parasites. Eur J Biochem 2003 Mar;270(6):1057-64.

492. Tetaud E, Giroud C, Prescott AR, Parkin DW, Baltz D, Biteau N, et al. Molecular characterisation of mitochondrial and cytosolic trypanothione-dependent tryparedoxin peroxidases in *Trypanosoma brucei*. Mol Biochem Parasitol 2001 Sep 3;116(2):171-83.

493. Reckenfelderbaumer N, Ludemann H, Schmidt H, Steverding D, Krauth-Siegel RL. Identification and functional characterization of thioredoxin from *Trypanosoma bruceibrucei*. J Biol Chem 2000 Mar 17;275(11):7547-52.

494. Schmidt A, Clayton CE, Krauth-Siegel RL. Silencing of the thioredoxin gene in *Trypanosoma bruceibrucei*. Mol Biochem Parasitol 2002 Nov-Dec;125(1-2):207-10.

495. Comini MA, Rettig J, Dirdjaja N, Hanschmann EM, Berndt C, Krauth-Siegel RL. Monothiol glutaredoxin-1 is an essential iron-sulfur protein in the mitochondrion of African trypanosomes. J Biol Chem 2008 Oct 10;283(41):27785-98.

496. Ceylan S, Seidel V, Ziebart N, Berndt C, Dirdjaja N, Krauth-Siegel RL. The dithiol glutaredoxins of african trypanosomes have distinct roles and are closely linked to the unique trypanothione metabolism. J Biol Chem 2010 Nov 5;285(45):35224-37.

497. Feng Y, Zhong N, Rouhier N, Hase T, Kusunoki M, Jacquot JP, et al. Structural insight into poplar glutaredoxin C1 with a bridging iron-sulfur cluster at the active site. Biochemistry 2006 Jul 4;45(26):7998-8008.

498. Marquez VE, Arias DG, Piattoni CV, Robello C, Iglesias AA, Guerrero SA. Cloning, expression, and characterization of a dithiol glutaredoxin from *Trypanosoma cruzi*. Antioxid Redox Signal 2010 Mar 15;12(6):787-92.

499. Reinders J, Sickmann A. Modificomics: posttranslational modifications beyond protein phosphorylation and glycosylation. Biomol Eng 2007 Jun;24(2):169-77.

500. Paulsen CE, Carroll KS. Orchestrating redox signaling networks through regulatory cysteine switches. ACS Chem Biol 2010 Jan 15;5(1):47-62.

501. Brandes N, Schmitt S, Jakob U. Thiol-based redox switches in eukaryotic proteins. Antioxid Redox Signal 2009 May;11(5):997-1014.

502. Dalle-Donne I, Rossi R, Colombo G, Giustarini D, Milzani A. Protein S-glutathionylation: a regulatory device from bacteria to humans. Trends Biochem Sci 2009 Feb;34(2):85-96.

503. Michelet L, Zaffagnini M, Massot V, Keryer E, Vanacker H, Miginiac-Maslow M, et al. Thioredoxins, glutaredoxins, and glutathionylation: new crosstalks to explore. Photosynth Res 2006 Sep;89(2-3):225-45.

504. Ghezzi P. Oxidoreduction of protein thiols in redox regulation. Biochem Soc Trans 2005 Dec;33(Pt 6):1378-81.

505. Sies H, Akerboom TP. Glutathione disulfide (GSSG) efflux from cells and tissues. Methods Enzymol 1984;105:445-51.

506. Mieyal JJ, Gallogly MM, Qanungo S, Sabens EA, Shelton MD. Molecular mechanisms and clinical implications of reversible protein S-glutathionylation. Antioxid Redox Signal 2008 Nov;10(11):1941-88.

507. Townsend DM, Manevich Y, He L, Hutchens S, Pazoles CJ, Tew KD. Novel role for glutathione S-transferase pi. Regulator of protein S-Glutathionylation following oxidative and nitrosative stress. J Biol Chem 2009 Jan 2;284(1):436-45.

508. Gallogly MM, Mieyal JJ. Mechanisms of reversible protein glutathionylation in redox signaling and oxidative stress. Curr Opin Pharmacol 2007 Aug;7(4):381-91.

509. Gao XH, Bedhomme M, Veyel D, Zaffagnini M, Lemaire SD. Methods for analysis of protein glutathionylation and their application to photosynthetic organisms. Mol Plant 2009 Mar;2(2):218-35.

510. Motohashi K, Kondoh A, Stumpp MT, Hisabori T. Comprehensive survey of proteins targeted by chloroplast thioredoxin. Proc Natl Acad Sci U S A 2001 Sep 25;98(20):11224-9.

511. Sturm N, Jortzik E, Mailu BM, Koncarevic S, Deponte M, Forchhammer K, et al. Identification of proteins targeted by the thioredoxin superfamily in *Plasmodium falciparum*. PLoS Pathog 2009 Apr;5(4):e1000383.

512. Balmer Y, Koller A, del Val G, Manieri W, Schurmann P, Buchanan BB. Proteomics gives insight into the regulatory function of chloroplast thioredoxins. Proc Natl Acad Sci U S A 2003 Jan 7;100(1):370-5.

513. Wong JH, Cai N, Balmer Y, Tanaka CK, Vensel WH, Hurkman WJ, et al. Thioredoxin targets of developing wheat seeds identified by complementary proteomic approaches. Phytochemistry 2004 Jun;65(11):1629-40.

514. Lemaire SD, Guillon B, Le Marechal P, Keryer E, Miginiac-Maslow M, Decottignies P. New thioredoxin targets in the unicellular photosynthetic eukaryote *Chlamydomonas reinhardtii*. Proc Natl Acad Sci U S A 2004 May 11;101(19):7475-80.

515. Rouhier N, Villarejo A, Srivastava M, Gelhaye E, Keech O, Droux M, et al. Identification of plant glutaredoxin targets. Antioxid Redox Signal 2005 Jul-Aug;7(7-8):919-29.

516. Fratelli M, Demol H, Puype M, Casagrande S, Villa P, Eberini I, et al. Identification of proteins undergoing glutathionylation in oxidatively stressed hepatocytes and hepatoma cells. Proteomics 2003 Jul;3(7):1154-61.

517. Lind C, Gerdes R, Hamnell Y, Schuppe-Koistinen I, von Lowenhielm HB, Holmgren A, et al. Identification of S-glutathionylated cellular proteins during oxidative stress and constitutive metabolism by affinity purification and proteomic analysis. Arch Biochem Biophys 2002 Oct 15;406(2):229-40.

518. Dixon DP, Skipsey M, Grundy NM, Edwards R. Stress-induced protein S-glutathionylation in *Arabidopsis*. Plant Physiol 2005 Aug;138(4):2233-44.

519. Hill BG, Bhatnagar A. Protein S-glutathiolation: Redox-sensitive regulation of protein function. J Mol Cell Cardiol 2011 Jul 20.

520. Cotgreave IA, Gerdes R, Schuppe-Koistinen I, Lind C. S-glutathionylation of glyceraldehyde-3-phosphate dehydrogenase: role of thiol oxidation and catalysis by glutaredoxin. Methods Enzymol 2002;348:175-82.

521. Zaffagnini M, Michelet L, Marchand C, Sparla F, Decottignies P, Le Marechal P, et al. The thioredoxin-independent isoform of chloroplastic glyceraldehyde-3-phosphate dehydrogenase is selectively regulated by glutathionylation. FEBS J 2007 Jan;274(1):212-26.

522. Lind C, Gerdes R, Schuppe-Koistinen I, Cotgreave IA. Studies on the mechanism of oxidative modification of human glyceraldehyde-3-phosphate dehydrogenase by glutathione: catalysis by glutaredoxin. Biochem Biophys Res Commun 1998 Jun 18;247(2):481-6.

523. Applegate MA, Humphries KM, Szweda LI. Reversible inhibition of alpha-ketoglutarate dehydrogenase by hydrogen peroxide: glutathionylation and protection of lipoic acid. Biochemistry 2008 Jan 8;47(1):473-8.

524. Ito H, Iwabuchi M, Ogawa K. The sugar-metabolic enzymes aldolase and triose-phosphate isomerase are targets of glutathionylation in *Arabidopsis thaliana*: detection using biotinylated glutathione. Plant Cell Physiol 2003 Jul;44(7):655-60.

525. Hondorp ER, Matthews RG. Oxidative stress inactivates cobalamin-independent methionine synthase (MetE) in *Escherichia coli*. PLoS Biol 2004 Nov;2(11):e336.

526. Rinna A, Torres M, Forman HJ. Stimulation of the alveolar macrophage respiratory burst by ADP causes selective glutathionylation of protein tyrosine phosphatase 1B. Free Radic Biol Med 2006 Jul 1;41(1):86-91.

527. Cross JV, Templeton DJ. Oxidative stress inhibits MEKK1 by site-specific glutathionylation in the ATP-binding domain. Biochem J 2004 Aug 1;381(Pt 3):675-83.

528. Prinarakis E, Chantzoura E, Thanos D, Spyrou G. S-glutathionylation of IRF3 regulates IRF3-CBP interaction and activation of the IFN beta pathway. EMBO J 2008 Mar 19;27(6):865-75.

529. Reynaert NL, van der Vliet A, Guala AS, McGovern T, Hristova M, Pantano C, et al. Dynamic redox control of NF-kappaB through glutaredoxin-regulated S-glutathionylation of inhibitory kappaB kinase beta. Proc Natl Acad Sci U S A 2006 Aug 29;103(35):13086-91.

530. Michelet L, Zaffagnini M, Marchand C, Collin V, Decottignies P, Tsan P, et al. Glutathionylation of chloroplast thioredoxin f is a redox signaling mechanism in plants. Proc Natl Acad Sci U S A 2005 Nov 8;102(45):16478-83.

531. Casagrande S, Bonetto V, Fratelli M, Gianazza E, Eberini I, Massignan T, et al. Glutathionylation of human thioredoxin: a possible crosstalk between the glutathione and thioredoxin systems. Proc Natl Acad Sci U S A 2002 Jul 23;99(15):9745-9.

532. Kehr S, Jortzik E, Delahunty C, Yates JR, Rahlfs S, Becker K. Protein S-Glutathionylation in Malaria Parasites. Antioxid Redox Signal 2011 Jul 7.

533. Jortzik E, Mailu BM, Preuss J, Fischer M, Bode L, Rahlfs S, et al. Glucose-6-phosphate dehydrogenase-6-phosphogluconolactonase: a unique bifunctional enzyme from *Plasmodium falciparum*. Biochem J 2011 Jun 15;436(3):641-50.

534. Reynaert NL, Ckless K, Guala AS, Wouters EF, van der Vliet A, Janssen-Heininger YM. *In situ* detection of S-glutathionylated proteins following glutaredoxin-1 catalyzed cysteine derivatization. Biochim Biophys Acta 2006 Mar;1760(3):380-7.

535. Mawatari S, Murakami K. Different types of glutathionylation of hemoglobin can exist in intact erythrocytes. Arch Biochem Biophys 2004 Jan 1;421(1):108-14.

536. Rossi R, Giustarini D, Milzani A, Dalle-Donne I. Membrane skeletal protein S-glutathionylation and hemolysis in human red blood cells. Blood Cells Mol Dis 2006 Nov-Dec;37(3):180-7.

537. Pastore A, Tozzi G, Gaeta LM, Bertini E, Serafini V, Di Cesare S, et al. Actin glutathionylation increases in fibroblasts of patients with Friedreich's ataxia: a potential role in the pathogenesis of the disease. J Biol Chem 2003 Oct 24;278(43):42588-95.

538. Wang J, Boja ES, Tan W, Tekle E, Fales HM, English S, et al. Reversible glutathionylation regulates actin polymerization in A431 cells. J Biol Chem 2001 Dec 21;276(51):47763-6.

539. Gallogly MM, Starke DW, Mieyal JJ. Mechanistic and kinetic details of catalysis of thiol-disulfide exchange by glutaredoxins and potential mechanisms of regulation. Antioxid Redox Signal 2009 May;11(5):1059-81.

540. Gao XH, Zaffagnini M, Bedhomme M, Michelet L, Cassier-Chauvat C, Decottignies P, et al. Biochemical characterization of glutaredoxins from *Chlamydomonas reinhardtii*: kinetics and specificity in deglutathionylation reactions. FEBS Lett 2010 Jun 3;584(11):2242-8.

541. Bedhomme M, Zaffagnini M, Marchand CH, Gao XH, Moslonka-Lefebvre M, Michelet L, et al. Regulation by glutathionylation of isocitrate lyase from *Chlamydomonas reinhardtii*. J Biol Chem 2009 Dec 25;284(52):36282-91.

542. Findlay VJ, Townsend DM, Morris TE, Fraser JP, He L, Tew KD. A novel role for human sulfiredoxin in the reversal of glutathionylation. Cancer Res 2006 Jul 1;66(13):6800-6.

543. Zaffagnini M, Michelet L, Massot V, Trost P, Lemaire SD. Biochemical characterization of glutaredoxins from *Chlamydomonas reinhardtii* reveals the unique properties of a chloroplastic CGFS-type glutaredoxin. J Biol Chem 2008 Apr 4;283(14):8868-76.

544. Chrestensen CA, Starke DW, Mieyal JJ. Acute cadmium exposure inactivates thioltransferase (Glutaredoxin), inhibits intracellular reduction of protein-glutathionyl-mixed disulfides, and initiates apoptosis. J Biol Chem 2000 Aug 25;275(34):26556-65.

545. Srinivasan U, Mieyal PA, Mieyal JJ. pH profiles indicative of rate-limiting nucleophilic displacement in thioltransferase catalysis. Biochemistry 1997 Mar 18;36(11):3199-206.

546. Gravina SA, Mieyal JJ. Thioltransferase is a specific glutathionyl mixed disulfide oxidoreductase. Biochemistry 1993 Apr 6;32(13):3368-76.

547. Peltoniemi MJ, Karala AR, Jurvansuu JK, Kinnula VL, Ruddock LW. Insights into deglutathionylation reactions. Different intermediates in the glutaredoxin and protein disulfide isomerase catalyzed reactions are defined by the gamma-linkage present in glutathione. J Biol Chem 2006 Nov 3;281(44):33107-14.

548. Frezard F, Demicheli C, Ferreira CS, Costa MA. Glutathione-induced conversion of pentavalent antimony to trivalent antimony in meglumine antimoniate. Antimicrob Agents Chemother 2001 Mar;45(3):913-6.

549. Ferreira Cdos S, Martins PS, Demicheli C, Brochu C, Ouellette M, Frezard F. Thiol-induced reduction of antimony(V) into antimony(III): a comparative study with trypanothione, cysteinyl-glycine, cysteine and glutathione. Biometals 2003 Sep;16(3):441-6.

550. Roberts WL, Berman JD, Rainey PM. *In vitro* anti Leishmanial properties of tri- and pentavalent antimonial preparations. Antimicrob Agents Chemother 1995 Jun;39(6):1234-9.

551. Ephros M, Bitnun A, Shaked P, Waldman E, Zilberstein D. Stage-specific activity of pentavalent antimony against *Leishmania donovani* axenic amastigotes. Antimicrob Agents Chemother 1999 Feb;43(2):278-82.

552. Shaked-Mishan P, Ulrich N, Ephros M, Zilberstein D. Novel Intracellular SbV reducing activity correlates with antimony susceptibility in *Leishmania donovani*. J Biol Chem 2001 Feb 9;276(6):3971-6.

553. Mukhopadhyay R, Rosen BP. Arsenate reductases in prokaryotes and eukaryotes. Environ Health Perspect 2002 Oct;110 Suppl 5:745-8.

554. Moutiez M, Quemeneur E, Sergheraert C, Lucas V, Tartar A, Davioud-Charvet E. Glutathione-dependent activities of *Trypanosoma cruzi* p52 makes it a new member of the thiol:disulphide oxidoreductase family. Biochem J 1997 Feb 15;322 (Pt 1):43-8.

555. Garzon E, Borges MC, Cordeiro-da-Silva A, Nacife V, Meirelles Mde N, Guilvard E, et al. *Trypanosoma cruzi* carrying a targeted deletion of a Tc52 protein-encoding allele elicits attenuated Chagas' disease in mice. Immunol Lett 2003 Oct 9;89(1):67-80.

556. Moutiez M, Aumercier M, Schoneck R, Meziane-Cherif D, Lucas V, Aumercier P, et al. Purification and characterization of a trypanothione-glutathione thioltransferase from *Trypanosoma cruzi*. Biochem J 1995 Sep 1;310 (Pt 2):433-7.

557. Ouaissi MA, Dubremetz JF, Schoneck R, Fernandez-Gomez R, Gomez-Corvera R, Billaut-Mulot O, et al. *Trypanosoma cruzi*: a 52-kDa protein sharing sequence homology with glutathione S-transferase is localized in parasite organelles morphologically resembling reservosomes. Exp Parasitol 1995 Dec;81(4):453-61.

558. Bethony JM, Cole RN, Guo X, Kamhawi S, Lightowlers MW, Loukas A, et al. Vaccines to combat the neglected tropical diseases. Immunol Rev 2011 Jan;239(1):237-70.

559. Creek DJ, Anderson J, McConville MJ, Barrett MP. Metabolomic analysis of trypanosomatid protozoa. Mol Biochem Parasitol 2011 Oct 19.

560. Paape D, Aebischer T. Contribution of proteomics of *Leishmania* spp. to the understanding of differentiation, drug resistance mechanisms, vaccine and drug development. J Proteomics 2011 Aug 24;74(9):1614-24.

561. Dubessay P, Ravel C, Bastien P, Crobu L, Dedet JP, Pages M, et al. The switch region on *Leishmania major* chromosome 1 is not required for mitotic stability or gene expression, but appears to be essential. Nucleic Acids Res 2002 Sep 1;30(17):3692-7.

562. Ilgoutz SC, Zawadzki JL, Ralton JE, McConville MJ. Evidence that free GPI glycolipids are essential for growth of *Leishmania mexicana*. EMBO J 1999 May 17;18(10):2746-55.

563. Mukherjee A, Roy G, Guimond C, Ouellette M. The gamma-glutamylcysteine synthetase gene of *Leishmania* is essential and involved in response to oxidants. Mol Microbiol 2009 Nov;74(4):914-27.

564. Murta SM, Vickers TJ, Scott DA, Beverley SM. Methylene tetrahydrofolate dehydrogenase/cyclohydrolase and the synthesis of 10-CHO-THF are essential in *Leishmania major*. Mol Microbiol 2009 Mar;71(6):1386-401.

565. Silverman JM, Chan SK, Robinson DP, Dwyer DM, Nandan D, Foster LJ, et al. Proteomic analysis of the secretome of *Leishmania donovani*. Genome Biol 2008;9(2):R35.1-21

566. Rukmangadachar LA, Kataria J, Hariprasad G, Samantaray JC, Srinivasan A. Two-dimensional difference gel electrophoresis (DIGE) analysis of sera from visceral *Leishmania*sis patients. Clin Proteomics 2011;8(1):4.

567. Daneshvar H, Wyllie S, Phillips S, Hagan P, Burchmore R. Comparative proteomics profiling of a gentamicin-attenuated *Leishmania infantum* cell line identifies key changes in parasite thiol-redox metabolism. J Proteomics 2011 Nov 28 *in press*

568. El Fadili K, Drummelsmith J, Roy G, Jardim A, Ouellette M. Down regulation of KMP-11 in *Leishmania infantum* axenic antimony resistant amastigotes as revealed by a proteomic screen. Exp Parasitol 2009 Sep;123(1):51-7.

569. Vergnes B, Gourbal B, Girard I, Sundar S, Drummelsmith J, Ouellette M. A proteomics screen implicates HSP83 and a small kinetoplastid calpain-related protein in drug resistance in *Leishmania donovani* clinical field isolates by modulating drug-induced programmed cell death. Mol Cell Proteomics 2007 Jan;6(1):88-101.

570. Creek DJ, Jankevics A, Breitling R, Watson DG, Barrett MP, Burgess KE. Toward global metabolomics analysis with hydrophilic interaction liquid chromatography-mass spectrometry: improved metabolite identification by retention time prediction. Anal Chem 2011 Nov 15;83(22):8703-10.

571. De Souza DP, Saunders EC, McConville MJ, Likic VA. Progressive peak clustering in GC-MS Metabolomic experiments applied to *Leishmania* parasites. Bioinformatics 2006 Jun 1;22(11):1391-6.

572. Olszewski KL, Llinas M. Central carbon metabolism of *Plasmodium* parasites. Mol Biochem Parasitol 2010 Feb;175(2):95-103.

573. Kaye P, Scott P. Leishmaniasis: complexity at the host-pathogen interface. Nat Rev Microbiol Aug;9(8):604-15.

574. Mehta SR, Huang R, Yang M, Zhang XQ, Kolli B, Chang KP, et al. Real-time in vivo green fluorescent protein imaging of a murine Leishmaniasis model as a new tool for *Leishmania* vaccine and drug discovery. Clin Vaccine Immunol 2008 Dec;15(12):1764-70.

575. Thalhofer CJ, Graff JW, Love-Homan L, Hickerson SM, Craft N, Beverley SM, et al. In vivo imaging of transgenic *Leishmania* parasites in a live host. J Vis Exp 2010(41).

576. Torres DC, Adaui V, Ribeiro-Alves M, Romero GA, Arevalo J, Cupolillo E, et al. Targeted gene expression profiling in *Leishmania braziliensis* and *Leishmania* guyanensis parasites isolated from Brazilian patients with different antimonial treatment outcomes. Infect Genet Evol 2010 Aug;10(6):727-33.

577. Fernandez-Gomez R, Esteban S, Gomez-Corvera R, Zoulika K, Ouaissi A. *Trypanosoma cruzi*: Tc52 released protein-induced increased expression of nitric oxide synthase and nitric oxide production by macrophages. J Immunol 1998 Apr 1;160(7):3471-9.

578. Allaoui A, Francois C, Zemzoumi K, Guilvard E, Ouaissi A. Intracellular growth and metacyclogenesis defects in *Trypanosoma cruzi* carrying a targeted deletion of a Tc52 protein-encoding allele. Mol Microbiol 1999 Jun;32(6):1273-86.

579. Lye LF, Owens K, Shi H, Murta SM, Vieira AC, Turco SJ, et al. Retention and loss of RNA interference pathways in trypanosomatid protozoans. PLoS Pathog 2010;6(10):e1001161.

580. Van Assche T, Deschacht M, da Luz RA, Maes L, Cos P. *Leishmania*-macrophage interactions: insights into the redox biology. Free Radic Biol Med 2011 Jul 15;51(2):337-51.

581. Garcera A, Barreto L, Piedrafita L, Tamarit J, Herrero E. Saccharomyces cerevisiae cells have three Omega class glutathione S-transferases acting as 1-Cys thiol transferases. Biochem J 2006 Sep 1;398(2):187-96.

582. Dalle-Donne I, Rossi R, Giustarini D, Colombo R, Milzani A. S-glutathionylation in protein redox regulation. Free Radic Biol Med 2007 Sep 15;43(6):883-98.

583. Xiong Y, Uys JD, Tew KD, Townsend DM. S-glutathionylation: from molecular mechanisms to health outcomes. Antioxid Redox Signal 2011 Jul 1;15(1):233-70.

584. Fratelli M, Demol H, Puype M, Casagrande S, Eberini I, Salmona M, et al. Identification by redox proteomics of glutathionylated proteins in oxidatively stressed human T lymphocytes. Proc Natl Acad Sci U S A 2002 Mar 19;99(6):3505-10.

585. Shenton D, Grant CM. Protein S-thiolation targets glycolysis and protein synthesis in response to oxidative stress in the yeast *Saccharomyces cerevisiae*. Biochem J 2003 Sep 1;374(Pt 2):513-9.

586. Zaffagnini M, Bedhomme M, Groni H, Marchand CH, Puppo C, Gontero B, et al. Glutathionylation in the photosynthetic model organism *Chlamydomonas reinhardtii*: a proteomic survey. Mol Cell Proteomics 2011 Nov 28 *in press*

587. Kehr S, Jortzik E, Delahunty C, Yates JR, 3rd, Rahlfs S, Becker K. Protein s-glutathionylation in malaria parasites. Antioxid Redox Signal 2011 Dec 1;15(11):2855-65.

588. Hashemy SI, Johansson C, Berndt C, Lillig CH, Holmgren A. Oxidation and S-nitrosylation of cysteines in human cytosolic and mitochondrial glutaredoxins: effects on structure and activity. J Biol Chem 2007 May 11;282(19):14428-36.

589. Li WF, Yu J, Ma XX, Teng YB, Luo M, Tang YJ, et al. Structural basis for the different activities of yeast Grx1 and Grx2. Biochim Biophys Acta 2010 Jul;1804(7):1542-7.

590. Gossage SM, Rogers ME, Bates PA. Two separate growth phases during the development of *Leishmania* in sand flies: implications for understanding the life cycle. Int J Parasitol 2003 Sep 15;33(10):1027-34.

591. Sacks DL, Pimenta PF, McConville MJ, Schneider P, Turco SJ. Stage-specific binding of *Leishmania donovani* to the sand fly vector midgut is regulated by conformational changes in the abundant surface lipophosphoglycan. J Exp Med 1995 Feb 1;181(2):685-97.

592. McConville MJ, Turco SJ, Ferguson MA, Sacks DL. Developmental modification of lipophosphoglycan during the differentiation of *Leishmania major* promastigotes to an infectious stage. EMBO J 1992 Oct;11(10):3593-600.

593. Sadlova J, Price HP, Smith BA, Votypka J, Volf P, Smith DF. The stage-regulated HASPB and SHERP proteins are essential for differentiation of the protozoan parasite *Leishmania major* in its sand fly vector, Phlebotomus papatasi. Cell Microbiol 2010 Dec;12(12):1765-79.

594. Davies CR, Cooper AM, Peacock C, Lane RP, Blackwell JM. Expression of LPG and GP63 by different developmental stages of *Leishmania major* in the sandfly *Phlebotomus papatasi*. Parasitology 1990 Dec;101 Pt 3:337-43.